

ACTA PATHOLOGICA ET MICROBIOLOGICA SCANDINAVICA

A PATHOLOGY

EDITORIAL BOARD

STEEN OLSEN DENMARK
J RAPOLA FINLAND
O BJARNASON ICELAND
K ARNESEN NORWAY
J L E ERICSSON SWEDEN

EDITOR IN-CHIEF

J CHR SUH

ADVISORY BOARD

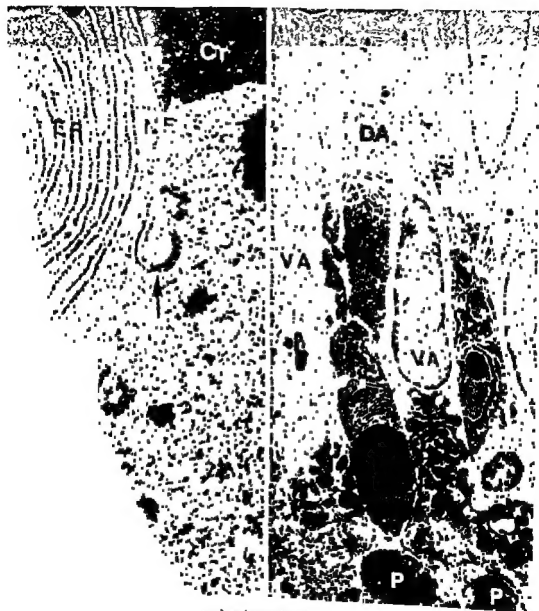
J RYGAARD DENMARK
J VISFELDT DENMARK
T NEVALAINEN FINLAND
L TEPPÖ FINLAND
G GEORGSSON ICELAND
J HALLGRIMSSON ICELAND
T HÖVIG NORWAY
O D LERUM NORWAY
T BERGE SWEDEN
K NILSSON SWEDEN

VOL 87A FASC. 1 JANUARY 1979

ISSN 0365-4384

MUNKSGAARD COPENHAGEN

Fig 4 Electron micrograph showing the basal part of the ameloblast layer and the adjacent cytoplasm of stratum intermedium cells (SI) To the left and to the right viable ameloblasts (VA) are seen Between them are two large nucleus-containing degenerating ameloblast fragments (DA1) Compare the rounded mitochondria (M1) of the degenerating cells with the mitochondria (M2) of the viable cells The stratum intermedium cells have engulfed two large ameloblast fragments (DA2) and are in the process of enwrapping the fragments marked DA1 with thin cytoplasmic extensions (arrows) X 9 600



Some of the fragments envelop small amounts of karyoplasm (arrows) ER endoplasmic cisternae with monodispersed ribosomes Cr

viable ameloblasts (VA) are intermingled with solitary degenerating phagosomes (P) are seen in the stratum intermedium X 7,700

SEQUENTIAL ULTRASTRUCTURAL CHANGES IN VINBLASTINE-INDUCED CELL DEATH OF SECRETORY AMELOBLASTS OF RAT INCISORS *IN VIVO*

H MOE

Anatomy Department C University of Copenhagen Denmark

Moe H Sequential ultrastructural changes in vinblastine induced cell death of secretory ameloblasts of rat incisors *in vivo* Acta path microbiol scand Sect A 87 1-9 1979

Secretory ameloblasts in the continuously growing incisors of the rat were used to study the sequential changes in a mature cell type degenerating after administration of vinblastine at a dosage of 2 mg per kg body weight. In less than half an hour nearly all microtubules vanished. This was succeeded by progressive displacement of the nuclei and disorganization of the cytoplasmic structure. After 1 to 3 hours attached and free polyribosomes were converted into monoribosomes. All these cytoplasmic changes were seen in viable as well as in necrotic cell. Between 5 and 6 1/2 hours after application of the drug degeneration of nuclei began. These changes from the outset indicated that a particular ameloblast had been drawn into a sequence of events which would ultimately lead to its death. The progressive alterations of the nucleus and cytoplasm of the degenerating cells and the concurrent fragmentation and elimination of the fragments are described.

Key words: Ameloblasts, vinblastine, cell death, ultrastructure.

H Moe, Anatomy Department C, Universitetsparken 1, DK-2100 Copenhagen Ø, Denmark.

Accepted as submitted 18 vi 78

Most cell systems in which the toxic effect on normal cells *in vivo* of non-lethal dosages of antineoplastic substances has been studied morphologically are heterogeneous. This often makes it difficult to identify early stages of injury and to state the sequence of events induced. The continuously growing incisors of the rat contain populations of stem cells, proliferating cells, differentiating cells and mature active cells arranged in compartments in succession. The ameloblasts constitute such a cell

at a dosage of 2 mg per kg body weight. They are used in the present work to study the sequential changes in non-dividing cells fatally injured by vinblastine.

MATERIAL AND METHODS

Mandibular incisors from 18 female SPF Wistar rats weighing about 100 g were used. The animals were injected intravenously with vinblastine sulfate (Velbe) at

enamel matrix is produced, the ameloblasts form a uniform layer of mature prismatic secretory cells. Many of these cells die in rats exposed to vinblastine

at 48 hours and 3 animals 72 hours after receiving vinblastine. 7 additional animals served as controls. The procedure for treatment and preparation of the material was as earlier described (Moe & Mikkelsen 1977a).

Founded 1924

Editor-in Chief J CHR SIM, M D, Copenhagen, Denmark
 Managing Editors JAKOB VISFELDT, M D and
 ERIK BRUMMERSTEDT, D V M
 Consultant for Illustrations MR AKSEL BIRCH-ANDERSEN
 Editorial Office c/o INGER DANIELSEN Secretary,
 Johnstrups Alle 6 DK 1923 Copenhagen V Denmark

Acta Pathologica et Microbiologica Scandinavica is intended for the prompt publication of original research in the fields of pathology, microbiology, and immunology. It is included in Current Contents, Excerpta Medica and Medlars.

Acta Pathologica et Microbiologica Scandinavica is a nonprofit making scientific journal. Since 1924 it has been published by the Scandinavian Societies for Medical Microbiology and Pathology. It appears in three sections: Section A Pathology, Section B Microbiology, and Section C Immunology.

Acta Pathologica et Microbiologica Scandinavica has subscribers in more than seventy countries throughout the world with a wide readership in the major research institutes, hospitals, laboratories, and specialist libraries.

EDITORIAL CORRESPONDENCE

All communications regard
 Editorial Office c/o Inger
 Denmark

SUBSCRIPTION

At present one annual volume of Section A, one of Section B and one of Section C (each section consisting of 6 issues appearing bimonthly) will contain a total of approximately 1400 pages. During the past few years approximately five free supplements have been issued annually. These supplements will be delivered separately to the subscribers by surface mail at no extra charge. The subscription price is

Sect A B and C	D kr 850 - plus postage	D kr 66 - (\$ 183.20 £ 91.60 DM 338.95)
Sect A	D kr 505 - plus postage	D kr 24 - (\$ 105.80 £ 52.90 DM 195.75)
Sect B	D kr 505 - plus postage	D kr 24 - (\$ 105.80 £ 52.90 DM 195.75)
Sect C	D kr 400 - plus postage	D kr 18 - (\$ 83.60 £ 41.80 DM 154.70)
Sect A and C (combined)	D kr 750 - plus postage	D kr 42 - (\$ 158.40 £ 79.20 DM 293.05)
Sect B and C (combined)	D kr 750 - plus postage	D kr 42 - (\$ 158.40 £ 79.20 DM 293.05)

Back numbers (whole volumes or single copies) are available
 NB All prices are subject to exchange rate fluctuation

© 1979 by Acta Pathologica et Microbiologica Scandinavica. All rights reserved.
 Reproduction in any form including microfilm without written permission of the Editor is prohibited.

Second class postage paid at Jamaica NY. Airfreight and mailing in the US by Publications
 Expediting Inc. Elmont NY 11003. Printed in Denmark.

SEQUENTIAL ULTRASTRUCTURAL CHANGES IN VINBLASTINE-INDUCED CELL DEATH OF SECRETORY AMELOBLASTS OF RAT INCISORS *IN VIVO*

H MOE

Anatomy Department C University of Copenhagen Denmark

Moe H Sequential ultrastructural changes in vinblastine induced cell death of secretory ameloblasts of rat incisors *in vivo* Acta path microbiol scand Sect. A 87 1-9 1979

Secretory ameloblasts in the continuously growing incisors of the rat were used to study the sequential changes in a mature cell type degenerating after administration of vinblastine at a dosage of 2 mg per kg body weight. In less than half an hour nearly all microtubules vanished. This was succeeded by progressive displacement of the nuclei and disorganization of the cytoplasmic structure. After 1 to 3 hours attached and free polyribosomes were converted into monoribosomes. All these cytoplasmic changes were seen in viable as well as in necrotic cell. Between 5 and 6 1/2 hours after application of the drug degeneration of nuclei began. These changes from the outset indicated that a particular ameloblast had been drawn into a sequence of events which would ultimately lead to its death. The progressive alterations of the nucleus and cytoplasm of the degenerating cells and the concurrent fragmentation and elimination of the fragments are described.

Key words: Ameloblasts, vinblastine, cell death, ultrastructure.

H Moe, Anatomy Department C, Universitetsparken 1, DK-2100 Copenhagen Ø, Denmark.

Accepted as submitted 18 vi 78

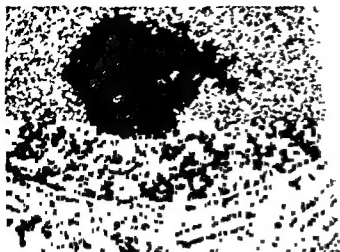
Most cell systems in which the toxic effect on normal cells *in vivo* of non-lethal dosages of antineoplastic substances has been studied morphologically are heterogeneous. This often makes it difficult to identify early stages of injury and to state the sequence of events induced. The continuously growing incisors of the rat contain populations of stem cells, proliferating cells, differentiating cells and mature active cells arranged in compartments in succession. The ameloblasts constitute such a cell

at a dosage of 2 mg per kg body weight. They are used in the present work to study the sequential changes in non-dividing cells fatally injured by vinblastine.

MATERIAL AND METHODS

Mandibular incisors from 18 female SPF Wistar rats weighing about 100 g were used. The animals were injected intravenously with vinblastine at a dosage of 2 mg per kg body weight. At 0, 1, 2, 4, 8 hours and 24 hours after injection the animals were sacrificed. At 0, 1, 2, 4, 8 hours and 24 hours after receiving vinblastine 7 additional animals served as controls. The procedure for treatment and preparation of the material was as earlier described (Moe & Mikkelsen 1977a).

enamel matrix is produced the ameloblasts form a uniform layer of mature prismatic secretory cells. Many of these cells die in rats exposed to vinblastine



RESULTS

Visible changes in the nucleus occurred relatively late after administration of vinblastine. Changes in the cytoplasm began early and were pronounced when the nuclear changes appeared. Very early (in less than half an hour) nearly all the microtubuli vanished. This was succeeded by progressive displacement of the nuclei, redistribution at random of most organelles, and arrested apical translocation of secretory granules. Later (1 to 3 hours after drug administration) the polyribosomes of the endoplasmic reticulum and of the cytoplasmic matrix were converted into monoribosomes and the number of cisternae in the Golgi complex began to increase from the normal three to five parallel cisternae to five to nine empty cisternae per complex. While the early cytoplasmic changes occurred in all secretory ameloblasts whether the cells would survive or not, the conversion of the polyribosomes into monodispersed ribosomes did not occur in all cells. It had occurred, however, in all ameloblasts in which nuclear degeneration took place (Fig. 1).

Nuclei with early necrotic features began to appear about 5 hours after administration of vinblastine. Their number increased rapidly during the following hour. $6\frac{1}{2}$ to 8 hours after drug administration nearly all injured nuclei were in an advanced state of necrosis.

The first change observed in the nuclei consisted of a peripheral accumulation of chromatin (Fig. 1). This became progressively denser and formed three to six oblong masses beneath the nuclear envelope (Fig. 2). These masses were further condensed and fused into two or three compact bodies often

situated at the nuclear poles (Figs. 2 and 3). In this position the shape of the bodies was approximately planoconvex. In a few nuclei the chromatin fused into a thick disc oriented transversely to the long axis. Finally the chromatin formed one or two large, dense, eccentrically placed globules (Fig. 4). The nucleoli were also condensed and often segregated into granular and fibrillar regions. They lay freely in the karyoplasm or were attached to a chromatin body (Figs. 3 and 4). At the conclusion of chromatin condensation the nuclear envelope disrupted into fragments of varying size and the karyoplasm became contiguous with the cytosol. During this process, fragments of the nuclear envelope frequently enveloped small amounts of karyoplasm or chromatin (Fig. 5). In advanced necrosis, rounded chromatin masses lay freely in the cytoplasm, often without identifiable remnants of the nuclear envelope.

Necrotic ameloblasts appeared singly (Fig. 6), in groups (Fig. 7) or in wide continuous areas (Fig. 8) of the ameloblast layer. When dense — — —

the distal lateral junctional complex and apical cell web were lost prior to the nuclear changes and the apical cell parts were often irregular or distorted and sometimes retracted. Concurrently with the nuclear alterations, the cytoplasm changed in organization and increased in density. Lamellar endoplasmic cisternae were early arranged into parallel or concentric arrays or disrupted into round vesicles (Figs. 2, 7 and 9). Golgi complexes were transformed into large clusters of closely packed vesicles (Fig. 10). Mitochondria became large and rounded (Fig. 4). Monoribosomes were attached to the membranes of the endoplasmic reticulum and scattered freely in the cytoplasm (Figs. 1, 5 and 9). Lipid droplets had formed in some cells (Fig. 10). Delimitation of organelles into autophagic vacuoles did not take place after the beginning of the nuclear changes.

Progressive fragmentation of the dying ameloblasts took place by invagination of the lateral cell membrane. All fragments were surrounded by intact cell membranes and many fragments assumed irregular or distorted shapes (Fig. 7). In areas where — — —

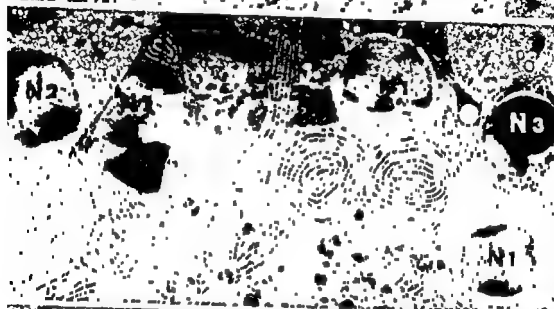
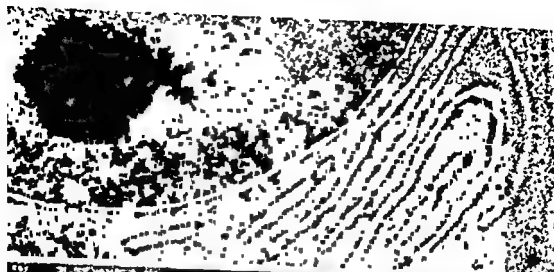
vacuoles engulfed the fragments by means of

In areas with extensive cell death, numerous

Fig. 1 Part of an ameloblast with incipient accumulation of chromatin (C) along the nuclear envelope and condensation of the nucleolus (Nu). The ribosomes of the endoplasmic cisternae, the nuclear envelope and the cytoplasmic matrix are monodispersed. X 32,000.

Fig. 2 Fragments of necrotic ameloblasts. N1 marks nuclei in early stage of degeneration with several oblong

Fig. 3 Ameloblasts with compact chromatin bodies at the nuclear poles. Nu, nucleolus. In the lower right corner the nuclear envelope is disintegrating. ER, lamellar endoplasmic cisternae in parallel arrays. X 11,400.



RESULTS

Visible changes in the nucleus occurred relatively late after administration of vinblastine. Changes in the cytoplasm began early and were pronounced when the nuclear changes appeared. Very early (in less than half an hour) nearly all the microtubuli vanished. This was succeeded by progressive displacement of the nuclei, redistribution at random of most organelles, and arrested apical translocation of secretory granules. Later (1 to 3 hours after drug administration) the polyribosomes of the endoplasmic reticulum and of the cytoplasmic matrix were converted into monoribosomes and the number of cisternae in the Golgi complex began to increase from the normal three to five parallel cisternae to five to nine empty cisternae per complex. While the early cytoplasmic changes occurred in all secretory ameloblasts whether the cells would survive or not, the conversion of the polyribosomes into monodispersed ribosomes did not occur in all cells. It had occurred however, in all ameloblasts in which nuclear degeneration took place (Fig. 1).

Nuclei with early necrotic features began to appear about 5 hours after administration of vinblastine. Their number increased rapidly during the following hour. 6 1/2 to 8 hours after drug administration nearly all injured nuclei were in an advanced state of necrosis.

The first change observed in the nuclei consisted of a peripheral accumulation of chromatin (Fig. 1). This became progressively denser and formed three to six oblong masses beneath the nuclear envelope (Fig. 2). These masses were further condensed and fused into two or three compact bodies often

Fig. 1 Part of an ameloblast with incipient accumulation of chromatin (Cr) along the nuclear envelope and condensation of the nucleolus (Nu). The ribosomes of the endoplasmic cisternae, the nuclear envelope and the cytoplasmic matrix are monodispersed. $\times 32,000$

Fig. 2 Fragments of necrotic ameloblasts. N1 marks nuclei in early stage of degeneration with several oblong peripheral chromatin masses. N2 marks nuclei in which the chromatin is further condensed and aggregated. N3 marks an advanced stage of nuclear degeneration in which the chromatin has aggregated into a dense globule. Concurrent with progressive nuclear degeneration the density of the cytoplasm has increased. $\times 7,300$

Fig. 3 Ameloblasts with compact chromatin bodies at the nuclear poles. Nu nucleolus. In the lower right corner the nuclear envelope is disintegrating. ER lamellar endoplasmic cisternae in parallel arrays. $\times 11,400$

situated at the nuclear poles (Figs. 2 and 3). In this position the shape of the bodies was approximately planoconvex. In a few nuclei the chromatin fused into a thick disc oriented transversely to the long axis. Finally the chromatin formed one or two large, dense, eccentrically placed globules (Fig. 4). The nucleoli were also condensed and often segregated into granular and fibrillar regions. They lay freely in the karyoplasm or were attached to a chromatin body (Figs. 3 and 4). At the conclusion of chromatin condensation the nuclear envelope disrupted into fragments of varying size and the karyoplasm became contiguous with the cytosol. During this process, fragments of the nuclear envelope frequently enwrapped small amounts of karyoplasm or chromatin (Fig. 5). In advanced necrosis rounded chromatin masses lay freely in the cytoplasm, often without identifiable remnants of the nuclear envelope.

Necrotic ameloblasts appeared singly (Fig. 6) in groups (Fig. 7), or in wide continuous areas (Fig. 8) of the ameloblast layer. When degeneration of the nucleus began, the cells usually extended throughout the entire thickness of the epithelium. However, the distal lateral junctional complex and apical cell web were lost prior to the nuclear changes and the apical cell parts were often irregular or distorted and sometimes retracted. Concurrently with the nuclear alterations the cytoplasm changed in organization and increased in density. Lamellar endoplasmic cisternae were early arranged into parallel or concentric arrays or disrupted into round vesicles (Figs. 2, 7 and 9). Golgi complexes were transformed into large clusters of closely packed vesicles (Fig. 10). Mitochondria became large and rounded (Fig. 4). Monoribosomes were attached to the membranes of the endoplasmic reticulum and scattered freely in the cytoplasm (Figs. 1, 5 and 9). Lipid droplets had formed in some cells (Fig. 10). Delimitation of organelles into autophagic vacuoles did not take place after the beginning of the nuclear changes.

Progressive fragmentation of the dying ameloblasts took place by invagination of the lateral cell membrane. All fragments were surrounded by intact cell membranes and many fragments assumed irregular or distorted shapes (Fig. 7). In areas where necrotic and vital cells were intermingled, the fragments were gradually displaced basally and phagocytized by the cells of the stratum intermedium which engulfed the fragments by means of thin cytoplasmic extensions (Fig. 4). Only Tomes processes and some apical fragments evaded basal displacement and degenerated very slowly in situ (Fig. 11).

In areas with extensive cell death, numerous

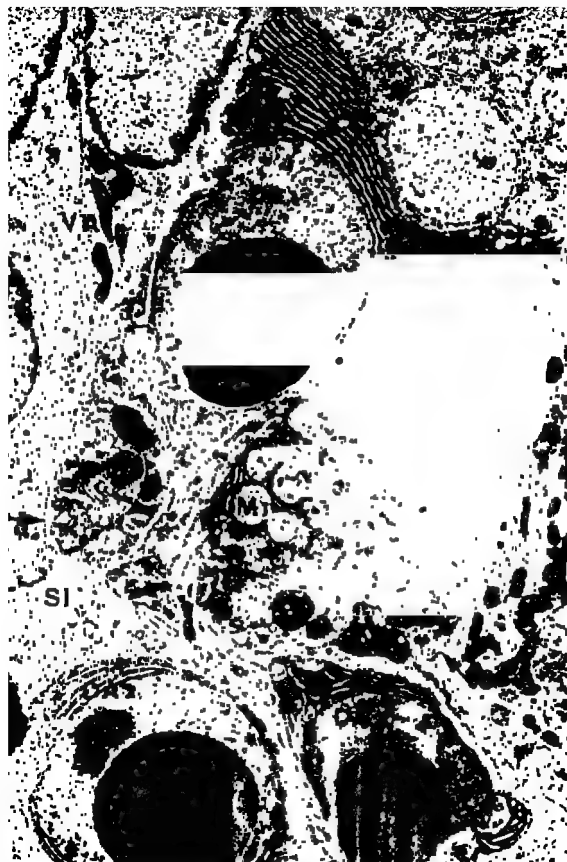
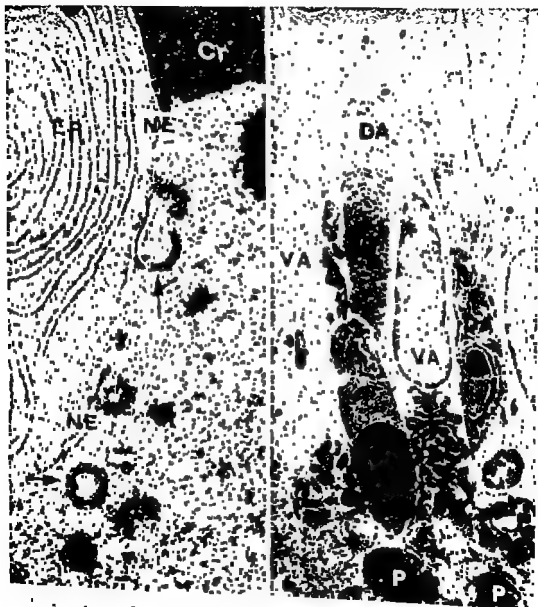


Fig 4 Electron micrograph showing the basal part of the ameloblast layer and the adjacent cytoplasm of stratum intermedium cells (SI) To the left and to the right viable ameloblasts (VA) are seen Between them are two large nucleus-containing degenerating ameloblast fragments (DA1) Compare the rounded mitochondria (M1) of the degenerating cells with the mitochondria (M2) of the viable cells The stratum intermedium cells have engulfed two large ameloblast fragments (DA2) and are in the process of enveloping the fragments marked DA1 with thin cytoplasmic extensions (arrows) X 9 000



Note the nuclear pores of the chromatin body X 30 000

Fig 6 This micrograph is from an area where viable ameloblasts (VA) are intermingled with solitary degenerating ameloblasts (DA) in the process of fragmentation Phagosomes (P) are seen in the stratum intermedium X 7,700

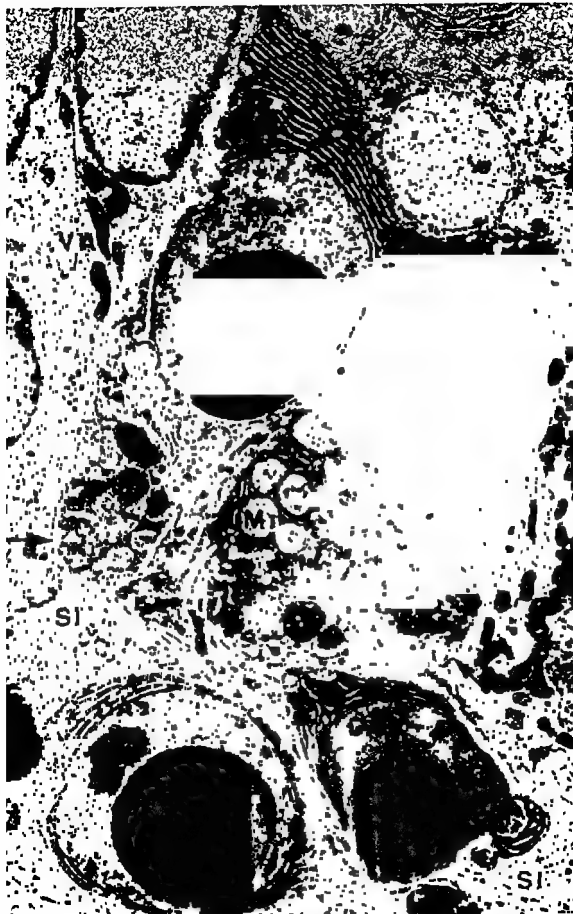
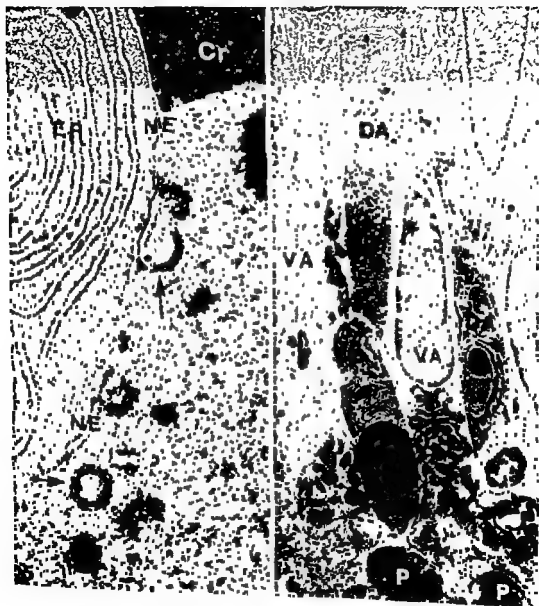


Fig 4 Electron micrograph showing the basal part of the ameloblast layer and the adjacent cytoplasm of stratum intermedium cells (SI). To the left and to the right viable ameloblasts (VA) are seen. Between them are two large nucleus-containing degenerating ameloblast fragments (DA1). Compare the rounded mitochondria (M1) of the degenerating cells with the mitochondria (M2) of the viable cells. The stratum intermedium cells have engulfed two large ameloblast fragments (DA2) and are in the process of entrapping the fragments marked DA1 with thin cytoplasmic extensions (arrows) X 9 000



Note the nuclear pores of the fragments (arrows). ER: endoplasmic reticulum (NE). Some of the fragments envelop small amounts of karyoplasm chromatin body X 30 000

Fig 6 This micrograph is from an area where viable ameloblasts (VA) are intermingled with solitary degenerating ameloblasts (DA) in the process of fragmentation. Phagosomes (P) are seen in the stratum intermedium X 7,700

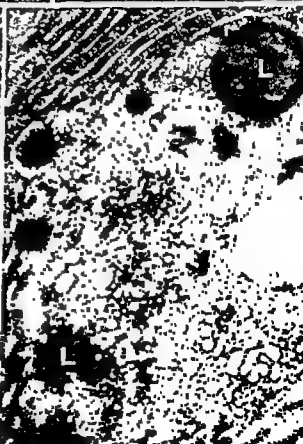


Fig 7 Fragments from the supranuclear part of a group of degenerating ameloblasts with parallel and concentric arrays of endoplasmic cisternae. The differences in density of the fragments indicate that the initial degeneration was not simultaneous. Some of the fragments are irregular or distorted. X 5 600

Fig 8 A small section of a large area with extensive cell death adjacent to the enamel matrix. Most fragments are small and round. The dark round bodies are condensed chromatin. Fragments of Tomes' processes are seen (arrows). X 3 100

Fig 9 Early degenerative changes of the endoplasmic reticulum consisting of organization of the lamellar cisternae into parallel arrays or disruption of the cisternae into round vesicles. The ribosomes are monodispersed. X 19 500

Fig 10 Degenerating Golgi area containing numerous closely packed small vesicles. L, lipid bodies. X 25 000

small fragments were formed (Fig 8). These fragments took a rounded form and were not removed. They underwent slow lysis *in situ* in 2 or 3 days.

Many of the fragments engulfed by the stratum intermedium cells were very large (Fig 4) and many cells of this layer engulfed several pieces of debris. Often the fragments were not in a very advanced stage of degeneration when phagocytized. After phagocytosis the phagosomes became progressively more condensed and thereafter dissolved. 24 hours after administration of the drug few phagosomes remained in the stratum intermedium and those present were usually empty or contained a little debris (Fig 12) and sometimes glycogen particles. Typical residual bodies were small and rare.

DISCUSSION

It was easy to identify incipient cell degeneration and to recognize the sequence of degenerative changes in the dying cells in the simple ameloblast layer. Analysis of the changes was facilitated because no foreign cells invaded the epithelium and most debris was removed by the well-defined stratum intermedium beneath the ameloblasts.

Whereas cytoplasmic changes commencing with the disappearance of microtubules and the elevation of nuclei already began a few minutes after the administration of vinblastine, nuclear changes began late (after about 5 hours) but indicated from the outset that a particular ameloblast had been drawn into a sequence of events which would ultimately lead to its death. The period within which nuclear degeneration set in was notably short, only about one and a half hours. Nuclear and cytoplasmic condensation, fragmentation and degradation thereafter progressed in a characteristic manner as described above. Where necrotic ameloblasts occurred solitarily or in small groups supported by ameloblasts, the fragments were

gradually dislocated basally, possibly by activity of the viable cells. The debris was thereafter engulfed by the cells of the stratum intermedium. The rapidity and completeness with which the stratum intermedium cells eliminated the phagosomes suggest that these cells in their few small lysosomes contain a complete set of enzymes for digestion of ameloblast debris. Where many or all the ameloblasts in a large area were necrotic, numerous small fragments were rapidly formed. This debris underwent lysis slowly *in situ*.

The type of degeneration in the secretory ameloblasts was similar to that described by Schweichel & Merker (1973) as type I necrosis in physiological cell death during morphogenesis, and by these authors and by Sadler & Cardell (1977) in embryonic tissues after application of various embryotoxic substances. Sadler & Cardell exposed mouse embryos to hydroxyurea, which inhibits ribonucleotide reductase, thereby inhibiting DNA synthesis, and described the changes in developing neuroepithelium in relation to time. They found chromatin condensation and cell fragmentation soon (1 to 2 hours) after administration of the drug. As in the vinblastine-injured ameloblasts, the nuclear changes were preceded by the breakdown of polyribosomes into monoribosomes, suggesting functional disturbances of the nucleus prior to visible alterations of the chromatin. The late effect of the microtubule-inhibitor vinblastine on the nuclear structure and ribosomal pattern compared to the rapid effect of hydroxyurea on these structures might suggest that the effect of vinblastine upon the nucleus is a consequence of the inhibition of the microtubular system. A direct interaction of vinblastine with replication, transcription or translation is also possible, however (see review by Creasey 1975).

In the present work the vinblastine dosage was 2 mg per kg body weight. This dose is usually not lethal, since the LD₅₀ value of intravenously

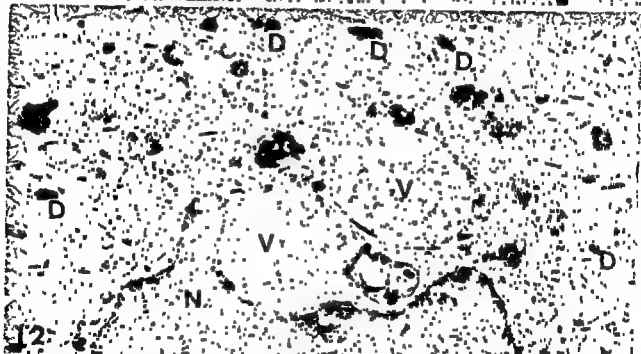


Fig 11 Apical part of the ameloblast layer 24 hours after vinblastine administration. Most of the ameloblasts in this area survived. Detached Tomes processes (arrow heads) and a large nucleus containing ameloblast fragment have evaded basal dislocation and are degenerating slowly in situ. In such old fragments many lipid droplets are seen (arrows). X 5,300.

Fig 12 Part of a stratum intermedium cell facing the base of the ameloblast layer, 24 hours after administration of vinblastine. Two large vacuoles (V) are seen, representing late phagosomes with a few debris remnants. N nucleus. D desmosomes. Most of the small round dark bodies are mitochondria. X 12,500.

administered vinblastine sulfate for rats weighing 105–140 g is 2.9 mg per kg (Todd et al 1975). Yet many secretory ameloblasts vanished and a reduced population of cells remained to conclude the

formation of the enamel. As was reported earlier (Moe & Mikkelsen 1977b), these surviving cells were also injured, however, and their activity had suffered both quantitatively and qualitatively.

REFERENCES

- 1 Creasey W A Vinca alkaloids and colchicine ■ Saniorelli A C & Johns D G (Ed) Antineoplastic and immunosuppressive agents part II Springer Verlag Berlin Heidelberg 1975 ■ 670-694
- 2 Moe H On the effect of vinblastine on ameloblasts of rat incisors *in vivo* 3 Acute and protracted effect on differentiating ameloblasts A light microscopical study Acta path microbiol scand Sect A 85 330-334 1977
- 3 Moe H & Mikkelsen H Light microscopical and ultrastructural observations on the effect of vinblastine on ameloblasts of rat incisors *in vivo* 1 Short term effect on secretory ameloblasts Acta path microbiol scand Sect A 85 73-88 1977a
- 4 Moe H & Mikkelsen H On the effect of vinblastine on ameloblasts of rat incisors *in vivo* Protracted effect on secretory ameloblasts A light microscopical study Acta path microbiol scand Sect A 85 319-329 1977b
- 5 Sadler T W & Cardell R R Ultrastructural alterations in neuroepithelial cells of mouse embryos exposed to cytotoxic doses of hydroxyurea Anat Rec 188 103-124 1977
- 6 Schweichel J U & Merker H J The morphology of various types of cell death in prenatal tissues Teratol 7 253-266 1973
- 7 Todd G C Gibson W R & Morton M M Toxicology of vindesine (desacetyl vinblastine amide) in mice rats and dogs J Toxicol Environ mental Health 1 843-849 1976

NUCLEAR SEGMENTATION IN GOITRE ASPIRATES

GÖRAN NILSSON

Dept of Medicine Central Hospital Västerås Sweden

Nilsson G Nuclear segmentation in goitre aspirates Acta path microbiol scand Sect A 87 11-13 1979

Nuclear segmentation was studied in fine needle aspirate smears from toxic and atoxic goitres. The smear technique implies a flattening of the nuclei on a slide which facilitates detection of nuclear segmentation. Such segmentation was found in 2.2% of the nuclei in toxic goitres and in 0.9% in atoxic goitres. The difference was highly significant $p < 0.001$. The segmented cells were usually of uniform appearance with one large and one small segment. Only very rarely were more than two segments seen.

Key words: Goitre aspirates, nuclear segmentation.

Göran Nilsson, Dept of Medicine, Central Hospital, S-721 89 Västerås.

Accepted and submitted 3 vii 78

Nuclear segmentation is a topic of traditional interest mainly to the haematologist. The neutrophil granulocyte is the classical cell type showing this phenomenon. Furthermore Norberg (1) has demonstrated some interesting characteristics of nuclear segmentation of mononuclear leucocytes in different experimental situations as well as the importance of contractile cytoplasmic proteins in this process. The segmented leukemic blast cells (Reider cells) are still another haematologic cell type in which nuclear segmentation is a conspicuous and interesting finding.

To the author's knowledge nuclear segmentation has not been described in nuclei from benign epithelial tissue. Such nuclei have a smoothly rounded contour - as opposed to the nuclei in blood leucocytes. Epithelial tissues are usually studied in histological sections. The cut-off nuclear segments as well as overlying cells in such sections make the study of nuclear segmentation technically much more difficult than in smears. The increasing use during recent years of fine needle aspirates from epithelial organs viz. thyroid, liver, kidney and prostata, implies a study of these organs with the smear technique.

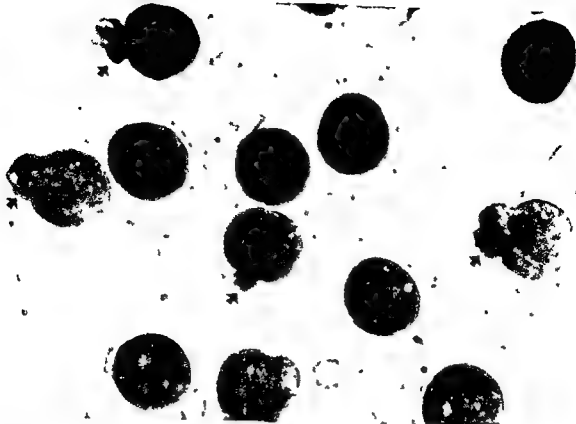
draw attention to the phenomenon of such segmentation which may be found in a small percentage of the cells in many types of benign epithelial tissue (for instance liver, kidney, prostata and thyroid). This paper concerns nuclear segmentation in goitre aspirate smears and a comparison between the frequency of nuclear segmentation in toxic goitres and benign non thyroiditis goitres. The purpose of the comparison was to elucidate the relationship if any between thyroid function and segmentation of goitre cell nuclei.

MATERIAL AND METHODS

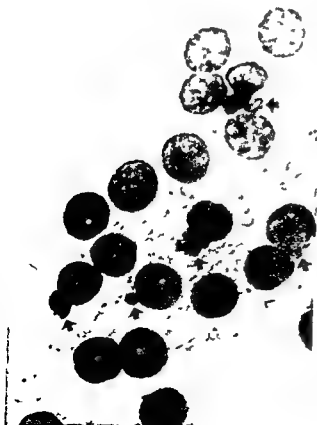
67 fine needle aspirates from toxic goitres (40 diffuse and 27 nodular) were studied. The diagnosis of hyperthyroidism had invariably been confirmed by clinical examination and laboratory values which always included increased serum thyroxine and T_3 resin uptake.

For comparison 50 non malignant, non thyroiditic goitre aspirates from nodular or diffuse goitres of euthyroid patients were examined. The euthyroidism of these patients was confirmed by clinical examination and demonstration of a normal level of serum thyroxine and T_3 resin uptake.

The biopsies were performed according to Soderstrom² with a fine needle with an outer diameter of 0.6-0.7 mm. The aspirated material was distributed as



Figs 1-2 Nuclear segmentation (arrows) in two cases of toxic goitres Basic magnification Fig 1 $\times 400$ Fig 2 $\times 256$



smears dried in the air and stained with the May Grunwald Giemsa technique. In a few cases Feulgen staining was done in order to visualize the chromatin distribution in the nuclei studied.

A nucleus was regarded as segmented when a separate segment was clearly indicated by indentations in the nuclear contour. For example see Fig 1-2. Five hundred nuclei from each aspirate were examined for nuclear segmentation.

RESULTS

The segmentation found in the preparations studied was of rather stereotype appearance (Figs 1-2). Only very rarely were more than two segments found. There was a great difference in size between the segments, the smaller segment seldom being more than one half the size of the larger one. Sometimes the smaller segment was more weakly stained than the larger one, suggesting that the chromatin in the smaller segment was more diluted than that of the larger segment. This finding was also confirmed in Feulgen stained preparations. The nuclear contour of the small segments was sometimes irregular and wavy compared with that of the larger segment. This sometimes gave the nucleus a "pomegranate" appearance.

Comparison between toxic and atoxic goitres showed a highly significant difference ($p < 0.001$).

between the frequency of segmented nuclei (mean \pm SEM 2.2 ± 0.3 per cent segmented nuclei for goitres. Corresponding figures for atoxic goitres 0.9 ± 0.2). No relationship was found between the frequency of segmented nuclei and age or sex and there was no difference between diffuse and nodular goitres in either of the groups of toxic or atoxic goitres.

DISCUSSION

An important question concerning the present findings is the possibility of artefacts during aspiration of the tissue or during preparation of the smear. Though the effect of such mechanism can not of course be ruled out the difference found between toxic and atoxic goitres argues strongly against such technical factors being the only cause of the nuclear segmentation observed.

It is known from the field of hematology that certain factors can be related to the segmentation phenomenon in leucocytes: (1) lack of vitamin B₁₂; (2) hereditary factors; (3) and contractile proteins. (4) Such proteins have been shown to regulate the radial segmentation of mononuclear cells.¹ Available data will not permit evaluation of the possible importance of these factors in epithelial tissues.

A phenomenon of nuclear budding, resembling the nuclear segmentation described above, has been demonstrated in cell cultures of various tissues (5, 6). This phenomenon is thought to be of importance for the nuclear-cytoplasmic communication as well as for the formation of micronuclei. The latter finding implies that a small nuclear segment is pinched off with the formation of small nuclei. Such small nuclei were seen only very rarely in the aspirate smears studied here.

The increased metabolic needs in thyrotoxicosis

reasonably imply a larger metabolite transport between nucleus and cytoplasm. The relationship between nuclear surface and volume of both cytoplasm and nucleus is rendered more favourable by segmentation of the nucleus. On the other hand the general enlargement of cells and cell nuclei in toxic goitres (7) tends to decrease the nuclear surface: cell volume ratio. It is therefore tempting to regard the increased frequency of segmented nuclei in toxic goitres as a consequence of increased nuclear volume and cell volume in this condition.

The work was supported by Axel Linder's foundation

REFERENCES

1. Norberg B. Contractile processes in human lymphocytes and monocytes from peripheral blood. *Scand J Haematol* 14 Suppl 141 1971.
2. Söderström N. Fine Needle Aspiration Biopsy Used as a Direct Adjunct in Clinical Diagnostic Work. Almqvist Wiksell Stockholm 1966.
3. Jones O P. Origin of neutrophils in pernicious anaemia (Cocks macropolycytes). *Arch Int Med* 60 1002 1937.
4. Urdet E. Eine neue sipp m t erblich - konstitutioneller Hochsegmentierung der Neutrophilen Kerne Schweiz Med Wschr 88 1000 1958.
5. Elston R N. Nuclear budding and micronuclei formation in human cells.
6. Ljungqvist A C & Yerganian G. Some observations on nuclear budding and nuclear extrusions in a chinese hamster cell culture. *J Natl Cancer Inst* 34 53 1965.
7. Nilsson G. Nuclear size classes in fine needle aspirates from toxic goitres. *Acta Endocr (Kbh)* 70 373 1972.

THE PROLIFERATIVE ACTIVITY OF MYOCARDIAL CAPILLARY WALL CELLS IN VARIOUSLY AGED SWIMMING-EXERCISED RATS

GUNNAR UNGE STURE CARLSSON ARNE LJUNGQVIST GÖRAN TORNÖLING and JAN
ADOLFSSON

The Departments of Pathology and Thoracic Medicine Karolinska sjukhuset Stockholm Sweden

Ungé G Carlsson S Ljungqvist A Tornöling G & Adolfsson J The proliferative activity of myocardial capillary wall cells in variously aged swimming-exercised rats Acta path microbiol scand Sect A 87 15-17 1979

Cellular proliferation was studied by incorporation of ^3H thymidine in the hearts of young adult and old swimming-exercised rats. The proliferative activity was measured by scintillation counting. The swimming exercise induced a significant proliferation of capillary wall cells in the younger age groups suggesting a neoformation of myocardial capillaries in these rats whereas no cell proliferation was recorded in the old rats.

Key words Myocardium capillary wall cells rats

Arne Ljungqvist Department of Pathology Karolinska sjukhuset S 104 01 Stockholm Sweden

Accepted as submitted 3 vii 78

A marked increase in capillary wall cell proliferation indicative of a capillary neoformation has previously been demonstrated in the heart of swimming-exercised adult rats (Ljungqvist and Unger 1973 Mandache *et al* 1972 and 1973). Others have found that young rats with experimental cardiac hypertrophy show a more pronounced cellular proliferation in the myocardial interstitial tissue than similarly treated old animals (Bloor and Leon 1970 Bloor Pasik and Leon 1970 and Neffgen and Korecki 1972) but the proliferating cells were not further specified. In the present investigation the proliferative activity of the myocardial capillary wall cells was studied in variously aged rats with swimming induced cardiac hypertrophy.

MATERIAL AND METHODS

Forty-eight male Sprague Dawley rats were used in the experiment. The animals were divided into three groups according to ages (Table 1). Half the number of animals in each age group were swimming-exercised 1 hour/day 5 days a week over a period of 3 weeks. The other half of each group of animals served as normal controls.

At the end of the experimental period the animals were weighed and given a single intravenous injection of ^3H thymidine (1 $\mu\text{Ci}/\text{nmol}$). In the young animals the dosage was 100 μCi in the adults 200 μCi and in the old animals 400 μCi .

The animals were sacrificed 15 minutes after the thymidine injections. The heart was quickly removed weighed and frozen at -20°C . After storage the heart was disintegrated in 0.5 M PCA with a Polytron ultrahomogenizer (Kinematica setting # 4). The homogenate was centrifuged (2000 rpm for 30 minutes $\pm 0^\circ\text{C}$) and the supernatant discarded. The pellet was resuspended in 0.5 M PCA and re-centrifuged. This washing procedure was repeated twice. The final pellet was hydrolyzed twice in 0.5 ml 0.5 M PCA at 80°C for 15 minutes and centrifuged. Samples of the clear supernatant were used for colorimetric determination of DNA according to Burton (1956) and measurement of radioactivity.

RESULTS

Table 1 shows that there was a decrease in body weight of young animals ($p < 0.005$) and an increase in heart weight in the old age group ($p < 0.05$). The heart weight/body weight ratio $\times 1000$ was increased in all experimental animals and this

TABLE 1 *Body Weights Heart Weights and Heart/Body Weight Ratios $\times 1000$ in Control (contr) and Swimming exercised Rats (exp) of Various Ages (I = Young II = Adult III = Old Rats)*

Group	Body weight (g)		Heart weight (mg)	Ratio
	Start	End		
I	contr 100	225 \pm 8	746 \pm 22	3.31 \pm 0.16
	exp 100	208 \pm 10**	769 \pm 41	3.69 \pm 0.11***
II	contr 200	308 \pm 14	938 \pm 38	3.04 \pm 0.21
	exp 200	299 \pm 10	971 \pm 65	3.24 \pm 0.20
III	contr 400	414 \pm 18	1191 \pm 79	2.86 \pm 0.13
	exp 400	416 \pm 16	1286 \pm 72*	3.08 \pm 0.14**

* Significantly different from control group ($p < 0.05$)

** Significantly different from control group ($p < 0.01$)

*** Significantly different from control group ($p < 0.001$)

increase was statistically significant in the young and old rats

The scintillation countings are presented in Table 2. There was a significantly increased ^3H thymidine incorporation in the young ($p < 0.005$) and adult ($p < 0.05$) rats, but not in the old rats.

DISCUSSION

Nuclear incorporation of thymidine is specific for DNA synthesizing cells (Cleaver 1967). The degree of thymidine incorporation is therefore used as a measure of cellular proliferative activity. In previous works we have shown on light and electron microscope autoradiograms that the vast majority of labelled cells in the hearts from adult rats

receiving ^3H thymidine consists of capillary wall cells and that only these cells increase their proliferative activity during swimming exercise suggesting a neoformation of capillaries (Ljungqvist and Unger 1973; Mandache *et al.* 1972 and 1973). The methods used in the present investigation therefore directly measure the proliferative activity of the capillary wall cells induced by swimming exercise in rats of various ages.

The present observation of an increased proliferative activity in the myocardial capillary walls of swimming-exercised young and adult rats but not of similarly treated old rats is in agreement with the semi quantitative estimations made by Bloor and Leon (1970) and Heflgen and Korecky (1972) on rats with cardiac hypertrophy secondary to exercise and anemia. These authors reported a higher number of capillaries and ^3H thymidine labelled interstitial cells in the hearts of young and adult rats than in the hearts of old rats.

It appeared that the swimming induced proliferative activity in the myocardial capillary walls was more intense in the young than in the adult rats. Whether this is a further age related phenomenon is difficult to assess in the absence of comparable degrees of cardiac hypertrophy in the two age groups. In fact the increase in heart weight of the adult rats was too low to be statistically significant. The importance of the present observations is therefore restricted to the finding that unlike the young and adult rats the old animals were unable to increase their myocardial capillary vasculature during swimming exercise despite the fact that their hearts became enlarged.

TABLE 2 *Measurements of Myocardial Radioactivity Following ^3H Thymidine Injections into Control (Contr) and Swimming Exercised Rats (Exp) of Various Ages (I = Young II = Adult III = Old Rats)*

Group	cpm/ μg DNA	Increase (%)
I	contr 23.75 \pm 7.72	124
	exp 53.12 \pm 30.29**	
II	contr 50.12 \pm 22.54	49
	exp 74.87 \pm 29.19*	
III	contr 91.12 \pm 33.05	10
	exp 100.25 \pm 35.99	

* Significantly different from control group ($p < 0.05$)

** Significantly different from control group ($p < 0.01$)

This study was supported by the *Swedish Medical Research Council* (project no B75 12% 716) and the *Research Funds of Karolinska Institutet*

REFERENCES

- Bloor C M & Leon A S Interaction of age and exercise on the heart and its blood supply *Lab Invest* 22 160-165 1970
- Bloor C M Pasik S & Leon A S Interaction of age and exercise on organ and cellular development *Am J Pathol* 58 185-199 1970
- Burton K Study of conditions and mechanism of diphenylamine reaction for colorimetric estimation of deoxyribonucleic acid *Biochemical Journal* 62 315-323 1956
- Cleaver J E Thymidine metabolism and cell kinetics *North Holland Research Monographs Frontiers of Biology* vol 6 Amsterdam North Holland publishing Co 1967
- Ljungqvist A & Unger G The proliferative activity of the myocardial tissue in various forms of experimental cardiac hypertrophy *Acta path microbiol scand Sect A* 81 233-240 1973
- Mandache E Unger G & Ljungqvist A Myocardial blood capillary reaction in various forms of cardiac hypertrophy *Virchows Arch Abt B Zellpath* 11 97-110 1972
- Mandache E Unger G Appelgren L E & Ljungqvist A The proliferative activity of the heart tissues in various forms of experimental cardiac hypertrophy studied by electron microscope autoradiography *Virchows Arch Abt B Zellpath* 12 112-122 1973
- Neffgen J F & Korecky B Cellular hyperplasia and hypertrophy in cardiomegalies induced by anaemia in young and adult rats *Circ Res* 30 104-113 1972

ULTRASTRUCTURAL FEATURES OF CULTURED HUMAN GLIA AND GLIOMA CELLS

V P COLLINS N FORSBY U T BRUNK J L E ERICSSON and B WESTERMARK

Department of Tumor Pathology Karolinska Institute Stockholm and Institute of Pathology and The Wallenberg Laboratory University of Uppsala Uppsala Sweden

Collins V P Forsby N Brunk U T Ericsson J L E & Westermark B Ultrastructural features of cultured human glia and glioma cells Acta path microbiol scand Sect A 87 19-28 1979

The fine structure of three lines of human normal glial cells and eight established lines of malignant glioma cells are described. The glial cell lines were ultrastructurally very similar whereas the glioma cell lines differed greatly from one another. In sparse proliferating cultures there were no consistent findings which distinguished the glioma cell lines as a group from the normal glial cells. Only in post confluent cultures could the consistently irregular cell surfaces and ruffling both at the cell periphery and centrally on the upper cell surface with associated pinocytosis distinguish the glioma from the post-confluent glial cultures which did not possess these properties. The common attributes of post confluent glioma cells reflect the cells continued proliferation. The glioma lines did display individual ultrastructural characteristics which appear to be stable the glioma lines having retained these during a number of years of continual passage.

Key words: Glia, glioma cells, cell lines, ultrastructure.

V P Collins Department of Tumor Pathology Karolinska sjukhuset S 104 01 Stockholm 60 Sweden

Accepted as submitted 29 v 78

Many studies have been carried out on the conventional transmission electron microscopic (TEM) structure of normal and malignant cells *in vivo* and *in vitro* (for recent reviews on the fine structure of normal and malignant cells *in vitro* see 8 and 17). No consistent fine structural differences have hitherto been noted. *In vivo* studies are complicated by a number of incalculable factors such as immunological reactions, anoxia etc. which obstruct an evaluation of the biological state of the cells under study. Adequate fixation of tissues can also be problematical. *In vitro* studies of cells derived from normal and malignant tissue of the same origin are thus of interest. The biological state of the cultured cells can be defined and optimal fixation conditions obtained all of which simplifies the interpretation of the findings.

A system of human normal glia and malignant

system have been described at various cell densities (7).

In the present study we examined the fine structure of ultrathin sections of human normal glia and malignant glioma cells cultivated *in vitro* at different cell densities. The cells were studied from 2 to 21 days following subcultivation.

MATERIAL AND METHODS

Collins V P and eight established lines of human malignant glioma cells (U 87 MG, U 118 MG, U 178 MG, U 251 MG, U 343 MG, U 373 MG, U 410 MG and U 563 MG) initiated from poorly differentiated

at

fc

m

cf - all cells of these lines have been previously

described (18 19 20) Passages of the glial cells in midphase II were used. All glioma lines show various degrees of diminished growth control *in vitro* and the selected lines were regarded as being representative of the 24 glioma lines which have so far been established. The cell lines were grown in Eagle's minimal essential medium (EMEM) supplemented with 10% calf serum and antibiotics. The cultures were incubated at 37°C in a humidified atmosphere containing 5% CO₂.

The cells were seeded in 60 mm plastic Petri dishes (Nuncclone®) at approximately 125 × 10³ cells per dish. Cell counting was performed with an electronic particle counter (Celloscope AB Lars Ijungberg Stockholm). The medium was renewed twice weekly. In order to exclude the possibility of alterations caused by insufficient nutrition, some glia and glioma lines were fed daily. The cultures were harvested for TEM studies at 2, 7, 14 and 21 days following subcultivation. Confluence of cells normally occurred 5 to 7 days following subcultivation.

Transmission Electron Microscopy (TEM)

The cell cultures were fixed *in situ* by the rapid exchange of the medium for the fixative solution consisting of 2% glutaraldehyde in 0.1 M Na cacodylate-HCl buffer with 0.1 M sucrose (pH 7.2, total osmolality 510 mOsm, vehicle osmolality 300 mOsm) (2, 4). The cultures were initially fixed at 37°C for 15 min in the cultivating incubators. They were then brought to room temperature for 45 min. The cells were subsequently postfixed in 1% OsO₄ in 0.15 M cacodylate buffer (pH 7.2) at room temperature for a further 90 min and dehydrated in a graded series of ethanol solutions (50%, 70%, 80%, 90%, 95% and 100% × 3). In the second change of 100% ethanol they were stained with 2% uranyl acetate for 10 minutes. The layers were then cut into squares with a razor blade, removed from the dishes by propylene oxide (1), washed in propylene oxide and embedded in Epon 812, as has been described previously (3). Following centrifugation and polymerization, ultrathin sections were cut with diamond knives on an LKB Ultratome and stained with lead citrate (16). The specimens were examined in a Siemens Elmiskop 1A or a Philips EM 201. All filament and microtubule measurements were carried out on films taken with the Philips EM 201 at × 40,000 magnification which was simultaneously calibrated by means of a replica grating.

RESULTS

Features Common to Glia and Glioma Cells

First we shall describe findings which apply equally to the normal glia and the malignant glioma lines. Cells in mitosis are excluded from the following account in which only interphase cells will be considered. The general shape, behaviour and surface morphology of these cell lines as studied with time lapse cinematography and scanning electron microscopy have been previously reported (7).

All cells were anchored by attachment plaques to the bottom of plastic dishes covered with microprecipitate (3). These attachment devices consisted of an osmophilic plaque just inside the cell membrane into which mainly approximately 7 nm microfilaments usually arranged in a bundle converged obliquely (Figs 4, 13 and 16). Single microtubules as well as filaments with diameters approaching 10 nm were also found in these structures (Fig. 16). Between such plaques the cells' lower membrane was usually suspended above the microprecipitate (Figs 2, 8, 10, 11 and 13). This was most pronounced in dense cultures. Such attachment plaques could be found anywhere along the lower cell surface. They were often observed at the end of the stabilized part of the leading lamella from where lamellipodia extended over the substratum or were elevated to form ruffles (Figs 6 and 9). Lamellipodia, whether formed at the tip of the leading lamella or on the upper surface of dense cultures of malignant glioma cells, did not show the presence of microtubules or definite filaments (Figs 6, 9 and 14) but simply contained cell sap and occasional ribosomes.

Cell junctions, when observed between the cells, showed a fine structure similar to that of desmosomes, even though they sometimes lacked one or

Fig. 1 Central part of proliferating glial cell in non confluent culture. Note the well developed Golgi apparatus (G), a micropinocytotic vesicle (mv) and an attachment plaque anchoring the cell to the microprecipitate (arrows). × 11,600.

Fig. 2 Portions of density growth inhibited glial cells. Note the secondary lysosomes, some of the residual body type (rb), the long straight cell appositions and the attachment plaques (arrows). The inset shows a junction between two such cells. × 11,400. Inset × 35,000.

Fig. 3 Tangentially sectioned upper surface of a glial cell showing the submembranous microfilament mat and some microtubules (arrows). × 29,600.

Fig. 4 Glial cell with attachment plaque showing numerous microfilaments. × 33,200.

Fig. 5 Glial cell containing a cilium (ci) with a diplosomal basal organization. × 24,800.

Fig. 6 Peripheral part of a proliferating glial cell showing a ruffling area with the formation of a pinocytotic vacuole (v). Note the attachment plaque at the foremost end of the leading lamella. × 17,900.

Fig. 7 Density growth inhibited glial cell at 21 days. Note the presence of an extracellular material, the fibers of which are orientated parallel to those in the cell. × 11,900.



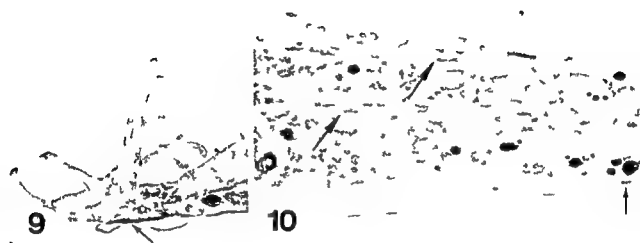


Fig 8 Preconfluent glioma cell (U 118 MG) Note the well developed Golgi areas (G) $\times 11,300$

Fig 9 Foremost tip of a leading lamella of a malignant glioma cell (U 373MG) Note the fine ruffles and the attachment plaque (arrows) $\times 6300$

Fig 10 Part of the leading lamella of a malignant glioma cell (U-343 MG) Note the microfilaments arranged under the upper cell membrane, as well as a bundle centrally in the cytoplasm (large arrows) An attachment plaque is also arrowed $\times 8300$

Fig 11 Dense culture of malignant glioma cells at 21 days (U 251 MG) Note the cell multilayer and the very irregular, interdigitating, cellular surfaces. At the upper surface of the multilayer can be seen a number of microvilli and lamellipodia. Three attachment plaques are arrowed $\times 4700$

more of the characteristics of this junction type. They were most frequently observed in the cultures at 21 days.

All cells contained — in their cell sap — microtubules approximately 24 nm in diameter, and filaments of variable diameters. The filaments were arranged in four different ways: (a) Tight bundles of straight microfilaments which had a diameter of, in the main, 7 nm and were generally oriented towards the perinuclear region and apparently originated in the attachment plaques (Figs 4, 13 and 16). Away from the plaques these bundles became dissociated and dispersed, in some cases, especially when located at the cell periphery they merged with the submembranous filament mat below the upper cell membrane. (b) A layer of straight microfilaments found mainly under, and parallel to, the upper cell membrane. These filaments also tended to be 7 nm in diameter (Figs 3 and 14). (c) More diffuse bundles of often wavy filaments were observed centrally in the cell, and almost exclusively found in the malignant cells (Fig 15). The diameters of these filaments varied between 5 and 10 nm. (d) Finally there occurred apparently randomly oriented single filaments in the perinuclear area: these were straight with diameters ranging between 5 and 10 nm. Microtubules were observed in close association with the filaments in all locations with the exception of the diffuse wavy bundles described above (Figs 3, 13, 16 and 17). The cellular contents of filaments appeared to increase in the later cultures, at 14 and 21 days.

An understanding of the orientation and spatial relationships of a number of the cell organelles is important for the interpretation of the micrographs. This is particularly true of the endoplasmic

reticulum (ER) and mitochondria, both of which lie mainly with their long axes parallel to the substratum. Thus, only sections parallel to the plane of the substratum will demonstrate, for example, the intricate connections of the ER, or the full extent of the often polymorphic forms of the mitochondria. This is also true of the submembranous microfilament mat which can be best demonstrated in tangential sections of the cell surface (Figs 3 and 17).

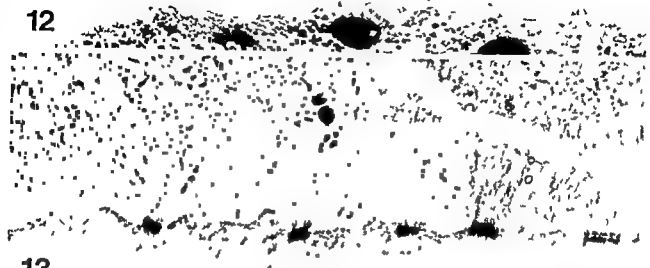
The rough ER, although the total extent varied greatly among the malignant lines, was rather evenly distributed throughout the cell in all the lines studied. Ribosomes were arranged as free polysomes or lined up along the ER. Occasional autophagosome-like structures were seen in all cell lines. The outer nuclear membrane could have a few attached ribosomes. Nuclear pores in all the lines were identical, orifice approximately 80 nm in diameter with an annular lamella, eight peripheral and one central granule (Fig 16). Microvilli were found to contain a bundle of approximately 7 nm microfilaments, as was also the case with the few sectioned microspikes. Single or solitary cilia were occasionally observed in all of the glial cell lines studied and in one of the malignant glioma lines (U 563 MG). They had a diplosomal basal organization, the few cross-sectioned examples seen having a 9 + 0 axial microtubule complex and they often lay in a tunnel-like plasma membrane invagination (Fig 5). The cultures which received new medium daily showed no differences from those which received medium twice weekly.

Normal Human Glial Cells, prior to Confluence

The three lines of glial cells were similar in all respects. At two days they were thinly spread over the microprecipitate (Fig 1) with a leading lamella, associated ruffling, and macropinocytotic vacuoles (Fig 6). The cells were attached to the substratum by a number of attachment plaques as described above. These were always rather large with an average size in cross-section of approximately 10 μ m (mean cross section of 75 glial cell attachment plaques measured at random). Attachment plaques were often observed at the foremost part of the leading lamella (Fig 6). These usually had distinct bundles of microfilaments. The leading lamella contained some mitochondria and secondary lysosomes, as well as rough ER and polysomes. The upper cell surface when sectioned obliquely, displayed a submembranous mat of filaments, the majority of which were approximately 7 nm in diameter. Microtubules were observed below these filament mats (Fig 3). A similar arrangement of microfilaments could be found on oblique sectioning of the



12



13



14

15



17

Fig 12 Dense culture of malignant glioma cells at 21 days (U 87 MG) Note the presence of intercellular material the fibres of which in some points seem to run parallel to those within the cells $\times 34\ 800$

Fig 13 Dense culture of malignant glioma cells at 14 days (U-410 MG) showing numerous attachment plaques containing microfilaments $\times 11\ 300$

Fig 14 Detail from the upper surface of a dense culture of U 373 MG at 14 days showing ruffling activity with the formation of micropinocytotic vacuoles (V) $\times 7600$

Fig 15 Detail from the cytoplasm of U 118 MG showing the loose wavy microfilament bundles which are a characteristic of this line $\times 17\ 400$

Fig 16 Detail of a glioma cell attachment plaque (U 410 MG) showing the bundles of microfilaments which are included in these structures Note also the presence of occasional microtubules (arrows) The section is cut tangentially beneath a nucleus A number of nucleopores can be seen in the upper part of the micrograph $\times 17\ 700$

Fig 17 Detail of the perinuclear area of a glioma cell (U 410 MG) showing a somewhat irregular nucleus with tangentially sectioned nucleopores and a submembranous mat of microfilaments Note the single microfilaments and microtubules in the perinuclear area $\times 8800$

cannot be classified among the more generally accepted cell junctions The frequency of such junctional devices increased with cell density One such junction is shown in the inset in Fig 2 On one or two occasions structures morphologically similar to tight junctions were observed between the glial cells The microfilament mat under the upper surface of the glial cells appeared to become more evident with increased cell density and could be very obvious at 21 days when the glial cells were completely inhibited from further growth (Fig 2) The attachment plaques were present as earlier but now with apparently less obvious bundles of microfilaments

At both 14 and 21 days a large amount of fibrous extra-cellular substance was noted Most of the fibres were approximately 10 nm in diameter and as a rule ran parallel to each other as well as to the submembranous microfilaments of the glial cells (Figs 7 and 12) In some sections continuity could be suspected between some extra and intracellular filaments

Malignant Glioma Cells - General Characteristics

The malignant glioma cell lines differed in many respects from one another Nevertheless they did show certain common characteristics some of which help to distinguish them as a group from the normal glial cells These distinguishing features became most prominent after the cells reached confluence

The sparse glioma cells had a general distribution of organelles similar to the glial cells They appeared never to spread as thinly as do glial cells in comparable cultures Prior to confluence the glioma cells had fairly regular and flat cell surfaces with various numbers of microvilli (Figs 8 and 10) They had leading lamellae with ruffling (Fig 9)

Post-confluent cultures on the other hand showed a number of characteristics almost specific for the glioma cells The cells in such cultures showed distinctly more

gl
in
th
the cell surfaces of adjacent cells intertwined to form complex cell surface appositions Few junctional devices were observed, however The frequency of junctions increased in the cultures at 14 and 21 days On the upper surface of such dense cultures which often

glioma cells could have rather large areas in their ground cytoplasm containing only filaments

cell sides and occasionally at the edge of the lower cell surface The perinuclear area contained numbers of randomly arranged microtubules and filaments (the latter varying in diameter between 5 nm and 10 nm) as well as secondary lysosomes sometimes of the residual body variety and mitochondria of various sizes and shapes The Golgi area was usually well developed and surrounded by coated and uncoated vesicles many of which presumably represented primary lysosomes Coated invaginations and submembranous vesicles probably representing micropinocytosis could occur all around the cell but seemed to be most frequent along the lower cell surface

Normal Glial Cells Post confluent

As the cultures became denser the following changes were noted The leading lamellae with their ruffles disappeared The cytoplasm of the cells overlapped (Fig 2) These overlappings resulted in large areas of cell membrane in appositions which tended to be straight (Fig 2) The number of secondary lysosomes increased Occasionally osmophilic plaques occurred just inside apposing membranes These were often dissociated from other structural arrangements the inter membrane gap being approximately 10-20 nm so that they

(Fig 15), microtubules, or even polysomes in the cellular ground substance

The malignant cells seemed to contain much larger amounts than glial cells of the loosely arranged bundles of wavy filaments which occurred centrally in the cell (Fig 15). Bundles of microtubules were also occasionally observed. The perinuclear area contained quantities of secondary lysosomes which invariably increased in number in the denser cultures. The Golgi zone was in general well developed and surrounded by many coated and uncoated vesicles. The nuclei were almost without exception irregular in shape (Fig 17).

The arrangement of the chromatin material varied from cell to cell. The nucleoli were generally attached to the nuclear membrane. Occasional dead cells or their organelles were seen in some of the dense cultures of malignant cells. These cellular components were found to be subject to phagocytosis by other cells. Even phagocytosis of whole nuclei was observed.

Malignant Glioma Cells: Variable Factors

The various cell lines have all been prepared for electron microscopy at different times during the last years. Thus, they have been subcultivated many times, in some cases many hundred times, during this period. Nevertheless, the various lines have, under the conditions studied, retained their morphological characteristics.

The frequency of attachment plaques was very variable, as was also the size of these structures. Nevertheless, their different components were constant as described above. Some of the lines, such as U-410 MG and U-251 MG, had large numbers of small attachment devices (Figs 11 and 13), while others had fewer which could either be large (U-118 MG) or small (U-87 MG). The cross sectional measurement of 75 randomly selected glioma cell attachment plaques from all glioma lines gave a range of 100 nm to 2 μ m. The incidence of these structures per substrate unit area appeared to increase greatly in the dense cultures. Some sections revealed cells with multiple attachment devices (Fig 13). The occurrence of cell junctional devices was also haphazard in most of the glioma lines they were but seldom observed and then only in dense cultures whereas in two (U-118MG and U-563 MG) they were a relatively frequent finding. The microfilamentous mat below the cells' upper surface membrane varied in its degree of development. In some lines it could be very obvious (e.g. U-87 MG) while in others it might be rudimentary and patchy (e.g. U-118 MG). Some lines had a similar microfilament mat above the lower cell membrane (U-373 MG).

The occurrence of the loosely arranged wavy filament bundles (5 nm–10 nm) varied greatly, one cell line (U-118 MG) presenting them as its most obvious attribute (Fig 15). The lines U-87 MG, U-178 MG and U-410 MG had the greatest quantities of rough ER. In lines U-178 MG and U-118 MG the rough ER had an unusual arrangement, being apparently tightly wrapped around the mitochondria.

The number of secondary lysosomes present in the growing cultures was greatest in U-410 MG and least in U-251 MG and U-563 MG. This difference was noted throughout the period of culture. The production of extracellular substance (often consisting of fibrous material with a fiber diameter of approximately 10 nm) reached a level equal to that of normal glial cells at 21 days in the case of line U-87 MG (Fig 12). The lines U-178 MG, U-410 MG, U-118 MG, U-343 MG and U-373 MG yielded this material in decreasing amounts, while no such material was produced by the lines U-251 MG and U-563 MG.

DISCUSSION

The present findings demonstrate yet again the homogeneity of the human glial cell lines cultivated *in vitro*, which could not here be differentiated on the basis of their ultrastructure. Observations of the glial lines have given almost identical results in many other studies. For example, their growth control characteristics are very similar (19), their production of glycosaminoglycans (10) and their behaviour and surface morphology at varying cell densities *in vitro* (7). The malignant cells, on the other hand, show a spectrum of appearances, and no two lines are identical in all respects. This was also the case in previous studies of other parameters, where the degree of deficient growth control of the malignant cell lines – as determined by the crowding index (19) – the production of glycosaminoglycans (10) and even the degree of surface activity (7), was variable. This variability among malignant cell lines *in vitro* despite derivation from tumours of the same histogenetic origin and degree of histopathological malignancy warrants attention. Studies where but a few malignant lines are compared with their normal counterparts should therefore, be interpreted with great caution. This variability can be of value in assessing which structures are probably essential for cell survival and proliferation *in vitro*. Those not common to all cells, both normal and malignant, are unlikely to be vital. It is noteworthy that the different lines of glioma cells retained their individual characteristics during cultivation *in vitro* during many years and

thus seem to be morphologically stable. Accordingly they reveal no tendency to transform into a common malignant type. The differences between the normal and malignant cells in this study were more quantitative than qualitative. One can postulate that some malignant glioma line may well be found to be identical with the glial cells as regards any one of the differences noted here. It is the observation of many different factors which at the last clearly differentiates the malignant glioma cells from the stable homogeneous morphological attributes of the glial cells; this differentiation is most easily achieved in the comparison of post-confluent cultures.

The attachment plaque which is common to all the normal and malignant cell lines has been likened to a hemi-desmosome (8) and its presence might be supposed to be related to the cells' ability to create such intercellular junctions. Our study does not support this notion since we observed cell lines with many attachment plaques (U 251 MG and U 563 MG) one of which was seldom found to form junctional devices (U 251 MG) while the other (U 563 MG) did so. Furthermore the lines U 118 MG and U 87 MG had but few attachment plaques yet the cells from the former line had relatively numerous junctional devices while those from the latter were seldom observed to form any at all. We also found microtubules to be a component of the attachment plaque which distinguishes this structure from the desmosome. It should be remembered however that gap junctions are very difficult to observe in ultrathin sections and if occurring may well have been overlooked.

It is interesting that our observations in the time lapse study previously reported (7) can be so closely correlated to our present findings. In that study the even and regular forward movement of U 251 MG suggested a continuous formation and breach of many attachment plaques; the presence of which has now been confirmed. The strength of intercellular adhesions as assessed by length and persistence of cytoplasmic projections when cells parted in

approximately 10 nm filamentous material will require further study. The parallelism frequently observed between these filaments and the intracellular filaments and various sections suggesting continuity is worthy of note. *Perdue* (13) described filaments of a similar diameter which appeared to pass through the surface membranes of cultured chick embryo fibroblasts. A similar extracellular microfibrillar mat resistant to collagenase in dense cultures of human foetal normal glial cells has been reported (12).

The fact that the cellular load of secondary lysosomes increases with density dependent inhibition of growth of glial cells to decrease again by dilution on cell division with return to logarithmic growth has been previously described and quantitated (5). A similar increase also appears to occur in glioma cells at terminal cell density when cell multiplication is at a minimum for these cells. The malignant cells' load of secondary lysosomes during logarithmic growth appeared to correlate inversely rather well with the malignant lines *C1* (19). This may be explained by the fact that malignant cell lines with high crowding indices will during routine culture seldom reach cell densities at which inhibition of growth would be considerable.

All the cells contained filaments with cross sectional diameters varying between 5 nm and 10 nm. The literature contains reports in which these filaments are divided up on the basis of their diameters and found to be in pure form in differing situations. We have not found this to be so. All locations studied could contain filaments of any diameter within the aforementioned range. Further studies will be required in order to define the significance of these structures for instance with the aid of various substances such as heavy meromyosin and cytochalasin B as well as immunological techniques.

The interpretation of our findings of the variable often rather irregular arrangements of filaments some of which were almost specific or characteristic for the malignant cell lines is difficult. We have made no observations which suggest obvious motile deficiencies in any of the lines. On the other hand control of this motility seems to be somewhat lacking. We previously described the form --

None of our ultrastructural findings e.g. the frequency of attachment plaques, the presence or absence of junctions or the production of extracellular material correlate with the degree of deficient growth control exhibited by the malignant lines as assessed by their crowding index (CI) at terminal cell density (19) and *B. Westermarck* (unpublished results). The amount of rough ER appeared however to correlate positively to the production of the extracellular substance. The nature of this

... as do the normal cells but transfer it to the upper cell surface. These facts may be related to the particular cellular fibrillar systems observed in the glioma cell lines. In this respect it is interesting to note that virus transformation *in vitro*

has been found in a number of studies to be associated with the disruption of the cells stress fibres (9, 14, 21)

In cultures of serum deprived glial cells we have observed the amounts of microfilaments to increase greatly while the cells are blocked in G1 (6). In this study we also perceived an apparent increase in intracellular filaments when both the normal and malignant cells reach densities at which density dependent growth inhibition will reach its maximum (18 and 19)

Supported by Stockholm's Cancer Society, the Swedish Medical Research Council and The Swedish Cancer Society

REFERENCES

- 1 Biberfeld P. A method for the study of monolayer cultures with preserved cell orientation and interrelationship. *J Ultrastruct Res* 25: 158-159 1968
- 2 Brunk U, Bell P, Collins P, Forsby N & Fredriksson B. A SEM of in vitro cultivated cells: osmotic effects during fixation. In Scanning Electron Microscopy. O Johari and I Corvin eds. IIT Research Institute, Chicago, Illinois: 379-386 1975
- 3 Brunk U, Ericsson J, L E, Ponten J & Westermark B. Specialization of cell surfaces in contact inhibited human glia like cells in vitro. *Exptl Cell Res* 67: 407-415 1971
- 4 Collins V P, Arboreli B & Brunk U. A comparison of the effects of three widely used glutaraldehyde fixatives on cellular volume and structure. *Acta Path Microbiol Scand Sect A* 85: 157-168 1977
- 5 Collins V P & Brunk U. Quantitation of residual bodies in cultured human glia cells during stationary and logarithmic growth phases. *Mech Ageing Dev* 8: 139-152 1978
- 6 Collins V P, Brunk U, T, Fredriksson B. A & Westermark B. The fine structure of growing and non growing whole glia cell preparations. *Cytobiologie*. In press 1978
- 7 Collins V P, Forsby N, Brunk U, T & Westermark B. The surface morphology of cultured human glia and glioma cells. A SEM and time lapse study at different cell densities. *Cytobiologie Eur J Cell Biol* 16: 52-62 1977
- 8 Franks L M & Wilson P D. Origin and ultrastructure of cells in vitro. *Int Rev Cytol* 48: 55-139 1977
- 9 Goldman R D, Yerna M J & Schloss J A. Localization and organization of microfilaments and related proteins in normal and virus transformed cells. *J Supramol Struct* 5: 155-183 1976
- 10 Glumetius B. Glycosaminoglycans in cultures of normal and malignant glial cells. *Acta Univ Upsal* 281 Uppsala 1977
- 11 Kernohan J W, Mabon R F, Siven H J & Adson A W. A simplified classification of the gliomas. *Proc of the staff meetings of the Mayo Clinic* 24: 71-75 1949
- 12 Macintyre E H, Ponten J & Valler A E. The ultrastructure of human and murine astrocytes and of human fibroblasts in culture. *Acta Path Microbiol Scand Sect A* 80: 267-283 1972
- 13 Perdue J F. The distribution ultrastructure and chemistry of microfilaments in cultured chick embryo fibroblasts. *J Cell Biol* 58: 265-283 1973
- 14 Pollack R, Osborn M & Weber K. Patterns of organization of actin and myosin in normal and transformed cultured cells. *Proc Nat Acad Sci USA* 72: 994-998 1975
- 15 Ponten J & Macintyre E. Long term culture of normal and neoplastic human glia. *Acta Path Microbiol Scand* 74: 465-486 1968
- 16 Reynolds E S. The use of lead citrate at high pH as an electron opaque stain in electron microscopy. *J Cell Biol* 17: 208-212 1963
- 17 Seman G & Dmochowski L. Ultrastructural characteristics of human tumor cells in vitro. In Human tumor cells in vitro. J Fogh ed. Plenum Press, New York 1975
- 18 Westermark B. Proliferation control of cultivated human glia like cells under steady state conditions. *Exptl Cell Res* 69: 259-264 1971
- 19 Westermark B. The deficient density dependent growth control of human malignant glioma cells and virus transformed glia like cells in culture. *Int J Cancer* 12: 438-451 1973
- 20 Westermark B, Ponten J & Hugosson R. Determinants for the establishment of permanent tissue culture lines from human gliomas. *Acta Path Microbiol Scand Sect A* 81: 791-805 1973
- 21 Wang E & Goldberg A R. Changes in microfilament organization and surface topography upon transformation of chick embryo fibroblasts with Rous sarcoma virus. *Proc Nat Acad Sci USA* 73: 4065-4069 1976

THE FINE STRUCTURE OF GROWING HUMAN GLIA AND GLIOMA CELLS

Whole Cell Preparations

V P COLLINS U T BRUNK B A FREDRIKSSON and ■ WESTERMARK

Department of Tumor Pathology Karolinska Institutet Stockholm and Institute of Pathology and Wallenberg Laboratory University of Uppsala Uppsala Sweden

Collins V P Brunk U T Fredriksson ■ A & Westermark ■ The fine structure of growing human glia and glioma cells. Whole cell preparations. Acta path microbiol scand Sect A 87 29-36 1979

Three lines of normal human glia cells and eight established lines of malignant glioma cells have been studied in the electron microscope (EM) using preparations of critical point dried whole cells sparsely grown on formvar-coated EM gold grids. The malignant cell lines showed a very varied morphology almost every line having its peculiarities as compared to the essentially identical normal glia lines. The major differences noted concerned the form of the leading lamellae number of microspikes and the distribution of organelles such as secondary lysosomes and mitochondria. No single consistent finding made it possible to differentiate the glioma cells as a group from the glia cells in sparse cultures. The findings of this study show some of the individual glioma cell lines to have characteristic cell surface structures. They were found to be identical with the findings in previous SEM studies suggesting the peculiarities of the individual malignant glioma lines to be stable and retained despite continual passage.

Key words: Glia glioma cells cell lines: ultrastructure

V P Collins Department of Tumor Pathology Karolinska sjukhuset S 104 01 Stockholm 60 Sweden

Accepted as submitted 4 vii 78

In previous studies we have described differences in the behaviour and morphology of a number of lines of normal human glia and malignant glioma cells *in vitro*. The major of these differences concerned (a) the degree of cell motility - including plasma membrane activity in the form of ruffling with associated pinocytosis - which appears to be greater in glioma cells particularly in post confluent cultures (3-8); (b) dependency on the presence of growth factors for proliferation which is absolute for glia cells (3-14); and (c) deficient density-dependent regulation of growth of the glioma cells (18).

The discrepancies in motility between the glia and glioma cells suggest changes from the normal in the

structure and/or function of the malignant cell's musculo skeletal system. Microtubuli and microfilaments which are the morphologically most easily identifiable components of this system have also been implicated in growth control (9). A number of reports have described radical changes in the cell's microfilament arrangement after virus transformation *in vitro* (1-10, 13, 15, 17). The general distribution of cell organelles and especially that of microtubuli and filaments is particularly difficult to study *in vitro* - but to obtain an overall view of the cellular arrangement and thus to complement our previous studies of conventional thin sections (7).

MATERIAL AND METHODS

Cell Lines and Culture Conditions

The investigation was carried out on three lines of diploid normal human glia cells (U-619 CG, U-787 CG, U-1160 CG), and eight lines of established human malignant glioma cells (U-87 MG, U-118 MG, U-178 MG, U-251 MG, U-343 MG, U-373 MG, U-410 MG and U-563 MG). The cell lines were established in culture as previously described (16, 19). Only early passages of the glia cells were used. All the cell lines were grown in Eagle's minimal essential medium (EMEM), supplemented with 10% calf serum and antibiotics.

The cells were seeded into 36 mm plastic Nunclon® petri dishes containing carbon stabilized, formvar covered, EM gold grids as described by Porter *et al.* (11, 20). The cell suspensions contained approximately 10 000 cells/ml and each dish received 2 ml. After 24 hours, during which time the cells attached and spread on the substrate, a few grids were removed and fixed as described below. At 48 and 72 hours further grids were removed and fixed. From previous studies (18) it is known that at these time points all cells were in log growth phase. The malignant lines, a selection from the 24 now established, were representative of all, as regards their growth characteristics (18).

Preparation for Transmission Electron Microscopy of Whole Cell Preparations

The grids were placed directly in 2% glutaraldehyde in 0.1 M Na-cacodylate-HCl buffer with 0.1 M sucrose (pH 7.3, total osmolality 510 mOsm, vehicle osmolality 300 mOsm) at 37° C for one hour and then at 4° C for up to one week (4). The grids were subsequently postfixed in 1% OsO₄ in 0.15 M cacodylate buffer for 90 minutes, stained in 2% uranyl acetate in water for 15 minutes, dehydrated in a graded series of ethanols and critical point dried from carbon dioxide in a Polaron 3000 apparatus. The grids with cells were subsequently stabilized by carbon evaporation and studied in a Jeol 100 C microscope with a side entrance goniometer, or in a Philips 201 microscope at 100 kV. Stereo pairs were photographed at various angles up to 20° depending on the magnification.

RESULTS

We will first describe the structures common to all cells studied. How characteristic these findings were for the various glia and glioma lines will be described in the following sections.

Lamellipodia which spread out over the substrate and formed ruffles, contained no filamentous structures or any organelles except occasional ribosomes (Figs 1-4). There was one exception and that was when lamellipodia were found in association with microfilament containing microspikes or microvilli (Fig. 3). Ruffle associated macropinocytotic vesicles could be observed just behind the ruffles or under transport to the perinuclear area (Fig. 3).

The leading lamella, from the tip of which the lamellipodia formed, was a stable area of cytoplasm stretching from the perinuclear area to the leading edge. It contained diffusely arranged microtubuli and filaments in different degrees of bundle formation. Various numbers of mitochondria and secondary lysosomes, as well as an invariably evenly distributed endoplasmic reticulum, were found in the leading lamella and the perinuclear region (Figs 1-5 and 9).

The mitochondria showed a large morphological spectrum in both the normal and the malignant cells. They could be branched or circular in form, or even have combinations of these forms (Figs 6-10 and 12). Microspikes and microvilli had approximately similar diameters, both contained a small bundle of microfilaments and differed only with respect to their length (Fig. 11). Both appeared «sticky» and could become attached to one another. Most cell-to-cell contacts showed no particular local cellular changes even when the cell cytoplasm overlapped, except for the almost invariable presence of microspikes (Fig. 5). Nothing reminiscent of a cell junction was observed. Occasionally, where it appeared that two cells attempted to draw apart, a number of microfilament-containing retraction fibrils could be seen. Retraction fibrils, which were present at the trailing end of the cell, also contained microfilament bundles. Microtubules could be visualized in the leading lamellae but no particular organization or orientation of these structures could

Fig. 1 Stereopair of micrographs showing a typical leading lamella of a glia cell (U-787 CG). Note the broad leading lamella and ruffles. A number of long microvilli and microspikes can be seen just behind the fine ruffles. The images can be fused with a stereo viewer. X 2 000.

Fig. 2 Stereopair of the leading lamella with small broken-up ruffling areas so characteristic of U-563 MG. Note the presence of many long microspikes in association with the ruffles. The leading lamella contains a very evenly distributed endoplasmic reticulum which can be seen as a fine network. A few mitochondria and some microvilli on the upper cell surface are also seen. X 1 920.

Fig. 3 Stereopair of the leading lamella of U-87 MG with broad lamellipodia and ruffles. A large number of macropinocytotic vesicles under transport in towards the electron dense perinuclear region can be seen as well as a number of secondary lysosomes, mitochondria and even microfilament bundles. Note the fine ruffle like structures do not appear to contain any filamentous structures here except at the arrow, where a little microvillus is placed on the ruffle and a fine bundle of microfilaments traverses the ruffle at this point. X 1 600.





Fig 4 Stereopair of a typical leading lamella of a U 251 MG with its very microspike rich tuft like ruffling areas. Note the leading lamella is almost completely lacking in any organelles except for the evenly distributed endoplasmic reticulum which is somewhat difficult to see and the ends of a few mitochondria protruding from the perinuclear area. X 1600

Fig 5 Stereopair of two glia cells in contact (U 619 CG). Note the overlapping of the cell cytoplasm, both having long microspike like structures. In the case of the microspikes of the cell lying under these be along the substratum whereas the microspikes of the cell being above stand upright. Note also the distribution of the cell organelles including mitochondria and secondary lysosomes which are spread out to the cell periphery. X 1600

Fig 6 The leading lamella near the perinuclear area of a cell of the line U 178 MG. A mitochondrion and endoplasmic reticulum hanging in the microtrabecular system are seen. The mitochondrion is relatively regular in shape and the cristae can clearly be observed. X 10000

be found. Another cell protrusion frequently observed was a very long thin structure which had a diameter similar to a microspike and contained a small microfilament bundle. They originated at the lateral edge of the cell and stretched out along the substrate. They could bend or branch and when they branched they always did so into two equally thick branches at an angle of approximately 120° (Fig 13).

The perinuclear area which was very much thicker than the more peripheral parts of the cell contained the greater part of the cell's mitochondria, secondary lysosomes and the Golgi zone. This area could be least well visualized and analyzed in this study. The cellular ground substance was similar to that described in other systems and named the microtrabecular system (10-18). Cells in mitosis were rounded with many retraction fibrils. The latter configuration did not permit visualization of internal cellular structures at 100 kV.

Glia Cell Lines

The three glia cell lines were very similar in their morphology and could not be differentiated from one another. The fine structure of intact glia cells has been previously described (6) and we will only report here on those findings which were of particular interest to this study in that they differed from the malignant glioma cells. The interphase glia cells were well spread with usually a single broad leading lamella with or without broad lamellipodia and ruffling at its distal end (Fig 1). Microspikes

were present in small numbers usually just behind or to one side of the ruffles. Microspikes or microvilli were very occasionally located at the tips of the lamellipodia. The mitochondria and secondary lysosomes were mainly arranged in the perinuclear area but could also be present in the leading lamella decreasing in number with increased distance from the nucleus. The leading lamella could contain long discrete bundles of microfilaments. Otherwise filaments were evenly arranged in a thin mat especially along the cell edges.

Malignant Glioma Cell Lines

The malignant glioma cell lines showed a wide morphological spectrum. They differed from one another as much as they did from glia cells. The general characteristics of the cells from the various lines are described below.

The leading lamellar lamellipodia formation could be similar to glia cells with broad lamellipodia (U 87 MG, U 410 MG) (Fig 3). Some lines had small lamellipodia which formed in a number of different areas (Figs 2 and 4) along the leading edge of the leading lamella. The latter was particularly characteristic of U 251 MG, U 343 MG and U 563 MG. The incidence of microspikes both contained in the lamellipodia and free standing varied greatly. U 251 MG showed the greatest numbers of lamellipodia containing microspikes (Fig 4) with U 563 MG having the next greatest numbers of

leading lamellae contained decreasing numbers of secondary lysosomes and mitochondria with increasing distance from the nucleus (U 87 MG, U 410 MG and U 178 MG) (Figs 3 and 9) while others contained almost no such organelles (Figs 2 and 4, U 251 MG and U 563 MG). The occurrence of microfilament bundles also varied in some lines being almost non-existent (Figs 2 and 4) while in other lines being quite evident (Fig 3). The occurrence of secondary lysosomes varied with the line. U 410 MG contained the greatest amounts while U 251 MG and U 563 MG contained but few. The other lines having intermediate numbers. Even the distribution of organelles in the perinuclear area varied. Again the lines U 251 MG and U 563 MG showed a very particular arrangement in this respect with the organelles - mostly mitochondria - being apparently tightly bound to the one side of the cell nucleus (Fig 8). Very few mitochondria were ever observed anywhere else in these cells (Figs 2 and 4).

The degree to which the glioma cells spread on the substratum was also very variable with the line

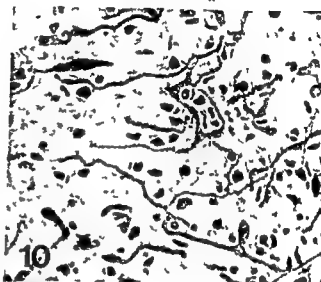
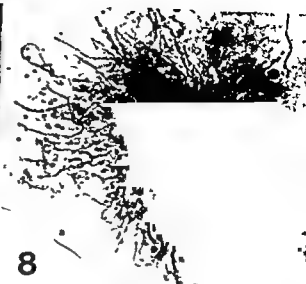


Fig 7 The perinuclear area of a glia cell (U 787 CG) showing the large numbers of electron dense secondary lysosomes and the evenly arranged mitochondria X 2 000

Fig 8 The perinuclear area of a U 563 MG cell which does not contain so many electron dense secondary lysosomes but a large bunch of mitochondria which seem tightly attached to one side of the nucleus. Compare with Fig 7 X 1 600

Fig 9 A leading lamella of a cell from the line U 373 MG with little active ruffling and a large number of microspikes. A number of bizarre mitochondria are located in the leading lamella. The endoplasmic reticulum can be seen to be evenly spread X 3 300

Fig 10 Perinuclear area of a glia cell (U 619 CG) showing mitochondria of all shapes and sizes also a number of electron dense secondary lysosomes in the microtubular system X 3 300

Fig 11 The edge of a cell with filopodia and a microvillus of the line U 562 MG. Note the fine thin bundles of microfilaments entering the bases of these structures. At the bottom of the picture endoplasmic reticulum can be seen X 10 000

Fig 12 A circular and a long mitochondrion showing cristae both hanging in the microtubular network X 26 000

Fig 13 The long thin filopodia which can extend from the lateral edge of the cell and bend or branch. Note the angle at which they do this and that a fine bundle of microfilaments enters the base of the structure to the left X 4 480

U 118 MG displaying the most rounded state which made the observation of the perinuclear area of these cells almost impossible. In general the perinuclear areas of the glioma cells were more difficult to visualize than those of the glia

DISCUSSION

In our studies of cultured normal human glia cells we have found the different glia lines to show strikingly similar characteristics both as to their behaviour and morphology as well as to their growth control attributes (7, 8, 18). This has again been confirmed in the present study. The malignant glioma cell lines on the other hand show a spectrum of morphologies all differing more or less from that of the glia cell lines (7, 8). The glioma lines also show various degrees of defective growth control (18).

In this study we have uncovered the internal cellular structures which lie beneath the surface

characteristics previously reported (8). No common factors by which all the malignant cell lines differ morphologically from their normal counterparts in sparse cultures have been detected. The only consistent finding which again varied in degree between the malignant lines was the difficulty in viewing the perinuclear area, owing to the glioma cells' apparently greater thickness and less well spread state. This is interesting since decreased cell spreading has been documented after virus transformation (2). To differentiate the lines on this basis is however almost impossible as all contain cells more or less well spread - for example in association with mitosis. The malignant glioma lines did individually have some rather characteristic qualities - for example the filopodia and microvilli.

have previously described this type of ruffling as being typical of U 251 MG (3). The same is true of the leading lamella and the lamellipodia forms of the other cell lines which have been previously described as seen in the SEM (8).

The arrangement of the malignant cell lines' filament systems varied, some showing the presence of microfilament bundles while others did not. Thus we have been unable to confirm in all the malignant glioma lines the findings of studies on virus transformed cells *in vitro* where transformation is associated with the disruption of the organization of stress fibres (1, 10, 13, 15, 17). The large variation we have found between the individual glioma lines in respect of every attribute studied is noteworthy (7, 8, 12, 18). This should be recalled when differences between single or a few malignant cell lines are found when comparing them with their normal counterparts. Such results should be interpreted with great caution.

The occurrence of electron dense secondary lysosomes was greatest in the malignant cell lines which show a relatively low crowding index (18). This may reflect the fact that they are more frequently growth inhibited to a greater or lesser degree thus permitting the accumulation of these structures as also occurs in glia cells under density dependent growth inhibition (5). Why the small

has its molecular explanation.

The bizarre mitochondrial morphology is worthy of note. Ultrathin sections very seldom show the true mitochondrial form (7) mitochondria appearing to be rod like bodies. Whether *in vitro* conditions somehow effect mitochondrial form is not established.

It is unfortunate that we cannot study post confluent cultures with the whole cell technique using standard electron microscopes since the cell density does not permit visualization of crowded cultures with an accelerating voltage of 100 kV. High voltage electron microscopy will be required for study under such conditions.

Supported by Stockholm Cancer Society and the Swedish Medical Research Council

REFERENCES

1. Altincub B & Steiner S. Altered microfilament structure during cellular transformation by murine sarcoma virus. *J Cell Biol* 67 7a 1975
2. Ambros V R, Chen L B & Buchanan J M. Surface ruffles as markers for studies of cell transformation by Rous sarcoma virus. *Proc Nat Acad Sci USA* 72 3144-3148 1975
3. Brunk U T, Schellens J P M, Westermark B & Collins V P. Effect of serum deprivation on ruffling activity, macropinocytosis and proliferation of cultivated human glia and glioma cells. *Cytobiologie Europ J Cell Biol* 15 275-284 1977
4. Collins V P, Arborgh B & Brunk U. A comparison of the effects of three widely used glutaraldehyde fixatives on cellular volume and structure. *Acta Path Microbiol Scand Sect A* 85 157-168 1977
5. Collins V P & Brunk U T. Quantitation of residual bodies in cultured human glia cells during stationary and logarithmic growth phases. *Mech Ageing Dev* 8 139-152 1978
6. Collins V P, Brunk U T, Fredriksson B A & Westermark B. The fine structure of growing and non growing whole glia cell preparations. *Cytobiologie Europ J Cell Biol* In press 1978
7. Collins V P, Forsb N, Brunk U T, Ericsson J L E & Westermark B. Ultrastructural features of cultured human glia and glioma cells. *Acta Path Microbiol Scand Sect A* 87 19-28 1979
8. Collins V P, Forsb N, Brunk U T & Westermark B. The surface morphology of cultured human glia and glioma cells. A SEM and time lapse study at different cell densities. *Cytobiologie Europ J Cell Biol* 16 52-62 1977
9. Edelman G M, Deustachio P, McClain D A & Jazwinska S M. Surface signals and cellular regulation of growth in Mitosis Facts and questions. Eds M Little et al. Springer Verlag 1977
10. Edelman G M & Yahare J. Temperature sensitive changes in surface modulating assemblies of fibroblasts transformed by mutants of Rous sarcoma virus. *Proc Nat Acad Sci U S A* 73 2047-2051 1976
11. Gershenbaum M R, Shay J H & Porter K R. The effects of cytochalasin B on BALB/3T3 mammalian cells cultured in vitro as observed by scanning and high voltage electron microscopy. *Scanning Electron Microscopy* 1974 pt III IIT Research Institute Chicago U S A pp 581-596
12. Glimelius B. Glycosaminoglycans in cultures of normal and malignant glial cells. *Acta Universitatis Upsalensis* 281 Uppsala 1977
13. Goldman R D, Yerna M J & Schloss J A. Localization and organization of microfilaments and related proteins in normal and virus transformed cells. *J Supramol Struct* 5 155-183 1976
14. Lindgren A, Westermark B & Ponten J. Serum stimulation of stationary human glia and glioma cells in culture. *Exptl Cell Res* 95 311-319 1975
15. Pollack R, Osborn M & Weber K. Patterns of organization of actin and myosin in normal and transformed cultured cells. *Proc Nat Acad Sci U S A* 72 994-998 1975
16. Ponten J & Macintyre E. Long term culture of normal and neoplastic human glia. *Acta Path Microbiol Scand* 74 465-486 1968
17. Wang E & Goldberg A R. Changes in microfilament organization and surface topography upon transformation of chick embryo fibroblasts with Rous sarcoma virus. *Proc Nat Acad Sci* 73 4065-4069 1976
18. Westermark B. The deficient density dependent growth control of human malignant glioma cells and virus transformed glia like cells in culture. *Int J Cancer* 12 438-451 1973
19. Westermark B, Ponten J & Hugosson R. Determinants for the establishment of permanent tissue culture lines from human gliomas. *Acta Path Microbiol Scand Sect A* 81 791-805 1973
20. Holosenich J J & Porter K R. Stereo high voltage electron microscopy of whole cells of the human diploid cell line WI-38. *Amer J Anat* 147 303-323 1976

TUMOURS IN ICELAND

1 Malignant Tumours of Skin - A Histological Classification

CHARLES K. MCKNIGHT and BJARKI MAGNUSSON

The Department of Pathology University of Iceland Reykjavik Iceland

McKnight C K & Magnusson B Tumours in Iceland 1 Malignant tumours of skin - a histological classification. *Acta path microbiol scand Sect A* 87 37-44 1979

Four hundred and eighty five primary malignant skin tumours submitted for histological diagnosis in Iceland during the period 1955-1974 were typed according to the WHO histological classification. The incidence of these tumours age adjusted to the World population was 12.6/100 000 in males and 11.0/100 000 in females. These are very low figures for a white population. The distribution by type among males was basal cell carcinoma 66.8%, squamous cell carcinoma 22%, malignant melanoma 7.2% and others 4%. Among females basal cell carcinoma 66.9%, malignant melanoma 20.8%, squamous cell carcinoma 10.2% and others 2.1%. The exposed areas of the body were affected much more frequently than other areas. The results support the theory that intensity of solar radiation is of major aetiological significance.

Key words: Skin tumours, primary malignant, solar radiation.

Bjarki Magnusson, Dept. of Pathology, University of Iceland, P.O. Box 150, 121 Reykjavik, Iceland.

Accepted as submitted 7 vii 78

This study was undertaken to investigate the pattern and incidence of primary skin malignancies in Iceland and to classify them in accordance with the World Health Organisation nomenclature as published in 1974 (9). The latter aim is part of this department's objective to classify all tumours occurring in Iceland in the period 1955-1974 according to the WHO International Histological Classification of Tumours.

The incidence of malignant skin tumours in Iceland is of particular interest owing to the country's extreme northern latitude (between 63° 23' and 66° 33' north) in view of the well known association between intensity of solar radiation and these tumours. Additional advantages of such a study in Iceland are the stability and homogeneity of the population and the well-organised reporting of all malignant tumours to the Icelandic Cancer Registry.

MATERIALS AND METHODS

Since 1954 the Icelandic Cancer Registry has listed all primary skin malignancies in Iceland.

All those reported) were considered in the study. The cancer registry is based on reports from all hospitals, private practices and institutes of radiology and the diagnostic files from autopsies and surgical specimens at the Department of Pathology of the University of Iceland which is the only laboratory for anatomical pathology in the country.

The authors the WHO I were cut from tissue blocks. Where more than one tumour was reported from the same person, they were considered to be separate only if distinct in histology and/or topography from other tumours in that person.

In addition to age specific rates the figures obtained were expressed as age standardised rates, standardised

TABLE 1 *Histological Types of Skin Cancer in Iceland Based on the WHO Classification in the Period 1955-1974 by Sex and Percentage*

Type of Cancer	Male		Female		Total	
	No	Percent	No	Percent	No	Percent
Basal Cell Cancer	167	66.8	157	66.9	324	66.8
Squamous Cell Cancer	55	22.0	24	10.2	79	16.3
Metatypical	2	0.8	1	0.4	3	0.6
Malignant Melanoma	18	7.2	49	20.8	67	13.8
Kaposi's Sarcoma	2	0.8	3	1.3	5	1.0
Dermatofibrosarcoma Protruberans	3	1.2	—	—	3	0.6
Fibrosarcoma	1	0.4	1	0.6	2	0.4
Syringocystadenocarcinoma Papilliferum	1	0.4	—	—	1	0.4
Sebaceous Adenocarcinoma	1	0.4	—	—	1	0.4
Total	250	100.0	235	100.2	485	100.3

TABLE 2 *Histological Sub-Types of Basal Cell Carcinoma Based on the WHO Classification in the Period 1955-1974 by Sex and Percentage*

Sub-type of Basal Cell Carcinoma	Male		Female		Total	
	No	Percent	No	Percent	No	Percent
Solid	100	60.0	98	62.4	198	61.1
Cystic	20	12.0	20	12.7	40	12.3
Adenoid	10	6.0	11	7.0	21	6.5
Adenoid-Cystic	4	2.4	2	1.3	6	1.9
Keratotic	6	3.6	1	0.6	7	2.2
Superficial Multicentric	14	8.4	15	9.6	29	9.0
Morphoea Like	11	6.6	7	4.5	18	5.6
Fibro-Epithelial	2	1.2	3	1.9	5	1.5
Total	167	100.2	157	100.0	324	100.1

both to the mean Icelandic population for the period and to the «world» population (4). The incidence for the decade 1955–1964 was then compared with that for the decade 1965–1974 to see if there was a significant difference between the two. Finally data on the intensity of global radiation in Iceland were obtained from the Icelandic Meteorological Office. Global radiation is short wave radiation both direct from the sun and reflected from the sky and clouds.

RESULTS

Histological slides were available from 501 tumours (496 patients). Sixteen of these were excluded as their origin was not from skin although they had been listed as such in the registry. The results of the typing of the remaining 485 primary malignant skin tumours are shown in Tables 1 and 2. In males basal cell carcinomas constituted two thirds (66.8%), squamous cell carcinomas 22% and malignant melanoma 7.2%.

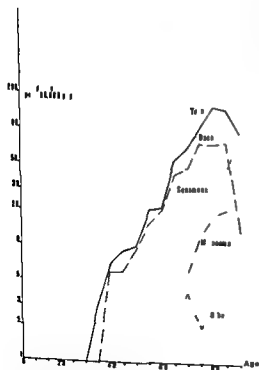


Fig 1 Age-specific incidence rates of the various types of primary malignant skin tumours among Icelandic males

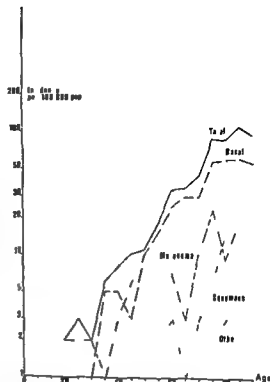


Fig 2 Age-specific incidence rates of the various types of primary malignant skin tumours among Icelandic females

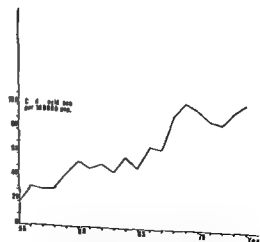


Fig 3 Crude incidence of naevi submitted for histological examination during the period 1955–1974, males and females combined, showing a marked increase over the 20 years

TABLE 3 *Anatomical Site of Squamous and Basal Cell Carcinomas 1955-1974 by Sex and Percentage*

Site	Male		Female		Total	
	Squamous No (%)	Basal No (%)	Squamous No (%)	Basal No (%)	Squamous No (%)	Basal No (%)
Scalp	—(—)	2 (1.2)	—(—)	2 (1.3)	—(—)	4 (1.2)
Neck	—(—)	9 (5.4)	2 (8.3)	4 (2.5)	2 (2.5)	13 (4.0)
Forehead	1 (1.8)	6 (3.6)	2 (8.3)	14 (8.9)	3 (3.8)	20 (6.2)
U Eyelid	—(—)	10 (6.0)	—(—)	6 (3.8)	—(—)	16 (4.9)
L Eyelid	3 (5.5)	20 (12.0)	—(—)	13 (8.3)	3 (3.8)	33 (10.2)
Nose	9 (16.4)	29 (17.4)	2 (8.3)	31 (19.7)	11 (13.9)	60 (18.5)
Cheek	6 (10.9)	23 (13.8)	4 (16.7)	14 (8.9)	10 (12.7)	37 (11.4)
Temple	3 (5.5)	11 (6.6)	—(—)	9 (5.7)	3 (3.8)	20 (6.1)
U Lip	—(—)	2 (1.2)	—(—)	2 (1.3)	—(—)	4 (1.2)
L Lip	2 (3.6)	—(—)	1 (4.2)	3 (1.9)	3 (3.8)	3 (0.9)
Ear	8 (14.5)	5 (3.0)	2 (8.3)	3 (1.9)	10 (12.7)	8 (2.5)
Face (N O S)	4 (7.3)	25 (15.0)	2 (8.3)	25 (15.9)	6 (7.6)	50 (15.4)
Head & Neck (Total)	36 (65.5)	142 (85.0)	15 (62.5)	126 (80.2)	51 (64.4)	268 (82.7)
Trunk	1 (1.8)	8 (4.8)	1 (4.2)	16 (10.2)	2 (2.5)	24 (7.4)
U Extremities (Ex Hand)	1 (1.8)	3 (1.8)	1 (4.2)	2 (1.3)	2 (2.5)	5 (1.5)
Hand	7 (12.7)	—(—)	3 (12.5)	1 (0.6)	10 (12.7)	1 (0.3)
L Extremities	4 (7.3)	3 (1.8)	1 (4.2)	1 (0.6)	5 (6.3)	4 (1.2)
Site Not Rec	6 (10.9)	11 (6.6)	3 (12.5)	11 (7.0)	9 (11.3)	22 (6.8)
Total	55 (100.0)	167 (100.2)	24 (100.0)	157 (99.8)	79 (99.9)	374 (99.8)

In females basal cell carcinomas also made up two thirds (66.9%) with malignant melanoma at 20.8% and squamous cell carcinoma 10.2%.

Tables 3 and 4 show the frequency of involvement of various anatomical sites for each histological type. The commonest site for both basal and squamous cell carcinomas was the head and neck, followed in frequency by the trunk for basal and the hand for squamous carcinoma. The lower limb was the commonest site for malignant melanoma in both sexes, followed by the neck and trunk. The number of other cancers was too low to permit any conclusions to be drawn about site.

The relationship between primary skin malignancy and age is shown in Table 5 and Figs 1 and 2. Uncommon before middle age, the incidence then rises sharply to reach its maximum of 107/100 000 (females) and 150/100 000 (males) during the eighth decade. The shape of the total curve was

produced mainly by the basal cell carcinoma curve. The male/female ratio for the various types is given in Table 6.

The age standardised rates for the two 10 year periods 1955-1964 and 1965-1974 were then compared to see if there was a significant difference in incidence between them (Table 7). Chi squared tests (7) were applied for each type and sex. The increase in basal cell carcinomas in females was significant to the 5 per cent level but insignificant for the other types in females and all types in males. For comparison and in order to estimate whether there had been an increase in surgical procedures of the skin in general, the annual crude incidence rates for all benign naevi submitted to the Department of Pathology over the twenty year period were calculated and are shown in Fig 3.

Finally Table 8 compares the incidence of primary malignant skin tumours from the Icelandic

² Cancer Registry with the recently published figures from other registries (10) The same areas are also compared with reference to annual mean global radiation and average daylight hours (11)

DISCUSSION

The incidence of primary skin malignancies in Iceland conforms to the established pattern of a decrease in incidence associated with an increase in latitude and a decrease in exposure to direct sunlight (2) Fig. 3 shows that with an increase in facilities over the years a steadily increasing number of skin blemishes have been removed and submitted for histological examination. This suggests that the increased reporting of basal cell carcinomas in females is probably related to an increase in minor cosmetic surgery rather than a true rise in incidence. With reference to Table 8 those areas with a large population and a high incidence of primary skin malignancy probably under report the incidence of these tumours in the registries (5). In a recent survey of the incidence of non melanoma skin cancer in four areas of the United States the rates were at least twice the figure quoted by the American Cancer Society (8) and in the Dallas Ft

Worth area of Texas the annual age adjusted incidence was 643/100 000 (males) and 286/100 000 (females) (8). In Iceland however with a small population (about 230 000) low incidence of primary skin malignancy and good reporting the figures are probably an accurate reflection of the true incidence.

Although the malignant tumours are relatively few the distribution by anatomical site and histological type is similar to that found in high incidence areas (5, 8, 12). Thus both basal and squamous cell carcinomas occur most frequently on the exposed parts of the body the head and neck being the site of about 83% of all basal cell carcinomas and 64% of all squamous cell carcinomas.

With 23% of the Icelandic population being employed in agriculture and fishing (3) it is surprising that the incidence of primary skin malignancies in males should not differ statistically from that in females in the same way as in many other countries (1, 5, 8, 12). If the carcinogenic effect of solar radiation is dose related the males should be over represented owing to the preponderance of males in out door occupations. The Icelandic results show that at low dosage the

TABLE 4 Anatomical Site of Malignant Melanoma and Other Skin Cancers 1955-1974 by Sex and Type

Site	Male		Female		Total	
	Melanoma No	Other (type)*	Melanoma No	Other (type)*	Melanoma No	Other (type)*
Face	4 (22.7%)	2 (Se, D)	7 (14.3%)	2 (K, K)	11 (16.4%)	4 (K, K, Se, D)
Neck/Trunk	5 (27.8%)	-	10 (20.4%)	-	15 (22.4%)	-
U. Extremity	2 (11.1%)	2 (S, D)	8 (16.3%)	1 (K)	10 (14.9%)	3 (K, D, S)
Foot	6 (33.3%)	1 (D)	7 (14.3%)	-	13 (19.4%)	1 (D)
L. Extremity (Ex Foot)	1 (5.6%)	2 (K, Sa)	17 (34.7%)	1 (Sa)	18 (26.9%)	3 (K, Sa, Sa)
Site Unknown	-	1 (K)	-	-	-	1 (K)
Total	18 (100.0%)	8	49 (100.0%)	4	67 (100.0%)	12

*Type K - Kaposi's Sarcoma
D - Dermatofibrosarcoma Protuberans
S - Syringocystadenocarcinoma Papilliferum
Sa - Sarcoma
Se - Sebaceous Adenocarcinoma

TABLE 5 Age Specific Incidence per 100 000 in Both Sexes for all Types of Skin Cancer 1955-1974 and Age Adjusted Incidence for Icelandic (1956-1975) and World Populations

Type of Cancer	Age Group																	Stand Iceland	Stand »World«
	0	1	5	10	15	20	25	30	35	40	45	50	55	60	65	70	75	80	85+
Total Skin Cancer (Male)	0	0	0	0	1	1	1	3	7	9	10	20	21	52	67	101	150	143	92
Total Skin Cancer (Female)	0	0	0	0	2	3	2	6	8	10	11	18	33	34	43	85	83	107	91
Basal Cell Cancer (Male)	0	0	0	0	0	1	1	1	6	6	9	15	20	41	46	74	73	75	13
Basal Cell Cancer (Female)	0	0	0	0	0	1	1	5	5	3	10	15	24	29	29	53	56	58	53
Squamous Cell Cancer (Male)	0	0	0	0	0	0	0	0	3	1	2	3	3	9	11	15	40	41	92
Squamous Cell Cancer (Female)	0	0	0	0	0	0	0	0	1	1	0	2	3	1	3	6	15	24	23
Malignant Melanoma (Male)	0	0	0	0	0	0	0	2	0	0	0	0	0	0	6	12	18	20	10
Malignant Melanoma (Female)	0	0	0	0	2	2	2	1	3	6	0	0	7	3	10	23	9	19	25
Other Cancer (Male)	0	0	0	0	0	0	0	0	0	1	0	0	0	2	4	2	4	7	0
Other Cancer (Female)	0	0	0	0	0	0	0	0	0	0	1	0	0	0	0	2	3	0	0

TABLE 6 *Male/Female Ratio of Average Annual Rates of Skin Cancer 1955-1974 Age Adjusted to World Population (4)*

Type	M/F Ratio
All Skin Cancer	1.2/1
Basal Cell Cancer	1.2/1
Squamous Cell Cancer	2.6/1
Malignant Melanoma	0.4/1
Other Cancer	3.0/1

relationship between amount of exposure and disease is not so marked.

The incidence of malignant melanoma while generally lower than that in other countries (6-10), is not as comparatively low as that of basal and squamous carcinomas. This lends support to the belief that the level of sunlight exposure while

important in the development of malignant melanoma is not as important as it is for the basal and squamous groups. Primary malignant skin tumours are not as important as a cause of morbidity in Iceland as in some other countries where for sheer weight of numbers they are excluded from the registries. In Icelandic males they rank 4th in order

TABLE 7 *Incidence per 100 000 of Various Types of Skin Cancer During the 10 Year Periods 1955-1964 and 1965-1974 Age Adjusted to World Population (4)*

	1955-1964		1965-1974	
	Males	Females	Males	Females
Basal cell	6.9	4.8	10.2	9.5
Squamous cell	2.7	0.7	2.6	1.1
Melanoma	0.4	1.6	1.1	2.9
Other	0.6	0.4	0.2	0.3

TABLE 8 *The Incidence of Skin Cancer per 100 000 in Various Areas of the World as Recorded by Cancer Registries (10) Compared with their Annual Mean Global Radiation Levels and Average Sunshine Hours per Day (11)*

Area	Non Melanoma Skin Cancer		Malignant Melanoma		Annual Mean Global Radiation cal/cm ² /day	Annual Average Sunshine hours per day
	Males	Females	Males	Females		
U.S.A. (Texas non-lauo)	119.9	75.5	3.4	4.8	408	10.3
Canada (Saskatchewan)	122.6	81.3	3.1	3.8	297	6.1
Canada (Newfoundland)	40.4	27.2	1.3	1.7	257	4.2
Denmark	34.4	24.5	3.5	6.0	239	4.8
Finland	24.4	30.5	2.9	3.4	235	5.2
England (Sheffield)	32.0	26.6	1.3	2.0	196	3.3
Scotland (Ayrshire)	44.1	38.6	2.7	3.4	207	3.5
Iceland	12.6	11.0	0.7	2.3	177	3.3

of frequency behind cancers of stomach, prostate, bronchus and colon, in females they rank 9th behind breast, stomach, cervix uteri, colon, thyroid, ovary, corpus uteri and bronchus (3)

In conclusion, these figures emphasize the low incidence of primary skin malignancies at high latitudes (2). Yet the histological types and their relative importance remain similar to those found in white populations in areas of higher solar radiation. The similarity in the rates for males and females suggest that at a low intensity of radiation, length of exposure is more erratic in inducing malignancy than at high exposure.

This investigation was supported by the *World Health Organisation*. The authors are grateful to *Hrafn Tullius M. D.* for his advice on statistical methods and to *Jonas Hallgrímsson M. D.* for his comments and help throughout the work.

REFERENCES

- 1 Atkinson L, Glezy J A, Riley-Young P S, Scott G C & Wigley S C. The epidemiology of cancer in Papua New Guinea. Department of Public Health Papua New Guinea 1974 pp 24-33
- 2 Belisario J C. Cancer of the skin. Butterworths London 1959 p 15-16
- 3 Bjarnason O. Cancer incidence in Iceland 1964-1972. In Waterhouse J, Muir C, Correa P & Powell J (Eds) Cancer incidence in five continents vol 3. International agency for research on cancer Lyon 1974 p 320
- 4 Doll R. Comparison between registries age standardised rates. In Waterhouse J, Muir C, Correa P & Powell J (Eds) Cancer incidence in five continents vol 3. International agency for research on cancer, Lyon 1976 pp 453-459
- 5 Lynch F N, Seidman H & Hammond E C. Incidence of cutaneous cancer in Minnesota. Cancer 25 83-91, 1970
- 6 Magnus A. Incidence of malignant melanoma of the skin in the five Nordic countries: significance of solar radiation. Int J Cancer 20 477-485 1977
- 7 Mantel N & Haenszel W. Statistical aspects of the analysis of data from retrospective studies of disease. J Nat Cancer Inst 22 719-748 1959
- 8 Scotto J, Kopf A W & Urbach F. Non melanoma skin cancer among caucasians in four areas of the United States. Cancer 34 1333-1338 1974
- 9 Ten Seldam R E J, Helwig E B, Sobin L H & Tortoni H. Histological typing of skin tumours. International histological classification of tumours No 12. World Health Organisation Geneva 1974
- 10 Waterhouse J, Muir C, Correa P & Powell J (Eds) Cancer incidence in five continents vol 3. International agency for research on cancer Lyon 1976
- 11 World Meteorological Organisation. Solar radiation and radiation balance data (the world network). Annual data 1969-1973. Part 2. USSR. Chief administration of the hydro meteorological service Leningrad 1976
- 12 Zagula-Waltz Z W, Rosenberg E W & Kashgarian M. Frequency of skin cancer and solar keratosis in a rural southern county as determined by population sampling. Cancer 34 345-349 1974

ULTRASTRUCTURE OF LIPOGRANULOMAS IN HUMAN FATTY LIVER

P. PETERSEN and P. CHRISTOFFERSEN

Medical Department A, Division of Hepatology, Rigshospitalet, and Department of Pathological Anatomy, Hvidovre Hospital, University of Copenhagen, Copenhagen, Denmark

Petersen P & Christoffersen P. Ultrastructure of lipogranulomas in human fatty liver. *Acta path microbiol scand Sect A* 87 45-49 1979

Lipogranulomas from severe fatty livers due to alcoholism, diabetes or overweight were examined in the electron microscope. When a fat droplet protrudes through the cell membrane of a liver cell, histiocytes and lymphocytes settle around it and a lipogranuloma is formed. Remnants of the liver cell may be seen between the fat droplet and the histiocytes. It is confirmed that the fat droplets are situated extracellularly in the fully developed lipogranulomas.

Key words: Liver, lipogranulomas, ultrastructure.

Palle Petersen, Medical Department A, Division of Hepatology, Rigshospitalet, 2100 Copenhagen Ø, Denmark.

Received 20 v 78 Accepted 23 vii 78

Lipogranulomas are granulomatous structures in liver tissue with fatty change. They comprise one or more extracellular lipid droplets surrounded by lymphocytes and histiocytes (1).

Lipogranulomas are most frequently found in severe alcoholic fatty livers (4) but may be found in other human steatotic conditions too, for example in fatty liver related to diabetes and/or overweight (2).

The appearance of lipogranulomas is correlated to the degree of histological and biochemical activity reflected in elevated level of serum aspartate transaminase (1).

An electron microscopic description of the small lipogranulomas is given in this paper with special emphasis on the earliest events of their formation.

MATERIAL AND METHODS

The material consists of eight percutaneous liver biopsies, all with severe fatty change and in addition containing several smaller lipogranulomas. The liver biopsies have been performed a m. Menghini in patients with chronic alcoholism alone or in combination with overweight and/or diabetes (7). The handling of the biopsies and the preparation for electron microscopic examination has been described previously (5, 6).

RESULTS

Eleven lipogranulomas were recognized in one μm thick toluidine blue stained sections from the eight biopsies. In all cases the lipogranulomas were of the small type and found in areas with many large fat droplets in the hepatocytes.

The fat droplets of the smallest lipogranulomas were partly intracellular, partly extracellular, as they were found to protrude from one side of the liver cell and were partly surrounded by histiocytes and lymphocytes (Fig. 1).

Slightly larger lipogranulomas consisted of an extracellular fat droplet surrounded by a few or more histiocytes (Figs. 2 and 5). Some of these lipogranulomas were seen to contain remnants of liver parenchymal cells between the fat droplet and the histiocytes (Fig. 3 and 4). When the histiocytes were situated directly adjoining the fat droplet, they always kept their membrane intact (Fig. 6). The lipid of the fat droplet was never seen to be phagocytized by the mesenchymal cells. In the cases investigated and collagen fibres were not found. Eosinophils, plasma cells and Ito cells were not found in connection with the granulomas.

The triglyceride of the fat droplets of lipogranulomas was of the same appearance as the triglyceride

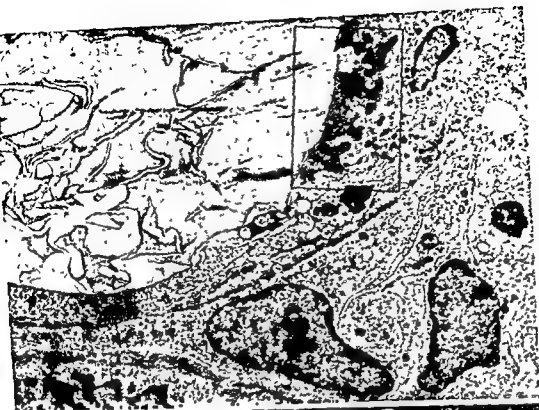
of frequency behind cancers of stomach, prostate bronchus and colon in females they rank 9th behind breast, stomach, cervix uteri colon, thyroid ovary, corpus uteri and bronchus (3)

In conclusion, these figures emphasize the low incidence of primary skin malignancies at high latitudes (2) Yet the histological types and their relative importance remain similar to those found in white populations in areas of higher solar radiation The similarity in the rates for males and females suggest that at a low intensity of radiation length of exposure is more erratic in inducing malignancy than at high exposure

This investigation was supported by the *World Health Organisation* The authors are grateful to *Hrafn Tulinius M D* for his advice on statistical methods and to *Jonas Hallgrímsson M D* for his comments and help throughout the work

REFERENCES

- 1 Atkinson L, Glezy J A, Reay Young P S, Scott G C & Wigley S C The epidemiology of cancer in Papua New Guinea Department of Public Health Papua New Guinea 1974 pp 24-33
- 2 Belisario J C Cancer of the skin Butterworths London 1959 p 15-16
- 3 Bjarnason O Cancer incidence in Iceland 1964-1972 In Waterhouse J, Muir C, Correa P & Powell J (Eds) Cancer incidence in five continents vol 3 International agency for research on cancer Lyon 1974 p 320
- 4 Doll R Comparison between registries age standardised rates In Waterhouse J, Muir C, Correa P & Powell J (Eds) Cancer incidence in five continents vol 3 International agency for research on cancer Lyon 1976 pp 453-459
- 5 Lynch F N, Seidman H & Hammond E C Incidence of cutaneous cancer in Minnesota Cancer 25 83-91, 1970
- 6 Magnus A Incidence of malignant melanoma of the skin in the five Nordic countries significance of solar radiation Int J Cancer 20 477-485 1977
- 7 Maniel N & Haenszel W Statistical aspects of the analysis of data from retrospective studies of disease J Nat Cancer Inst 22 719-748 1959
- 8 Scott J, Kopf A W & Urbach F Non melanoma skin cancer among caucasians in four areas of the United States Cancer 34 1333-1338 1974
- 9 Ten Seldam R E J, Helwig E B, Sobin L H & Torloni H Histological typing of skin tumours International histological classification of tumours No 12 World Health Organisation Geneva 1974
- 10 Waterhouse J, Muir C, Correa P & Powell J (Eds) Cancer incidence in five continents vol 3 International agency for research on cancer Lyon 1976
- 11 World Meteorological Organisation Solar radiation and radiation balance data (the world network) Annual data 1969-1973 Part 2 USSR Chief administration of the hydro meteorological service Leningrad 1976
- 12 Zagula Maly Z W, Rosenberg E W & Ashkanian M Frequency of skin cancer and solar keratosis in a rural southern county as determined by population sampling Cancer 34 345-349 1974



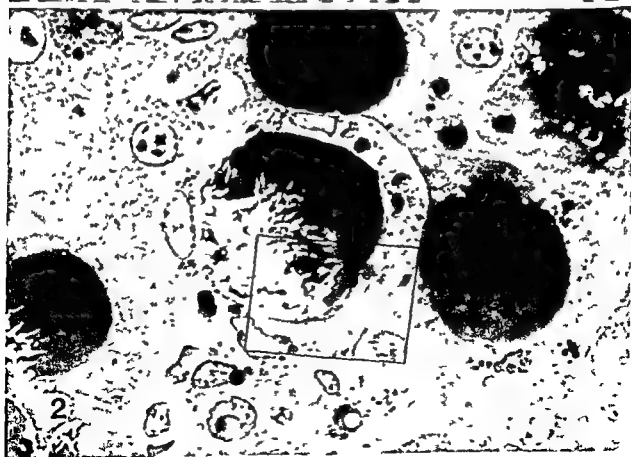
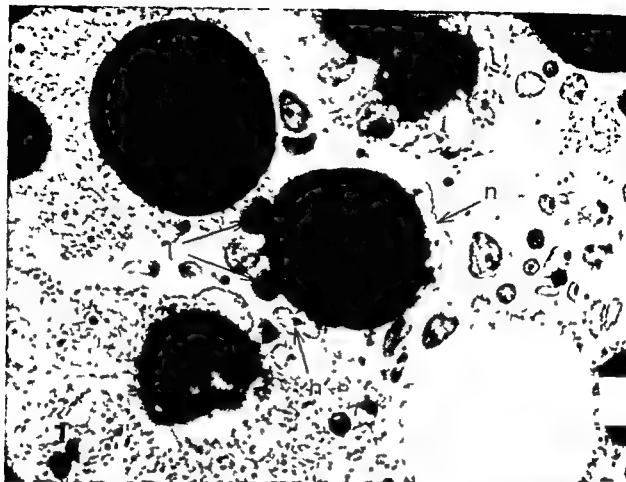


Fig 1 Fat droplets in liver cells. A fat droplet below the middle of the picture is seen to be surrounded by lymphocytes (l) and histiocytes (h) on one side and remnants of a liver parenchymal cell with a nucleus (n) on the other side.

1 μ m thick section of EPON embedded material
Toluidine blue stain $\times 1260$

Fig 2 Lipogranuloma between liver cells. The fat droplet is surrounded by histiocytes which sharply demarcate the lipogranuloma. Some of the fat of the droplets has been extracted.

1 μ m thick section of EPON embedded material
Toluidine blue stain $\times 1260$

Fig 3 Electronmicrograph from part of the lipogranuloma shown in frame in Fig. 2. Part of the liver cell is shown in the frame.

Uranyl acetate and lead citrate staining $\times 5600$

Fig 4 The remnants of the liver cell shown in Fig. 3. Degenerated mitochondria (m) are closely packed together towards the lipid droplet (l). Some of the organelles of adjacent histiocytes are also seen.

Uranyl acetate and lead citrate staining $\times 21000$

Fig 5 A fat droplet of a lipogranuloma surrounded by many histiocytes.

1 μ m thick section of EPON embedded material
Toluidine blue stain $\times 1260$

Fig 6 Electron micrograph of parts of two neighbouring histiocytes shown in the frame in figure 5. The membranes of the histiocytes are seen to be in direct contact with the fat droplet.

Uranyl acetate and lead citrate staining $\times 21000$

of the fat droplets of the parenchymal cells of the same biopsy. Extracted areas and accumulations of little black granules were seen in the droplets just as in the liver cells.

DISCUSSION

Since the first description of lipogranulomas which were produced in rats fed a choline deficient diet (3) lipogranulomas have been thought to arise through the coalescence of fat droplets from several liver cells and being contemporaneously enclosed by a layer of epithelial cells derived from dedifferentiated parenchymal cells (3).

Lipogranulomas in human liver are described by Leen et al (4) as large extracellular fatty cysts producing an inflammatory reaction composed of lymphocytes and an exudate. Christoffersen et al

describe small lipogranulomas (type 1 and type 2) as large extracellular vacuoles surrounded by histiocytes, lymphocytes and sometimes eosinophils (1). This composition of the smaller lipogranulomas has been confirmed in the present electron microscopic study. In 1 μ m thick sections we have seen that the most probably way the lipogranulomas arise is that the fat droplet of a liver cell protrudes through one side of the cell and lymphocytes and histiocytes then react to this stimulus and settle around the fat droplet.

In the further development of lipogranulomas the fat droplet is surrounded by histiocytes on all sides but liver cell remnants may still be seen between the histiocytes and the fat droplet.

The histiocytes do not engulf the fat as is seen from the fact that the fat of the lipogranulomas is always situated outside the cell boundaries of the histiocytes.

The fate of the enclosed fat cannot be followed in this study, but the fat might be accessible to circulating lipolases and in this manner be eliminated.

It has been shown that the small lipogranulomas usually disappear without sequelae and this is in accordance with the fact that we did not demonstrate any tendency for formation of collagen fibers.

The big lipogranulomas (type 3) were not available in the material and the significance of these structures for the development of fibrosis cannot be evaluated.

REFERENCES

- 1 Christoffersen P, Brandstrup O, Juhl E & Poulsen P. Lipogranulomas in human liver biopsies with fatty change. *Acta path microbiol scand Sect A* 79: 150-158 1971.
- 2 Christoffersen P & Petersen P. Morphological features in fatty liver. *Acta path microbiol scand Sect A* 82: 255-263 1974.
- 3 Leen C M, Zinke M R, White T J & Grossi A M. Clinical observations on the fatty liver. *Arch Int Med* 92: 527-541 1953.
- 4 Petersen P. Lipid droplets in fatty liver. *Acta path microbiol scand Sect A* 82: 255-263 1974.
- 5 Petersen P. Abnormal mitochondria in hepatocytes in human fatty liver. *Acta path microbiol scand Sect A* 85: 413-420 1977.
- 6 Petersen P. Fatty liver in patients with moderate alcohol consumption, diabetes mellitus and overweight. *Scand J Gastroent* 12: 781-784 1977.

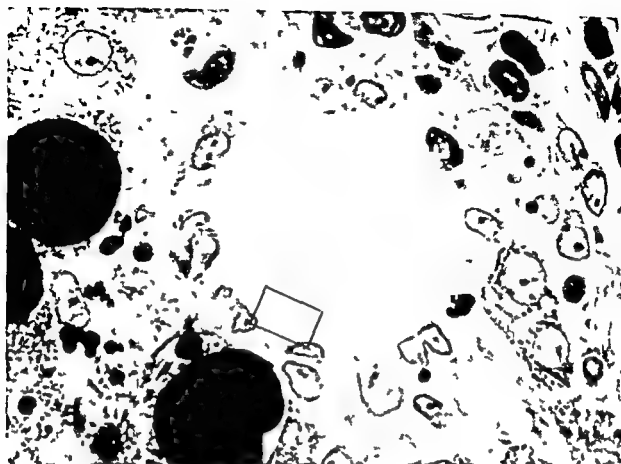


TABLE 3 *Distribution of Alcoholic Hepatitis*

2 biopsy \ 1 biopsy	Without alcoholic hepatitis	Slight alcoholic hepatitis	Moderate alcoholic hepatitis	Severe alcoholic hepatitis	
Without alcoholic hepatitis	49	1	1	0	51
Slight alcoholic hepatitis	3	2	1	0	6
Moderate alcoholic hepatitis	0	1	1	1	3
Severe alcoholic hepatitis	0	0	0	2	2
	52	4	3	3	62

$$r = 0.73 \quad p < 10^{-6}$$

TABLE 5 *Distribution of Cholestasis*

2 biopsy \ 1 biopsy	No cholestasis	Slight cholestasis	Moderate cholestasis	Severe cholestasis	
No cholestasis	46	0	0	0	46
Slight cholestasis	1	5	0	0	6
Moderate cholestasis	1	2	2	1	6
Severe cholestasis	0	0	0	4	4
	48	7	2	5	62

$$r = 0.91 \quad p < 10^{-6}$$

TABLE 4 *Distribution of Cirrhosis*

2 biopsy \ 1 biopsy	No septa or cirrhosis	Septa	Suspicion of cirrhosis	Demonstrated cirrhosis	
No septa or cirrhosis	41	2	0	0	43
Septa	3	2	0	1	6
Suspicion of cirrhosis	0	0	2	1	3
Demonstrated cirrhosis	0	0	2	8	10
	44	4	4	10	62

$$r = 0.83 \quad p < 10^{-6}$$

TABLE 6 *Distribution of the Biopsy Pairs with Regard to the Size of the Portal Tracts*

2 biopsy \ 1 biopsy	Normal size	Slight enlargement	Moderate enlargement	Pronounced enlargement	
Normal size	10	7	0	0	17
Slight enlargement	5	7	6	0	18
Moderate enlargement	0	3	4	5	12
Pronounced enlargement	0	0	1	2	3
	15	17	11	7	50

$$r = 0.64 \quad p < 10^{-6}$$

routine staining methods used at the pathological department. The same pathologist (P.B.) described and graded all the biopsies. The answers were ordinary descriptive ones, though with specified grading terms, and were later on transferred to diagrams. This was done to give the study the best possible resemblance to the diagnostic routine procedure.

Before the investigation was started, a minimal size requirement was established before the biopsies were allowed to enter the investigation. Biopsies comprising 1-3 pieces had to be at least 1 cm in length and biopsies composed of 4 or more parts had to be at least 1 1/2 cm. There were 10 biopsies (7%) originating from 8 biopsy pairs, which did not fulfil the criteria; they were considered insufficient and therefore excluded from the material. After this, 62 biopsy pairs remained.

Some pathological conditions were represented in only a few of the biopsies and in the following the results have been limited to the most frequently occurring changes. Because of scanty representation, malignancy and piecemeal necroses, among other lesions, had to be excluded.

The histological changes were semiquantitatively graded into 1) none, 2) few or slight, 3) some or moderate and 4) many or pronounced. The results were placed in $n \times m$ tables with separate entries for the first and second biopsy of a pair. Kendall's rank correlation test with tied ranks (9) was used statistically. The rank correlation coefficient, τ , and its significance were calculated for each $n \times m$ table. This coefficient of correlation has the same limits (from -1 to +1) and the same meaning as the usually-employed (Pearson) correlation coefficient r .

RESULTS

The distribution of the degrees of steatosis is shown in Table 1. »Scattered liver cells with fatty change« means a condition in which only a few per cent of the liver cells are transformed. »Slight, moderate and severe steatosis« indicates that under 1/3, between 1/3 and 2/3, and over 2/3 of the hepatocytes respectively, are transformed.

Table 2 demonstrates the number and distribution of Mallory bodies in the biopsy pairs. The grouping used here is similar to that mentioned above, viz. an estimated division into three equal parts is made.

The alcoholic hepatitis is graded according to the number of necrotic liver cells containing Mallory's hyalin and surrounded by neutrophil granulocytes. A schematic division is shown in Table 3.

Table 4 gives a survey of the distribution of the biopsy pairs with regard to the disturbance of the lobular architecture, amount of connective tissue in the lobules and formation of regeneration nodules. The diagnosis »septa« means star-shaped portal tracts with formation of interlobular septa but still

TABLE 1 Distribution of Steatosis

2 biopsy \ 1 biopsy	2 biopsy					1 biopsy
	No steatosis	Scattered liver cells with fatty change	Slight steatosis	Moderate steatosis	Severe steatosis	
No steatosis	20	6	1	0	0	27
Scattered liver cells with fatty change	3	3	1	0	0	7
Slight steatosis	0	2	14	2	0	18
Moderate steatosis	0	0	1	6	1	8
Severe steatosis	0	0	0	0	2	2
	23	11	17	8	3	62

$$\tau = 0.82 \quad p < 10^{-6}$$

TABLE 2 Distribution of Mallory Bodies

2 biopsy \ 1 biopsy	2 biopsy				1 biopsy
	No Mallory bodies	Few Mallory bodies	Some Mallory bodies	Many Mallory bodies	
No Mallory bodies	30	6	2	1	39
Few Mallory bodies	4	3	2	1	10
Some Mallory bodies	1	1	3	3	8
Many Mallory bodies	0	1	1	3	5
	35	11	8	8	62

$$\tau = 0.58 \quad p < 10^{-6}$$

TABLE 11 *Distribution of Acidophilic Bodies*

2 biopsy \ 1 biopsy	No acidophilic bodies	Few acidophilic bodies	Some acidophilic bodies	Many acidophilic bodies	
No acidophilic bodies	39	5	0	0	44
Few acidophilic bodies	2	1	0	0	3
Some acidophilic bodies	0	1	2	0	3
Many acidophilic bodies	0	0	0	0	0
	41	7	2	0	50

$$\tau = 0.51 \quad p < 0.0003$$

without regeneration nodules. «Suspicion of cirrhosis» indicates increased amounts of connective tissue forming active septa combined with incipient segregation of liver cell groups. This group includes two biopsy pairs with the diagnosis of «chronic aggressive hepatitis with transition in cirrhosis».

The distribution of cholestasis is shown in Table 5. Cholestasis means that at least one bile thrombus located in a bile canaliculus or a portal tract bile duct is observed. If bile coloured pigment is present in the cytoplasm of the liver cells only this biopsy is placed in the diagram as «no cholestasis». «Slight cholestasis» indicates single small scattered bile thrombi. «moderate» means many small «severe» is used for many large thick dense thrombi that occur in the bile canaliculi and/or in the bile ducts.

Bianchi *et al* (2) and De Groote *et al* (7) describe a range of single components that must be estimated before the diagnosis of one of the varieties of hepatitis is made. These are among others for the portal tracts 1) the size 2) the amount of inflammatory cells 3) the amount of connective tissue 4) the degree of bile-duct proliferation and in the lobules 5) the number of focal necroses and 6) the number of acidophilic bodies. It is not possible to give exact limitations for the degrees of the changes of the portal tracts unless a total quantitative analysis of the lesions is made but we wanted to be able to correlate the results of this study with the estimated semiquantitative methods used in the daily routine work. The lesions of focal necroses and acidophilic bodies are graded in such a way that

«few» means less than 2, «some» between 2 and 5, and «many» more than 5 per lobules on average. The mutual relations between the biopsy pairs concerning the six mentioned changes are given schematically in Tables 6-11. In this part of the study the portal tracts were necessary for the estimation of the changes, and therefore cases of cirrhosis had to be excluded. This left only 50 biopsy pairs.

The calculated values of τ are given below each Table and range from +0.50 to +0.91. This is a statistical expression of the fact — revealed by close inspection of the Tables — that e.g. the percentage of identical grading of pairs varied from 58 to 92. Cholestasis (0.91), cirrhosis (0.83) and steatosis (0.82) show the highest values of τ , while the lowest results are found for the bile-duct proliferation of the portal tracts (0.50) and the number of acidophilic bodies in the lobules (0.51). All the calculated values of τ are highly significant.

DISCUSSION

All the examined pathological changes display a certain difference in the grading of two biopsies taken simultaneously from the same patient. This

— — — — —

considered e.g. the pathologist may not exercise the same concentration while observing different biopsies, or he may not interpret an observation in the same way from time to time (observer error). In this study it is not possible to decide how much of the observed variation within the biopsy pair depends on sampling error and how much of the variation comes from observer error. A difference in size of the two biopsies will be of great importance for the differences in interpretation. The observer will always have a better impression of the severity of a lesion when the biopsy is relatively large.

Rourke & Stewart (11) have performed biochemical analyses on wedge biopsies while Billing *et al* (3) have investigated the distribution of steatosis both biochemically and histologically by taking needle biopsies in 18 different locations from autopsy livers. Both have found as we have that steatosis is uniformly distributed.

In the present material there is an excellent correlation in the lesions of the interdependent biopsies with regard to septal formation and cirrhosis. Braunstein (4) has correspondingly reported that a surprisingly fine agreement is found between the changes of cirrhosis in post mortem liver biopsies taken from different areas. The remaining variation is presumably due to the sliding

TABLE 7 *Distribution of the Biopsy Pairs with Regard to the Amount of Inflammatory Cells of the Portal Tracts*

2 biopsy \ 1 biopsy	No increase	Slight increase	Moderate increase	Pronounced increase	
No increase	13	3	1	0	17
Slight increase	2	14	3	0	19
Moderate increase	1	4	7	1	13
Pronounced increase	0	0	0	1	1
	16	21	11	2	50

$\tau = 0.64 \quad p < 10^{-6}$

TABLE 9 *Distribution of the Biopsy Pairs with Regard to the Bile Duct Proliferation of the Portal Tracts*

2 biopsy \ 1 biopsy	No bile duct proliferation	Slight bile duct proliferation	Moderate bile duct proliferation	Pronounced bile duct proliferation	
No bile duct proliferation	15	4	2	0	21
Slight bile duct proliferation	6	8	2	0	16
Moderate bile duct proliferation	2	3	2	1	8
Pronounced bile duct proliferation	0	1	0	4	5
	23	16	6	5	50

$\tau = 0.50 \quad p < 0.00006$

TABLE 8 *Distribution of the Biopsy Pairs with Regard to the Amount of Connective Tissue of the Portal Tracts*

2 biopsy \ 1 biopsy	No increase	Slight increase	Moderate increase	Pronounced increase	
No increase	25	5	0	0	30
Slight increase	6	7	3	0	16
Moderate increase	0	0	4	0	4
Pronounced increase	0	0	0	0	0
	31	12	7	0	50

$\tau = 0.61 \quad p < 0.000005$

TABLE 10 *Distribution of Focal Necroses*

2 biopsy \ 1 biopsy	No focal necroses	Few focal necroses	Some focal necroses	Many focal necroses	
No focal necroses	15	5	0	0	20
Few focal necroses	8	14	1	0	23
Some focal necroses	0	1	4	1	6
Many focal necroses	0	0	1	0	1
	23	20	6	1	50

$\tau = 0.61 \quad p < 0.00003$

- 14 Soloway R D Baggenstoss A H Schoenfield L J & Summerskill W H J Observer error and sampling variability tested in evaluation of hepatitis and cirrhosis by liver biopsy Amer J Dig Dis 16 1082-1086 1971
- 15 Wagoner G Ulevitch H Gall E A & Schiff L Biopsy of needle-specimen of liver tissue VI Comparison of findings on biopsy and an autopsy Amer J Clin Path 21 338-341 1951
- 16 Waldstein S S & Santo P B Accuracy of sampling by needle biopsy in diffuse liver disease Arch Path 50 326-328 1950

transition between chronic hepatitis and cirrhosis. In these stages the observer often has an impression of incipient formation of liver cell groups without real proof of regeneration nodules. Soloway *et al* (14) found a fairly large disagreement in the presence and degree of cirrhosis when several liver biopsies were taken simultaneously at different angles from the site of puncture. In the same investigation they noticed an excellent correlation between the discoveries of hepatitis.

Christoffersen (6) mentions two kinds of Mallory bodies of which the characteristic type 2 is easy to identify. However, type 1 can very readily be confused with other cytoplasmic components and this is probably an important reason for the disagreement in the grading of the number of Mallory bodies in the biopsy pairs.

In alcoholic hepatitis focal necroses with granulocytes are of greatest importance, whereas Mallory bodies have no longer the same significance in identification, which probably influenced the difference in results of Tables 2 and 3.

Acidophilic bodies are easy to identify because of their distinct red round regular structure with a surrounding clear halo. If one disregards those biopsy pairs in which acidophilic bodies do not occur in both biopsies, it appears from the Table that a fairly poor agreement exists, but only 11 biopsy pairs contain acidophilic bodies and no biopsies with «many» are observed. Therefore a conclusion is uncertain because the frequency and the degree of severity of the lesion are too small in the present material.

A relative low correlation of the lesions of portal tracts is found even inside the limited area of a needle biopsy. Usually there is a gradual transition from the slightest to the most severe changes. This is probably the main reason for the difference found in the various pathological changes of the portal tracts.

All the calculated values of the correlation coefficient r show good to excellent agreement between the lesions investigated in the biopsy pairs. However, it must be emphasized that a large value of r may depend on a large number of biopsy pairs being located in the upper left square of the Tables, which means that most of the biopsies do not include the lesion examined. Therefore the high value of r may be based on the fact that it is easier for an observer to register no change than to grade a lesion.

A number of lesions are not included in this account because of their scanty representation in the present material. One of the more important of these was malignant tissue, which occurred in only three of the sufficient biopsy pairs. Malignancy was

diagnosed in both biopsies of two patients. In one patient only one of the biopsies showed malignant tissue. Christian (5) and several others have pointed out that needle biopsies are not particularly useful for demonstrating localized lesions in the liver, but others including Sherlock (13) emphasize that it is surprising how often metastases and other circumscribed lesions are present even in needle biopsies.

In evaluating liver biopsies one must emphasize the lesions with the fewest errors (sampling + observer). The results of the present investigation show that most changes give a reliable basis for the histo-pathological diagnosis.

Acknowledgement is made to the Danish Medical Research Council for statistical advice.

REFERENCES

1. Baron E. Aspiration for removal of biopsy material from the liver. *Arch Int Med* 63: 276-289, 1939.
2. Bianchi L, De Groote J, Desmet V J, Gedigk P, Korb G, Popper H, Poulsen H, Scheuer P J, Schmid M, Thaler H & Wepler W. Morphological criteria in viral hepatitis. *Lancet* 1: 333-337, 1971.
3. Billing B H, Conlon H J, Hein D E & Schiff L. The value of needle biopsy in the chemical estimation of liver lipids in man. *J Clin Invest* 32: 214-225, 1953.
4. Braunstein H. Needle biopsy of the liver in cirrhosis. *Arch Path* 62: 87-95, 1956.
5. Christian E. An evaluation of needle biopsy of the liver. *Amer J Med* 13: 689-703, 1952.
6. Christoffersen P. Light microscopic features in liver biopsies with Mallory bodies. *Acta path microbiol scand* 80: 705-712, 1972.
7. De Groote J, Desmet V J, Gedigk P, Korb G, Popper H, Poulsen H, Scheuer P J, Schmid M, Thaler H, Uehlinger E & Wepler W. A classification of chronic hepatitis. *Lancet* 2: 626-628, 1968.
8. Kendall M G. Rank correlation methods. 4th ed. Griffin London 1970. pp. 45-56.
9. Menghini G. One second needle biopsy of the liver. *Gastroenterology* 35: 190-199, 1958.
10. Rourke G M & Stewart J D. Composition of the liver: Its uniformity with respect to the concentration of certain biochemical constituents in different parts of the same liver. *Arch Path* 33: 603-606, 1942.
11. Sanchez G C, Baunsgaard P & Lundborg C J. (To be published).
12. Sherlock S. Aspiration liver biopsy: Technique and diagnostic application. *Lancet* 249: 397-401, 1945.

- 14 Soloway R D Bogenstoss A H Schoenfield L J & Summerskill W H J Observer error and sampling variability tested in evaluation of hepatitis and cirrhosis by liver biopsy Amer J Dig Dis , 16 1082-1086 1971
- 15 Wagoner G Ulevitch H Gall E A & Schiff L Biopsy of needle-specimen of liver tissue VI Comparison of findings on biopsy and at autopsy Amer J Clin Path . 21 338-341, 1951
- 16 Waldstein S S & Szanto P B Accuracy of sampling by needle biopsy in diffuse liver disease Arch Path 50 326-328, 1950

transition between chronic hepatitis and cirrhosis. In these stages the observer often has an impression of incipient formation of liver cell groups without real proof of regeneration nodules. *Soloway et al* (14) found a fairly large disagreement in the presence and degree of cirrhosis when several liver biopsies were taken simultaneously at different angles from the site of puncture. In the same investigation they noticed an excellent correlation between the discoveries of hepatitis.

Christoffersen (6) mentions two kinds of Mallory bodies, of which the characteristic type 2 is easy to identify. However, type 1 can very readily be confused with other cytoplasmic components, and this is probably an important reason for the disagreement in the grading of the number of Mallory bodies in the biopsy pairs.

In alcoholic hepatitis focal necroses with granulocytes are of greatest importance, whereas Mallory bodies have no longer the same significance in identification which probably influenced the difference in results of Tables 2 and 3.

Acidophilic bodies are easy to identify because of their distinct red, round regular structure with a surrounding clear halo. If one disregards those biopsy pairs in which acidophilic bodies do not occur in both biopsies, it appears from the Table that a fairly poor agreement exists but only 11 biopsy pairs contain acidophilic bodies, and no biopsies with »many« are observed. Therefore a conclusion is uncertain, because the frequency and the degree of severity of the lesion are too small in the present material.

A relative low correlation of the lesions of portal tracts is found even inside the limited area of a needle biopsy. Usually there is a gradual transition from the slightest to the most severe changes. This is probably the main reason for the difference found in the various pathological changes of the portal tracts.

All the calculated values of the correlation coefficient r show good to excellent agreement between the lesions investigated in the biopsy pairs. However, it must be emphasized that a large value of r may depend on a large number of biopsy pairs being located in the upper left square of the Tables which means that most of the biopsies do not include the lesion examined. Therefore the high value of r may be based on the fact, that it is easier for an observer to register no change than to grade a lesion.

A number of lesions are not included in this account because of their scanty representation in the present material. One of the more important of these was malignant tissue, which occurred in only three of the sufficient biopsy pairs. Malignancy was

diagnosed in both biopsies of two patients. In one patient only one of the biopsies showed malignant tissue. *Christian* (5) and several others have pointed out that needle biopsies are not particularly useful for demonstrating localized lesions in the liver, but others including *Sherlock* (13) emphasize that it is surprising how often metastases and other circumscribed lesions are present even in needle biopsies.

In evaluating liver biopsies one must emphasize the lesions with the lowest errors (sampling + observer). The results of the present investigation show that most changes give a reliable basis for the histopathological diagnosis.

Acknowledgement — made to the Danish Medical Research Council for statistical advice.

REFERENCES

1. *Baron E* Aspiration for removal of biopsy material from the liver. *Arch Int Med* 63: 276-289 1939.
2. *Bianchi L, De Groote J, Desmet V J, Gedigk P, Korb G, Popper H, Poulsen H, Scheuer P J, Schmid M, Thaler H & Wepler W* Morphological criteria in viral hepatitis. *Lancet* 1: 333-337 1971.
3. *Billing B H, Conton H J, Hein D E & Schiff L* The value of needle biopsy in the chemical estimation of liver lipids in man. *J Clin Invest* 32: 214-225, 1953.
4. *Braunstein H* Needle biopsy of the liver in cirrhosis. *Arch Path* 62: 87-95 1956.
5. *Christian E R* An evaluation of needle biopsy of the liver. *Amer J Med* 13: 689-703 1952.
6. *Christoffersen P* Light microscopical features in liver biopsies with Mallory bodies. *Acta path microbiol scand* 80: 705-712 1972.
7. *De Groote J, Desmet V J, Gedigk P, Korb G, Popper H, Poulsen H, Scheuer P J, Schmid M, Thaler H, Uehlinger E & Wepler W* A classification of chronic hepatitis. *Lancet* 2: 626-628 1968.
8. *Iversen P & Roholm K* On aspiration biopsy of the liver with remarks on its diagnostic significance. *Acta med Scand* 102: 1-16 1939.
9. *Kendall M G* Rank correlation methods. 4th ed. Griffin London 1970. p. 45-56.
10. *Menghini G* One second needle biopsy of the liver. *Gastroenterology* 35: 190-199 1958.
11. *Rourke G M & Steuart J D* Composition of the liver. Its uniformity with respect to the concentration of certain biochemical constituents in different parts of the same liver. *Arch Path* 33: 603-606 1942.
12. *Sanchez G C, Baunsgaard P & Lundborg C J* (To be published).
13. *Sherlock S* Aspiration liver biopsy. Technique and diagnostic application. *Lancet* 249: 397-401 1945.

BILATERAL BONE-MARROW EXAMINATIONS IN SMALL-CELL ANAPLASTIC CARCINOMA OF THE LUNG

FRED R. HIRSCH, HEINE H. HANSEN and BO HAINAU

Department of Chemotherapy RII V and Department of Pathology Finsen Institute Copenhagen Denmark

Hirsch Fred R, Hansen Heine H & Hainau B. Bilateral bone marrow examinations in small-cell anaplastic carcinoma of the lung. *Acta path microbiol scand Sect. A* 87 59-62 1979

Bilateral bone marrow examinations from the posterior iliac crests were routinely performed as a pretreatment staging procedure in 111 consecutive patients with small-cell anaplastic carcinoma of the lung. Bone marrow involvement was found in 20 patients (22.5%) in 9 (10.1%) only on one side and in 11 (12.4%) on both sides. Aspiration was found to be significantly superior to biopsy being positive in 25 examinations as compared with 14 positive biopsies. Compared with unilateral bone-marrow examination the positive findings increased by approximately 30%. Bilateral bone marrow examinations are recommended in patients in whom the detection of bone marrow metastases will have therapeutic implications.

Key words: Small-cell carcinoma of the lung, bone marrow examination, staging.

Fred R. Hirsch, Department of Pathology, Finsen Institute, 49 Strandboulevarden, DK 2100 Copenhagen, Denmark.

Received 17 III 78 Accepted 1 VII 78

Small-cell anaplastic carcinoma of the lung (sm a c) is known to disseminate very early and widely as evidenced by staging procedures such as mediastinoscopy, unilateral bone marrow examination and peritoneoscopy with liver biopsy (Selawry & Hansen 1973).

Using unilateral examination of the bone marrow from the posterior iliac crest as an initial staging procedure, the incidence of bone marrow involvement may vary from 17% to 47% depending on the selection of patients (Eagan *et al* 1974, Hansen 1974, Abeloff *et al* 1976, Choi & Carey 1976, Anner & Drewinko 1977, Hirsch *et al* 1977).

In studies of patients with malignant lymphoma (Bunning *et al* 1975) an increase in positive results was observed when examinations were performed from both posterior iliac crests. The present report presents the results of a study investigating bilateral bone marrow examinations from the posterior iliac crests in patients with small-cell anaplastic carcinoma of the lung.

MATERIAL AND METHODS

From June 1976 to August 1977, bilateral bone-marrow examinations were performed as part of the pretreatment staging in a consecutive series of 101 untreated patients with small-cell anaplastic carcinoma of the lung (sm a c) referred for treatment to the Finsen Institute, Copenhagen.

The primary diagnosis of sm a c was based on material obtained by bronchial biopsy and/or mediastinoscopy and/or scalene lymph node biopsy. The material available for diagnosis was reviewed by the same pathologist (B. H.). All patients routinely underwent the following minimal pre-treatment staging procedures: clinical examination, chest radiography, peritoneoscopy with liver biopsy and bilateral bone marrow examinations of material from the posterior iliac crests.

The bone marrow examination was performed by using a Radner needle (Dombrowsky *et al* 1974). After local anaesthesia of the skin, subcutaneous tissue and periosteum, the needle was inserted through the skin. Penetration of the compact portion of the bone was accomplished by gentle taps with a hammer. Touch imprint was made from each biopsy specimen. The biopsy procedure was in all cases followed by bone marrow aspiration from the same side. Several smears

rapy and surgery) in this disease this procedure seems less important today than just few years ago. However, if the use of localized treatment is part of the overall therapy and this is based on the stage of the disease bilateral bone marrow examinations may still play a role - however minor, considering that only 4.5% of all patients as demonstrated in this study would be erroneously classified if only an unilateral bone marrow examination is performed. The bilateral bone marrow examinations might be important in monitoring the disease during treatment and in particular in early recognition of progression of the disease because the histological evaluation of the bone marrow is more sensitive in the detection of metastases from sm a c than skeletal radiography and/or bone-scan (Hansen 1974).

In addition the investigation emphasized the observation made in our earlier studies viz that aspiration is superior to biopsy in the detection of bone marrow involvement in sm a c of the lung a finding which is in contrast to the observations made for lymphoma and many other solid tumours (Grahn et al 1966; Han et al 1971; Rosenberg 1971; Contreras et al 1972; Bearden et al 1974; Brunning et al 1975; Lake Lewin et al 1975). The superiority of the aspiration in detecting malignant cells from sm a c in the bone marrow is in agreement with the findings in acute leucemias (Ulan et al 1971). It may be a question of obtaining a larger quantity of bone marrow in the aspirations as compared with biopsy specimens (Ioannides & Rykin 1976).

This question could be solved by a comparison of different needles giving rise to specimens of different sizes (McFarland & Dameshek 1958; Ellis et al 1964; Siavem 1967; Jamshidi et al 1971; Schaadt & Fischer 1974; Helleberg Rasmussen & Søndergaard Petersen 1975; Landys & Stenram 1975). More likely however is the superiority of the aspiration in sm a c due to the limited amount of fibrous stroma usually present in these tumours or to low degree of intercellular cohesion as compared with other solid tumours.

This study was supported by grants from *Esper and Olga Boel's foundation*.

REFERENCES

- Abeloff M D, Ellinger D S, Baylin S B and Hazzra T. Management of small cell carcinoma of the lung. Therapy staging and biochemical markers. *Cancer* 38: 1394-1401 1976.
- Anner R M & Drenth B. Frequency and significance of bone marrow involvement by metastatic solid tumors. *Cancer* 39: 1337-1344 1977.
- Bearden J H, Ratkin G A & Colman C A. Comparison of the diagnostic value of bone marrow biopsy and bone marrow aspiration in neoplastic disease. *J clin Path* 27: 738-740 1974.
- Brunning R H, Bloomfield C D, McKenna R H & Peterson L. Bilateral trephine bone marrow biopsies in lymphoma and other neoplastic diseases. *Ann Intern Med* 82: 365-366 1975.
- Choi C H & Carey R W. Small cell anaplastic carcinoma of the lung. Reappraisal of current management. *Cancer* 37: 2651-2657 1976.
- Contreras E, Ellis E D & Lee R E. Value of the bone marrow biopsy in the diagnosis of metastatic carcinoma. *Cancer* 29: 778-783 1972.
- Dombrowsky P, Horn A M, Hainau B, Hansen H H & Nissen A I. The Radney needle a bone marrow biopsy device. *Scand J Haemat* 12: 270-273 1974.
- Eagan R T, Maurer L H, Forcier R J & Tulloh M. Small cell carcinoma of the lung. Staging paraneoplastic syndromes treatment and survival. *Cancer* 33: 527-532 1974.
- Ellis L D, Jensen D N & Westerman V P. Needle biopsy of bone marrow. *Arch Intern Med* 114: 213-221 1964.
- Grahn J, Pool J L & Mayer K. Comparative study of bone marrow aspiration and biopsy in patients with neoplastic disease. *Cancer* 19: 1898-1900 1966.
- Han T, Stulman L & Roque A L. Bone marrow biopsy in Hodgkin's disease and other neoplastic diseases. *J Amer Med Ass* 217: 1239-1241 1971.
- Hansen H H. Bone metastases in lung cancer. Thesis Copenhagen Munksgaard 1974.
- Hansen H H & Mugg A M. Early detection of bone marrow invasion in oat-cell carcinoma of the lung. *N Engl J Med* 284: 962-963 1971.
- Helleberg Rasmussen J & Søndergaard Petersen H. Bone marrow biopsy with the Bordier trephine. *Scand J Haematol* 14: 123-128 1975.
- Hirsch F, Hansen H H, Dombrowsky P & Hainau B. Bone marrow examination in the staging of small-cell anaplastic carcinoma of the lung with special reference to subtyping. *Cancer* 39: 2563-2567 1977.
- Ioannides K & Rykin A M. A comparative study of histologic sections of bone marrow obtained by aspiration and by needle biopsy (abstr). *Am J clin Pathol* 65: 267 1976.
- Jamshidi K, Windschitl H E & Swaim H R. A new biopsy needle for bone marrow. *Scand J Haemat* 8: 69-71 1971.
- Lake Lewin D, Tange C K & Grey G F. Metastatic tumor in bone marrow biopsy. *New York State Journal of Med* 75: 1008-1011 1975.
- Landys K & Stenram U. Bone marrow biopsy of the posterior iliac crest with Gidlund's instrument in malignant diseases. *Scand J Haematol* 15: 104-108 1975.

were made from the aspirate, and the remainder was allowed to clot. The biopsy specimen had an overall size of 3–10 mm in length and 1–5 mm in diameter.

After fixation in formalin and decalcification with »CALCIFIX«* for 15–30 minutes, the biopsy specimen was placed in running water for about 10 minutes, and then dehydrated and embedded in paraffin. Finally, it was sectioned and stained with haematoxylin-eosin.

The aspiration material contained, on average, 10 ml. The clot was fixed in formalin, dehydrated and embedded in paraffin, sectioned and finally stained with haematoxylin-eosin and »Perls' Prussian blue«. The smears from the aspiration and the touch imprint were fixed in methanol and stained with May-Grunwald-Giemsa and then air dried and covered with a slip. The smears were in addition stained with »Perls' Prussian blue«.

The bone marrow specimens were examined by the same pathologist (B.H.). The fact that sm.a.c. tends to crush readily and show »crush phenomena« makes it sometimes difficult to distinguish the tumour cells from an unspecific reaction of surrounding tissue with infiltration of traumatic haemopoietic cells. For this reason, only identified isolated neoplastic cells compatible with sm.a.c. unrelated to crush zones were evaluated as positive bone marrow specimen. On account of the frequent finding of traumatic cells in the smears and imprints, it was decided that only tumour cells in the sections of the clot and biopsy specimens should be interpreted as a positive finding.

Following the staging procedures the patients included in the study were subsequently staged as having either »loco-regional« disease (i.e. no clinically demonstrable disease outside one lung including the mediastinal and supraclavicular lymph nodes) or »extensive« disease.

Fischer's exact test was used in the statistical analysis.

* Prepared by Kunz Instruments A/S Copenhagen

RESULTS

Bone-marrow examination was performed in 101 patients, of whom 12 were excluded from the study, 10 because of inadequate samples from one of the two sides, and 2 because the bone marrow examination was performed only on one side.

TABLE 1 Bilateral Bone-Marrow Examinations in the Pretreatment Staging of Small-Cell Anaplastic Carcinoma of the Lung (in 89 Patients)

No evidence of malignancy		Evidence of malignancy			
		Bilateral		Unilateral	
No	%	No	%	No	%
89	77.5	11	12.4	9	10.1

TABLE 2 Comparison between Biopsy and Aspiration in 25 Positive Bone-Marrow Examinations of Small Cell Anaplastic Carcinoma of the Lung

Both biopsy and aspiration positive		Only aspiration positive		Only biopsy positive	
No	%	No	%	No	%
14	56*	11	44*	0	0

* $p < 0.002$

The study thus included 89 patients, 60 men and 29 women, with a median age of 60 years. Tumour cells were identified in the bone-marrow in 20 patients (22.5%) (Table 1). In 9 patients, tumour cells were found only on one side. Two of these patients had other evidence of extensive disease. Thus, 4 of the 89 patients (4.5%) would have been classified as having »loco-regional« disease if only unilateral bone-marrow examination was performed. Three of the 11 patients with bilateral bone marrow involvement of malignant cells had other evidence of »extensive« disease.

Representative material was present both in clot sections of the aspirate and the sections of the biopsy specimen in 25 examinations, while in the remaining 15 positive specimens, material was present only either in the sections of the clot or in the biopsy.

Tumour cells were present in both the aspirate and the biopsy specimens in 14 of 25 examinations (56%), while the aspirate alone was positive in 11

($p < 0.002$)

DISCUSSION

The tendency of sm.a.c. to disseminate very early to the iliac crest was recognized by Hansen & Muggia in 1971, and it is now well established also from several other studies using ipsilateral bone marrow examination.

The present study demonstrates that by doing a second contralateral examination, the yield of positive examinations increase by approximately 30%.

Today, the indications for performing a bone-marrow examination in the initial staging of patients with sm.a.c. depend on the modality of therapy to be applied. Because of the increasing general use and effectiveness of systemic treatment as compared with localized treatment (e.g. radiothe-

EFFECT OF VARIOUS ROUTINE CYTOPREPARATORY TECHNIQUES ON NORMAL UROTHELIAL CELLS AND THEIR NUCLEI

M E BEYER BOON M J A VAN DER VOORN DEN HOLLANDER P W ARENTZ
C J CORNELISSE A SCHABERG and C H FOX

Department of Pathology University Medical Center Leyden the Netherlands and the Institute for
Pathology Karolinska Institute Stockholm Sweden

Beyer Boon M E. Voorn-den Hollander M J A van der Arentz P W Cornelisse C J
Schaberg A & C H Fox Effect of various routine cytopreparatory techniques on normal urothelial
cells and their nuclei Acta path microbiol scand Sect A 87 63-69 1979

Nuclear and cytoplasmic sizes of cells in permanent, stained smear preparations differ from those in unfixed unstained cells. In air-dried MGG-stained smears the area of the nucleus is 50% larger and that of the cytoplasm 30% larger. In wet fixed Papanicolaou stained smears the nucleus is 10-30% and the cytoplasm is 15-55% smaller. The shrinkage in the wet fixation method is dependent on the concentration of the ethyl alcohol applied. The staining method has relatively little influence on nuclear and cytoplasmic size. The three-dimensional appearance of the smeared stained cells is also dependent on the cytopreparatory technique applied. In the methods with air-drying the nuclei and cells are flat and in the wet fixation method more spherical. In the methods with air-drying the nuclear-cytoplasmic ratio is larger than that seen with the wet fixation methods.

Key words Urothelial cells cytopreparation

M E Beyer Boon, Department of Pathology University Medical Center Leyden The Netherlands

Received 12 vi 78 Accepted 10 vii 78

Urinary cytology is important in the early diagnosis of cancer and more objective cytologic criteria for determining malignancy would probably improve the reliability of this approach. Nuclear and cellular size are suitable cellular descriptors (6-9) for this purpose but may vary with the cytopreparatory technique used. Changes in cell size due to preparatory techniques has predominantly been concerned with histological methods (3-13). Shrinkage in various fixatives has been reported in unstained preparations of cells or cell cultures but not in permanent stained smear preparations (11-12).

We have investigated the nuclear and cytoplasmic sizes of normal piriform urothelial cells in smears prepared by routine cytopreparatory techniques and compared the results with those obtained in unstained unfixed cell suspensions. Such quantitative morphometrical studies can provide data

about the variability of the size of cells of the same type in one preparation and also between cells in preparations obtained with different techniques. The findings can provide a basis for the development of rational standardized cell preparation techniques suitable for further cytometrical studies.

MATERIAL AND METHODS

Cells from bladder scrapings from patients without urothelial disease were taken at autopsy within 6 hours after death. No post mortem changes were detected. These cells were suspended in a balanced salt solution (310 mOsm) and the size of the piriform cells was measured immediately or permanent cell preparations were made as follows:

- 1 Direct smear scraped cells air-dried for 19 min. May-Grunewald Giemsa (MGG) stain (1-3 min in May-Grunewald stain rinsed with diluted Giemsa stain (MGG) for 12 min rinsed with distilled water air-dried and mounted in Euparal pH buffer 6.8).

- 20 *McFarland, W & Domeshek, W* : Biopsy of bone marrow with the Vim-Silverman needle *J Amer Med Ass* 166 1464-1466, 1958
- 21 *Rosenberg, S* Hodgkin's disease of the bone marrow *Cancer Research* 31. 1733-1736, 1971.
- 22 *Schaadt, O & Fischer, S* : Cristabiopsi med en ny knoglebiopsinål *Ugeskr Læg* 136 1739-1740, 1974
- 23 *Selawry, O S & Hansen H H* In Holland J F & Frei, E, III (eds), *Cancer Medicine*, Lea & Febiger Philadelphia, 1473-1518, 1973
- 24 *Stavem, P* A new bone marrow biopsy needle *Scand J Haemat* 4 158-160, 1967

TABLE 2 Nuclear and Cellular Size and Nuclear Cytoplasmic Ratio of Fxfrm Epithelial Cells Subjected to Various Cytopreparatory Techniques

Cell preparation and staining technique	N	Nuclear area	Cellular area	N/C ratio
1 Air-dried MGG	300	95 (± 11.0) μ^2	277 (± 63.6) μ^2	0.37 (± 0.086)
2 50% ethyl alcohol Papanicolaou	300	49 (± 8.9) μ^2	176 (± 46.3) μ^2	0.30 (± 0.073)
3 96% ethyl alcohol Papanicolaou	300	32 (± 6.4) μ^2	114 (± 36.7) μ^2	0.29 (± 0.063)
4 Spray fixative Papanicolaou	300	40 (± 9.7) μ^2	131 (± 47.3) μ^2	0.31 (± 0.072)
5 Methanol acetic acid Papanicolaou	300	78 (± 8.6) μ^2	-	-
6 No fixation no staining phase-contrast microscopy	100	60 (± 12.0) μ^2	703 (± 72.3) μ^2	0.34 (± 0.057)

\pm values are the standard deviation

The accuracy of the measurements were partially dependent on the size of the measured object when the same object was measured 50 times the results were as follows 10.3 (± 1.9) μ^2 25.3 (± 2.1) μ^2 37.0 (± 2.6) μ^2 98.2 (± 2.7) μ^2 and 191.1 (± 2.3) μ^2 . The inaccuracy of the measurements of cells in suspension was relatively large due to floating of the cells during the procedure. These measurements were somewhat limited by the resolution of the cursor a problem since reduced with an improved tablet.

To study the effect of prefixing cells with methanol and their subsequent flattening the nuclei of cells in suspension was measured following methanol acetic acid fixation and compared to values of cells that were prefixed on a slide with the methanol fixative. The cells in suspension had a nuclear area of 37 μ^2 with a SD of 11.1 while those on the slide had a nuclear area of 78 (SD 4.7) μ^2 .

If cells were treated with 96% ethanol or spray fixative and measured before staining and mounting there was a slightly higher value for the nuclear area 46 (SD 10.1) μ^2 for 96% ethanol and 53 (SD 10.2) μ^2 for spray fixative.

When cells were given the same fixation but different stains i.e. fixation in methanol followed by staining in either Papanicolaou or MGG nuclear areas of MGG cells were 92 (SD 7.8) μ^2 with cytoplasmic areas of 277 (SD 35.3) μ^2 while Papanicolaou stained cells had a nuclear area of 80 (SD 8.2) μ^2 and a cytoplasmic area of 269 (SD 76.1) μ^2 .

DISCUSSION

Cytopreparatory techniques can result in both smaller and larger nuclear and cytoplasmic areas compared with unstained unfixed cells in suspension. These procedures can be broken down into separate steps each of which has an effect on the smeared fixed and stained cells on the microscope slide.

The extremely large size of cells air-dried before further treatment is doubtless due to the extreme pressures exerted on cellular structures by the surface tension of a drop.

Staining with methanol and acetic acid followed by air-drying gave larger nuclear areas than were found in unfixed cells but smaller ones than in cells that were air-dried only. Two major contributions to this effects are the lower surface tension of the methanol acetic acid mixture (1082 dynes per sq. cm in air for 50% MeOH [7]) and the hardening of the nuclear structures by the dehydrating effect of the organic solvents.

None of the fixation or preparation methods commonly employed for diagnostic cytology preserve the exact dimensions of cells. Although it is quite possible to preserve the exact morphology of cells by cross linking fixatives such as glutaraldehyde [7] or dimethylsuberimide among others there has been little use of these fixatives in clinical cytology. The results reported here indicate that the

- 2 Direct smear scraped cells fixed in 50% ethyl alcohol for 1 hr Papanicolaou stain according to Koss (10)
 - 3 Direct smear scraped cells fixed in 96% ethyl alcohol for 1 hr Papanicolaou stain
 - 4 Direct smear scraped cells were fixed on the slide with a spray fixative (80 ml poly-ethyleneglycol mol weight 300 690 ml isopropanol 170 ml acetone 60 ml distilled water) then immersed for 15 min in 96% ethyl alcohol followed by Papanicolaou stain
 - 5 Cell suspension a cell suspension was fixed for 1 hr in 1 ml solution of 48% methanol and 5% glacial acetic acid (final modified after Esposti et al 2 5) This suspension was centrifuged for 10 min at 2000 rpm the supernatant decanted and one drop of the sediment placed on a glass slide and the slides were then dried and stained according to Papanicolaou
- Method 1 is an air dry method methods 2 3 and 4 are wet fix methods and method 5 is a combination of the two

Measurements

The nuclear and cytoplasmic areas were measured with a graphic digitizing tablet interfaced to a PDP 12 computer (Digital Equipment Corporation Maynard Mass USA) Cells were examined under a microscope equipped with a camera lucida drawing tube The cursor of the graphic tablet which has a light emitting diode was viewed through the camera lucida in the microscopic field the projected image could be traced by moving the cursor The electronic signals of the cursor were converted to coordinates by the specially constructed interface and these coordinates were fed into the computer to calculate the area of the outlined field Thus while the movement of the cursor was done manually the rest of the procedure was (fully) automated

The attachment of cells to the microscope slide after air drying was observed by reflexion interference contrast microscopy with a Leitz (E Leitz Wetzlar Germany) Diavert microscope equipped with suitable optics

In each smear the cytoplasm and nucleus of 300 piniform cells were measured with the exception of the

methanol acid Papanicolaou smears in which only the nucleus was measured because the margins of the cytoplasm were too indistinct

RESULTS

The specimens contained predominantly piniform cells which have an oval nucleus with most of the cytoplasm at either end of the long axis of the nucleus (Fig 2) When the material was prepared the same way there was little variation in the size of these piniform cells in two smears from the same scraping and little difference between the piniform cells of three individuals (Table 1)

The cellular and nuclear sizes obtained with the various cell preparation techniques are shown in Table 2 The variation of the nuclear size ranged from a mean of $32 \mu^2$ (96% ethyl alcohol Papanicolaou) to $95 \mu^2$ (air-dried MGG) whereas the native mean size of the nuclei was $60 \mu^2$ (Table 2 1 3 6) There was a slight but statistically insignificant difference between the nuclear size of the cells in 96% ethyl alcohol and cells prepared with the spray fixative the mean values being 32 and $40 \mu^2$ respectively (Table 2 3 4) However variation of the ethyl alcohol concentration resulted in significant differences (0.01 confidence level) (Table 2 2 3) with a mean of $49 \mu^2$ for cells fixed with 50% ethyl alcohol as compared with $32 \mu^2$ for 96% ethyl alcohol The differences between the two methods using air drying also proved to be significant (Table 2 1 5) as were those between the fixed and unfixed cells The change in cytoplasmic areas were approximately similar However the nucleus/cytoplasm ratio differed to some degree for the various techniques (from a mean of 0.29 for native wet fixed Papanicolaou stained cells to a mean of 0.37 for air dried MGG stained cells) The histograms of the measurements are shown in Fig 1

TABLE 1 Variation in the Nuclear Size of Piniform Urothelial Cells between Three Individuals

Cell preparation and staining	Nuclear area \pm SD	Nuclear area \pm SD	Nuclear area \pm SD
Air dried MGG	$96 (\pm 11.1) \mu^2$	$97 (\pm 11.0) \mu^2$	$93 (\pm 11.1) \mu^2$
96% ethyl alcohol Papanicolaou	$32 (\pm 6.3) \mu^2$	$32 (\pm 7.9) \mu^2$	$33 (\pm 5.4) \mu^2$
Spray fixative Papanicolaou	$39 (\pm 9.4) \mu^2$	$42 (\pm 10.4) \mu^2$	$39 (\pm 9.8) \mu^2$
Esposti's fixative combined with 96% ethyl alcohol Papanicolaou	$42 (\pm 5.5) \mu^2$	$42 (\pm 5.7) \mu^2$	$42 (\pm 4.9) \mu^2$

the greatest amounts of shrinkage of the nuclear diameter and of cytoplasmic dimensions. Fixation in 50% ethanol is somewhat less distorting. The reasons for this difference are probably complex as have been noted by others (4, 13). The osmolarity for 50% ethanol exceeds the osmotic pressure of a 5.0 M sodium chloride solution and that of 96% ethanol is much greater (17). The mechanics of alcohol fixation probably involve a rapid influx of alcohol through the increasingly disrupted cellular membrane structure. The volume of the cell probably increases initially through solvation of the water in the cell by alcohol. At least in low alcohol concentrations. An initial swelling has been observed in methanol fixation by Bloom and Friberg (3) and by Siering (13) which was confirmed in our observations on cells fixed in methanol acetic acid where nuclear areas increased 22% after 1 hr immersion in methanol acetic acid and then decreased to about 5% less than the unfixed cells. Bloom and Friberg found that methanol alone among the primary alcohols induced swelling of tissues for histological preparations and that shrinkage increa-

sed with molecular size of the alcohol used as fixative, which they interpreted to be associated with the solubilities of lipids in the higher alcohols. Another possibility is that the polarity of the solvents is inversely related to shrinkage; that is, that the more polar the solvent, the faster the penetration of the cell and the faster the solvation of cellular structures. Cellular water in turn leaves the cell by diffusion and the cellular contents become progressively more dehydrated. This is probably only another factor in a very complex series of events.

The majority of papers on fixation changes describe volume changes in tissue (1, 12, 14, 15).

preparations where the most commonly observed changes are two-dimensional rather than three-dimensional as found in blocks of tissue.

Fixation with either spray fixative (isopropanol-acetone) or 96% ethanol results in more spherical nuclei than in air-dried preparations. This is demonstrated by the photomicrographs (Fig. 3 a, b) where the nucleus of the cells cannot be brought into full focus with a 100 \times objective (N.A. 1.30). No doubt part of the differences between nuclear areas in the various preparations is influenced by

further
xylene
further

followed by aqueous extraction in Giemsa buffer and then by another air-drying step. When cells were fixed in methanol and stained with either MGG or with Papanicolaou there were only slight changes in the nuclear and cytoplasmic areas indicating that staining is not a major factor in the size changes.

The attachment of cells to the slides after air drying does not involve a large area of cell membrane being attached to the glass itself, although there is some evidence that individual portions of the cell surface do become cemented to the glass surface. Reflection interference microscopy shows that the cells settle out on the slide and are gradually pressed flat on the slide by the evaporating liquid. There does not appear to be a flattening of the cell. The cell attaches at the rest of the cytopla.

One curious finding is that the variation in N/C ratio was shown by the standard deviation is less in



Fig. 2 Air-dried MGG stained uniform urothelial cells. This photomicrograph shows the complete cytoplasm and nucleus because the cell is at one level (i.e. flat) $\times 1250$.

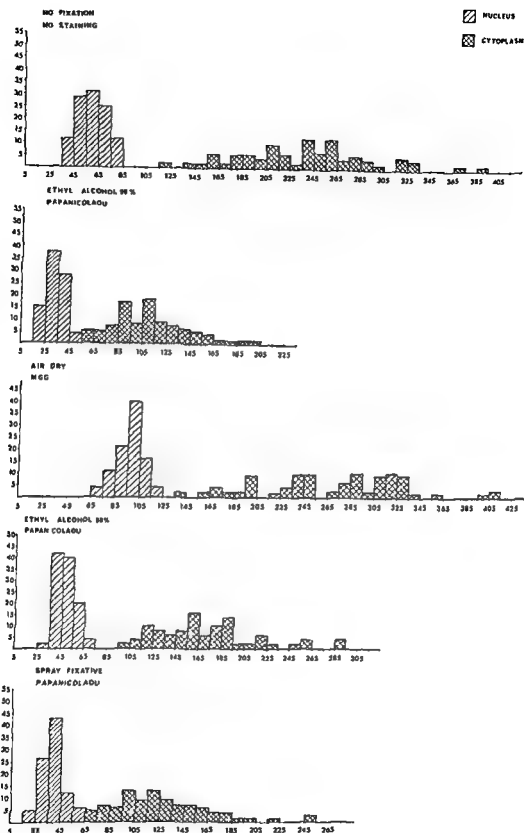


Fig 1 Histograms showing the nuclear areas of unstained unfixed cells and fixed stained cells in permanent smear preparations obtained with several cytopreparatory techniques

methods for cell preparation can affect not only the dimensions of the cytoplasm and the nucleus, but the nuclear cytoplasmic ratio as well. What effects

these variations have on the subjective judgement of cellular atypias is unclear.

Direct fixation of cells in 96% ethanol results in



a



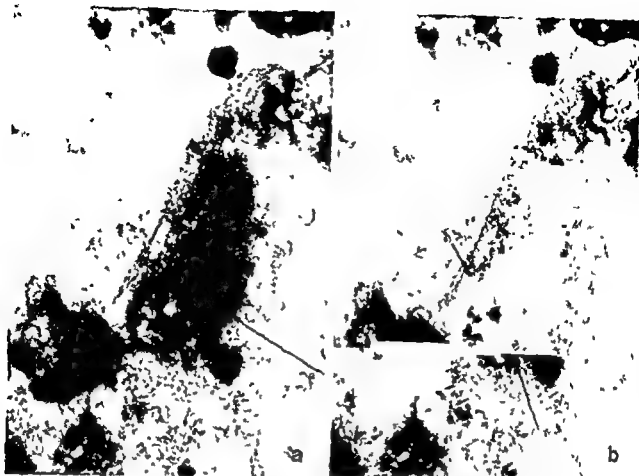
b

Figs 4a & b Reflexion interference photomicrograph of puriform cells from the bladder taken as the cells (4a) dried on the slide (4b)

- 9 Kern W H Bales C E Webster W W
Cytologic evaluation of transitional cell carcinoma
of the bladder *J Urol* 100 616-622 1968
- 10 Allen L G Diagnostic cytology and its histopatho-
logic bases J B Lippincott Co Philadelphia 2nd
Ed 1968
- 11 Krishna D Shrinkage of animal cells due to
fixatives *Nature* 161 202-203 1948
- 12 Lodin Z Mares J Karusek J & Skrmanova P
Studies on the effect of fixation on nervous tissue II
Changes of sizes of nuclei of nervous cells after
fixation and after further histological treatment of
the nervous tissue *Acta histochem* 28 297-312
1967
- 13 Siering H Schädigung cytologischer Präparate
durch verschiedene Fixierungsmittel *Acta Med
Scand* 149 229-236 1954
- 14 Stohrer H Der Einfluss der Fixierung auf das
Volumen der Organe *Zeits f Wissen Mikroskopie*
23 14-25 1908
- 15 Tarkhan A A The effects of fixatives and other
reagents on cell size and tissue bulk *J R Micr Soc*
51 387-400 1931
- 16 Vassar P S Hards J M Brooks M E

Hagenberger B Seaman G & Physicochemical
effects of aldehydes on the human erythrocyte *J
Cell Biol* 53 809-821 1972

- 17 Weast R C Handbook of Chemistry and Physics
49th ed The Chemical Rubber Co Cleveland
Ohio USA 1968



Figs 3a & b Umbrella cells (fixed in 96% ethyl alcohol and Papanicolaou stained) photographed at two focus levels. The nucleolus of the upper nucleus is in focus in Fig. 3a (arrow) but not in Fig. 3b. The nucleolus and chromatin clumps of the lower nucleus are in focus in Fig. 3b (arrows) but not in Fig. 3a.

unfixed cells than in fixed ones. This phenomenon may be related to changes that occur at the time of fixation such as shrinkage and agonal changes.

Fixation induced size changes are not completely understood and are highly complicated (7). The results of our investigations illustrate more than they explain the complexity of the problems involved, but we believe that fixation of cells is an extremely important factor in subsequent judgments of cytomorphology that has been too little reckoned with in quantitative microscopy and in attempts at cytology automation. We feel that studies such as this should precede any attempt to make quantitative image analysis of cells.

REFERENCES

1. Bahr G F, Blum G, Friberg U. Volume changes of tissue in physiological fluids during fixation in osmium tetroxide or formaldehyde and during subsequent treatment. *Exp Cell Res* 12: 342-355 1957.
2. Beyer Bonn M E. The efficacy of urinary cytology. Thesis chapter II. PP 46-53. 1977. W. D. Meinema Delft.
3. Bloom B & Friberg U. Shrinkage during fixation and embedding of histological specimens. *Acta Morph Neerlandica Scand* 1: 12-20. 1956-58.
4. Donaldson H H. Preliminary observations on some changes caused in the nervous tissues by reagents commonly employed to harden them. *J Morph* 11: 123-129. 1894.
5. Foxen P L, Moberger G, Zantek J. The analysis of Feulgen stained cell nuclei from transverse sections of the urinary bladder. *J Histochem* 22: 1977.
6. Forss S D, Kaalhus O. Computer assisted image analysis of Feulgen stained cell nuclei from transverse sections of the urinary bladder. *J Histochem* 22: 1977.
7. Foxen P L. Cytochemical analysis of neoplastic transformation of vertebrate cell populations. *Cancer Res* 36: 1536-1561. 1976.
8. Hopwood D. Fixatives and fixation. A review. *Histochem J* 1: 323-360. 1969.

ELECTRON MICROSCOPY OF NEPHROPATHIA EPIDEMICA CELL NUCLEI IN KIDNEY BIOPSIES

Y. COLLAN and J. LAHDEVIRTA

Department of Pathology and the Third Department of Medicine University of Helsinki Helsinki
Finland

Collan Y & Lahdevirta J Electron microscopy of nephropathia epidemica Cell nuclei in kidney
biopsies Acta path microbiol scand Sect. A 87 71-77 1979

Ultrastructural changes in cell nuclei were studied in kidney biopsies from 18 patients suffering from Nephropathia epidemica. Three patients showed small nuclear particles in a large aggregate in a few cells of the distal tubule. The particles had a diameter of about 30 nm and their occurrence was not associated with intravenous glucose infusions. Large light nuclear bodies were numerous in the nuclei of both interstitial and tubular cells. Many showed strands of darker material about 35 nm in diameter at their center. Nuclear vesicles with varying amounts of membrane debris were seen in both tubular and interstitial cells. Occasional interstitial lymphocytes showed abnormal margination of chromatin. Of the changes observed the small nuclear particles are not found in kidney biopsies in other conditions and it is possible that they are aggregates of viral protein.

Key words Nephropathia epidemica haemorrhagic fever kidney nucleus inclusions electron microscopy

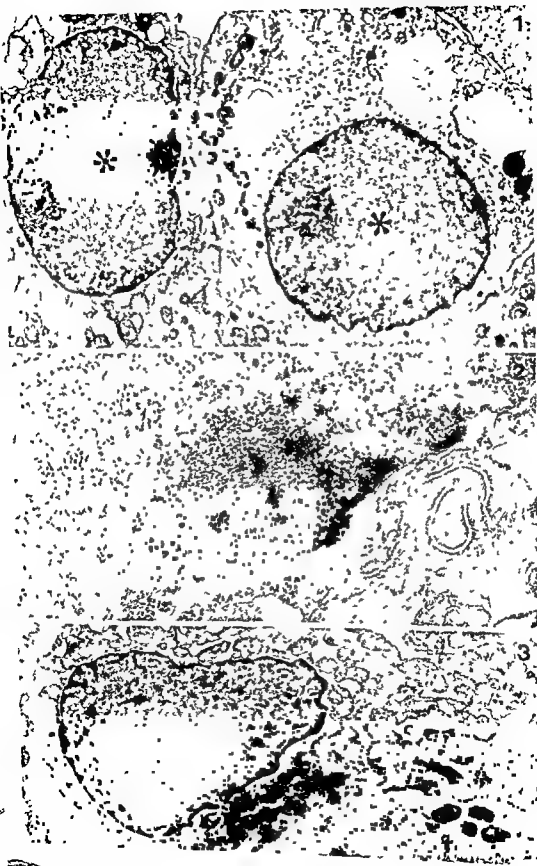
Yrjö Collan Department of Pathology University of Helsinki Haartmaninkatu 3 SF-00290 Helsinki 29
Finland

Accepted as submitted 21 viii 78

The most recent studies (Lee and Lahdevirta 1978) suggest that Nephropathia epidemica (Lahdevirta 1971) which occurs in north western Europe is related to Korean haemorrhagic fever (haemorrhagic fever with renal syndrome epidemic haemorrhagic fever) as originally speculated by Gajdusek (1953 1962). The causative agent of Korean haemorrhagic fever - probably a virus - has been isolated by Lee *et al* (1978) but the pathogenetic mechanisms underlying the changes in kidney tissue in these two diseases are not clear. We have studied cell nuclei in kidney biopsies of patients suffering from Nephropathia epidemica to look for evidence of viral interference.

MATERIAL AND METHODS

The material consisted of 20 biopsies from 18 patients taken during and after the acute stage of the disease (Collan *et al* 1978). Clinical diagnosis was based on typical symptoms and signs of the disease (Lahdevirta 1971). Five biopsies were taken 3-9 days, eight biopsies 10-19 days, five biopsies 20-35 days and two biopsies 3.5 and 6.5 months after the onset of fever. The biopsies were fixed in 3% phosphate buffered glutaraldehyde (pH 7.3) for three hours, transferred into 0.2 molar phosphate buffered sucrose solution and kept there for 1-6 days at +4° C. Following this each piece was postfixated in 1% phosphate buffered osmium tetroxide for 1 hour, then dehydrated and embedded in Epon. Ultrathin sections were cut with glass knives and stained with 1% uranyl acetate in 50% ethanol and with lead



citrate. Semi thin 1 μ m thick sections were also cut and stained with 1% methylene blue in 1% sodium borate solution. The ultrathin sections were studied with a Hitachi HS 7S electron microscope.

RESULTS

Small nuclear particles were seen in three patients who were biopsied 6, 9 or 13 days after the onset of fever. The particles formed aggregates in the nuclei of distal tubular cells only. Such aggregates were rare; they were seen in 1–5 cells in the biopsies, and only once in two adjacent cells (Fig. 1). At low magnification the aggregates were light areas against a background of normal nuclear texture (Figs. 1 and 3). Higher magnification showed small particles about 30 nm in diameter (Figs. 2 and 4A). The cells containing these nuclear structures usually showed dilatation of the cisterna of the RER and SER but no corresponding aggregates were found in the cytoplasm.

Light nuclear bodies were seen in proximal and distal tubular cells and interstitial cells (Figs. 4B and 5A). The nucleus sometimes contained several nuclear bodies. Many were light, hazy, and finely fibrillar areas in the nucleoplasm, but others showed, in addition, dark strands suggestive of chromatin at the center. However, the dark strands were composed of coarser material than the interchromatin granules of the nuclei, and were about 35 nm thick.

Nuclear vesicles were seen in both tubular and interstitial cells. The vesicles were usually simple membrane bound vacuoles with homogenous watery contents. Budding of the nucleoplasm into the vesicles resulted in membrane bound globules of nucleoplasm. Often there were dense aggregates of chromatin immediately outside these nuclear vesicles (Fig. 5B). Occasionally the nuclear vesicles contained a large amount of membrane debris (Fig. 6A), possibly the result of active budding. Abnormal chromatin aggregation was rare and only found in a few interstitial lymphocytes which showed margination of the nuclear chromatin (Fig. 6B).

DISCUSSION

Viral nucleocapsids produced in the nuclei often form aggregates which show indistinct borders and at low magnification appear lighter than the surrounding nuclear chromatin (Raine *et al.* 1973; Iwasaki and Koprowski 1974). The small nuclear particles we described could be nucleocapsids or parts of nucleocapsids, e.g. aggregates of protein molecules of the nucleocapsid. It is not likely that they are composed of nucleic acid because they stained lighter than the nuclear chromatin or interchromatin granules. The size of these particles was about 30 nm. Glycogen granules may have varying appearance and glycogen is sometimes found as β particles of the size of the particles we observed in the nuclei (Sheldon *et al.* 1962; Renel 1964). However, the particles we found stained lighter than glycogen. Uranyl acetate in water can dissolve glycogen out of samples but we used uranyl acetate in ethanol and short staining times. In addition, small nuclear particles were also seen in sections stained with lead citrate alone. In glycogen storage disease one finds glycogen both in the cytoplasm and in the nuclei (Sheldon *et al.* 1962). The cells with the nuclear inclusions in our samples however, were practically free of ultrastructurally detectable cytoplasmic glycogen. Because some of the patients we studied had received intravenous transfusions during their stay in the hospital we checked whether the patients with the small nuclear particles had been subjected to heavy glucose loads which could have resulted in abnormal glycogen accumulation. None had received intravenous glucose solutions but two patients who did not show these particles had been given 5% glucose in saline on the day of arrival at hospital. The particles we found were the size of papova viruses (Granboulan *et al.* 1963; Bastian 1971). That the small nuclear particles were observed in biopsies from three patients only does not exclude the possibility that they are of viral origin and linked with the aetiology of the condition. The experience we have of nuclear inclusions in viral infections such as cytomegalic disease, is that in many cases extensive search is

Fig. 2 Higher magnification of part of Fig. 1. Note the light staining particles in the nuclear sap. Part of the nucleolus is seen at the center of the figure. 37500 \times .

Fig. 3 Epithelial cell of a distal tubule. Note dilatation of the cisterna of the SER and RER. The nucleus shows an aggregate of small nuclear particles. There is no membrane surrounding the aggregate. The cytoplasm is practically free of glycogen. From a case of Nephropathia epidemica 9 days after the onset of fever. 9400 \times .

Fig 4A Higher magnification of Fig 3 The particles are shown in more detail They are roughly round and about 30 nm in diameter There are lighter areas containing sap between them 64000 x

Fig 4B Nucleus of an interstitial cell in Nephropathia epidemica There are several light nuclear bodies present (arrows) In the most central body dark about 35 nm thick tubular structures are present From a case of Nephropathia epidemica 3 days after the onset of fever 10500 x

Fig 5A Light nuclear body Note the lighter periphery and darker aggregates in the center There is also a membrane bound structure in the body (arrow) This is possibly an invagination of the inner leaflet of the nuclear membrane From a case of Nephropathia epidemica 11 days after the onset of fever 24500 x

Fig 5B Nuclear vesicle in an epithelial cell of the distal tubule The vesicle is surrounded by a single membrane (inner leaflet of the nuclear membrane) Two round bodies seem to bud off from the inner surface of the vesicle (open arrows) Note dark aggregates of chromatin at the site of constriction of the nuclear vesicle (thin arrows) From a case of Nephropathia epidemica 3 days after the onset of fever 46000 x

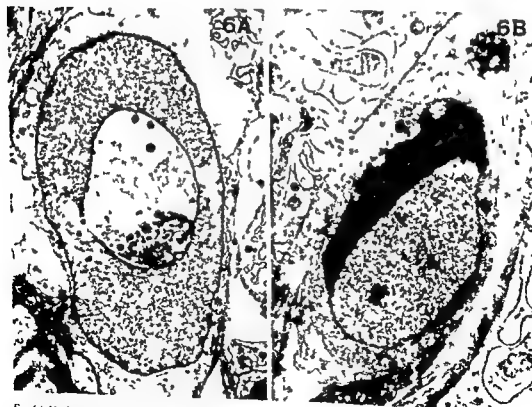


Fig 6A Nuclear vesicle with membranous debris in an interstitial cell of a patient with Nephropathia epidemica This vesicle is probably a further stage of an active budding process (cf Fig 5B) The vesicles have probably been produced by the inner leaflet of the nuclear membrane From a case of Nephropathia epidemica 17 days after the onset of fever 6400 x

Fig 6B A lymphocyte with margination of nuclear chromatin present in the interstitial kidney tissue of a patient with Nephropathia epidemica 9 days after the onset of fever This kind of margination may occur in viral infections 12000 x

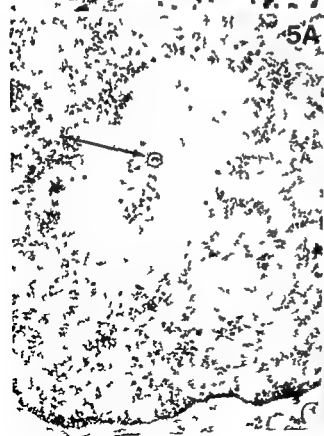


Fig 4A Higher magnification of Fig 3 The particles are shown in more detail They are roughly round and about 30 nm in diameter There are lighter areas containing sap between them 64000 \times

Fig 4B Nucleus of an interstitial cell in Nephropathia epidemica There are several light nuclear bodies present (arrows) In the most central body dark about 35 nm thick tubular structures are present From a case of Nephropathia epidemica 3 days after the onset of fever 10500 \times

Fig 5A Light nuclear body Note the lighter periphery and darker aggregates in the center There is also a membrane-bound structure in the body (arrow) This is possibly an invagination of the inner leaflet of the nuclear membrane From a case of Nephropathia epidemica 11 days after the onset of fever 24500 \times

Fig 5B Nuclear vesicle in an epithelial cell of the distal tubule The vesicle is surrounded by a single membrane (inner leaflet of the nuclear membrane) Two round bodies seem to bud off from the inner surface of the vesicle (open arrows) Note dark aggregates of chromatin at the site of constriction of the nuclear vesicle (thin arrows) From a case of Nephropathia epidemica 3 days after the onset of fever 46000 \times



vesicle is
produced
onset of f 11 0000 \times

Nephropathia epidemica, 17 days after the

Fig 6B
Nephrop
12000 \times

necessary before inclusions are found in surgical biopsies or autopsy specimens. Needle biopsies of kidney tissue are much smaller and under corresponding conditions need not contain inclusions in all cases.

Light nuclear bodies were first described by de The *et al* (1960). Since their report corresponding structures have been found in numerous tumours and experimental conditions (Boutelle *et al* 1967, Krishan *et al* 1967). The function of these bodies is not known. Light nuclear bodies also occur in kidney biopsies from patients with other diseases (Runeberg *et al* 1975) and we have seen them in a wide variety of conditions. Maiztegui *et al* (1975) showed that in Argentine haemorrhagic fever these bodies bound fluorescein-labelled ascitic fluid hyperimmune to Junin virus. The latter observation suggests that the numerous light nuclear bodies we found in NE might also in one way or other be linked with viral activity. Iwasaki *et al* (1973) found nucleocapsids of a paramyxovirus in nuclear light bodies in cultured brain cells from two cases of multiple sclerosis. Also Granboulan *et al* (1963) showed SV40 viruses inside nuclear bodies.

Nuclear vesicles of various types are not necessarily signs of viral activity, but viruses are occasionally seen inside intranuclear vesicles (Skinner and Mizell 1972). Margination of nuclear chromatin might be associated with cell necrosis or mitosis. However, it is also linked with viral activity (Baringer and Nathanson 1972, Giddens 1975). We did not find virus-like particles in the nuclei that show margination of chromatin, but we do not think that this is enough evidence to exclude the possibility that margination is caused by viral activity.

In conclusion, our study of the nuclei showed numerous changes that are not generally considered normal in kidney biopsies. Many of the changes have been described in other conditions, but the small nuclear particles suggest a more specific link with NE. It is possible that they are composed of viral protein produced during the course of infection in this disease.

The financial support given by Sigrid Juselius Foundation and the Academy of Finland is gratefully acknowledged.

REFERENCES

- 1 Baringer J R & Nathanson N. Parvovirus hemorrhagic encephalopathy of rats. Electron microscopic observations of the vascular lesions. *Lab Invest* 27: 514-522 1972.
- 2 Bastian F O. Papova like viruses in a human brain tumor. *Lab Invest* 25: 169-175 1971.

- 3 Boutelle M, Kalfat S R & Delarue J. Ultrastructural variations of nuclear bodies in human diseases. *J Ultrastruct. Res* 19: 474-486 1967.
- 4 Collan Y, Lahdevirta J & Jokinen E. J. Electron microscopy of Nephropathia epidemica. Glomerular changes. *Virchows Arch (Pathol Anat)* 377: 121-144, 1978.
- 5 Gajdusek D C. Acute infectious hemorrhagic fevers and mycotoxicoses in the Union of Soviet Socialist Republics. 140 pages. U.S. Army Medical Service Graduate School Medical Science Publication No. 2, Washington. Walter Reed Army Medical Center, 1953.
- 6 Gajdusek D C. Virus hemorrhagic fevers. Spec reference to hemorrhagic fever with renal syndrome (Epidemic hemorrhagic fever). *J Pediatr* 60: 84-857, 1962.
- 7 Giddens W E Jr. Replication of Herpesvirus stans in cultured lymphocytes of infected monkeys (*Aotus trivirgatus*). *Lab Invest* 32: 492-502, 1975.
- 8 Granboulan N, Tourner P, Wicker R & Bernhardt W. An electron microscope study of the development of SV40 virus. *J Cell Biol* 17: 423-442, 1963.
- 9 Iwasaki Y, Koprowski H, Muller D, terMeulen A & Adcock Y M. Morphogenesis and structure of a virus in cells cultured from brain tissue from two cases of multiple sclerosis. *Lab Invest* 28: 494-500 1973.
- 10 Iwasaki Y & Koprowski H. Cell to cell transmission of virus in the central nervous system. I. Subacute sclerosing panencephalitis. *Lab Invest* 31: 187-196 1974.
- 11 Krishan A, Usman B G & Hedley-White E T. Nuclear bodies. A component of cell nuclei in hamster tissues and human tumors. *J Ultrastruct. Res* 19: 563-572 1967.
- 12 Lahdevirta J. Nephropathia epidemica in Finland. A clinical, histological and epidemiological study. *Ann Clin Res* 3: Suppl 8: 1-154 1971.
- 13 Lee H W & Lahdevirta J. Personal communication 1978.
- 14 Lee H W, Lee P W & Johnson K M. Isolation of the etiologic agent of Korean hemorrhagic fever. *J Infect Dis* 137: 298-308 1978.
- 15 Maiztegui J I, Laguens R P, Cossio P M, Casanova M B, de la Vega M T, Riancho J, Segal A, Fernandez N J & Arana R M. Ultrastructural and immunohistochemical studies in five cases of Argentine hemorrhagic fever. *J Infect Dis* 132: 35-43 1975.
- 16 Raine C S, Feldman L A, Sheppard R D & Bornstein M B. Subacute sclerosing panencephalitis virus in cultures of organized central nervous system. *Lab Invest* 28: 627-640 1973.
- 17 Revel J P. Electron microscopy of glycogen. *J Histochem Cytochem* 12: 104-114 1964.
- 18 Runeberg L, Collan Y, Jokinen E, J. Lahdevirta J & Aro A. Hypomagnesemia due to renal disease of unknown etiology. *Am J Med* 59: 873-881 1975.

Sheldon H Silverberg M & Kerner I On the differing appearance of intranuclear and cytoplasmic glycogen in liver cells in glycogen storage disease J Cell Biol 13 468-473 1962

Skinner M S & Miell M The effect of different temperatures on herpesvirus induction and replica-

tion in Lucké tumor explant. Lab Invest. 26 671-681 1972

- 21 deThe G Rivière M & Bernhard W Examen au microscope électronique de la tumeur VX2 du lapin domestique dérivée du papilloma de Shope Bull Assoc Franc Canc 47 570-584 1960

INFLUENCE OF 4-AMINOPYRAZOLOPYRIMIDINE ON MORPHOLOGY, SYNTHESIS OF TRIGLYCERIDE AND PROTEIN AND THEIR SECRETION IN RAT HEPATOCYTES

GRETE NORDBY and BERIT SCHREINER

Institute for Nutrition Research School of Medicine University of Oslo Blindern Oslo Norway

Nordby G & Schreiner B Influence of 4 aminopyrazolopyrimidine on morphology synthesis of triglyceride and protein and their secretion in rat hepatocytes Acta path microbiol scand Sect A 87 79-85 1979

The influence of 4 aminopyrazolopyrimidine (4 APP) on morphology and on synthesis and secretion ability of isolated rat hepatocytes was investigated. 4 APP was found to inhibit both the synthesis and secretion of proteins. The synthesis of triglycerides was unaffected by 4 APP while the secretion of triglycerides was markedly reduced. Transmission electron microscopy revealed that 4 APP induced morphological changes in the smooth membrane systems: the smooth endoplasmic reticulum and the Golgi apparatus. The possibility that 4 APP inhibits lipoprotein formation by inhibition of the apoprotein synthesis is discussed.

Key words: 4 aminopyrazolopyrimidine, hepatocytes, lipoproteins, ultrastructure.

Grete Nordby, Institute for Nutrition Research, School of Medicine, University of Oslo, P O Box 1046 Blindern, Oslo 3, Norway.

Received 23 I 78 Accepted 23 vii 78

The hepatic lipids are secreted as lipoproteins and studies have therefore been performed to evaluate a possible correlation between an impaired hepatic protein synthesis and the development of a fatty liver. Experiments with different inhibitors of protein synthesis *in vivo* may or may not lead to a fatty liver (3, 4, 12, 18). These divergent results have raised the question whether an accumulation of hepatic triglycerides is caused by an inhibition of lipoprotein release or by an increased mobilization of free fatty acids from the adipose tissue (13).

In rats administration of 4 aminopyrazolopyrimidine (4 APP) produces fatty livers (14) with reduced plasma levels of triglycerides (TG), cholest-

17) As one avoids possible effects on other organs and as rate of synthesis and secretion is more easily measured in an *in vitro* system than in experiments on living animals we have used isolated rat hepatocytes in our effort to study the effect of 4 APP.

Recently we have found (9) that isolated hepatocytes incubated with 4 APP in the medium show a decreased secretion of lipoproteins and other secretory proteins. A reduced secretion of lipoproteins may as previously mentioned be due to a reduced synthesis of the protein part of the lipoproteins. If the TG synthesis is unaffected by the 4 APP, an accumulation of TG in the cells can be expected. In this study we have measured the protein and TG synthesis and the secretion of these substances under the influence of 4 APP. During a short incubation period the cells will not have time to

might be expected to disturb the protein synthesis. *In vivo* studies with 4 APP have given ambiguous answers as to whether the effect is connected with the synthesis or the secretion of proteins or both (5

TABLE 2 The Effect of 4 APP on Trgl cer de Synthesis and Secretion

	synthesized triglycerides (μ moles/liver)	secreted triglycerides (μ moles/liver)
control	none	76
2 h	108	171
4 h		
4 APP (0.1 mg/ml)	none	46
2 h	106	73
4 h		

The hepatocytes were incubated in the medium RPMI 1640 with HEPES added to a final concentration of 60 mM lactate to 10 mM and pyruvate = 1 mM. At zero time after 2 and 4 hours samples of the cell suspension were homogenized in a Dounce homogenizer and the concentration of TG in the homogenates was determined. Other samples were centrifuged and the concentration of TG in the media was determined. The synthesis and secretion of TG per liver were calculated.

synthesized and secreted into the medium. Table 1 shows that addition of 4 APP to the medium led to a decreased synthesis of labelled proteins. After 2 hours of incubation the radioactivity of the secreted proteins was 80% and after 5 hours 68% of the control value.

The portion of synthesized proteins which was secreted into the medium was

synthesized in the control medium. In the 4 APP containing medium 25% of the radioactivity of the synthesized proteins was recovered in the medium.

As we know neither the specific activity of the intracellular proteins nor the specific activity of the secreted proteins, we cannot calculate how much of the synthesized proteins is secreted.

The effect of 4 APP on TG synthesis and secretion. During the first 2 hours of incubation a secretion but no net synthesis of TG was observed in the control hepatocytes. After 4 hours of incubation these cells synthesized TG but the secretion of TG exceeded the synthesis (Table 2). 4 APP did not influence the synthesis of TG in the hepatocytes. However, the secretion was reduced to about 43% of the control value after 4 hours.

Electron Microscopy

and Golgi apparatus. Golgi apparatus and Golgi-derived vesicles contained VLDL-like particles (Fig. 11) with varying electron density (11).

The cells contained more autophagic vacuoles than immediately after isolation. Usually a few large lipid droplets were seen while glycogen was absent.

VLDL-like particles were never observed inside the Golgi apparatus. Golgi-derived vesicles with VLDL-like particles were frequently found. Some of these vesicles contained in addition to VLDL, very electron-dense deposits that resembled small lipid droplets (Fig. 4). Very small vesicles were pinched off from the cis-cisternae (Fig. 5). We frequently observed a body with a very distinct surrounding membrane and contents resembling SER elements. The membrane in some instances seemed to be multilayered as a result of tight packing of membranes.

b) *0.1 mg/ml* The most striking feature in cells incubated with 0.1 mg/ml 4 APP was large areas of accumulations of vesicles in close proximity to disordered fragments of cisternae with smooth membranes (Fig. 2a, b, 6, 7). Such areas were found in nearly all the cells sectioned through the nuclear area, i.e. approximately at the equatorial plane. They

Neither regular Golgi apparatuses nor vesicles with VLDL-like particles were found. No changes in the other organelles were observed. A few of the cells contained large lipid droplets.

MATERIAL AND METHODS

Chemicals

Bovine albumin (essentially free from fatty acids) prepared from fraction V, collagenase Type I, HEPES (N-2 hydroxyethylpiperazine-N'-2 ethanesulfonic acid) and 4-aminopyrazolopyrimidine were obtained from Sigma Chemicals Co., St. Louis, Mo., U.S.A. Boehringer, Mannheim, Germany, supplied enzymes and substrates for the determination of triglycerides. Nutrition medium RPMI 1640 was obtained from Flow Laboratories, Irvine, U.S.A. [^{14}C] protein hydrolysate, 54 mCi/mAtom was purchased from Radiochemical Centre, Amersham, England. Radioactivity was measured in a Packard Tri Carb liquid scintillation spectrometer, using Diluene (Packard Instrument Co., Ill., U.S.A.) as liquid scintillator medium. Counting efficiency was determined by the channels ratio method and was approximately the same in all samples.

Preparation and Incubation of Rat Hepatocytes

Male Wistar rats were fed ordinary laboratory chow and water *ad libitum*. The hepatocytes were isolated and incubated as described earlier (10). The control medium consisted of RPMI 1640 with HEPES added to a final concentration of 60 mM lactate to 10 mM and pyruvate to 1 mM. To add 4-APP a stock solution was prepared by dissolving 4 APP (3 mg/ml) in the incubation medium with pH lowered to 2.5. This solution was then added to the basic medium to a final concentration of 0.015 mg/ml or 0.1 mg/ml. To enable us to compare our *in vitro* results with those obtained *in vivo* (6, 8, 17) doses in the same order of magnitude as those used in *in vivo* studies were chosen. Before use the pH of all the media was adjusted to pH 7.45. The osmolality was approximately 300 mOsm. To measure protein synthesis and secretion [^{14}C] protein hydrolysate was added to the incubation media (20 ml/ml) before the incubation was started.

Biochemical Procedures

Protein synthesis or secretion was measured as follows. The proteins in a 400 μl cell suspension or a cell-free medium were precipitated with an equal volume of ice cold trichloroacetic acid (10% w/v). The precipitate was washed four times with trichloroacetic acid (5% w/v). The radioactivity in the precipitate was counted (16). The glycerol of the triglycerides was determined according to the method of Wieland (19) and measured fluorimetrically.

Electron Microscopy

The isolated hepatocytes were processed for electron microscopy after incubation for 3 hours with or without 4 APP (0.015 mg/ml or 0.1 mg/ml). The cells were fixed according to Arborgh *et al.* (2) and embedded in Epon 812. From each cell suspension several samples were embedded, and two blocks from each group were chosen for sectioning. Sections were collected from different levels of the blocks. They were stained with lead citrate and examined in a Siemens Elmiskop 1A electron microscope at 80 kV.

RESULTS

Several experiments on the effect of 4-APP upon synthesis and secretion of TG and radioactive protein were performed. The rate of synthesis and secretion in the control cells differed somewhat in the experiments, and the magnitude of the effect of 4-APP also varied to some extent. However the effect of 4-APP was principally the same in all experiments. The results from one typical series are presented.

The effect of 4-APP on protein synthesis and secretion. During incubation with radioactive amino acids in the medium, labelled proteins were

TABLE 1 The Effect of 4 APP on Protein Synthesis and Secretion

	Synthesized radioactive protein cpm/ml hepatocytes	secreted radioactive protein cpm/ml hepatocytes
control		
2 h	31400	6100
5 h	51900	19200
4-APP (0.1 mg/ml)		
2 h	25000	2700
5 h	35600	8800

The hepatocytes were incubated in the medium RPMI 1640 with HEPES added to a final concentration of 60 mM lactate to 10 mM pyruvate to 1 mM and with [^{14}C] protein hydrolysate (20 μl /ml medium). At zero time and after 2 and 5 hours samples of the cell suspension were mixed with trichloroacetic acid. Other samples were centrifuged and the radioactive proteins in the medium were precipitated with trichloroacetic acid. The incorporation of labelled amino acids into protein per mill hepatocytes was calculated.

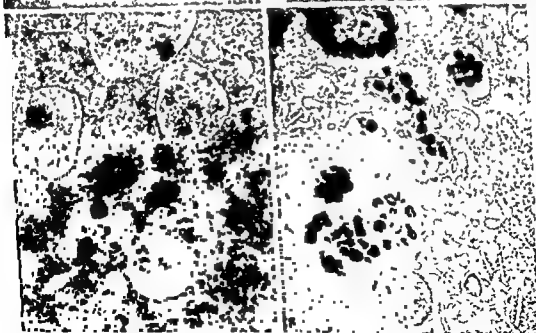
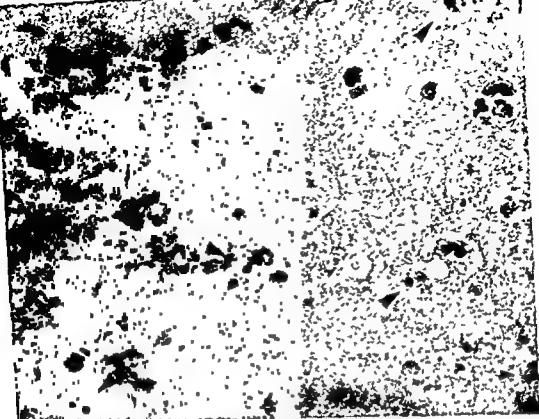
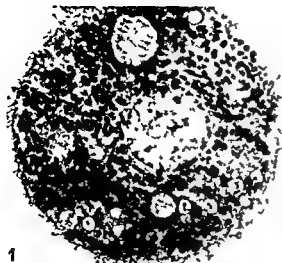


Fig. 6 & 7 From a hepatocyte incubated for 3 h with 4 APP (0.1 mg/ml)

Fig. 6 Area with vesicles and disordered fragments of cisternae with smooth membranes. Vesicles with lipid like droplets (arrowheads) $\times 18\,000$

Fig. 7 Higher magnification of part of the same area $\times 36\,000$

Fig. 8 + VLDL from a control hepatocyte incubated for 2 h at 37° C $\times 36\,000$



1



2a



2b



Fig 1 Control hepatocyte incubated for 3 h at 37° C $\times 2\,000$

Figs 2a & 2b Hepatocytes incubated for 3 h with 4-aminopyrazolopyrimidine (0.1 mg/ml). Note areas with vesicles and disordered fragments of cisternae (arrowheads) $\times 2\,000$

Fig 3 5 From hepatocytes incubated for 3 h with 4-APP (0.015 mg/ml)

Fig 3 Golgi apparatus with flattened cisternae curled up in a semicircle (arrowhead) $\times 39\,000$

Fig 4 Golgi-derived vesicles with lipoprotein particles. Note lipid-like droplets in the vesicles (arrowhead) $\times 39\,000$

- 6 Henderson J F & Junga I G Effects of 4 aminopyrazolo (3-4-d) pyrimidine and 1 methyl-4 aminopyrazolo (3-4-d) pyrimidine on nucleic acid purine metabolism in ascites tumors. *Cancer Res* 21 173-177 1961
- 7 Iwamoto A & Martin Jr D W Inhibition of cell growth and of biosynthesis by allopurinol and 4 aminopyrazolo (3-4-d) pyrimidine. A comparative study. *Biochem Pharmacol* 23 3199-3209 1974
- 8 Mjos O D, Faergeman O, Hamilton R L & Havel R J Characterization of remnants produced during the metabolism of triglyceride rich lipoproteins of blood plasma and intestinal lymph in the rat. *J clin Invest* 56 603-615 1975
- 9 Nordby G Secretion of lipids and lecithin cholesterol acyltransferase (LCAT) from isolated rat hepatocytes. In Peeters H (ed) *Protides of Biological Fluids*. Pergamon Press, New York, 209-212 1977
- 10 Nordby G, Berg T, Ahrén M & Åhrum A R Secretion of Lecithin Cholesterol Acyltransferase from isolated rat hepatocytes. *Biochim Biophys Acta* 450 69-77 1976
- 11 Nordby G, Schreiner B, Berg T & Åhrum A R The effect of D galactosamine on LCAT secretion and morphological structures in isolated rat hepatocytes. *Acta path microbiol scand Sect A* 85 839-849 1977
- 12 Sabesin S M Effects of acetoxycycloheximide on the metabolism of hepatic triglycerides in the rat. *Exp Mol Pathol* 25 227-235 1976
- 13 Sabesin S M & Koff R S D Galactosamine hepatotoxicity IV. Further studies of the pathogenesis of fatty liver. *Exp Mol Pathol* 24 425-434 1976
- 14 Scholler J, Philips F S & Sternberg S S Production of fatty livers by 4 aminopyrazolo (3-4-d) pyrimidine. Toxicological and pathological studies. *Proc Soc exp Biol Med* 93 398-402 1956
- 15 Scholler P O Protein degradation in isolated rat hepatocytes is inhibited by ammonia. *Biochem Biophys Res Comm* 66 44-52 1975
- 16 Selkin P O Incorporation of radioactive amino acids into protein in isolated rat hepatocytes. *Biochim Biophys Acta* 442 391-404 1976
- 17 Shiff T S, Rheim P S & Edler H A Effects of high sucrose diets and 4 aminopyrazolopyrimidine on serum lipids and lipoproteins in the rat. *J Lipid Res* 12 596-603 1971
- 18 Stein O, Bar-On H & Stein Y Lipoproteins and the liver. In Popper H & Schaffner F (eds) *Progress in Liver Disease* vol IV. Grune & Stratton, New York, 45-62 1972
- 19 Wuland O Glycerol UV Method. In Bergmeyer H U (ed) *Methods of enzymatic analysis* 3 ed vol 3. Chemie Weinheim Academic Press, New York, 1404-1409 1974

DISCUSSION

In this study we have found that 4 APP inhibited both the synthesis and secretion of labelled proteins. In animals receiving 4 APP *Shiff et al* (17) found that incorporation of labelled amino acids into lipoproteins and plasma proteins was depressed while incorporation of labelled amino acids into total liver proteins was unaltered one or three hours after injection of the radioactive amino acids. In contrast to these findings we found that 4 APP inhibited liver protein synthesis. This effect was especially pronounced after five hours of incubation. By our method the secreted proteins were included when the synthesis of radioactive proteins was measured. This may partly account for the difference in results obtained by *Shiff* and his group and by us. In our study we have found the highest effect of 4 APP upon the incorporation of labelled amino acids into secreted proteins. This may be due to a higher production rate of these proteins. One cannot however ignore that 4 APP may have an additional effect on the protein secretion as such.

During incubation of hepatocytes 2-4% of the cell proteins are degraded to amino acids per hour (15) and the specific activity of the intracellular amino acid pool will diminish as degradation goes on. We have calculated the incorporation of radioactive amino acids into proteins when measuring the effect of 4 APP upon protein synthesis and secretion. Any change in the rate of degradation will also influence the specific activity of the amino acid pool and consequently may give a false picture of the rate of protein synthesis. We have found that 4 APP decreases the protein degradation (unpublished results). The inhibitory effect of 4 APP on protein synthesis and secretion is therefore probably somewhat underestimated in our study.

Our results showed that the synthesis of TG was unaffected by 4 APP while the secretion of TG was markedly reduced. As a consequence TG was accumulated in the cells. This is in agreement with earlier findings that TG in serum is decreased while TG in liver is increased (5, 14, 17). Protein secretion and TG secretion were inhibited almost to the same extent. In our study with isolated rat hepatocytes we have avoided any possible effect of an altered influx of fatty acids upon lipoprotein metabolism. It is reasonable to presume that the effect of 4 APP upon TG secretion is caused by a primary deficiency of apoprotein and hence a disturbed production of lipoproteins.

The morphological changes in the 4 APP treated cells are apparently connected with the smooth membranes of the cells while the rough membranes look unaffected. Thus with a small dose of 4 APP

the Golgi apparatuses were frequently found but they were not producing VLDL. With a higher dose however neither the usual Golgi cisternae and saccules nor vesicles with VLDL like particles were observed. The lack of secretory vesicles containing nascent VLDL is in accordance with observations on livers from 4 APP treated rats (8). According to *Alexander et al* (1) the nascent TG rich lipid particles originate in SER while apoprotein B and other possible VLDL apoproteins are delivered from RER. A specialized tubule system connects the endoplasmic reticulum to the Golgi apparatus where the nascent lipoprotein undergoes concentration and further glycosylation. The morphological changes we observe in the 4 APP treated cells can be interpreted as a disturbance in this tubular region between the endoplasmic reticulum and the Golgi apparatus. Instead of Golgi derived vesicles with nascent VLDL there are vesicles with unknown contents. We assume that the vesicles contain the TG rich lipid produced in the SER inasmuch as we know that the TG synthesis is undisturbed by the 4 APP. The electron-dense deposits of the vesicles resemble small osmophilic lipid droplets. This observation supports the assumption that the lipid synthesis is undisturbed.

Our biochemical and electron microscopic results from isolated hepatocytes may suggest that 4 APP treatment does not affect the production of the lipid part of the lipoprotein while the production of apoprotein is reduced. In this way rats treated with 4 APP will accumulate lipids in their livers and subsequently develop fatty livers.

The authors are grateful to Torhild M. Lund and Tivoli Bøker for excellent technical assistance.

REFERENCES

1. Alexander C A, Hamilton R L & Havel R J. Subcellular localization of B apoprotein of plasma lipoprotein in rat liver. *J Cell Biol* 69: 241-263, 1976.
2. Arborgh B, Bell P, Brunk L & Collins J P. The osmotic effect of glutaraldehyde during fixation. A transmission electron microscopy scanning electron microscopy and cytochemical study. *J Ultrastruct Res* 56: 339-350, 1976.
3. Bar-On H, Stein O & Stein Y. Multiple effects of 4 APP on liver metabolism. *Acta 110* 444-452, 1976.
4. Farber E. Ethionine fatty liver. *Advan Lipid Res* 5: 119-183, 1967.
5. Henderson J F. Studies on fatty liver induction by 4 aminopyrazolopyridimidine. *J Lipid Res* 4: 68-74, 1963.

BRIEF REPORT

CARCINOMA IN SITU OF TESTIS IN TESTICULAR FEMINIZATION SYNDROME

Axel E. Skakkebaek

The Laboratory of Reproductive Biology and Fertility Clinic University Department of Obstetrics and Gynaecology Rigshospitalet Copenhagen ■ Denmark

Skakkebaek N E Carcinoma in situ of testis in testicular feminization syndrome. Acta path microbiol scand Sect. A 87 87-89 1979

A light microscopical study of an excised testis from a 14½ year-old girl with incomplete type of testicular feminization syndrome revealed a carcinoma in-situ pattern in a part of the gonad. An identical histological pattern has repeatedly been demonstrated in infertile men who developed gross testicular germ cell tumours. It is suggested that germ cell carcinomas in patients with testicular feminization syndrome may be preceded by this characteristic intratubular germ cell abnormality.

Key words: Carcinoma in situ, testicular neoplasm, testicular feminization syndrome.

Skakkebaek N E The Laboratory of Reproductive Biology and Fertility Clinic University Department of Obstetrics and Gynaecology Rigshospitalet Copenhagen ■ Denmark

Received 2 ix 78 Accepted 9 x 78

Patients with testicular feminization syndrome run a high risk of developing germ cell tumours (Morris & Mahesh 1963 ■ Connell *et al* 1973) although the true incidence is difficult to assess because many patients are treated with prophylactic orchiectomy. It has recently been shown that germ cell tumours may be preceded by a carcinoma in situ pattern of the seminiferous tubules in some infertile men (Nielsen *et al* 1974 Niesch, Bachmann & Hedinger 1977 Skakkebaek 1972 Skakkebaek 1978). In order to evaluate the role of carcinoma in situ in the testes of patients with testicular feminization we have commenced a light microscopical study of the germ cells in testes which have been removed from patients with testicular feminization.

In one of five testes we have detected a carcinoma in situ pattern.

Material and Methods

The patient, a 14½ year-old girl with testicular feminization syndrome and 46 XY chromosome complement was born with an enlarged clitoris. Other external genitalia were as in a normal female. The left gonad was removed when the patient had a left herniotomy at the age of 2½. Microscopy was reported as infantile testis

At the age of 14½ the patient was first seen in our clinic owing to virilization, and the right testis was excised. Approximately half of the organ was prepared for endocrinological and ultrastructural studies (Pedersen *et al* to be published). The other half was used for the present light microscopical study. The tissue was fixed in Cleland's fixative, embedded in Paraplast, sectioned serially at 4 µm and stained with iron haematoxylin and eosin.

Results

All seminiferous tubules were well preserved with little hyalinization of the membranes of the seminiferous tubules. In approximately 15 per cent of the tubules a characteristic carcinoma in situ pattern was found (Fig. 1). The tubules contained atypical germ cells which were located along the tubular wall. The nuclei were round (approximately 10 µm in diameter) and contained 1-4

chromosomes. The tubules contained fully-differentiated Sertoli cells only.

The number and morphology of the Leydig cells in the interstitial tissue were similar to those of normal men

Discussion

The finding of seminiferous tubules with carcinoma in situ of the germ cells in a patient with testicular feminization syndrome is not surprising since as many as 5-20 per cent of patients with this disease may develop germ cell tumours of their testes (Morris & Mahesh 1963; O'Connell *et al.* 1973). However I have not been able to find a previous report on this subject.

Because the gonad was removed it was not possible to obtain information on subsequent invasive tumour growth in the present case. However there is evidence to suggest that approximately 70 per cent of infertile men in whom a testicular biopsy has revealed carcinoma in situ of the germ cells will subsequently develop seminomas, teratomas or other types of germ cell tumours within five years of their first biopsy (Skakkebaek & Berthelsen 1978). A similar correlation between carcinoma in situ and growth of invasive germ cell tumours may exist in the testicular feminization syndrome.

References 1 Morris J M & Mahesh B Am J Obstet Gynec 87 731-747 1963 - 2 Nielsen H Nielsen M & Skakkebaek A E Acta path microbiol scand A 82 235-248 1974 - 3 Auesch Buchmann I H & Hedinger C Schweiz med Wschr 107 795-801 1977 - 4 O'Connell M J Ramsey H F Whang Peng J & Wieruck P H Am J med Sci 265 321-333 1973 - 5 Pedersen H Sjarup J & Skakkebaek N E Endocrinological and ultrastructural studies of gonadal function in patients with testicular feminization syndrome in preparation - 6 Skakkebaek A E Lancet ii 516-517 1972 - 7 Skakkebaek A E Histopathology 2 157-170 1978 - 8 Skakkebaek A E & Berthelsen J G Lancet ii 204-205 1978



Fig. 1 Excised testis. Section of the part containing carcinoma in situ.

a) Note the homogenous pattern of the seminiferous tubules. $\times 150$.

b) Same as a). Higher magnification showing atypical germ cells (G) along the basement membrane and Sertoli cell (S). $\times 375$.

ACTA PATHOLOGICA ET MICROBIOLOGICA SCANDINAVICA

Section **A** PATHOLOGY

EDITORIAL BOARD

STEEN OLSEN DENMARK
J RAPOLA FINLAND
O BJARNASON ICELAND
K ARNESEN NORWAY
J L E ERICSSON SWEDEN

EDITOR IN CHIEF
J CHR SHIM

ADVISORY BOARD

J RYGAARD DENMARK
J VISFELDT DENMARK
T NEVALAINEN FINLAND
L TEPPÖ FINLAND
G GEORGSSON ICELAND
J HALLGRIMSSON ICELAND
T HOVIG NORWAY
O D LÆRUM NORWAY
T BERGE SWEDEN
K NILSSON SWEDEN

VOL 86 A FASC 1-6 1978

MUNKSGAARD COPENHAGEN

INDEX

VOL. 86 A FASC 1-6 1978

Mabo Kristian	285	Faarup Poul	409
Mabo Kristian	293	Fenger Claus	225
Almeren Helena	337	Fennestad K L	251
Amtrup F	273	Fossberg Tor Magne	121
Andersen Johan	205	Fox Cecil H	131
Andersson Gunnar	17	Francis Dorthe	389
Aparisi Tomas	157	Francis Dorthe	393
Arbogh Bengt	143	Francis Dorthe	397
Arbogh Bengt	157	Franssila A	483
Arro E	257	Frederiksen P	461
Asklund C	273	Gad Adel	21
Auer Gert	131	Gothlin Gustav	157
Baunsgaard P	273	Gothman Lars	21
Bergman Bo	245	Græm Niels	499
Bergmann S	70	Grude Tove Helliesen	437
Bertheussen K J	90	Grude Tove Helliesen	513
Bichel P	461	Grude Tove Helliesen	523
Bjarnason O	483	Hagmar Bjorn	231
Blomquist E	257	Hamberg H	487
Bohle A	375	Hansen Birgit Fischer	241
Boquist Lennart	313	Hansen Jens Peder Hart	36
Boquist Lennart	331	Hansen Jens Peder Hart	185
Breistein Liv Stray	121	Hansen Knud Bendix	285
Brunk U	45	Hansen Knud Bendix	293
Brunk U	257	Hansen L	273
Brunk U	487	Haugen Åge	101
Bruun L	251	Haugen Åge	415
Carlsson Jorgen	45	Heby Olle	17
Carlsson S	82	Helweg Larsen Karin	499
Carlsson S	117	Hestbech J	195
Carlsson S	297	Hiltunen R	265
Christensen H E	273	Hultcrantz Rolf	143
Christensen J A	375	Jakobsen C	273
Christensen N	251	Jakobsson Sten W	401
Christoffersen Per	495	Jakubowski H D	375
Clausen Per P	383	Jarlstedt Jan	111
Collan Y	265	Jensen Herluf	409
Collins Peter	45	Jensen Jørn	205
Diemer V H	90	Jensen N K	273
Døskeland Stein Ole	121	Jørgensen Leif	1
Ekfors T O	25	Johansson Sonny	333
Elling Folmer	409	Johansson Sonny	505
Enzell C	135	Jokinen E J	265
Ericsson Jan L E	157	Jones Dean P	401
Ericsson Jan L E	487	Jordo Lars	111

Published by the
Scandinavian Societies for Microbiology and Pathology

•
Acta Pathologica
et Microbiologica
Scandinavica
1978

All rights reserved

Reproduction in any form
including microfilm without written permission
of the Editor is prohibited

Distributed by Munksgaard
International Booksellers and Publishers Ltd
35 Norre Sogade DK 1370 Copenhagen K, Denmark

Printed by
bording grafik a/s
Copenhagen

Adipositas liver morphology alcoholism diabetes mellitus	495	Cystadenoma of ovary versus ovarian tumours histochemistry electron microscopy mucous substances	303
Alcoholic beverages amino acid incorporation cerebellum cerebrum liver rat malnutrition	111	Cystic fibrosis sulphated glycoproteins	83
Alcoholism liver morphology diabetes mellitus adipositas	495	Cytoplasmic proteins cell membranes fluorescent labelling	131
Alloxan pancreatic B-cells sensitivity <i>in vivo</i> inorganic phosphate acid-base balance	313	Diabetes mellitus liver morphology alcoholism adipositas	495
Alpha 1 antitrypsin globules liver PAS non glycogenic globules	325	Diphosphonate cartilage calcification matrix	211
Alveolar epithelial cells transthoracic aspiration biopsy	397	Dipyridamole DNA-synthesis heart, skeletal muscle	82
Ameloblastoma, jaw Swedish Cancer Registry	337	Dura solitary plasmacytoma extracerebral	21
Amyloidosis, ureter neoplasm	357	Early infarction Nitro-BT coronary thrombosis sudden death	279
Anal transitional zone macroscopic demonstration	225	Endothelial cells aorta local alterations rabbit	1
Anaplastic carcinoma salivary gland neoplasms Greenland eskimos	185	Eskimo Greenland cervical cancer	36
Aorta, endothelial cells focal alterations rabbit	1	Eskimos Greenland salivary gland neoplasms anaplastic carcinoma	185
Argyrophil and argentaffin cells histogenesis mucinous ovarian cystadenoma ultrastructure	471	Fibroblasts human diploid tobacco smoke condensation	135
Argyrophil and argentaffin cells mucosa histology ovary mucinous cystadenoma	463	Fine needle aspirates sputum micronuclei	201
Aspiration biopsy flow cytometry DNA prostate carcinoma prostate cytology clinical stages	461	Flow cytometry DNA prostate carcinoma aspiration biopsy prostate cytology clinical stages	461
Aspiration biopsy transthoracic	389	Gastric adenocarcinoma gastric epithelium ultrastructure	87
Aspiration biopsy transthoracic	393	Gastric epithelium gastric adenocarcinoma ultrastructure	87
Aspiration biopsy transthoracic alveolar epithelial cells	397	Glia cells cultured human ageing <i>in vitro</i> phage III phenomenon plasma membrane motility scanning electron microscopy time-lapse film	257
Bone tumours chondrosarcoma ultrastructure alkaline phosphatase ATPase	157	Gliomas neurinomas scanning electron microscopy cell culture	101
Bone turn-over hypothyroidism morphometric and dynamic studies	56	Gliomas neurinomas transmission electron microscopy cell culture cytoskeleton	415
Breast cancer tissue oestrogen sensitivity <i>in vitro</i> oestrogen receptors	169	Glomerulonephritis crescent nephritis renal failure immunosuppression	409
Cancer of the larynx histological grading reproduction	499	Glomerulonephritis immunofluorescent microscopy kidney disease	531
Cardiac myocytes rat light microscopy anoxia suspension membrane permeability histological sections	403	Glomerulonephritis immunofluorescent microscopy kidney disease	543
Cartilage diphosphonate calcification matrix	211	Glomerulonephritis ultrastructure	379
Cell culture electron microscopy proliferation ruffling membranes ultrastructure carcinoma graphy	45	G	201
Cell death serum polyamines putrescine spermidine Ehrlich ascites tumour	17	G	36
Cell membranes cytoplasmic proteins fluorescent labelling	131	G	185
Cerebral ventriculography pulmonary excretion macrophages	90	Hamartomas, biliary liver needle biopsy von Meyenburg complexes microhamartomas	93
Cervical cancer eskimo Greenland	36	Heart autopsy ischemic heart disease Nitro-BT test quantitation	241
Cervix carcinoma methylcholanthrene mouse immunological marker <i>pro can kinase cyclic</i> AMF chromosomes	121	Heart, hypertensive damage acute arterial vessels	199
Cervix uteri histopathologic diagnosis reliability	273	Heart, osteogenic sarcoma thrombocytopenia	505
Chondrosarcoma bone tumours ultrastructure alkaline phosphatase ATPase	157	Heart skeletal muscle dipyridamole DNA-synthesis	82
Colonic metaplasia intestinal metaplasia human stomach	351	Hepatitis B-surface antigen, liver tissue orcein staining immunoperoxidase staining	383
Coronary thrombi early infarction Nitro-BT sudden death	279	Histiocytoma fibrous, malignant, soft tissue tumour fibrosarcoma malignant atypical fibrosarcoma	25

Jung B	487	Nørgaard Tove	409
Kalland Terje	121	Nørgaard Tove	427
Kjær T B	461	Normann T	483
Klemi P J	303	Østergaard Karen	279
Klemi P J	465	Olesen O Vendelin	195
Klemi P J	471	Olsen Finn	199
Klunken L	90	Olsen Tom Skyhøj	361
Knutson Folke	245	Olsen Tom Skyhøj	367
Kutti Jack	505	Olsson Lars Bertil	505
Lahdevirta J	265	Olsson Rlof	111
Lærum Ole Didrik	101	Petersen Falle	495
Lærum Ole Didrik	415	Pilotti Å	135
Larsen Svend	531	Poulsen H Skovgaard	169
Larsen Svend	543	Præstholm J	90
Larsen Tove Eeg	437	Rajs Jovan	401
Larsen Tove Eeg	451	Rantakokko V	25
Larsen Tove Eeg	513	Rasmussen J	273
Larsen Tove Eeg	523	Reintoft Ingermarie	273
Larsson Åke	211	Reintoft Ingermarie	325
Larsson Åke	337	Révesz J	331
Larsson Sven Erik	211	Ringertz N	483
Larsson S E	331	Ringsted J	273
Litwin J	135	Risberg Bjorn	14
Ljungqvist A	82	Rolla Gunnar	83
Ljungqvist A	117	Rolschau J	273
Ljungqvist A	297	Ryd Walter	231
Locklund Birgitta	131	Saxén E	483
Lorentzon R	331	Sonju Torlef	83
Ludwigsen Erik	319	Sørensen Finn Hanberg	319
Meistrup Larsen Karen Inger	499	Starklint H	273
Meistrup Larsen Uggi	499	Sundstrom C	173
Melander Stig	14	Svendsen Einar	1
Melsen B	63	Teglbjærg P Stubbe	87
Melsen B	70	Teglbjærg P Stubbe	351
Melsen B	83	Thommesen N	93
Melsen F	56	Thommesen N	273
Melsen F	63	Thommesen P	461
Melsen F	70	Thomsen K	195
Meyer D S	375	Thomsen Per	383
Mikkelsen Flemming	36	Tornling G	82
Mikkelsen Flemming	185	Tornling G	117
Moesner J	273	Tornling G	297
Mosekilde L	56	Ueland Per Magne	121
Mosekilde L	63	Unge G	82
Mosekilde L	70	Unge G	117
Neuenhofer J	375	Unge G	297
Nevalainen T J	303	Vrang J	273
Nevalainen T J	471	Westermarck B	257
Nickels Juha	14	Willems Jan Silvester	131
Nielsen H Overgard	351	Willen Helena	21
Nielsen Nils Højgaard	36	Willen Helena	357
Nielsen Nils Højgaard	185	Willen Roger	21
Nilsson A	331	Zeiterberg Anders	131
Nilsson Goran	201		
Nilsson K	173	A See Ae	Æ See Ae
Nilsson Ulf	157	Ø See Oe	Ö See Oe
			Å See Aa

Salivary gland neoplasms: anaplastic carcinoma Greenland eskimos	185	microscopy proliferation ruffling membranes	45
Serum polyamines putrescine spermidine cell death Ehrlich ascites tumour	17	Tobacco smoke condensate human diploid fibro- blasts	135
Soft tissue tumour fibrous histiocytoma malig- nant fibroxanthoma malignant atypical fi- broxanthosarcoma	25	Trophoblastic tumour uterine neoplasms	14
Stomach human intestinal metaplasia colonic metaplasia	351	Ureter neoplasm amyloidosis	357
Sudden death early infarction Nitro-BT coronary thrombi	279	Urinary tract infection ileal conduit urinary diversion pyelonephritis renal abscesses au- topsy	245
Swedish Cancer Registry ameloblastoma	337	Urothelial hyperplasia phenacetin mechanical per- foration	333
Thrombocytopenia osteogenic sarcoma heart	505	Uterine neoplasms trophoblastic tumour	14
Thyroid cancer histologic classification observer variation quality control in histopathology	483	X irradiation cultured human cells plasma mem- brane motility scanning electron microscopy time lapse filming	487
Time lapse cinematography cell culture electron			

Histomorphometric studies iliac crest bone structure	70	Melanoma lymphocyte infiltration prognosis	523
Histomorphometry iliac bone errors	63	Membranes ruffling cell culture electron microscopy proliferation time lapse cinematography	45
Histopathologic diagnosis reliability cervix uteri	273	Microangiography hypertrophied myocardium vascular pattern	297
Hypertensive damage acute arterial vessels heart	199	Microthrombosis megakaryocytes intravascular coagulation	285
Hypothyroidism bone turn over morphometric and dynamic studies	56	Murine tumours syngeneic metastases ascites tumours	23
Ileal conduit urinary diversion urinary tract infection pyelonephritis renal abscesses autopsy	245	Myocardial capillary vasculature physical exercise rat	117
Iliac bone histomorphometry errors	63	Myocardium hypertrophied vascular pattern microangiography	297
Iliac crest bone structure histomorphometric studies	70	Nephritis crescent glomerulonephritis renal failure immunosuppression	409
Immunofluorescent microscopy kidney disease glomerulonephritis	531	Nephropathia epidemica renal biopsy electron microscopy immunohistology renal sequelae	265
Immunofluorescent microscopy kidney disease glomerulonephritis	543	Neurinomas gliomas scanning electron microscopy cell culture	101
Intestinal metaplasia colonic metaplasia human stomach	351	Neurinomas gliomas transmission electron microscopy cell culture cytoskeleton	415
Intravascular coagulation megakaryocytes micro thrombosis	285	Nitro BT test heart autopsy ischemic heart disease quantitation	241
Iron overload liver rat electron microscopy	143	Oestrogen receptors breast cancer tissue oestrogen sensitivity <i>in vitro</i>	169
Ischemic heart disease heart autopsy Nitro BT test quantitation	241	Oestrogen sensitivity <i>in vitro</i> breast cancer tissue oestrogen receptors	169
Juxtaglomerular apparatus renal hypertension juxtaglomerular contact areas macula densa basal area	375	Osteogenic sarcoma heart thrombocytopenia	505
Kidney disease immunofluorescent microscopy glomerulonephritis	531	Ovarian mucinous cystadenoma argyrophil and argentaffin cells histogenesis ultrastructure	471
Kidney disease immunofluorescent microscopy glomerulonephritis	543	Ovarian mucinous cystadenoma argyrophil and argentaffin cells mucin histochemistry	465
Kidney enzymes proximal kidney tubule histochemistry salt depletion salt load	427	Ovarian tumours serous cystadenoma of ovary histochemistry electron microscopy mucosal substances	303
Kidney tubule proximal histochemistry kidney enzymes salt depletion salt load	427	Pancreas pancreas autopsies	361
Larynx cancer of histological grading reproducibility	499	" " " " "	367
Leukaemia megakaryocytes	293	" " " " "	313
Lithium rat kidney focal cortical fibrosis light microscopy	195	" " " " "	333
Liver alcoholic beverages amino acid incorporation cerebellum cerebrum rat malnutrition	111	Plasmacytoma extraskelatal solitary dura	21
Liver alpha 1 antitrypsin globules PAS non glycosidic globules	325	Plasma membrane motility cultured human cells X irradiation scanning electron microscopy time lapse filming	487
Liver morphology alcoholism diabetes mellitus adipositas	495	Pleural effusion disease rabbit viral infection histopathology	251
Liver needle biopsy biliary hamartomas von Meyenburg complexes microhamartomas	93	Prostatic carcinoma flow cytometry DNA aspiration biopsy prostatic cytology clinical stages	451
Liver rat iron overload electron microscopy	143	Pulmonary excretion cerebral ventriculography macrophages	90
Liver tissue hepatitis B surface antigen orcein staining immunoperoxidase staining	383	Rat kidney lithium focal cortical fibrosis light microscopy	195
Lymph nodes specimen radiography carcinoma colon rectum	285	Renal biopsy nephropathia epidemica electron microscopy immunohistology renal sequelae	265
Lymphomas human malignant cell lines	173	Renal biopsy post streptococcal glomerulonephritis differential cell count morphometry	319
Megakaryocytes intravascular coagulation micro thrombosis	285	Renal hypertension juxtaglomerular apparatus juxtaglomerular contact areas macula densa basal area	175
Megakaryocytes leukaemia	293		
Melanoma cell type pigmentation atypia mitotic count prognosis	513		
Melanoma classification growth patterns	451		
Melanoma classification prognosis	437		

ovary gland neoplasms anaplastic carcinoma		microscopy proliferation ruffling membranes	
Greenland eskimos	185		45
um polyamines putrescine spermidine cell		Tobacco smoke condensate human diploid fibro-	
death Ehrlich ascites tumour	17	blasts	135
ft tissue tumour fibrous histiocytoma malig-		Trophoblastic tumour uterine neoplasms	14
nant, fibroanthoma, malignant, atypical fi-		Ureter neoplasm amyloidosis	357
broxanthosarcoma	25	Urinary tract infection renal conduit urinary	
omach human intestinal metaplasia colonic		diversion pyelonephritis renal abscesses au-	
metaplasia	351	topsy	245
dden death early infarction Nitro BT coronary		Urothelial hyperplasia phenacetin mechanical per-	
thrombi	279	foration	333
edish Cancer Registry ameloblastoma	337	Uterine neoplasms trophoblastic tumour	14
thrombocytopenia osteogenic sarcoma heart	505	X irradiation cultured human cells plasma mem-	
thyroid cancer histologic classification observer		brane motility scanning electron microscopy	
variation quality control in histopathology	483	time lapse filming	487
time lapse cinematography cell culture electron			

- Supplement 264 *Korhonen Matti O*: Adenocarcinoma of the Uterine Cervix. An evaluation of the available diagnostic methods. Pp 59 1978 (Section A)
- Supplement 265 *Hærem Jørgen W*: Sudden unexpected Coronary Death. The Occurrence of Platelet Aggregates in the Epicardial and Myocardial Vessels of Man. Pp 47 1978 (Section A)
- Supplement 266 *Koch Christian*: Bactericidal Activity of Human Neutrophil Granulocytes. Studies in clinical disorders with the in vitro bactericidal test. Pp 63 1978 (Section C)
- Supplement 267 *Svendsen Ulrik Gerner*: The Importance of the Thymus for Hypertension and Hypertensive Vascular Disease in Rats and Mice. Pp 15 1978 (Section A)
- Supplement 268 *Lindström Clas G*: Experimental Colo Rectal Tumours in the Rat. A histopathologic study with special reference to normal anatomy and to immunologic and radiographic aspects. Pp 75 1978 (Section A)
- Supplement 269 *Krogh Palle*: Causal Associations of Mycotoxic Nephropathy. Pp 28 1978 (Section A)
- Supplement 270 *Clemmesen Johannes Johannes*: Fibiger. Gongylonema and Vitamin A in Carcinogenesis. Pp 13 1978 (Section A)
- Supplement 271 *Berthold Peter and Berthold Claes H*: Immuno Electron Microscopic Identification of a Dental Plaque Microorganism - *Streptococcus mutans*. Pp 37 1978 (Section B)

DENSITY DETERMINATIONS OF HUMAN PARATHYROID GLANDS BY DENSITY GRADIENTS

GÖRAN ÅKERSTRÖM HÅKAN PERTOFT LARS GRIMELIUS and HENRY JOHANSSON

Departments of Surgery and Pathology University Hospital and Department of Medical and Physiological Chemistry The Biomedical Center University of Uppsala Uppsala Sweden

Åkerström G Pertoft H Grimelius L & Johansson H Density determinations of human parathyroid glands by density gradients Acta path microbiol scand Sect A 87 91-96 1979

The densities of human parathyroid glands were measured in density gradient columns of various media Percoll (an aqueous colloidal solution of polyvinylpyrrolidone-coated silica) equilibrated to 300 mOsm with sodium chloride was found to be the ideal gradient medium for density measurements of tissues with a density >1.0 g/ml which includes most parathyroid glands The densities of the glands varied between 0.96 and 1.06 g/ml Density measurements in gradients of Percoll were simple and reproducible and were made with an accuracy of approximately 0.001 g/ml In other gradient media (aqueous solutions of sucrose and Ficoll and organic solvents) there was a drift in density caused by osmotic or lipid solvating effects of the media For measurements of densities <1.0 g/ml no ideal gradient medium was found but a silicon oil or carbon tetrachloride/kerosene gradient could be used with somewhat reduced accuracy It is concluded that the density gradient technique with the use of Percoll is potentially useful as a complement to routine histopathological parathyroid diagnosis as glandular density is a good indicator of the relative proportions of parenchymal and fat tissue

Key words Parathyroid glands density determinations

Göran Åkerström Department of Surgery University Hospital 75014 Uppsala Sweden

Accepted as submitted 24 vii 78

Density determinations have recently been suggested as a tool in parathyroid diagnosis (Åkerström *et al* 1977 and 1979 & Wang & Rieder 1978) These determinations are based on the differences in density between the two main glandular components - parenchymal and fat cells Thus glandular density reflects the distribution between the two components and also indirectly the parenchymal tissue content Density measurements should therefore be of value as a contribution to parathyroid diagnosis as the parenchymal cell mass is probably the best indicator of the endocrine activity The usefulness of such measurements in clinical practice however is dependent upon the availability of a simple and accurate technique

One of the most sensitive and simple methods of determining the densities of biological tissues is probably the density gradient column technique (Oster & Yamamoto 1963 Åkerström *et al* 1977)

The liquids most often used in density gradients are various organic solvents which however may interfere with the integrity of the tissues e.g. by dissolving lipids Solutions of sucrose Ficoll and alcohol can exert osmotic pull on the water of the tissue leading to dehydration (Oster & Yamamoto 1963) Percoll an aqueous colloidal solution of polyvinylpyrrolidone-coated silica was recently introduced for density gradient centrifugation (Pertoft & Laurent 1977) In contrast to other gradient media the osmotic pressure of Percoll is low It can be increased simply by adding salt

The aim of this study was to compare Percoll with other gradient media in density measurements on parathyroid glands This was done by determining drift curves in gradients made of different liquids Changes in the tissues caused by the gradient liquids could easily be disclosed by following the position of the material in the column as a function of time The effect of osmotic pressure

SUPPLEMENTS

- Supplement 264 *Korhonen, Matti O* Adenocarcinoma of the Uterine Cervix An evaluation of the available diagnostic methods Pp 59 1978 (Section A)
- Supplement 265 *Hærem, Jørgen W* Sudden, unexpected Coronary Death The Occurrence of Platelet Aggregates in the Epicardial and Myocardial Vessels of Man Pp 47 1978 (Section A)
- Supplement 266 *Koch, Christian* Bactericidal Activity of Human Neutrophil Granulocytes Studies in clinical disorders with the in vitro bactericidal test Pp 63 1978 (Section C)
- Supplement 267 *Svendsen, Ulrik Gerner* The Importance of the Thymus for Hypertension and Hypertensive Vascular Disease in Rats and Mice Pp 15 1978 (Section A)
- Supplement 268 *Lindström, Clas G* Experimental Colo-Rectal Tumours in the Rat A histopathologic study with special reference to normal anatomy and to immunologic and radiographic aspects Pp 75 1978 (Section A)
- Supplement 269 *Krogh, Palle* Causal Associations of Mycotoxic Nephropathy Pp 28 1978 (Section A)
- Supplement 270 *Clemmesen, Johannes Johannes Fibiger* Gongylonema and Vitamin A in Carcinogenesis Pp 13 1978 (Section A)
- Supplement 271 *Berthold, Peter and Berthold, Claes-H* Immuno Electron Microscopic Identification of a Dental Plaque Microorganism - *Streptococcus mutans* Pp 37 1978 (Section B)

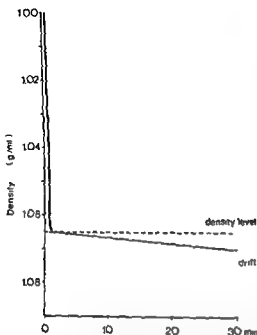


Fig 1 The behaviour of a tissue in a density column. The tissue sinks rapidly to its buoyant density level. If the gradient medium interferes with the tissue there will be a more or less pronounced drift in density with time.

10 to 60 sec depending on the size of the object. The only exception was the fall in the silicon gradient, which was prolonged for up to 5 min due to the... gradient the same density value was recorded within the accuracy of the technique.

The second phase consisted of a drift in density which was more or less pronounced. Following the drift frequent density readings were made during the first 30 min. In some gradients the drift was registered for up to 3 h.

Comparison of the Buoyant Densities Measured in Different Gradients

When the same gland was measured in different gradients the initial buoyant density was almost the same irrespective of the gradient liquid used. However in liquids with a pronounced drift the reading of the proper density level was greatly disturbed.

Measurements in Organic

an
No

bromobenzene/kerosene. A similar but less marked effect was seen in carbon tetrachloride/kerosene. When the effect was followed for up to 3 h, it could be seen that the fat tissue was influenced more than the glandular tissue, in accordance with the explanation that the drift is due to extraction of lipids from the tissue specimens or penetration of the gradient medium into lipid compartments.

Measurements in Silicon Oil

Fat tissue was studied in silicon oils and the drift in density was negligible (Fig. 3). The equilibration of the tissue in the column was slow, owing to the high viscosity of silicon. The high viscosity also made this gradient more easily subject to convection and somewhat less stable than other gradients when used repeatedly.

Measurements in Aqueous Gradients

Curves showing the density drift of parathyroids in gradients of sucrose, Ficoll and Percoll are given in Fig. 4. The change in density of the tissue was clearly related to the osmolarity of the gradient medium (see Fig. 5). In sucrose gradients, tissues with an original density of <1.03 drifted towards lower densities, and those with original densities of >1.03 moved towards higher densities. The osmolarity of sucrose at a density of 1.034 is 300 mOsm/l, which is the physiological osmolarity of

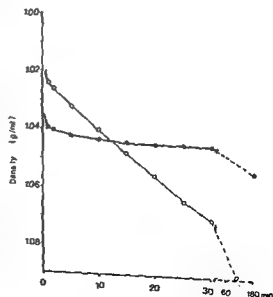


Fig 2 Density drift of parathyroid glands in organic solvents.

○—○ bromobenzene/kerosene
●—● carbon tetrachloride/kerosene

variations in the gradient could also be more thoroughly investigated by studying drift curves in Percoll columns of different osmolarities

As parathyroid glands sometimes contain fat tissue in such an amount that the density is less than 1.0 g/ml gradient liquids that can be used for estimation of densities below 1.0 g/ml were also investigated

MATERIALS AND METHODS

Tissues

Human parathyroid glands (weight 12–90 mg) and pieces of human fat tissue (weight 10–100 mg) were obtained from operation or autopsy cases. These tissues cover the density range 0.91–1.06 g/ml (Åkerström *et al.* 1979 a)

Chemicals

Bromobenzene, carbon tetrachloride, kerosene and sucrose (analytical reagent grade) were purchased from AB Kobo, Stockholm, Sweden. Ficoll[®] and Percoll[™] were obtained from Pharmacia Fine Chemicals AB, Uppsala, Sweden, and silicon oils from Dow Corning, Brussels, Belgium.

Gradient Formation

Using an automatic variable gradient former (MSE Crawley, England) linear density gradients (35–40 cm high) were made in glass cylinders from two liquids of different densities.

Gradients in the density range 1.00–1.08 g/ml were obtained by mixing water for a salt solution) with 20% (w/w) sucrose, 28% (w/w) Ficoll or 80% (v/v) Percoll* dissolved in water for the corresponding salt solution).

Gradients in the density range 0.92–1.00 g/ml were made by mixing the two types of silicon oil 200/5 cs and 510/50 cs. Organic solvents were used for the complete density range 0.92–1.08 g/ml. These gradients were made from carbon tetrachloride/kerosene (1.49 v/v) and carbon tetrachloride/kerosene (1.18 v/v) or alternatively from bromobenzene/kerosene (1.26 v/v) and bromobenzene/kerosene (1.14 v/v).

Bacterial growth in aqueous gradients was prevented by the addition of 0.02% sodium azide to the solutions.

Calibration of the Columns

The gradients were calibrated with ~ 50 µl drops of solutions insoluble in the gradient liquids (Ficoll, Percoll and sucrose gradients were calibrated with organic solvents, Silicon oil gradients were calibrated with mixtures of methanol and glycol). Organic solvent gradients were calibrated with sucrose solutions. The densities of the test solutions were determined in a DMA 02C digital density meter (Anton Paar, Graz, Austria). Ocular registration of the position of a drop in the gradient could be made with an accuracy of ± 1 mm, which allowed a precision in the calibration of 0.001 g/ml. As this accuracy was sufficient for our purpose, cathetometer readings were considered unnecessary (with

cathetometer readings the density can be estimated with an accuracy of 10⁻¹ g/ml Oster & Yamamoto 1963). A more convenient calibration was achieved with special coloured spheric glass floats with a diameter of approximately 4 mm (Scientific Glass Co, Bloomfield, New Jersey, USA). The densities of the floats were correct within 0.001 g/ml when tested against calibration solutions.

The gradients were recalibrated at frequent intervals and the stability was very good even when in constant use they remained linear for as long as 3–6 months.

To evaluate the effect of temperature, the column was calibrated at room temperature (+20° ± 1°C) and at +4°C.

Determination of Osmolarity

The osmolarity of aqueous gradient media was determined as a function of density by estimating the freezing point depression with an osmometer (Advanced Instruments Inc, Newton Highlands, Mass, USA).

Determination of Tissue Densities

Parathyroid glands and pieces of fat tissue were allowed to sink in the gradients and their positions were registered at the end of the fall (Oster & Yamamoto 1963). Any drift in position was recorded by frequent readings for 30 min–3 h.

The influence of the osmolarity of the gradient medium on the tissue density was tested in Percoll columns with osmolarities of 200, 300, 400, 600 and 800 mOsm/l, respectively. The osmolarity of a pure Percoll solution is 10 mOsm/l and the adjustments were made by addition of sodium chloride (Periofi & Laure 1977).

Penetration of Tissues by Percoll

Penetration of parathyroid glands and fat tissue by Percoll was tested with the use of ¹²⁵I labelled Percoll (Periofi & Kjellen 1978). Small pieces of the respective tissues (weight 32 to 85 mg) were incubated in the radioactive solution (2.2 × 10⁶ cpm/3 ml) for time varying between 30 min and 26 h. They were then washed lightly three times in physiological saline and transferred into 3 ml plastic tubes and the ¹²⁵I radioactivity was counted in a Packard model 578 auto gamma scintillation spectrometer with a well type crystal detector.

RESULTS

General Aspects of Density Measurements of Biological Material in a Gradient Column

The movement of an object in the density column is illustrated in Fig. 1. In the first phase the material sank rapidly to its buoyant density level, i.e. within

* Density of undiluted Percoll without additives = 1.130 g/ml

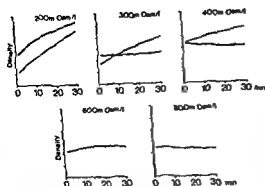


Fig 6 Density drift of parathyroid glands in Percoll gradients of different osmotic pressures (Density scale in interval 0.001 g/ml)

— fresh parathyroid glands
- - - parathyroid glands autolysed for 24-48 h

300 mOsm/l) it became rehydrated and a drift towards its original density was observed

Effect of Temperature on Tissue Densities

When the same tissue was placed in a Percoll gradient at 20°C or 4°C the difference in density was approximately 0.004 g/ml. Normal variations at room temperature will therefore have only an insignificant effect on the measurements

Penetration of the Tissues by Percoll

Both parathyroid glands and fat tissue were exposed to radioactive Percoll for varying lengths of time. The amount of radioactivity found in the tissues was low and changed very little with time (Table 1) indicating that the radioactivity derived from Percoll which had adsorbed to the surface

rather than from diffusion of Percoll into the tissue. If Percoll had equilibrated evenly through the whole tissue and with the same concentration as in the gradient, the radioactive counts would have been in the order of 10^4 cpm.

Results of Density Estimations of Parathyroid Glands and Fat Tissue

The parathyroid glands investigated varied in density between 0.96 and 1.06 g/ml, higher values being recorded for glands rich in parenchymal cells and lower ones for those rich in fat.

The fat tissue varied in density between 0.92 and 0.96 g/ml, with a mean value of $0.93 \text{ g/ml} \pm 0.01$.

DISCUSSION

The density gradient column technique was found to be a simple and sensitive method for measuring the density of biological tissues. With 0.4 m high columns, density values that were accurate within 0.001 g/ml were obtained simply by ocular determination of the position of the object at equilibrium. The use of coloured glass floats made the calibration of the gradients easy and the results reproducible. The measurements could be made at

any medium with density up to 1.1 M NaCl. The density of fresh parathyroid glands remained constant when they were floating in the Percoll gradient for 24 h.

TABLE 1 Penetration of ^{125}I Percoll in Two Parathyroid Glands and Two Pieces of Fat Tissue Incubated for Different Lengths of Time in 3 ml of 23% (w/w) ^{125}I Percoll with a Radioactivity of 2.2×10^4 cpm/3 ml

Tissue	Weight (mg)	Radioactivity cpm			
		30 min	60 min	18 h	26 h
Parathyroid gland	32	32	30	41	49
Parathyroid gland	41	30	30	61	111
Fat	82	41	72	28	37
Fat	111	56	77	52	90

indicated that no Percoll entered the tissue. An advantage was that in dehydrated glands normal hydration was restored in the Percoll gradient, which simplified the biological sampling before the measurements.

The Percoll gradients could also be used as tissue osmometers. By varying the sodium chloride concentration in the gradient it was possible to titrate out the osmolality of the medium, which was approximately in equilibrium with that of the tissue. The present technique clearly demonstrates the effects of osmotic pressure variations on registered tissue density. These effects should also be kept in mind in density determinations using centrifugation techniques (Pertoff & Laurent 1977).

For measurements of human tissue densities of less than 1.0 g/ml, no similar ideal gradient liquid was found. Silicon oil did not interact noticeably

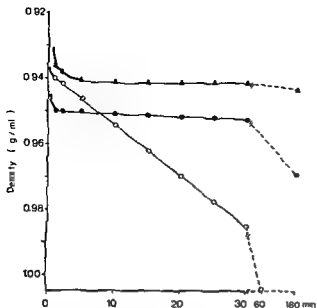


Fig 3 Density drift of fat tissue in organic solvents and silicon oils

○—○ bromobenzene/kerosene
●—● carbon tetrachloride/kerosene
▲—▲ silicon oil

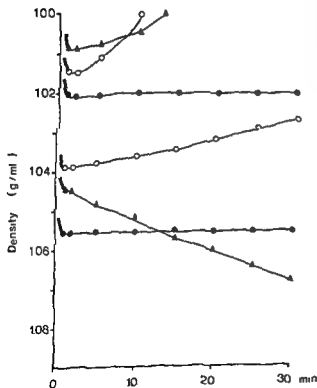


Fig 4 Density drift of parathyroid glands in aqueous media

▲—▲ sucrose
○—○ Ficoll
●—● Percoll

the parathyroid gland (see below). Apparently, tissue becomes hydrated at low and dehydrated at high osmolarities. The behaviour in Ficoll is similar, although the osmolarity in this gradient never exceeded the physiological osmolarity, while in Percoll an upward drift for all measured glands was observed. Ficoll gradients can of course be made isotonic if a salt gradient is applied, but no attempt was made to do this.

The experiment with Percoll described in Fig 5 was performed with a sodium chloride concentration of 0.15 M all through the column (300 mOsm/l). As seen in Fig 5, this gave an almost constant osmolarity in the gradient, as the contribution of Percoll is very low (Perloff & Laurent 1977). Under these conditions, no drift was observed during the observation period.

Determination of the Iso-Osmolar Conditions for Parathyroid Glands in Percoll

The possibility of keeping the osmolarity constant throughout a Percoll gradient was utilized by titrating out the iso-osmolar salt concentration of the tissue. Fresh and autolysed tissues were studied in density columns containing sodium chloride at different concentrations. As seen in Fig 6, fresh glands had osmolarities of about 300 mOsm/l, while glands autolysed for 24–48 h had osmolarities of 600–800 mOsm/l.

An observation with some practical relevance was made on partly dried tissues. It is sometimes difficult to prevent evaporation in the sampling of tissues. However, when partly dried tissue was studied in a gradient medium with an osmolarity of

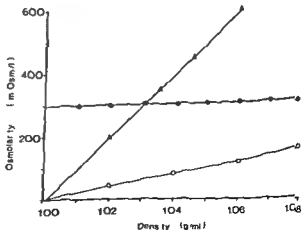


Fig 5 Osmolarity in aqueous gradients as a function of density

▲—▲ sucrose
○—○ Ficoll
●—● Percoll

ASCITES TUMORS IN CBA MICE

2 Ultrastructural Aspects on Ascites Conversion

WALTER RYD and BJÖRN HAGMAR

Institute of Pathology and Department of Clinical Cytology Sahlgren Hospital Göteborg Sweden

Ryd W & Hagmar B Ascites tumors in CBA mice 2 Ultrastructural aspects on ascites conversion
Acta path microbiol scand Sect A 87 97-107 1979

We have studied four syngeneic murine tumors a fibrosarcoma a squamous cell carcinoma and their two ascites-converted counterparts by transmission electron microscopy The ascites tumors were

disseminated junctions This we think is a prerequisite for ascites growth But the ascites tumors show no peculiar ultrastructural features in comparison with other undifferentiated malignant tumors We found no morphological cell alterations by the enzymatical dissociation procedure used to bring the solid tumors into suspension Differences between the AS and AA tumors can be ascribed to differences in proliferation rates

Key words Ascites tumors ultrastructure CBA mice

W Ryd Dept of Clinical Cytology Sahlgren Hospital 413 45 Göteborg Sweden

Received 19 iv 78 Accepted 8 viii 78

Ascites tumors are used in many fields of experimental tumor research because they have certain advantages over solid tumors (cf Klein G 1951 Klein E 1955) Most importantly these tumors grow fast and are easily harvested in large amounts The dispersion procedures applied to solid

tumors in CBA mice primarily to study metastasis formation (Hagmar and Ryd 1978 Ryd and Hagmar 1978)

The transformation of solid tumors to ascites

It still remains to be discovered about how ascites conversion affects other properties of the tumors especially their morphology metastasizability and pattern of metastasis all of which may differ significantly from those of their solid progenitors (Mellgren *et al* 1966 Hagmar 1974 a-c) The factors governing metastasis spread present in particular an area in which research must treat new ascites tumors as distinct from their solid ancestors (Hagmar and Ryd 1974)

The present study describes the ultrastructure of four tumors with known transplantability and metastasizing properties a fibrosarcoma and a squamous cell carcinoma and their ascites transformed counterparts All four tumors were studied in syngeneic CBA mice

tumors are cells proliferate singly or in small aggregates intraperitoneally (i.p.) There is no need for enzymatical or mechanical dispersion procedures to obtain a cell suspension Consequently ascites tumors are more suitable than solid tumors for studies on cell surface characteristics growth

with the tissues and is therefore preferable to organic solvents. The high viscosity of silicon oil however prolongs the measurements and the gradient is more easily subjected to convection when used for repeated measurements. Organic solvents exhibit fat solvating and perhaps also dehydrating effects (Miller & Gasek 1960). These effects were considerably less pronounced in carbon tetrachloride/kerosene gradients than with bromobenzene/kerosene. Neither silicon oil nor organic solvents normalized dehydrated tissue. The accuracy of measurements in these liquids is therefore somewhat reduced.

The technique described in this report has already been used in our department in the histopathological evaluation of parathyroid glands. Biopsies of parathyroid adenomas and hyperplastic glands examined hitherto have all shown a higher density than normal glands. In a simultaneous investigation of the parenchymal cell content of glands with an image analyzing computer technique (Grimelius *et al.* 1978) a linear correlation between glandular density and parenchymal cell content has been demonstrated (Åkerström *et al.* to be published 1979). The density gradient technique can therefore be used for rapid determination of the relative parenchymal cell content of parathyroid glands. The simplicity and reproducibility of the method suggest that it could be useful in routine parathyroid diagnosis. Further evaluation is needed however to establish the correlation between density and parenchymal cell content for different parathyroid glands. Thereafter it should be possible to determine the exact density - i.e. parenchymal cell content - that distinguishes normal and abnormal parathyroid glands.

Supported by the Swedish Medical Research Council project No B77 17X 04787 02 and project No 03X 04

REFERENCES

- 1 Miller G I & Gasek J Mc G. Drift of drops in density gradient columns. *Anal Biochem* 1 78-87 1960
- 2 Oster G & Yamamoto M. Density gradient techniques. *Chemical Reviews* 63 257-268 1963
- 3 Pertofi H & Laurent T C. in *Methods in cell separation* (N Catsimpoolas ed) Vol 1 25-65 Plenum Press New York 1977
- 4 Pertofi H & Kjellen L. Radioactive labelling of Percoll. *Anal Biochem* 88 283-284 1978
- 5 Wang C & Rieder S V. A density test for the
 6 Lundqvist H. Estimation of the parenchymal cell content of the parathyroid gland using density gradient columns. *prel report Acta path microbiol Scand Sect A* 85 555-557 1977
- 7 Åkerström G, Grimelius L, Fridh C & Johansson H. Estimation of parenchymal cell mass of parathyroid glands by a volumetric technique (accepted for publ.) *Ups J Med Sci* 1979 a
- 8 Grimelius L, Åkerström G, Johansson H & Lundqvist H. Estimation of parenchymal cell content of human parathyroid glands using the image analysing computer technique. *Am J Pathol* 93 793-799 1978
- 9 Åkerström G, Grimelius L, Johansson H, Lund

TABLE 2 Summary of Ultrastructural Features of the MCB21 and MCB31 Tumours in Solid Form (SS/SC) Solid Asclates Form (AS) and Asclates Form (AA)

	21-SS	21-AS	21-AA	31-SC	31-AS	31-AA
Differentiation	undiff	undiff		spinocell	undiff	
Cell size μm	8-15	10-15	15-22	15-20	10-18	12-25
Form of nucleus	ovoid slightly irregular	ovoid slightly irregular	beanshaped	irregular	beanshaped slightly irregular	beanshaped
Number of nucleoli	1-3	1-3	1-3	1-2	1-2	1-2
Polysomes/ribosomes	++	+++	+++	+++	+++	+++
RER	+	+	+	+	+	+
Golgi complex	+	++	++	+	++	++
Mitochondria no per section	10-20	20-40	20-50	15-30	15-30	20-40
Microfilaments	++ unorganized	+++ unorganized	+++ unorganized	+++ tonofilaments	+++ unorganized	+++ unorganized
Intercell junctions	no	no	no	desmosomes	no	no
Intercell collagen	+	+		+	+	
Microvilli/ruffles						
Solid tumor	+	(+)		++	+	
Suspens on	+	(+)	++	++	+	++
Blebs	++	+	+	++	+	+

Many cells contain an unorganized meshwork of filaments (≈ 10 nm) concentrated in the perinuclear region. Microfilaments (≈ 6 nm) occur predominantly submembranously. The tumor cells do not form any intercellular junctions and are never closer to each other than about 200 Å. The intercellular gap is sometimes as wide as 2 μm . In this space there are small amounts of collagen and granular deposits. The cells have a few short microvilli or ruffle like protrusions. Usually there are 3-5 such projections not longer than 2 μm in central sections.

The tumor cells in enzymatically produced suspensions are spherical and have an eccentrically located nucleus. The ribosomes are mainly single and not aggregated in polysomes as in the solid tumor. Other cytoplasmic organelles look like those in the solid tumors.

In SEM most of the cells are spherical and only a few are ovoid or irregular (Fig. 5). SS cells show considerable variation in the appearance of the cell surface. Some SS cells are smooth and naked, others are covered with small projections and a few blebs.

The MCB21 AS tumor is similar to the SS tumor. AS cells however contain more polysomes and single ribosomes. The Golgi complex is better developed and larger, composed of 3-5 stacks of flattened sacs. There are more mitochondria in AS cells but their morphology resembles those in SS cells. Unorganized filaments are more numerous in AS. In sections from solid tumors AS cells have even fewer ruffle or microvilli like protrusions (< 3 μm) than SS cells. The intercellular space in AS however is similar to that in SS (Fig. 2).

The only intracellular difference between MCB21 AS in suspension and in solid form is a disaggregation of the polysomes in the dissociated cells.

In SEM the AS cells are usually spherical (Fig. 6). The cell surface is slightly irregular and has low ridges. Only a few cells have some short microvilli (< 1 μm). About 25 per cent of the cells have blebs. We have seen no ruffle like projections.

MCB21 AA cells (diameter 12-15 μm) are larger than both SS and AS cells. The cytoplasmic organelles are similar to those in AS cells except that microtubuli, which are present in all cell types, are more prominent in AA. The ribosomes occur

MATERIAL AND METHODS

The solid tumors, MCB21 and MCB31, were induced in syngeneic CBA mice by gastric feeding of 20 methylchoanthrene (Hagmar and Ryd 1978). MCB21-SS (solid sarcoma) was originally a differentiated fibrosarcoma. But by repeated s.c. transplantations it has become less differentiated and more polymorphic. MCB31-SC (solid carcinoma) was at first a well differentiated squamous cell carcinoma. It has also grown less differentiated during transplantations, but it has kept its spinocellular pattern and is still moderately differentiated and keratin producing in gen. 38. To obtain ascites tumors from 21-SS and 31-SC we followed the method described by G. Klein (1951) i.e. serial i.p. transplantation of tumor mince. When after several transplantations the tumors become transplantable with ascites only and fulfil certain criteria (Hagmar 1974 a) we consider them ascites tumors. The first transplant generation of the MCB21 and 31 ascites tumors (MCB21-AA and MCB31-AA) correspond to the solid gen. 26 and 45 respectively. Both tumors grow as solid tumors when transplanted intramuscularly (i.m.) or subcutaneously (s.c.) (AS-tumor = ascites solid).

In our present work, we studied the SS/SC tumors and AS tumors both in solid form and in enzymatically-

produced suspensions. Table 1 gives the transplant generation used and number of days after transplantation. The solid tumors were fixed *in situ* by cardiac or aortic perfusion. Tumor-bearing animals were anesthetized with ether and the thorax opened. Warm (37°C) fixative (2.5% glutaraldehyde containing 0.10 M sucrose and 0.10 M Na cacodylate) (Collins *et al.* 1977) was used, with a perfusion pressure of about 100 cm H₂O. The pH of the fixative was 7.2, the total osmotic pressure 560 mOsmol and the osmotic pressure of the vehicle (sucrose and Na cacodylate) 300 mOsmol.

We produced tumor cell suspensions from solid tumors according to Wietjes and Prop (1970) using pronase, collagenase and hyaluronidase. After enzyme treatment the cells were spun down and fixed as ascites tumor cells (*vide infra*).

The ascites tumor cells were harvested from ether-anesthetized mice and immediately fixed by injection into warm (37°C) glutaraldehyde with Na-cacodylate and sucrose.

For transmission electron microscopy, samples from all solid tumors and tumor cell suspensions were postfixed in OsO₄, dehydrated and embedded in Epon. Ultrathin sections were stained with uranyl acetate and lead citrate.

For scanning electron microscopy, fixed cells in suspensions of SS/SC, AS and AA were allowed to settle onto albumin-coated cover slips. The cells were dehydrated with ethanol and acetone and dried by the critical point method using liquid CO₂ (Polaron). The dehydration schedule was 50 and 70% ethanol, 70, 75, 80, 85, 90, 95, 100% acetone. The ethanol or acetone was changed several times at each step. After drying the specimens were covered with a 360 Å thick gold film in a sputter ion equipment (Polaron E5000). The acceleration voltage in the electron microscopes was 60 kV for TEM and 10–20 kV for SEM.

TABLE 1 Transfer Generations of the MCB21 and MCB31 Tumors Used for Transmission and Scanning Electron Microscopy

	TEM solid tumor suspension		SEM
MCB21 SS	61 (22) 63 (13)	68 (21)	41 (21) 68 (22)
MCB21 AS	3 (18) 13 (8)	6 (13)	6 (13) 9 (8)
MCB21 AA		6 (7) 8 (6) 8 (7)	8 (6) 43 (6)
MCB31 SC	41 (21) 45 (16)	49 (17)	40 (17) 49 (18)
MCB31 AS	16 (8) 18 (8)	6 (13)	5 (13) 6 (13)
MCB31 AA		7 (6) 17 (7) 19 (7)	7 (6) 7 (6) 26 (7)

The AS tumors were always investigated in the first generation after s.c. ascites injection and the figures indicate the AA generation used to produce the tumor. Figures in brackets give the tumor growth time in days.

RESULTS

A summary of the results is given in Table 2.

MCB21

MCB21-SS comprised of polymorphic 10–15 µm cells. As seen in TEM they have a large nucleus with prominent nucleoli (Fig. 1). The cytoplasm contains a large amount of ribosomes both as polysomes and single ribosomes. The RER and the Golgi complexes (1–3 stacks) are poorly developed. In central sections the cells usually show 10–20 mitochondria which are very irregular and which vary from spherical to rod shaped (2–3 µm long). The density and length of the mitochondrial cristae also vary. Ballooned and degenerated mitochondria are regularly seen, as are the debris of mitochondria in phagosomes. Such abnormal mitochondria occur frequently in solid tumors but the mitochondrial changes seem to be reversible and to reflect a lack of adequate nutrition (Bernhard 1969, Birbeck 1976).



Fig 5 MCB21 SS (gen 41) The variation in cell surface features is evident: naked cells; cells with short microvilli; ridges and/or blebs are seen. $\times 3500$

Fig 6 MCB21 AS (gen 9) The cells have a slightly irregular surface with few or no microvilli. $\times 3300$

Fig 7 MCB21 AA (gen 43) All cells have short microvilli with a slight variation in number. $\times 2500$

Fig 8 MCB31 SC (gen 40) The cells vary: either naked or covered with microvilli or blebs. $\times 3000$

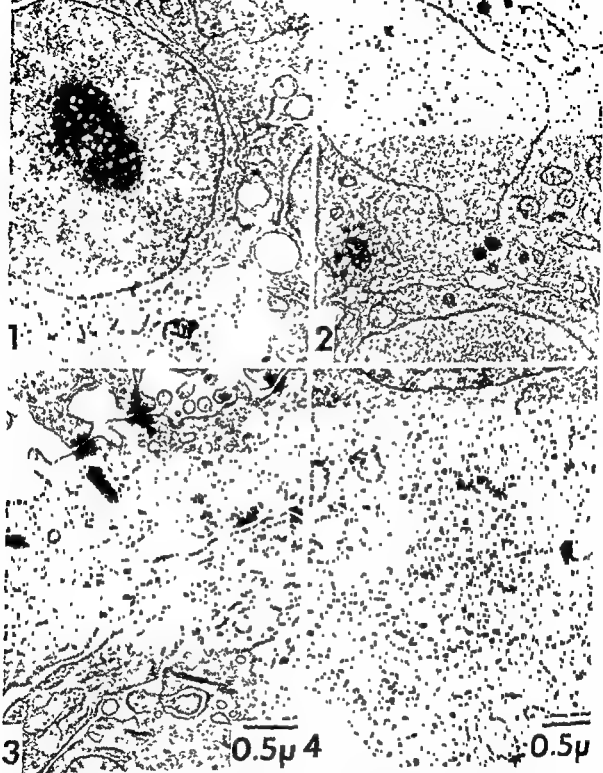


Fig 1 MCB21-SS (gen 61) The tumor cells have large nuclei with prominent nucleoli. A few microvilli protrude into the intercellular space which is narrow in this picture. No intercellular junctions are seen $\times 7000$

Fig 2 MCB21-AS (gen 13) The nucleoli are large and their diameters exceed half the cell diameter. The cell protrusions into the intercellular space are fewer than in 21-SS $\times 10000$

Fig 3 MCB31-SC (gen 41) The spinocellular differentiation of this tumor is evident, with numerous desmosomes and tonofilament bundles. Near the upper margin there are many microvilli in the intercellular space. Note the desmosome on a microvillus near the upper right corner $\times 24000$

Fig 4 MCB31-AA (gen 19) The cells have a well-developed Golgi complex. A microtubule runs longitudinally $\times 24000$



Fig 11 The picture shows a MCB31 AS tumor cell without microvilli but with a few blebs. The intracellular organelles are well preserved. Compare with fig 12 and 13. $\times 14000$



Fig 12 MCB31 AS (gen. 13). Most cells are smooth but some cells have blebs or microvilli. $\times 2400$



Fig 13 MCB31-AA (gen. 26). All cells have short microvilli. The number of villi is more constant than on 31 SC cells (fig. 8). $\times 4900$



9



10

Fig 9 MCB21-AA (gen 8) The Golgi complex adjacent to the nucleus is well developed. Note the meshwork of microfilaments in the center of the cell $\times 12500$

Fig 10 MCB31-AS (gen 18) The intercellular space is as irregular as in SC (fig 7), but no desmosomes are observed. In the upper left corner a nucleus is cut peripherally and the pores in the nuclear membrane are clearly visible. The Golgi complex in that cell is rather well developed. To the left of the Golgi apparatus there are some filaments $\times 13000$

al 1968), in benign cells *in vivo* (Ghadially and Roy 1969) and *in vitro* (Biberfeld 1971). The accumulation of filaments has been interpreted on the one hand as a degenerative phenomenon (Ghadially 1975) or on the other as an indication of increased metabolic activity in an active or neoplastic state (Hamed and Morgan 1972). Our findings would seem to support the latter hypothesis.

The AS cells in enzymatically produced suspensions have much fewer microvilli than the corresponding AA cells. We do not think that this difference in cell surface morphology reflects a damage to AS-cells. Transplantability tests with enzyme treated AA-cells and enzymatically dissociated AS-cells do not indicate any serious cell damage, but the cells grow from the same cell number as untreated AA cells (Ryd and Hagmar 1978, Ryd in preparation). The viability of enzyma-

Boeryd et al (1968) reported that the MCG1-AS tumor has a wider intercellular space than MCG1-SS. Yoshida (1964) described AS tumors as a colony of free cells in a pre-existing normal stroma. This is a finding we cannot confirm in our systems, where normal stroma cells were conspicuously absent. Of course there may be differences among ascites tumors in this respect. E. Klein (1955) reported that some ascites tumors always grow up as a suspension, while others give rise to a solid peritoneal carcinosis if the cell inoculum is small. This result, in turn, may depend on each tumor's ability to elicit stroma formation and establish stable cell contacts. By our present methods, we detected only occasional macrophages in the tumors.

If the cohesive forces were lower in AS tumors

duced number of microvilli on AS cells may effect a lower proliferation rate (*vide supra*) but may also be due to cellular effects of the enzymes used in the dissociation procedure. Widely used for dissociation of both solid tissue and *in vitro* growing cells proteolytic enzymes such as trypsin and pronase are known to alter both the cell surface and intracellular structures (Edwards and Fogh 1959, Waymouth 1974, Masson-Pévet et al 1976). Yet in our systems, the number of cell protrusions in the solid tumors is similar to the number of microvilli and ridges on the same

Fu
mi

damage such as swelling of mitochondria and degranulation of the RER (Waymouth 1974, Masson-Pévet et al 1976). There is however a disaggregation of polysomes into single ribosomes. Such a disaggregation is generally considered to indicate a lowered protein metabolism (Ghadially 1975). During the dissociation procedure, pieces of tumor are devoid of their perfusion and kept in a balanced salt solution without serum. We think this slows down the cell metabolism which in turn, disaggregates the polysomes. The absence of morphological alterations by the enzymes we use would agree with Waymouth (1974) and with Masson-Pévet et al (1976). It must be kept in mind however that enzymes may alter cell membranes chemically if not morphologically by digesting surface material or by adhering to cell surfaces (cf Waymouth 1974, Hagmar and Ryd 1975).

The intercellular space is similar in our SS-SC and AS tumors. In this respect our results agree with Bergstrand and Ringertz (1960). However,

fact have a greater tendency to spread by the lymph than 21-SS (Hagmar and Ryd 1978). Between the MCB31 tumors the difference is even more evident. 31-AS gives rise to lymph node and pulmonary metastases, while 31-SC does not metastasize at all. MCB31-SC and AS are transplantable *iv* with equal cell doses (Ryd and Hagmar 1978), so it is unlikely that the differences in spontaneous metastasizability depend on differences in cell survival among released cells. Instead, we must ascribe the increased tendency of AS tumor spread to a difference in cell release from the solid primaries. Since the stroma appears to be similar in all tumors, we think that loss of intercellular cohesion among tumor cells (Coman 1954, Birbeck 1976) is greater in AS tumors. Specifically, we noted the lack of desmosomes in 31-AS. We think that loss of stable intercellular junctions is a pre requisite for conversion of a solid tumor into ascites form. E. Klein (1955) demonstrated that this conversion implies the selection of a genetically altered tumor cell clone.

Microvilli are dynamic structures of the cell surface and are considered a membrane store. They increase in number in S and G2 (Knutton et al 1975) and they diminish in number when circulating cells get trapped in tissue (van Ewijk et al 1976) or when cells settle onto a surface, even though the total cell surface is unaltered (Erickson and Trinkaus 1976).

To give rise to tumor metastases, circulating tumor cells must overcome the electronegative repulsive forces between the tumor cell surface and the endothelium. Weiss (1967) has suggested that this is done by surface protrusions like ruffles and microvilli. Sindelar et al (1975) found ultrastructural evidences that *iv* injected tumor cells first

both as polysomes and single ribosomes in the same proportion as in the solid AS tumor (Fig 9)

In SEM the cells are spherical with short microvilli ($<2\text{ }\mu\text{m}$) and ridges evenly distributed over the cell surfaces (Fig 7). The number of microvilli varies among different cells but AA cells have far more microvilli than both AS and SS cells in suspension. A few AA cells ($<5\%$) have blebs which cover the entire cell surface. Few cells have ruffles.

MCB31

MCB31 SC cells are large with a diameter of $15\text{--}20\text{ }\mu\text{m}$. The nucleus is wrinkled. The cytoplasm contains many polysomes and free ribosomes. The RER and the Golgi complex are poorly developed. There are many tonofilament bundles generally surrounding the nucleus. But there are also bundles running at right angles to the cell surface terminating in prominent desmosomes (Fig 3). The cell surface is uneven with broad ribosomes containing projections which make the extracellular space irregular. Our impression is that collagen although present is scantier than in 21-SS. In addition to ribosome-containing extensions many microvilli ruffles ($<2\text{ }\mu\text{m}$, $5\text{--}10/\text{section}$) protrude into the intercellular space.

Except for a disaggregation of polysomes the SC cells in suspension are quite similar to the cells in solid tumors.

In SEM tumor cells in enzymatically produced suspensions are spherical. The configuration of the cell surface varies but most cells have many microvilli ($<3\text{ }\mu\text{m}$). About thirty per cent of the cells have blebs. No ruffles appear (Fig 8).

MCB31 AS cells are smaller than SC cells, being $10\text{--}18\text{ }\mu\text{m}$ in diameter. The nucleus is bean shaped and not as convoluted as in SC. The Golgi complex is larger than in SC and composed of 5–6 stacks of flattened sacs (the SC cell holds 1–3 stacks). There are numerous unorganized whorls of filaments especially in the perinuclear region. There are no tonofilament bundles or desmosomes. So the tumor in contrast to 31-SC lacks spinocellular differentiation. The extracellular space is similar to that in SC except that it lacks intercellular junctions. Microvilli ruffles however are much scarcer and shorter ($<1\text{ }\mu\text{m}$) in AS cells (Fig 10).

The AS cells in suspension contain mainly single ribosomes while the tumor cells in the solid tumor mainly contain polysomes.

In suspension the AS cells in SEM show a smooth surface or just a few ridges. Only occasional cells have short microvilli or blebs (Fig 11, 12).

MCB31 AA cells are large ($12\text{--}25\text{ }\mu\text{m}$) and spherical. The cytoplasmic organelles are similar to

those in AS cells. As in MCB21 microtubuli are more prominent in AA cells than in SC and AS cells. Where a centriole is observed microtubuli often run towards it (Fig 4).

In SEM all AA cells have short microvilli and low ridges. The average AA cell has as many villi as an SC cell does but among the AA cells the variation is less and the villi are shorter (Fig 13).

In agreement with our light microscopy studies (Hagmar and Ryd 1978) we found almost no stroma in the tumors except for scattered small blood vessels. Nor have we seen any virus particles in the tumor cells.

DISCUSSION

MCB21 SS is histologically a de-differentiated fibrosarcoma and its ultrastructural appearance agrees with other poorly differentiated fibrosarcomas (Clarke 1969).

MCB31 SC retains a squamous cell differentiation through serial transplantation (Ryd and Hagmar 1978). This is confirmed by electron microscopy where we find tonofibrils and well-developed desmosomes. MCB31 AS however is a quite undifferentiated tumor like the other ascites tumor MCB21 AS.

The cells of the two AS tumors have a larger Golgi complex than that found in the corresponding SS/SC cells. The AS cells also contain more mitochondria and ribosomes. We interpret these differences as a part of a more rapid cell proliferation and membrane turn over in the AS tumor. The RER is small in all tumors; none of them seems to show secretory activity.

The AA cells of both tumors appear larger than the corresponding AS cells. This finding agrees with cell volume determinations (Ryd and Hagmar 1978). The AA cells also contain more mitochondria than the AS cells and in addition have more microvilli. We know that the cell volume increases when cells enter the S and G₂ phase and the number of microvilli increases in G₂ (Knutson et al 1975). Thus the differences between AA and AS cells may also be interpreted as arising from differences in cell proliferation. This is reasonable since the AA cells were fixed in a phase of logarithmic cell proliferation while the AS cells were taken from solid tumors. Here we know that cell division is logarithmic only in well vascularized parts of the tumors (Tannock 1968).

The AS and AA cells have many filaments concentrated in the perinuclear region. Such filaments are described in other tumor cells (Brandes et al 1966; Bergstrand and Ringertz 1960; Boerj et

- Hagmar B & Ryd W MCG101 AA a new ascites tumor in C57 mice 4 Influence of enzyme treatment on transplantability and some *in vitro* characteristics Acta path microbiol scand Sect. A 83 328-338 1975
- Hagmar B & Ryd W Metastasis spread from syngeneic murine tumors Establishment of a test protocol for comparisons between ascites tumors and their progenitors Acta path microbiol scand Sect. A 86 231-239 1978
- Hamed K & Morgan D A Papillary adenocarcinoma of endometrium with psammoma bodies Cancer 29 1326-1335 1972
- Klein E Transformation of solid into ascites tumors Almqvist & Wiksells Boktryckeri AB Uppsala 1955
- Klein G The production of ascites tumors in mice and their use in studies on some biological and chemical characteristics of neoplastic cells Almqvist & Wiksells Boktryckeri AB Uppsala 1951
- Knutson S Sumner M C B & Pasternak C A Role of microvilli in surface changes of synchronized P815Y mastocytoma cells J Cell Biol 66 568-576 1975
- Masson Pevet M Jongsma H J & de Bruyne J Collagenase and trypsin-dissociated heart cells A comparative ultrastructural study J mol cell cardiol 8 747-757 1976
- Mellgren J Bartholdsson E Boeryd B & Norrby K A spontaneously metastasizing 20 methylcholant hrene induced rhabdomyosarcoma and its transformation to ascites form in the CBA mouse Acta path microbiol scand 68 535-546 1966
- Ryd W & Hagmar B Ascites tumors in CBA mice Comparisons between two new tumors a carcinoma and a sarcoma in solid and ascites form Manuscript 1978
- Sindelar W Tralka T S & Ketcham A Electron microscopic observations on formation of pulmonary metastases J Surg Res 18 137-161 1975
- Tannock J F The relation between cell proliferation and the vascular system in a transplanted mouse mammary tumour Br J Cancer 22 258-273 1968
- Waymouth C To disaggregate or not to disaggregate Injury and cell disaggregation transient or permanent? In vitro 10 97-111 1974
- Weiss L The cell periphery metastasis and other contact phenomena North Holland Publishing Company Amsterdam, 1967
- Wiepjes G J & Prop F J A Improved method for preparation of single-cell suspensions from mammary glands of adult virgin mouse Exptl cell res 61 451-454 1970
- Yoshida T Ascites tumors - Yoshida sarcoma and ascites hepatoma(s) Nat Cancer Inst Monograph 16 1964

adhere to the capillary endothelium by pseudopods and ruffle like protrusions

The AA tumor cells in this study are generally covered with microvilli and ridges, while the AS tumor cells in enzymatically produced suspensions are almost naked. In spite of this difference, the injected AS cells have the same virulence and the same tumor distribution pattern as the corresponding AA cells (Ryd and Hagmar 1978). This finding suggests that if cell protrusions are responsible for tumor cell adhesion to the endothelium they are not necessarily the same as microvilli on circulating cells. New protrusions may be formed when the tumor cells are trapped in capillaries (Domagala and Koss 1977).

Summing up our results, these ascites tumors present themselves as undifferentiated tumors. They do not possess peculiar ultrastructural features not present in other undifferentiated tumors. In contrast to its solid progenitor, MCB31-SC, MCB31-AS represents a dedifferentiated cell clone without desmosomes. Other ultrastructural differences between the ascites tumors and their progenitors may largely be ascribed to different growth kinetics in the tumors. The surface characteristics of the solid tumors may also be affected by enzymatic procedures required to bring the cells into suspension. We detected no specific such changes by our present methods, but the question will be further investigated by ultrastructural cytochemistry on our different tumor lines.

Dr Ulf Brunk and his collaborators are gratefully acknowledged for help and advice on scanning and transmission electron microscopy. We thank Miss Marianne Bremner and Miss Agneta Jacobsson for skilful technical assistance and Mrs Ann Cairn Bjornhede for typing the manuscript. Ass. prof. Michel Mullin has helped us to correct the English text.

The investigations were supported by grants from the Swedish Society of Medical Sciences and the Swedish Cancer Society No 465 B75 06X.

REFERENCES

Bernhard W. Ultrastructure of the cancer cell. In Lima de Faria A. (Ed.) North Holland Publ. Co. Amsterdam 1969.
 Bergstrand A & Ringert N. Electron microscopic examination of the MCIM tumor I and II. J Nat. Cancer Inst. 25: 501-545 1960.
 Biberfeld P. Cytotoxic interaction of phytohemagglutinin-stimulated blood lymphocytes with monolayer cells. A study by light and electron microscopy. Cell Immunol. 2: 54-72 1971.

Birbeck M S C. Ultrastructure of tumor cells. In: Found of oncology. Symington T & Carter R C (Ed.) Witham Heinemann medical books Ltd London 1976.
 Boerdy B, Lundin P M, Norrby K & Schelin U. Ultrastructure of a mouse sarcoma in its solid, enzymatically dissociated and ascitic forms. Int. J. Cancer. 3: 283-290 1968.
 Brandes D, Schonfeld B, Slusser R & Anton E. Studies of L1210 leukemia. I. Ultrastructure of solid and ascites cells. J. Nat. Cancer Inst. 37: 467-471 1966.
 Clarke M A. The fine structure of methylcholanthrene induced tumors in mice. Cancer. 24: 147-157 1969.
 Collins V P, Arbores B & Brunk U. A comparison of the effects of three widely used glutaraldehyde fixatives on cellular volume and structure. A TEM, SEM, volumetric and cytochemical study. Acta path. microbiol. scand. Sect. A. 85: 157-168 1977.
 Coman D R. Mechanisms responsible for the origin and distribution of blood borne metastases. A review. Cancer Res. 13: 397-404 1954.
 Domagala W & Koss L G. Configuration of surfaces of human cancer cells in effusions. A scanning electron microscopic study of microvilli. Virchows Arch. B. Cell Path. 26: 27-42 1977.
 Edwards G A & Fogh J. Micromorphologic changes in human amnion cells during trypsinization. Cancer Res. 19: 608-611 1959.
 Erickson C A & Trinkaus J P. Microvilli and blebs as sources of reserve surface membrane during cell spreading. Exp. Cell Res. 99: 375-384 1976.
 van Ewijk W, Brons N H C & Rozing J. Scanning electron microscopy of homing and recirculation lymphocyte populations. Cell Immunol. 19: 245-261 1975.
 Ghadially F N. Ultrastructural pathology of the cell. A text and atlas of physiological and pathological alterations in cell fine structure. Butterworths London 1975.
 Ghadially F N & Roy S. Ultrastructure of synovial joints in health and disease. Butterworths London 1969.
 Hagmar B. MCG101 AA, a new ascites tumour in C3H biol. scand. Sect. A. 82: 369-378 1974 b.
 Hagmar B. MCG101 AA, a new ascites tumour in C3H mice. 2. Protocol of *in vivo* transplantation studies in comparison with the solid (SS) and solid ascites (AS) tumours. Acta path. microbiol. scand. Sect. A. 82: 369-378 1974 b.
 Hagmar B. MCG101 AA, a new ascites tumour in C3H mice. 3. Studies of the spontaneous metastasis formation from the resectable solid ascites tumour in comparison with the solid tumour of origin. Acta path. microbiol. scand. Sect. A. 82: 379-385 1974 c.
 Hagmar B & Ryd W. Alterations of transplantation characteristics and metastasis patterns by ascites transformation of solid sarcomas. Abstracts 11th Int. Cancer Congress 636-637 1974.

THE ULTRASTRUCTURE OF LIPOSARCOMA

A Study of 10 Cases

LARS-GUNNAR KINDBLOM and JOHAN SAVE SÖDERBERGH

Department of Pathology Sahlgren's hospital University of Göteborg Sweden

Kindblom L G & Save Soderbergh J The ultrastructure of Liposarcoma A study of 10 cases Acta path microbiol scand Sect. A 87 109-121 1979

An ultrastructural study of 10 liposarcomas is reported. Four of the liposarcomas were wholly or predominantly of well-differentiated lipoma like or fibrosing type 3 of myxoid type 2 of round cell type and 1 of pleomorphic type. The well-differentiated lipoma like liposarcomas showed cells with a few large lipid droplets few organelles and a peripherally located fairly large nucleus. The well-differentiated liposarcomas of fibrosing type revealed mostly spindle-shaped fibroblast like cells with abundant rough endoplasmic reticulum and inconspicuous lipid inclusions surrounded by collagen. One well-differentiated liposarcoma contained an area which was similar to brown adipose tissue and hibernoma. The spindle and stellate shaped cells of the myxoid liposarcomas showed abundant rough endoplasmic reticulum and large smooth membraned vacuoles filled with moderately dense amorphous material which appeared to be extruded extracellularly by rupture of the vacuoles. Cytoplasmic lipid droplets were seen in most cells but were much less prominent than in the well-differentiated lipoma like liposarcomas. Ultrastructurally there were many similarities between the myxoid and round cell liposarcoma indicating a close relationship between the two types. The pleomorphic liposarcoma revealed cells with one or more large irregular nuclei numerous large vacuoles after dissolved lipids abundant dilated cisternae of rough endoplasmic reticulum and rounded electron-dense bodies corresponding to PAS positive hyalin globules seen in the light microscope. The ultrastructural study suggests that the variegated cellular appearance of the different subtypes of liposarcoma reflects the wide cellular spectrum seen during the differentiation of adipose tissue and supports the view that all liposarcomas histogenetically represent a single entity.

Key words Liposarcoma ultrastructure

L G Kindblom Department of Pathology II Sahlgren's hospital S-413 45 Göteborg Sweden

Received 5 vi 78 Accepted 7 ix 78

Liposarcoma is probably one of the most common malignant soft tissue tumours and several large series of cases have been studied with particular reference to the clinical radiographic and light microscopic appearances and prognosis (Eninger & Winslow 1962 Reszel *et al* 1966 Kindblom *et al* 1975). Liposarcomas may show considerable variation in histologic appearance and prognosis from highly differentiated lipoma like recurring but not metastasizing tumours to pleomorphic tumours which have a great tendency to metastasize and a bad prognosis. Histologically 4 main subtypes have been recognized well-differentiated of lipoma like and/or fibrosing type myxoid

round-cell and pleomorphic liposarcoma all of which may appear in pure or mixed forms (WHO Eninger *et al* 1969 Kindblom *et al* 1975).

Few ultrastructural studies of liposarcoma have previously been reported. Altogether 5 liposarcomas examined electron microscopically have been described and illustrated (Scarpelli & Greider 1962 Razuk *et al* 1971 Kalderon & Fethiere 1973 Flenker 1976). Two of these were of myxoid type and 1 of pleomorphic type but the histologic subtypes of the other 2 were not given in the report.

cacodylate buffer pH 7.2 for 4 hours and 4°C, washed in cold buffer, post fixed with 1 per cent OsO_4 for 1 hour and thereafter prepared in the same way as the OsO_4 fixed material. In 2 cases only formalin fixed tissue was available from which small pieces were washed in 0.1 M sodium cacodylate buffer for 24 hours, fixed for 3 hours in ice-cold 1 per cent OsO_4 in cacodylate buffer and prepared as previously described. Only paraffin-embedded material was available in 2 cases. Small tumour pieces from selected areas of 20–50 micron thick sections from the paraffin blocks were carefully deparaffinized in xylene, hydrated in decreasing concentrations of ethanol and finally washed in cacodylate buffer, fixed in 1 per cent OsO_4 and prepared as described above. One micron thick sections were stained with toluidine blue and silver to grey thin sections were stained with uranyl acetate and lead citrate prior to examination in a Philips 200 electron microscope.

RESULTS

Light Microscopic Appearance

Well-differentiated liposarcoma Four tumours were wholly or predominantly of well-differentiated type (cases 1, 2, 3 and 4). Lipoma like areas revealed mostly univacuolated fat cells of variable sizes with slight nuclear pleomorphism, the nuclei were hyperchromatic and enlarged and occasionally contained vacuoles so-called »Lochkerner«. The number of atypical multivacuolated lipoblasts varied considerably from tumour to tumour and within different areas of the same tumour (Fig. 1). The

liposarcoma (case 1) also included areas of fibrosing type and another (case 2) was predominantly of this type. Intermingling with dense broad collagen bundles in these tumours were rather large cells with indistinct cytoplasmic borders and hyperchromatic nuclei. The predominantly fibrosing well-differentiated liposarcoma showed only a few scattered atypical multivacuolated lipoblasts. This tumour (case 2) contained areas of poorly differentiated nuclei suggestive of the presence of intracytoplasmic lipid droplets.

These small multivacuolated cells were closely associated with a prominent network of small capillaries.

Myxoid liposarcoma Three tumours were wholly or predominantly of myxoid type (cases 5, 6 and 7)

and 2 others, being predominantly of well-differentiated and round cell type (case 4 and 9) respectively, included some myxoid areas. The myxoid liposarcomas were characterized by an abundant, basophilic mucoid matrix containing fusiform or stellate cells with indistinct cytoplasmic borders and a prominent plexiform network of delicate capillary-like vessels. In some areas, the mucoid matrix coalesced to form round or oval spaces, the so-called pooling phenomenon (Enzinger & Winslow 1962) (Fig. 3). The number of multivacuolated lipoblasts varied from tumour to tumour and within different areas of the same tumour. Most multivacuolated lipoblasts were fairly small and often arranged around the delicate vessels (Fig. 4).

Round cell liposarcoma Two tumours were predominantly of round cell type (cases 8 and 9) and one, predominantly myxoid (case 7), included areas of this type. The round cell liposarcomas were characterized by closely associated fairly small, rounded or oval shaped cells usually with a single cytoplasmic vacuole (Fig. 5). Characteristic atypical multivacuolated lipoblasts were generally few in number. There was usually little or no intercellular mucoid substance in the highly cellular areas of the tumours although areas of myxoid type and intermediate round cell and myxoid type were found.

Pleomorphic liposarcoma The pleomorphic liposarcoma (case 10) contained extremely pleomorphic, multivacuolated lipoblasts, some of them huge, with several irregular hyperchromatic nuclei (Fig. 6). Cytoplasmic hyaline eosinophilic and PAS positive, diastase resistant globules were frequently seen (Fig. 7). Mitotic figures were frequent, some being polyploid.

Electron Microscopic Appearance

Well-differentiated liposarcoma The tumour cells varied considerably in size and general appearance from large cells, 100 μ in diameter or more with a single large, lipid inclusion occupying most of the cytoplasm and a peripherally displaced nucleus.

showing a central or eccentric oval nucleus with smooth outlines, a homogeneous heterochromatin and a single distinct nucleolar region. The cytoplasmic lipid droplets were rounded in shape and lacked limiting membrane. Numerous smooth-surfaced vesicles and large vacuoles were found within the cytoplasm, containing an amorphous material of varying density, frequently seen close to the cell surface. Mitochondria were round

The present investigation is an electron microscopic study of 10 liposarcomas representing all 4 types. The light microscopic and ultrastructural features of the various types are correlated. Ultrastructural similarities between the different subtypes and between these and embryonal and mature adipose tissue are emphasized and support a common histogenesis for the various subtypes of liposarcoma.

MATERIAL

The material for the study comprised clinical histories, operative specimens, formalin fixed tumour tissue, tissue blocks, routine histologic sections, 1 micron thick sections of Epon embedded tumour tissue and ultrathin sections for electron microscopy. Eight of the 10 liposarcomas were cases concurrently examined at the Department of Pathology, Sahlgrenska Hospital, Göteborg, Sweden, between 1970 and 1975. The other 2 cases were obtained from other departments of pathology in Sweden.

All tumours were surgical specimens and 6 of them were primarily fixed and prepared for ultrastructural examination; of the other 4, only formalin fixed tumour

tissue or paraffin embedded material was available.

The clinical data concerning the age and sex of the patients, tumour site and size as well as histologic subtype and fixation technique are presented in Table 1.

METHODS

Five micron thick sections of formalin fixed and paraffin embedded tumour tissue were stained according to the haematoxylin van Gieson method and with haematoxylin and eosin. Gordon's and Sweet's silver impregnation was used for the demonstration of reticulin fibre and the PAS stain according to McManus with and without prior diastase digestion to study the presence of glycogen.

In 2 cases, small pieces of tumour tissue were embedded in glycol methacrylate and 1-2 micron thick sections were stained according to the haematoxylin van Gieson method and with haematoxylin and eosin.

For electron microscopy, small pieces from 6 of the tumours were immediately put into ice cold buffer, OsO_4 fixed for approximately 2 hours, dehydrated in ethanol, embedded in Epon 812 and cut in an LKB Ultratome III. In 3 of the cases, small pieces were also immersed in 2.5 per cent glutaraldehyde in 0.1 M

TABLE 1. Clinical Data, Histologic Subtype and Fixation of 10 Liposarcomas

Case	Sex	Age (years)	Tumour site	Tumour size (cm)	Histologic subtype of liposarcoma	Fixation
1	M	61	Right axillary region	8 × 7	Well differentiated lipoma like and fibrosing	OsO_4
2	M	76	Right thigh	15 × 10	Well differentiated fibrosing	Formaldehyde paraffin embedded - OsO_4
3	F	49	Left thigh	14 × 8 × 4 1/2	Well differentiated lipoma like with a fibroma like area	Formaldehyde - OsO_4
4	M	50	Right leg	7 × 6	Well differentiated lipoma like with myxoid areas	Formaldehyde - OsO_4
5	M	29	Right thigh	18 × 8 × 8	Myxoid	OsO_4
6	M	59	Right groin	9 × 8 × 6	Myxoid	Glutaraldehyde - OsO_4
7	M	43	Left thigh	16 × 8 × 7	Predominantly myxoid with round-cell areas	Glutaraldehyde - OsO_4
8	F	58	Left thigh	18 × 12 × 11	Round-cell	Glutaraldehyde - OsO_4
9	F	50	Right thigh	13 × 7 × 4	Round-cell with myxoid areas	OsO_4
10	F	73	Right thigh	15 × 14 × 12	Pleomorphic	Formaldehyde paraffin embedded - OsO_4

Fig 1 Case 1 Well-differentiated lipoma like liposarcoma with atypical multi vacuolated lipoblasts intermingling with unvacuolated polymorphic fat cells H&E $\times 120$

Fig 2 Case 2 Sclerosing area of a well-differentiated liposarcoma with distinct networks of wavy fibrils with the staining reaction of collagen closely associated with nuclei Van Gieson $\times 300$

Fig 3 Case 5 Myxoid liposarcoma showing a plexiform capillary vascular pattern stellate or fusiform cells some of which show cytoplasmic vacuoles and myxoid spools H&E $\times 120$

Fig 4 Case 5 One micron thick section of Epon-embedded myxoid liposarcoma Most tumour cells contain several small or one or two large lipid droplets Many tumour cells are intimately associated with the delicate capillaries Toluidine blue $\times 400$

ed or spherical in shape and occasionally filamentous They all revealed a relatively simple internal structure In cells with abundant lipid inclusions there were a few short parallel profiles of rough endoplasmic reticulum and no distinct Golgi apparatus was found In the cells resembling mature fat cells the cytoplasmic organelles were few and concentrated in the perinuclear region where the

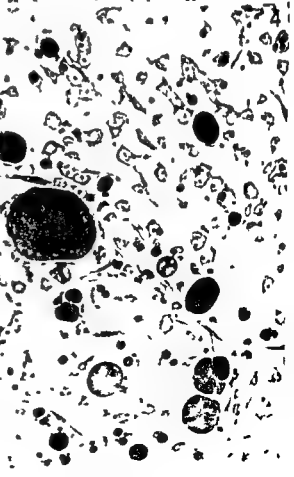
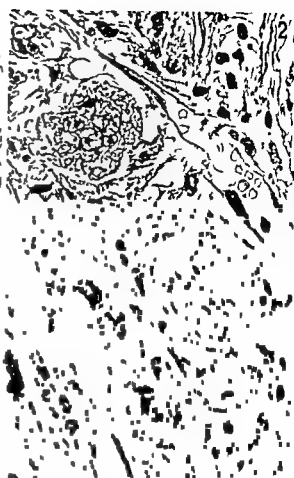
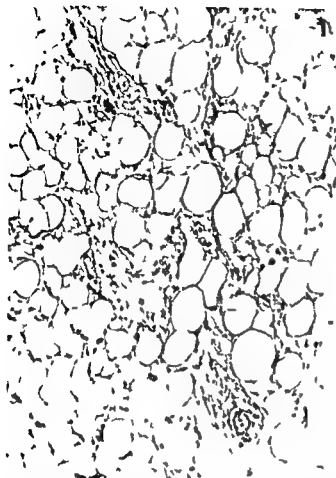
cytoplasm was most abundant Aggregates of dense particles 20-30 nm in diameter resembling glycogen were found within the cytoplasm without any distinct relation to cytoplasmic organelles

The plasma membranes were in many cells completely or partly surrounded by a thin less dense zone of amorphous material identified as a basement membrane



Fig 5 Case 8 Round-cell liposarcoma composed of closely packed rounded cells mostly with one small cytoplasmic vacuole H&E, $\times 120$

Fig 6 Case 10 Pleomorphic liposarcoma showing prominent cellular and nuclear pleomorphism and several large atypical multi vacuolated lipoblasts H&E $\times 120$





clearly outside the cytoplasmic membranes often filling irregular intercellular spaces formed between the cells which showed long closely-entwining cytoplasmic extensions

The hibernoma like areas found in the light microscope within one of the well-differentiated liposarcomas (case 3) were composed of small cells 20-40 μ in diameter with a centrally located nucleus and numerous cytoplasmic lipid inclusions. The lipid inclusions were characteristically small and fairly equal in size and appeared as more or less empty vacuoles because of the poor fixation in this case (Fig 10). However in some areas the highly osmophilic lipid material was preserved and appeared to lack a lining membrane. Within the cytoplasm were abundant mitochondria of variable

Fig 9 Case 1 Detail of a spindle shaped tumour cell showing segments of rough endoplasmic reticulum and mitochondria. The cell is closely associated with collagen and the plasma membrane is partly surrounded by basement membrane like material $\times 25,000$

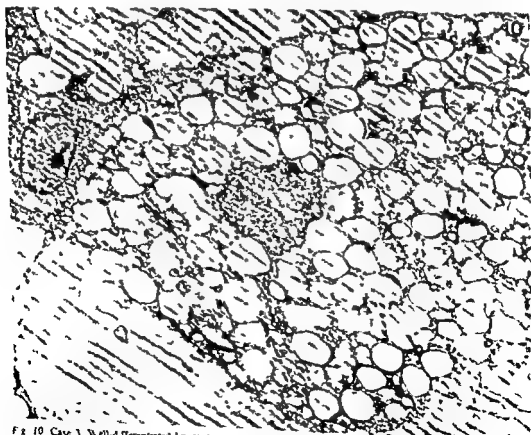


Fig 10 Case 3 Well-differentiated liposarcoma hibernoma like area. A rounded cell with a central nucleus and numerous uniform vacuoles, presumably lipid inclusions $\times 4,000$ Formalin fixation



The tumour cells in case 2 and within fibrosing areas of case 1 could be identified by their fusiform shape with centrally placed elongated nuclei. The cytoplasm of these cells contained only small highly osmiophilic inclusions resembling lipids abundant vesicles and smooth surfaced vacuoles containing a less dense amorphous material. In contrast to the lipid rich cells, numerous prominent systems of rough endoplasmic reticulum and also some large Golgi zones were found. Closely associated with these cells were abundant collagen fibres (Fig 9) which formed broad bundles. The ultrastructural examination of the peculiar area of case 2 which in the light microscope suggested the presence of intracytoplasmic collagen, was hampered by the fact that only paraffin-embedded material was available. The cytoplasmic membranes were frequently disrupted, but many cellular details were rather well preserved. The abundant network of fibres seen in the light microscope was identified as collagen. Ultrastructurally, however, the collagen fibre bundles closely associated with the cells appeared to be

Fig 7 Case 10 Pleomorphic liposarcoma showing cytoplasmic PAS positive hyalin globules PAS $\times 700$

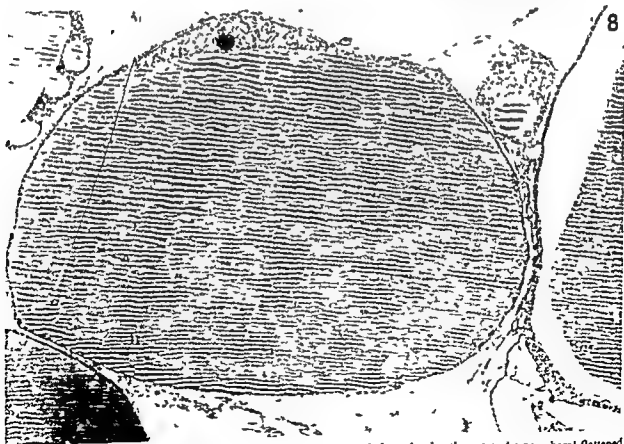


Fig 8 Case 4 Well differentiated liposarcoma Fat cell with a single large lipid inclusion and a peripheral flattened nucleus $\times 5000$ Formalin fixation



Fig 11 Case 6 Myxoid liposarcoma. **A** An irregularly shaped tumour cell with prominent cytoplasmic extensions and delicate slender projections. The cytoplasm contains abundant lipid inclusions and some vacuoles close to the plasma membrane $\times 11\,500$. **B** Cytoplasmic extensions containing finely-dispersed dense particles resembling glycogen, lipid droplets and peripheral vacuoles, some of which appear to have ruptured $\times 27\,000$. Glutaraldehyde fixation.

diameter, with a centrally located nucleus. The nucleus was characteristically ovoid and indented and showed a coarse chromatin pattern with heterochromatin peripherally and one or two prominent nucleoli (Figs 15 and 16). The cytoplasmic details were similar to those of the myxoid liposarcomas in many respects, i.e. the abundance of vacuoles varying in size and contents was the most prominent feature. As in the myxoid liposarcomas the rough endoplasmic reticulum was often distended and ended into cisternae filled with a moderately dense material, similar to that contained in most free vacuoles. There were cells containing vesicles and vacuoles lying around Golgi zones. Occasional cells contained a few large lipid droplets, which occupied most of the cell volume (Fig. 15), while in most cells the lipid inclusions were less prominent. Mitochondria were abundant and very variable in



Fig 12 Case 6 Myxoid liposarcoma. Detail of a tumour cell containing tubular rough endoplasmic reticulum continuous with ribosome-studded cisternae (arrows) filled with amorphous or granular material of varying density. Some small lipid droplets are seen $\times 19\,000$.

also observed. The internal structure was simple with short cristae. Abundant dense particles resembling glycogen were often found within the cytoplasm (Fig. 11B) and occasionally also appeared within the nucleus. The peripheral cytoplasm was digitated and formed slender projections. Basement membrane like material completely or partly surrounded the cells but the thickness varied and in some areas was absent. The extracellular spaces contained an abundant amorphous, moderately dense material and few collagen fibres. No desmosomes were seen in the junctions between tumour cells. Cells were seen to be closely associated with tightly-packed endothelial lined capillaries.

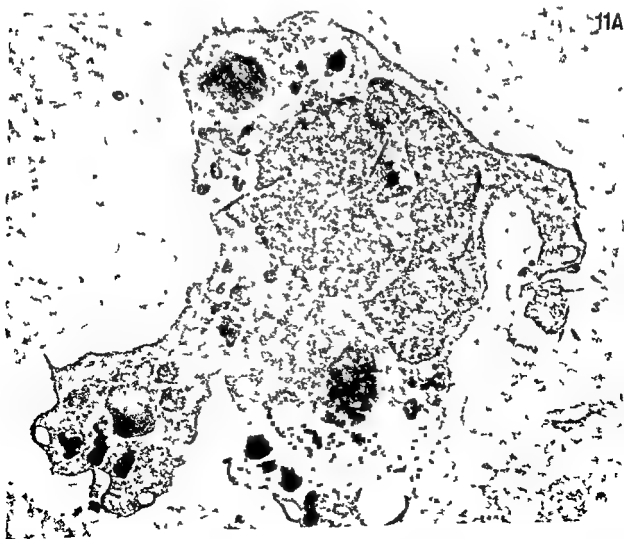
Round-cell liposarcoma. The cells of the round-cell liposarcomas were rounded or oval, 15–40 μ m in

size and shape mostly spherical or rod shaped but also filamentous frequently surrounding the lipid inclusions. Neither endoplasmic reticulum nor Golgi apparatus could be clearly identified. These cells were intimately associated with endothelial cells of the prominent capillary bed. Intercellular collagen was not found in this area of the tumour.

Myxoid liposarcoma Ultrastructurally the cells of the myxoid liposarcomas were characteristically irregular in shape, stellate or elongated with numerous slender or plump cytoplasmic extensions, most cells being less than 25 μ in largest diameter (Fig. 11 A). The nuclei showed characteristically deep indentations so that in section the cell sometimes appeared multinucleated. The heterochromatin was usually finely dispersed and one or two prominent nucleoli were found. The most striking cytoplasmic feature was the abundance of membrane bound vacuoles and vesicles, mostly containing a moderately electron-dense material (Fig. 11 B). These vacuoles were often closely associated with rough endoplasmic reticulum and

in places similar vacuoles clearly emerged from the tail end of distended rough endoplasmic reticulum (Fig. 12). Some of these vacuoles were ribosome-studded while the free vacuoles were outlined by a smooth membrane. Many large vacuoles were found close to the plasma membrane. In some cells they appeared to be ruptured and the contents to be extruded into the extracellular space which showed abundant amorphous material of the same density as the vacuole content (Fig. 13 A and B). The number and size of lipid inclusions varied considerably from cell to cell within one and the same tumour but all cells contained some highly osmophilic droplets without a lining membrane (Fig. 11 A).

There was a moderate amount of free ribosomes and rough endoplasmic reticulum appearing as short parallel profiles and only occasionally a small distinct Golgi apparatus was found. The mitochondria were variable in size and shape, being rod shaped, oval or peanut shaped. Long filamentous mitochondria (Fig. 14) sometimes angulated were





16.

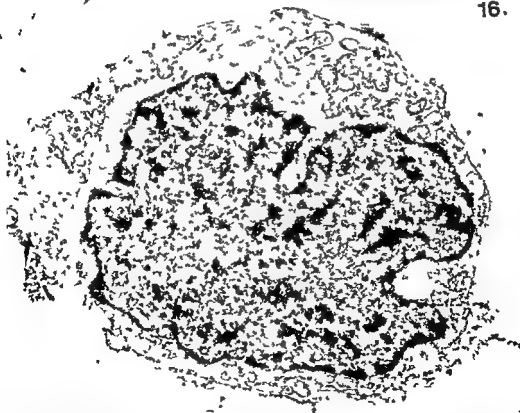


Fig 15 Case 9 Round-cell liposarcoma. A group of ovoid and round cells showing indented nuclei and numerous cytoplasmic vacuoles with few lipid inclusions. The cells contain many mitochondria, some of which are filamentous. $\times 3,500$ OsO₄ fixation.

Fig 16 Case 8 Round-cell liposarcoma. A rounded tumour cell with a large indented nucleus, prominent mitochondria and some vacuoles. The cell is partly surrounded by a basement membrane like structure. $\times 19,000$ OsO₄ fixation.



Fig 13 Case 6 A & B Myxoid liposarcoma Details from a cell surface with multiple vacuoles some of them in the process of rupturing $\times 49\,000$ Glutaraldehyde fixation



Fig 14 Case 5 Myxoid liposarcoma Filamentous mitochondria and smooth membrane lined vacuoles $\times 45\,000$ OsO₄ fixation

shape and size some of them were very long and filamentous measuring up to $3\ \mu$ in length. The internal structure was mostly simple although occasionally long cristae following an irregular sometimes longitudinal course, were found. Diffusely dispersed or aggregated dense particles resembling glycogen were present in most cells. The majority of cells contained cytoplasmic filaments (Fig 16) running parallel to the long axis of the cells or arranged concentrically around vacuoles.

Basement membrane like structures were often prominent (Fig 16) and in areas appeared multilayered. Individual cells were closely apposed without demonstrable desmosome structures. Inter-cellular spaces were filled with an amorphous moderately dense material and scarce intercellular collagen. As in myxoid liposarcomas, the cells were often closely associated with endothelial cells of the capillary bed.

Pleomorphic liposarcoma Since only formaldehyde fixed and paraffin-embedded material was available in this case the preservation was rather poor, and many cellular details could not be discerned. The tumour cells varied in size the largest being $150\ \mu$ in diameter. The cells contained one or occasionally 2 or more nuclei which showed one or more prominent nucleoli and frequently deep

1965) It is of interest to note that filamentous sometimes exceedingly long mitochondria were found in all types in the present study and predominated in some cells of the myxoid and round-cell type. The presence of cytoplasmic glycogen most prominent in the myxoid and round-cell liposarcomas is similar to that observed in the middle stages of differentiation of the adipose cell. Another cellular detail which resembles that of the differentiating adipocyte is the presence of basement membranes (Apolitano 1965) which partly or completely surrounded some cells in most of the tumours in the present series.

The prominent cellular changes which occur during the differentiation of the ordinary white adipose cell from a primitive stem cell apparently indistinguishable from a fibroblast to the mature signet ring fat cell have been studied in detail

various stages seen during the differentiation of ordinary adipose cells. The present study suggests that the different subtypes of liposarcoma originate from a single line of cells and this supports the view that all liposarcomas should be considered histogenetically to represent a single entity although very variable in appearance. The variegated cellular appearance of liposarcomas is believed to be a reflection of the wide cellular spectrum seen during the differentiation of adipose tissue.

This investigation was supported by grants from the Swedish Cancer Society (530 B75 03X).

The technical assistance of Miss Margareta Evaldsson is gratefully acknowledged.

REFERENCES

Enliert H T Culbertson J D Rochlin D B & Brady L W Liposarcoma. A clinical and pathological study of 53 cases. *Cancer* 13 932-950 1960

- Eninger F M & Winslow D J Liposarcoma. A study of 103 cases. *Virchows Arch Path Anat* 335 367-388 1962
- Enzinger F M Lattes R & Torlone H Histological typing of soft tissue tumours. International Classification of Tumors No 3 World Health Organization Geneva 1969
- Fleaker H Myxoid liposarcoma. Light and electron microscopic investigation. *Virchows Arch Path Anat* 371 171-176 1976
- Gould V Joa W Gould N & Soto J Comparative ultrastructure of hibernomas and myxoid and pleomorphic liposarcomas (Abstract). *Lab Invest* 34 36 1976
- Greenlee T K Jr & Riss R The development of the rat flexor digitorum tendon. A fine structure study. *J Ultrastruct Res* 18 354-376 1967
- Kalderon A E & Fethere W Fine structure of two liposarcomas. *Lab Invest* 28 60-69 1973
- Kindblom L G Angervall L & Siendensen P Liposarcoma. A clinicopathologic, radiographic and prognostic study. *Acta path microbiol scand Sect A suppl* 253 1975
- Levine G Hibernoma. An electron microscopic study. *Human Pathol* 3 351-359 1972
- Napolitano L The fine structure of adipose tissue. In Reynolds A E & Cahill G F (editors) *Handbook of physiology* section 5 Adipose tissue. Waverly Press Baltimore 1965 pp 109-123
- Ratuk M A Urschel H C Race G J Kingsley W B & Paulson D L Liposarcoma of the mediastinum. Case report and review of the literature. *J Thorac Cardiovasc Surg* 61 819-826 1971
- Resel P A Soule E H & Coventry M B Liposarcoma of the extremities and limb girdles. A study of two hundred twenty two cases. *J Bone Joint Surg* 48 A 229-244 1966
- Scarpelli D G & Greider M H A correlative cytochemical and electron microscopic study of a liposarcoma. *Cancer* 15 776-789 1962
- Seemayer T A Knaack J Wang N S & Ahmed M N On the ultrastructure of hibernoma. *Cancer* 36 1785-1793 1975
- Taxt J B & Battjara H Malignant fibrous histiocytoma. An electron microscopic study. *Cancer* 40 254-267 1977

indentations. The cytoplasm revealed numerous, large, empty spaces, probably previously occupied by lipids which were dissolved during processing. Rough endoplasmic reticulum was abundant and in areas formed a dense network. Segments of the rough endoplasmic reticulum were distended and filled with a moderately electron dense material. The hyalin, PAS positive globules seen in the light microscope within the cytoplasm appeared ultrastructurally as rounded, electron-dense bodies, up to 10 μ in diameter, without any limiting membranes or definite relation to any cytoplasmic structures. Strands of fibrillar material, 300–350 nm thick, with a 90 nm axial periodicity were observed in a few tumour cells.

DISCUSSION

Ultrastructurally, the cells of the well-differentiated lipoma-like liposarcomas characteristically showed a few, large, lipid droplets, relatively few organelles and often an eccentric or peripherally located, fairly large nucleus with a prominent nucleolus. Many of these ultrastructural features are similar to those found in the later, »multilocular« stages in the development of ordinary white adipose cells. In fact, within these tumours occasional univacuolated tumour cells were also found which closely resembled ordinary mature signet ring fat cells (Napolitano 1965).

The empty, intranuclear vacuoles frequently seen in the light microscope, giving the »Möckherne« appearance, were not observed ultrastructurally. However, the large lipid inclusions of the multiloculated tumour cells frequently made deep impressions in the nucleus. The »Möckherne« observed by light microscopy might have been caused by the sectioning of such scalloped nuclei.

The cells of the well-differentiated liposarcoma of fibrosing type clearly differed from those of the lipoma like type being spindle shaped with abundant rough endoplasmic reticulum and closely associated with collagen. Thus the cells ultrastructurally in many respects resembled fibroblasts (Greenlee & Ross 1967). However, some lipid inclusions were seen in most cells and intermingled with the spindle cells were occasional cells with prominent lipid droplets such as those seen in the well-differentiated lipoma like liposarcomas suggesting a relationship between the 2 subtypes. In fact, in the light microscope well-differentiated liposarcoma often contains both lipoma-like and fibrosing areas poorly demarcated from each other (Kindblom *et al* 1975).

The liposarcoma of the well-differentiated type in the present series, which included the hibernoma-

like area, has previously been described in a report of a Swedish National Series of liposarcoma studies by one of us, although the ultrastructural examination was not reported then (Kindblom *et al* 1971). The intimate association with capillaries, the centre nucleus, the size and amount of lipid inclusions as well as the abundance of mitochondria in the present case is similar to that described in brown adipose tissue and hibernoma (Napolitano 1966, Levine 1972, Seemayer *et al* 1975). Since the tumour was located deep in the thigh, it is unlikely that the hibernoma-like area is ordinary brown adipose tissue included within the liposarcoma but rather forms an integral part of the neoplasm.

The myxoid liposarcomas could be clearly distinguished ultrastructurally from the well-differentiated liposarcomas. The lipid inclusions were usually much less prominent and of smaller size. The presence of smooth membraned vacuoles containing moderately dense amorphous or granular material and ribosome-studded cisternae contiguous with the tail ends of the rough endoplasmic reticulum containing similar material, was characteristic and might suggest that the abundant mucosubstances seen light-microscopically were produced in the rough endoplasmic reticulum.

Ultrastructurally there were many similarities between the myxoid and round-cell liposarcoma although the cells were generally smaller and the systems of vacuoles were less prominent in the latter type. There was no evidence of any relationship ultrastructurally between round-cell liposarcoma and brown adipose tissue as was once suggested (Enterline *et al* 1960). The frequent occurrence of mixed and intermediate forms indicates a relationship between myxoid liposarcoma and round-cell liposarcoma (Kindblom *et al* 1975). The present ultrastructural observations further support such a relationship between myxoid and round-cell liposarcoma.

The abundant grey to dark large cytoplasmic granules seen in the pleomorphic liposarcoma correspond to the eosinophilic, hyalin globules observed in the light microscope. These structures were reported as being frequent in pleomorphic liposarcoma and are believed to be degenerative in nature (cf Kindblom *et al* 1975). Similar cytoplasmic granules have been reported in other tumours such as malignant fibrous histiocytoma and ultrastructurally have been considered to be lysosomal in origin (Taxy & Battifora 1977).

During the development of the mature adipose cell, the appearance of the mitochondria changed. Initially they were predominantly spherical and in the late stages more filamentous, maintaining a relatively simple internal structure (Napolitano

(5) It is of interest to note that filamentous reticles exceedingly long mitochondria were found in all types in the present study and dominated in some cells of the myxoid and round-cell type. The presence of cytoplasmic glycogen is most prominent in the myxoid and round-cell liposarcomas similar to that observed in the middle stages of differentiation of the adipose cell. Other cellular detail which resembles that of the differentiating adipocyte is the presence of basement membranes (Napoli 1965) which partly completely surrounded some cells in most of the tumours in the present series.

The prominent cellular changes which occur during the differentiation of the ordinary white lipose cell from a primitive stem cell apparently distinguishable from a fibroblast to the mature myeloid fat cell have been studied in detail (Napoli 1965). The tumour cells of the different types of liposarcoma in this series show many cellular details which seem to follow closely the various stages seen during the differentiation of ordinary adipose cells. This is in

that all liposarcomas should be considered histogenetically to represent a single entity although very variable in appearance. The variegated cellular appearance of liposarcomas is believed to be a reflection of the wide cellular spectrum seen during the differentiation of adipose tissue.

This investigation was supported by grants from the Swedish Cancer Society (530 B75 03X).

The technical assistance of Miss Margareta Elvén is gratefully acknowledged.

REFERENCES

- Eninger H T, Culbertson J D, Rochlin M B & Brady L H Liposarcoma. A clinical and pathological study of 53 cases. *Cancer* 13 932-950 1960
- Eninger F M & Winslow D J Liposarcoma. A study of 103 cases. *Virchows Arch Path Anat* 335 367-388 1962
- Eninger F M, Lattes R & Torione H Histological typing of soft tissue tumours. International Classification of Tumors No 3. World Health Organization Geneva 1969
- Flenker H Myxoid liposarcoma. Light and electron microscopic investigation. *Virchows Arch Path Anat* 371 171-176 1976
- Gould V, Joa W, Gould N & Sato J Comparative ultrastructure of hibernomas and myxoid and pleomorphic liposarcomas (Abstract). *Lab Invest* 34 36 1976
- Greenlee T K Jr & Ross R The development of the rat flexor digitorum tendon. A fine structure study. *J Ultrastruct Res* 18 354-376 1967
- Kalderon A E & Fethiere W Fine structure of two liposarcomas. *Lab Invest* 28 60-69 1973
- Kindblom L G, Angervall L & Svendsen P Liposarcoma. A clinicopathologic, radiographic and prognostic study. *Acta path microbiol scand Sect A suppl* 253 1975
- Levine G Hibernoma. An electron microscopic study. *Human Pathol* 3 351-359 1972
- Napoli L The fine structure of adipose tissue. In Reynolds A E & Cahill G F (editors) *Handbook of physiology* section 5 Adipose tissue. Waverly Press Baltimore 1965 pp 109-123
- Raebuk M A, Urschel H C, Race G J, Kingsley W B & Paulson D L Liposarcoma of the mediastinum. Case report and review of the literature. *J Thorac Cardiovasc Surg* 61 819-826 1971
- Resel P A, Soule E H & Coventry M B Liposarcoma of the extremities and limb girdles. A study of two hundred twenty two cases. *J Bone Joint Surg* 48 A 229-244 1966
- Scarpelli D G & Greider M H A correlative cytochemical and electron microscopic study of a liposarcoma. *Cancer* 15 776-789 1962
- Seemayer T A, Knaack J, Wang N S & Ahmed M N On the ultrastructure of hibernoma. *Cancer* 36 1785-1793 1975
- Taxy J B & Battifora H Malignant fibrous histiocytoma. An electron microscopic study. *Cancer* 40 254-267 1977

FOCAL ENDOTHELIAL CELL INJURY IN RABBIT AORTA, AGGRAVATION OF INJURY BY 2 DAYS OF CHOLESTEROL FEEDING

EINAR SVENDSEN

Institute of Medical Biology University of Tromsø Tromsø Norway

Svensden E. Focal endothelial cell injury in rabbit aorta: aggravation of injury by 2 days of cholesterol feeding. *Acta path microbiol scand Sect. A* 87 123-130 1979

A randomized morphometric study of «spontaneous» endothelial cell injury in rabbit aorta was performed blindly. Four different areas of the aorta were sampled in a standardized fashion and examined by scanning electron microscopy. The finding of protruding endothelial cells was taken as sign of injury. The endothelial cell injury was focal and in the sampled areas particularly prevalent in the distal part of the lesser curvature of the aortic arch and the distal lip of intercostal artery orifices. In the area between two intercostal artery orifices on the same side of the midline injured cells were only exceptionally found. Rabbits fed a 2% cholesterol diet for 2 days showed an increase in protruding cells particularly at the intercostal artery orifices. It is concluded that the endothelial cell injury in rabbit aorta may be caused by local factors determining the focal nature and by systemic factors such as acute hypercholesterolemia.

Key words: Endothelial cell injury, aorta, cholesterol, rabbit.

Einar Svendsen, Institute of Medical Biology, University of Tromsø, N 9000 Tromsø, Norway.

Received 20 vi 78. Accepted 15 ix 78

Several reports deal with spontaneous endothelial cell injury (2, 22, 28). The question arises: what mechanisms are responsible for this injury? Several indirect observations indicate that endothelial cell injury is particularly located at certain sites. Thus Wright (33) reported increased mitotic activity in the proximity of branching orifices in the aorta of guinea pigs. Packham *et al* (20) and others (4, 5, 16, 19) showed increased permeability along the lesser curvature of the aortic arch and in association with branching sites in the aorta of several species. Platelet deposition and microthrombi have been observed in the same areas (10, 15, 16, 20).

days of cholesterol feeding in swine. Heber *et al* (32) demonstrated endothelial cell injury in cholesterol fed rabbits developing atherosclerotic plaques.

By scanning electron microscopy it is possible to identify injured endothelial cells (28) because an early sign of injury is bulging of the nuclear area creating a protruding spindle-shaped form of the cells (2, 6, 28). That has made it possible to measure the frequency of injured endothelial cells at various sites under various circumstances. The present study aims at answering the following questions by using morphometry on scanning electronmicrographs.

1. Can it be confirmed by direct measurements that injury of endothelial cells particularly occurs in certain predilection sites in rabbit aorta?

2. Can it be likewise confirmed that short term cholesterol feeding accentuates this injury?

A preliminary investigation based on light microscopy (30) gave affirmative answers to these questions.

in rabbits fed cholesterol. Shimamoto *et al* (26) reported edematous swelling and increased occurrence of «bridge like structures» even after a single dose of cholesterol per os. Florentin *et al* (7) showed increased mitotic activity of the endothelium after 3

MATERIAL AND METHODS

Altogether 24 male New Zealand white rabbits were used. All were provided by the same breeder and kept in our laboratory on standard low fat rabbit pellet diet (Karin pellets Felleskjøpet Trondheim) for about four weeks prior to use. All animals were about 6 months of age weighing from 3.5 to 3.8 kg. The animals were divided into 2 equal groups: one group was fed a 2% cholesterol diet mixed up with crushed rabbit pellets (BDH Chemicals Ltd, Poole, England); the other group got crushed rabbit pellets without addition and served as control group. The diets as well as water were given *ad libitum* for 2 days.

The animals of both groups were assigned a code number based on a random number table. The cholesterol fed animals ate from 3–8 g of pure cholesterol during the 2 days. The mean serum cholesterol level in the experimental group after 2 days of cholesterol rich diet was 149.25 mg percent. In the control group the mean serum cholesterol was 34.5 mg percent. The animals were sacrificed by a perfusion technique described earlier (28). After careful dissection specimens were taken from the aorta for scanning electron microscopy from the same areas as described earlier (28): that is from the distal part of the lesser curvature of the aortic arch, from the area around the second and the sixth pair of the intercostal artery orifices and from the area between two intercostal artery orifices on the same side. The specimens were processed as described previously (28).

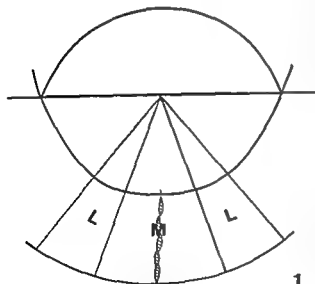


Fig. 1. Schematic representation of an intercostal artery orifice as seen in scanning electron microscopy. From the midpoint of the line drawn across the orifice one central sector of 40 degrees (M) and two lateral (L) of twenty degrees each spread out in distal direction. A curved line parallel with the lower lip of the orifice at a distance corresponding to 5 endothelial cells limits the sector fields.

Specimens from animals of the cholesterol group as well as of the control group were mixed and scanning electron microscopy was done on a Hitachi HHS 100 Scanning electron microscope. At the time of microscopy the specimens still carried their code number and the investigator did not know to which group the individual specimens belonged. In specimens from the lesser curvature of the aortic arch and between intercostal artery orifices 8 pictures in a series at a magnification of 200 \times from the central part of the specimens were taken. In specimens from the intercostal artery orifices 4 pictures including the distal lip of each orifice were taken. The photos were mounted in montages on a stiff cardboard. On the montages from the aortic arch and from the area between two intercostal artery orifices the central part were framed out in a standard fashion. On the montages of the intercostal artery orifice a horizontal line was drawn through the centre of the orifice (Fig. 1). A line perpendicular to this was drawn at the lowest point of the distal lip. From the base of this perpendicular three radiating lines were drawn in distal direction creating a central angle of 40 degrees and two lateral of 20 degrees each as shown in Fig. 1. A curved line parallel with the circumference of the edge of the lower lip at a distance corresponding to the length of 5 endothelial cells was drawn. Together with the radiating lines the curved line limited 3 segmental fields: one central at approximately the same size as the sum of the two lateral ones (Fig. 1).

A morphometric study was carried out by placing upon the montages a transparent point counter with a distance 0.5 mm between the points. Points falling upon protruding endothelial cells within the framed areas were counted out as well as the total number of points. The ratio of points for protruding cells over total points gave an index. When all indexes were calculated the code was broken and a statistical analysis of the two groups for each site of the aorta was performed. The two-sided Wilcoxon test was chosen in order to avoid the assumption that the endothelial cell injury index is normally distributed.

RESULTS

In the area between two intercostal artery orifices the intima of both control and cholesterol fed animals was characterized by moderately marked folds running in long unsharp waves as described earlier (29). In this area protruding endothelial cells could be seen only exceptionally (Fig. 2).

In specimens taken from the lesser curvature of the aortic arch of both animal groups abundant protruding endothelial cells were seen (Fig. 3). Only scattered platelets were found.

Just distal to the lower lip of the intercostal artery orifices of both animal groups many protruding endothelial cells appeared. They were particularly frequent in the central field. The area of protruding cells often created a triangular area with the base at



the edge of the lower lip of the orifice and the top reaching down stream at varying distance from the edge, seldom more than corresponding to the length of 6 endothelial cells (Fig 4) Furthermore clefts in the intima in the direction of the long axis of the aorta at the edge of the distal lip of the intercostal artery orifices were frequently seen (Fig 5) Dispersed corpuscular elements mainly platelets or even small thrombi could appear distal to the intercostal artery orifices (Fig 6)

The morphometric study gave the following results In the control group as well as in the cholesterol fed group the prevalence of injured endothelial cells in the framed areas was higher in the aortic arch and distal to the intercostal artery orifices compared with the area between two intercostal artery orifices where the number of injured cells was extremely low (Fig 7) These differences were statistically significant (Table 1)

Cholesterol feeding for two days resulted in an increase of injured endothelial cells in all areas counted (Fig 7) A statistical analysis including all sites in the cholesterol group against all sites in the control group revealed a statistically significant

Fig 2 Scanning electron microscopy from the area between two intercostal artery orifices on the same side of the midline Parallel intimal folds running in longitudinal direction are seen Protruding endothelial cells are lacking in this area From control animal 360 x

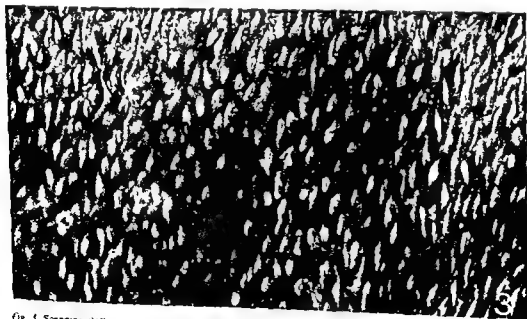


fig 3 Scanning electron microscopy from the lesser curvature of the aortic arch of rabbit aorta. Many spindle shaped protruding endothelial cells are seen From control animal 360 x

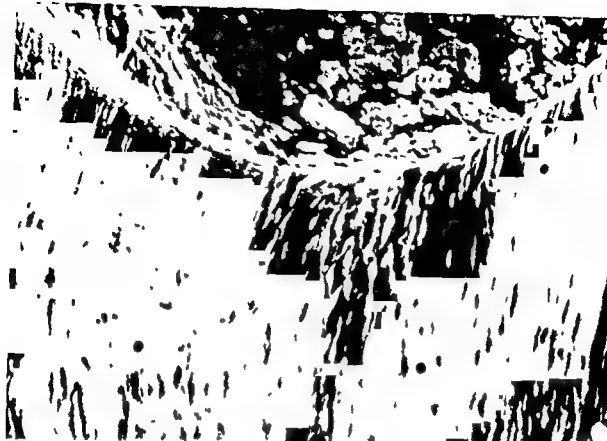


Fig 4 Scanning electron microscopy of rabbit aorta from the area distal to an intercostal artery orifice. Centrally wedge shaped area with numerous protruding endothelial cells are seen. From cholesterol fed animal 380 \times

Fig 5 Scanning electron microscopy of the distal area of an intercostal artery orifice. In the central part protruding endothelial cells are seen. Furthermore there are clefts located at the lower edge of the orifice (single arrows). Notice the well formed intimal folds at the outset of the intercostal artery (double arrows). From cholesterol fed animal 380 \times

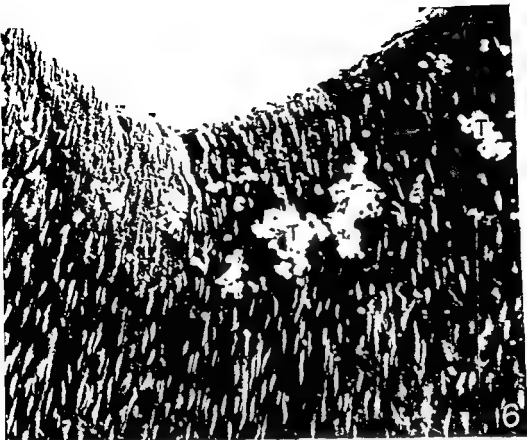


Fig 6 Scanning electron microscopy of the area distal to an intercostal artery orifice. Abundant protruding endothelial cells are seen. Small platelet thrombi (T) are deposited below the distal edge of the orifice. From control animal. 380 \times .

increase of protruding injured endothelial cells (Table 2). When comparing each site in the cholesterol fed animals with control animals, statistical significance was obtained for the area distal to the intercostal orifices (Table 2) but not for the other areas.

DISCUSSION

The protruding endothelial cells described in this paper are similar to those reported by other authors (21, 22, 24) and according to previous findings (28) they should be considered as injured cells. The distribution of protruding injured endothelial cells in rabbit aorta was not uniform but focal. The injured cells occurred particularly at sites which correspond to areas in which other authors have shown increased mitotic rate (5, 33), increased permeability (4, 16, 19, 20), platelet deposition and microthrombi (10, 15, 16, 20). The results of this study strengthen the theory that focally increased mitotic activity, increased permeability and platelet

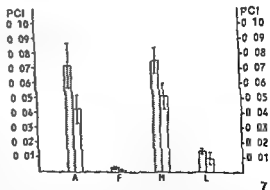


Fig 7 Diagram showing the prevalence of protruding injured endothelial cells with \pm one standard error of the mean at various sites in rabbit aorta. The hatched bars represent the standard error.

intercostal artery orifice. L, lateral area distal to an intercostal artery orifice.

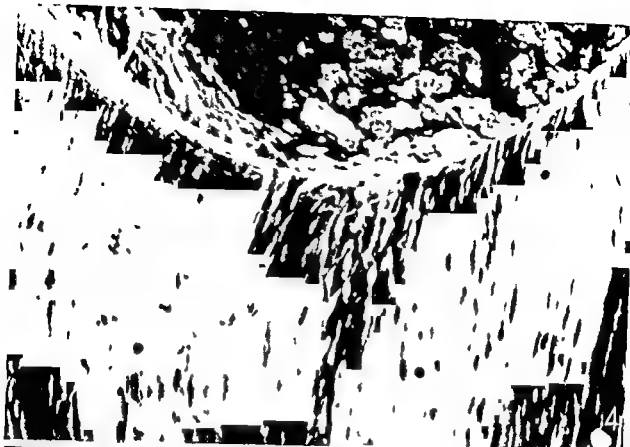


Fig 4 Scanning electron microscopy of rabbit aorta from the area distal to an intercostal artery orifice. Centrally a wedge shaped area with numerous protruding endothelial cells are seen. From cholesterol fed animal. 380 \times

Fig 5 Scanning electron microscopy of the distal area of an intercostal artery orifice. In the central part many protruding endothelial cells are seen. Furthermore there are clefts located at the lower edge of the orifice (single arrows). Notice the well formed intimal folds at the outset of the intercostal artery (double arrows). From cholesterol fed animal. 380 \times

TABLE 1 *Prevalence of Protruding Injured Endothelial Cells in Rabbit Aorta at Less Curvature (A) Lower Lip of Intercostal Artery Medial Segment (M) and Lateral Segment (L) against Sites between Two Intercostal Arteries at the Same Side (F)*

Cholesterol fed group			Control group		
Area A versus area F	n = 12	p < 0.01	Area A versus area F	n = 12	p < 0.01
Area L versus area F	n = 12	p < 0.01	Area L versus area F	n = 12	p < 0.01
Area M versus area F	n = 12	p < 0.01	Area M versus area F	n = 12	p < 0.01

Two tailed Wilcoxon test. The capital letters symbolize the same areas as in fig. 7

deposition are associated with focal endothelial cell injury

There may be several mechanisms responsible for the focal endothelial cell injury. It is reasonable to consider flow disturbance as an important factor. The distal area of the branching orifices is probably a site of high shear stress as pointed out by Fry (9). The other predilection site, the lesser curvature of the aortic arch, represents a bend where boundary layer separation with eddy formation may occur (8, 12, 31). The presence of shallow intimal pits in this area is in accordance with this view (29). Transient reactions of platelets caught in eddies may play a role through release of injuring substances (11, 14, 17). Only scattered platelets however were observed in this study. This could be due to the perfusion technique. The present study lends no direct support to the role of blood platelets. Only 2 days of cholesterol feeding causes a significant over all increase of protruding injured endothelial cells. The injury is more pronounced at the predilectional sites, particularly distal to the lower lip of the intercostal artery orifices where the difference between the cholesterol fed animals and control animals was statistically significant. Also in the lesser curvature of the aortic arch the cholesterol fed animals showed more protruding cells than the control animals but the difference between the groups for this area alone was not statistically

significant. This area however is less defined and the sampling from this area could not be as precise and standardized as the sampling from the orifices.

The demonstrated increase of endothelial cell injury makes it reasonable to conclude that the locally induced endothelial cell injury can be aggravated by a systemic stimulus such as an acute hypercholesterolemia induced by only two days of cholesterol rich diet.

Previous reports have demonstrated that the initial atherosclerotic lesions in rabbits have the same predilection sites as shown here for endothelial cell injury (1, 23). The present observations support the theory that endothelial cell injury plays a major role for the initiation of atherosclerotic lesions in these animals (2). The observation that diet induced acute hypercholesterolemia may cause aggravation of the «physiological» focal injury suggests that the role of hypercholesterolemia for production of atherosclerotic lesions is not only saturation of the intima with lipid. The excess plasma cholesterol may also have a direct «toxic» effect upon the endothelial cells. Previous reports support this assumption (3, 26, 27, 30).

In the initial stages of the injury contraction of the cell could be an important event. This was first suggested by Shimamoto & Sunaga (25). Henriksen *et al.* (13) have shown increased susceptibility of endothelial cells in vitro challenged to serum from

TABLE 2 *Prevalence of Protruding Injured Endothelial Cells at Standardized Sites in Rabbit Aorta. Comparison between Cholesterol fed Group and Control Group*

Cholesterol fed animals versus control	All areas	n = 24	0.05 > p > 0.02
Cholesterol fed animals versus controls	Area A	n = 24	p > 0.1
Cholesterol fed animals versus controls	Area F	n = 24	p > 0.1
Cholesterol fed animals versus controls	Area M	n = 24	0.05 > p > 0.02
Cholesterol fed animals versus controls	Area L	n = 24	0.05 > p > 0.02

Two tailed Wilcoxon test. A, F, L and M symbolize the same areas as in fig. 7

patients with hypercholesterolemia type 2 and low density lipoproteins. It is reasonable to suggest that acute hypercholesterolemia could make the endothelial cells more vulnerable to the factors operating at the local level.

I owe my gratitude to Prof. I. Jørgensen for advice and reading the manuscript, Prof. A. Westlund for advice concerning the statistical analysis, Anne Gro Grothe and Kirsti Renne for technical assistance and Dagny Madsen Fauske for typing the manuscript.

REFERENCES

1. Anitschkow N. Über die Atherosklerose der Aorta beim Kaninchen und über deren Entstehungsbedingungen. *Beitr. z. Path.* 59: 306-349, 1914.
2. Björkerud S & Bondjers G. Endothelial integrity and viability in the aorta of the normal rabbit and rat as evaluated with dye exclusion tests and interference contrast microscopy. *Atherosclerosis* 15: 285-300, 1972.
3. Bliock A, Björkerud S, Brattsand R, Hansson G K, Hansson H A & Bondjers G. Endothelial structure in rabbits with moderate hypercholesterolemia. *Acta path. microbiol. Scand. Sect. A* 85: 671-682, 1977.
4. Caplan B A, Gerrits R G & Schwartz C J. Endothelial cell morphology in focal areas of *in vivo* Evans blue uptake in the young pig aorta. *Exp. Mol. Pathol.* 21: 102-117, 1974.
5. Caplan B A & Schwartz C J. Increased endothelial cell turnover in areas of *in vivo* Evans blue uptake in the pig aorta. *Atherosclerosis* 17: 401-417, 1973.
6. Elemer G, Kerensy T & Jelinek H. Scanning (SEM) and transmission (TEM) electron microscopic studies on post ischemic endothelial lesions following recirculation. *Atherosclerosis* 24: 219-232, 1976.
7. Flemming R A, Ham S C, Lee A T, Lee K J & Thomas H A. Increased mitotic activity in aortas of swine. *Arch. Path.* 88: 463-469, 1969.
8. Fox J A & Hugh A E. Localization of atheroma: A theory based on boundary layer separation. *Brit. Heart J.* 78: 388-399, 1966.
9. Friess L. Certain chemorheologic considerations regarding the blood vascular interface with particular reference to coronary artery disease. *Suppl. IV to Circulation*. Vols. XXXIX and XL. IV: 38 IV, 59, 1969.
10. Geissinger H D, Mustard J F & Russell H C. The occurrence of microthrombi on the aortic endothelium of swine. *Can. Med. Assoc. J.* 87: 405-408, 1962.
11. Goldsmith H L. The flow model particles and blood cells and its relation to thrombogenesis. *Space T. 11* (ed). Progress in Hemostasis and Thrombosis. Vol. I. 97-139, 1972.
12. Gutstein H H & Schneck D J. *In vitro* boundary layer studies of blood flow in branched tubes. *J. Atheroscler. Res.* 7: 295-299, 1967.
13. Henriksen T, Evensen S A & Carlander B. Injury of endothelial cells in culture induced by low density lipoproteins. VIII International Congress on Thrombosis and Haemostasis. July 1, 1977. Philadelphia, USA.
14. Hughes A & Tonks R S. Intravascular platelet clumping in rabbits. *J. Path. Bact.* 84: 379-390, 1962.
15. Jørgensen L, Hørem J H & Moe N. Platelet Thrombosis and non traumatic intimal injury in mouse aorta. *Thrombos. Diathes. Haemorrh.* 29: 470-489, 1973.
16. Jørgensen L, Packham M A, Russell H C & Mustard J F. Deposition of formed elements of blood on the intima and signs of intima injury in the aorta of rabbit, pig and mouse. *Lab. Invest.* 27: 341-350, 1972.
17. Jørgensen L, Hovig T, Russell H C & Mustard J F. Adenosine diphosphate induced platelet aggregation and vascular injury in swine and rabbits. *Am. J. Path.* Vol. 61, No. 2: 161-176, 1970.
18. Magnani B & Coccheri S. Sulla patogenesi della aterosclerosi dietetica nel coniglio. Significato dei fenomeni di alterata permeabilità vascolare. *Giorn. clin. med.* 41: 1103-1119, 1960.
19. McGill H C, Geer J C & Holman R L. Sites of vascular vulnerability in dogs demonstrated by Evans blue. *Arch. Path. and Lab. Med.* 64: 303-311, 1957.
20. Packham M A, Russell H C, Jørgensen L & Mustard J F. Localized protein accumulation in the wall of the aorta. *Exp. Mol. Path.* 7: 214-232, 1967.
21. Reid M A & Bowyer D E. Scanning electron microscopy. Morphology of aortic endothelium following injury by endotoxin and during subsequent repair. *Atherosclerosis* 26: 319-328, 1977.
22. Reid M A & Bowyer D E. The morphology of aortic endothelium in haemodynamically stressed areas associated with branches. *Atherosclerosis* 26: 181-194, 1977.
23. Roach W, Fletcher J & Cornhill J F. The effect of the duration of cholesterol feeding on the development of sudanophilic lesions in the rabbit aorta. *Atherosclerosis* 25: 1-11, 1976.
24. Shimamoto T. An introduction to the investigation of atherosclerosis. *Thrombosis and Hemostasis*. 26: 1-11, 1976.
25. Shimamoto T & Sunaga T. Contraction of endothelial cells as a key mechanism in atherosclerosis. *Proc. Japan Acad.* 48: 633-639, 1972.
26. Shimamoto T, Yamashita T, Humano F & Sunaga T. Scanning and transmission electron microscopic observation of endothelial cells in the

- normal condition and in initial stages of atherosclerosis *Acta Path Jap* 21 (1) 93-119 1971
- 27 *Silkworth J B McLean B & Stehbens W E* The effect of hypercholesterolemia on aortic endothelium studied en face *Atherosclerosis* 22 335-348 1975
 - 28 *Svendsen E & Jorgensen L* Focal »spontaneous« alterations and loss of endothelial cells in rabbit aorta *Acta path microbiol scand Sect A* 86 1-13 1978
 - 29 *Svendsen E & Jorgensen L* Intimal pits of aorta in rabbits. Imprints of vortices of blood flow? *Acta path microbiol scand Sect A* 85 25-32 1977
 - 30 *Svendsen E & Jorgensen L* Loss of endothelial cells in rabbit aorta following short term cholesterol feeding. IV International Symposium on Atherosclerosis Aug 24-28 1976 Tokyo Japan
 - 31 *Texon M* The hemodynamic concept of atherosclerosis *Bull NY Acad Med* 36 263-274 1960
 - 32 *Weber G Fabbrini E Capacciole E & Res L* Repair of early cholesterol induced aortic lesions in rabbits after withdrawal from short term atherogenic diet *Atherosclerosis* 22 565-572 1975
 - 33 *Wright H P* Mitosis patterns in aortic endothelium *Atherosclerosis* 15 93-100 1972

A RETROSPECTIVE HISTOLOGICAL STUDY OF 669 CASES OF PRIMARY CUTANEOUS MALIGNANT MELANOMA IN CLINICAL STAGE I

4 *The Relation of Cross-sectional Profile Level of Invasion Ulceration and Vascular Invasion to Tumour Type and Prognosis*

TOVE EEG LARSEN and TOVE HELLIESEN GRUDE

Institute of Pathology University of Oslo Rikshospitalet Oslo 1 Norway and the Norwegian Radium
Hospital Oslo 3 Norway

Larsen T E & Grude T H A retrospective histological study of 669 cases of primary cutaneous malignant melanoma in clinical stage I 4 The relation of cross sectional profile level of invasion ulceration and vascular invasion to tumour type and prognosis *Acta path microbiol scand Sect A* 87 131-138 1979

A selected series of 669 primary cutaneous malignant melanomas stage I was studied. The series includes 86 lentigo maligna melanomas 259 superficial spreading malignant melanomas 194 nodular malignant melanomas and 130 unclassifiable malignant melanomas. The cross sectional profile level of invasion ulceration and vascular invasion were graded. The relation of these features to each other and to tumour type was studied by χ^2 tests. The prognostic value was also studied. The most common finding was a slightly elevated surface level III of invasion no ulceration and no vascular invasion. Most of these tumours were superficial spreading malignant melanomas. A good prognosis was associated with a flat cross sectional profile level II of invasion, no ulceration and no vascular invasion. A poor prognosis was associated with marked protrusion of the surface level IV-V of invasion ulceration and vascular invasion. Lentigo maligna melanomas tended to be more benign while nodular malignant melanomas tended to be more malignant than the average. A superficial spreading malignant melanoma could vary in either direction. The prognostic value of level of invasion and ulceration was found to be greater than that of tumour type. The prognostic importance of invasion no further than level III is stressed. Level of invasion ought to be reported to the clinician as well as the tumour type.

Key words Melanoma cross-sectional profile level of infiltration ulceration vascular invasion prognosis

T E Larsen Institute of Pathology Rikshospitalet Oslo 1 Norway

Received 10 ix 78 Accepted 20 ix 78

The method of selection of 669 primary malignant melanomas (MM) of the skin in clinical stage I (256 men and 413 women) has been reported by Iversen *et al* (1975) and by Larsen & Grude (1978a). Clark's histological classification (Clark 1967) was used. We found 86 lentigo maligna melanoma (LM) 259 superficial spreading malignant melanoma (SSM) 194 nodular malignant melanoma (NM) and 130 unclassifiable malignant melanoma (UM). The 3 types of MM had a significantly different prognosis.

In other previous papers (Larsen & Grude 1978 b and c) we reported our findings concerning the interrelation of various tumour cell features (i.e. cell type pigmentation, atypia and mitotic count) tumour associated lymphocyte infiltration and ulceration to each other as well as to tumour type and prognosis.

The present paper deals with some features related to the local expanding and invasive growth of the tumour i.e. cross sectional profile level of invasion ulceration and vascular invasion.

METHODS

The specimens were studied independently by each of the authors without access to any clinical information. The results were then compared and agreement was reached in most cases. Information about survival was provided later by the *Cancer Registry of Norway*.

Cross-sectional Profile

We classified the profile according to the system described by *Beardmore et al* (1970). The various subclasses are illustrated in Fig 1. When the superficial part of the tumour was missing the expression unclassifiable was used.

Level of Invasion

Clark's system (Fig 2) was used as described by *Clark et al* (1969) and *McGovern et al* (1973). When the deepest part of the tumour was missing the term unclassifiable was used.

Ulceration

Ulceration was defined as loss of the epidermis superficial to the tumour which had occurred *in vivo*. Intraepidermal erosions were excluded. We did not try to exclude fresh injuries in the manner of *Little* (1972).

We classified ulceration as present (+) or not present (-). When the superficial part of the tumour was missing ulceration was registered as unclassifiable.

Vascular Invasion

This feature was classified as present (+) or not present (-). We found it impossible and unnecessary to distinguish between blood and lymph vessels like *Hornstein & Weidner* did (1973) and in agreement with

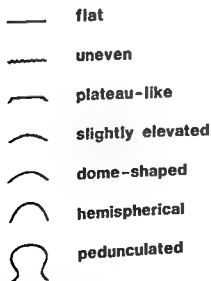


Fig 1 The gradation of cross sectional profile according to *Beardmore & Little* (1970)

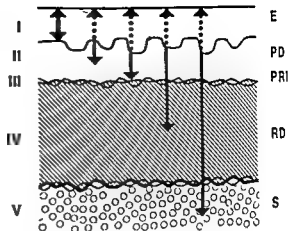


Fig 2 The gradation of level of invasion according to *Clark et al* (1969)

Fisher & Fisher (1964). Neither did we distinguish between invasion of clusters of cells and single cells. Vascular invasion was considered certain only when the suspected tumour cells were lying in an endothelial lined space (*Little* 1972, *McGovern et al* 1973). In doubtful cases the term unclassifiable was used.

RESULTS

Grading, Prognostic Value and Relation to Tumour Type

Cross-sectional Profile

The relative frequency of the different grades of protrusion of the tumour surface is illustrated in Fig 3. The slightly elevated tumours were the most frequent (165 ~ 24.7%).

The observed cumulative survival rates are also shown in Fig 3. The survival rates gradually decrease with increasing protrusion of the tumour surface. The main impression is that there is a significantly different survival between cases with every second of the subclasses after both 5 and 10 years of observation, e.g. uneven surfaced vs dome-shaped MM, dome shaped vs pedunculated MM, slightly elevated vs hemispherical MM (not after 10 years). There is no significant difference in the survival of MM patients with flat, plateau-like and slightly elevated surfaces. The survival for each tumour type has not been studied.

Among the 86 LMM as many as 83 (96.5%) were not more than slightly elevated. None were hemispherical or pedunculated. On the other hand 89 (45.9%) of the 194 NMM were hemispherical or pedunculated, while only 8 were flat or slightly elevated. The SMM showed all grades of protrusion.

Cross-sectional profile

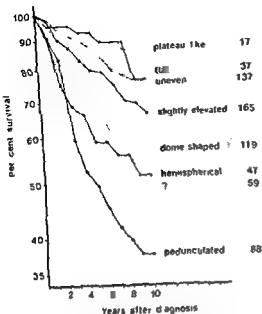


Fig 3 Survival curves illustrating the observed cumulative survival rates according to cross sectional profile

Vascular Invasion

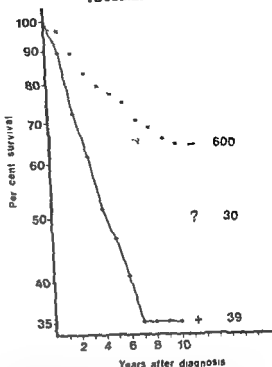


Fig 5 Survival curves illustrating the observed cumulative survival rates according to ulceration. Ulceration present — + No ulceration — — Ulceration undetermined — ?

Level of invasion

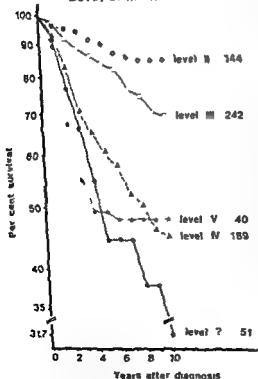


Fig 4 Survival curves illustrating the observed cumulative survival rates according to level of invasion

Level of invasion

The relative frequency of the various levels can be seen in Fig 4. The largest group was level III (242—36.2%). More than half of the cases (389—58.2%) invaded no deeper than level III.

The figure also shows the observed cumulative survival rates according to level of invasion. Three MM with level I of invasion are not illustrated. The prognosis becomes worse with increasing level of infiltration. There is a significantly different survival after both 5 and 10 years of cases with MM invading level II vs III, level III vs IV and level IV vs V (not after 10 years).

There was a strong tendency of LMM to be limited to level II (61—70.9%). Only 5 (5.8%) LMM invaded level IV and none level V. As a contrast, 82 (47.1%) of the NMN invaded level IV.

We have shown in an earlier paper (Larsen & Grude 1978a) that there is a highly significant

METHODS

The specimens were studied independently by each of the authors without access to any clinical information. The results were then compared and agreement was reached in most cases. Information about survival was provided later by the *Cancer Registry of Norway*.

Cross-sectional Profile

We classified the profile according to the system described by *Beardmore et al* (1970). The various subclasses are illustrated in Fig 1. When the superficial part of the tumour was missing the expression unclassifiable was used.

Level of Invasion

Clark's system (Fig 2) was used as described by *Clark et al* (1969) and *McGovern et al* (1973). When the deepest part of the tumour was missing the term unclassifiable was used.

Ulceration

Ulceration was defined as loss of the epidermis superficial to the tumour which had occurred in vivo. Intraepidermal erosions were excluded. We did not try to exclude fresh injuries in the manner of *Little* (1972).

We classified ulceration as present (+) or not present (-). When the superficial part of the tumour was missing ulceration was registered as unclassifiable.

Vascular Invasion

This feature was classified as present (+) or not present (-). We found it impossible and unnecessary to distinguish between blood and lymph vessels like *Hornstein & Weidner* did (1973) and in agreement with

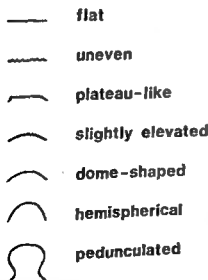


Fig 1 The gradation of cross-sectional profile according to *Beardmore & Little* (1970)

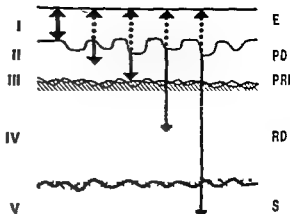


Fig 2 The gradation of level of invasion according to *Clark et al* (1969)

Fisher & Fisher (1964). Neither did we distinguish between invasion of clusters of cells and single cells. Vascular invasion was considered certain only when the suspected tumour cells were lying in an endothelial lined space (*Little* 1972, *McGovern et al* 1973). In doubtful cases the term unclassifiable was used.

RESULTS

Grading, Prognostic Value and Relation to Tumour Type

Cross-sectional Profile

The relative frequency of the different grades of protrusion of the tumour surface is illustrated in Fig 3. The slightly elevated tumours were the most frequent (165 ~ 24.7%).

The observed cumulative survival rates are also shown in Fig 3. The survival rates gradually decrease with increasing protrusion of the tumour surface. The main impression is that there is a significantly different survival between cases with every second of the subclasses after both 5 and 10 years of observation, e.g. uneven-surfaced vs dome-shaped MM, dome-shaped vs pedunculated MM, slightly elevated vs hemispherical MM (not after 10 years). There is no significant difference in the survival of MM patients with flat, plateau like and slightly elevated surfaces. The survival for each tumour type has not been studied.

Among the 86 LMM as many as 83 (96.5%) were not more than slightly elevated. None were hemispherical or pedunculated. On the other hand, 11 (45.9%) of the 194 NMM were hemispherical or pedunculated, while only 8 were flat or slightly elevated. The SMM showed all grades of protrusion.

TABLE 1 *The Relationship between Cross Sectional Profile Level of Infiltration Ulceration Vascular Invasion and Tumour Type*

Features compared	(X ²)	X ² *	Df**	P***	Obvious trends among the determinate grades and types
Level of infiltration/ tumour cell type	(36.01)	16.31	9	>0.05	Ø
Vascular invasion/ tumour type	(51.53)	15.93	6	<0.02	(+ invasion ~ NVM)
Vascular invasion/ atypia	(19.03)	15.90	3	<0.01	+ invasion ~ + + + atypia
Vascular invasion/ level of infiltration	(137.31)	33.31	8	<0.001	+ invasion ~ level V
Vascular invasion/ ulceration	(144.40)	36.45	4	<0.001	+ invasion ~ ulceration
Ulceration/tumour type	(88.30)	61.96	6	<0.001	+ ulceration ~ NVM - ulceration ~ LMM
Level of infiltration/ atypia	(96.74)	82.98	12	<0.001	level II ~ atypia + Level IV-V ~ atypia + + +
Ulceration/cross sectional profile	(274.95)	122.86	10	<0.001	+ ulceration ~ pedunculated - ulceration ~ flat uneven plateau like
Level of infiltration/ mitotic count	(143.93)	125.57	12	<0.001	level II ~ Mc + Level V ~ Mc + + +
Level of infiltration/ tumour type	(250.34)	209.41	12	<0.001	level II ~ LMM level IV-V ~ NVM
Cross-sectional pro- file/tumour type	(279.15)	235.89	15	<0.001	flat/uneven ~ LMM hemispherical ~ NVM pedunculated
Cross sectional profile/ level of infiltration	(365.95)	265.46	15	<0.001	flat uneven ~ level I-II plateau like ~ level IV domeshaped ~ level IV pedunculated ~ Level V

* The indeterminate grades and types eliminated

** Degrees of freedom

*** The complete tables are available from the author

cells may be roughly measured by the mitotic count which has been considered in one of the earlier papers (Larsen & Grude 1978 b). The significant relationship between mitotic count and level of invasion is illustrated in Table 1. The immune response of the patient may be indicated by the tumour-associated lymphocyte infiltration. This feature and the significant tendency of lymphocytes to disappear (fading or blocking of the immune response[†]) when level IV is reached has been discussed previously (Larsen & Grude 1978 c).

Cross sectional Profile. This feature was the easiest to grade. Its prognostic trend (Fig. 3) was in

agreement with the findings of Little (1972). A large number of subclasses seems to be unnecessary as the difference in survival is significant only between cases in every second class.

The highly significant tendency of LMM to be flat and of NVM to be hemispherical or pedunculated (Table 1) is in agreement with the findings of Clark (1967).

Level of invasion. The limited number of sections from each case may cast doubt on our grading of level of invasion. However, as far as we know the most of our available sections include a central transsection of the tumour (Larsen & Grude

Ulceration

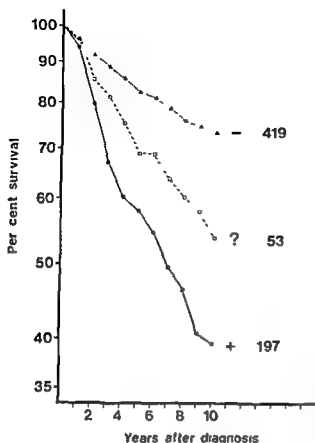


Fig 6 Survival curves illustrating the observed cumulative survival rates according to vascular invasion. Vascular invasion present + No vascular invasion - - - Vascular invasion indeterminate - ?

difference in the cumulative specific survival rates according to tumour type. However, when we concentrate on MM, level III there is no longer any significant difference in the prognosis of patients with LMM vs SMM and SMM vs NMM. In fact, there is only barely significant difference between cases with LMM and NMM. In contrast, if we take one particular tumour type, the difference in survival at level III vs IV is significant at both 5 and 10 years after diagnosis for the SMM and NMM, but not for the LMM (only 5 cases invade level IV).

Ulceration

Fig 5 shows that we found 197 (29.5%) ulcerated MM, i.e. no ulceration was the most common finding.

The observed cumulative survival of patients is significantly worse with ulcerated MM than without at both 5 and 10 years after diagnosis.

Only 5 (5.8%) of the LMM were ulcerated versus 58 (22.4%) of the SMM and 91 (46.9%) of the NMM. When we look at the survival of these patients, there is no significant difference concerning those with LMM (only 5 cases) versus SMM and SMM versus NMM after 5 and 10 years observation.

Vascular Invasion

We found vascular invasion in only 39 (5.8%) cases, i.e. no vascular invasion was the most common finding.

The observed cumulative survival rates are illustrated in Fig. 6. The presence of vascular invasion carries a significantly poor prognosis at both 5 and 10 years after diagnosis.

None of the LMM, 12 (4.6%) of the SMM and 21 (10.8%) of the NMM showed vascular invasion. These figures are too small to investigate the survival according to tumour type.

The Relationship Between the Different Features Including Tumour Cell Type, Atypia and Mitotic Count

Table 1 illustrates the results of χ^2 tests* concerning these various relationships. Because of the strong linkage of some of the indeterminate grades and types to each other we have chosen to eliminate these groups when evaluating the χ^2 value without changing the degrees of freedom. The obvious trends in the relationship between the determinate grades and types appear from the table**.

* A multiple regression analysis will be published later.

** The complete tables are available from the author.

DISCUSSION

Cross-sectional Profile and Level of Invasion

These two features both represent the mass of tumour tissue, something which is also indicated by both the tumour diameter (Breslow 1970, Little 1972, Franklin et al 1975) and the thickness of the tumour (Breslow 1970, Hansen & McCarten 1974, Wanabe et al 1975). We have not measured either the diameter or the height of the tumour.

The mass of the tumour is the result of a balance between tumour cell proliferation and loss, whether either mechanically from the surface, by cell movement into vessels or by cell death (e.g. for immunological reasons). The proliferation of MM

The incidence of vascular invasion in our series is low (5.8%). Only Little (1972) gives a lower incidence of 0.7% (which is probably too low). The many artificial clefts around tumour cells made this feature difficult to study. This problem may be responsible for the higher incidence (10–37%) in other studies (Sondergaard & Hou Jensen 1977; Cochran 1968; Hornstein & Weidner 1973).

The high prognostic significance of vascular invasion in our series is further in agreement with the findings in the studies mentioned above. Knutson *et al.* (1971) could not confirm this.

Vascular invasion was found in the superficial part of the tumour in most of our 39 cases. Most of these tumours invaded level IV–V as described by Elias *et al.* (1977). Ulceration was present in 28 of these 39 cases (Table 1). This corresponds well with the theory that long, thin walled, dilated blood and lymph capillaries are easily penetrated by tumour cells (Hornstein & Weidner 1973). Under normal conditions such vessels are found in the upper part of the dermis (level II–III). Further, such vessels are found in the granulation tissue which results from ulceration of the tumour surface and in the stroma of the tumour as a result of the production of an angiogenic factor by the MM itself (for further references see Urbach & Graham 1962; Hubler & Wyl 1976).

Finally there is a moderately significant relationship between vascular invasion and grade of atypia (grade +++ ~ invasion). This is in agreement with the findings of Engell (1959) and of Urbach & Graham (1962) concerning non melanotic tumours.

Concerning the limitation of the X² test we refer to the discussion in previous papers (Uarsen & Trude 1978 b) and c). Because of the uncertain results of this analytical method used in these papers as well as in the present one the need of a multiple regression analysis is obvious. The results of such will be published later.

CONCLUSIONS

1) The following histological features indicate a good prognosis: flat cross-sectional profile, level I or II of invasion, no ulceration and no vascular invasion. Features which indicate a bad prognosis are: a heavy protrusion of the tumour surface, level IV–V of invasion, ulceration and vascular invasion.

2) The most common findings were slightly elevated surface together with level III of invasion, no ulceration and no vascular invasion. Most of these tumours were superficial spreading malignant melanomas.

3) When a lentigo maligna melanoma diverged from this common picture it was usually in the benign direction. When nodular malignant melanoma diverged from the common picture it was usually in the malignant direction. When a superficial spreading malignant melanoma diverged it might be in either direction.

4) Level of infiltration and ulceration had greater prognostic value than tumour type. The prognostic importance of invasion no further than level III is stressed. Level of invasion ought to be reported to the clinician as well as the tumour type.

We are grateful to Professor O. H. Larsen and Dr A. Magnus, Cancer Registry of Norway, for valuable help and advice.

REFERENCES

- Allen A. C. & Spitz S. Melanoma: Diagnosis and prognosis. *Cancer* 6: 11–45, 1953.
- Beardmore G. L. Primary cutaneous polypoidal non-susceptible melanomas in Queensland. *Aust. J. Derm.* 18: 73–76, 1977.
- Beardmore G. L., Quinn R. L. & Little J. H. Malignant melanoma in Queensland. *Pathology* 105: fatal cutaneous melanomas. *Pathology* 2: 277–286, 1970.
- Breslow A. Thickness, cross-sectional areas and depth of invasion in the prognosis of cutaneous melanoma. *Ann. Surg.* 172: 902–908, 1970.
- Breslow A. Tumour thickness, level of invasion and node dissection in stage I cutaneous melanoma. *Ann. Surg.* 182: 572–575, 1975.
- Clark W. H. A classification of malignant melanoma in man correlated with histogenesis and biologic behavior. In: Montagna W. (Ed.) *Advances in biology of the skin. The pigmentary system*, 1 ed, vol. 8. Pergamon Press, Oxford, 1967, p. 621–647.
- Clark W. H., From L., Bernardino E. A. & Mihm M. C. The histogenesis and biologic behavior of primary human malignant melanomas of the skin. *Cancer Research* 29: 705–726, 1969.
- Cochran A. J. Histology and prognosis in malignant melanoma. *J. Path.* 97: 459–468, 1969.
- Donellan M. J., Seemayer T., Huys A. G., Mike V. & Strong E. W. Clinicopathologic study of cutaneous melanoma of the head and neck. *Amer. J. Surg.* 124: 450–455, 1972.
- Elias E. G., Didolkar M. S., Goel J. P., Forrester J. F., Valenzuela L. A., Pickett S. L. & Moore R. H. A clinicopathologic study of prognostic factors in cutaneous malignant melanoma. *Surg. Gynecol. Obstet.* 144: 327–334, 1977.
- Fisher B. & Fisher E. R. Biologic aspects of cancer-cell spread. *Proc. Nat. Cancer Conf.* vol. 5, J. B. Lippincott, Co., Philadelphia, 1964, p. 105–121.
- Fitzpatrick P. J., Brown T. C. & Reid J. Malignant melanoma of the head and neck. A clinicopathologic study. *Can. J. Surg.* 15: 90–101, 1972.

1978a) In a prospective study of MM (Larsen 1978) the deepest level of invasive growth was always seen in the central part of the tumour, unless there were changes indicating clinical tumour regression in this area. Finally, Hermanek *et al* (1976) in fact found that the study of 1-2 blocks from a MM was enough to evaluate the level of invasion. We consider, therefore, our findings to be reliable. However, we sometimes found it difficult to distinguish between two neighbour levels. Other investigators mention the same problem (Breslow 1975, Wanebo *et al* 1975, Steigleder & Kleine 1977).

We found the same incidence of level III as Hermanek *et al* (1976) but we have a higher incidence of level II and a lower one of level IV-V. This is probably mainly due to a higher incidence of NMM in the German series of MM, clinical stage I than in ours (53% vs 29%) see below.

Level of invasion bears no relation to tumour cell type. Its relation to mitotic count and atypia (Table 1) is however, highly significant. This is in agreement with the finding that the mitotic count indicates the tumour cell proliferation and that the degree of atypia measures the malignant properties of the tumour cells. The time factor (age of the MM before removal) has however not been considered.

As expected we found a highly significant trend in the relationship between cross sectional profile and level of invasion (Table 1) i.e. that pedunculated MM invade mainly level IV-V. An exception to this rule is the pedunculated MM level II-III. Little (1972) and later Beardmore (1977) found that the prognosis of these cases is as poor as that of MM level V. We have 31 such cases in our series which show a 5 year survival rate of 74% and a 10 year survival rate of 65%. This is not worse than that of all MM level III. We have no explanation of this difference unless we have included some juvenile melanomas in this group.

The prognostic significance of level of invasion (Fig. 4) and its relation to tumour type (Table 1) in our series is in agreement with that in earlier studies (for further references see Clark *et al* 1969, McGovern 1970, Little 1972, Donellan *et al* 1972, Hermanek *et al* 1976, Sondergaard & Hou-Jensen 1977).

Hermanek *et al* (1976) pointed out that level of invasion is more important to the prognosis of MM than the tumour type according to Clark's system. Our study confirms this. Breslow (1970) prefers to measure the tumour thickness. We recommend that at least level of invasion is reported to the clinician as well as the tumour type. Further it seems extremely important that the tumour does not penetrate level III. There is a significant difference

in the survival rates (Fig. 4) when moving from level III to IV both at 5 years and 10 years after diagnosis. This trend is significant in each particular tumour type.

The highly significant trend of LMM to show usually a small mass of low grade malignant tumour tissue and of NMM to show usually a large mass of high grade malignant tumour tissue while SMM may vary in either direction may well explain the difference in survival according to tumour type.

Ulceration

The incidence of ulcerated MM in our series (29.5%) correspond well with the 30% of the MM clinical stage I of Pakkanen (1977) but is somewhat lower than that of studies including MM with known metastases (e.g. Cochran 1968, 46%).

The prognostic significance of ulceration in our series (Fig. 5) is in agreement with most earlier studies (for further references see Cochran 1968, Little 1972, Huvois *et al* 1974, Sondergaard & Hou-Jensen 1977, Knutson *et al* (1971) and Eljas *et al* (1977), however did not find any prognostic significance of this feature.

The prognostic significance of ulceration seems to be greater than that of tumour type. This might merely be due to a large mass of tumour (Table 1) as pointed out by McGovern *et al* (1973) and Franklin *et al* (1975). Heavily protruding tumours may easily be injured. Allen & Spitz (1953) found however, a higher incidence of ulceration among small fatal MM than among small nonfatal MM. Correspondingly Petersen *et al* (1962) found a highly prognostic significance of ulceration at one particular level of invasion. We have studied the prognostic importance of ulceration in tumours with a flat or slightly elevated surface. These cases show significantly lower survival rates of ulcerated than of non ulcerated tumours at both 5 and 10 years after diagnosis. This indicates that the mere presence of an ulceration is a prognostic important feature independently of the size of the tumour and the tumour type.

It is our impression that ulceration and vascular invasion often coexist (see below). The poor prognosis of ulcerated tumours may be due to a high incidence of vascular invasion.

Vascular invasion

The presence of intravascular tumour cells is by no means proof that a malignant tumour has metastasized (for further references see Fisher & Fisher 1964). One might however, expect some prognostic significance especially if the vascular invasion is found in only one or a few blocks of the tumour independently of its size.

HISTOLOGICAL CHANGES IN TESTICULAR BIOPSIES FROM CHRONIC ALCOHOLICS WITH AND WITHOUT LIVER DISEASE

P T BOESEN J LINDHOLM C HAGEN M BAHNSEN and N FABRICIUS-BJERRE

The Institute of Pathology and Medical Department III Kommunehospitalet, Copenhagen and Medical Department F Copenhagen County Hospital Glostrup Denmark

Boesen P T Lindholm J Hagen C Bahnsen & Fabricius Bjerre N Histological changes in testicular biopsies from chronic alcoholics with and without liver disease Acta path microbiol scand Sect A 87 139-142 1979

Testicular and liver biopsies were obtained from thirty consecutive patients at the age of 30 to 64 years with chronic alcoholism (daily consumption of 72 g of alcohol or more for at least five years). The spermatogenesis was normal in 12 patients (40 per cent) moderately reduced in 15 patients (50 per cent) and severely reduced in 3 patients (10 per cent). No relation between the presence of liver disease as assessed by histological examination of the liver biopsy and the impairment in the spermatogenesis could be demonstrated.

Key words Spermatogenesis versus chronic alcoholism liver

Poul T Boesen Institute of Pathology Kommunehospitalet, DK 1399 Copenhagen K Denmark

Received 23 vii 78 Accepted 6 x 78

Early investigations on testicular histology in patients with alcoholic cirrhosis of the liver reported changes in the testes mainly confined to the germinal epithelium (4-13). At that time the cause was thought to be a combined effect of liver disease and direct toxicity of alcohol on the testes, since the changes were more pronounced in the patients with cirrhosis than in those without.

Later the liver disease, especially the alcoholic cirrhosis, was thought to be the dominating if not the only cause of reduced spermatogenesis (1, 8-9). Elevation in serum concentration of estrogens caused by an impaired ability of the liver to conjugate these hormones was thought to cause the spermatogenic reduction.

Recent studies of the pituitary testicular function have raised serious doubts about the role of liver diseases as the main cause of testicular changes in chronic alcoholism (5, 6, 11, 12).

We have studied the light microscopy findings in testicular biopsies in patients with chronic alcoholism and correlated the findings to the liver histology.

MATERIAL AND METHODS

The material comprised biopsies from the testes and liver of thirty consecutive patients with chronic alcoholism aged 30 to 64 years admitted to a medical ward.

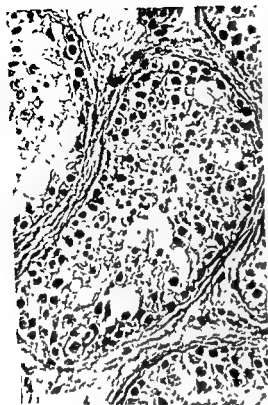
... was 4-5 times this amount for 10-15 years. They were informed about the biopsy procedures and agreed to participate. Patients with primary testicular disorders, severe liver disease, clinical signs and/or symptoms of other endocrine diseases as well as patients receiving ...

... and cut in serial sections (6 μ m - approximately 50 sections).

The light microscopy was performed ...

h
n
st

- Franklin J D, Reynolds V H & Page, D L Cutaneous melanoma A Twenty-year retrospective study with clinicopathologic correlation *Plast Reconstr Surg* 56 277-285, 1975
- Hansen M G & McCarten, A B Tumor thickness and lymphocytic infiltration in malignant melanoma of the head and neck *Am J Surg* 128 557-561, 1974
- Hermanek P, Hornstein, O P, Tonak, J & Weidner, F Malignes Melanom Invasionstiefe und Melanomtyp *Beitrage Pathol* 157 269-282, 1976
- Hornstein, O P & Weidner, F Untersuchungen zur prognostischen Bedeutung der »Stromareaktion« beim malignen Melanom I Vascularisation und Prognose Virchows Arch Abt A Path Anat 359 67-76, 1973
- Hubler, W R & Wolf, J E Melanoma Tumor angiogenesis and human neoplasia *Cancer* 38 187-192, 1976
- Huvs A G, Shah, J P & Miké, V Prognostic factors in cutaneous malignant melanoma A comparative study of long term and short term survivors *Human Pathology* 5 347-357, 1974
- Iversen O H, Larsen T E, Grude, T H & Magnus K Histological classification of malignant melanoma in relation to prognosis and cytogenesis Proceedings of The Sixth International Symposium on the Biological Characterization of Human Tumours *Excerpta medica international congress series* No 375, Amsterdam 1975, p 260-273
- Knutson C O, Hori J M & Spratt, J S Melanoma *Curr Probl Surg* No 12 1-55, 1971
- Larsen T E The classification of primary cutaneous malignant melanoma A prospective study of 60 cases using Clark's classification *Acta Path Microbiol Scand Section A* 86 451-459 1978
- Larsen T E & Grude T H A retrospective histological study of 669 cases of primary cutaneous malignant melanoma in clinical stage I I Histological classification sex and age of the patients localization of tumour and prognosis *Acta Path Microbiol Scand Section A* 86 437-450 1978
- Larsen T E & Grude T H A retrospective histological study of 669 cases of primary cutaneous malignant melanoma in clinical stage I 2 The relation of cell type, pigmentation, Atypia and mitotic count to histological type and prognosis *Acta Path Microbiol Scand Section A*, 86 513-522, 1978
- Larsen, T E & Grude, T H A retrospective histological study of 669 cases of primary cutaneous malignant melanoma in clinical stage I 3 The relation of tumour-associated lymphocyte infiltration and sex and sex, tumour cell type, pigmentation cellular atypia, mitotic count depth of invasion ulceration tumour type and prognosis *Acta Path Microbiol Scand Section A*, 86 523-530, 1978
- Little, J H Histology and prognosis in cutaneous malignant melanoma In McCarthy, W H (Ed) International cancer conference, Sydney 1972 Melanoma and skin cancer, Proceedings, 1st ed Bligh, C N, Government Printer, Sydney 1972, pp 107-119
- McGovern V J The classification of melanoma and its relationship with prognosis *Pathology* 2 85-88 1970
- McGovern V J, Mihm M C, Bailly, C Booth J C, Clark, W H, Cochran A J, Hardy, E G, Hicks J D, Levene, A, Lewis, M G, Little, J H & Milton G W The classification of malignant melanoma and its histologic reporting *Cancer* 32 1446-1457, 1973
- Pakkanen, M Clinical appearance and treatment of malignant melanoma of the skin *Ann Chir Gynaecol* 66 21-30, 1977
- Petersen, N C, Bodenham D C & Lloyd O G Malignant melanomas of the skin A Study of the origin, development, aetiology spread, treatment and prognosis Part I *Brit J Plast. Surg* 15 49-94 1962
- Siegleider, G K & Kleime W Vertikaler Durchmesser (Dicke) und Prognose beim malignen Melanom *J Hautkr* 52 969-972, 1977
- Søndergaard K & Hou-Jensen K Histologi og prognose ved kutant malignt melanom *Ugeskrift for Læger* 139 2993-2996 1977
- Urbach F & Graham J H Anatomy of human skin tumour capillaries *Nature* 194 652-654 1962
- Wanebo H J, Woodruff J & Forner J G Malignant melanoma of the extremities A clinicopathologic study using levels of invasion (microstage) *Cancer* 35 666-676 1975



were also studied. The following components of the testicular tissue have been semiquantitatively assessed

- 1 The germinal epithelium
- 2 The lamina propria of the seminiferous tubules
- 3 The interstitial tissue

The testicular biopsies were divided into three groups based upon the spermatogenesis as judged by the testicular biopsy score count method (3). According to this method each tubular cross section is given a score from 10-1 according to the following criteria: score 10 = normal epithelium; Score 9 = disorganised epithelium; Score 8 = only few spermatozoa present; Score 7 = no spermatozoa but many spermatids present; Score 6 = no spermatozoa and only few spermatids present; Score 5 = no spermatozoa no spermatids but many spermatocytes present; Score 4 = no spermatozoa no spermatids and only few spermatocytes present; Score 3 = only spermatogonia present; Score 2 = no germ cells but Sertoli cells present; Score 1 = no cells present.

In each biopsy 50 tubular cross sections were given a score and the mean score (MS) was calculated. Biopsies with a MS of 8.00 or more were considered normal while those from 4.00 to 8.00 were called moderately reduced spermatogenesis. Biopsies with a mean score of less than 4.00 were designated severely reduced spermatogenesis.

The tubular lamina propria was examined for fibrosis.

In the interstices special attention was paid to whether alterations in number and morphology of the Leydig cells were present. It was also registered if fibrosis or inflammatory reaction was present.

At the time of the testicular biopsy a percutaneous liver biopsy was performed by the Menghini technique (in one case only minimal liver tissue was available and no definite diagnosis could be made).

The liver tissue was fixed in neutral formalin, embedded in paraffin and cut in serial sections (6 μ m - 50 sections). Haematoxylin and eosin stained sections were studied as well as additional sections stained for collagen fibres, reticulin fibres, iron, PAS positive material and pyroninophile substance.

The biopsies were examined and divided into three main categories:

- 1 Normal
- 2 Steatosis without cirrhosis
- 3 Cirrhosis

The non cirrhotic liver biopsies with less than five per cent of the liver cells showing fatty change were considered within normal limits. The remaining biopsies were divided into three groups according to the degree of steatosis: mild, moderate and severe. Only in three biopsies was alcoholic hepatitis found and no subgrouping on this point was performed.

The liver and testicular biopsies were examined without any knowledge of the clinical or hormonal status of the patients.

TABLE 1 Correlation between Spermatogenesis and Liver Histology

Spermatogenesis		Liver histology	
I	Normal Mean age and range (years) 47.8 (30-56)	12	Normal 2 Steatosis 8 Cirrhosis 2
II	Moderately reduced Mean age and range (years) 51.9 (31-46)	15	Normal 3 Steatosis 5 Cirrhosis 6 Unsuitable 1
III	Severely reduced Mean age and range (years) 52.3 (43-60)	3	Normal 1 Steatosis 0 Cirrhosis 2
Total		30	30

RESULTS

As shown in Table 1 there was a marked variation in the spermatogenesis with 40 per cent of the biopsies appearing normal (Fig. 1). In the remaining biopsies fifteen (50 per cent) showed moderately reduced spermatogenesis (Fig. 2) while only three (10 per cent) showed severely reduced spermatogenesis (Fig. 3 and 4). The ages of the patients in the three groups were not significantly different.

The lamina propria of the seminiferous tubules showed only minimal fibrosis in 21 biopsies while in 8 cases there was moderate fibrous thickening and in only one case severe fibrosis.

Fig. 1 Cross section of seminiferous tubules with presence of all germ cell types including mature spermatozoa. The lamina propria is only slightly fibrotic and the interstices are edematous. Haematoxylin and eosin $\times 250$.

Fig. 2 Cross section of seminiferous tubules with disorganized germinal epithelium and predominance of spermatocytes but no mature spermatozoa. The lamina propria is only minimally fibrotic and the interstices show a slightly increased number of Leydig cells. Example of moderately reduced spermatogenesis. Haematoxylin and eosin $\times 250$.

Fig. 3 and 4 Cross section of seminiferous tubules with few germ cells (spermatogonia). The lamina propria is slightly fibrotic and the interstices are edematous but show no Leydig cell hyperplasia. Examples of severely reduced spermatogenesis. Haematoxylin and eosin $\times 100$ (Fig. 3) and $\times 250$ (Fig. 4).

INFLUENCE OF SURFACE LIPIDS ON SKIN CARCINOGENESIS IN RATS

E. ARFFMANN and N. HJØRNE

Departments of Pathology and Clinical Chemistry Aalborg Hospital North Aalborg Denmark

E. Arfmann & N. Hjerne: Influence of surface lipids on skin carcinogenesis in rats. *Acta path. microbiol. scand. Sect. A* 87: 143-149, 1979.

Skin tumours were induced in female Wistar SPF rats by different polycyclic aromatic hydrocarbons (PAHs): benzo[a]pyrene (BaP), benzo[a]anthracene (BaA), dibenz[a,h]anthracene (DBA) and 3

values were BP. Half of the animals in each group underwent skin-surface lipid extraction (SSLE) before the application of carcinogen. SSLE did not influence the cumulative number of rats with skin tumours during an observation period of 15 months nor the type of tumours induced. The lipid extraction however increased the latency period and decreased the rate of tumour development when BP and MCA acted as carcinogens. On the contrary, SSLE enhanced the rate of tumour production by DMBA and reduced the latency period. The role of sebum and its composition in skin carcinogenesis is discussed and an explanation of the different influence of SSLE on BP and MCA carcinogenesis is contrasted to DMBA carcinogenesis is sought in differences in metabolic activation of the carcinogens.

Key words: Surface lipids, skin carcinogenesis, rats

E. Arffmann Department of Pathology Aalborg Hospital North P.O. box 361 DK 9100 Aalborg Denmark

Received 17 Jul 78 Accepted 1 Mar 79

The sensitivity to chemical carcinogens of the skin of rats differs from that of mice Berenblum (1959):

skin carcinogen among polycyclic hydrocarbons but fewer chemicals prove carcinogenic for the skin of rats (Cherry & Glucksmann 1971)

Glavind & Christensen (1967, 1969) observed that surface lipids of the skin of rats normally contain substantial amounts of peroxides. In contrast only small amounts were found in the skin surface lipids of mice, hamsters, guinea-pigs and rabbits. The difference was explained by the fact that the rat is the only common rodent which excretes large amounts of linoleic acid in the skin-surface.

The very low peroxide content in skin surface lipids of mice has later been confirmed (Arffmann & Glavind 1974). The different composition of the surface lipids in rats implies the presence of autooxidative processes which may have a destructive action on the carcinogenic hydrocarbons explaining the relative protection of the skin, as suggested by Glavind & Christensen (1969). The present study was undertaken to investigate the effect of SSLE on skin carcinogenesis in rats using various carcinogenic hydrocarbons.

MATERIAL AND METHODS

Animals Female Wistar SPF rats (number 4)

In one third of the cases slight fibrosis and chronic inflammation was present in the interstitial tissue as well as a minimal increase in the number of Leydig cells. Table 1 also shows the distribution of the 30 consecutive liver biopsies. As in the testicular biopsies the histological findings varied considerably, with the largest group (approximately 40 per cent) showing various degree of steatosis.

The fatty change in the liver biopsies (classified as steatosis without cirrhosis) was almost identical in eleven of the thirteen biopsies, namely mild steatosis, while the remaining two showed moderate and severe steatosis. No relation between the degree of steatosis and reduction in spermatogenesis could be demonstrated.

Six liver biopsies were normal and ten showed cirrhotic liver tissue. The three cases of alcoholic hepatitis were all found in patients with cirrhosis.

Spermatogenesis and liver histology have been compared (Table 1). In six patients with normal liver histology only two had intact spermatogenesis. Of the remaining 4 patients three had moderately reduced spermatogenesis and one severely reduced spermatogenesis.

DISCUSSION

Since the beginning of this century reduced spermatogenesis in chronic alcoholics with cirrhosis of the liver has been well recognized (4, 13). The original concept that alcohol has a toxic effect on the testes was apparently forgotten and several studies incriminated the hepatic insufficiency as the cause of spermatogenetic reduction (1, 8, 9). A recent report (10) demonstrating sterility and abnormal seminal fluid in chronic alcoholic males without advanced liver disease again raised the question of whether alcohol *per se* also is toxic to testicular tissue. Alcohol is known to be toxic to various tissues such as liver, myocardium, hematopoietic and nervous tissue etc. but the mode of action of alcohol is not known. Data suggesting that alcohol might act directly on the testes have recently been reported (2, 11, 12) and several mechanisms for the action of alcohol have been suggested.

However, no satisfactory explanation has been given for the marked difference in spermatogenesis in patients with the same degree of liver disease. The almost identical degree of steatosis precluded any evaluation of the relation between spermatogenesis and degree of steatosis. Our investigations show that alcohol seems to affect the germinal epithelium while the changes in the tubular lamina propria (fibrosis) and in the interstices (fibrosis, chronic inflammation and Leydig cell abnormalities) were inconspicuous.

No relationship between liver disease (especially cirrhosis) and testicular changes could be demonstrated. The finding that four patients (14 per cent) with normal liver histology had either severely or moderately reduced spermatogenesis suggests that alcohol *per se* has a direct toxic effect on the testes. Most likely reduced spermatogenesis in chronic alcoholics is due to a combined effect of alcohol and hepatic disease as a previous investigation has demonstrated spermatogenetic disorders in non-alcoholic liver disease (8).

REFERENCES

1. Bennett H S, Baggenstoss A H & Bull H R. The testis, breast and prostate of men who die of cirrhosis of the liver. *Am J clin Path* 70: 814-828 1950.
2. Gotliao Teles A, Anderson D G, Burke G H. Biologically active androgens and oestradiol in men with chronic liver disease. *Lancet* i: 173-177 1973.
3. Johnsen S G. Testicular Biopsy Score Count—A Method for Registration of Spermatogenesis in human testes. *Hormones* 1: 1-24 1970.
4. Kyrle J. Über Strukturveränderungen im menschlichen Hodenparenchym. *Verh Dtsch path Gesellsch* 13: 391-395 1909.
5. Lindholm J, Fabricius Bjerre N, Hagen C, Bahnsen M, Boiesen P. Pituitary testicular function in patients with chronic alcoholism. *European Journal of Clinical Investigation*. Accepted for publication.
6. Lindholm J, Fabricius Bjerre N, Bahnsen M, Boiesen P, Hagen C & Christensen T. Sex steroids and sex hormone binding globulin in males with chronic alcoholism. *European Journal of Clinical Investigation*. Accepted for publication.
7. Pearce A G F. *Histochemistry* ed 3 vol 1 p 602 London 1968.
8. Morrione T G. Effect of estrogens on the testis in hepatic insufficiency. *Arch Path* 37: 39-43 1944.
9. Rafter L J. Hepatic cirrhosis and testicular atrophy. *Arch Int Med* 80: 397-407 1947.
10. Van Thiel D H, Gavaler J S & Lester R. Ethanol inhibition of vitamin A metabolism in the testis.
11. Goldman M D. Alcohol induced testicular atrophy: an experimental model for hypogonadism occurring in chronic alcoholic men. *Gastroenterology* 69: 326-332 1975.
12. Van Thiel D H, Lester R & Shinn R J. Hypogonadism in alcoholic liver disease: evidence for a double effect. *Gastroenterology* 67: 1188-1199 1974.
13. Wechselbaum A. Über Veränderungen der Hoden bei chronischem Alkoholismus. *Verh Dtsch path Gesellsch* 13: 391-395 1909.

Standard curve A series of standards representing 5 10 20 30 and 40 $\mu\text{mole/l}$ is prepared by pipetting into 10 ml volumetric flasks 250 500 1000 1500 and 2000 μl respectively of the Fe^{+++} standard 200 $\mu\text{mole/l}$ and filling to the mark with Fe^{++} solution 200 $\mu\text{mole/l}$

After thoroughly mixing the absorbances of the solutions are measured at 500 nm against the reagent blank and the corresponding values of concentrations and absorbances are plotted into a coordinate system with the concentration as the abscissa and the absorbance as the ordinate

Observation of tumour development All animals were examined in two weeks interval and the number size

and distribution of tumours noted Only tumours measuring $2 \times 2 \text{ mm}$ or more were counted in

Animals were sacrificed when the skin tumours were clinically malignant and influenced their general state Surviving animals were killed after 15 months in experiment

Autopsy was performed on all rats and included a histologic examination of the skin and when indicated of internal organs

RESULTS

Table 1 presents the average results of determining total skin surface lipids and peroxides in the

TABLE 1 Lipoperoxide Content and Total Amount of Skin Surface Lipids from Random Groups of Female Wistar SPF rats

Group	Animal weight g ¹⁾	Mg fat ¹⁾ extracted/rat on		Peroxide $\mu\text{equival}^{1)}/\text{rat on}$	
		1st day	2nd day	1st day	2nd day
1 b	253.3	79.7	28.6	5.4	0.9
2 b	272.4	79.1	27.8	3.0	0.7
3 b	250.0	86.1	26.3	1.5	0.9
4 b	254.7	82.1	30.1	2.9	0.8

Extraction with acetone was performed on two consecutive days

¹⁾ Average values from 15 consecutive extractions on fully grown animals

TABLE 2 Skin Tumour Induction in Female Wistar SPF Rats by Topical Application of Carcinogenic Hydrocarbons with or without Preceding Skin Surface Lipid Extraction (SSLE)

Group	Treatment (total dose/rat)	No of rats	Survivors at the appearance of the first skin tumour	Cumulative no of rats with skin tumours ^{*)}	Days to first skin tumour
1 a	BP 150 mg	10	10	8	280
b	- - + SSLE	10	4	3	303
2 a	DBA 112.5 mg	10		0	
b	- - + SSLE	10		0	
3 a	MC 125 mg	10	10	9	238
b	- - + SSLE	10	6	6	280
4 a	DMBA 30 mg	10	10	9	183
b	- - + SSLE	10	8	8	155

¹⁾ Benzo(a)pyrene

²⁾ Dibenz(a,h)anthracene

³⁾ 1,3 Methylcholanthrene

⁴⁾ 7,12 Dimethylbenzo(a)anthracene

^{*)} Minimal size $2 \times 2 \text{ mm}$

mixture from Korn og Foderstofkompagniet Copenhagen) with water ad libitum. The experiment started when the animals were 56 to 63 days old.

Carcinogens The carcinogenic hydrocarbons used were benzo(a)pyrene (BP), 3-methylcholanthrene (MCA) and 7,12-dimethylbenzo(a)anthracene (DMBA) (Sigma Chemical Company) and dibenz(a,h)anthracene (DBA) (Koch Light Ltd). They were solved in acetone (pro analysis Merck) to obtain saturated and clear solutions. The resulting concentrations all w/v were 0.25 per cent for DBA, 0.5 per cent for MCA and 1.0 per cent for BP. A higher concentration could have been obtained with DMBA but it was decided to use a 1 per cent solution as with BP.

Experimental procedures Eighty animals were randomly distributed in 4 groups of 20 each i.e. one group for each carcinogen. In the individual groups the carcinogen solution was dropped with a syringe pipette in a volume of 0.25 ml on the hindmost half of the dorsal skin of the animals after shaving off the hair. The carcinogen was administered at two weeks interval and each animal received a total of 20 applications of the 0.25 ml acetone solution.

Each of the 4 main groups was divided into two subgroups of 10 rats each 'a' and 'b'. The 'a' subgroups were treated as mentioned above, the 'b' subgroups had in addition their skin surface lipids extracted before the application of carcinogen.

Extraction of skin surface lipids was performed as described in detail by Glavind & Christensen (1967). The main steps of this procedure are anesthesia of the rats with ether and immersion of the animals' body in acetone (pro analysis Merck). All animals of the same 'b' subgroup were extracted with the same 300 ml portion of acetone. The extraction was performed at two weeks interval and on two consecutive days. The carcinogen application was made on the 2nd day immediately after evaporation of the acetone from the skin.

The animal room was lit by fluorescent lamps giving 0.096 per cent of ultra violet rays. The light was put on for 12 hours in every 24. The animals of the 'b' subgroups had a peroral supplement of vitamin E (d- α -tocopherol acetate, Hoffmann-La Roche & Co.) given separately in an alcoholic solution (daily amount 8-9 mg per animal for 5 days = 1 week) to give partial protection against autooxidation of the skin surface lipids.

Determination of lipoperoxides

Reagents

1. Ammoniumthiocyanate solution (max storage time 2 weeks)
Ammoniumthiocyanate (Merck 1213) 6.0 g
Ethanol 99% up to 100 ml
2. Chloroform thiocyanate solution (max storage time 2 weeks)
Chloroform (Merck 2445) 250 ml
Ammoniumthiocyanate solution 250 ml
3. Fe+++ standard stock solution 20 mmole/l (to be kept in darkness) 0.585 g
Iron powder (Merck 3819) 50 ml
Hydrochloric acid 10 mole/l

- Hydrogenperoxide 30% 2 ml
Distilled water up to 500 ml
- The iron powder is dissolved in the hydrochloric acid and the hydrogenperoxide is added. Surplus of peroxide is destroyed by boiling for 5 min. The water is added.
4. Fe+++ standard 200 μ mole/l (to be made immediately before use)
Fe+++ standard stock solution 20 mmole/l 250 μ l
Chloroform thiocyanate solution up to 25 ml
 5. Fe++ stock solution 40 mmole/l (max storage time 2 weeks at 0-5°C)
a. { Bariumchloride dihydrate (Merck 1719) 0.89 g
Distilled water up to 50 ml
b. { Ferrous sulphate heptahydrate (Merck 3965) 1.11 g
Distilled water up to 50 ml
Hydrochloric acid conc (Merck 317) 2 ml

a and b are mixed and the hydrochloric acid is added. The mixture is filtered through an ash free filter paper.

6. Fe++ solution 200 μ mole/l (to be made immediately before use) 125 μ l
Fe++ stock solution 40 mmole/l 25 ml
Chloroform thiocyanate solution up to 25 ml

Method

Samples: the acetone-extract from one group of animals (approx. 300 ml) is filtered and a suitable aliquot (which by experience is known to contain approx. 10 mg of surface lipids) is transferred into a pre-weighed flask. The content is evaporated into dryness in vacuo at a temperature not exceeding 35°C. The flask is weighed again to determine the exact amount of lipids (1 gram). The residue is re-dissolved in a suitable volume (8 ml at least 6 ml) of chloroform and after complete dissolution 5.0 ml is transferred into a graduated test tube with a total volume of about 15 ml.

5 ml of ammoniumthiocyanate solution is added and the volume of the content is noted. Nitrogen is passed through the solution for 15 minutes. 50 μ l of Fe++ stock solution 40 mmole/l is added and the nitrogen pass is continued for another 3 minutes. The volume of the content is checked and if necessary established by addition of chloroform.

The absorbance of the solution is finally read spectrophotometrically at 500 nm against the reagent blank.

The corresponding Fe+++ concentration is found from the standard curve and the peroxide index (meq peroxide/1000 g lipid) is calculated from the following equation:

$$\text{Peroxide index} = \frac{\text{Fe}^{+++}\text{-conc} \times B}{S \times A}$$

Reagent blank: A mixture of 5.0 ml chloroform, 5.0 ml ammoniumthiocyanate solution and 50 μ l Fe++ stock solution 40 mmole/l.

oma components occurred in only two cases. The BP treated group took an intermediate position as to tumour type induced. In 8 of 13 rats dying with tumours (of any size) squamous cell tumours with cellular atypia dominated, five infiltrated the panniculus carnosus three the corium only. But 5 of these cases included basal cell tumour areas and in addition 4 animals of the group died with small basalomas as the predominant tumour lesion. One of the 13 rats died with a benign squamous cell papilloma.

Significant differences as to tumour types did not appear between animals undergoing SSLE and those left untreated before the carcinogen application.

Figure 1 demonstrates the rate of tumour development benign and malignant in the various groups expressed by the number of tumours per animal alive at any time. The graph has two curves for each of the three tumour inducing carcinogens one for each animal subgroup. The starting point of each curve reflects the latency periods which are specified in Table 2. The curves demonstrate that a shorter induction period is followed by a faster rate of tumour development. It is evident that DMBA is the most potent carcinogen in our experiment, as shown both by length of latency period and steepness of curves. It is also clearly shown that MCA is more potent than BP. The terminal decline of the curve for the DMBA + SSLE treated subgroup is due to a confluence of tumours which made it impossible to define the individual tumours.

Malignant tumours in other sites than the skin were rare and seen only in animals treated with DMBA. Three rats had adenocarcinoma of the mamma, one rat an endometrial carcinoma and one rat an ear-duct carcinoma metastasizing to the pleura.

DISCUSSION

It appears from Table 1 that the extraction procedure leads to a significant reduction of the total amount of skin-surface lipids and of their peroxide content in all animal groups. The effect of vitamin E given as a dietary supplement and leading to a decrease of the peroxide content was anticipated on the basis of earlier observations (Glavin & Christensen 1967, 1969; Lo & Black 1973) and not checked in this study.

The total of 20 applications of carcinogen was chosen because this number was found optimal by Glucksmann & Cherry (1971) for the induction of epithelial tumours in the dorsal skin of rats when DMBA was administered weekly in a 1 per cent solution. Accordingly almost 90 per cent of our rats

treated with DMBA died with carcinoma of the skin.

When our results are given as cumulative numbers of animals bearing tumours, benign or malignant, there is no significant difference between animals whose skin has been deprived of surface lipids and animals not treated before carcinogen application (Table 2). Table 1 shows, however, that a difference emerges when induction periods are compared. After application of BP and MCA the first skin tumour appeared earlier in the animal subgroups that had the carcinogen administered without pre-treatment of the skin, especially within group 3. Conversely, by SSLE the induction of the first tumour after DMBA painting was accelerated with 28 days.

These differences are confirmed and extended by Figure 1, which shows a more rapid development in number of tumours per rat when MCA and BP are administered without preceding SSLE, while this treatment on the contrary seems to enhance the production of skin tumours when followed by DMBA application.

Two factors may be of importance for the observed results: namely the amount of fat on the surface of the skin and the peroxide content in this fat.

Sebum is produced by the sebaceous glands and serves as a natural vehicle in chemical carcinogenesis of the skin. It has been supposed that the thick layer of keratinized epidermis in rats might inhibit the absorption of carcinogens. This possible explanation of the apparent resistance to tar cancer in these animals found some support in Watson's experiments (1933) which indicated that preliminary treatment of the skin of rats with a lipid extract to facilitate absorption might increase the carcinogenic effect of tar. Arundell *et al.* (1969) tested DMBA

on normal and on sebaceous gland deficient mice. In addition, the latency period for the development of skin carcinomas was longer in the aseptic mice. These experimental observations indicate that sebaceous glands and their secretion product may play some, although not a critical, role in skin carcinogenesis.

In the present study the longer latency period and the lower rate of tumour production after MCA or BP application to acetone treated skin compared with the application to untreated skin might be due to the removal of sebum as a supposedly important vehicle substance. This explanation, however, seems

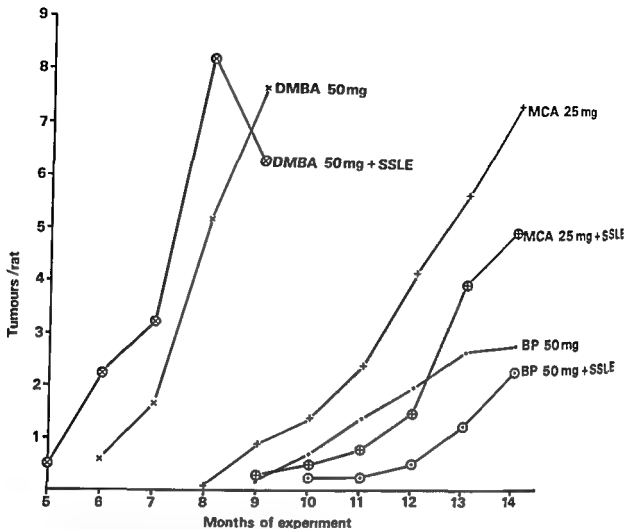


Fig 1 Tumour induction in the skin of rats by topical application of various polycyclic aromatic hydrocarbons with or without preceding skin surface lipid extraction (SSLE)

Total doses of the carcinogens applied are given

The rate of tumour development is expressed as the average number of tumours benign and malignant per rat alive at monthly intervals from the 5th to the 14th month of the experimental period

DMBA = 7.12 dimethylbenz[*a*]anthracene

MCA = 3 methylcholanthrene

BP = benzo[*a*]pyrene

individual groups of rats. Animal weights and total amounts of extracted fat on the 1st and the 2nd days do not differ significantly from group to group. The peroxide content calculated per rat is distinctly higher in animal group 1b than in the other groups but on the 2nd day the lower values are equal. Lipid amounts and peroxide contents are lower than found by Glavind & Christensen (1967, 1969) in male Wistar rats.

In Table 2 the skin tumour induction is expressed by means of the number of tumour bearing rats and the latency period. Unfortunately, quite many rats died during the anesthesia, and this reduced the subgroups.

DBA induced only a single skin tumour, a basalioma occurring in the a subgroup and meas-

ring less than 2 mm. In the remaining groups the tumour types varied significantly with the carcinogen applied. In the MCA treated group (group 3) 14 of the 15 tumour bearing animals died with basaliomas as the most advanced malignant tumours. 2 with a squamous cell component in the tumour. Only one rat had a pure squamous cell carcinoma. In contrast 12 of 17 animals with tumours in group 4 (DMBA treated) died with advanced squamous cell carcinomas often keratinizing. Three had papillomas with cellular atypia as in carcinomas and downgrowth in the corium but without invasion in the panniculus carnosus. The remaining 2 tumour-bearing rats had sarcoma of the skin. Two carcinomas and one sarcoma were metastasizing. In the DMBA treated group basa-

- 11 *Kiljunen A* Mitotic activity in normal and malignant epidermal tissue of the rat *Acta path microbiol scand Suppl 112* 1956 p 65-83
- 12 *Lo W b & Black H S* Inhibition of carcinogen formation in skin irradiated with ultraviolet light *Nature (Lond)* 246 489-491 1973
- 13 *Tomsak R L & Cook R T* Metabolism of 7 12 dimethylbenzo[a]anthracene by normal and regenerating rat livers *Brit J Cancer* 35 713-721 1977
- 14 *Turuso V S (ed)* Pathology of Tumours in Laboratory Animals Volume I - Tumours of the rat Part 1 IARC Scientific Publications No 5 Lyon 1973 p 7
- 15 *Watson A F* Experimental skin tumours in the rat produced by tar *J Path Bact* 36 251-256 1933
- 16 *Wattenberg L W* Inhibition of carcinogenic and toxic effects of polycyclic hydrocarbons by phenolic antioxidants and ethoxyquin *J nat Cancer Inst* 48 1423-1430 1972
- 17 *Yang S K McCourt D W Leut J C & Gelboin H V* Benzo[a]pyrene diol epoxides: Mechanism of enzymatic formation and optically active intermediates *Science* 196 1199-1201 1977

not likely in view of the enhancing influence of the surface lipid extraction on tumour development when DMBA is applied

Liperoxides on the other hand might exert a more specific action in skin carcinogenesis. An earlier study (Arffmann & Glavind 1974) demonstrated a promoting potency of two oxygen containing derivatives of unsaturated fatty acids on the induction of skin tumours in mice, and this property might be acting in the present experiment when BP and MCA are initiators. DMBA is a much more potent carcinogen to rat skin and consequently a promoting action of liperoxides may not be able to manifest itself.

Another more specific effect of the peroxides in sebum might be an oxidation of the applied polycyclic hydrocarbons. Experimental evidence has accumulated that most of the carcinogenic hydrocarbons exert their action through oxidative metabolites. The principal biologically active form of benzo(a)pyrene is supposed to be a diol epoxide derivative (Yang *et al.* 1977), and experiments using co administration of a potent inhibitor of epoxide hydrolase(s) with MCA showed an increase in carcinogenic effect of the polycyclic hydrocarbon strongly supporting the view that an epoxide is the proximate or possibly ultimate carcinogen (Burki *et al.* 1974).

It is uncertain at present whether or not DMBA must be metabolically activated to become carcinogenic (Tomsak & Cook 1977). Berry *et al.* (1977) confirmed that the presence of a potent epoxide hydrolase inhibitor increased the tumour efficacy of BP and MCA but had no effect on DMBA initiation in mice. Wattenberg (1972) observed in his experiments that concomitant application of antioxidants did not significantly protect against initiation of neoplasia in the mouse skin by DMBA. These various observations support the contention that DMBA is carcinogenic in the absence of oxidative metabolism and this may partly explain why in our experiment SSLE showed different effects on carcinogenesis by DMBA than by BP and MCA.

Our results include a difference in tumour type with the applied carcinogen. The induction of predominantly well-differentiated squamous cell carcinomas by DMBA is in accordance with other observations (Berenblum 1949) while the frequency of basalomas is higher after MCA application than earlier reported by some (Kiljunen 1956) and lower after DMBA application than generally observed (Tursova 1973). These differences may be due to the longer intervals between applications and the lower total dose of carcinogens used in our experiment.

The present report shows a rather moderate effect

of SSLE on skin carcinogenesis by polycyclic hydrocarbons in female rats. A more marked effect may be expected if male animals excreting larger amounts of sebum and showing higher peroxide values in the skin surface lipids are used.

The authors are grateful to the late John Glavind Ph.D. Copenhagen for his valuable advice.

Tocopherol acetate was kindly supplied by Hoffmann La Roche & Co. and the solutions were prepared by the Dispensary of the Aalborg Hospital.

This work was supported by a grant from the Danish Cancer Society.

REFERENCES

- 1 Arffmann E & Glavind J. Carcinogenicity in mice of some fatty acid methyl esters - I. Skin application. Acta path. microbiol. scand. Section 4 82: 127-136 1974.
- 2 Arundell F D, Karasik M A & Gates A H. 7,12-dimethyl benzantracene tumor induction in mutant (hairless, asebic and hairless, asebic) mice. J. Invest. Derm. 52: 119-125 1969.
- 3 Berenblum I. The carcinogenic action of 9,10-dimethyl 1,2 benzantracene on the skin and subcutaneous tissues of the mouse, rabbit, rat and guinea pig. J. nat. Cancer Inst. 10: 167-174 1949.
- 4 Berry D L, Slaga T J, Viole A, Wilson A M, DiGiovanni J, Juchau M R & Selkirk J A. Effect of trichloropropene oxide on the ability of polycyclic aromatic hydrocarbons and their α -keto epoxides to initiate skin tumors in mice and to bind to DNA in vitro. J. nat. Cancer Inst. 58: 1051-1055 1977.
- 5 Burki K, Stomung T A & Bresnick E. Effects of an epoxide hydrolase inhibitor on in vitro binding of polycyclic hydrocarbons to DNA and on skin carcinogenesis. J. nat. Cancer Inst. 52: 785-788 1974.
- 6 Burki K, Wheeler J E, Akamatsu T, Scribner J E, Candelas G & Bresnick E. Early differential effects of 3-methylcholanthrene and its α -keto epoxide on mouse skin. Possible implication in the two stage mechanism of tumorigenesis. J. nat. Cancer Inst. 51: 967-976 1974.
- 7 Cherry C P & Glucksmann A. The influence of carcinogenic dosage and of sex on the induction of epitheliomas and sarcomas in the dorsal skin of rats. Brit. J. Cancer 25: 544-564 1971.
- 8 Glavind J & Christensen F. Influence of nutrition and light on the peroxide content of the skin surface lipids of rats. Acta derm. venerol. 47: 339-344 1967.
- 9 Glavind J & Christensen F. Further studies on the peroxidation of the surface lipids of the skin of rodents. Acta derm. venerol. 49: 536-546 1969.
- 10 Glucksmann A & Cherry C P. The effect of variation in carcinogenic dosage on the induction of tumours in the dorsal and vulval skin of female rats. Brit. J. Cancer 25: 735-745 1971.

PROLACTIN AND 3-METHYLCHOLANTHRENE INDUCED CERVICAL CARCINOMA EFFECT OF BROMOCRIPTINE

JOHN-GUNNAR FORSBERG and LIV STRAY BREISTEIN

Institute of Anatomy University of Bergen Norway

Forsberg J G & Stray Breistein L. Prolactin and 3 methylcholanthrene induced cervical carcinoma
Effect of bromocriptine Acta path microbiol scand Sect. A 87 151-156 1979

Female mice of the NMRI strain were injected with estradiol for the first five days after birth (estrogenized animals) and ovariectomized at the age of 6-9 weeks. One week later a cotton thread impregnated with 3 methylcholanthrene was inserted into the uterine cervix. Starting on the day of insertion of the thread and for a further 6 days the females were injected with estradiol (E) ovine prolactin (P) or 2-bromo- α -ergokryptine mesylate (bromocriptine). Controls were injected with vehicles only. The animals were killed 4 or 8 weeks after insertion of the thread and the uterine cervix was serially sectioned. A combined treatment with E₂ and P resulted in an increased incidence of invasive epithelial lesions in the uterine cervix. This incidence was higher than in controls or females injected with either hormone separately. Bromocriptine reduced the incidence of invasions and this reduction could not be restored to the control level by a simultaneous treatment with E₂ and/or P. Finally the incidence of invasive lesions in the control group of estrogenized females was higher than that reported in an earlier study using non-estrogenized females.

Key words: Cervical carcinoma, mouse, incidence of carcinoma, prolactin, estradiol, bromocriptine.

J G Forsberg, Institute of Anatomy, Årstadveien 19, N-5000 Bergen, Norway.

Received 20 II 78 Accepted 22 XI 78

Human uterine cervical carcinoma is a disease which still has many unsolved biological components (1-7). During recent years the importance of type 2 herpes simplex virus has been in the center of interest (11). Generally speaking, hormonal factors have not been considered of importance for human cervical carcinoma, but many studies have been devoted to the influence of hormones on experimentally induced cervical carcinomas in e.g. mouse (Akre and Bjørro (10) summarized earlier studies in the latter experimental field and presented their own results on dimethyl benzantracene induced cervical carcinomas (WLO mice) which indicated that progesterone and testosterone had a protecting effect while ethynylestradiol was a promoting agent.

However, in other studies estrogens have been described as tumor promoters, as not affecting carcinogenesis and finally as retarding carcinogenesis and invasive growth (5). In an earlier study we compared the development of 3 methylcholanthrene (MCA) induced cervical carcinomas in normal NMRI mice and in mice injected with estradiol in the neonatal life (estrogenized females). We found that the early incidence of invasive lesions was higher in the estrogenized females as compared with normal females (5). The adult estrogenized females have large areas with a columnar epithelium in the uterine cervix (4) and they also have an abnormal endogenous hormonal pattern due to a disturbed hypothalamic-pituitary regulation (8). Thus, two factors could contribute to the higher incidence of

RESULTS

The results are presented in TABLE I where the number of specimens with different stages of epidermoid carcinomas are given for the different treatment groups. As can be seen only two examples of adenocarcinomas were found. The histological pictures of the different Stages of epidermoid carcinomas as well as of an adenocarcinoma are given in Fig. 2-5. As a rule the Stages II and III lesions can be characterized as well differentiated squamous carcinomas and only one example of a poorly-differentiated Stage III tumor was found.

The different treatment groups, the females of which were killed 4 weeks after insertion of the MCA thread, can be grouped into three larger separate groups: the highest incidence of invasive epithelial lesions is seen in the group of females injected with E₂/P; females injected with E₂ or P have only about the same incidence as the controls; the third group consists of the females injected with CB 154 alone or in some types of combination with

E₂ and/or P. There is a striking similarity in incidence of invasive lesions in the latter four treatment groups (TABLE I), and this incidence is lower than in any of the other four treatment groups studied at 4 weeks. Controls and females injected with E₂ or P have the same incidence of invasive lesions; females injected with E₂ and P in combination have an increased, and those injected with CB 154 alone or in combination with hormones have a decreased incidence of invasions.

At 8 weeks there are interesting changes in the incidence figures as compared with the 4 weeks groups. Females injected with both E₂ and P have the same incidence at 4 and 8 weeks but the trend is toward a higher Stage scoring at 8 weeks. The same holds true for females injected with P alone. However, for the two groups injected with CB 154 in addition to P, or E₂ and P, the incidence has increased as compared with the 4-weeks figures. There is one difference between these two groups: the group E₂/P, CB 154 contains only Stage I lesions while in the group P, CB 154 there are Stage II and Stage III lesions in addition.

TABLE I. Incidence of Invasive Lesions in Cervical Preparations from Different Treatment Groups

Treatment	Stage I	Stage II	Stage III	Adeno carcinoma	Total no of animals studied	% with invasion
<i>4 weeks</i>						
C	7	2				
E ₂ /P	13 ¹⁾	1		1	21	48
E ₂	9				20	70
P	8 ²⁾	1			21	43
CB 154	4	2			20	45 ²⁾
E ₂ /P CB 154	5	1			21	29
E ₂ CB 154	5				22	27
P CB 154	3	1			21	24
					20	25
<i>8 weeks</i>						
E ₂ /P CB 154	8					
E ₂ /P	3	3	3		12	67
P CB 154	2 ¹⁾	2	3		13	69
P	1	3	3		18	39
			3	1	17	47

¹⁾ One cervical preparation had a small adenocarcinoma in addition.

²⁾ One questionable lesion is included in Stage I and in the percentage given.

C Controls injected with vehicles only
 E Estradiol 17 β
 P Prolactin
 CB 154 2-bromo-*n*-ergokryptine mesylate

invasive lesions in the estrogenized females: a pronounced epidermization process taking place as a result of local irritation (5) and/or an abnormal hormonal pattern. Our interest was focused on estradiol and prolactin. In a following study (6), normal female mice were ovariectomized and a cotton thread impregnated with MCA was inserted into the uterine cervix. During the week following insertion of the thread the animals were injected with estradiol, ovine prolactin or progesterone, alone or in combinations. The females were killed the day after the last hormone injection or 22 days later. Females injected with estradiol and prolactin in combination had a higher incidence of invasive lesions compared with controls or females injected with each hormone separately.

In the present study we have used ovariectomized, neonatally estrogenized females. The aim of the study was two-fold: to investigate the role of the epidermization process taking place after insertion of the cotton thread with MCA (5) by comparing the »basal« incidence of invasive lesions in these females with the same incidence in nonestrogenized normal females previously reported (6), and secondly, to study the importance of the endogenous prolactin level, which was postulated to be regulated in estrogenized females in a way differing from that in normal females (9). For the latter reason we used the plasma prolactin decreasing drug bromocriptine (CB 154).

MATERIAL AND METHODS

The females used belong to a closed stock of NMRI mice. Within 24 hours after birth the newborn females were separated from the male siblings and litters of 7-9 females were nursed by one single mother. Starting on the day of birth the female pups were injected subcutaneously with 5 µg estradiol 17β (E₂, Sigma Chemical Co.) in 0.025 ml olive oil. The injections were repeated on the following four days after birth. The neonatally estradiol injected animals are termed »estrogenized« females.

The E₂ injected females were ovariectomized at the age of 6-9 weeks. One week later they were laparotomized under ether anaesthesia and a cotton thread impregnated with a mixture of beeswax and 3-methylcholanthrene (MCA, Sigma Chemical Co.) was inserted into the uterine cervix according to the method described earlier (5). As earlier the average MCA content of the thread was about 0.6 mg. The animals were divided into different treatment groups: injections starting on the day of laparotomy and continuing for a further 6 days. During the treatment period groups of females were given daily subcutaneous injections of E₂ (5 µg in 0.025 ml saline with 1% ethanol), ovine prolactin (P, 5 µg in 0.1 ml Parker 199, Sigma Chemical Co.) or 2

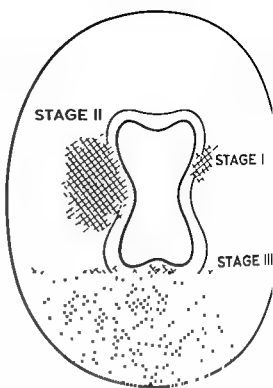


Fig. 1 Schematic illustration of a cross section through the uterine cervix indicating the principles of Stage scoring

bromo-ergokryptine mesylate (CB 154 or bromocriptine, kindly supplied by Sandoz Products, Basle, 50 µg in 0.05 ml 5% tartaric acid). Injections with CB 154 were repeated twice a day with a 12 hours interval. The three substances mentioned were injected alone or in different combinations (TABLE 1) and in such a way that one female injected with one active substance alone was also injected in addition with the solvents for the two other substances. Controls were injected with solvents for all three substances.

Four or 8 weeks after insertion of the cotton thread the females were killed by cervical dislocation. The uterine cervix was dissected out and fixed in Bouin's fluid. Only those females with the cotton thread in situ position were used. After conventional dehydration in ethanol and paraffin embedding the cervical preparations were serially sectioned and stained in haematoxylin and eosin. The section series were studied independently by both authors, twice by one author, and the absence or presence of invasive lesions were recorded. In case of the presence of lesions they were classified according to the histological picture as well differentiated, poorly differentiated or anaplastic squamous carcinomas or as adenocarcinoma. Moreover the degree of infiltration of the cervical wall was registered according to a stage division illustrated in Fig. 1. The smallest invasions were classified as Stage I; a typical example is given in Fig. 2 when the invasion engaged up to about half of the cervical wall it was classified as a Stage II lesion; a larger invasion in several cases reaching the mesothelial surface of the cervix was classified as a Stage III lesion.

RESULTS

The results are presented in TABLE I where the number of specimens with different stages of epidermoid carcinomas are given for the different treatment groups. As can be seen only two examples of adenocarcinomas were found. The histological pictures of the different Stages of epidermoid carcinomas as well as of an adenocarcinoma are given in Fig. 2-5. As a rule the Stages II and III lesions can be characterized as well differentiated squamous carcinomas and only one example of a poorly-differentiated Stage III tumor was found.

The different treatment groups, the females of which were killed 4 weeks after insertion of the VCA thread, can be grouped into three larger separate groups: the highest incidence of invasive pitheal lesions is seen in the group of females injected with E₂-P; females injected with E₂ or P have only about the same incidence as the controls; the third group consists of the females injected with CB 154 alone or in some types of combination with

E₂ and/or P. There is a striking similarity in incidence of invasive lesions in the latter four treatment groups (TABLE I) and this incidence is lower than in any of the other four treatment groups studied in 4 weeks. Controls and females injected with E₂ or P have the same incidence of invasive lesions; females injected with E₂ and P in combination have an increased incidence and those injected with CB 154 alone or in combination with hormones have a decreased incidence of invasions.

At 8 weeks there are interesting changes in the incidence figures as compared with the 4 weeks groups. Females injected with both E₂ and P have the same incidence at 4 and 8 weeks but the trend is toward a higher Stage scoring at 8 weeks. The same holds true for females injected with P alone. However, for the two groups injected with CB 154 in addition to P, or E₂ and P, the incidence has increased as compared with the 4 weeks figures. There is one difference between these two groups: the group E₂-P-CB 154 contains only Stage I lesions while in the group P-CB 154 there are Stage II and Stage III lesions in addition.

TABLE I. Incidence of Invasive Lesions in Cervical Preparations from Different Treatment Groups

Treatment	Stage I	Stage II	Stage III	Adeno-carcinoma	Total no of animals studied	% with invasion
<i>4 weeks</i>						
C	7	2				
E ₂ -P	13 ¹⁾	1		1	21	48
E ₂	9				20	70
P	8 ²⁾	1			21	43
CB 154	4	2			20	45 ¹⁾
E ₂ + CB 154	5	2			21	29
E ₂ -CB 154	5				22	27
P-CB 154	3	1			21	24
					20	25
<i>8 weeks</i>						
E ₂ -P-CB 154	8					
E ₂ -P	3	3	3		12	67
P-CB 154	2 ¹⁾	2	3		13	69
P	1	3	3		18	39
				1	17	47

¹⁾ One cervical preparation had a small adenocarcinoma in addition.

²⁾ One questionable lesion is included in Stage I and in the percentage given.

C Controls injected with vehicles only
 E₂ Estradiol 17 β
 P Prolactin
 CB 154 2-bromo- α -ergokryptone mesylate

invasive lesions in the estrogenized females a pronounced epidermization process taking place as a result of local irritation (5) and/or an abnormal hormonal pattern. Our interest was focused on estradiol and prolactin. In a following study (6), normal female mice were ovariectomized and a cotton thread impregnated with MCA was inserted into the uterine cervix. During the week following insertion of the thread the animals were injected with estradiol, ovine prolactin or progesterone, alone or in combinations. The females were killed the day after the last hormone injection or 22 days later. Females injected with estradiol and prolactin in combination had a higher incidence of invasive lesions compared with controls or females injected with each hormone separately.

In the present study we have used ovariectomized, neonatally estrogenized females. The aim of the study was two-fold: to investigate the role of the epidermization process taking place after insertion of the cotton thread with MCA (5) by comparing the «basal» incidence of invasive lesions in these females with the same incidence in nonestrogenized normal females previously reported (6), and secondly, to study the importance of the endogenous prolactin level which was postulated to be regulated in estrogenized females in a way differing from that in normal females (9). For the latter reason we used the plasma prolactin decreasing drug, bromocriptine (CB 154).

MATERIAL AND METHODS

The females used belong to a closed stock of NVRI mice. Within 24 hours after birth the newborn females were separated from the male siblings and litters of 7-9 females were nursed by one single mother. Starting on the day of birth the female pups were injected subcutaneously with 5 µg estradiol 17β (E₂; Sigma Chemical Co) in 0.025 ml olive oil. The injections were repeated on the following four days after birth. The neonatally estradiol injected animals are termed «estrogenized» females.

The E₂ injected females were ovariectomized at the age of 6-9 weeks. One week later they were laparotomized under ether anaesthesia and a cotton thread impregnated with a mixture of beeswax and 3-methylcholanthrene (MCA; Sigma Chemical Co) was inserted into the uterine cervix according to the method described earlier (5). As earlier the average MCA content of the thread was about 0.6 mg. The animals were divided into different treatment groups: injections starting on the day of laparotomy and continuing for a further 6 days. During the treatment period groups of females were given daily subcutaneous injections of E₂ (5 µg in 0.025 ml saline with 1% ethanol), ovine prolactin (P; 5 µg in 0.1 ml Parker 199; Sigma Chemical Co) or 2

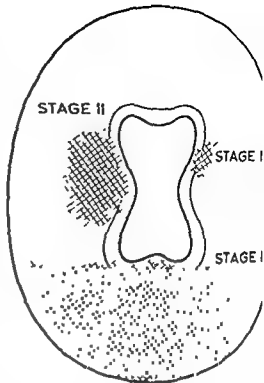


Fig. 1. Schematic illustration of a cross section through the uterine cervix indicating the principles of scoring.

bromo- α -ergokryptine mesylate (CB 154 or bromocriptine kindly supplied by Sandoz Products Basle, 50 µg/0.05 ml 5% tartaric acid). Injections with CB 154 were repeated twice a day with a 12 hours interval. The substances mentioned were injected alone or in different combinations (TABLE I) and in such a way that female injected with one active substance alone was injected in addition with the solvents for the two other substances. Controls were injected with solvents for three substances.

Four or 8 weeks after insertion of the cotton thread the females were killed by cervical dislocation. The uterine cervix was dissected out and fixed in Bouin's fluid. Only those females with the cotton thread in position were used. After conventional dehydration in ethanol and paraffin embedding the cervical preparations were serially sectioned and stained in haematoxylin and eosin. The section series were studied independently by both authors, twice by one author, and the absence or presence of invasive lesions were recorded. In case of presence of lesions they were classified according to histological picture as well differentiated poorly differentiated or anaplastic squamous carcinomas or adenocarcinoma. Moreover the degree of infiltration of the cervical wall was registered according to a subdivision illustrated in Fig. 1. The smallest invasions were classified as Stage I; a typical example is given in Fig. 2. When the invasion engaged up to about half of the cervical wall it was classified as a Stage II lesion; a large invasion in several cases reaching the mesothelial surface of the cervix was classified as a Stage III lesion.

DISCUSSION

The highest incidence of invasive lesions in the uterine cervix of ovariectomized estrogenized females killed 4 weeks after insertion of the MCA thread occurred in the group injected with both E_2 and P for one week after insertion of the MCA thread. The incidence in this group was higher than in both controls injected with vehicles only or in females treated with E_2 or P alone. The incidence in the latter three groups was higher than in the groups injected with CB 154 alone or in combination with E_2 , P or E_2 and P.

As CB 154 is an inhibitor of prolactin release (3) it was a *a priori* thought that if CB 154 reduced the incidence of invasive lesions it would be possible to restore this effect by using exogenous prolactin. In fact this was not the result. There are two possible explanations for this: either CB 154 has an effect on its own in some mechanism essential for development of the invasive lesions or exogenous ovine prolactin cannot in this system substitute for reduced level of endogenous prolactin. According to the first alternative CB 154 could influence some hitherto unknown mechanisms in the MCA induction of cervical carcinomas e.g. resulting in an increased MCA detoxification or reduced metabolism. The second alternative implies that ovine prolactin cannot restore all the effects of endogenous prolactin withdrawal but it should be effective together with E_2 in non-CB 154 treated females with a "normal" level of mouse prolactin.

We have earlier demonstrated that the mouse cervicovaginal epithelium is a target organ for prolactin.

CB 154 induced reduction of the specific cell product (9). The problems could be solved by using mouse prolactin; this however is impossible in this type of experiments. A more fruitful way should be to study the CB 154 effect on the uptake and metabolism of MCA.

According to the classic model CB 154 inhibits prolactin secretion both in the pituitary and hypothalamic levels being a dopamine receptor agonist (3). In animals where the cyclic gonadotropin secretion is suppressed by high plasma prolactin cyclicity can be induced after CB 154 treatment.

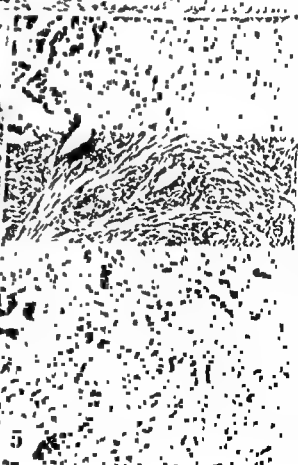
(3) In juvenile PMIS treated rats CB 154 inhibits the preovulatory LH surge (3). CB 154 is a weak α adrenoreceptor stimulator and inhibitor and its action on 5 HT vascular receptors is weak. It antagonises ergometrine stimulation of uterus (2). None of the parameters mentioned seem to be a likely explanation for the CB 154 effect on induction of cervical carcinomas.

It can be questioned whether all the invasions grouped in Stage I are of real malignant character or linked to a concomitant inflammatory reaction. The real malignant character is stressed by the progressive higher Stage scoring with time as demonstrated for instance by the treatment groups E_2 , P and P at 4 and 8 weeks. Moreover in the latter time tumor pieces have been grafted subcutaneously into newborn female mice where they grow rapidly to an enormous size finally killing the host animal but not metastasizing (Forsberg and Breistein unpublished results).

The results from this study are in line with those previously reported using non-estrogenized females (6). A combined treatment with E_2 and P increases the incidence of invasive lesions 4 weeks after insertion of the MCA thread. At that time E_2 and P in combination result in about the same incidence in both types of animals. However nonestrogenized females (controls or those injected with E_2 or P only) had a lower incidence of invasions in 4 weeks than the corresponding estrogenized ones in the present study. Thus the combined E_2 , P effect is more striking in nonestrogenized than in estrogenized females. Besides hormonal factors the strong epidermization process taking place in estrogenized females after insertion of the MCA thread has been considered a factor of importance for the rapid development of invasions (5). This extensive epidermization takes place in the large regions with a columnar epithelium in the uterine cervix of neonatally estradiol injected females (4). The epidermization process could be a factor favouring the development of invasive lesions and explaining the higher basal incidence in the estrogenized females as compared with nonestrogenized females. In both cases E_2 and P injected simultaneously increase the incidence but this increase is most pronounced in nonestrogenized females.

Fig 2-5 The histological appearance of a section from a control female 4 weeks after injection with E_2 , P and CB 154. Poorly differentiated type. Female. A Stage III adenocarcinoma.

the cervix
a female
one of the
x 190
x 190



DISCUSSION

The highest incidence of invasive lesions in the uterine cervix of ovariectomized estrogenized females killed 4 weeks after insertion of the MCA thread occurred in the group injected with both E_2 and P for one week after insertion of the MCA thread. The incidence in this group was higher than in both controls injected with vehicles only or in females treated with E_2 or P alone. The incidence in the latter three groups was higher than in the groups injected with CB 154 alone or in combination with E_2 , P or E_2 and P.

As CB 154 is an inhibitor of prolactin release (3) it was *a priori* thought that if CB 154 reduced the incidence of invasive lesions it would be possible to restore this effect by using exogenous prolactin. In fact this was not the result. There are two possible explanations for this: either CB 154 has an effect on its own in some mechanism essential for development of the invasive lesions or exogenous ovine prolactin cannot in this system substitute for reduced level of endogenous prolactin. According to the first alternative CB 154 could influence some hitherto unknown mechanisms in the MCA induction of cervical carcinomas e.g. resulting in an increased MCA detoxification or reduced metabolism. The second alternative implies that ovine prolactin cannot restore all the effects of endogenous prolactin withdrawal but it should be effective together with E_2 in non-CB 154 treated females with a normal level of mouse prolactin.

We have earlier demonstrated that the mouse cervicovaginal epithelium is a target organ for prolactin influencing production of a specific cell product. In this test system rat prolactin free from growth hormone contamination could restore the CB 154 induced reduction of the specific cell product (9). The problems could be solved by using mouse prolactin this however is impossible in this type of experiments. A more fruitful way should be to study the CB 154 effect on the uptake and metabolism of MCA.

According to the classic model CB 154 inhibits prolactin secretion both at the pituitary and hypothalamic levels being a dopamine receptor agonist (3). In animals where the cyclic gonadotrophin secretion is suppressed by high plasma prolactin cyclicity can be induced after CB 154 treatment

(3). In juvenile PMS treated rats CB 154 inhibits the preovulatory LH surge (3). CB 154 is a weak α adrenoreceptor stimulator and inhibitor and its action on 5 HT vascular receptors is weak. It antagonises ergometrine stimulation of uterus (2). None of the parameters mentioned seem to be a likely explanation for the CB 154 effect on induction of cervical carcinomas.

It can be questioned whether all the invasions grouped in Stage I are of real malignant character or linked to a concomitant inflammatory reaction. The real malignant character is stressed by the progressive higher Stage scoring with time as demonstrated for instance by the treatment groups E_2 , P and P at 4 and 8 weeks. Moreover in the latter time tumor pieces have been grafted subcutaneously into newborn female mice where they grow rapidly to an enormous size finally killing the host animal but not metastasizing (Forsberg and Breistein unpublished results).

The results from this study are in line with those previously reported using non-estrogenized females (6). A combined treatment with E_2 and P increases the incidence of invasive lesions 4 weeks after insertion of the MCA thread. At that time E_2 and P in combination result in about the same incidence in both types of animals. However nonestrogenized females (controls or those injected with E_2 or P only) had a lower incidence of invasions at 4 weeks than the corresponding estrogenized ones in the present study. Thus the combined E_2 , P effect is more striking in nonestrogenized than in estrogenized females. Besides hormonal factors the strong epidermization process taking place in estrogenized females after insertion of the MCA thread has been considered a factor of importance for the rapid development of invasions (5). This extensive epidermization takes place in the large regions with a columnar epithelium in the uterine cervix of neonatally estradiol injected females (4). The epidermization process could be a factor favouring the development of invasive lesions and explaining the higher basal incidence in the estrogenized females as compared with nonestrogenized females. In both cases E_2 and P injected simultaneously increase the incidence but this increase is most pronounced in non-estrogenized females. It must be stressed that the ovine prolactin used may contain a contamination with growth hormone influencing the results.

Fig 2-5 The histological appearance of different types of invasive lesions. Fig 2 shows a poorly differentiated type from a control female 4 weeks after insertion of the MCA thread. Fig 3 shows a poorly differentiated type injected with E_2 , P and CB 154 4 weeks after insertion of MCA thread. Fig 4 shows a Stage III adenocarcinoma from a female injected with E_2 and P and killed 8 weeks after insertion of the MCA thread. Fig 5 shows a Stage III adenocarcinoma from a female injected with E_2 , P and CB 154 4 weeks after insertion of the MCA thread.

REFERENCES

- 1 *Coppleson, L W & Brown B* Observations on a model of the biology of carcinoma of the cervix. A poor fit between observation and theory. *Am J Obstet Gynecol* 122 127-136, 1975
- 2 *Flückiger, E* The pharmacology of bromocriptine. In *Bayliss R I S, Turner, P, Maclay, W P*, Eds. Pharmacological and clinical aspects of bromocriptine (Parlodel). MCS Consultants, Turnbridge Wells, 1976 pp 12-26
- 3 *Flückiger, E* Effects of bromocriptine on the hypothalamo-pituitary axis. *Acta Endocrinol (Kbh)* Suppl 216 111-117, 1978
- 4 *Forsberg J-G* The development of atypical epithelium in the mouse uterine cervix and vaginal fornix after neonatal oestradiol treatment. *Br J Exp Pathol* 50 187-195, 1969
- 5 *Forsberg J-G & Stray Breistein L* Carcinogenesis with 3-methylcholanthrene in uterine cervix of mice treated neonatally with estrogen. *J Natl Cancer Inst* 49 155-172, 1972
- 6 *Forsberg, J-G & Stray Breistein L* A synergistic effect of oestradiol and prolactin influencing the incidence of 3-methylcholanthrene induced cervical carcinomas in mice. *Acta path microbiol scand Sect A*, 84 384-390, 1976
- 7 *Foulds L* Neoplastic Development Vol 2 Academic Press London New York, 1975 pp 109-162
- 8 *Gorski R A, Harlan, R E & Christensen L W* Perinatal hormonal exposure and the development of neuroendocrine regulatory processes. *J Toxicol Environ Health* 3 97-121, 1977
- 9 *Kalland T, Daskeland S-O & Forsberg J G* The content of a specific cell product in the vaginal epithelium of normal and neonatally estrogenized mice: its dependence on an estradiol prolactin interaction. *Endocrinology* 99 1548-1553, 1976
- 10 *Mylre E & Bjoro A* Hormones and cervical cancer. Universitetsforlaget Oslo 1971
- 11 *Rawls W E & Adam E* Herpes simplex viruses and human malignancies. In *Hiatt H H, Watson J D & Winston J A*, Eds. Origins of Cancer Book B Mechanisms of Carcinogenesis. Cold Spring Harbor Laboratory 1977, pp 1133-1155

CARBONIC ANHYDRASE ACTIVITY IN MOUSE ENDOCRINE PANCREAS

L. BOQUIST and S. HAGSTRÖM

Department of Pathology University of Umeå Umeå Sweden

Boquist L. & Hagstrom S. Carbonic anhydrase activity in mouse endocrine pancreas. *Acta path microbiol scand Sect. A* 87 157-164 1979

Histochemical staining for carbonic anhydrase (CAH) was demonstrated in the mouse pancreas. Light microscopically a strong reaction for CAH was found in the B-cell region of the islets in blood vessels inside and outside the islets and in centroacinar cells and ductules. In contrast no distinct reaction was seen in the peripheral A and D-cell regions of the islets or in the cytoplasm of the acinar cells. A weak irregular staining could however be observed in some nuclei of the acinar parenchyma. A newly-developed ultrastructural modification disclosed a distinct reaction in a varying number of the secretory granules of the B-cells whereas a sparse irregularly-distributed reaction was observed in the nuclei and cytoplasmic ground substance and in association to the plasma membranes and microvilli of these cells. The CAH reaction was in all portions of the pancreas abolished by acetazolamide. The specificity of the results is discussed. The findings are suggested to indicate presence of a true CAH activity in the B-cells of the mouse pancreas.

Key words: Carbonic anhydrase, pancreatic islets, B-cells, mouse, electron microscopy.

L. Boquist, Department of Pathology, University of Umeå, S 901 87 Umeå, Sweden.

Received 11 vii 78 Accepted 28 vii 78

In published reviews on pancreatic islet histochemistry there is either no information about the existence or non-existence of carbonic anhydrase (CAH) (EC 4.2.1.1) activity in the endocrine pancreas (Schäfer 1958; Larsson & Volk 1962; Aris 1963; Czepis & Gregoire 1971; Hellman & Täljedal 1972; Lange 1973; Boquist 1977) or upon is given of an unspecific reaction interpreted

been accepted by other authors (Aarhønen & Korhonen 1965).

with the aim of studying the CAH reaction in the endocrine pancreas of mice from the colonies used in current diabetes research in this laboratory using Hansson's (1967 and 1968) light microscopic method which is considered specific for CAH (Lönnerholm 1974). A new electron microscopic modification for CAH is also described. There is no previous ultrastructural report of CAH activity in the exo- or endocrine pancreas of any species.

MATERIAL AND METHODS

Non-diabetic adult C57BL/6J +/+ mice were used. They were from a local stock kept under standard laboratory conditions at a constant temperature of 22°C.

In some species suggested to indicate a false positivity of the Kurata method (Fand et al 1959). Using the modified Hauser (1958) method Blegvad (1964) observed an intense CAH reaction in pancreatic islets from different species including mouse. However, the specificity of the Hauser method has



Fig 1 Photomicrograph demonstrating intense CAH reaction in the B cell region of a mouse islet. No distinct reaction is seen in the peripheral A and D cell regions of the islet. The acinar parenchyma exhibits only a weak irregular nuclear staining $\times 450$



Fig 2 Strong CAH reaction in B-cell region of a pancreatic islet and in erythrocytes and blood vessels (B) and in one pancreatic ductule (D) outside the islet. A distinct reaction is seen in the A and D-cell regions of the islet. The acinar tissue possesses only a weak irregular nuclear staining $\times 400$

The animals had free access to water and a standard laboratory ration.

The animals were killed and specimens were immediately taken from the pancreas and processed for CAH according to Hansson (1967 and 1967) using cryostat sections post fixed in cooled acetone. The specificity of the staining reaction was checked by incubation of the sections in the presence of 10 μ M acetazolamide (Diamox $\text{\textcircled{C}}$ Cyanamid International, Lederle Lab, Dept. Wayne, New Jersey, U.S.A.).

An attempt was made to localize CAH electron microscopically using the modification described by Cross (1970). Since however this modification gave unsatisfactory results a new ultrastructural technique was developed based upon the Hausler and Hansson methods for light microscopic demonstration of CAH. The details of this new modification are as follows: Small tissue cubes $1 \times 1 \times 1$ mm were fixed in 2.5% glutaraldehyde in 0.2 M sucrose and 0.05 M phosphate buffer (pH 7.4) for 2 hours at 4°C . After rinsing in 0.05 M phosphate buffer the cubes were minced with glass knives and the minced tissue was placed on Millipore filters which were floated on Hausler medium for 1 to $1\frac{1}{2}$ hours. Acetazolamide (10 μ M) was added to this medium in control experiments carried out in order to check the specificity of the staining reaction. After rinsing in distilled water the tissue was placed for 1



Fig 3 Control section subjected to acetazolamide demonstrating absence of CAH reaction in pancreatic islet (I), ductules (D) and acinar parenchyma (A).

stained with toluidine blue were used. The thin sections were either stained with

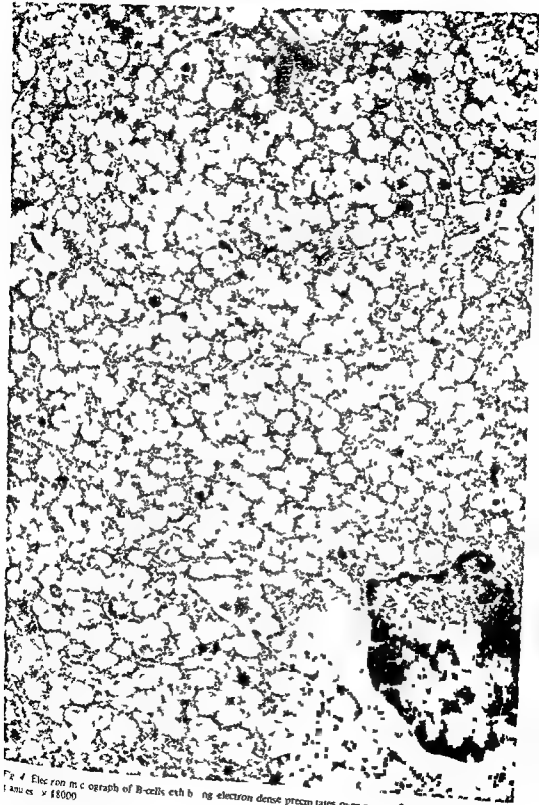


Fig. 4. Electron micrograph of B-cells exhibiting electron dense precipitates over some of the numerous secretory granules. $\times 18000$



Fig 1 Photomicrograph demonstrating intense CAH reaction in the B cell region of a mouse islet. No distinct reaction is seen in the peripheral A and D-cell regions of the islet. The acinar parenchyma exhibits only a weak irregular nuclear staining $\times 450$



Fig 2 Strong CAH reaction in B-cell region of a pancreatic islet and in erythrocytes and blood vessels (B) and in one pancreatic ductule (D) outside the islet. No distinct reaction is seen in the A and D-cell region of the islet. The acinar tissue possesses only a weak irregular nuclear staining $\times 400$

The animals had free access to water and a standard laboratory ration.

The animals were killed and specimens were immediately taken from the pancreas and processed for CAH according to Hansson (1967 and 1967) using cryostat sections post fixed in cooled acetone. The specificity of the staining reaction was checked by incubation of the sections in the presence of 10 μ M acetazolamide (Diamox \oplus Cyanamid International, Lederle Lab, Dept Wayne, New Jersey, U.S.A.).

An attempt was made to localize CAH electron microscopically using the modification described by Cross (1970). Since however this modification gave unsatisfactory results, a new ultrastructural technique was developed based upon the Hausler and Hansson methods for light microscopic demonstration of CAH. The details of this new modification are as follows. Small tissue cubes, $1 \times 1 \times 1$ mm, were fixed in 2.5% glutaraldehyde in 0.2 M sucrose and 0.05 M phosphate buffer (pH 7.4) for 2 hours at 4°C . After rinsing in 0.05 M phosphate buffer, the cubes were minced with glass knives and the minced tissue was placed on Millipore filters which were floated on Hausler medium for 1 to $1\frac{1}{2}$ hours. Acetazolamide (10 μ M) was added to this medium in control experiments carried out in order to check the specificity of the staining reaction. After rinsing in distilled water, the tissue was placed for 1 minute in 1% $(\text{NH}_4)_2\text{S}$, rinsed again in distilled water, transferred to 95% ethanol, and then to absolute alcohol. Embedding was carried out in Epon 812. Thick sections stained with toluidine blue were used for identification of the islets. The thin sections were either stained with

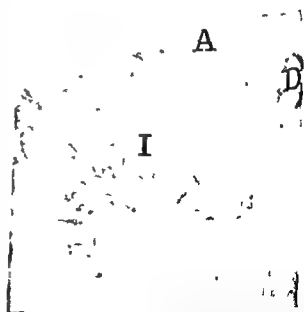


Fig 3 Control section subjected to acetazolamide demonstrating absence of CAH reaction in pancreatic islet (I), ductules (D) and acinar parenchyma (A) $\times 450$

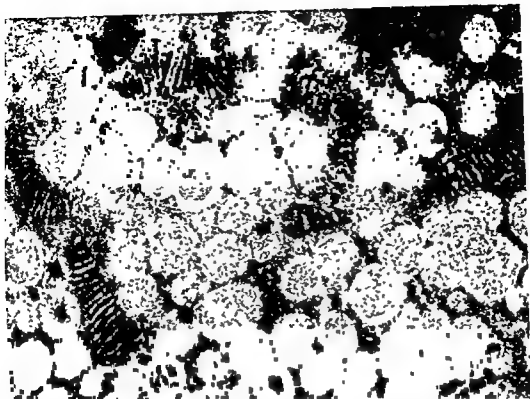


Fig 6 Portion of B cell cytoplasm showing precipitates over central or peripheral portion of some secretory granule cores. No precipitates are seen in mitochondria. Free ribosomes are demonstrated. The β granules exhibit finely granular cores of rather low density. $\times 36000$

the epithelium of the pancreatic ductules exhibited a strong although somewhat irregularly-distributed reaction. Control sections treated with acetazolamide exhibited absolutely no reaction in any portions of the pancreas including the islets (Fig. 3).

The reaction in the endocrine pancreas was localized to the B-cell region in the central portion of the islets whereas the islet periphery, in which the A- and D-cells are situated, showed no distinct reaction (Fig. 1 and 2).

The ultrastructural study was directed to the islet parenchymal cells. The B-cells possessed distinct, highly electron-dense precipitates in association to some of the secretory granules (Fig. 4). The number of secretory granules exhibiting precipitates varied considerably in different cells. In most cells only a minor portion of the granules possessed precipitates. Most precipitates were confined to the periphery of the core and the so-called halo of the β -granules (Fig. 5). In many granules the precipitates were seen in the whole halo whereas they were localized to

some portion of the halo circumference in other granules. In still other granules the precipitates were situated in a more or less central position over the granule core (Figs. 6 and 7).

In addition, a sparse number of irregularly distributed precipitates was occasionally seen in the nuclei and in the cytoplasmic ground substance of the B-cells. Precipitates were also found in association to the plasma membranes and microvilli (Fig. 7). No unequivocal precipitates were found in mitochondria (Fig. 6) or other organelles, with the exception of the

for electron microscopy. The secretory granules of the B-cells, on the other hand, exhibited somewhat lower electron-density than that which is known to be present in B-cells of islets subjected to standard electron microscopic technique.

Control sections subjected to acetazolamide exhibited no precipitation at all (Fig. 8).

uranyl acetate and lead citrate, or were left unstained, and were then viewed in a Siemens Elmiskop 1A or 101

RESULTS

Light microscopically, a strong histochemical reaction for CAH was found in the pancreatic islets (Fig

1) In contrast, no reaction was observed in the cytoplasm of the acinar cells. A weak, irregular staining could, however, be found in the nuclei of some acinar cells. An intense reaction was also seen in blood vessels and erythrocytes, both inside and outside the islets (Fig. 2). The centroacinar cells and

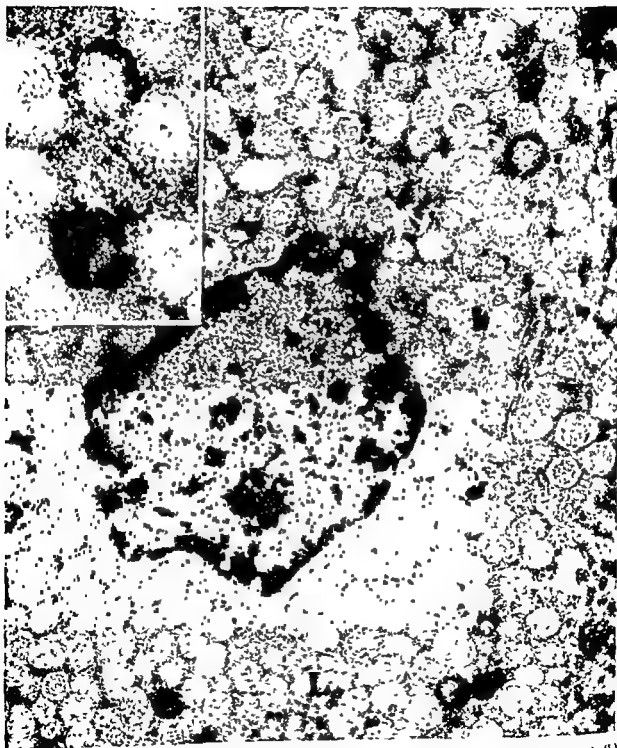


Fig. 5 B-cell possessing electron dense precipitates in the halo of some secretory granules. A lysosomal body (L) without precipitates is shown $\times 24000$. Inset demonstrates higher magnification of precipitates localized to the periphery of the core and most of the halo of two β granules $\times 43000$.

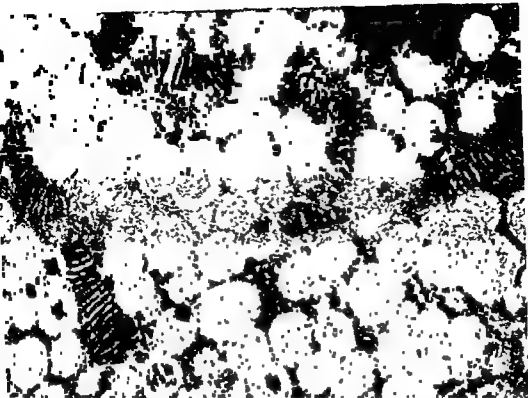


Fig 6 Portion of B-cell cytoplasm showing precipitates over central or peripheral portion of some secretory granule cores. No precipitates are seen in mitochondria. Free ribosomes are demonstrated. The β granules exhibit finely granular cores of rather low density. $\times 36000$

the epithelium of the pancreatic ductules exhibited a strong although somewhat irregularly-distributed reaction. Control sections treated with acetazolamide exhibited absolutely no reaction in any portions of the pancreas including the islets (Fig 3).

The reaction in the endocrine pancreas was localized to the B-cell region in the central portion of the islets, whereas the islet periphery in which the A and D-cells are situated showed no distinct reaction (Fig 1 and 2).

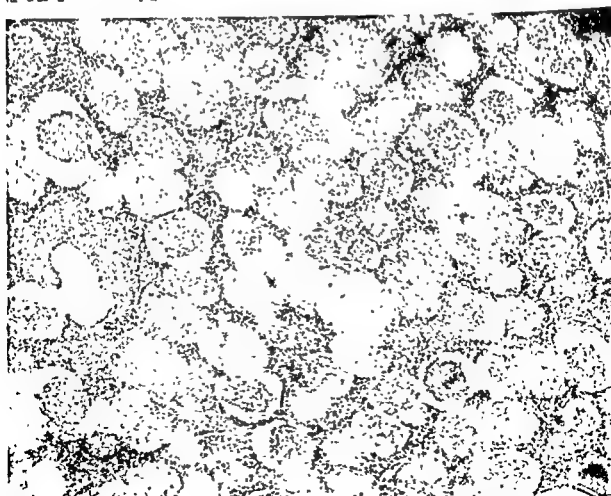
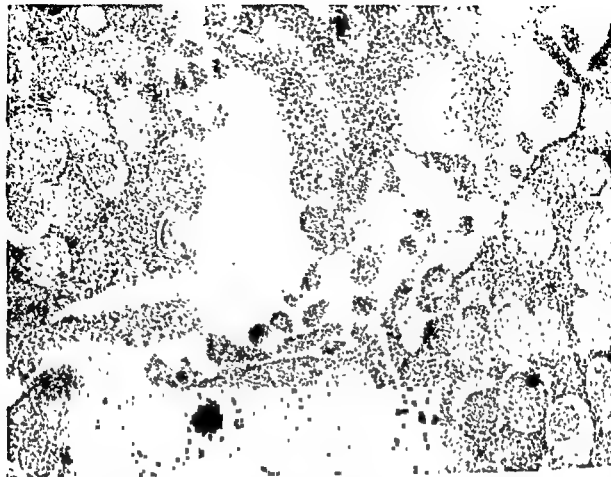
The ultrastructural study was directed to the islet parenchymal cells. The B-cells possessed distinct, highly electron-dense precipitates in association to some of the secretory granules (Fig 4). The number of secretory granules exhibiting precipitates varied considerably in different cells. In most cells only a minor portion of the granules possessed precipitates. Most precipitates were confined to the periphery of the core and the so-called halo of the β granules (Fig 5). In many granules the precipitates were seen in the whole halo, whereas they were localized to

some portion of the halo circumference in other granules. In still other granules the precipitates were situated in a more or less central position over the granule core (Figs 6 and 7).

In addition, a sparse number of irregularly-distributed precipitates was occasionally seen in the nuclei and in the cytoplasmic ground substance of the B-cells. Precipitates were also found in association to the plasma membranes and microvilli (Fig 7). No unequivocal precipitates were found in mitochondria (Fig 6) or other organelles, with the exception of the secretory granules.

No obvious precipitates were observed in the A- or D-cells of islets subjected to standard technique for electron microscopy. The secretory granules of the B-cells, on the other hand, exhibited somewhat lower electron-density than that which is known to be present in B-cells of islets subjected to standard electron microscopic technique.

Control sections subjected to acetazolamide exhibited no precipitation at all (Fig 8).



DISCUSSION

The results of the present study confirm the report of *Bleyl* (1964) of a strong reaction for CAH in the pancreatic islets of mice and conform to the finding of CAH in the endocrine pancreas also of other species (*Fand et al* 1959). However in contrast to the report of *Bleyl* (1964) of a stronger reaction in the region of the A-cells than in that of the B-cells the light microscopically observed activity in the present studied islets was intense in the B-cell area but absent from the A- and D-cell regions. This was confirmed ultrastructurally.

The question then arises whether the CAH activity in the islets represents an unspecific reaction or whether it signifies true CAH activity. *Fand et al* (1959) using the *Aurata* method (1953) regarded the islet reaction for CAH as physiologically surprising and theoretically unexpected, and *Bleyl* (1964) proposed that the reaction in the islets disclosed by the modified *Hausler* reaction (1958) was unspecific and ascribed it to precipitation of bivalent zinc ions not bound to the enzyme but to insulin and glucagon.

Hansson's method (1967 and 1968) was light microscopically applied in the present study. It represents a modification of the *Hausler* method allowing shorter incubation times and abolishment of the staining by micromolar concentrations of specific inhibitors of CAH, e.g. acetazolamide. *Hansson* —

was inhibition by acetazolamide.

Thus the use of *Hansson's* method in the present study would seem to minimize the risk of unspecific results. The fact that no activity at all was found in pancreatic tissue subjected to acetazolamide supports the view that the CAH activity in the islets is specific.

If the CAH activity in the islets was merely due to the presence of zinc bound to insulin and glucagon (*Bleyl* 1964) one would rather expect a diffuse reaction in the islets also in the A-cell area (but not in D-cells and PP-cells?). However the reaction was confined to the B-cell region of the present studied non-diabetic mice. Furthermore although crystalline insulin contains chemically bound zinc (*Scott & Fisher* 1935) and rhombohedral zinc insulin crystals are composed of two zinc ions

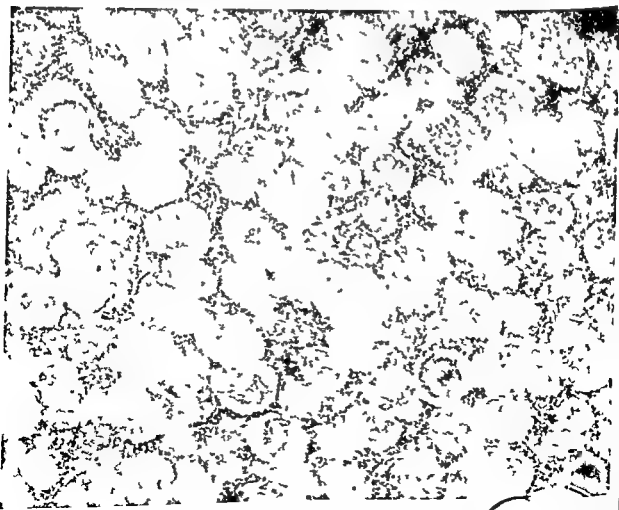
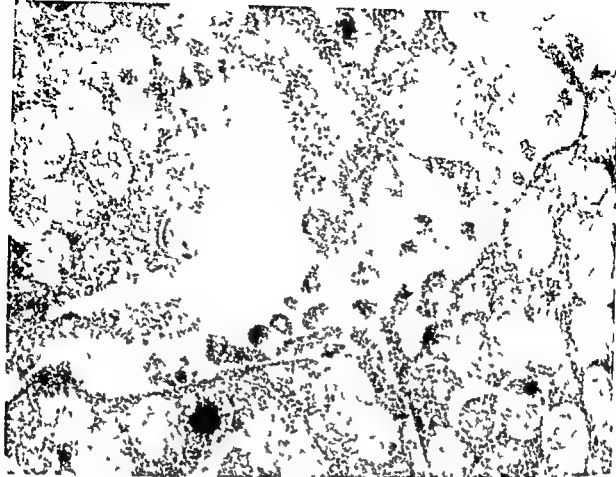
and six insulin molecules (*Adams et al* 1969) it is not known whether zinc is bound to insulin in the β granules although this remains a possibility (*cf. Boquist* 1977). Therefore one can not directly accept the view (*Fand et al* 1959) that the CAH activity in the islets represents zinc not associated with CAH. Moreover if the islet CAH activity were unspecific it is difficult to explain why there is a distinct activity in the islets but no reaction at all in the cytoplasm of the acinar cells. Finally the results of the ultrastructural studies disclosing CAH activity mainly and distinctly localized to only one kind of organelle, viz. the β granules suggest that the CAH activity in the islets is specific.

A discrepancy may seem to exist between the strong light microscopic staining reaction in the islets and the ultrastructural finding of electron dense precipitates only in some secretory granules in the B-cells. However this phenomenon is not unexpected since similar light and electron microscopic differences may exist when other kinds of histochemical methods, e.g. those for zinc, are applied in islet studies (*Boquist* 1977). Moreover in the present study precipitates were ultrastructurally found not only in secretory granules but also to some extent in nuclei, cytoplasmic ground substance and in association to plasma membranes and microvilli. These precipitates like those in blood vessels have conceivably contributed to the strong staining reaction observed in the light microscopic sections.

It is not clear why only some of the secretory granules in the B-cells possessed precipitates. However also in this respect comparison with the results of other histochemical methods shows that this is not an unusual phenomenon. Thus precipitates indicating presence of zinc (*Boquist* 1977) or calcium (*Herman et al* 1973, *Schafer & Kloppel* 1974, *Boquist* 1977) are localized to only a portion of the total number of secretory granules in the B-cells. Variations in the pattern and intensity of precipitation seem to be related to the functional state of the B-cells (*Schafer & Kloppel* 1974). It is believed that the secretory granules containing precipitates are in a different stage (presecretory stage?) of functional activity than those which possess no precipitates (storage stage?). If the observed differences in the pattern of precipitation in the B-cells were merely due, e.g. to a poor

Fig. 7 Interstitial area in B-cell region demonstrating precipitates over central or peripheral portion of β granule cores and in microvilli protruding into an electron lucent intercellular space. $\times 38000$.

Fig. 8 Control section subjected to acetazolamide demonstrating absence of precipitates over secretory granules in B-cell cytoplasm. $\times 38000$.



RESPONSE OF PULMONARY (CIRCULATING) MEGAKARYOCYTES TO EXPERIMENTALLY INDUCED CONSUMPTION COAGULOPATHY IN RABBITS

KNUD BENDIX HANSEN KRISTIAN AABO and OLAF MYHRE JENSEN

University Institute of Pathology Århus Amtssygehus 8000 Århus C Denmark

Hansen K. B. Aabo K. & Myhre Jensen O. Response of pulmonary (circulating) megakaryocytes to experimentally induced consumption coagulopathy in rabbits. Acta path. microbiol. scand. Sect. A 87 165-172 1979

The effects of slow temporary infusion of a tissue thromboplastin solution into the superior vena cava on pulmonary as well as circulating megakaryocytes were studied in 40 rabbits (2-48 hours after infusion) and related to 6 noninfused and 7 infused with normal saline. This is a simple and specific method of inducing a fall in blood platelet levels and thereby an activation of thrombocytopoiesis and megakaryocytopoiesis. The induced intravascular coagulation is probably counterbalanced by an activated fibrinolysis allowing the animals to survive the infusion and thereby offering the possibility of studying the long term effects. An increase to about 300% of the normal values in circulating as well as pulmonary megakaryocytes was found 20 and 24 hours after the onset of the infusions respectively. The number of circulating and pulmonary megakaryocytes, showing great individual variations, however dropped to normal levels within 28 hours after onset of the infusions, which means that megakaryocytes remain detectable for less than eight hours in the lungs. No increase was found in pulmonary megakaryocytes in the control (saline infused) group. In our opinion the entrance of megakaryocytes from the bone marrow into the blood circulation is an incidental event; the number in the circulation reflecting the activity of megakaryocytopoiesis. This experiment supports our suggestion that intravascular coagulation is one of the major pathophysiological mechanisms leading to an increase in pulmonary megakaryocytes.

Key words: Megakaryocytopoiesis, thromboplastin infusion, intravascular coagulation.

Knud Bendix Hansen, University Institute of Pathology, Århus Amtssygehus, 8000 Århus C.

Received 19 viii 78 Accepted 3 xii 78

Since 1893 (Aschoff) it has been a well known fact that certain abnormal conditions are connected with increased amounts of pulmonary as well as circulating megakaryocytes, but not until recently has this been related to the occurrence of intravascular coagulation in these pathologic conditions as the major pathophysiological mechanism (Aabo and Hansen (1978)). Different more or less specific methods, such as infusion of platelet specific antiserum (Gabriele *et al* (1967a), Ebbe *et al* (1968a), Rolovic *et al* (1970) and Odell *et al* (1971)), exchange transfusion with homologous platelet-depleted blood (Harker (1966, 1968), Ebbe *et al* (1968a, 1968b), Pennington *et al* (1970) and

Odell *et al* (1971)), simple bleeding (Gabriele *et al* (1967b) and Odell *et al* (1962)) and infusion of endotoxin (Beller *et al* (1969) and Seeler *et al* (1969)) have been used in studies on megakaryocyte and platelet kinetics in order to cause thrombocytopoiesis and thereby stimulate the megakaryocyte and thrombocytopoiesis. Several investigators have shown that infusion of thromboplastin induces a state of hypercoagulability and defibrination with excessive consumption of ~ blood
of 119
(1970)

In an autopsy series we have recently demonstrated a significant correlation between manifest

penetration of fixatives, one would expect to find signs of degeneration in the B-cells, or areas completely devoid of precipitates: this was not the case.

The possible functional significance of CAH in the B-cells remains to be explained. Since it is known that changes in hydrogen ion concentration may affect the insulin secretion *in vivo*, presence of CAH in the B-cells may facilitate, or be a prerequisite for rapid alterations in the intracellular hydrogen ion concentration, which in turn may play a role in insulin secretion. Alterations in hydrogen ion concentration may be of importance in experimental diabetes (Boquist 1978). The view of a role of CAH in the islets is supported by the report of CAH activity also in another endocrine gland, namely the anterior pituitary of rats (Kimura & McLeod 1975). The results of the present study are believed to indicate a true CAH activity in the B-cells of the mouse pancreas.

Supported by grants from the Swedish Medical Research Council (Project No. 718).

REFERENCES

- Adams M J, Blundell T L, Dodson E J, Dodson G, Vijayan M, Baker E N, Harding M H, Hodgkin D C, Rimmer B & Shear S: Structure of rhombohedral two zinc insulin crystals. *Nature (Lond)* 224: 491-495 1969.
- Arvy L (Ed): *Histo-enzymologie des glandes endocrines. Les activités enzymatiques du tissu langerhansien*. Gauthier Villars Editeur Paris pp 105-118 1963.
- Bleyl U von: Zur spezifität des histochemischen Carboanhydrasenachweises im Inselorgan der Bauchspeicheldrüse. *Histochemie* 4: 286-311 1964.
- Boquist L: Histochemistry and electron microscopy of islets. In: *The diabetic pancreas* (eds W Volk and K F Wellman) Plenum Publ Corp pp 129-169 1977.
- Boquist L: Pancreatic B-cell sensitivity to alloxan *in vivo*. Study of antagonizing compounds, serum inorganic phosphate and acid base balance. *Acta Path Microbiol Scand Sect A* 86: 313-318 1978.
- Cro
- Fand S B, Levine J H & Erwin H L: A reappraisal of the histochemical method for carbonic anhydrase. *J Histochem Cytochem* 7: 27-33 1959.
- Gepts W & Gregoire F: Quantitative histochemistry of the endocrine pancreas. In: *Recent advances in quantitative histo and cytochemistry. Methods and applications* (eds U C Dubach and U Schmidt) Berne: Hans Huber pp 284-311 1971.
- Gossner W von: Die vergleichende Morphologie Langerhansschen Inseln. *Histochemie der Langerhansschen Inseln*. In: *Handbuch des Diabetes mellitus. Band I. Pathophysiologie und Klinik* (ed F Pfeiffer) J F Lehmanns Verlag München pp 87 1969.
- Hansson H P J: Histochemical demonstration of carbonic anhydrase activity. *Histochemie* 11: 128 1967.
- Hansson H P J: Histochemical demonstration of carbonic anhydrase activity in some epithelia for active transport. *Acta Physiol Scand* 73: 434 1968.
- Herman L, Sato T & Hales C N: The electron microscopic localization of cations to pancreatic islets of Langerhans and their possible role in insulin secretion. *J Ultrastruct Res* 42: 298-311 1972.
- Häusler G: Zur Technik und Spezifität des histochemischen Carboanhydrasenachweises im Modellversuch und in Gewebsschnitten von Rattenmilien. *Histochemie* 1: 29-47 1958.
- Hellman B & Tahjedal I B: Histochemistry of pancreatic islet cells. In: *Handbook of physiology* (eds D F Steiner and N Freinkel) Williams & Wilkins Company Baltimore Maryland pp 9110 1972.
- Kimura H & MacLeod R M: Evidence for existence of two isozymes of carbonic anhydrase in the anterior pituitary gland of female rats. *J Biol Chem* 248: 1933-1938 1973.
- Korhonen L A & Korhonen E: Histochemical demonstration of carbonic anhydrase activity in mast cells. *Experientia (Basel)* 21: 628-629 1965.
- Kurata Y: Histochemical demonstration of carbonic anhydrase activity. *Stain Technol* 28: 231-232 1953.
- Lange R H: Histochemistry of the islets of Langerhans. In: *Handbuch der Histochemie* (eds W Graumann and K Neumann) Gustav Fischer Verlag Stuttgart Vol VIII/1 pp 1-283 1973.
- Laarås S S & Volk B W: The pancreas in human and experimental diabetes. Grune and Stratton New York and London pp 21-59 1962.
- Lonnerholm G: Carbonic anhydrase histochemistry: critical study of Hansson's cobalt phosphate method. *Acta Physiol Scand Suppl* 418 1974.
- Maren T H: Carbonic anhydrase. *Chemistry physiology and inhibition*. *Physiol Rev* 47: 595-78 1967.
- Schofer H J & Moppel G: The significance of calcium in insulin secretion. Ultrastructural studies of the secretory granules of the β -cells of the rat pancreas. *Arch A Path*.
- Scharle W von: Histochemie des Inselapparates. *Acta Histochemica* 6: 93-132 1958.
- Scott D A & Fisher A M: Crystalline insulin. *Biochem J* 29: 1048-1054 1935.

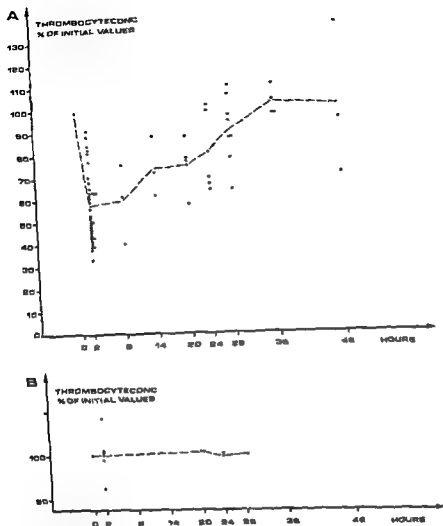


Fig 1 Thrombocyte Counts before (0 hours) and after (2 hours) Infusion of A Thromboplastin B Physiological Saline and immediately before Sacrifice in 40 and 7 Rabbits respectively

a fall in platelet count in the thromboplastin infused animals the mean initial value being 200×10^4 per μ l (166-260) and the mean value immediately after infusion being 112×10^4 per μ l (86-144) which is an average decrease to 58% of the initial values. The platelet counts gradually increased until initial values were reached 36 hours after the thromboplastin infusion had been initiated (Figure 1A). In seven rabbits infused with physiological saline no reduction in platelet count could be observed (Figure 1B).

Megakaryocytes in the pulmonary blood vessels. We found a wide range in the number of pulmonary megakaryocytes. the six rabbits not

infused (normal values) had values from 3 to 39 megakaryocytes per cm^2 lung tissue (Table 1). In the rabbits infused with thromboplastin, the number of pulmonary megakaryocytes remained unchanged during the first 20 hours after infusion but then at 24 hours there was a sudden increase to 300% of the normal values from a mean value of 18 megakaryocytes per cm^2 to a mean value of 55 megakaryocytes per cm^2 (18-86) (Table 1 and Figure 2A). Twenty-eight hours after the infusion values had again dropped to - further - seven animals showed no increase during the period of

intravascular coagulation and an increased number of megakaryocytes in the pulmonary blood vessels (Aabo and Hansen (1978)) In order to study this relation under standardized circumstances, 40 male rabbits were infused with a thromboplastin solution.

MATERIAL AND METHODS

Fifty-three male rabbits (white country race), weighing 3-4 kg, were used Forty rabbits were infused with thromboplastin, seven with physiological saline (0.9%) and six sacrificed without infusion Blood samples were drawn from the superior vena cava or the right atrium through a polyethylene catheter for determination of fibrinogen, platelet and megakaryocyte concentrations The rabbits were killed by intravenous injection of nembutal (10 ml 5% solution) at various periods after infusion Autopsies were performed immediately, and tissue specimens were obtained from both lungs, kidneys, liver and spleen The sections were then fixed in formaldehyde (4% neutral, phosphate buffered), embedded in paraffin wax and sliced at 6-7 microns The tissue sections were stained with haematoxylin-eosin (HE), periodic-acid-Schiff (PAS) and phosphotungstic acid-haematoxylin (PTAH) The degree of thrombosis and the number of megakaryocytes in lung tissue sections were estimated (Aabo and Hansen (1978))

Anesthesia After ear-vein injection of nembutal (2 mg/kg 1% solution) the rabbits were anesthetized with Halothane 1.0-1.5 liters per min, N₂O 4 liters per min and O₂ 2 liters per min on open face mask.

Thromboplastin Infusion (Albrechtsen et al (1970)) 20 ml of a solution of thromboplastin (Roche Laboratories), adjusted to initiate coagulation of rabbit plasma in nine seconds were infused through a polyethylene catheter operatively placed in the external jugular vein extending to the superior vena cava or right atrium

Using a motor pump the infusion lasted approximately two hours during which the rabbits were kept anesthetized Blood samples were drawn immediately before and after the infusion (0 and 2 hours) and the catheter was removed At various time intervals (8 hours up to 48 hours) after the infusion and immediately before sacrificing the animals, the catheter was again introduced into the superior vena cava in order to draw blood samples

Saline Infusion 20 ml of physiological saline (0.9%) were infused into the superior vena cava or the right atrium over a period of two hours The procedure including blood sampling, was identical with that used in the thromboplastin experiment

Fibrinogen concentrations were measured by a precipitation method (Gram (1921))

Platelet concentrations were determined by the use of a Thomas counting chamber

Megakaryocytes in central venous blood (3 ml samples) were counted after being prepared by a saponin haemolysis-leucoconcentration technique (Tinggaard Jensen 1971) using circular Millipore filters (type SC) with a pore size of 8 microns (three filters per 3 ml sample) and stained by Papanicolaou's method

RESULTS

Fibrinogen concentrations and platelet counts Fibrinogen concentrations, all of which showed a decrease (20-90%) during the infusion of thromboplastin, were estimated in eleven rabbits The mean initial value was 11.6 ymol per liter (7.3-25.8), and the mean value immediately after infusion was 5.4 ymol per liter (2.8-8.1) The average value after infusion of thromboplastin was 52% of the initial values There was also registered

TABLE 1 Megakaryocyte Number per cm² Lung Tissue at Different Times after Infusion of Thromboplastin in 40 Rabbits and in 6 Rabbits not Infused (Normal values)

Time of sacrifice	Megakaryocyte number per cm ² lung tissue								Mean	S D
	Single values									
0 hours	03	08	09	10	39	39			18	17
2 hours	05	16	21						14	08
8 hours	08	09	10						09	01
14 hours	02	04	05	12	20				09	07
20 hours	03	05	05	21	22				11	09
24 hours	18	20	38	69	76	79	86		55	29
28 hours	02	03	04	05	08	09	14	35	10	10
36 hours	05	07	12	16					10	05
48 hours	03	03	07	07	33				11	13

S D = Standard Deviation

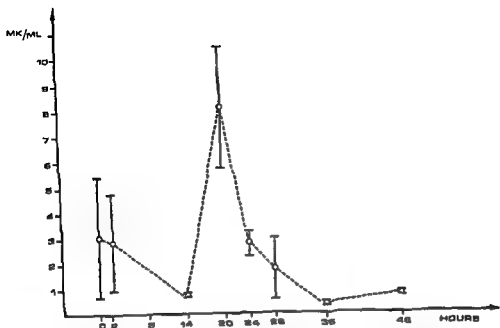


Fig 3 Megakaryocyte Number per ml Central Venous Blood before (0 hours) and after (2 hours) Infusion of Thromboplastin and immediately before Sacrifice in 13 Rabbits Mean \pm S D (Standard Deviation)

observation (Table 2 and Figure 2B) We found no difference between the right and the left lung regarding the number of pulmonary megakaryocytes

Megakaryocyte number in central venous blood was determined in thirteen of the thromboplastin infused rabbits The megakaryocyte number increased from the initial average of 3.1 per ml (0.7-8.0) to an average of 8.2 per ml (6.3-9.7) twenty hours

after onset of infusion (Figure 3) No alterations in the percentage distribution of cytoplasmatic megakaryocytes and naked nuclei were observed

Thrombosis Twenty-three of the forty rabbits infused with thromboplastin had thrombi in the larger pulmonary arteries (Figure 4), and microthrombosis was observed only in one rabbit There was no correlation between incidence of thrombi and time after onset of infusion Of the seven rabbits

TABLE 3 Megakaryocyte Number per 3 ml Central Venous Blood before (0 hours) and after (2 hours) Infusion of Thromboplastin and immediately before Sacrifice in 13 Rabbits

Time of sacrifice	Megakaryocyte number per 3 ml central venous blood														Mean
	Single values														
0 hours	02	03	03	05	06	06	07	07	08	09	19	20	24		09
2 hours	01	01	04	04	06	07	08	09	10	11	13	17	19		08
14 hours	02	02													02
20 hours	19	29													24
24 hours	06	08	09	09											08
28 hours	03	03	09												05
36 hours	01														01
48 hours	02														02

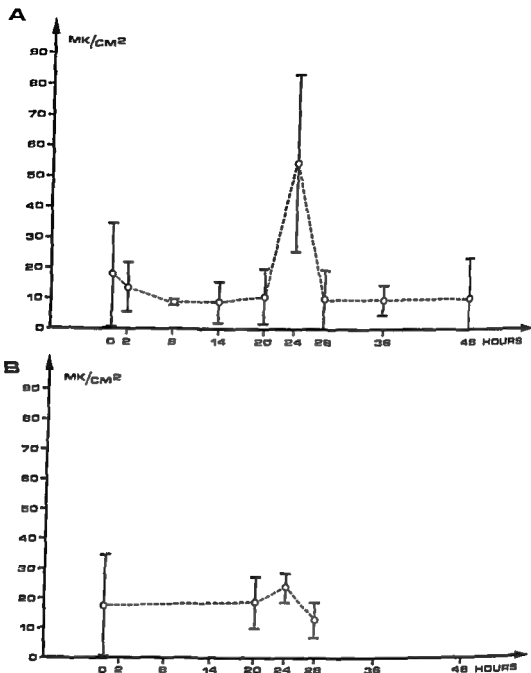


Fig 2 Megakaryocyte Number per cm² Lung Tissue in 47 (40 + 7) Rabbits at Different Times after Infusion of A Thromboplastin B Physiological Saline and in 6 Rabbits not Infused (Normal Values) Mean \pm S D (Standard Deviation)

TABLE 2 Megakaryocyte Number per cm² Lung Tissue at Different Times after Infusion of Normal Saline in 7 Rabbits and in 6 Rabbits not Infused (Normal Values)

Time of sacrifice	Megakaryocyte number per cm ² lung tissue						Mean	S D
	Single values							
0 hours	03	08	09	10	39	39	18	17
20 hours	13	25					19	09
24 hours	18	27	28				24	05
28 hours	08	17					13	06

S D = Standard Deviation

the bone marrow when the megakaryocytopoiesis is moderately stimulated. Owing to an increased maturation rate mature megakaryocytes will accumulate in the bone marrow 20-24 hours after stimulation of the megakaryocytopoiesis and if the passage from the marrow to the blood is incidental this can explain the increase in circulating and pulmonary megakaryocytes found in our study.

As mentioned the increase in platelets began within the first 8-14 hours after the infusion of thromboplastin was initiated and before pulmonary and circulating megakaryocyte number had increased. This initial increase in blood platelets could be explained by inflow of platelets from a platelet pool in the bone marrow or in the spleen. The initial platelet level was not reached until after the number of circulating and pulmonary megakaryocytes had returned to normal. We therefore assume that the final platelet production was due to fragmentation of circulating megakaryocyte cytoplasm pinched off more or less *in toto* intravascularly (macroplatelets) (Aabo and Hansen (1979)).

In our study the megakaryocytes seemed to disappear from the lungs in less than eight hours. This is in accordance with Tierch (1967) who found that megakaryocytes spend a maximum of six hours in the lungs. The fate of the circulating megakaryocytes has been much debated. Only few investigators e.g. Wright (1910) have found degenerating megakaryocytes in the bone marrow or in the blood and newer investigations have not been able to demonstrate degenerating megakaryocytes either in the bone marrow (Behnke (1968)) or in the blood (Tinggaard Pedersen (1974)). Because only very few megakaryocytes from central venous blood show signs of degeneration (Aabo and Hansen (1978)) and only few megakaryocytes pass the capillary bed of the lungs (Scheinin and Korumemi (1963)) and Kallnikos Maniatis (1969) it seems likely that the disintegration must take place in the lungs as was also assumed by Tinggaard Pedersen (1976). We never observed degenerative forms in histologic sections of lung tissue; this might be due to the difficulty in distinguishing them from other cells in the lung capillaries or the fact that degenerative forms are smaller in size and thus able to pass the capillary bed finding their final determination in other parts of the reticuloendothelial system.

REFERENCES

1 Aabo K & Hansen K B Megakaryocytes in pulmonary bloodvessels. I Incidence at autopsy clinicopathological relations especially to disseminated intravascular coagulation. Acta path microbiol scand Sect. A 88 283-291 1978

2 Aabo K & Hansen K B New aspects of the morphology of circulating megakaryocytes in rabbits. Acta path microbiol scand Sect. A 87 173-177 1979

3 Albrechtsen O & Brakman P & Astrup T The defibrination syndrome in rabbits following infusion of tissue thromboplastin in the jugular vein. Thromb Diath Haemorrh 24 113-128 1970

4 Aschoff L Über capillare Embolien von riesenkernhaltigen Zellen. Virch Arch Path Anat Physiol Klin Med 134 11-24 1893

5 Behnke O An electron microscope study of the megakaryocytes of the rat bone marrow. I The development of the demarcation membrane system and the platelet surface coat. J Ultrastruct. Res 24 412-433 1968

6 Beller F K Graeff H & Gorstein F Disseminated intravascular coagulation during the continuous infusion of endotoxin in rabbits. Amer J Obstet Gyn 103 544-554 1969

7 Bond V P Kinetics of megakaryocyte proliferation. Proc Soc Biol 111 177-182 1962

8 Gabriele G de & Pennington D G Physiology of the regulation of platelet production. Brit J Haemat 13 202-209 1967

9 Gabriele G de & Pennington D G Regulation of platelet production. Thrombopoietin. Brit J Haemat 13 210-215 1967

10 Gram H C Studier over fibrinogenmængden i menneskets blod og plasma. Thesis. København 1921

11 Harker L A Megakaryocyte Alterations in Thrombopoiesis. Blood 28 1014-1014 1966

12 Harker L A Kinetics of thrombopoiesis. J Clin Invest 47 458-465 1968

13 Hume R West J T Malmgren R A & Cline J A Kinetics of thrombopoiesis. J Clin Invest 47 458-465 1968

14 Kallnikos Maniatis A Megakaryocytes and platelets in central venous and arterial blood. Acta Haemat 42 330-335 1969

15 Kaufmann R M Ara R Pollack S Crosby W H & Doberneck R Origin of pulmonary megakaryocytes. Blood 25 767-773 1965

16 Odell T T McDonald T P & Asano M Response of rat megakaryocytes and platelets to bleeding. Acta Haemat 27 171-179 1962



Fig 4 Evidence for Coagulation in Pulmonary Blood Vessels in Thromboplastin Infused Rabbits Thrombus in a Larger Artery

infused with normal saline, none had thrombi in the pulmonary blood vessels. No micro- or macrothrombosis was found in livers, spleens or kidneys.

DISCUSSION

Slow infusion of thromboplastin is a simple and specific method of initiating intravascular coagulation (Albrechtsen *et al.*, 1970) and thereby consumption of blood platelets and fibrinogen. This leads to a transitory reduction in blood platelet levels and makes it possible to study thrombocytopoiesis and megakaryocytopoiesis as well. Other methods have been described in the past, but these seem to be more complicated or unspecific. Simple bleeding stimulates not only megakaryocytopoiesis but also erythro- and leukopoiesis, and changes the haemodynamic balance. Exchange transfusion with homologous platelet depleted blood is a complicated procedure, which may entail mechanical alteration of the reinfused blood. Infusion of platelet specific antiserum leads to severe reduction in blood platelet values and may affect the megakaryocytes in the bone marrow, owing to common antigenic properties of platelets and megakaryocytes (Witte (1955) and Rologic *et al.* (1970)).

Albrechtsen *et al.* (1970) found a mean reduction in the platelet count of approximately 58% and a mean decrease in the fibrinogen concentration of approximately 60% after infusion of thromboplastin. Our values (42% reduction in platelets and 48% reduction in fibrinogen values) are similar, showing that we have reproduced their experimental model, in which a defibrination syndrome following infusion of tissue thromboplastin in the

jugular vein of rabbits was convincingly demonstrated.

Decrease in fibrinogen concentration and platelet counts in all the rabbits infused with thromboplastin, without alteration in blood platelet levels after infusion with normal saline, indicates that tissue thromboplastin is able to initiate a consumption coagulopathy, through macro- and microthrombosis was found in relatively few animals. This is probably due to a compensatory activation of the fibrinolysis, breaking down fibrin at the same rate as it is formed in the pulmonary vascular bed. This finding is supported by Albrechtsen *et al.* (1970), who found a decrease in euglobulin activity and plasminogen activity after the thromboplastin infusion.

While several investigators have dealt with megakaryocytes in the blood as well as in the bone marrow, after stimulation of the megakaryocytopoiesis, no one has reported the response in pulmonary megakaryocytes to experimentally-induced intravascular coagulation. In our study an increase in the number of pulmonary megakaryocytes was found 24 hours after infusion of thromboplastin while no increase was observed after infusion of saline. This indicates that the increase is a response to the infused thromboplastin and not to the procedure itself. The observation is further supported by the increase in circulating megakaryocytes in central venous blood 20 hours after infusion of thromboplastin also found in this study. The great individual variation in pulmonary megakaryocyte number as well as in the number in central venous blood cannot be due to a diurnal pattern described by Hume *et al.* (1964), as all our rabbits in the different time-interval groups were studied (sacrificed) at the same time of the day. Tinggaard Pedersen (1971, 1973) also reported a great individual variation in megakaryocyte number in central venous blood in rats, and he found a maximum increase in the number 24 hours after surgery (1972). Megakaryocyte proliferation time in the bone marrow of rats is found to be 40-60 hours (Ebbe *et al.* (1965, 1968b), Odell *et al.* (1969) and Feinendegen *et al.*, 1962) and in rabbits 32-36 hours (Cooney *et al.* 1965). These maturation rates refer to normal states and are reduced when the thrombocytopoiesis is stimulated. Odell *et al.* (1969) reported a reduction in the maturation time of approximately seven hours by infusing platelet specific antiserum into rats. Our findings indicate that the megakaryocyte maturation time in rabbits may be reduced to approximately 20-24 hours in stimulated thrombocytopoiesis. Only mature megakaryocytes were found in the blood and the lung capillaries, so it seems that only mature forms leave

NEW ASPECTS OF THE MORPHOLOGY OF CIRCULATING MEGAKARYOCYTES IN RABBITS

KRISTIAN AABO AND KNUD BENDIX HANSEN

University Institute of Pathology Århus Amtssygehus 8000 Århus C Denmark

Aabo K & Hansen K B New aspects of the morphology of circulating megakaryocytes in rabbits
Acta path microbiol scand Sect A 87 173-177 1979

Circulating cytoplasmatic megakaryocytes isolated from central venous blood of rabbits by a saponin haemolysis leuco-concentration technique were found to have two morphological appearances a globular and an oblong form referring to the shape of the cells as a whole as well as to the shape of the nuclei. The nucleus was either centrally or peripherally located. Of the megakaryocytes observed 40% were cytoplasmatic and 60% naked nuclei. Regressive changes in the residual nucleus was observed only 4.5% showing karyorrhexis or karyolysis. Megakaryoblasts and promegakaryocytes were never encountered. The average megakaryocyte content per ml central venous blood was 3.8 (range 0-10). A not previously described cytoplasmatic ligating process in which the nucleus seemed to move out of the cytoplasm forming a naked nucleus and leaving the total cytoplasm intact was observed. We call this phenomenon 'nucleus escape'. The function and fate of the intravascular megakaryocytes are briefly discussed.

Key words: Megakaryocyte morphology, nucleus escape.

Knud Bendix Hansen, University Institute of Pathology, Århus Amtssygehus, 8000 Århus C, Denmark.

Received 19 viii 78 Accepted 3 xii 78

Since Aschof (1893) observed megakaryocytes in lung capillaries the origin, function and fate of the cells in the blood have been a matter of debate. They have both in animals and in human beings been isolated from peripheral blood (Oelhofen 1914, Minot 1922, Whitby 1948, Efrati *et al* 1960, Herbeval *et al* 1962, Milani *et al* 1962, Wurst 1963, Hume *et al* 1964, Hirota 1966, Melamed *et al* 1966, Breslow *et al* 1968, Karpas *et al* 1969, Dago *et al* 1971) as well as from central venous and arterial blood (Scheinin *et al* 1963, Kaufman *et al* 1965, Kallnikos Maniatis 1969, Tinggaard Pedersen 1971, 1974).

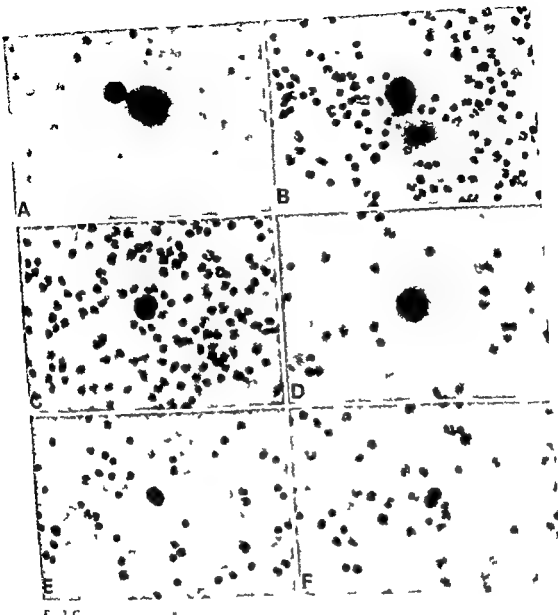
Circulating megakaryocytes have been described as giant cells with multi-lobulated nuclei surrounded by varying amounts of cytoplasm which may appear more or less irregularly (Kaufman *et al* 1965, Kallnikos Maniatis 1969, Tinggaard Pedersen 1971) or as cytoplasmatic-depleted residual nuclei (naked nuclei). The cytoplasmatic megakaryocyte is most frequently encountered in central

venous blood and rarely in central arterial or peripheral venous blood which implies a production of blood platelets in the lung capillaries (Scheinin *et al* 1963, Kaufman *et al* 1965, Kallnikos Maniatis 1969, Tinggaard Pedersen 1974). Also the naked nucleus is found in fewer numbers in blood from the arterial side of the pulmonary circulation as compared to the venous side. This has led to the suggestion that megakaryocytes released into the blood from the bone marrow degenerate in the lung capillaries. The present study was undertaken in order to examine in more detail the morphology of circulating megakaryocytes.

MATERIAL AND METHODS

Central venous blood from rabbits (three 1 ml samples from each) drawn through a polyethylene catheter operatively placed in the right atrium was prepared by a saponin haemolysis leuco-concentration technique (Tinggaard Pedersen 1971). Millipore filters (type SC

- 22 Odell, T T, Jackson C W, Friday, T T & Charska, D E Effects of thrombocytopenia on megakaryocytopoiesis *Brit J Haemat* 17 91-101, 1969
- 23 Odell, T T, Jackson C W & Friday, T J Assay of megakaryocytopoiesis in thrombocytopenic rats *Brit J Haemat* 21 233-240, 1971
- 24 Pedersen, N T Circulating megakaryocytes in blood from the inferior vena cava in adult rats *Scand Haemat* 8 223-230, 1971
- 25 Pedersen, N T The increase in the number of circulating megakaryocytes and blood platelets in the rats after surgery *Scand J Haemat* 11 71-77, 1973
- 26 Pedersen N T The pulmonary vessels as a filter for circulating megakaryocytes in rats *Scand J Haemat* 13 225-231, 1974
- 27 Pedersen, N T Undersøgelser over cirkulerende megakaryocyter Thesis, København, 1976
- 28 Pennington D G & Olsen T E Megakaryocytes in states of altered platelet production *Brit J Haemat* 18 447-463, 1970
- 29 Pirkle, H C, Anderson, H C, McHugh J J & Allen V G Production of intravascular clotting in the rabbit by intravenous injection of blood thromboplastin *Am J Path* 35 710-711 1959
- 30 Pirkle, H C, Wallace J G & Allen V G Experimental intravascular clotting *Arch Path* 74 370-374, 1962
- 31 Rolovic, Z, Baldini M & Dameshek W Megakaryocytopoiesis in experimentally induced immune thrombocytopenia *Blood* 35 178-188 1970
- 32 Scheinin T M & Korvunemi A P Megakaryocytes in the pulmonary circulation *Blood* 22 82-87 1963
- 33 Seeler, R A, Forman, E N, Bolger J E, Abildgaard, C E & Schulman I Induction of intravascular coagulation and renal cortical necrosis in rabbits by simultaneous injection of thromroast and endotoxin *Brit J Haemat* 16 501-505, 1969
- 34 Stalker, A L, Brown, L J, Hall, J & Blench S M Studies in experimental defibrination *Microvasc Res* 1 287-294, 1969
- 35 Tverdy, G Über den kreislauf und über die erneuerung der megakaryozyten in den lungen der maus *Arztl Forsch* 21 389-391, 1967
- 36 Witte, S Megakaryozyten und thrombocytopoese bei der experimentellen thrombocytopenischen purpura *Acta Haemat* 14 215-230 1955
- 37 Wright, J H The histogenesis of platelets *J Morphol* 21 263-278, 1910



cytoplasmic megakaryocytes with more or less abundant

globular or elongated with multiple lobules and located either centrally or peripherally. Usually a high number of lobules were present and frequently located in a rosette like fashion. The chromatin was coarsely fragmented with a tendency to accumulate in the periphery of the lobules. The cytoplasm was gritty in the Papanicolaou stain without the characteristic granules of the Romanowsky Wright stain. Frequently a brush border like surface coat was observed (Fig 1 A B).

The cytoplasmic megakaryocyte is a large cell (fifty to several hundred μm). Two morphological appearances were identified a globular (Fig 1 III) and an oblong form (Fig 1 D). The nuclei were also

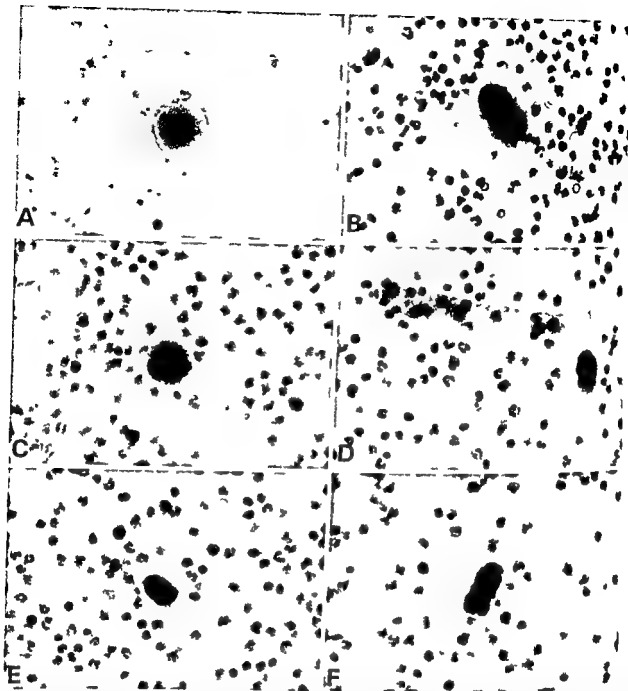


Fig 1 Circulating Megakaryocytes A B Globular Megakaryocytes with Abundant Cytoplasm and a Brush Border like Surface Coat C Globular Megakaryocyte with Less Cytoplasm D Oblong Megakaryocyte with Abundant Cytoplasm being Pinched off in Toto E F Naked Nuclei One without Cytoplasm and One with a Narrow Rim of Cytoplasm

diameter 47 mm pore size 8 γ) were stained by the Papanicolaou method (one filter per 1 ml blood sample) Megakaryocytes and leukocytes were well preserved and the megakaryocytes could easily be identified by their size and characteristic morphology The slides with millipore filters were screened at a magnification of 25 \times obj

RESULTS

The average megakaryocyte content per ml central venous blood from twenty two normal albino rabbits was 3.8 (range 0-16) 40% had more or less cytoplasm and 60% were naked nuclei Megakaryoblasts and promegakaryocytes were never encountered

Circulating megakaryocytes by far the largest cells in the blood were principally recognized as

- 2 Behnke O An electron microscope study of the megakaryocytes of the rat bone marrow I The development of the demarcation membrane system and the platelet surface coat J Ultrastruct. Res 24 412-433 1968
- 3 Behnke O An electron microscope study of the megakaryocytes of the rat bone marrow II Some aspects of platelet release and microtubules J Ultrastruct. Res 26 111-129 1969
- 4 Breslow A Kaufman R M & Lawsky A R The effect of surgery on the concentration of circulating megakaryocytes and platelets Blood 32 393-401 1968
- 5 Dago C Karpas C M Pincus L Tytun A & Oppenheim A Circulating megakaryocytes A quantitative observation in normal subjects by age and sex Acta Cytol 15 410-413 1971
- 6 Efrati P & Roentgen L The morphology of buffy coat in normal human adults Blood 16 1012 1019 1960
- 7 Hansen K B Aabo K & Myhre Jensen O Response of Pulmonary (Circulating) Megakaryocytes to Experimentally Induced Consumption Coagulopathy in Rabbits Acta path microbiol scand Sect. A 87 165-172 1979
- 8 Herbeval H Duheille J Cuny G & Guerci O La megacaryocytemie des cancéreux Ann Med Nancy 1 894 903 1962
- 9 Hirota Y Studies on megakaryocyte nuclei in peripheral blood Acta Haem Jap 29 833-844 1966
- 10 Hume R West J T Malmgren R A & Chu E 4 Quantitative observations of circulating megakaryocytes in the blood of patients with cancer New Engl J Med 270 111 117 1964
- 11 Kallimkos Maniatis A Megakaryocytes and platelets in central venous and arterial blood Acta Haemat 42 330-335 1969
- 12 Karpas C M Dago C Oppenheim A & Cheng L Significance of circulating megakaryocytes in the peripheral blood of patients with cancer Acta Cytol 13 142-148 1969
- 13 Kaufman R M Auro R Pollack S & Crosby W H Circulating megakaryocytes and platelet release in the lung Blood 26 720-731 1965
- 14 Melamed M R Clifton E E Mercer C & Koss L G The megakaryocyte blood count. Amer J Med Sci 252 301-309 1966
- 15 Mihani A & Passaleva A Caratteristiche morfologiche dei megacariociti circolanti nel vecchio e nel giovane G Geront 10 615-620 1962
- 16 Minot G R Megakaryocytes in the peripheral circulation J Exper Med 36 1-8 1922
- 17 Oelthafen H Über Knochenmarkriesen Zellen im stromenden Blut Folia Haemat 18 171-206 1914
- 18 Pedersen N T Circulating megakaryocytes in blood from the inferior vena cava in adult rats Scand J Haemat 8 223-230 1971
- 19 Pedersen N T The increase in the number of circulating megakaryocytes and blood platelets in the rat after surgery Scand J Haemat 11 71-77 1973
- 20 Pedersen N T The pulmonary vessels as a filter for circulating megakaryocytes in rats Scand J Haemat 13 225-231 1974
- 21 Scheinin T M & Korvunemi A P Megakaryocytes in the pulmonary circulation Blood 22 82-87 1963
- 22 Tierdy G Über den kreislauf und über die erneuerung der megakaryozyten in den lungen der maus Arch Forsch 21 389-391 1967
- 23 Tierdy G Etude de megacaryocytes pulmonaires dans un cas de carcinome bronchique Ann Anat Path 15 361-368 1970
- 24 Whitby L The significance of megakaryocytes in the peripheral circulation Blood 3 934-938 1948
- 25 Wright J H The histogenesis of platelets J Morphol 21 263 278 1910
- 26 Wüst G Über das Vorkommen von Megakaryozyten in stromenden Blut. Folia Haemat 8 421-435 1963
- 27 Yamada E The fine structure of megakaryocytes in the mouse spleen Acta Anat. 29 267-290 1957

Ligation of the cytoplasm could be more or less total (Fig 2 A, B), and occasionally the nucleus seemed to move out of the cytoplasm, forming a naked nucleus and leaving the total cytoplasm intact (Fig 2 A, C, D). We have called this form of total pseudopodial ligation *nucleus escape phenomenon*.

The nuclear lobules of the residual megakaryocyte (the naked nucleus) were densely packed, and frequently the nucleus was pycnotic without visible lobulation (Fig 2 E). Usually the cytoplasm was lacking, but occasionally a narrow rim of cytoplasm was visible (Fig 1 F). Only four megakaryocytes (1.5%) showed karyorrhexis and karyolysis (Fig 2 F).

DISCUSSION

The variation in shape of the circulating cytoplasmic megakaryocytes, which has also been described by others (Herbeval *et al* 1962, Kaufman *et al* 1965, Tinggaard Pedersen 1971) may be due to an active ameboid capacity to form pseudopods or it might be an expression of the space conditions in the bone marrow, as the megakaryocytes are maturing, forming the cytoplasm. When seen in organs the shape of the intravascular megakaryocytes may simply reflect the space conditions in the capillary bed.

Two different ways of platelet-formation in the bone marrow have been described. Wright (1910) introduced the so-called pseudopodial theory, according to which numerous long thin pseudopods are formed projecting into the sinusoids of the marrow where they are pinched off and later fragmented into platelets. This process was electron microscopically verified by Behnke (1969). The other theory was advanced by Yamada (1957) according to whom the cytoplasm *in situ* is

smaller pseudopodial buds described by Wright were never observed. This might be the explanation of the variation in cytoplasmic mass in megakaryocytes with the same nuclear size and supports the theory of Yamada. It therefore seems reasonable that both ways of platelet formation actually occur.

Under certain circumstances an increased release of megakaryocytes from the bone marrow into the circulation takes place (Hansen *et al* 1978). Many of these megakaryocytes may be slightly immature regarding the development of the surface connecting demarcation membrane system (Behnke 1968) and after being released into the blood, their cytoplasm may fragment at places where the development of the demarcation membrane system is most comple-

ted. Whether or not the demarcation of the cytoplasmic bits (*agiant platelets*) is terminated fragmenting the bits into platelets when they are separated from the nucleus, is not known. On the other hand it has been demonstrated that an intravascular platelet production occurs in the lungs (Scheinin *et al* 1963, Kaufman *et al* 1965, Kallimkos-Mamatis 1969, Tinggaard Pedersen 1974). This production may be due to pulmonary cytoplasmic megakaryocytes alone but possibly also to fragmentation of larger cytoplasmic fragments led to the lungs by the blood.

We observed a special cytoplasm ligating process in which the nucleus is moving out of the cytoplasm, analogous with the formation of the erythrocyte from the orthochrome erythroblast. This process, which has not been described earlier, may be an expression of total pseudopodial ligation and is called *nucleus escape phenomenon*.

Under normal circumstances 40% of the megakaryocytes in central venous blood in rabbits (this study), rats (Tinggaard Pedersen 1971, 1973) and human beings (Mihani *et al* 1962, Scheinin *et al* 1963, Kaufman *et al* 1965) are cytoplasmic megakaryocytes and the rest naked nuclei. How much of the total amount of megakaryocytes in the marrow that migrate into the blood and whether it is only the cytoplasmic megakaryocytes or also naked nuclei that pass into the blood is not known. As the naked nuclei found in central venous blood might have released their cytoplasm on their way to the right atrium.

Only very few megakaryocytes pass the capillary bed of the lungs (Kallimkos-Mamatis 1969, Tierhøj 1970, Tinggaard Pedersen 1974) which indicates that they do at least to a certain extent, degenerate in the pulmonary capillaries. Furthermore megakaryocytes only remain detectable in the lungs for 6-8 hours (Tierhøj 1967, Hansen *et al* 1978) suggesting a degeneration during this time. No other investigators have described degenerating megakaryocytes in the blood and in our material only very few (1.5%) showed regressive signs (karyorrhexis and karyolysis) when isolated from central venous blood. They may be degenerating cells released from the bone marrow or recirculating cells escaped from the lungs. The final disintegration of the megakaryocytes may happen in the lungs or in other parts of the reticuloendothelial system.

REFERENCE

1. Aschoff L. Über capillare Embolie von riesenkernhaltigen Zellen. *Virch Arch Path Anat Physiol klin Med* 134: 11-24, 1891.

POLYPOID CYSTITIS

A Catheter Associated Lesion of the Human Bladder

PETER EKELOUND and SONNY JOHANSSON

Geriatric clinic I Vasa hospital and Department of Pathology II Sahlgrens hospital University of Göteborg Göteborg Sweden

Ekelund P & Johansson S Polypoid cystitis a catheter associated lesion of the human bladder Acta path microbiol scand Sect A 87 179-184 1979

Histopathological examination of the urinary bladders of 63 patients dying in a geriatric clinic was performed. In 40 of 51 patients who had been treated with a urinary catheter histological changes of polypoid cystitis were found. In 34 of the bladders the lesion engaged the posterior wall which corresponds to the localization of the tip of the catheter. The frequency of polypoid cystitis increased with increasing time of catheter treatment and reached its peak by three months. After that time the frequency was relatively constant. The frequency of polypoid cystitis seemed not to be influenced by bacterial urinary tract infection. Urothelial atypia was not seen after catheter treatment.

Key words: Urinary bladder catheter polypoid cystitis

Sonny Johansson Department of Pathology II University of Göteborg Sahlgrens hospital S 413 45 Göteborg Sweden

Received 13 XI 78 Accepted 5 XII 78

A number of inflammatory and reactive lesions with a characteristic histological appearance in the human bladder have been described e.g. cystitis cystica and glandularis follicular cystitis interstitial cystitis radiation cystitis giant cell cystitis and malakoplakia (Koss 1974). Polypoid cystitis is a term used by Friedman & Ash (1959) for a vesical growth which may simulate neoplasm macroscopically but was considered to be inflammatory degenerative and reactive in origin. They illustrated a case in a 23 year-old man without apparent cause which Koss (1974) considered to be exceptional. The present study is a histopathological examination of the urinary bladder from 63 consecutive patients dying in a geriatric clinic.

MATERIAL AND METHODS

Sex and age. Thirty four of the patients were males and 19 females with a mean age of 79 years (range 45-99). Twelve of the patients had never been treated with a urinary catheter the remaining patients had used

catheters for varying lengths of time. The charts and the clinical records were examined with particular reference to diseases of the urinary tract especially urinary tract infection.

Morphological methods. Thirty minutes after the patients were declared dead by a physician the urinary bladder was filled with 150 cc 4 per cent formaldehyde solution in order to achieve acceptable histological fixation. The pelvic organs were removed en bloc the urinary bladder was bisected and inspected and multiple sections were taken from the urethra and prostate trigone posterior wall dome and left and right lateral walls. Five µm sections were stained with hematoxylin and eosin and according to Weigert - van Gieson.

RESULTS

Clinical results. The patients were old and had often several major diseases e.g. 19 of them had malignant tumours in a terminal stage and 33 patients suffered from cardiovascular diseases including diabetes hypertension and cerebral hemorrhage or infarction.

POLYPOID CYSTITIS

A Catheter Associated Lesion of the Human Bladder

PETER EKELUND and SONNY JOHANSSON

Geriatric clinic I Vasa hospital and Department of Pathology II Sahlgrenska hospital University of
Göteborg Göteborg Sweden

Ekelund P & Johansson S Polypoid cystitis: a catheter associated lesion of the human bladder. *Acta path microbiol scand Sect. A* 87: 179-183 1979

Histopathological examination of the urinary bladders of 63 patients dying in a geriatric clinic was performed. In 40 of 51 patients who had been treated with a urinary catheter histological changes of polypoid cystitis were found. In 34 of the bladders the lesion engaged the posterior wall which corresponds to the localization of the tip of the catheter. The frequency of polypoid cystitis increased with increasing time of catheter treatment and reached its peak by three months. After that time the frequency was relatively constant. The frequency of polypoid cystitis seemed not to be influenced by bacterial urinary tract infection. Urothelial atypia was not seen after catheter treatment.

Key words Urinary bladder catheter polypoid cystitis

Sonny Johansson Department of Pathology II University of Göteborg Sahlgrenska hospital S-413 45
Göteborg Sweden

Received 13 xi 78 Accepted 5 xii 78

A number of inflammatory and reactive lesions with a characteristic histological appearance in the human bladder have been described e.g. cystitis cystica and glandularis follicular cystitis interstitial cystitis radiation cystitis giant cell cystitis and malakoplakia (Koss 1974). Polypoid cystitis is a term used by Friedman & Ash (1959) for a vesical growth which may simulate neoplasm macroscopically but was considered to be inflammatory degenerative and reactive in origin. They illustrated a case in a 23 year-old man without apparent cause which Koss (1974) considered to be exceptional. The present study is a histopathological examination of the urinary bladder from 63 consecutive patients dying in a geriatric clinic.

catheters for varying lengths of time. The charts and the clinical records were examined with particular reference to diseases of the urinary tract, especially urinary tract infection.

Morphological methods Thirty minutes after the patients were declared dead by a physician the urinary bladder was filled with 150 cc 4 per cent formaldehyde solution.

wall dome and left and right lateral walls. Five μ m sections were stained with hematoxylin and eosin and according to Weigert - van Gieson.

RESULTS

Clinical results The patients were old and had often several major diseases eg 19 of them had malignant tumours in a terminal stage and 33 patients suffered from cardiovascular diseases including diabetes hypertension and cerebral hemorhage or infarction.

MATERIAL AND METHODS

Sex and age Thirty four of the patients were males and 19 females with a mean age of 79 years (range 45-99). Twelve of the patients had never been treated with a urinary catheter the remaining patients had used

TABLE 1 *The Correlation between Time of Catheter Treatment and Incidence of Urinary Tract Infection in 64 Patients*

Urinary tract infection	Time of catheter treatment (months)							Total
	0	<1	1-3	3-6	6-12	12-24	>24	
Negative	9	6(4)	3(3)	1(1)	1(1)	0	0	20
Positive	3	7(4)	7(6)	4(3)	6(4)	8(7)	8(7)	43
Total	12	13	10	5	7	8	8	63

The numbers within brackets indicate patients with polypoid cystitis

TABLE 2 *The Frequency of Different Histopathological Changes of the Urinary Bladder and Prostate in 64 Patients after Different Times of Catheter Treatment*

Morphological lesion	Time of catheter treatment (months)						
	0 n = 12	<1 n = 13	1-3 n = 10	3-6 n = 5	6-12 n = 7	12-24 n = 8	>24 n = 8
Polypoid cystitis	—	8	9	4	5	7	7
von Brunn's nest	5	5	5	2	4	3	4
Severe inflammation with contracted bladder	2	—	1	3	—	1	4
Diverticuli	1	1	2	—	—	1	3
Squamous metaplasia	2			1	2		1
Bladder calculi				1			1
Follicular cystitis			1				
Benign prostatic hyperplasia	6	6	3	1	3	4	3
Prostatic adenocarcinoma		2	2			1	3
»Normal« bladder	7	2	1	—	—	—	—

In 43 patients urinary tract infection was recorded (positive urine cultures or urine sediment) and in 20 patients this could not be verified. Three of 12 patients who had not been treated with a Foley catheter had bacterial urinary tract infection. Table 1 gives the correlation between time of catheter treatment and urinary tract infection. The incidence of urinary tract infection seems to increase with increasing time of catheter treatment. All the patients who had had a urinary catheter for 12 months or more had urinary tract infection. Nine of the 11 catheter treated patients without evidence of bacterial urinary tract infection had polypoid cystitis.

Morphological results Macroscopical lesions of the urinary bladder were seen in twelve cases. The pathological area exhibited polypoid or bullous lesions up to 0.5 cm in diameter. The mucosa

Altogether polypoid cystitis (see below) was found in 40 bladders: 22 men and 18 women. In 28 of the patients the lesion was only microscopical. The frequency and localization of polypoid cystitis is given in Table 3. Thus in 34/40 cases the polypoid cystitis involved the posterior wall (Fig. 1). All the three patients who had involvement of the entire bladder had been using catheters for more than six months. Polypoid cystitis was not found in any of the patients who had not been using a urinary catheter.

Microscopically the lesions were polypoid, sometimes bullous or papillary (Figs. 2-4). Urothelial hyperplasia of mild degree was frequently found and the urothelium often contained small microabscesses. The underlying lamina propria was oedematous, often with abundant inflammatory cells, particularly polymorphous leucocytes and lymphocytes. In association with the oedematous areas an increased number of capillaries and sometimes larger ectatic vessels were seen. Signs of recent and old hemorrhage were also common (Fig.



Fig. 1. Localization of the tip of the catheter in the posterior wall.



Fig 2 Combined polypoid and papillary lesion after 4 months of catheter treatment Htx & eo $\times 90$



Fig 3 Bullous lesion with urothelial hyperplasia prominent oedema and mild inflammation after 2 months of catheter treatment Htx & eo $\times 120$

TABLE 3 The Frequency and Localisation of Polypoid Cystitis in 51 Patients Treated with a Urinary Bladder Catheter

Localisation	No of patients (n = 51)
Trigone	3
Trigone + posterior wall	6
Posterior wall	18
Trigone + posterior wall + dome	1
Posterior wall + dome	6
Dome	3
Entire bladder	3



Fig 4 Polypoid lesion with inflammatory oedema and abscesses in the urothelium after 4 months of catheter treatment. Htx & eo $\times 90$

Sometimes particularly in patients who had been using a permanent catheter for more than six months the lesions appeared to be more organized with prominent fibrosis and collagen formation (Fig 6). Urothelial atypia was not seen.

DISCUSSION

The present study demonstrated that a majority of catheter treated patients had characteristic histological changes in the bladder. The lesion seemed to be more frequent and to involve a larger area of the bladder with increasing time of catheter treatment. Thus the mucosa was polypoid, bullous or papillary, the urothelial lining often mildly hyperplastic and the lamina propria oedematous with abundant capillaries (Figs 2-4). Signs of hemorrhage and inflammation were frequently seen (Fig 5). The lesion resembles partly polypoid cystitis which has been described by Friedman & Ash (1959) in a 23 year-old man. It also resembles what they and Koss (1974) call bullous cystitis particularly when the

oedematous bullous changes dominate. We suggest that the name of the lesion should be polypoid cystitis because the polypoid lesions dominate. In the majority of cases polypoid cystitis engaged the posterior wall (Table 3) an area in close contact



Fig 5 Partly polypoid lesion with extensive hemorrhage and inflammation after 5 months of catheter treatment. Htx & eo $\times 90$



Fig 2 Combined polypoid and papillary lesion after 4 months of catheter treatment Htx & eo $\times 90$



Fig 3 Bullous lesion with urothelial hyperplasia, prominent oedema, and mild inflammation after 2 months of catheter treatment Htx & eo $\times 120$

EFFECTS OF CYCLOPHOSPHAMIDE ON OPEN, GRANULATING SKIN WOUNDS IN RATS

HENRIK WIE INGOLV BRUASET and THOMAS ECKERSBERG

Department of Pathology Dental Faculty and Institute for Surgical Research Rikshospitalet University of Oslo Norway

Wie H Bruaset I & Eckersberg Th Effects of cyclophosphamide on open granulating skin wounds in rats Acta path microbiol scand Sect A 87 185-192 1979

The effect of cyclophosphamide on the healing of open cutaneous wounds was studied in rats. Following intraperitoneal injections of 25 mg/kg body weight every second day for 9 days only about 7% of the wounds were completely covered by epithelium after 15 days whereas in the control animals 60% of the wounds were completely epithelialized. Measurements of wound diameters in circular skin wounds revealed unhealed wound areas in the drug-treated animals which were significantly larger than those of the control animals. Cyclophosphamide was found to reduce the occurrence of H³ labelled cells in the granulation tissue when evaluated after 11 days. At 15 days there was no difference in the labelling frequency between treated and control animals indicating reversal of the drug effect.

Key words: Autoradiography, cyclophosphamide, rat, skin, wound healing.

Henrik Wie, Dental Faculty, University of Oslo, Geitmyrsvei 71, Oslo 4, Norway.

Accepted as submitted 20 x 78

Cyclophosphamide has a detrimental effect on cells at a high mitotic rate when administered in therapeutic and toxic doses. The effect is dose dependent (Hill 1975) and is most clearly observed in growing tumours in the intestinal mucosa (Calabresi & Parks 1975) in the matrix cells of the hair follicles of the scalp in man (Lee *et al* 1973) and in the hemopoietic system (Host 1966, Valerius *et al* 1968, Lev *et al* 1973).

Proliferation and differentiation of cells are prominent features in wound healing and a retarding effect of the drug on these processes could be expected. There is however no general agreement in the literature as to the effect of cyclophosphamide on the healing of surgical wounds. Lentini *et al* (1956), Host & Nissen Meyer (1960), Stales *et al* (1962), Mutti & Dedl (1966) and Calnan & Davies (1968) found no effect of the drug on the progress of healing while Des Prez & Kuhn (1960), Hoppe (1962), Mangione & Taverna (1964), Romanowski & Kubicki (1967), Aarppinen & Mäkitiemi

(1970) and Cohen *et al* (1975) reported a retardation of the healing of surgical wounds. In the present study the effects of cyclophosphamide on the healing of open granulating skin wounds were studied in order to further elucidate this problem.

MATERIALS AND METHODS

Forty-eight-day-old male Wistar/AF/Han/Nol SPF rats were used. Two brother animals were kept in each cage, one randomly selected for drug treatment, the litter mate for control and given standard animal pellets (Bj nr 3155 Mellesentralen 1/S Oslo) and water *ad libitum*. The animals were weighed every second day throughout the experimental period. Mean initial weight was 194 ± 14 g.

Following ether anaesthesia the proximal dorsal part of the tail was shaved and circular wounds comprising the cuts and subcutaneous tissues were inflicted with a hollow punching instrument having a diameter of 8 mm. A thin spray of sulphathiazol powder and a covering film of Nobecutan® (Bofors) were applied to the fresh wounds.

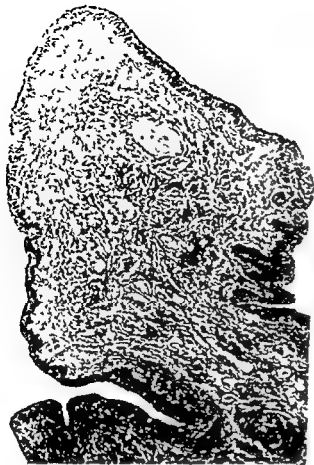


Fig 6 Organized polypoid lesion with marked fibrosis and collagen formation after 18 months of catheter treatment Hix & eo $\times 45$

with the tip of the catheter (Fig 1). The development of polypoid cystitis is probably caused by mechanical irritation by the catheter tip. This irritation does not seem to produce squamous metaplasia, a common finding in patients with chronic cystitis, particularly in combination with stone formation. This may indicate that not only the chronic irritation but also the material of the catheter may be of importance for the development of polypoid cystitis. Other reactive lesions such as von Brunn's nests or cystitis glandularis did not seem to be more frequent in patients with

permanent urinary catheters. Neither was urothelial atypia seen.

Urinary tract infection did not seem to play a major role in the development of polypoid cystitis, since the majority of catheter-treated patients without infection also developed the lesion (Table 1). It appears that the time of catheter treatment was important in the development of the lesions. Those within one month, early lesions were found in approximately 50 per cent of the patients, in comparison with approximately 90 per cent from three months and onwards.

Polypoid cystitis is probably what the urologist recognizes as «catheter cystitis». At cystoscopy, almost all urologists find no difficulty in distinguishing it from a bladder tumour. This explains why the lesion is rarely biopsied and therefore not histologically well recognized. Histologically, it would not seem possible to differentiate a biopsy taken from a lesion in Fig 1 from an ordinary papilloma. The importance of polypoid cystitis from a clinical point of view is difficult to evaluate and needs further investigation. Polypoid cystitis may act as a *locus minoris resistentiae* and be of importance in recurrences of urinary tract infection. Long-standing lesions seem to be organized, fibrotic and probably irreversible and may influence the function of the bladder. The histological appearance of early lesions, particularly when oedema is dominating, would suggest that they are reversible.

We thank Dr Per Arvidqvist, Geriatric clinic I, Väasa hospital, for encouragement to perform the present study. We also thank Miss Karin Karlsson and Miss Yvonne Malmfors for skilful technical assistance.

REFERENCES

1. Friedman N B & Ish J E. Tumors of the urinary bladder. AFIP Sect VI and VIII. Fascicle 31. Washington 1959.
2. Kerr L G. Tumors of the urinary bladder. AFIP Second series. Fascicle 11. Washington 1975.

EFFECTS OF CYCLOPHOSPHAMIDE ON OPEN, GRANULATING SKIN WOUNDS IN RATS

HENRIK WIE INGOLV BRUASET and THOMAS ECKERSBERG

Department of Pathology Dental Faculty and Institute for Surgical Research Rikshospitalet University of Oslo Norway

Wie H Bruaset I & Eckersberg Th Effects of cyclophosphamide on open granulating skin wounds in rats Acta path microbiol scand Sect A 87 185-192 1979

The effect of cyclophosphamide on the healing of open cutaneous wounds was studied in rats. Following intraperitoneal injections of 25 mg/kg body weight every second day for 9 days only about 7% of the wounds were completely covered by epithelium after 15 days whereas in the control animals 60% of the wounds were completely epithelialized. Measurements of wound diameters in circular skin wounds revealed unhealed wound areas in the drug-treated animals which were significantly larger than those of the control animals. Cyclophosphamide was found to reduce the occurrence of H^3 -labelled cells in the granulation tissue when evaluated after 11 days. At 15 days there was no difference in the labelling frequency between treated and control animals indicating reversal of the drug effect.

Key words: Autoradiography, cyclophosphamide, rats, skin wound healing.

Henrik Wie Dental Faculty University of Oslo Gentmyrsvei 71 Oslo 4 Norway

Accepted as submitted 20 x 78

Cyclophosphamide has a detrimental effect on cells at a high mitotic rate when administered in therapeutic and toxic doses. The effect is dose dependent (Hill 1975) and is most clearly observed in growing tumours in the intestinal mucosa (Calabresi & Parks 1975) in the matrix cells of the hair follicles of the scalp in man (Lee *et al* 1973) and in the hemopoietic system (Host 1966, Valeriote *et al* 1968, Lee *et al* 1973).

Proliferation and differentiation of cells are prominent features in wound healing and a retarding effect of the drug on these processes could be expected. There is however no general agreement in the literature as to the effect of cyclophosphamide on the healing of surgical wounds. Lentini *et al* (1956), Host & Nissen (1960), Staley *et al* (1962), Mutti & Dede (1966) and Calnan &

(1970) and Cohen *et al* (1975) reported a retardation of the healing of surgical wounds. In the present study the effects of cyclophosphamide on the healing of open granulating skin wounds were studied in order to further elucidate this problem.

MATERIALS AND METHODS

Forty-eight-day-old male Wistar/AF/Han/Mol SPF rats were used. Two brother animals were kept in each cage, one randomly selected for drug treatment, the litter mate for control and given standard animal pellets (B1 or 3155 Molleventralen I/S Oslo) and water *ad libitum*. The animals were weighed every second day throughout the experimental period. Mean initial weight was 194 ± 14 g.

of the
ho on pull mg instrument having a diameter of 8 mm. A thin spray of sulphathiazol powder and a covering film of Nobecutan® (Bofors) were applied to the fresh wounds.

Cyclophosphamide (Sendovan® Pharmacia Uppsala Sweden) was dissolved in sterile water and 25 mg/kg body weight were injected intraperitoneally every second day for 9 days the first injection given when inflicting the wound. This dose was found convenient after preliminary studies. Control animals received corresponding injections of isotonic vehicle.

The animals were killed by a blow on the head or by exsanguination. The wound with adjacent part of the dorsum and tail was excised and fixed in a 4% formaldehyde solution. After fixation a 2 mm transverse piece of tissue comprising the broadest part of the wound was removed, prepared and embedded. Five μ m thick sections were cut and stained using the Harris hematoxylin/eosin and Goldner Masson staining techniques. The diameter of the non epithelialized part of the wound was examined and measured in a Leitz microscope provided with a graded screen. The total magnification was calculated by means of an object micrometer.

In 48 rats (24 treated and 24 controls) the wounds were examined after 11 days. The transverse diameter of the non epithelialized part of the wounds was measured.

In 30 rats (15 treated and 15 controls) the wounds were examined after 15 days of healing. The criterion for healing was full epithelial covering of the wound bed (yes/no).

In 18 rats (8 treated, 8 controls and 2 control of background emission) autoradiographic studies were performed and the wounds were examined 11 and 15 days after infliction. H^3 thymidine (spec. activity 5 Ci/mM and radioactive concentration 1.0 mCi/ml) 1.0 μ Ci/g body weight was injected intraperitoneally 60 minutes prior to sacrifice (Skougaard 1965). After sacrifice the wounds with surroundings were removed and fixed in Lavdowsky's fixative. Slides were prepared for autoradiography using the dipping technique (Kodak Nuclear Track Emulsion NTB 2) (Gilhuus-Moe 1969). After exposure the slides were developed and stained with Harris hematoxylin. Counting of labelled cells was performed in the granulation tissue according to the method described by Hick & Paumgarner (1967) and modified for the present study. Labelled cells were counted in 20 view fields per animal using the following procedure: between the granulation tissue and the adjacent differentiated connective tissue of full thickness skin wounds an easily discernible border line is visible in the microscope. This border line was used as starting point and the counting was performed just below the epithelial coverage and proceeded at right angles to the border line always from left to right.

Twenty germ free rats (10 treated and 10 controls) were included in the study in order to rule out the possibility that wound infection might influence the interpretation of the results. Germ free rats (Wistar/AF/Han, Zentralinstitut für Versuchstierzucht, Hannover, Linden) with mean initial weight 236 ± 15 g were kept in commercially available plastic cages according to standard procedures (Snyder Lab, Division of Snyder Manufacturing Company Inc., Philadelphia, Ohio). The air to the cages was filtered and materials taken into the

cages were sterilized by autoclaving. Absence of germs was controlled by weekly incubations of faeces etc. at room temperature and at 36°C using blood agar, agar agar, Sabouraud medium and thioglycolate medium. No growth of germs could be detected during the experimental period. The rats were fed Norwegian standard diet for rats with vitamins and water *ad libitum*. The wounds were examined after 11 days and preparation of microscopic specimens and autoradiographic techniques were similar to those described above.

Statistical Analysis

Means and standard deviations were calculated and significant differences were estimated by the Wilcoxon two sample test. Differences were considered significant if $p \leq 0.05$ (Diem & Lentner 1975).

RESULTS

A distinct retardation of growth was found in all animals receiving cyclophosphamide when compared to controls. The mean increase of body weight in the treated animals was 13.90 ± 11.5 g and in the placebo animals 32.75 ± 7.9 g during 11 days ($p < 0.005$). In animals observed for 15 days there seemed to occur an increase in the growth rate of the medicated animals from the 10th day. This increase which amounted to about 5 g above naive values coincided with the discontinuation of the cyclophosphamide treatment.

When full epithelial coverage of the wound bed was used as criterion for healing 7% of the treated wounds and 60% of the control wounds were healed after 15 days.

Measurements of wound diameters after 11 days (Fig. 1) showed a mean value of 2.0 ± 0.82 mm in the treated animals and 1.1 ± 0.94 mm in control animals ($p < 0.027$). The wound measurements in control animals constitute two separate groups (Fig. 1): one with wound diameters between 0 and 0.8 mm and the other with diameters between 1.3 and 3.2 mm. In the latter group 4 control animals had diameters exceeding those of their treated counterparts. A slight inflammatory reaction was seen in the wounds belonging to this group of control animals.

Apart from these few cases the wounds in the control group healed without complications. The scab persisted in some of the wounds while in others it was lost at the time the animal was killed. In most cases the persistence of the scab coincided with the occurrence of larger wound diameters and signs of inflammatory reactions in the wounds.

Healing occurred at a slightly slower rate in the test animals than in the control animals. This was evidenced by a more frequent persistence of the scab, a larger scab and a broader non-epithelialized

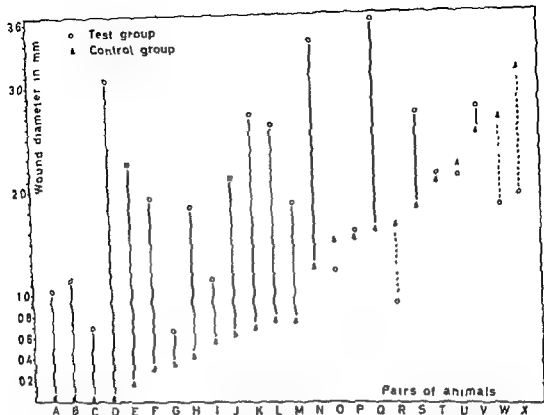


Fig 1 Wound diameters in circular skin wounds arranged according to measurements in the control animals. Observation period 11 days. Cyclophosphamide dosage 25 mg/kg given every second day and discontinued on day 9. Vertical lines connect treated and non treated brothers. Significant difference $p < 0.027$.



Fig 2
and of
Cycloph

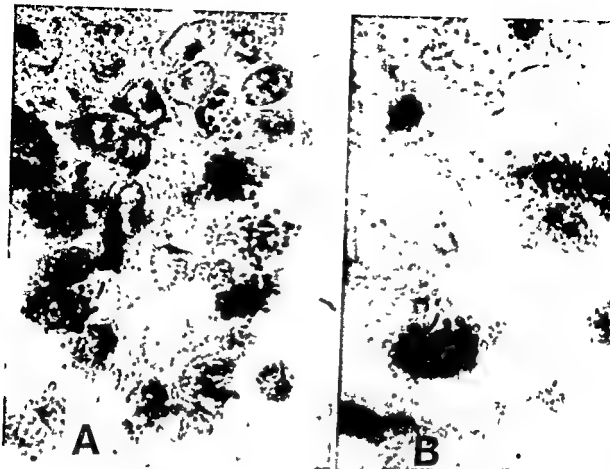
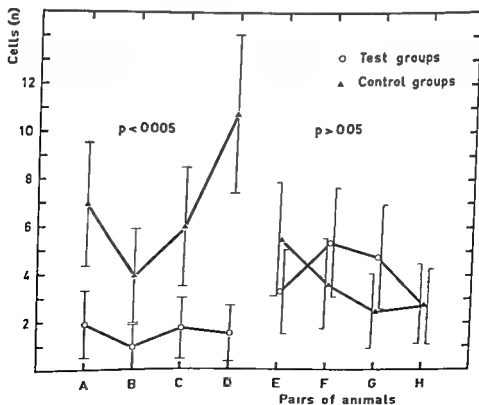


Fig 7 Photomicrographs showing H^3 labelled cells in epithelial hyperplasia of the wound margin (A) and in the granulation tissue (B) in a cyclophosphamide treated animal observation period 11 days. Note heavy labelling of basal epithelial cells and the sparsely labelled granulation tissue. Hematoxylin ($\times 2975$ oil immersion)



wound area. In a large number of wounds in the treated group the epidermis showed hyperplastic reactions at the wound margins. This was also seen in the control wounds but to a much lesser degree (Fig 2).

Autoradiographic observations

Microscopic examination showed intense labelling of the epithelial cells in the hyperplastic downgrowths and rete pegs of the epidermis (Fig 3A). As the cell proliferation of the epithelium however is confined to the basal layers and the epithelial offshoots are irregular in size and shape counting of labelled cells was performed only in the granulation tissue. The occurrence of labelled cells (Fig 3B) seemed to be greater in the periphery of the wound than towards the central part. This tendency was not always present and the material is too small to provide any definite conclusions.

The mean labelled cell count of the treated and control animals after 11 days was 1.5 and 6.9 respectively ($p < 0.005$) which indicates a distinct retarding effect from the drug on the proliferating cell populations of the granulation tissue (Fig 4). After 15 days the mean labelled cell count of the treated animals was 4.06 whereas in the control rats there was a mean of 3.6 labelled cells per view field ($p > 0.05$).

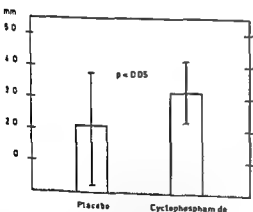


Fig 1. Germ free rat. Histograms of the wound diameter in treated and control animals. Dose of cyclophosphamide 5 mg/kg injected intraperitoneally every second day for 9 days. Control animals were given saline injections. Observation period 11 days.

Fig 4. H³-labelled cells 15 days after wounding. Control animals were given

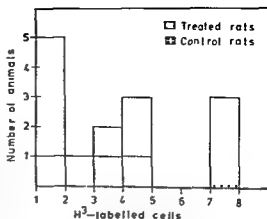


Fig 6. Germ free rats. Frequency histograms of the number of H³-labelled cells per view field in the granulation tissue. Cyclophosphamide dose 25 mg/kg injected intraperitoneally every second day for 9 days. Control animals were given saline injections. Observation period 11 days. Significant difference $p < 0.05$.

Germ free Animals

One control animal was obviously ill and two treated animals died during the experiments. These animals were excluded from the study.

The mean weight increase of the treated animals was 4.6 ± 11.3 g and the corresponding value in the control group was 0.6 ± 11.5 g, i.e. no significant difference in the weight changes of the two groups.

The average wound diameter (Fig 5) in the cyclophosphamide animals 3.19 ± 0.96 mm was found to be significantly larger ($p < 0.05$) than that of the placebo rats (2.01 ± 1.78 mm).

The mean count of H³-labelled cells in the granulation tissue of the cyclophosphamide and placebo animals was calculated to be 2.2 ± 1.1 and 4.9 ± 7.3 per view field respectively ($p < 0.05$) (Fig 6).

DISCUSSION

The results of the present study have revealed that cyclophosphamide in the employed dose schedule has a retarding effect on the contraction and epithelial covering of granulating skin wounds and on the proliferating cell populations in wound granulation tissue. The results from the experiment

days. Control animals were given

with germ-free animals indicate that this retardation is caused by the drug and not by an initial infection.

It was expected that 25 mg/kg given every second day for 9 days though being a high and intense dose schedule, would be well tolerated by the animals. Based on white blood cell counts after various doses of the drug in rats, the present dose schedule is assumed to be within therapeutic range in man.

Using daily doses of 15 and 25 mg/kg for 11 days De Prcz & Liehn (1960) found that wound tensile strength was diminished and there was a slight delay in the «take» of skin autografts. In open wounds fibroplasia was retarded. These findings are in accordance with the results of the present study. Also the findings of Hoppe (1962) are in agreement with the present results as regards the formation of granulation tissue and retarded wound contraction. Similar observations were made by Mangione & Taverna (1964) on osseous callus formation and by Romatowski & Lubicki (1967) on the healing of wounds in cancer-inoculated mice, and by Karpinen & Mälarinen (1970) and Cohen *et al.* (1975) in incisional wounds in rats. On the other hand Bocckl & Karrer (1963) after single doses of 20 and 80 mg/kg of cyclophosphamide in rats, Calnan & Davies (1965) after daily doses of 7.5 mg/kg in rats, Mutti & Dede (1966) after daily doses of 10 and 15 mg/kg in rabbits found no significant delay of wound healing. From studies in man reports are also conflicting as to what extent cyclophosphamide produces a deleterious effect on the healing of wounds. Host & Nissen Meyer (1960) and Lentini *et al.* (1967) found no delay as evaluated by clinical criteria while Haas (1962) reported an increase in the prevalence of fistulae from the hypopharynx after cancer surgery in cyclophosphamide treated patients. Differences in the dosage and in the general condition of the patients caused by the tumour may explain these discrepancies.

All treated animals except the germ free group showed significantly lower weight increases than corresponding controls. This observation poses the question as to what extent starvation and retarded growth may be detrimental to the healing process. Howes *et al.* (1933) reported that caloric restrictions over a short time period did not appreciably affect the healing response in adult rats whereas Stahl (1965) found delayed healing in rats fed a low protein diet. Cohen *et al.* (1975) found that wound healing proceeded normally in mice with negative nitrogen balance following terminal stage of cancer disease.

The autoradiographic observations have revealed marked differences between treated and untreated animals. On the basis of these results some features

pertaining to the mechanism of action of cyclophosphamide are evident when comparing the autoradiographic data with those of the wound measurements and the histologic examinations.

- 1) In the 11-day series reduced mitotic rate in the granulation tissue coincided with a low rate of healing.
- 2) In the 11-day series reduced mitotic rate in the granulation tissue coincided with a higher frequency of epithelial hyperplasias in the wound margins.
- 3) In the 15-day series there was no difference in the labelling frequency of the granulation tissue between test animals and control animals.

The proliferation of granulation tissue cells is reduced under the influence of cyclophosphamide as shown from autoradiographic observations. The explanation of a concomitant occurrence of epithelial hyperplasia in the wound margins, retardation of epithelial covering of the wound surface and the reduction of connective tissue constituents is obscure.

Removal of epithelial continuity may act as a stimulant to epithelial growth (e.g. disturbances of chalone equilibrium Iversen & Bjerknes 1963). For the normal migration and differentiation of the epithelial cells an interaction is supposed to be necessary between the new connective tissue and epidermis (Tarin & Croft 1970). One suggestion might therefore be that under the influence of drugs that inhibit the formation of proper granulation tissue this interaction is faulty resulting in a reduced migratory rate.

The effect might also concern the contractile process of the healing wound. It is possible that the drug by inhibiting the proliferation of the connective tissue cells will reduce the speed of wound contraction (Abercrombie *et al.* 1961). Another and perhaps additional explanation may be the influence of a continuous medication of cyclophosphamide on the stem cell populations of the polymorphonuclear leukocytes. It has been shown by Vizard *et al.* (1964) that the migration of epidermis follows a band of polymorphonuclear leukocytes on the wound surface. The continuous leukopenia induced by the long term medication of the drug may reduce this band to such a degree that migration is inhibited (Vizard *et al.* 1964).

The observation of a higher degree of epithelial hyperplasias in the wound margin in the treated animals as compared to controls may be explained as an inductive effect from cyclophosphamide on the epithelial cells as has been observed in the bladder epithelium (Koss 1967). Another reasonable hypothesis however is that the hyperplasias are merely indications of a greater immaturity of the

wounds in the treated groups than in the control animals as a manifestation of the retardation of the wound healing process (Ordman & Gilman 1966)

In the present investigation most of the standard wounds in the control animals were completely epithelialized 15 days after wounding. At this time the proliferation rate in the granulation tissue of the treated animals was not different from that of controls animals. The counting values after 11 days gave a ratio between treated and control animals of 0.22 which means marked influence from the drug. A comparison between treated and untreated animals at 11 and 15 days thus strongly indicates a reversal of the mitotic inhibition of cyclophosphamide.

The study was supported by the Norwegian Research Council for Science and Humanities and Norwegian Society for Fighting Cancer.

REFERENCES

- Abercrombie M, James D W & Hencombe J F. The role of contraction in the repair of excised wounds of skin. In: Wound healing. Proceedings of a symposium held on 12-13 Nov. 1959 at the Royal College of Surgeons of England. Ed by H Strome. Pergamon Press, Oxford 1961, pp 10-25.
- Boeckl O & Kurrer A. Gefährden Cytostatika abdominale Eingriffe. Wchen klin Wschr 75: 37-40 1963.
- Calabresi P & Purks R E Jr. Cytotoxic drugs, hormones and radioactive isotopes. In: The pharmacological basis of therapeutics. Ed by L S Goodman & A Gilman. Macmillan Co., New York 1975, pp 1262-1264.
- Calman J & Davies A. The effect of methotrexate (amethopterin) on wound healing. An experimental study. Brit J Cancer 19: 505-512 1965.
- Cohen S C, Gatznick H L, Johnson R A & Guldin A. Effects of cyclophosphamide and adriamycin on the healing of surgical wounds in mice. Cancer 36: 1277-1281 1975.
- DePre J D & Auer L. The effect of cytosine (cyclophosphamide) on wound healing. Plast reconstr Surg 36: 301-308 1960.
- Dim A & Lentner C (eds). Documenta Geigy. Scientific tables. 7th ed. Ciba-Geigy Ltd, Basel 1975, p 810.
- Gilhaus M O. Fractures of the mandibular condyle in the growth period. Thesis. Universitetsforlaget, Oslo 1969, pp 180-183.
- Huys E. Möglichkeiten und Grenzen der Chemotherapie maligner Tumoren aus hals-nasen-ohrenärztlichen Sicht. HNO (Berl) 10: 129-136 1962.
- Hill D L. A review of cyclophosphamide. Charles C. Thomas Publisher, Springfield, Illinois, U.S.A. 1975, pp 172-189.
- Hoppe J. Der Einfluss verschiedener cytostatischer Substanzen auf die Granulationsgewebsbildung experimentell gesetzter Wunden. Verh dtsh Ges inn Med 68: 259-262 1962.
- Howes E L, Briggs H, Shea R & Harvey S C. Effect of complete and partial starvation on the rate of fibroplasia in the healing wound. Arch Surg 27: 846-858 1933.
- Hest H. Comparative effects of cyclophosphamide, nitrogen mustard and total body irradiation on survival and on white blood cells in rats. Radiat Res 37: 638-651 1966.
- Hest H & Hissen Meyer R. A preliminary clinical study of cyclophosphamide. Cancer Chemother Rep 9: 47-50 1960.
- Iversen O H & Bjerknes R. Kinetics of epidermal reaction to carcinogens. Universitetsforlaget, Oslo 1963.
- Karppinen V & Mälariniemi H. Vascular reactions in healing laparotomy wound under cytosol treatment. Acta Chir Scand 136: 675-680 1970.
- Koss G. A light and electron microscopic study of the effects of a single dose of cyclophosphamide on various organs in the rat. I. The urinary bladder. Lab Invest 16: 44-65 1967.
- Lee Cheng Chun, Castles Th R & Kintner Loren D. Single-dose toxicity of cyclophosphamide (NSC 262 711) in dogs and monkeys. Cancer Chemother Rep Part 3: 4: 51-76 1973.
- Lentin M, Nambiar R & Brennan T G. Arterial perfusion of the breast with cytotoxic drugs. Brit J Surg 54: 519-521 1967.
- Mangiame F & Taverna L. Influenza di alcuni farmaci antiblastici alcuni effetti antimetaboliti sul processo di riparazione dei focolai di frattura (Ricerche sperimentali). Boll Soc ital Biol sper 40: 1711-1712 1964.
- Muth P & Dedo A. Influenza del trattamento con
- Ordman L J & Gilman T. Studies in the healing of cutaneous wounds. I. The healing of incisions through the skin of pigs. Arch Surg 93: 857-882 1966.
- Romatonowski M & Kubicki B. Effect of cytostatic drugs and hydrocortisone on healing of surgical wounds in mice inoculated with Ehrlich's cancer. Pol Tyg lek 22: 1971-1973 1967.
- Slauguard U R. Cell population kinetics of the gingival epithelium. Thesis. Rhodos Cph 1965, pp 15-23, 50-52.
- Stahl S S. The healing of experimentally induced gingival wounds in rats on prolonged nutritional deprivations. J Periodont 36: 283-287 1965.
- Staley Ch J, Kukral J C & Preston R B. Effect of antineoplastic drugs on experimental wound healing. Surg Forum 13: 35-36 1962.
- Tarun D & Crifi C B. Ultrastructural studies of wound healing in mouse skin. II. Dermoepidermal interrelationships. J Anat (Lond) 106: 79-91 1970.

- 28 Valeriote, F A Collings, D C & Bruce, W P
Hematological recovering in the mouse following
single doses of gamma radiation and cyclophospha-
mide Rad Res 33 501-511, 1968
- 29 Vitziam C B Matoltss, A G & Mescon H
Epithelialization of small wounds J invest Derm
43 499-507 1964
- 30 Wick, G & Paumgariner, G Autoradiographische
Untersuchungen am reparativen Granulations-
gewebe lathyritischer Ratten Med Pharmacol exp
16 561-566, 1967

MECHANICAL PROPERTIES AND HYDROXYPROLINE CONTENT OF CONNECTIVE TISSUE IN POROUS CERAMIC IMPLANTS

HENRIK WIE and EVA I BECK

Institute for Surgical Research Rikshospitalet University of Oslo Norway

Wie Henrik and Beck Eva I Mechanical properties and hydroxyproline content of connective tissue in porous ceramic implants Acta path microbiol scand Sect A 87 193-200 1979

The present study describes a model applying ceramic implants (Al₂O₃) for *in vivo* studies of connective tissue regeneration Two types of implants have been developed a one piece model for histological examination and chemical analyses and a two piece implant which can also be used for mechanical testing of connective tissue When these were implanted subcutaneously on the back of rats a correlation was found between the mechanical strength and the hydroxyproline content of connective tissue in the implants The peak synthesis occurred between the 7th and the 14th day after implantation and a plateau was reached for both strength increases and hydroxyproline formation between the 14th and the 21st days For histological examination the implants were embedded in plastic materials and prepared as hard tissue specimens The model presented can be applied to study connective tissue regeneration in normal and pathological conditions including studies of the effects of various drugs on connective tissue

Key words Ceramic implants hydroxyproline mechanical properties regeneration

Henrik Wie Dental Faculty University of Oslo Geitmyrsvn 71 Oslo 4 Norway

Received 20 x 78 Accepted 6 xii 78

Tissue ingrowth into implanted materials has been used to study wound healing and regeneration on a molecular level Alloplastic materials such as wire mesh cylinders silicate powder synthetic sponges carrageenine gauze cotton wool and viscose cellulose sponges have been used (Viljanto 1964) A method for measuring the mechanical strength of the new connective tissue bridging the gap between two connected cellulose implants in order to correlate mechanical properties directly to the collagen content was introduced by Viljanto (1964) Common to all these methods is a rich production of granulation tissue available for histological examination and chemical analysis Most previous methods have however been suffering from the disadvantage that connective tissue formation has been followed by resorptive processes The tissue reaction in and around the implants has been essentially a foreign body reaction often accompanied by abscess formation

and necrosis The connective tissue produced in these implants may therefore be qualitatively and quantitatively different from that found in a clean surgical wound

During recent years a porous ceramic material (Al₂O₃) has been introduced in orthopedic and dental surgical research as a means of attaching prosthetic devices directly to the skeletal system by ingrowth of connective tissue and bone (Hulbert *et al* 1970 1972 Lyng *et al* 1973 Pedersen *et al* 1974) This material has been shown by several authors to be highly inert when implanted into muscle or bone tissue of mammals (Hulbert *et al* 1972 Homsy *et al* 1973) The physical properties have been studied by Lemons & Richardson (1975) who found a completely interconnected major pore network with pore diameters above 75 µm

The aim of the present study has been to evaluate an inert ceramic material (Al₂O₃) as a model for studies of connective tissue regeneration The early ingrowth into these inert implants has been

evaluated by determining the mechanical strength and the hydroxyproline content in the implant connective tissue at various time intervals after implantation

MATERIALS AND METHODS

Implant Material

Ceramic implants were supplied by the Central Institute of Industrial Research Oslo Norway Manufacturing procedure and chemical composition were as described by Lyng et al (1973)

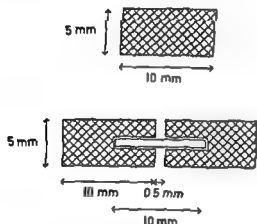


Fig 1 The implant model Schematic drawing of a longitudinal section through a one piece (A) and a two piece (B) ceramic implant

Cylindrical pieces for implantation were drilled out of the fired material with a diamond core bur to a diameter of 5 mm and cut to 10 mm length with a diamond saw. This type of implant is intended for biochemical analyses (Fig 1A)

In order to obtain collagen fibres comparable to the new connective tissue bridging the gap of an incised wound a rod shaped space keeper made from non porous ceramic material with identical composition was placed in a drilled axial blind channel in the implant pieces. Two implants were connected end to end by the rod keeping them at a constant distance of 0.5 mm (Fig 1B). This type is intended both for chemical analyses and for mechanical testing.

Cleaning and sterilizing procedure before implantation were in accordance with the technique used by Hulbert et al (1972). Weighing was performed on a Mettler analytical balance (E Mettler Zurich Switzerland) with a reading accuracy of 0.1 mg.

The porous ceramic material had a pore volume of 40%, a compressive strength of 300 kp/cm² and a channel diameter of 100–750 µm. The mean dry weight of the one piece implants was 0.458 ± 0.024 g.

Animals

Seventy seven male outbred Wistar/Al/Han/Mol SPF rats aged 48 days and weighing 180–190 g at the start of the experiments were used. The animals were kept single in stainless steel wiremesh cages and housed in rooms with automatic regulation of light (17 h light, and 12 h dark), temperature (22–23°C) and relative humidity (55%). The rats were given standard animal pellets (B1 nr 3155 Molesentralen I/S Oslo) and water *ad libitum*. For the experiments the animals were randomly divided into groups of seven rats.

Surgical Procedure

After intramuscular anesthesia (Hypnorm® Mekes) the backs of the animals were shaved and cleaned with 0.5% chlorhexidine gluconate in 70% ethyl alcohol. The implantation was performed using a standardized procedure.

- A A transversal skin fold was raised with two surgical tweezers and the incision made between them in a caudal direction from between the scapulae of the animals. Thus a 6 cm longitudinal midline incision including the cutis and the subcutaneous muscle was obtained. Maintaining strictly sterile surgical conditions a pouch was prepared with artery forceps on one or both sides of the median line and the implants were inserted after being submerged in sterile saline. The wounds were closed.
- B

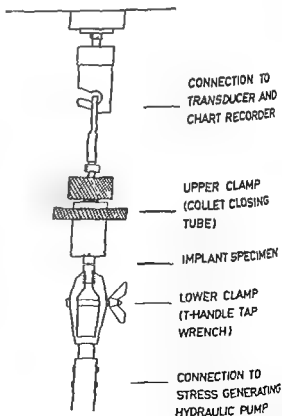


Fig 2 The two piece implant model with rod mounted in special clamps for mechanical testing of connective tissue

with 6 interrupted sutures of 3-0 black braided silk and left undressed.

The animals were killed by a blow on the head and cervical dislocation.

Mechanical Measurements

Ceramic implants were collected from the animals by carefully dissecting the implants free from the connective tissue capsule so that only tissue from inside the pores and in the space between the two joined implants was tested.

The tensile strength measurements of connective tissue between double implants were performed immediately after removal from the animals. One end of the implants was mounted in a specially designed circular clamp at the immobile part of a standard electrohydraulic tensile strength tester (Type 7-1/1 A/B Lorentz & Weir, Stockholm, Sweden). The other end was connected to the mobile part by means of a screw clamp (Fig. 2). The tensile strength tester was run at a constant strain rate (5 mm/min) and the load values were transferred by a transducer to a Riken Denshi chart recorder (Riken Denshi Co. Ltd Tokyo, Japan Model SP 5 B).

Biochemical Analysis

After stretching the implants were placed in acetone for dehydration and defatting or they were stored frozen (-70°C) until subjected to chemical analysis.

The implants were extracted in acetone for one week with daily changes of acetone and then dried in an oven at 35°C . After drying excess tissue adhering to the implants was easily scraped off before weighing to constant weight. The dry weight of the new connective tissue inside the implants was calculated as the difference between the net weight of the ceramic implants before insertion and the dry weight of the specimens after defatting.

After crushing the implants to a suitable crushing degree was attained.

The ground specimens were placed in ampules for hydrolysis. To each ampule was added 4 ml 6N HCl. The ampules were sealed and autoclaved at 125°C for 18 hours. After cooling at room temperature the hydrolysate was filtered through a fritted glass disk and transferred to analysis vials for analysis of total hydroxyproline using the direct acid method of Firschein (1969).

The extractability of collagen by 6 N HCl on uncrushed ceramic implants was tested in a series of seven 10-day-old implants. Conditions for hydrolysis and determination of total hydroxyproline were similar to those for the crushed material.

Samples for solubility fractionation were homogenized in a tissue grinder with 4 ml 0.5 M NaCl. The homogenate was centrifuged at 4°C for 10 min and the supernatants obtained were pooled and called the salt-soluble fraction.

The precipitate was homogenized in 8 ml cold 0.5 M citric acid buffer (pH 3.6) extracted, centrifuged and washed with the buffer solution. The pooled supernatants obtained were called the acid-soluble fraction. The remaining precipitate was called the insoluble fraction.

The fractions were then hydrolysed in 10 ml 6 N HCl by autoclaving at 125°C for 4 hours and subjected to analyses for total hydroxyproline using the method of Firschein (1969).

Histological Procedures

Implant specimens for histological examination were fixed in 10% formalin, embedded in methyl methacrylate (Conkie 1965) and cut in a Gilling machine in sections of approximately 150 μm . The sections were then ground down to a thickness of about 80 μm and stained with Paragon 1301 (Paragon PS 1301, Paragon C & Co Inc, Bronx, NY, USA).

Statistical Analysis

Median with 25 and 75 fractiles was used to express the average and dispersion of the measured values. Statistical significance was calculated using the Wilcoxon two sample test and differences were considered significant if $p \leq 0.05$ (Diem & Lentner 1975).

RESULTS

Mechanical Properties of Connective Tissue in Ceramic Implants

The tensile strength of the tissue bridging the gap of the two piece implants was measured on the 3rd, 7th, 14th and 21st days. The strength of the implant tissue increased almost linearly with time up to 14 days after implantation (Fig. 3). Thereafter the slope of the curve levelled off.

Total Hydroxyproline Content per Two Piece Ceramic Implant and per mg Dry Weight

As illustrated in Fig. 4 and Fig. 5 there was a rapid increase of hydroxyproline content of the implants from the 3rd to the 14th day ($p < 0.05$). Between the 14th and the 21st days no further increases were observed ($p > 0.05$).

Fractionation Studies

Solubility fractionation of connective tissue in the ceramic implants was done in order to test the feasibility of the method for fractionation techniques. Fractionation was performed on the 3rd, 5th, 7th, 10th, 14th and 21st days after implantation (Fig. 6).

The salt-soluble fraction showed a small increase from the 3rd to the 10th day. Between the 10th and the 21st days hydroxyproline levels were unaltered.

No significant changes were seen in the acid-soluble fraction before the 7th day. From the 7th day a significant increase was observed up to the

evaluated by determining the mechanical strength and the hydroxyproline content in the implant connective tissue at various time intervals after implantation

MATERIALS AND METHODS

Implant Material

Ceramic implants were supplied by the Central Institute of Industrial Research Oslo Norway Manufacturing procedure and chemical composition were as described by Lyng et al (1973)

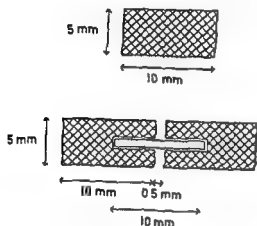


Fig 1 The implant model Schematic drawing of a longitudinal section through a one piece (A) and a two piece (B) ceramic implant

Cylindrical pieces for implantation were drilled out of the fired material with a diamond core bur to a diameter of 5 mm and cut to 10 mm length with a diamond saw. This type of implant is intended for biochemical analyses (Fig 1A)

In order to obtain collagen fibres comparable to the new connective tissue bridging the gap of an incised wound a rod shaped space keeper made from non porous ceramic material with identical composition was placed in a drilled axial blind channel in the implant pieces. Two implants were connected end to end by the rod keeping them at a constant distance of 0.5 mm (Fig 1B). This type is intended both for chemical analyses and for mechanical testing.

Cleaning and sterilizing procedure before implantation were in accordance with the technique used by Hulbert et al (1977). Weighing was performed on a Mettler analytical balance (E Mettler Zurich Switzerland) with a reading accuracy of 0.1 mg.

The porous ceramic material had a pore volume of 60% a compressive strength of 300 kp/cm² and a channel diameter of 100–750 μ m. The mean dry weight of the one piece implants was 1458 ± 0.024 g.

Animals

Seventy seven male outbred Wistar/Al/Han/M¹ SPF rats aged 48 days and weighing 180–190 g at the start of the experiments were used. The animals were kept single in stainless steel wiremesh cages and housed in rooms with automatic regulation of light (12 h light and 12 h dark) temperature (22–23°C) and relative humidity (55%). The rats were given standard animal pellets (B1 nr 3155 Møllecentralen I/S Oslo) and water *ad libitum*. For the experiments the animals were randomly divided into groups of seven rats.

Surgical Procedure

After intramuscular anesthesia (Hypnorm[®] Melv) the backs of the animals were shaved and cleaned with 0.5% chlorhexidine gluconate in 70% ethyl alcohol. The implantation was performed using a standardized procedure.

- A A transversal skin fold was raised with two surgical tweezers and the incision made between them in a caudal direction from between the scapulae of the animals. Thus a 6 cm longitudinal midline incision included the cutis and the subcutaneous muscle was obtained. Maintaining strictly sterile surgical conditions a pouch was prepared with artery forceps on one or both sides of the midline and the implants were inserted after being submerged in sterile saline. The wounds were closed.
- B

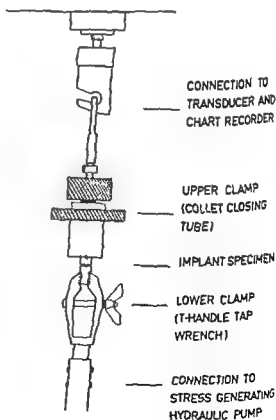


Fig 2 The two piece implant model with rod mounted in special clamps for mechanical testing of connective tissue

4th day ($p < 0.05$) whereas no significant increase as found between the 14th and the 21st day ($p > 0.05$)

The insoluble fraction reached $5.5 \mu\text{g}$ hydroxyproline per mg dry weight already on the 3rd day after implantation and a significant increase of this

fraction was found up to the 14th day. During the period from the 7th to the 14th day there was a doubling of the hydroxyproline content of the insoluble fraction ($p < 0.05$). Between the 14th and the 21st day there were no further increases of the insoluble fraction ($p > 0.05$)

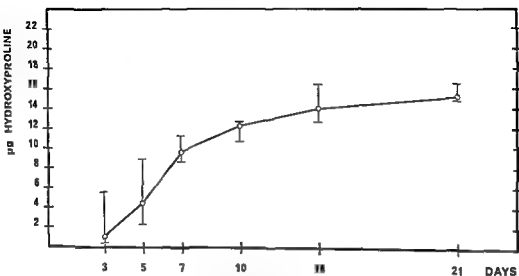


Fig 5 Hydroxyproline $\mu\text{g}/\text{mg}$ connective tissue dry weight in ceramic implants at various time intervals after implantation. Median values with 25 and 75 fractiles indicated

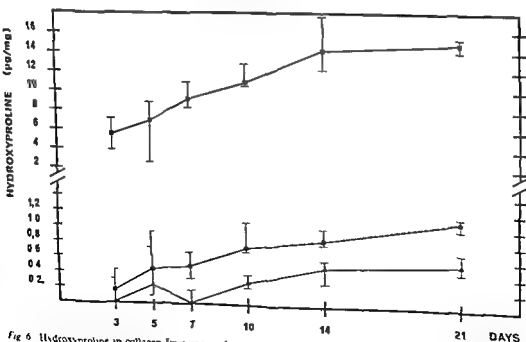


Fig 6 Hydroxyproline in collagen fractions $\mu\text{g}/\text{mg}$ dry weight of connective tissue in ceramic implants. Median values with 25 and 75 fractiles indicated. \circ — \circ 0.5 M NaCl soluble fraction \triangle — \triangle 0.5 M citric acid soluble fraction \square — \square 6 M HCl soluble fraction (insoluble)

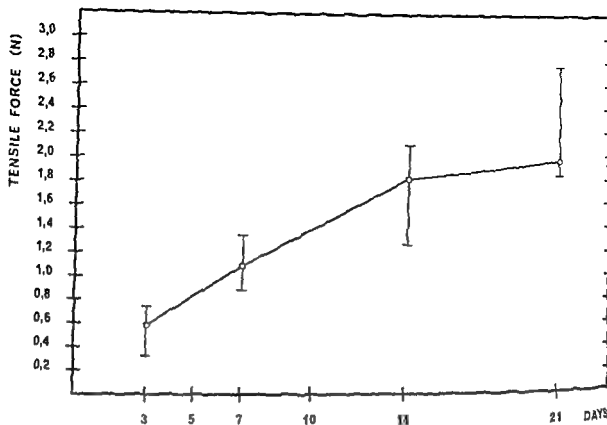


Fig 3 Tensile strength in newtons (N) of connective tissue in ceramic implants at various time intervals after implantation Median values with 25 and 75 fractiles indicated

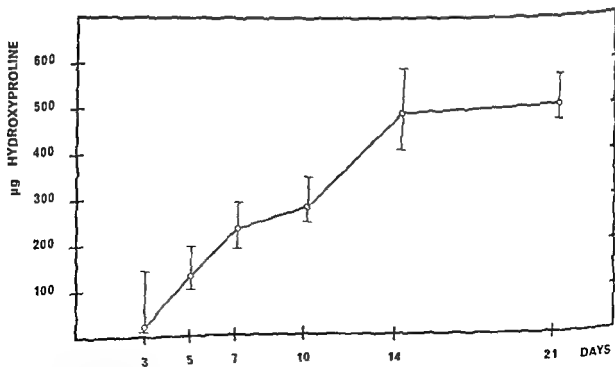


Fig 4 Total hydroxyproline per double ceramic implant after direct acid hydrolysis on crushed material in various time intervals after implantation Median values with 25 and 75 fractiles indicated

1974) The standard deviation of the mean weight of the implants was about 5%. This percentage reflects differences in the pore volume as the variation of the external dimensions of the implants was negligible. Salvatore *et al* (1961) investigated the influence of pore size on the extent of tissue ingrowth into polyurethane sponges and found the highest yield in the sponges with the smallest pore size. Nilles *et al* (1974) studied the influence of the density of a porous void metal composite (VMC) on tissue ingrowth after implantation in goat femora and found the best tissue penetration in the 30% dense material less in the 45% and least in the 75% material. The density of the present material is about 40% which approximates well to the porosity giving the better yield in the study of Nilles *et al* (1974).

Physical factors such as the elasticity of the implant material, the shape of the pores and the surface tension between the tissue fluid and the walls of the implant pores have been postulated to play a role in the formation of the new connective tissue. Surface tension decreasing agents did not however influence the speed of granulation tissue formation in cellulose sponges (Jantinen & Viljanto 1965).

The accuracy of the present tensile strength testing equipment has been studied on steel rods by Engesæter *et al* (1978) who found a standard deviation of about 1% indicating that rather accurate measurements can be performed. This deviation represents limitations of the load transducer, the amplifier, the chart recorder, the tensile testing machine and variations in the steel rods.

The direction of the stretching forces on the test specimen must be kept constant throughout the stretching procedure (Birk 1973). This has been secured by the central rod in the present model. The friction of the rod against the wall of the channel was found to be below the sensitivity of the transducer/chart recorder (i.e. 0.05 N). Therefore, without affecting the magnitude of the load necessary to rupture the collagen fibres, the rod keeps the implant specimen in the correct position relative to the main force direction.

The difference in the modulus of elasticity between the implant material and the collagen fibres may affect the testing of mechanical properties of connective tissue with the present model. This difference may influence the range of variation in the test results. A mean standard deviation as low as 8% was however obtained for maximum stress measurements.

In the present study the strength of the granulation tissue has been measured up to the 21st day after implantation. Viljanto (1964) tested the

strength of the sponge granulation tissue only up to the 12th day — which was the limit of his method owing to the mechanical properties of the sponge material. The present material with a compressive strength of 300 kp/cm² is able to withstand the testing of far stronger tissues.

It is evident from the present results that the increase in mechanical strength is lower during the period 14 to 21 days than in the preceding 7-day period. This observation seems to agree well with the peak of hydroxyproline synthesis in the ceramic implants which appears before the 14th day. This is in accordance with the findings of Jackson (1957) for carrageenin granuloma but contrary to the observations of Schilling *et al* (1969) who found a rapid linear increase of total hydroxyproline up to 4 weeks in the granulation tissue of wire mesh cylinders in dogs.

Previous reports as to the relative proportions of the collagen fractions at different time intervals during ingrowth into porous implants seem to differ slightly from the present results. Our data present an increase of the acid soluble fraction between the 7th and the 14th day after implantation whereas Viljanto (1964) failed to find any increase in this fraction. The salt soluble fraction seems to increase up to the 10th day while there is a rapid increase in the insoluble fraction up to the 14th day and a slower synthesis rate between the 14th and the 21st days. This is contrary to the observations of Viljanto (1964) who found significant increase of insoluble collagen up to 60 days. This discrepancy might be explained by differences in the compatibility of the implant materials. It has been suggested that non-inert materials will initiate and maintain a hyperplastic type of wound reaction (Conten *et al* 1967). This reaction will protract the normal regeneration and give a longer and greater productive phase than inert implant materials and clean surgical wounds. Studies pertaining to normal surgical wound healing should therefore be carried out on inert implant materials or on the wound itself.

REFERENCES

1. Bhaskar S N, Cutright D E, Knapp M J, Beasley J D, Pere B & Driskell T D. Tissue reaction to infrabony ceramic implants. *Oral Surg* 31: 282-289, 1971.
2. Conkle D. Plastic embedding in routine histology. *Acta Anat.* 60: 531-538, 1965.
3. Conten H, Straumann F & Paschke E. Grundlagen der Alloplastik mit Metallen und Kunststoffen. Georg Thieme Stuttgart 1967 pp. 125-147.
4. Dem K & Lentner C (eds). *Documenta Geigy*

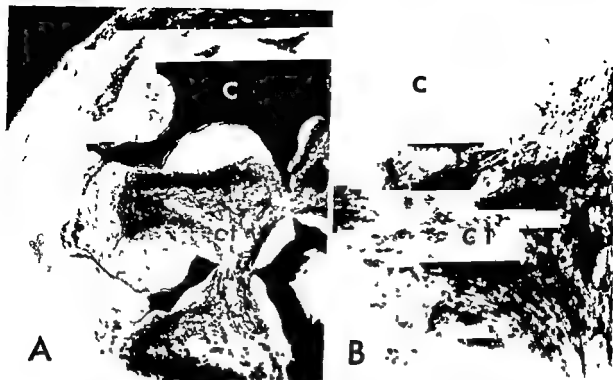


Fig 7 Tissue ingrowth (A) into the ceramic implant material ($\times 87$) Paragon stained ground sections B—higher magnification of connective tissue in the implant pores ($\times 220$) C = implant material Ct = connective tissue

All three fractions show almost parallel slopes of the curves indicating that their relative proportions are unaltered during the present observation period.

The direct acid method for determination of total hydroxyproline (Firschein 1969) did not give significantly different yields whether the material was assayed directly after the ceramics were crushed or after the material was homogenized and fractionated.

Extraction by 6 M HCl without crushing the implants yielded about 94% of the total hydroxyproline in the implants when compared with values obtained after crushing the ceramic material.

Histological studies

A preliminary histological study was included in order to evaluate tissue penetration and foreign body reaction in the implants. The ingrowth of connective tissue appeared most pronounced along the periphery of the implants at the earliest observation periods. After 14 and 21 days the fibrous tissue gradually reached the deeper parts of the implants. No foreign body giant cells were seen (Fig 7).

DISCUSSION

The present paper introduces an inert ceramic material Al_2O_3 as a model for studying regeneration of connective tissue. The model provides a

simple method for testing both mechanical properties and chemical composition of the tissue formed in the pores of the implanted material.

Most implantation models proposed for studying regeneration and wound healing in connective tissue are made from resorbable materials. Such materials will probably initiate a chronic inflammation and a foreign body reaction in the tissues penetrating the model (Björkman 1964). These adverse reactions may be caused by impurities in the model material or by degradation products released during resorption of the implant material (Homsy *et al* 1973).

The porous alumina material used in the present study has been found to be well tolerated by various living tissues (Bhaskar *et al* 1971, Hulbert *et al* 1972, Ling *et al* 1973). No foreign body reaction has been observed (Bhaskar *et al* 1971, Pedersen *et al* 1974). Schachtschabel & Blencke (1976) investigated the effect of pulverized glass-ceramic on the DNA and protein synthesis in monolayer cultures of human fibroblasts and found that these parameters were unaffected while pulverized plastic materials significantly retarded the production of

Varying pore size is probably the greatest source of error in quantitative essays with the present model. Both mechanical properties and the extent of tissue ingrowth will be affected by the pore size and the density of the implant material (Nilles *et al*

SURFACE ULTRASTRUCTURE OF HUMAN ARTERIES WITH SPECIAL REFERENCE TO THE EFFECTS OF SMOKING

A BYLÖCK, G BONDJERS, I JANSSON and H A HANSSON

Departments of Medicine Gynaecology and Histology University of Göteborg Göteborg Sweden

Bylöck A Bondjers G Jansson I & Hansson H A Surface ultrastructure of human arteries with special reference to the effects of smoking. Acta path microbiol scand Sect A 87 201-209 1979

The surface ultrastructure of uterine arteries from 20 women was studied with scanning electron microscopy. Specimens were excised and fixed under pressure shortly after removal of the uterus during hysterectomy. Two groups of patients were selected: non smokers and women who smoked more than 15 cigarettes a day. The prevalence of seven different morphological criteria was evaluated without knowledge of the smoking habits of the patients. Endothelial cells were usually well demarcated and distributed with their length axis parallel to that of the artery. The cell nucleus was revealed by a gentle bulging into the lumen and cell borders by the presence of rows of microvilli. Inter- and intracellular holes along the cell borders were more common in arteries from smokers whereas microvilli were more common on the cell surfaces of arteries from non smokers. These differences might be related to cell injury. Previous studies indicate that holes are more frequent in injured than in non injured cells whereas the surface of injured cells is often smoother than that of non injured cells. Therefore these data may be taken to suggest that smoking can lead to endothelial injury in man.

Key words: Arteries, human, ultrastructure, smoking.

Anders Bylöck, Department of Histology, University of Göteborg, Fack S 400 33 Göteborg 33, Sweden.

Received 18 ix 78 Accepted 18 xii 78

A number of significant risk factors for ischemic heart disease may cause injury to the arterial endothelium (see reviews Ross & Glomset 1973 Björkerud 1975). Endothelial injury may elicit repair responses in the subendothelial arterial tissue with an increased mitotic activity in arterial smooth muscle cells. If the repair response does not lead to healing of the arterial intima, the result is arterial thrombosis.

In experimental animals, arterial endothelial injury leads to the deposition of lipids, especially cholesterol, in the arterial tissue even in animals with low serum cholesterol levels (Bondjers 1972 1975). Furthermore, the risk for formation of mural thrombosis is increased after endothelial injury (Mustard 1977). Recently the hypothesis

was proposed that certain risk factors for ischemic heart disease may lead to atherosclerosis by causing endothelial injury (Bondjers *et al* 1977). One such risk factor might be hypertension (Björkerud & Eriksson 1976). Other risk factors, such as hypercholesterolemia (Bondjers *et al* 1978) and diabetes, could be connected with the disease by retarding repair processes (Bondjers *et al* 1977).

During the last ten years it has been assumed that cigarette smoking could lead to endothelial injury (Asmussen & Kjeldsen 1975 Astrup & Kjeldsen 1974) but the experimental basis for this assumption was recently questioned because there were insufficient controls (Hugod *et al* 1977). In the present study the relationship between smoking and endothelial injury was investigated by scanning electron microscopy.

- Scientific tables 7th ed Ciba Geigy Ltd Basel 1975 pp 180
- 5 Engesæter L B Ekeland A & Langeland N Methods for testing the mechanical properties of the rat femur *Acta orthop Scand* 49 512-518 1978
 - 6 Firschein H E Collagen and mineral dynamics in bone *Clin Orthop* 66 212-225 1969
 - 7 Homsy C A Kent J N & Hinds E C Materials for oral implantation - biological and functional criteria *J Am Dent Ass* 86 817-832 1973
 - 8 Hulbert S F Young F A Matthews R S Klawitter J J Talbert C D & Stelling F H Potential of ceramic materials as permanently implantable skeletal prostheses *J Biomed Mater Res* 4 433-456 1970
 - 9 Hulbert S F Morrison S J & Klawitter J J Tissue reaction to three ceramics of porous and non porous structures *J Biomed Mater Res* 6 342-374 1972
 - 10 Jackson D S Connective tissue growth stimulated by carrageenin 1 The formation and removal of collagen *Biochem J* 65 277-284 1957
 - 11 Lyng S Sudmann E Hulbert S F & Sauer B W Fixation of permanent orthopaedic prosthesis Use of ceramics in the tibial plateau *Acta Orthop Scand* 44 694-701 1973
 - 12 Nilles J L Karagianis M T & Wheeler A R Porous titanium alloy for fixation of knee prosthesis *J Biomed Mater Res Symposium No 5* pp 319-328 1974
 - 13 Pedersen A N Haanas H R & Lyng S Tissue ingrowth into mandibular intrabony porous ceramic implants *Int J Oral Surg* 3 158 165 1974
 - 14 Salvatore J E Gilmer W S Kaslgaran M & Barbee W R An experimental study of the influence of pore size of implanted polyurethane sponges upon subsequent tissue formation *Surg Gynecol & Obstet* 112 463-468 1961
 - 15 Schachtschabel D O & Blencke B A Effect of pulverized implantation materials (Plastic and glass ceramic) on growth and metabolism of mammalian cell cultures *Eur Surg Res* 8 71-80 1976
 - 16 Schilling J A White B A Lockhart M S & Shurley H M Wound healing in the dog *Am J Surg* 117 330-337 1969
 - 17 Ludik A Functional properties of collagenous tissues In *International review of connective tissue research* (ed D A Hall & D S Jackson) Vol 6 Academic Press New York and London 1973 pp 127-215
 - 18 Viljanto J Biochemical basis of tensile strength in wound healing *Acta Chir Scand Suppl* 333 1964 pp 43-48 55-56
 - 19 Vantunen E & Viljanto J Tensile strength of new connective tissue formed in pretreated viscose cellulose implants *Ann Med exp Fenn* 43 157 259 1965

twenty patients were investigated and the material was classified as described below.

The uterus was removed *in toto* immediately after interruption of the blood flow. It was immersed in Ringer's glucose solution at room temperature and brought to the laboratory. The main uterine arteries at both sides were cannulated and the endothelium was subjected to a dye exclusion test with Evans blue in buffered saline (Bjorkerud & Bondjers 1972) to identify areas with injured endothelium. The dye was washed out with Ringer's glucose solution after the test. The Ringer's solution was replaced by Karnovsky's fixative (Karnovsky 1965) and perfusion was continued at a pressure of 100 mm Hg for at least one hour. The artery was excised and dried according to the critical point method (Anderson 1951). Amyl acetate was used as the intermediate and carbon dioxide as the transitional fluid. The samples were coated with gold in a sputtering equipment and studied in a Jeol JSM 35, a Zeiss Novascan or a Jeol 100 CX Temscan scanning electron microscope with an accelerating voltage of 15-25 kV.

The specimens were studied especially with regard to the presence of (1) fibrin, (2) erythrocytes, (3) surface folding, (4) surface discontinuities, (5) spindle formed surface cells, (6) bulging cuboidal so-called cobble stone cells and (7) cell surface microprocesses. The prepara-

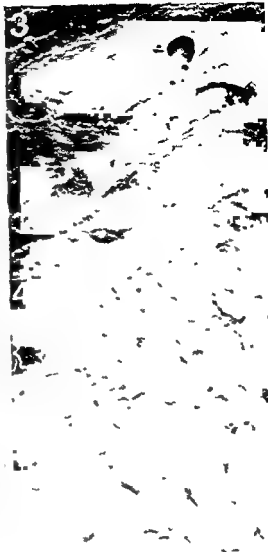


Fig 3 A normal appearance of endothelial cells with borders demarcated by an increased frequency of surface projections. A few discontinuities are also present. One erythrocyte is seen close to a conglomerate probably representing a few platelets (Smoker 48 years old) 1500x.

Fig 4 Normal endothelium with a moderate increase of surface projections (Smoker 43 years old) 1000x.

All figures show scanning electron micrographs of uterine arteries prepared for microscopy as stated in materials and methods.

Fig 1 A low power view of the surface. The transverse folds are seen.



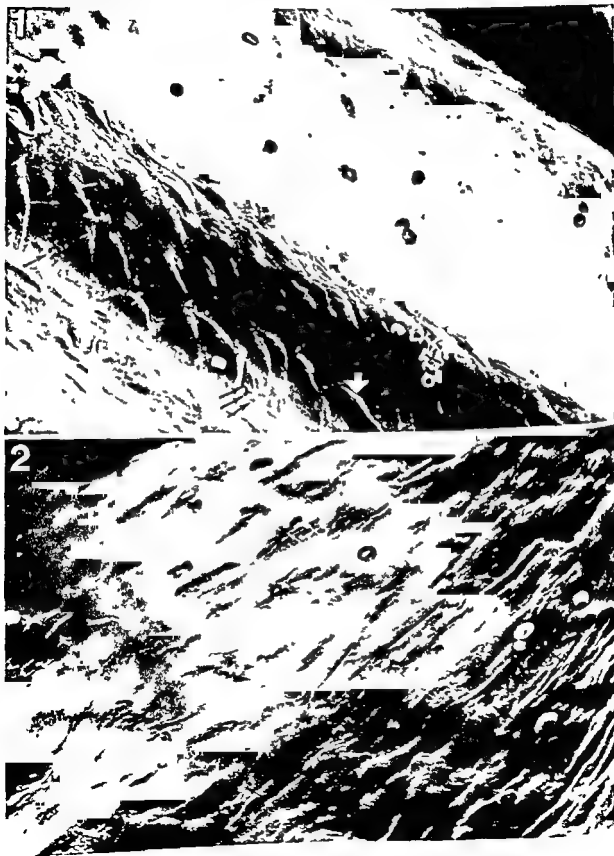
Fig 2 A survey of a surface with a smooth appearance. Surface projections at the cell borders. A few erythrocytes (black arrows) and a single large bulging more cuboidal discontinuity are present in areas marked with double

MATERIAL AND METHODS

Human uterine arteries were obtained as peroperative biopsies during hysterectomy due to uterine myoma.

The patients were selected at the department of gynaecology and consisted of two groups - women who

did not smoke and women who smoked more than 10 cigarettes a day. Patients with hypertension, hyperproteinemia and diabetes were excluded from the study. Only specimens from patients where the preliminary diagnosis of benign myomas was confirmed by histopathological investigations were included in the study.



To avoid bias in the morphological investigations all material was studied without knowledge of the patients' smoking habits. These were revealed after a total of twenty patients were investigated and the material was classified as described below.

The uterus was removed *in toto* immediately after interruption of the blood flow. It was immersed in Ringer's glucose solution at room temperature and brought to the laboratory. The main uterine arteries at both sides were cannulated and the endothelium was subjected to a dye exclusion test with Evans blue in buffered saline (Bjorkerud & Bondjers 1972) to identify areas with injured endothelium. The dye was washed out with Ringer's glucose solution after the test. The Ringer's solution was replaced by Karnovsky's fixative (Karnovsky 1965) and perfusion was continued at a pressure of 100 mm Hg for at least one hour. The artery was excised and dried according to the critical point method (Anderson 1951). Amyl acetate was used as the intermediate and carbon dioxide as the transitional fluid. The samples were coated with gold in a sputtering equipment and studied in a Jeol JSM 35, a Zeiss Novascan or a Jeol 100 CX Temscan scanning electron microscope with an accelerating voltage of 15.25 kV.

The specimens were studied especially with regard to the presence of (1) fibrin, (2) erythrocytes, (3) surface folding, (4) surface discontinuities, (5) spindle formed surface cells, (6) bulging cuboidal so-called cobble stone cells and (7) cell-surface microprocesses. The prepara-

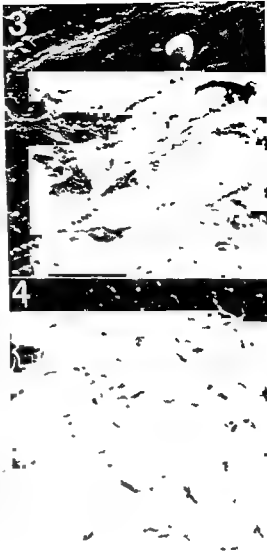


Fig 3 A normal appearance of endothelial cells with borders demarcated by an increased frequency of surface projections. A few discontinuities are also present. One erythrocyte is seen close to a conglomerate probably representing a few platelets (Smoker 48 years old) 1500x

Fig 4 Normal endothelium with a moderate increase of surface projections (Smoker 43 years old) 1000x

All figures show scanning electron micrographs of uterine arteries prepared for microscopy as stated in materials and methods.

Fig 1 A low power view of the surface. The transverse folds are covered with normal endothelium among which a spindle shaped cell is present. nature structure

Fig 2 A survey of a surface with a smooth appearance. Individual cells are demarcated by an increased frequency of surface projections at the cell borders. A few erythrocytes are seen as well as intercellular surface discontinuities (black arrows) and a single large bulging more cuboidal cell (white arrow). Platelets associated with surface discontinuities are present in areas marked with double black arrows (Smoker 48 years old) 800x



Fig 5a This picture shows endothelial cells with well-demarcated cell borders. The cell surface is covered with small processes (Non-smoker, 37 years old) 1200 \times

Fig 5b Endothelial cells with clearly visible borders indicated by rows of microvilli-like structures. Such structures are also seen scattered over the surface. At intercellular borders small holes are occasionally seen (Non-smoker, 37 years old) 3500 \times

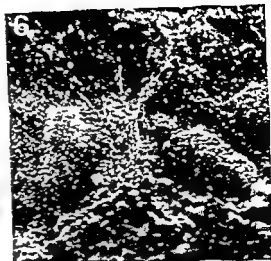


Fig 5c A high power view showing cell borders with rows of microvilli like structures (arrows) Small processes are seen scattered over the endothelial cell surface (Non smoker 45 years old) 10 000x

Fig 6 This picture shows cuboidal cells in an area subjected to increased hemodynamic trauma The nuclei are easily seen and holes at the borders between adjacent cells can be noted (Smoker 38 years old) 2500x

tions were rated with respect to each of these characteristics according to a scale with five degrees (0 + + + + + + + + +) As mentioned above these ratings are made without knowledge of the smoking habits of the patient

RESULTS

General Observations

In nine of the arteries the surface structure was more uneven than in the others The folds of the uterine arteries were transversely oriented apparently owing to underlying intimal structures Figure 1 depicts the surface structure of an artery with some transverse folds They are covered with endothelium of normal appearance Occasionally a few scattered spindle shaped cells and cobble stone cells were also observed The arterial endothelium was mostly rather smooth (Figs 2-4) There was a concentration of processes at the border between adjacent endothelial cells The position of the nucleus was revealed by a centrally located bulging into the vascular lumen (Figs 3 4) In some preparations the cell surface was covered with a large number of small processes (0.5-2 microns in diameter see Figs 5 a-c)

Intermingled with several normal cells cells with an aberrant surface structure were observed A few holes with a diameter of 0.1-2 microns were observed in one type of such cells (Fig 3) Other cells were cuboidal (Figs 2 6 8) and looked like cobble-stones paving the arterial surface Spindle

shaped cells were found with varying frequency in most preparations (Fig 7) Occasionally large intercellular surface discontinuities were observed (Fig 7)

Characteristic changes in surface topography were found in the vicinity of branching points (Figs 8 9) Large swollen cuboidal cells (Fig 8) contained surface discontinuities especially in the region surrounding the nucleus Thrombotic material was

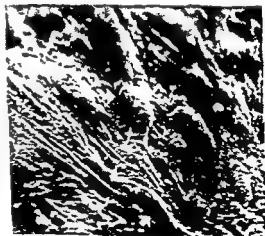


Fig 7 The cells in this area are spindle shaped The nuclei are clearly visible and bulge into the lumen (arrow) Intercellular borders are easily discerned Holes are also noted between adjacent endothelial cells (Smoker 38 years old) 1000x



Fig 8 This field of view is from the neighbourhood of an artery branching point (upper right corner). Several erythrocytes are present as well as a bulging cuboidal cell with surface discontinuities seen both at the cell membrane as well as intercellularly (Smoker 44 years old) $\times 500$

often found in such regions. Furthermore spindle shaped cells with an abnormally disposed length axis were frequently observed. These cells appeared partially detached from the surrounding and underlying arterial tissue (Fig 9) and were intermingled with other cells types. Cells within these areas had a more normal general surface structure and were smaller than those in adjacent intact areas of uterine arteries.

Smokers versus Non Smokers

In Table 1 the prevalence of various structural characteristics in smokers and non smokers is presented. Fibrin was found on the surface of arteries from three non smokers but not on the surface of arteries from other women. There was no difference between the two groups as to frequency of erythrocytes (Fig 1 and 8) and folds (Fig 1). Surface discontinuities and holes (Fig 2 and 8) were more common in smokers than in non smokers. Spindle shaped cells (Fig 7 and 9) were as common in smokers as in non smokers and the presence of

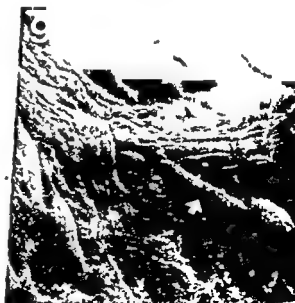


Fig 9 This area is located close to a branching point which is in the upper half of the field of view. Spindle-shaped cells are present (white arrow) (Smoker 47 years old) $\times 500$

TABLE 1 Structural Characteristics of the Arterial Endothelium in Smokers and Non Smokers as Observed with the Scanning Electron Microscope

	Fibrin	Erythrocytes	Surface folding	Surface discontinuities	Spindle shaped cells	Cobble stone cells	Processes	
	++++	+++	0	++++	++	+	+	NON SMOKERS
	++++	++	+	0	0	0	++++	
	0	+	0	++	++	0	++	
	0	+	+	++	+	0	++++	
	0	+	0	0	+++	0	++	
	0	0	0	0	++++	0	+	
	+	++	++	++	++	++++		
	0	+	0	++	++++	++	++	
	0	0	0	++	++	0	++++	
		+	++	++	++	++	+	
	0	++	+	+	++	++	+	SMOKERS
		+	++	++++	0	++	+	
	0	0	0	++++	+	+	0	
	0	+	0	++	++	++	++	
		+	0	++	++	++	++	
	0	+	0	++++	+	++	+	
	0	++	++	++	++++	+	+	
	0	+	++	++++	++	+	0	
	0	++	+	++++	++	+	0	
	0	+	0	++++	0	0	0	
Significance	n s	n s	n s	p<0.02	n s	n s	p<0.05	

schers test)*

Idem & Hedel 1975)

*Preparations were Rated (0 + + + + + + + + +) with Regard to the Prevalence of the Characteristics without knowledge of Patients smoking Habits

cobble-stone cells (Figs 6 and 8) did not differ statistically between the groups. However total absence of such cells was found in 6 out of 11 non smokers but only in 1 out of 9 smokers. Cell processes (Fig 5b) were more common in arteries from non-smokers than in those from smokers.

One woman in the non smoking group was considerably older than the other. Exclusion of the observations made on material obtained from her did not affect conclusions concerning differences between smokers and non smokers.

DISCUSSION

The surface structure of the human arterial biopsies conformed to that of animal arteries as described in previous reports (Bjorkerud 1975, Clark & Glasgow 1975, Bonders et al 1977, Bjlock et al 1977, Bjorkerud et al 1979). Thus the majority of

endothelial cells were elongated with the nucleus slightly bulging into the lumen and had their cell borders demarcated by an increased frequency of surface projections. As in animal arteries surface cells with an aberrant morphology were also observed in the human artery biopsies. One type of such luminal cells was spindle shaped and was most common in the vicinity of branches. The structure of these cells resembled most of all that of cells that have been subjected to mechanical manipulations (Reidy & Bowyer 1977). However they are observed even in areas where mechanical trauma ad exter-

is caused by the hemodynamic strain *in vivo* (Bjlock et al 1977, Bjorkerud et al 1979). Another cell type encountered both in human and animal arterial biopsies was larger and bulged slightly into the lumen of the arteries. In addition such cells were

also especially frequent near branching points. These cells have a general appearance similar to that of injured cells which are stained when a dye exclusion test is performed (Bjorkerud & Bondjers 1972). However, the relationship between the main endothelial cell population and spindle-shaped and swollen cells is still obscure. At present we can only conclude that the presence of these three cell types is a reproducible finding not only in animal arteries but also in arterial biopsies from man.

There are obvious difficulties in evaluating the significance of aberrations from the normal structure, since it is easy to induce artifacts during preparation. To decrease the possibility that such artifacts were given a biological significance, we chose to study the material without any knowledge of the smoking habits of the patients. Results from previous studies on the effect of smoking have been misinterpreted owing to the fact that morphological characteristics were evaluated by an investigator who knew which specimens were taken from smokers (Hugod *et al.* 1977). Obviously, the approach we have made with a blind evaluation of the material decreases the sensitivity of the method.

The structural characteristics we elected to study on a semiquantitative scale were selected on the basis of previous studies by scanning electron microscopy (Bjorkerud *et al.* 1979, Bylock *et al.* 1977, Bondjers *et al.* 1977). Spindle-formed surface cells and cobble-stone cells have been observed in the vicinity of branching-points at sites of experimentally-induced injury and at other sites where an increased frequency of injured endothelial cells has been established by independent methods (Bondjers *et al.* 1977). Thrombotic material was also observed at such sites. Inter cellular and cell membrane localized holes were observed between spindle-formed cells and on the surface of cobble stone cells. Cell surface processes varied in frequency with serum cholesterol levels (Bjorkerud *et al.* 1979). They were also less frequent on the surface of swollen cells (Bylock *et al.* 1977, Bondjers *et al.* 1977, Bjorkerud *et al.* 1979). However the presence of such processes might also indicate preparative hypoxemia (Bjorkerud *et al.* 1979).

An increased frequency of surface discontinuities and a decreased frequency of surface projections were found in the arteries of smokers as compared to non smokers. In previous studies we have observed that surface discontinuities are typical for areas with injured endothelium (Bondjers *et al.* 1977, 1978). For practical reasons fixation of the human arterial specimens could not be started until about 30 minutes after removal of the uterus. During this interval, surface projections may well have been induced, if results from studies on rabbit

aortae are relevant for human material. Accordingly, the presence of such projections may be regarded as normal, and the absence of such projections in smokers as an indication of decreased reactivity due to hypoxemia.

If a decreased frequency of surface projections as well as an increased frequency of surface discontinuities in smokers is regarded as an effect of cellular injury, it may seem surprising that we did not find any significant differences in the estimates of the frequency of spindle-formed or cobble stone cells. However, in earlier evaluations of the different methods that are available for quantitation of endothelial injury we concluded that scanning electron microscopy is not as suitable as the dye exclusion test (Bjorkerud & Bondjers 1972, Bondjers *et al.* 1978). Therefore the present results should encourage further studies with cell counting after a dye exclusion test in order to corroborate the impression that an increased frequency of surface discontinuities together with a decreased frequency of cell processes is the result of a true cellular injury from smoking.

In conclusion the present results suggest the possibility that the integrity of the arterial endothelium is decreased by smoking. This may be one factor which can explain the association between various manifestations of atherosclerotic arterial disease and smoking. However the possibility that smokers have an increased frequency of injured endothelial cells should be further investigated by more quantitative methods.

Supported by grants from the Swedish Medical Research Council (2543/4531), the Swedish National Association against Chest and Heart Diseases, the Swedish Tobacco Research Council and the University of Goteborg.

REFERENCES

- Anderson T R. Techniques for preservation of the fine structure in preparing specimens for the electron microscope. *Trans N Y Acad Sci* 13: 130-134 1951.
- Asmussen I & Kjeldsen A. Intimal ultrastructure of human umbilical arteries. *Circ Res* 36: 579-589 1975.
- Astrup P & Kjeldsen K. Carbon monoxide smoking and atherosclerosis. *Med Clin North Amer* 59: 323-350 1974.
- Bjorkerud S. Relationship of endothelium to smooth muscle overview. *Adv Exp Med Biol* 57: 180-204 1975.
- Bjorkerud S & Bondjers G. Endothelial integrity and viability in the aorta of the normal rabbit and rat as evaluated with dye exclusion tests and interference

ud S Bondjers G Bylock A & Hansson G K
dies of arterial endothelial integrity with the dye
lusion test - a review Functional and compara
anatomy of arteries vol 1 C J Schwartz (ed)
um Press New York In press 1979

ud S & Eriksson L O Strain injury adaption
l repair in hypertensive macroangiopathy »The
renal Hypertensive Disease A Symposium« G
rie & H van Cauwenberge (eds) Masson Inc
New York, Paris Barcelona Milan pp 39-49
16

rs G Endothelial integrity and cholesterol
asfer in the aorta of the rabbit Elanders
teborg 1972

rs G Cholesterol accumulation and removal in
rimal and atherosclerotic arterial tissue In Blood
f Arterial Wall in Atherogenesis and Arterial
rombosis J G A J Hautvast R J J Hermus &
van der Haas (eds) Brill Leiden pp 55-67 1975

rs G Brattsand R Bylock A Hansson G K &
rkerud S Endothelial integrity and atherogene
in rabbits with moderate hypercholesterolaemia
tery J 395-408 1977

rs G Björkerud S Brattsand R Bylock A
ansson G K & Hansson H A Endothelial injury
normo-cholesterolaemic and hypercholesterolaem
c rabbits International conference on Atheroscle
sis L A Carlson R Paoletti & G Weber (eds)
ven Press New York pp 567-573 1978

Bylock A Björkerud S Brattsand R Hansson G K
Hansson H A & Bondjers G Endothelial structure
in rabbits with moderate hypercholesterolaemia a
Scanning Electron Microscopic Study Acta Path
Microbiol Scand Sect A 85 671-682 1977

Clark J M & Glagov S Luminal surface of distended
arteries by scanning electron microscopy elimina
ting configurational and technical artifacts Br J Exp
Path 57 129-135 1975

Hugod C Hawkins L Kjeldsen K Thomsen H K &
Astrup P The influence of carbon monoxide on
intimal morphology Abstract Int Conf on Athe
rosclerosis p 167 1977

Karnovsky M J A formaldehyde glutaraldehyde fixa
tive of high osmolality for use in electron micro
scopy J Cell Biol 27 137A 1965

Mustard J F Moore S Packham M A & Kinlough
Rathbone R L Platelets thrombosis and athero
sclerosis Progr Biochem Pharmacol 13 312-325
1977

Oden A & Wedel H Arguments for Fisher's
permutation test Ann Statistics 3 518-520 1975

Reidy M A & Bowser D E Scanning electron
microscopy of arteries Atherosclerosis 26 181-
194 1977

Ross R & Glomset J A Atherosclerosis and the
arterial smooth muscle cell Science 180 1332-
1339 1973

also especially frequent near branching points. These cells have a general appearance similar to that of injured cells which are stained when a dye exclusion test is performed (Bjorkerud & Bondjers 1972). However the relationship between the main endothelial cell population and spindle shaped and swollen cells is still obscure. At present we can only conclude that the presence of these three cell types is a reproducible finding not only in animal arteries but also in arterial biopsies from man.

There are obvious difficulties in evaluating the significance of aberrations from the normal structure since it is easy to induce artifacts during preparation. To decrease the possibility that such artifacts were given a biological significance we chose to study the material without any knowledge of the smoking habits of the patients. Results from previous studies on the effect of smoking have been misinterpreted owing to the fact that morphological characteristics were evaluated by an investigator who knew which specimens were taken from smokers (Hugod *et al* 1977). Obviously the approach we have made with a blind evaluation of the material decreases the sensitivity of the method.

The structural characteristics we elected to study on a semiquantitative scale were selected on the basis of previous studies by scanning electron microscopy (Bjorkerud *et al* 1979, Bylock *et al* 1977, Bondjers *et al* 1977). Spindle formed surface cells and cobble stone cells have been observed in the vicinity of branching points at sites of experimentally induced injury and at other sites where an increased frequency of injured endothelial cells has been established by independent methods (Bondjers *et al* 1977). Thrombotic material was also observed at such sites. Intercellular and cell membrane localized holes were observed between spindle formed cells and on the surface of cobble stone cells. Cell surface processes varied in frequency with serum cholesterol levels (Bjorkerud *et al* 1979). They were also less frequent on the surface of swollen cells (Bylock *et al* 1977, Bondjers *et al* 1977, Bjorkerud *et al* 1979). However the presence of such processes might also indicate preparative hypoxemia (Bjorkerud *et al* 1979).

An increased frequency of surface discontinuities and a decreased frequency of surface projections were found in the arteries of smokers as compared to non smokers. In previous studies we have observed that surface discontinuities are typical for areas with injured endothelium (Bondjers *et al* 1977, 1978). For practical reasons fixation of the human arterial specimens could not be started until about 30 minutes after removal of the uterus. During this interval surface projections may well have been induced if results from studies on rabbit

aortae are relevant for human material. Accordingly the presence of such projections may be regarded as normal and the absence of such projections in smokers as an indication of decreased reactivity due to hypoxemia.

If a decreased frequency of surface projections as well as an increased frequency of surface discontinuities in smokers is regarded as an effect of cellular injury it may seem surprising that we did not find any significant differences in the estimates of the frequency of spindle formed or cobble-stone cells. However in earlier evaluations of the different methods that are available for quantitation of endothelial injury we concluded that scanning electron microscopy is not as suitable as the dye exclusion test (Bjorkerud & Bondjers 1972, Bondjers *et al* 1978). Therefore the present results should encourage further studies with cell counting after a dye exclusion test in order to corroborate the impression that an increased frequency of surface discontinuities together with a decreased frequency of cell processes is the result of a true cellular injury from smoking.

In conclusion the present results suggest the possibility that the integrity of the arterial endothelium is decreased by smoking. This may be one factor which can explain the association between various manifestations of atherosclerotic arterial disease and smoking. However the possibility that smokers have an increased frequency of injured endothelial cells should be further investigated by more quantitative methods.

Supported by grants from the Swedish Medical Research Council (2543, 4531), the Swedish National Association against Chest and Heart Diseases, the Swedish Tobacco Research Council and the University of Göteborg.

REFERENCES

- Anderson T R. Techniques for preservation of the free structure in preparing specimens for the electron microscope. *Trans N Y Acad Sci* 1973; 130-144.
- 1951.
- Asmussen I & Aejelsoen A. Intimal ultrastructure of human umbilical arteries. *Circ Res* 1975; 36: 579-589.
- 1975.
- Astrup P & Aejelsoen A. Carbon monoxide smoking and atherosclerosis. *Med Clin North Amer* 1977; 323-350.
- 1974.
- Bjorkerud S. Relationship of endothelium to smooth muscle overview. *Adv Exp Med Biol* 1978; 57: 181-204.
- 1975.
- Bjorkerud S & Bondjers G. Endothelial integrity and viability in the aorta of the normal rabbit and rat evaluated with dye exclusion tests and interference

- contrast microscopy *Atherosclerosis* 15 285-300 1972
- Björkerud S, Bondjers G, Bylock A & Hansson G K Studies of arterial endothelial integrity with the dye exclusion test - a review. Functional and comparative anatomy of arteries vol 1 C J Schwartz (ed) Plenum Press New York In press 1979
- Björkerud S & Eriksson L O Strain injury adaptation and repair in hypertensive macroangiopathy. The Arterial Hypertensive Disease A Symposium G Rorive & H van Cautenberge (eds) Masson Inc New York Paris Barcelona Milan pp 39-49 1976
- Björkerud S Endothelial integrity and cholesterol transfer in the aorta of the rabbit. *Elanders Göteborg* 1972
- Björkerud S Cholesterol accumulation and removal in normal and atherosclerotic arterial tissue. In *Blood and Arterial Wall in Atherogenesis and Arterial Thrombosis* J G A J Hautvast, R J J Hermus & F van der Haar (eds) Brill Leiden pp 55-67 1975
- Björkerud S, Brattsand R, Bylock A, Hansson G K & Björkerud S Endothelial integrity and atherogenesis in rabbits with moderate hypercholesterolaemia. *Artery* 3 395-408 1977
- Björkerud S, Björkerud S, Brattsand R, Bylock A, Hansson G K & Hansson H A Endothelial injury in normo-cholesterolaemic and hypercholesterolaemic rabbits. International conference on Atherosclerosis L A Carlson, R Paoletti & G Weber (eds) Raven Press New York pp 567-573 1978
- Bylock A, Björkerud S, Brattsand R, Hansson G K, Hansson H A & Bondjers G Endothelial structure in rabbits with moderate hypercholesterolaemia: a Scanning Electron Microscopic Study. *Acta Path Microbiol Scand Sect A* 85 671-682 1977
- Clark J M & Glasgow S Luminal surface of distended arteries by scanning electron microscopy: eliminating configurational and technical artifacts. *Br J Exp Path* 57 129-135 1975
- Hugod C, Hawkins L, Kjeldsen K, Thomsen H K & Astrup P The influence of carbon monoxide on intimal morphology. Abstract. Int Conf on Atherosclerosis p 167 1977
- Karnovsky M J A formaldehyde glutaraldehyde fixative of high osmolality for use in electron microscopy. *J Cell Biol* 27 137A 1965
- Mustard J F, Moore S, Packham M A & Kinlough Rathbone R L Platelets, thrombosis and atherosclerosis. *Progr Biochem Pharmacol* 13 312-325 1977
- Oden A & Wedel H Arguments for Fisher's permutation test. *Ann Statistics* 3 518-520 1975
- Reidy M A & Bowyer D E Scanning electron microscopy of arteries. *Atherosclerosis* 26 181-194 1977
- Ross R & Glumet J A Atherosclerosis and the arterial smooth muscle cell. *Science* 180 1332-1339 1973

STRUCTURAL CHANGES AND ABILITY TO RELEASE RENIN IN AUTO- AND ALLO- TRANSPLANTS OF MOUSE SUBMAXILLARY GLANDS

POUL FAARUP and JENS BING

The University for Experimental Medicine and Renal Laboratory the University Institute of
Pathological Anatomy Copenhagen

Faarup P & Bing J Structural changes and ability to release renin in auto and allo transplants of
mouse submaxillary glands Acta path microbiol scand Sect A 87 211-216 1979

In mice having a high renin content in the submaxillary glands allo and autotransplantation of the
gland showed identical histological changes of the tissue comprising disappearance of acini and
intercalated ducts as well as a reduction in the number and size of granules in the granulated ducts. No
structural signs of rejection were found. Adenomas possibly originating in the granulated ducts were
frequently present in the transplanted glands. The renin content of autotransplanted glands was
invariably much higher than in allotransplants and after noradrenaline injection renin was released
only from autotransplants never from allotransplants. Blockade of the renin system was accordingly
followed by a decrease in blood pressure only in mice with autotransplants.

Key words Submaxillary glands transplants renin release

P Faarup The University Institute for Experimental Medicine Nørre Alle 71 DK 2100 Copenhagen
Denmark

Accepted as submitted 23 XII 78

The presence of extremely high concentrations of
a renin like substance in the submaxillary glands of
male mice was first demonstrated by *Werk et al*
(1957) and has since been confirmed by many
investigators (see *Ganun et al* 1977). The enzyme is
concentrated in the granules of the granulated ducts
(*Bing and Faarup* 1965 and *Chiang et al* 1968).
Little or no renin being found in other parts of the
glands. The aim of the present investigation was to
study the morphology of auto and allo transplants
of the glands and to elucidate their ability to secrete
renin and influence the blood pressure.

lary glands were removed and cut into pieces about
1 x 1 x 1 mm which were suspended in sterile physio-
logical saline. Half the suspension corresponding to one
gland was immediately injected intraperitoneally into
the donor the other half was similarly injected into
another previously submaxillary-sialo adenectomized
mouse. Penicillin treatment was repeated 24 hours after
the transplantation. The mice were in most cases kept for
1 to 2 months before the functional effect of the
transplantations was studied these differences in time
had no influence on the results.

Histopathology The microscopical structure of the
transplanted submaxillary glands was investigated just
after the termination of the

MATERIAL AND METHODS

Mice Male albino mice of the State Serum Institute
strain A 67 maintained chiefly by outbreeding but with
some inbreeding. Body weight 48-60 g. Before the
transplantations donors and recipients were pretreated
with penicillin. Under aseptic conditions the submaxil-

lary glands were removed and cut into pieces about
1 x 1 x 1 mm which were suspended in sterile physio-
logical saline. Half the suspension corresponding to one
gland was immediately injected intraperitoneally into
the donor the other half was similarly injected into
another previously submaxillary-sialo adenectomized
mouse. Penicillin treatment was repeated 24 hours after
the transplantation. The mice were in most cases kept for
1 to 2 months before the functional effect of the
transplantations was studied these differences in time
had no influence on the results.

normal glands were imbedded in Epon One micron thick sections were stained by toluidine blue for a detailed inspection of the histological changes present in the transplanted glands

The histological investigation was performed without knowing whether the glands were autotransplants or allotransplants in order to evaluate whether systematic histological changes could be demonstrated in the two different types of transplants

Functional studies were performed on conscious mice. At least 2 hours before the experiments the previously sialoadenectomized mice were nephrectomized and had a catheter inserted into one femoral artery under brief ether anaesthesia. They were thereafter placed in restraining cages.

Blood pressure was recorded using a Tybjerg Hansen transducer and a Servogor 511 recorder.

The ability of the transplants to secrete renin was tested by intraarterial injection of 1 µg/kg noradrenaline which provokes renin release from the submaxillary glands (Menzle *et al.* 1974) after pretreatment with dihydralazine (Nepresol[®] Ciba). Blockade of the renin system was in most experiments performed by injection of 3 mg/kg of the converting enzyme inhibitor SQ

20 881 and in 2 mice of the competitive angiotensin II inhibitor Saralysin.

Plasma and tissue renin concentrations given in Goldblatt Units (GU) $\times 10^{-3} \times \text{ml}^{-1}$ or g^{-1} were determined using the antibody trapping radioimmuno assay for angiotensin (Poulsen and Jørgensen 1974). In order to study the renin content of transplants the omentum was removed 1 to 2 months after the transplantation in 14 mice on which no morphological or functional studies were performed.

RESULTS

1 Histopathology

1 Autotransplanted submaxillary glands The 10 autotransplanted submaxillary glands invariably showed pronounced structural changes of the parenchyma. In all the transplants the acini and the intercalated ducts were markedly atrophied leaving in the parenchyma nearly only granulated and intralobular ducts (Fig. 1). The cells from the granulated ducts systematically had a somewhat



content of the granulated duct cells in section. Toluidine Blue stained $\times 420$

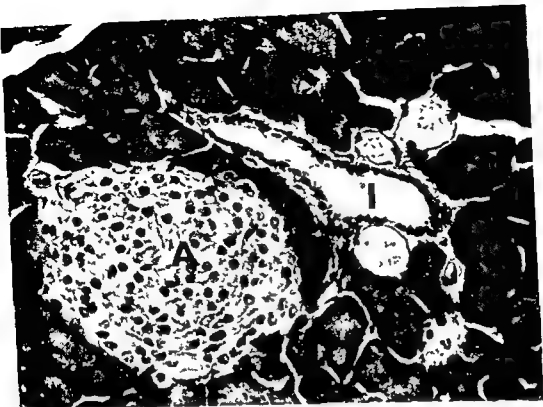


Fig. 2. Autotransplanted submaxillary gland in which the granulated ducts (G) form the main part of the gland. Due to the transplantation the acini and the intercalated ducts are atrophied and the interstitial tissue very sparse. An adenoma (A) is present and similar cells (arrow) are found closely related to cells of a granulated duct. I - intralobular duct (PAS $\times 360$).

lowered content of cytoplasmic granules which were of a smaller diameter but the number of granules in the cells could vary considerably in different areas of the tissue. In PAS stained sections the granules systematically appeared less chromophil than in the normal glands. In addition slight variations in nuclear size and slight pyknosis of the nucleus were focally present in the granulated ducts. No significant structural changes were seen in the intralobular ducts. Necrotic cells, interstitial edema, fibrosis or cellular infiltration were never observed. In 1 of the 10 specimens a few small PAS positive extracellular hyaline globules were seen interstitially. Often the surrounding fatty tissue showed slight focal infiltration comprising lymphocytes, macrophages, neutrophils and a few plasma cells.

In 9 out of the 10 specimens investigated multiple small adenomatous tumors were present in the parenchyma (Fig. 2) in which the cells were of the same average size as those of the granulated ducts. The nuclei were somewhat smaller and the cytop-

lastm was pale finely granulated. Identical cells could be found as solitary cells in the granulated ducts (Fig. 3).

In semithin plastic imbedded sections of the autotransplanted glands the lack of acini and of nearly all intercalated ducts was confirmed (Fig. 1). Besides the granulated ducts contained cells similar in morphology to those found in the adenomas (Figs. 2 and 3).

2. Allotransplanted submaxillary glands. In the 9 allotransplanted submaxillary glands the structural changes of the parenchyma were mainly identical with those of the autotransplanted glands, including atrophy of acini and of intercalated ducts, adenoma formation (present in 8 out of 9 specimens) and connective tissue changes. The only exception was a somewhat more frequent presence of extracellular PAS positive hyaline globules in the sparse interstitium of the allotransplanted glands, as this was seen in 6 out of the 9 transplants.

Vascular changes or rejection like changes were never observed. The allotransplanted and autotrans-

normal glands were imbedded in Epon One micron thick sections were stained by toluidine blue for a detailed inspection of the histological changes present in the transplanted glands

The histological investigation was performed without knowing whether the glands were autotransplants or allotransplants in order to evaluate whether systematic histological changes could be demonstrated in the two different types of transplants

Functional studies were performed on conscious mice. At least 2 hours before the experiments the previously sialoadenectomized mice were nephrectomized and had a catheter inserted into one femoral artery under brief ether anaesthesia. They were thereafter placed in restraining cages

Blood pressure was recorded using a Tybjaerg Hansen transducer and a Servogor 511 recorder

The ability of the transplants to secrete renin was tested by intraarterial injection of 1 µg/kg noradrenaline which provokes renin release from the submaxillary glands (Menzie *et al.* 1974) after pretreatment with dihydralazine (Nepresol[®] Ciba). Blockade of the renin system was in most experiments performed by injection of 3 mg/kg of the converting enzyme inhibitor SQ

20 881 and in 2 mice of the competitive angiotensin II inhibitor Saralasin

Plasma and tissue renin concentrations given in Goldblatt Units (GU) $\times 10^{-3} \times \text{ml}^{-1}$ or g^{-1} , were determined using the antibody trapping radioimmuno assay for angiotensin (Poulsen and Jørgensen 1974). In order to study the renin content of transplants the omentum was removed 1 to 2 months after the transplantation in 14 mice on which no morphological or functional studies were performed

RESULTS

1 Histopathology

1 Autotransplanted submaxillary glands The 10 autotransplanted submaxillary glands invariably showed pronounced structural changes of the parenchyma. In all the transplants the acini and the intercalated ducts were markedly atrophied leaving in the parenchyma nearly only granulated and intralobular ducts (Fig. 1). The cells from the granulated ducts systematically had a somewhat

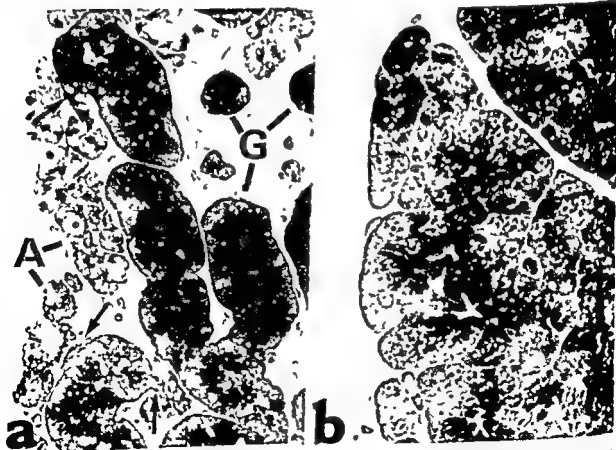


Fig. 1. Submaxillary gland (a) in which the usual compartments of the gland are readily identified in contrast to (b) in which the acini and the intercalated ducts are atrophied and the granular size and shape of the cells from the intralobular ducts (Semihoff 1974).

section Toluidine Blue stained $\times 400$

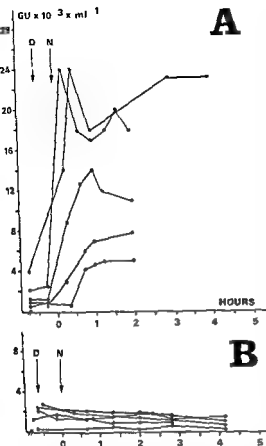


Fig 4 Changes in the plasma renin concentration with time after injection of noradrenaline (N) preceded by injection of dihydropyridine (D) in auto (A) and allo-transplanted (B) mice. The values for one of the autotransplanted mice are not given in A because the plasma renin concentration was high ($43 \text{ GU} \times 10^{-3} \times \text{ml}^{-1}$) before the injection of noradrenaline but even this mouse exhibited a marked (9.3 fold) postinjection increase in renin concentration. The ordinate shows the renin concentration in $\text{GU} \times 10^{-3} \times \text{ml}^{-1}$ and the abscissa the time in hours before and after the noradrenaline injection.

The atrophic changes of the acini and of the intercalated ducts found in both groups of mice are probably related to the inhibition of excretory function in the transplants. The granulated ducts in which the renin content of the gland has been found located were reasonably well preserved in the transplants although the granular content as well as the size of the granules in the cells were systematically diminished and the granules less PAS positive than in normal glands. In allotransplanted mouse salivary glands Hoshino and Lin (1968) also found

that the acinar portions of the glands had disappeared. Besides they reported a common occurrence of polycystic and adenomatous hyperplasia but found no true adenomas of the glands. In our work polycystic as well as adenomatous hyperplasia of the glands were completely absent. The constant appearance of multiple adenomas – the first one as early as 10 days following transplantation – in the glandular parenchyma is as yet unexplained (Fig 2). However the adenomas probably originated in the cells of the granulated ducts in which solitary typical adenoma cells were seen (Fig 3).

Ability to form and release renin. Contrary to the identical morphology of the auto- and allo-transplants their ability to form and secrete renin was quite different. This was shown by the much higher renin content in the majority of autotransplants than in allotransplants. In accordance with this finding all the autotransplanted mice were found to release renin after injection of noradrenaline while renin release was not found in any of the allotransplanted mice (Fig 4 A and B). The role of the renin release from the autotransplants in blood pressure regulation was shown by the decrease in pressure which followed blocking of the renin system.

In conclusion despite similar regressive structural changes in auto- and allo-transplanted submaxillary glands a high renin content and a renin release affecting the blood pressure levels were present only in autotransplanted glands.

This study was supported by grants from King Christian X's Foundation and the Foundation of the Insurance Companies of 1951. The authors are also grateful to Dr Alan W. Castillon, The Norwich Pharm. Co. New York, and to Dr S. J. Lucania, The Squibb Institute, New Jersey, U.S.A. for generous gifts of Saralasin and Squibb 20 881. The skilful technical assistance of Mrs V. Myland Smith is thankfully acknowledged.

REFERENCES

- Bing J & Faarup P. Location of renin (or a renin like substance) in the submaxillary glands of albino mice. *Acta path. et microbiol. scandinav.* 64: 203–212, 1965.
- Burnstone W S. Histochemical comparison of naphthol AS phosphates for the demonstration of phosphatases. *J. Nat. Cancer Inst.* 20: 600–612, 1958.
- Chang T S, Erdos E G, Mwa I, Tague L & Coulson J J. Isolation from a salivary gland of granules containing renin and kallikrein. *Circ. Res.* 27: 507, 1968.
- Franks L M & Knowles M A. The structure of tumors derived from mouse submandibular gland epithelium.

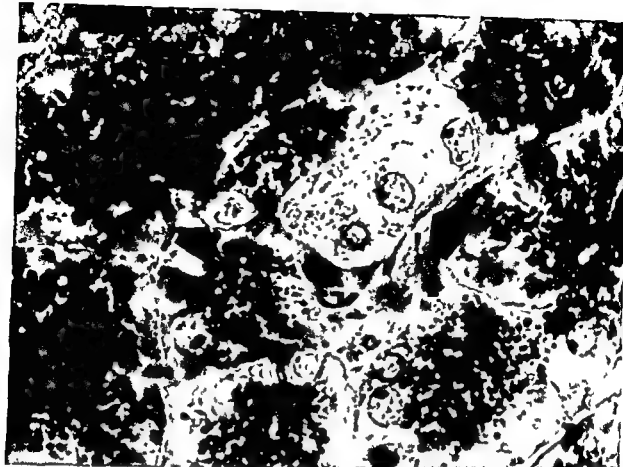


Fig. 3 Autotransplanted submaxillary gland in which the granulated duct (G) includes cells (arrows) of a structure similar to that of the adenomas found in transplanted glands (Semithin section Toluidine Blue stained $\times 1450$)

planted glands too were of the same histological structure in the semithin plastic imbedded sections

II Functional Studies

The effect of noradrenaline on the plasma renin concentrations was studied in 6 auto and 5 allo transplanted previously sialoadenectomized and nephrectomized mice. In all the autotransplanted mice noradrenaline injection provoked a significant ($p < 0.01$) increase in plasma renin concentration (Fig. 4 A) which remained quite unaffected in the allotransplanted mice (Fig. 4 B).

The effect on the blood pressure of blockade of the renin system also differed markedly in the above mentioned auto and allo transplanted mice. Both groups reacted with permanent hypotension to dihydralazine and with a brief marked pressor response to injection of noradrenaline. But while the

The renin concentration in extirpated omental tissue was determined in 7 auto and in 7 allotransplanted mice. In 5 of the 7 autotransplanted mice the mean concentration was 940 (range 203–1800) Goldblatt Units (GU) $\times 10^{-3} \times g^{-1}$ contrasting with values of 15 and 27 in the remaining 2 biopsies from the omentum of autotransplanted mice. In the omental biopsies from the 7 allotransplanted mice the mean renin concentration was 15 (range 2–48) GU $\times 10^{-3} \times g^{-1}$ and thus markedly lower than in the majority of biopsies from autotransplanted mice.

DISCUSSION

Structural changes of the transplanted glands In the present study identical histological changes were found in the autotransplants and allotransplants. The lack of rejection like structural changes in the allotransplanted animals indicates a significant degree of inbreeding among the mice investigated.

ced in 3 and fell only slightly (3 and 5 in 11.6 and 11.8 of the 5 allotransplanted mice.

CELL PROLIFERATION IN NORMAL AND DISEASED GASTRIC MUCOSA

Autoradiography after in vitro Continuous Labelling with Tritiated Thymidine

O HART HANSEN AA JOHANSEN J K LARSEN and L B SVENDSEN

Departments of Surgical Gastroenterology and Pathology Bispebjerg Hospital and Finsen Laboratory
Finsen Institute Copenhagen Denmark

Hart Hansen O Johansen Aa Larsen J K & Svendsen L B Cell proliferation in normal and diseased gastric mucosa. Autoradiography after *in vitro* continuous labelling with tritiated thymidine. Acta path microbiol scand Sect A 87 217-222 1979

The rate of gastric epithelial cell proliferation was studied in healthy volunteers and in patients with different degrees of gastritis. Endoscopic biopsies from the antral and fundic part of the stomach were incubated *in vitro* with ^3H thymidine for 30, 120 and 210 minutes respectively. Autoradiographs were prepared and the percentage of DNA synthesizing cells (labelling index) in the progenitor cell region was estimated. From the successive labelling indices the rate of entry of cells into DNA-synthetic phase (S phase) and the duration of the S phase could be estimated. All the biopsies were classified according to the degree of gastritis. The mean (\pm SEM) length of the S-phase was found to be 7.4 ± 1.3 hours in antral mucosa and 7.2 ± 0.4 hours in fundic mucosa. There was no significant difference between the S-phase duration in normal mucosa, superficial gastritis, mild atrophic gastritis and severe atrophic gastritis. This observation suggests that the labelling index can be used as an expression for the rate of cell proliferation in human gastric mucosa. A significant correlation between the labelling indices and the degree of gastritis was found in both antral and fundic mucosa. In six cases labelling indices estimated by cell counts performed on longitudinal or cross sections of foveolae were compared. There was no significant difference between the results obtained by the two different counting techniques.

Key words: Gastric mucosa, gastritis, cell division, autoradiography, ^3H thymidine.

O Hart Hansen, Department of Surgery D, Bispebjerg Hospital, DK-2400 Copenhagen NV, Denmark.

Received 3 xi 78 Accepted 8 i 79

The role of cell proliferation has in recent years become an increasingly important segment of research in digestive diseases (7). The technique of *in vitro* labelling with ^3H thymidine of mucosal biopsy specimens in combination with autoradiography has been found useful in studying cell proliferation kinetics in human gastric mucosa (3, 10, 18). In the autoradiographs the percentage of DNA synthesizing cells in the progenitor cell region (labelling index) can be estimated. The labelling index is approximately proportional to the proliferation rate of the cell population. On the assumption that the duration of the DNA synthetic phase (S phase) does not differ in the patients studied, The duration of S-phase seems to be fairly constant, but detailed

measurements have only been carried out in a limited number of subjects (2, 3, 14, 22). *In vivo* measurements derived from labelled mitosis curves have been performed in a few seriously ill patients (14, 22), but because of ethical considerations *in vivo* labelling with DNA-precursors generally must be

and using a similar *in vitro* double labelling technique it was possible for Bleiberg et al (2) and Castrop & Fuchs (3) to measure the S phase duration in human gastric mucosa. In a preliminary study we tried to estimate the S-phase duration in gastroscopic biopsies, using double labelling techniques with successive incubation with ^3H -thymidine

- lium transformed in vitro *B J Cancer* 37 240, 1978
- Ganten, D., Schelling, P. & Ganten U* Tissue isorenins. In Genest J., Koiw, E. & Kurchel, O. Hypertension, New York 1977 p 240
- Hoshino, A. & Chung Der Lin* Hyperplasia-inducing factor in mouse salivary gland isografts *Cancer Res* 28 2556-2558, 1968
- Menzie, J. W., Michelakis A. M. & Yoshida, H* Sympathetic nervous system and renin release from submaxillary glands and kidneys *Amer J Physiol* 227 1281-1284, 1974
- Pearse, A. E. G.* Histochemistry, 3 ed vol 1 J & A Churchill, London 1968
- Poulsen A. & Jorgensen J* An easy radioimmunological microassay of renin activity, concentration and substrate in human and animal plasma and tissues based on angiotensin I trapping by antibody *J Clin Endocrinol Metab* 39 816-825 1974
- Werle, E., Vogel R. & Goldel, L. F.* Über ein blutdrucksteigerndes Prinzip in Extrakten aus der Glandula Submaxillaris der weissen Maus *Arch. exp. Path. Pharm* 230 236 1957

CELL PROLIFERATION IN NORMAL AND DISEASED GASTRIC MUCOSA

Autoradiography after in vitro Continuous Labelling with Tritiated Thymidine

O. HART HANSEN, A. A. JOHANSEN, J. K. LARSEN and L. B. SVENDSEN

Departments of Surgical Gastroenterology and Pathology Bispebjerg Hospital and Finsen Laboratory
Finsen Institute Copenhagen Denmark

Hart Hansen O, Johansen Aa, Larsen J K & Svendsen L B. Cell proliferation in normal and diseased gastric mucosa. Autoradiography after *in vitro* continuous labelling with tritiated thymidine. *Acta path microbiol scand Sect A* 87 217-222 1979.

The rate of gastric epithelial cell proliferation was studied in healthy volunteers and in patients with different degrees of gastritis. Endoscopic biopsies from the antral and fundic part of the stomach were incubated *in vitro* with ^3H thymidine for 30, 120 and 210 minutes respectively. Autoradiographs were prepared and the percentage of DNA synthesizing cells (labelling index) in the progenitor cell region was estimated. From the successive labelling indices the rate of entry of cells into DNA synthetic phase (S phase) and the duration of the S-phase could be estimated. All the biopsies were classified according to the degree of gastritis. The mean (\pm SEM) length of the S phase was found to be 7.4 ± 0.3 hours in antral mucosa and 7.2 ± 0.4 hours in fundic mucosa. There was no significant difference between the S phase duration in normal mucosa, superficial gastritis, mild atrophic gastritis and severe atrophic gastritis. This observation suggests that the labelling index can be used as an expression for the rate of cell proliferation in human gastric mucosa. A significant correlation between the labelling indices and the degree of gastritis was found in both antral and fundic mucosa. In six cases labelling indices estimated by cell counts performed on longitudinal or cross sections of foveolae were compared. There was no significant difference between the results obtained by the two different counting techniques.

Key words: Gastric mucosa, gastritis, cell division, autoradiography, ^3H thymidine.

O. Hart Hansen, Department of Surgery II, Bispebjerg Hospital, DK-2400 Copenhagen NV, Denmark.

Received 3 xi 78 Accepted 8 i 79

The role of cell proliferation has in recent years become an increasingly important segment of research in digestive diseases (7). The technique of *in vitro* labelling with ^3H thymidine of mucosal biopsy specimens in combination with autoradiography has been found useful in studying cell proliferation kinetics in human gastric mucosa (3, 10, 18). In the autoradiographs the percentage of DNA synthesizing cells in the progenitor cell region (labelling index) can be estimated. The labelling index is approximately proportional to the proliferation rate of the cell population on the assumption that the duration of the DNA synthetic phase (S phase) does not differ in the patients studied. The duration of S phase seems to be fairly constant but detailed

measurements have only been carried out in a limited number of subjects (2, 3, 14, 22). *In vivo* measurements derived from labelled mitosis curves have been performed in a few seriously ill patients (14, 22) but because of ethical considerations *in vivo* labelling with DNA precursors generally must be avoided in man. In dog gastric mucosa Willems *et al.* (21) demonstrated good agreement between *in vivo* and *in vitro* estimates of the kinetic parameters and using a similar *in vitro* double labelling technique it was possible for Bleiberg *et al.* (2) and Castrop & Fuchs (3) to measure the S phase duration in human gastric mucosa. In a preliminary

- lium transformed in vitro **B** *J Cancer* 37 240 1978
- Ganten D Schelling P & Ganten U* Tissue isorenins In Genest J Koiv E & Kurchel O Hypertension New York 1977 p 240
- Hoshino K & Chung Der Lin* Hyperplasia inducing factor in mouse salivary gland isografts *Cancer Res* 28 2556-2558 1968
- Menzie J B Michelakis A M & Yoshida H* Sympathetic nervous system and renin release from submaxillary glands and kidneys *Amer J Physiol* 227 1281-1284 1974
- Pearse A E G* Histochemistry 3 ed vol 1 J & A Churchill London 1968
- Poulsen K & Jørgensen J* An easy radioimmunochemical microassay of renin activity concentration and substrate in human and animal plasma and tissues based on angiotensin I trapping by antibody *J Clin Endocrinol Metab* 39 816-825 1974
- Werle E Vogel R & Goldel L F* Über ein blutdrucksteigerndes Prinzip in Extrakten aus der Glandula Submaxillaris der weissen Maus *Arch exp Path Pharm* 230 236 1957

index. This error was reduced by use of a previously described equation for correction (11, 12)

Continuous Labelling

In the 3 volunteers and in 11 of the patients 3 antral and 3 fundic biopsies were taken near each other. In 2 other patients with Menetrier's disease only biopsies from the fundic part were obtained. The biopsies were incubated with ^3H thymidine for 30, 120 and 210 minutes respectively and the labelling indices were estimated as described above. From this continuous labelling experiment the rate of entry of cells into S-phase could be estimated as the slope (r_s) of a regression line based on the three successive labelling indices. When only two biopsies were suitable for counting the regression was based on the labelling indices of the two specimens. The duration of S (T_s) was then calculated from the formula for a steady state situation

$$T_s = \text{LI}/r_s$$

where LI = the initial labelling index which measures the fraction of cells in S phase at any time (1)

The turnover time (T_{ot}) which is defined as the time taken for all cells in a given population to be replaced (1) was then calculated from the equation

$$T_{ot} = T_s/\text{LI} \times 100$$

Blind evaluation of the autoradiographs for morphological analysis was performed by one of the authors (a J) and the histological classification was carried out as described before (10). Both in antral and fundic mucosa the degree of gastritis was classified into 4 groups: 1) normal gastric mucosa, 2) superficial gastritis, 3) mild atrophic gastritis and 4) severe atrophic gastritis.

Comparison of Counting Procedures

The labelling indices estimated by cell counts performed on cross sections and longitudinal sections of

foveolae were compared in fundic mucosa from 6 patients. In each patient 5 endoscopic biopsies were taken near each other in the fundic part of the stomach. After incubation for 30 minutes with ^3H thymidine 2 of the biopsies were treated and cell counts performed as described above. The remaining biopsies were carefully oriented under a dissecting microscope so that serial sectioning could be carried out parallel to the direction of the gastric pits. In these specimens the number of labelled cells and the total number of cells in the proliferation compartment (= progenitor cell region) were counted as described by Lipkin *et al.* (14). The approximate boundaries of the proliferation compartment are defined by the location of the uppermost and the lowest labelled cells in the crypt cell column.

Statistical Analysis

For statistical evaluation an analysis of variance, the Mann-Whitney rank sum test and the Wilcoxon test for pair differences were used.

RESULTS

The labelling index. For this reason T_s could not be measured in antral mucosa from one of the patients. The S phase duration in antral and fundic mucosa according to histological classification is noted in Tables 1 and 2. The range of T_s was rather wide (5.5–10.8 hours) but there was no statistically significant difference between T_s in the different groups of gastritis or between T_s in antral and fundic mucosa. In contrast the labelling indices were significantly enhanced with increasing degrees of gastritis in both types of mucosa ($p < 0.01$). As a result the turnover time was found to be shorter in

TABLE 1 Initial Labelling Index (LI), S phase Duration (T_s) and Turnover Time (T_{ot}) in Antral Mucosa*

Histological classification	No. of subjects	LI (per cent)	T_s (hours)	T_{ot} (hours)
Normal mucosa	3	11.7 ± 0.5	7.6 ± 0.3	85.4 ± 2.5
Superficial gastritis	7	11.3 ± 0.7	6.9 ± 0.3	62.6 ± 5.4
Mild atrophic gastritis	2	14.9 ± 0.4	7.6 ± 0.2	51.1 ± 2.9
Severe atrophic gastritis	1	19.4	10.0	51.8
Total	13	—	7.4 ± 0.3	—

* Results are means \pm SEM

and ^{14}C thymidine or with a weak and a high dose of ^3H -thymidine as described by Bleiberg *et al* (2). Unfortunately, we found it extremely difficult to distinguish between the differently labelled cells.

In experimental investigations on different tissues the method of continuous labelling with ^3H -thymidine has been found well suited for estimation of the kinetic parameters (1, 17). The present autoradiographic study was performed in order to estimate the S phase duration in human antral and fundic mucosa with different degrees of gastritis after *in vitro* continuous labelling of endoscopic biopsies. Furthermore, labelling indices estimated by cell counts performed on longitudinal or cross sections of foveolae were compared.

MATERIAL AND METHODS

After informed consent 3 healthy volunteers and 19 patients were studied. There were 9 women and 13 men with ages ranging from 22 to 72 years. In all subjects gastroscopy was performed in the morning after 12 hours of fasting using a fiberoptic gastroscope (Olympus GIF D or GIF K). Through the gastroscope biopsies were obtained from the lesser curvature in the antral part of the stomach (2 cm above the pylorus) and from the greater curvature high in the fundic part.

Autoradiographic Procedure

The specimens were immediately incubated in a shaking water bath at 37°C in 5 ml of Eagle's basal medium with Hanks salts (Flow Laboratories, Rockville, USA) containing $20\text{ }\mu\text{Ci}$ per ml of ^3H -thymidine (Radiochemical Centre, Amersham, England, specific activity 22–26 Ci per mmole). The pH was adjusted to 7.3–7.4 with sodium bicarbonate. After incubation for 30 minutes the biopsies were washed in unlabelled medium for 10 minutes, fixed in Bouin's solution for one hour, embedded in paraffin and serially sectioned in $4\text{ }\mu\text{m}$. The slides were then coated with liquid photographic emulsion (Ilford K) exposed for two weeks at 4°C , developed and stained with haematoxylin and eosin.

In the autoradiographs (Fig. 1) the background labelling was random and low, rarely exceeding 1 grain per $100\text{ }\mu^2$. The cells were considered labelled if they had 5 or more grains over the nucleus. The number of labelled cells as well as the total number of cells in all cross sections of foveolae containing one or more labelled cells were counted blindly. Every third section of the serially sectioned biopsy material was surveyed. In each specimen a minimum of 1000 cells was counted and the percentage of labelled cells (labelling index) was estimated. When only cross sections containing labelled cells are taken into consideration the labelling index will be overestimated because those cross sections through the progenitor cell region that do not have labelled cells will not be included in the estimation of the labelling

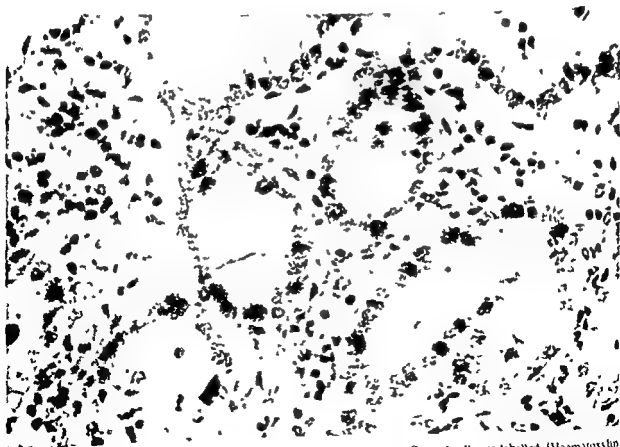


Fig. 1. Autoradiograph of an endoscopic biopsy of human gastric mucosa. Several cells are labelled (Haematoxylin and eosin $\times 250$).

duration for determination of the length of the S phase is based on the assumption that the cell population is asynchronous and that the maximal time of incubation is less than the duration of $G_2 + M$ -phase - otherwise some of the labelled cells will have divided. The first assumption seems to be fulfilled by a lack of circadian rhythm as found in canine and human gastric mucosa (12, 20) indicating the asynchronous nature of the proliferating

epithelial cell population within the stomach. The duration of $G_2 + M$ -phase has been estimated to be 1-4 hours in human fundic mucosa (3, 7) and 6 hours in intestinalized gastric mucosa (22). In the present study no labelled mitoses were observed suggesting a G_2 -duration of more than 3 hours which means that the second assumption also is met. The presence of radioactive thymidine may disturb the cell cycle by a delay or arrest of the cells in G_2 and M-phase (8, 15) which to some degree could explain the lack of labelled mitoses. However, the increase in labelling index from 120 to 210 minutes of incubation with 3H thymidine was similar to the increase from 30 to 120 minutes indicating that the rate of entry of cells into S phase remained unaffected.

The duration of S phase in the epithelial cells of the fundus has been reported to be within the range of 7-10 hours; the latter is an *in vivo* measurement derived from a labelled mitosis curve (14) while the shorter periods were obtained using *in vitro* double labelling techniques (2, 3). The 7 hour S phase found in the present study is in agreement with these results. There was no significant difference between the S phase duration in the patients studied, which accords with previous observations (3, 7) and suggests that the labelling index can be used as an expression for the rate of cell proliferation.

A significantly greater number of cells synthesizing DNA and a higher mitotic activity have been observed in the pyloric antrum as compared to the fundic mucosa (11, 12, 13). Thus the similar S-phase duration found in the two types of mucosa may signify a more rapid cell turnover in antral than in fundic mucosa.

If observations can be sufficiently prolonged continuous labelling may be used to determine the growth fraction of a cell population (1). Unfortunately the ability of human gastric mucosa to survive in culture systems is limited and the glandular elements show degenerative changes by 12 hours (19) suggesting that *in vitro* continuous labelling cannot be prolonged sufficiently for this purpose. Since the growth fraction of the progenitor cells in human gastric mucosa is unknown the cell cycle duration cannot be calculated. Instead the turnover

time which represents the time required for the total replacement of a number of cells equal to that initially present in the tissue was estimated in this study.

In chronic atrophic gastritis a gradual disappearance of parietal and chief cells from the gastric mucosa is typical (4, 9). Atrophic gastritis is associated with a high epithelial cell loss (5) and as in previous investigations (7, 10) an enhanced rate

finding that maximal acid output decreases with increasing rates of cell proliferation (10). These observations may indicate that an important part of the mechanisms underlying atrophic gastritis is a severe cell loss which does not permit the normal cell maturation and differentiation. In patients with atrophic gastritis Chiao & Weisberg (4) found no specific ultrastructural changes in the parietal or chief cells suggesting that the loss of these cells takes place into the lumen of the stomach.

Previous autoradiographic studies demonstrated that the DNA-synthesizing cells in normal fundic mucosa are situated in the base of the gastric pits and in the lower part of the

the present investigation.

The labelling indices estimated in cross sections of foveolae were similar to those measured by *Castrup & Fuchs* (3) in longitudinal sections of foveolae. However in the endoscopic biopsies we found it rather difficult to obtain a sufficient number of well-oriented longitudinally cut gastric pits and glands for accurate estimation of the labelling index. Therefore we prefer to estimate the number of DNA synthesizing cells in cross sections of foveolae. Using this method cell counts are easy to perform, the observer variance is small and the results are reproducible (11). The similar results obtained by the two different counting techniques suggest that both methods can be used in the study of cell proliferation kinetics in human gastric mucosa and that the results of such studies can be compared.

REFERENCES

1. Aherne W A, Camplejohn R S & Wright N A. An Introduction to Cell Population Kinetics. Edward Arnold, London, 1977, p 37.
2. Bleiberg H, Ma nguei P, Vandenhende J & Galand P. Mesure autoradiographique de la

TABLE 2 Initial Labelling Index (LI) S phase Duration (T_s) and Turnover Time (T_{α}) in Fundic Mucosa*

Histological classification	No of subjects	LI (per cent)	T_s (hours)	T_{α} (hours)
Normal mucosa	3	10.0 ± 1.4	6.1 ± 0.6	62.7 ± 7.9
Superficial gastritis	4	10.5 ± 0.8	7.6 ± 1.1	75.3 ± 15.0
Mild atrophic gastritis	4	12.6 ± 0.6	7.8 ± 0.8	62.9 ± 7.1
Severe atrophic gastritis	3	17.3 ± 0.6	6.5 ± 0.2	37.6 ± 7.1
Mb Menetrier	2	16.6 ± 3.4	7.6 ± 0.3	48.3 ± 11.8
Total	16	—	7.2 ± 0.4	—

* Results are means \pm SEM

TABLE 3 Labelling Indices (LI) Estimated on Basis of Cell Counts Performed on Longitudinal and Cross Sections of Foveolae in Human Fundic Mucosa

Patient	Histological diagnosis	Longitudinal sections		Cross sections	
		Total cell count	LI (%)	Total cell count	LI (%)
RB	Normal mucosa	789	11.0	1678	9.8
WA	Superficial gastritis	742	10.3	1851	11.4
HB	Severe atrophic gastritis	837	17.2	1424	19.9
TM	Severe atrophic gastritis	676	14.1	1647	14.7
AR	Superficial gastritis	924	11.4	2034	10.6
EO	Superficial gastritis	596	10.2	1894	12.6
Mean		761	12.4	1754	13.2

* The labelling indices measured in cross sections of foveolae are corrected by a previously described equation for correction (10, 12)

atrophic gastritis and Menetrier's disease than in normal gastric mucosa. Labelled mitoses were not observed in any of the biopsies and parietal and chief cell labelling was not seen.

In Table 3 the labelling indices estimated on the basis of cell counts in longitudinal and cross sections of foveolae are compared. Measurements in gastric pits oriented longitudinally from the surface down to the fundic glands were based on a smaller number of cells. Furthermore, the lowest portion of the progenitor cell region appeared in cross section in most of the specimens and therefore the «longitudinal» counts were incomplete to some degree. Nevertheless, there was no significant difference between the results obtained by the different counting procedures. In normal mucosa and in

superficial gastritis labelled cells were found at the bases of the gastric pits and in the isthmuses of the glands and only few labelled cells were seen in the midportion of the pits. In atrophic gastritis the progenitor cell region was extended and included labelled surface epithelial cells.

DISCUSSION

The present results indicate that the biopsy specimens kept their proliferative characteristics during the time of incubation and suggest that *in vitro* continuous labelling can be used for estimation of the kinetic parameters in human gastric mucosa. The method of continuous labelling of short

BRIEF REPORT

INFANTILE VAGINAL TUMOUR WITH ALPHA FETOPROTEIN SYNTHESIS

B Nørgaard Pedersen¹⁾ C J Lundborg²⁾ A M Laurson¹⁾ and I Hagerstrand¹⁾

¹⁾ Department of Clinical Chemistry Sønderborg Hospital Sønderborg ²⁾ Institute of Pathology and
³⁾ Department of Paediatric Diseases Odense University Hospital Odense Denmark

Nørgaard Pedersen B Lundborg C J Laurson A M & Hagerstrand I Infantile vaginal tumour with alpha Fetoprotein synthesis Acta path microbiol scand Sect A 87 223-226 1979

A 17 month old girl with a vaginal embryonal carcinoma (germ cell tumour) is reported. Alpha fetoprotein (AFP) was elevated before treatment in blood and vaginal fluid. Normal levels of AFP in blood and vaginal fluid were found after radiation and combination chemotherapy. By an indirect immunoperoxidase staining AFP was demonstrated in tumour tissue. 24 month-old local recurrence was preceded by a slight increase in serum AFP and AFP could also be demonstrated in vaginal fluid and vaginal smears.

Key words: Infantile vaginal tumour, endodermal sinus tumour, alpha fetoprotein.

B Nørgaard Pedersen, Department of Clinical Chemistry, Sønderborg Hospital, DK 6400 Sønderborg, Denmark.

Received 2 x 78 Accepted 21 x 79

Endodermal sinus tumour (EST) (yolk sac tumour) is a rather rare and clinically highly malignant tumour occurring in both the gonads (ovary and testis) and in various extragonadal sites.

The EST concept was first described by Teilmann in 1959 and was further developed in his fundamental studies in 1965 and 1971 about the histogenetic relationship and classification of these germ cell tumours. Recently it has been shown that gonadal and extragonadal germ cell tumours may produce AFP and/or human chorionic gonadotropin (HCG) (5, 6). Presence of vitelline components in the tumour tissue seems to be the cause of the AFP synthesis, whereas the HCG production is closely correlated to the presence of choriocarcinoma elements or so-called 'giant cells' in the tumour. 17 cases of typical infantile vaginal ESTs have previously been reported (1, 2, 3, 4). Atha *et al* (1) reported one case and quoted 12 others from the literature thought to be ESTs instead of clear cell carcinomas, with which they were previously often confused. Gibson (2) has briefly described three cases and Rich *et al* (3) recently mentioned a consultation case of a vaginal EST tumour in a 10 month-old infant where serum AFP was positive before excision of the tumour and negative afterwards.

The present study refers to a case of infantile vaginal tumour with increased levels of AFP in blood and vaginal fluid before treatment. Normal levels were found

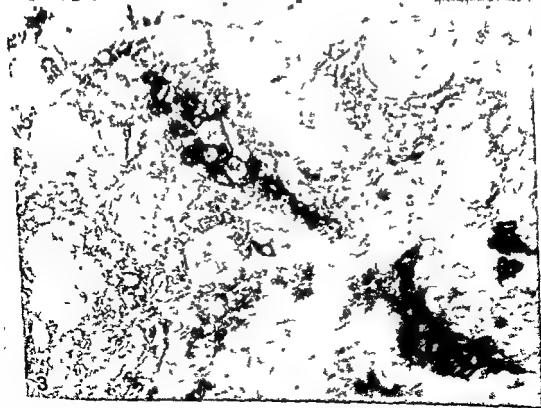
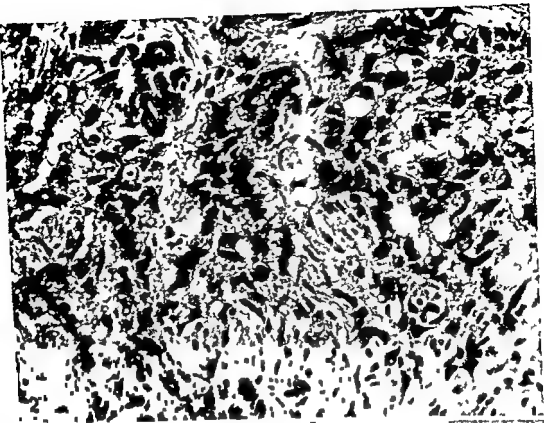
during treatment. Local recurrence of the tumour was forewarned by increased levels of AFP in both blood, and vaginal fluid.

Material and Methods

Serum, urine and a few samples of vaginal fluid and faeces were taken before treatment after radiation therapy and during the combination chemotherapy regime. The samples were either analysed immediately or stored at -20° C. A tumour tissue biopsy was also performed before therapy and smears were obtained after recurrence of the tumour.

was especially suitable for longitudinal profile studies of several sera from the same patient but also for demonstration of AFP in tumour tissue specimens, i.e. radioimmuno-electrophoresis (RRIE). RRIE was carried out as described elsewhere (5) and RRIE was carried out on the same gel plates by placing the microscopic slides directly upon the RRIE gel plate.

- proliferation cellulaire a differents niveaux du tractus digestif normal et pathologique Rev Europ Etud Clin Biol 16 233-239 1971
- 3 *Castrup H J & Fuchs A* Zur Zellerneuerung bei entzündlichen Magenschleimhautveränderungen Dtsch med Wschr 99 892-895 1974
- 4 *Chiao S F & Weisberg H* Ultrastructure of the gastric mucosa in patients with atrophic gastritis and pernicious anemia Gastroenterology 59 36-45 1970
- 5 *Craft D N & Cotton P B* Gastro Intestinal Cell Loss in Man Digestion 8 144-160 1973
- 6 *Deschner E E Winawer S J & Lipkin M* Patterns of Nucleic Acid and Protein Synthesis in Normal Human Gastric Mucosa and Atrophic Gastritis J Nat Cancer Inst 48 1567-1574 1972
- 7 *Deschner E E & Lipkin M* Proliferation of Epithelial Cells of the Gastrointestinal Tract in Cancer and Related Diseases In Glass G B J (Ed) Progress in Gastroenterology vol 3 Grune & Stratton New York 1977 pp 53-72
- 8 *Ehmann U A Williams J R Nagle W A Brown J A Belli J A & Lett J T* Perturbations in cell cycle progression from radioactive DNA precursors Nature 258 633-636 1975
- 9 *Faber A* Gastritis and its consequences Oxford University Press London 1935
- 10 *Hansen O Hart Johansen Aa Larsen J A Pedersen T & Svendsen L B* Relationship between gastric acid secretion histopathology and cell proliferation kinetics in human gastric mucosa Gastroenterology 73 453-456 1977
- 11 *Hansen O Hart Pedersen T & Larsen J K* A method to study cell proliferation kinetics in human gastric mucosa Gut 16 23-27 1975
- 12 *Hansen O Hart Pedersen T & Larsen J A* Cell proliferation kinetics in normal human gastric mucosa Gastroenterology 70 1051-1054 1976
- 13 *Liang I* Mitotic activity of gastric mucosa Acta path microbiol scand 72 43-63 1968
- 14 *Lipkin M Sherlock P & Bell B* Cell proliferation in the gastrointestinal tract of man II Cell renewal in stomach ileum colon and rectum Gastroenterology 45 721-729 1963
- 15 *Marz R Zylka J M Plagemann P G W Erle J Howard R & Sheppard J R* G₂ + M arrest of cultured mammalian cells after incorporation of tritium labelled nucleosides J Cell Physiol 90 18 1977
- 16 *McDonald W C Trier J S & Everett A B* Cell proliferation and migration in the stomach duodenum and rectum of man radioautographic studies Gastroenterology 46 405-417 1964
- 17 *Potten C S Kovacs L & Hamilton E* Continuous labelling studies on mouse skin and intestine Cell Tissue Kinet 7 271-283 1974
- 18 *Tanaka J* Autoradiographic studies on the cell proliferation of the human gastric mucosa in supravital condition Acta Path Jap 18 307-317 1968
- 19 *Trier J S* Organ-culture methods in the study of gastrointestinal mucosal function and development N Engl J Med 295 150-155 1976
- 20 *Willems G* Factors controlling cell proliferation in gastroduodenal mucosa In Glass G B J (Ed) Progress in gastroenterology vol 3 Grune & Stratton New York 1977 pp 29-51
- 21 *Willems G Galand P & Chretien J* Autoradiographic studies on cell population kinetics in the gastric and rectal mucosa A comparison between *in vitro* and *in vivo* methods Lab Invest 23 635-639 1970
- 22 *Winawer S J & Lipkin M* Cell proliferation kinetics in the gastrointestinal tract of man IV Cell renewal in the intestinalized gastric mucosa J Nat Cancer Inst 42 9-17 1969



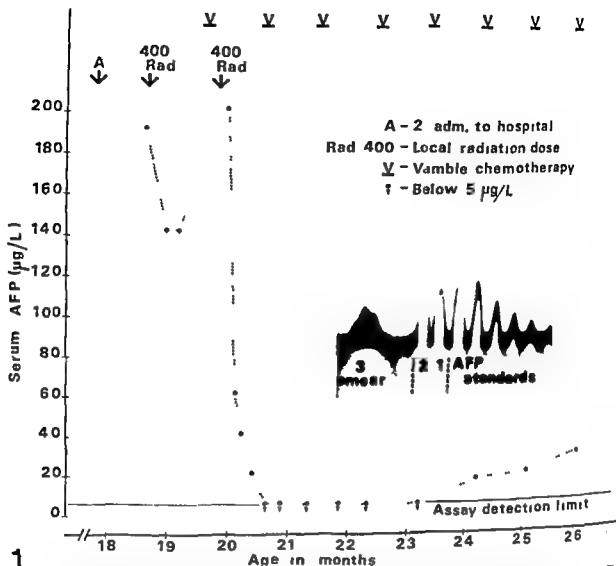


Fig 1 Serial AFP levels in a 17 month old girl with a primary vaginal tumour before and during treatment. The upper AFP limit of the normal range in adults is 20 µg/l. The detection limit of the PEG RIA is 5 µg/l. Inset: Autoradiography of radiorocket immunoelectrophoresis of 1 Serum before treatment (160 µg/l), 2 Vaginal fluid before treatment (720 µg/l) and 3 A vaginal smear obtained after tumour recurrence.

Immunohistochemical staining procedure for demonstration AFP was carried out as a three layer bridge technique according to the method of Palmer *et al* (7) for alpha₁ antitrypsin and AFP. Staining controls were performed with non immune rabbit sera. First antibody: Rabbit immunoglobulins against human alpha₁ fetoprotein (10-008). Second antibody: Swine immunoglobulins against rabbit serum IgG (21-090). Third antibody: DAKO PAP (horseradish peroxidase rabbit antiperoxidase complexes (Z 113). The first antibody was used in dilution 1/20 and the second and third antibodies in dilution 1/50. The antibodies are commercially available (Dako Immunoglobulins, Copenhagen).

Case Report

The patient was a 17 month-old girl admitted to hospital because of recurrent vaginal bleeding. She was born at term after an uncomplicated pregnancy. Birth weight 4300 g, length 55 cm. Her medical history was unremarkable until 15 months old. She was then admitted to the regional hospital because of bloodstaining of the diaper. A urinary tract infection was diagnosed and treated 2 months later. The patient again was submitted to hospital because of recurrent vaginal bleeding. At physical examination she appeared normal, developed and in good health. At gynecological examination in general anesthesia a 1 × 1½ cm tumour was

Fig 2 The tumour showed infiltrating cords of epithelial cells. Hc × 375

Fig 3
cords

in some tumour

PRIMARY CARCINOMA OF THE LIVER

A Histological Study of 52 Cases from Denmark

KAI NØRREDAM

Medical Department F Glostrup Hospital DK 2600 Glostrup

Nørredam Kai Primary carcinoma of the liver. A histological study of 52 cases from Denmark. Acta path microbiol scand Sect. A 87 227-236 1979

Among 7763 autopsies performed in Greater Copenhagen in 1973 there were 309 cases of cirrhosis of the liver and 52 cases of primary carcinoma of the liver (PCL). Of the latter 45 were hepatocellular carcinoma (HCC), 4 combined HCC and cholangiocarcinoma (CCC) and 3 CCC. HCC was found in 7.8 per cent of the cirrhotic livers and was in 57.1 per cent accompanied by cirrhosis. The criteria of WHO, Peters (modified) and Anthony were used for classification. The degree of differentiation of the tumours was estimated using the criteria of WHO and Edmondson. The apparently small number of CCC may be due to the fact that this tumour is often overdiagnosed at the expense of HCC. The incidence of combined tumours is probably higher than generally assumed. The reticulin stain was found very valuable in HCC both for descriptive and diagnostic purposes. In contrast to the situation in sub-Saharan Africa where hepatitis B virus is incriminated as the most important etiologic factor of HCC, it was found in the present study that alcoholism was a very essential cause of cirrhosis and thereby of HCC.

Key words: Primary carcinoma of the liver, cirrhosis, Denmark.

K. Nørredam, Medical Department F, Glostrup Hospital, DK 2600 Glostrup, Denmark.

Accepted as submitted 21/79

During the last two decades several methods of classifying primary carcinoma of the liver (PCL) have been proposed. Newest and most applied are the ones by WHO (Anthony *et al* 1978), Anthony (1973) and Peters (1976). The purpose of the present investigation is to describe the histological and cytological structure of PCL in a material from Denmark and use these 3 classifications. Further to evaluate the relation of PCL to cirrhosis and finally to correlate the findings with the results of a similar study from Malawi in South East Africa (Nørredam 1977 B).

MATERIAL AND METHODS

The study was carried out in the Department of Pathology, Glostrup Hospital, Denmark. The material consisted of 52 cases of primary carcinoma of the liver, which had been referred to the Department of Pathology for histological examination. The cases were selected from the files of the Department of Pathology, Glostrup Hospital, Denmark, for the period 1970-1978.

embedded in paraffin, sectioned and stained with the following techniques: Haematoxylin and eosin (H & E), van Gieson, Hansen periodic acid-Schiff (PAS) before and after digestion with diastase and staining for reticulin (Gordon & Sweet 1936), iron (Perls 1867), copper (Lillie & Fullmer 1976) and orcein (Shikata *et al* 1974). In some cases Alcian blue staining was used.

The hepatocellular carcinomas were typed according to WHO's criteria (Anthony *et al* 1978) (Table 1) to a modification of Peters' method (Peters 1976) (Table 2) and according to Anthony (1973). The degree of differentiation of the tumours was estimated using the criteria described by WHO (Anthony *et al* 1978) and Edmondson (1958) (Table 3).

The cholangiocarcinomas were typed according to WHO's classification (Anthony *et al* 1978).

Cirrhosis was recorded in cases where the liver was changed by a diffuse process characterized by fibrosis and replacement of the normal liver tissue by structurally abnormal nodules in accordance with WHO's criteria (Anthony *et al* 1977).

The following changes in the parenchyma were graded from 0 (not recognizable) to + + + + inflammation.

found projecting from the posterior vaginal wall 1 cm above the introitus. There were no signs of local infiltration outside the vagina. The tumour was whitish and friable. Secretions from the tumour were collected by washing of the vaginal lumen with 4 ml of sterile saline and a biopsy specimen was taken. Further investigations did not show distant metastases. Before treatment elevated levels of serum AFP were found (160 µg/l) (Fig. 1). Serum human chorionic gonadotropin was normal. AFP was also markedly high (720 µg/l) in the 4 ml fluid obtained by the vaginal washing procedure (Fig. 1) but was not found in faeces or urine. It was decided to avoid mutilating surgery and the patient was therefore treated with local radiotherapy (400 + 400 rad) and combination chemotherapy with VAMBLE (Vinblastin, Actinomycin D, Methotrexate and Bleomycin). During treatment the serum AFP level fell below detection limit. At 24 months of age a slight increase in serum AFP was found and a further increase was observed two months later (Fig. 1). AFP could also be demonstrated in the vaginal fluid (45 µg/l) and in vaginal smears (Fig. 1). These findings were interpreted as indicative of a local tumour recurrence. However it was not possible to demonstrate local recurrence nor distant metastases by clinical examination, by X-ray examination or by Co 57 bleomycin scintigraphy. The Chemotherapeutic regime was changed to Vincristine, Adriablastine and Cyclofosamide.

The biopsy specimen (10 × 6 × 5 mm) from the vaginal tumour showed infiltrating cords of epithelial cells in a loose connective tissue. The border between stroma and tumour cells was not distinct and the tumour cells seemed to be poorly connected (Fig. 2). Between tumour cells vacuoles and eosinophilic substance appeared. The latter contained in periodic acid Schiff staining positive globules which were resistant to diastase and thus non-glycogenic. Immunohistochemical staining for alpha-fetoprotein was positive in such intercellular spaces and inside tumour cells next to the spaces (Fig. 3). Mitoses were not uncommon. No differentiation of tumour cells similar to endodermal sinus structures were observed but the described appearance is in agreement with a pattern which is partly seen in most endodermal sinus tumours. Diagnosis: Embryonal Carcinoma.

Discussion

In this case report of a 17 month old girl with a primary vaginal tumour AFP seems to satisfy most of

the ideal criteria of a tumour marker. AFP could be demonstrated in serum and vaginal fluid before treatment and by an immunoperoxidase staining in tumour biopsy specimens. A distinct positive staining could be obtained in several tumour cells and in the areas close to these cells. Furthermore serum AFP levels accurately predicted the clinical response as well as lack of response to therapy. During the local tumour recurrence AFP could be demonstrated again in vaginal fluid and in vaginal smears. Fig. 1 shows the importance of performing frequent serum AFP assays especially during the initial treatment, and also in the follow up period when blood AFP have become normal or below the detection limit 5 µg/l of the assay. During this period AFP estimation should be made every month. Tumour recurrence may thus be detected several months before the presence of clinical symptoms thus significantly reducing the delay of additional therapy.

In conclusion detection of AFP in blood and tissue in primary infantile vaginal germ cell tumour may give additional information about the disease activity during therapy.

This study was supported by the Danish Cancer Society and Fonden for Lægevidenskabelig Forskning ved Sygehusene i Ringkøbing Ribe og Sønderjylland Amt.

- References 1 Allyn D L, Silverberg S G & Salhen A M. Cancer 27: 1231-1238 1971 - 2 Gibson A. M. Arch. dis. childh. 48: 163 1973 - 3 Jih T, Shirai R, Naka A & Matsumoto S. Gann 65: 215 226 1974 - 4 Norris H J, Bagley G P & Taylor H B. Arch. Path. 90: 473-479 1970 - 5 Aagaard Pedersen B. Human Alpha-fetoprotein: A Review of Recent Methodological and Clinical Studies. In: Scand. J. Immunol. Vol. 5 Suppl. 4. Universitetsforlaget Oslo 1976 - 6 Aagaard Pedersen B, Albrechtsen R & Teilmann G. Acta path. microbiol. scand. Sect. A 81: 573-589 1975 - 7 Palmer P E, Safavi H and Wolfe H J. Am. J. Clin. Path. 65: 575-582 1976 - 8 Ratcliffe J G, Burt R W, Baird G M, Campbell A M, Barter D A C & Willoughby M L. N. Scand. J. Immunol. 7 Suppl. 8: 1978 - 9 Teilmann G. Cancer J. 1092-1105 1959 - 10 Teilmann G. Acta path. microbiol. scand. 64: 407-429 1965 - 11 Teilmann G. Special Tumours of Ovary and Testis. Comparative Gynecology. J B Lippincott & Co. Philadelphia 1968 - 12 G. Brit. J.

PRIMARY CARCINOMA OF THE LIVER

A Histological Study of 52 Cases from Denmark

KAI NØRREDAM

Medical Department F Glostrup Hospital DK 2600 Glostrup

Nørredam Kai Primary carcinoma of the liver A histological study of 52 cases from Denmark Acta path microbiol scand Sect A 87 227-236 1979

Among 7763 autopsies performed in Greater Copenhagen in 1973 there were 309 cases of cirrhosis of the liver and 52 cases of primary carcinoma of the liver (PCL). Of the latter 45 were hepatocellular carcinoma (HCC), 4 combined HCC and cholangiocarcinoma (CCC) and 3 CCC. HCC was found in 7.8 per cent of the cirrhotic livers and was in 57.1 per cent accompanied by cirrhosis. The criteria of WHO, Peters (modified) and Anthony were used for classification. The degree of differentiation of the tumours was estimated using the criteria of WHO and Edmondson. The apparently small number of CCC may be due to the fact that this tumour is often overdiagnosed at the expense of HCC. The incidence of combined tumours is probably higher than generally assumed. The reticulin stain was found very valuable in HCC both for descriptive and diagnostic purposes. In contrast to the situation in sub-Saharan Africa where hepatitis B virus is incriminated as the most important etiologic factor of HCC it was found in the present study that alcoholism was a very essential cause of cirrhosis and thereby of HCC.

Key words: Primary carcinoma of the liver, cirrhosis, Denmark.

K. Nørredam, Medical Department F, Glostrup Hospital, DK 2600 Glostrup, Denmark.

Accepted as submitted 2:79

During the last two decades several methods of classifying primary carcinoma of the liver (PCL) have been proposed. Newest and most applied are the ones by WHO (Anthony *et al* 1978), Anthony (1973) and Peters (1976). The purpose of the present investigation is to describe the histological and cytological structure of PCL in a material from Denmark and use these 3 classifications. Further to evaluate the relation of PCL to cirrhosis and finally to correlate the findings with the results of a similar study from Malawi in South East Africa (Nørredam 1977 B).

MATERIAL AND METHODS

The study is retrospective, comprising all the cases that came to autopsy in 1973 in the 8 institutes of pathology affiliated to the hospitals in Greater Copenhagen. One to 5 tissue blocks from liver parenchyma as well as from tumour tissue were fixed in 10 per cent formalin

embedded in paraffin, sectioned and stained with the following techniques: Haematoxylin and eosin (H & E), van Gieson, Hansen periodic acid Schiff (PAS) before and after digestion with diastase and staining for reticulin (Gordon & Sweet 1936), iron (Perls 1867), copper (Lillie & Fullmer 1976) and orcein (Shikata *et al* 1974). In some cases Alcian blue staining was used.

The degree of differentiation of the tumours was estimated using the criteria described by WHO (Anthony *et al* 1978) and Edmondson (1958) (Table 3).

The cholangiocarcinomas were typed according to WHO's classification (Anthony *et al* 1978).

Cirrhosis was recorded in cases where the liver was changed by a diffuse process characterized by fibrosis and replacement of the normal liver tissue by structurally abnormal nodules in accordance with WHO's criteria (Anthony *et al* 1977).

The following changes in the parenchyma were graded from 0 (not recognizable) to + + + + inflammation.

found projecting from the posterior vaginal wall 1 cm above the introitus. There were no signs of local infiltration outside the vagina. The tumour was whitish and friable. Secretions from the tumour were collected by washing of the vaginal lumen with 4 ml of sterile saline and a biopsy specimen was taken. Further investigations did not show distant metastases. Before treatment elevated levels of serum AFP were found (160 µg/l) (Fig. 1). Serum human chorionic gonadotropin was normal. AFP was also markedly high (720 µg/l) in the 4 ml fluid obtained by the vaginal washing procedure (Fig. 1) but was not found in faeces or urine. It was decided to avoid mutilating surgery and the patient was therefore treated with local radiotherapy (400 + 400 rad) and combination chemotherapy with *VAMBLE* (Vinblastin, Actinomycin D, Methotrexate and Bleomycin). During treatment the serum AFP level fell below detection limit. At 24 months of age a slight increase in serum AFP was found and a further increase was observed two months later (Fig. 1). AFP could also be demonstrated in the vaginal fluid (45 µg/l) and in vaginal smears (Fig. 1). These findings were interpreted as indicative of a local tumour recurrence. However it was not possible to demonstrate local recurrence nor distant metastases by clinical examination by X-ray examination or by Co⁵⁷ bleomycin scintigraphy. The Chemotherapeutic regime was changed to Vincristine, Adriablastine and Cyclophosphamide.

The biopsy specimen (10 × 6 × 5 mm) from the vaginal tumour showed infiltrating cords of epithelial cells in a loose connective tissue. The border between stroma and tumour cells was not distinct and the tumour cells seemed to be poorly connected (Fig. 2). Between tumour cells vacuoles and eosinophilic substance appeared. The latter contained in periodic acid Schiff staining positive globules which were resistant to diastase and thus non-glycogenic. Immunohistochemical staining for alpha-fetoprotein was positive in such intercellular spaces and inside tumour cells next to the spaces (Fig. 3). Mitoses were not uncommon. No differentiation of tumour cells similar to endodermal sinus structures were observed but the described appearance is in agreement with a pattern which is partly seen in most endodermal sinus tumours. Diagnosis: Embryonal Carcinoma.

Discussion

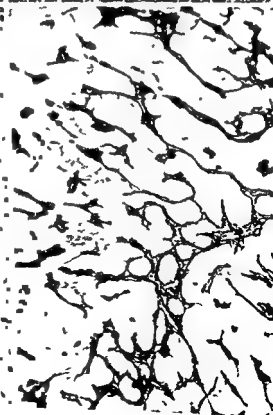
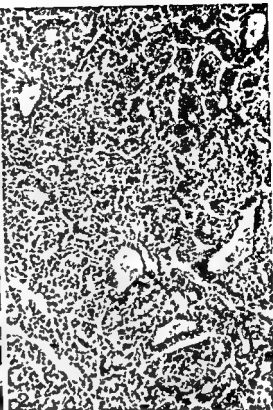
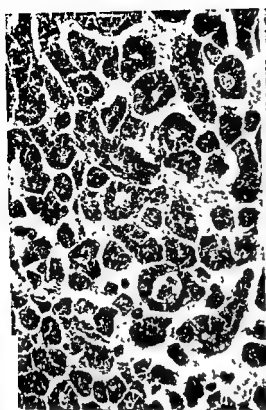
In this case report of a 17 month old girl with a primary vaginal tumour AFP seems to satisfy most of

the ideal criteria of a tumour marker. AFP could be demonstrated in serum and vaginal fluid before treatment and by an immunoperoxidase staining in tumour biopsy specimens. A distinct positive staining could be obtained in several tumour cells and in the areas close to these cells. Furthermore serum AFP levels accurately predicted the clinical response as well as lack of response to therapy. During the local tumour recurrence AFP could be demonstrated again in vaginal fluid and in vaginal smears. Fig. 1 shows the importance of performing frequent serum AFP assays especially during the initial treatment and also in the follow up period when blood AFP have become normal or below the detection limit 5 µg/l of the assay. During this period AFP estimation should be made every month. Tumour recurrence may thus be detected several months before the presence of clinical symptoms thus significantly reducing the delay of additional therapy.

In conclusion detection of AFP in blood and tissue in primary infantile vaginal germ cell tumour may give additional information about the disease activity during therapy.

This study was supported by the Danish Cancer Society and 'Fonden for Lægevidenskabelig Forskning ved sygehusene i Ringkøbing-Ribe og Sønderjylland Amt'.

- References** 1 Allyn D L, Silverberg S G & Salber A M. *Cancer* 27: 1231-1238 1971 - 2 Gibson A, M. *Arch. dis. childh.* 48: 163 1973 - 3 Itoh T, Shirai R, Naka A & Matsumoto S. *Cann.* 65: 215-226 1974 - 4 Norris H J, Bagley G P & Taylor I B. *Arch. Path.* 90: 473-479 1970 - 5 Norgaard Pedersen B. Human Alpha-fetoprotein: A Review. Recent Methodological and Clinical Studies. In: *Scand. Immunol. Vol. 5, Suppl. 4*. Universitetsforlaget, Oslo 1976 - 6 Norgaard Pedersen B, Albrechtsen R, Teilm G. *Acta path. microbiol. scand. Sect. A* 8: 573-589 1975 - 7 Palmer P E, Safavi H and Wolf H J. *Am. J. Clin. Path.* 65: 575-582 1976 - 8 Ratcliffe J G, Burt R W, Baird G M, Campbell M, Barter D A C & Willoughby M L N. *Scand. Immunol.* 7: Suppl. 8: 1978 - 9 Teilm G. *Cancer* 1: 1092-1105 1959 - 10 Teilm G. *Acta path. microbiol. scand.* 64: 407-429 1965 - 11 Teilm G. Special Tumours of Ovary and Testis. Comparative Pathology and Histological Identification. J B Lippincott Comp. 1971 and 1976 - 12 Vince J D, McManus T J, Ferguson Smith M A & Ratcliffe J G. *Brit. J. Obstet. Gynaec.* 82: 718-727 1975



tion (polymorphnuclear leucocytes, lymphocytes, plasma cells, eosinophils, total), bile duct proliferation and presence of iron in connective tissue, liver cell necroses (focal piecemeal, confluent), acidophil bodies, Mallory bodies, globular hyalin fat iron, bile intra- and extracellularly, glycogen, inflammation (polymorphnuclear leucocytes, lymphocytes, plasma cells, eosinophils, total), sinusoid dilatation, lipofuscin, nodules with dysplasia and adenomatous regeneration in the parenchyma, and tumour thrombi

Using the same grading the following changes in the tumour tissue were recorded Mallory bodies, globular hyalin, intranuclear inclusion bodies, bile intra and extracellularly, glycogen, fat necrosis haemorrhage, mitoses, the amount of collagenous and reticular connective tissue and pleomorphism

The patients' hospital files were examined, with special regard to the occurrence of alcoholism, previous acute hepatitis and hepatitis B associated surface antigen (HBsAg) in serum. Information about these 3 conditions was available in all 28 and 1 case respectively

RESULTS

Classification

The tumours were histologically classified into 45 cases of hepatocellular carcinoma (HCC), 4 cases of combined HCC and cholangiocarcinoma (CCC) and 3 of CCC

Histological Structure of HCC

HCC as well as the HCC-component of combined tumours are included in this group

Classification according to WHO According to their dominating histological features the tumour could be divided into trabecular/sinusoidal (5 cases compact (33 cases) and scirrus (1 case). Characteristically, all the tumours contained at least histological features (Table 1)

In the cases recorded as trabecular/sinusoidal the tumour tissue consisted of trabeculae covered with reticulin and endothelial cells and separated by blood-filled, sinusoidal cavities (Fig. 1). In a few specimens a small amount of collagenous fibre were seen between the endothelial cells and the tumour cells

In the pseudoglandular type, lumina with a wide range of form and size, and sometimes containing bile, were seen (Fig. 2)

A compact pattern was seen in 44 cases. In most cases, however, there were also trabecular/sinusoidal or pseudoglandular structures. The compact tumour tissue consisted of closely packed trabeculae with no intervening sinusoids covered with reticulin, and separated by collagenous connective tissue, containing few small blood vessels (Figs. 3 and 4). The amount of connective tissue varied from slight to moderate. Only 1 typical scirrus was found

TABLE 1 Distribution of 4 Histological Patterns in 49 Cases of HCC Including the HCC-components of 4 Combined Tumours After WHO (Anthony et al 1978)

	Not present	Little	Moderate	Much	All
Trabecular/sinusoidal	27	8	9	5	49
Pseudoglandular (acinar)	27	11	6	5	49
Compact	5	4	7	33	49
Scirrus	46	2	0	1	49

TABLE 2 Distribution of 9 Histological Patterns in 49 Cases of HCC Including the HCC components of 4 Combined Tumours. Modification of Peters' Classification (Peters 1976)

	Not present	Little	Moderate	Much	All
Microtrabecular	2	5	9	33	49
Macrotrabecular	30	6	8	5	49
Acinar	30	9	8	2	49
Ductal	46	3	0	0	49
Pseudoglandular	38	8	3	0	49
Adenoid	44	4	1	0	49
Papillary	48	1	0	0	49
Cirrhotomimetic	38	2	4	5	49
Connective tissue	3	27	16	3+	49

+ One of the 3 was a scirrhous

Fig 1 HCC The trabeculae are covered with endothelial cells and separated by sinusoids. Acini are seen in some of the trabeculae. WHO grade 1, Edmondson grade 2. H & E $\times 210$

Fig 2 HCC The trabeculae are separated by narrow sinusoids. Cavities are seen in some of the trabeculae, producing a pseudoglandular pattern. WHO grade 2, Edmondson grade 2. H & E $\times 210$

Fig 3 HCC The tumour tissue is compact, consisting of closely set microtrabeculae, separated by a moderate amount of collagenous connective tissue. WHO grade 1, Edmondson grade 2. H & E $\times 210$

Fig 4 HCC Same area as Fig 3. The microtrabeculae are coated with reticulin and separated by collagenous connective tissue. The reticulin is absent or extremely scarce inside the trabeculae. Reticulin stain $\times 210$

Fig 5 HCC The tumour tissue contains large amounts of collagenous connective tissue with disseminated islands and strands of malignant cells forming a scirrhous. WHO grade 3, Edmondson grade 4. H & E $\times 210$

Fig 6 HCC The tumour tissue is comprised partly of macrotrabeculae (periphery) partly of microtrabeculae (centre). Reticulin stain $\times 210$

Fig 7 HCC In this bizarre tumour the H & E gives the impression of almost complete lack of structure. WHO grade 3, Edmondson grade 3. H & E $\times 210$

Fig 8 HCC Same area as Fig 7. The tumour tissue forms a conspicuous microtrabecular pattern. Reticulin stain $\times 210$

while in 2 other cases small scirrus areas were seen (Fig 5).

Classification according to Peters A slight modification of this classification was used (Table 2). The tumour tissue was always composed of trabeculae, usually 2 to 10 cells wide (microtrabeculae) (Figs 3 and 4) but sometimes up to 100 cells thick (macrotrabeculae) (Fig 6). They were always

coated with reticulin which was absent or extremely scarce inside the trabeculae. In case of macrotrabeculae this gave a reticulin-deficient all over impression, strongly contrasting with benign liver parenchyma.

In anaplastic and highly pleomorphic tumours where H & E gave the impression of complete lack of structure the reticulin stain showed a distinctly trabecular pattern (Figs 7 and 8).

Structures with cavities may, according to Peters (1976) be divided into acinar, ductal, pseudoglandular and adenoid, which were all represented in the present material (Table 2). One tumour contained areas with a papillary structure.

Eleven tumours were more or less cirrhotomimetic.

Classification according to Arthory The tumours could be divided into hepatic (35 cases), adenoid (6 cases), pleomorphic (4 cases), clear-cell (3 cases) and scirrus types (1 case).

Other Features In a number of cases, at the border between parenchyma and tumour, trabeculae were seen which at one end consisted of cells that showed signs of malignancy and at the other end consisted of cells without such signs (Fig 9). The reticulin stain showed that these trabeculae were continuous (Fig 10). In some cases the transition between cells with and cells without criteria of malignancy was abrupt, in others more inconspicuous.

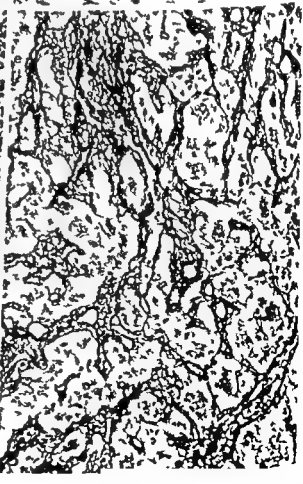
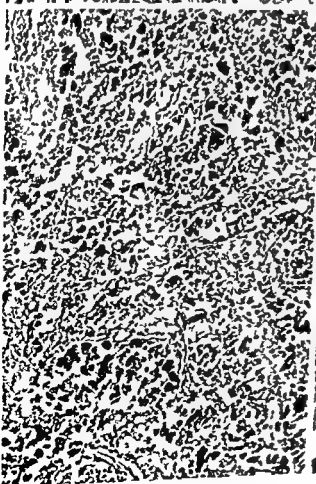
In 33 cases necroses were seen that affected larger parts of the tumour tissue at random. Besides, very frequently necroses were observed that were localized to the central parts of the trabeculae.

Haemorrhages of various size were seen in the tumour tissue in 8 cases. Tumour thrombi were found in the veins of parenchyma in 15 cases. Peliosis like areas were observed in 1 case.

The lack of inflammatory reaction in the tumour tissue was characteristic. However, in 1 case there

TABLE 3 The Grade of Differentiation of 45 Cases of HCC and 3 of CCC. In the 4 Cases of Combined Tumours both Components are Included. An Account of Edmondson's Criteria Has Been Given in a Previous Work (Nørredam 1977 B)

		Grade 1	Grade 2	Grade 3	Grade 4	All
HCC	WHO	17	22	10		49
	Edm	7	III	18	5	49
CCC	WHO	1	5	1		7
	Edm	1	3	3	0	7



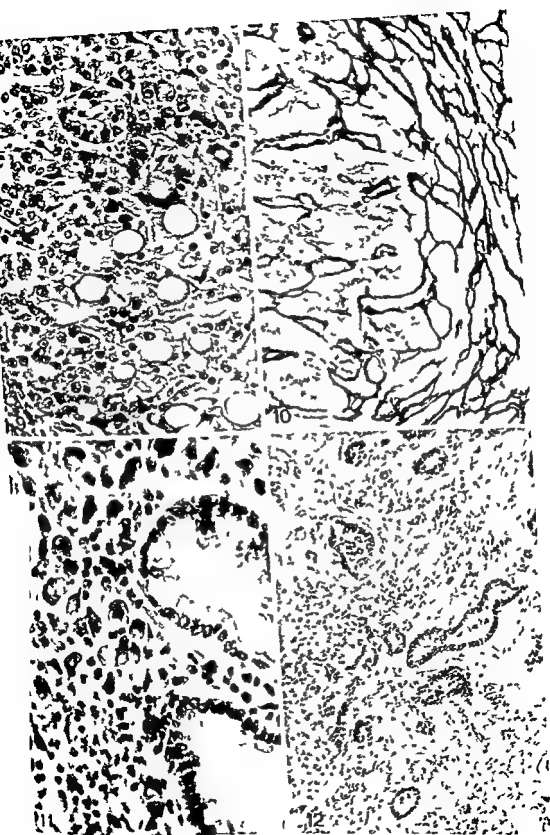


TABLE 4 Sex and Age of 52 Patients with PCL Related to the Histological Type and to the Presence of Cirrhosis and Alcoholism

	Number	Age range (mean)	Cirrhosis	Alcoholism	Type of PCL
Males	31	41-94 (66.8)	18 (29)	10	HCC
	3	58-77 (67.3)	1 (2)	1	Combined
	1	71	1 (1)	1	CCC
Total	35	41-94 (67.0)	20 (32)	12	
Females	14	53-82 (69.1)	6 (13)	1	HCC
	1	67	0 (1)	0	Combined
	2	74-77 (75.5)	1 (2)	0	CCC
Total	17	53-82 (69.8)	7 (16)	1	
Grand total	52	41-94 (67.9)	27 (48)	13	

In brackets under cirrhosis the number of cases where the presence of this condition could be verified

was a heavy infiltration with lymphocytes, and in 1 other case neutrophil granulocytes were seen occupying the centrilobular necroses

Grade of Differentiation and Cytology of HCC

The results of grading are seen in Table 3. The grade of differentiation sometimes varied from one area of a specimen to another, but never extremely so.

The tumours showed minimal, mild and moderate pleomorphism in 13, 14 and 18 cases, respectively. In another 4 cases the cytological picture was so pleomorphic that the tumour was bizarre (Fig. 7).

Characteristically, there was much less glycogen in tumour tissue than in parenchyma. Only in 3 cases were important amounts of glycogen found, corresponding to areas with clear-cells. There were no tumours that consisted exclusively of clear-cells.

The tumour cells contained fat in 10, Mallory bodies in 8 and lipofuscin in 3 cases. In 2 cases PAS-positive, diastase-resistant intracytoplasmic bodies with a morphology characteristic of alpha-1-antitrypsin deficiency were seen. In 3 cases orcin-positive ground glass change was found in the cytoplasm of a few malignant cells. Weakly PAS-positive globular hyalin, mainly intracellularly, was seen in 14 cases. Bile was found intracellularly in 2 extracellularly in 9 cases, the latter in the lumina of the acini. Intracellular inclusions, shown by electron microscopy to be cytoplasmic invaginations (Nørredam, unpublished work) were found in 19 cases, they were most frequent in the least differentiated tumours. No iron or copper was found in tumour tissue.

Histological Structure of CCC

In the 4 combined tumours the 2 types of tumour tissue were mixed at random: the quantity of each varying from area to area (Fig. 11). The 3 CCC and the CCC-components of the 4 combined tumours showed the following characteristics. The tumour tissue was usually embedded in abundant amounts of collagenous connective tissue (Fig. 12). It presented as an adenocarcinoma with predominance of tubular and acinar structure (Figs. 11 and 12). There were no compact or trabecular forms. Structures resembling Hering's canals were observed occasionally, but no tumours consisting exclusively of such structures (cholangiolocarcinomas) were found. Three of the tumours were papillary in places.

The individual acini and tubuli were coated with

Fig. 9 HCC Transitional zone between tumour tissue and parenchymal cells. The trabeculae are often continuous showing cells with criteria of malignancy in one end and cells without at the other end. WHO grade 1 Edmondson grade 2 H & E $\times 525$

Fig. 10 Same area as Fig. 9. In some places the trabeculae of tumour tissue are continuous with those of the parenchyma. Reticulin stain $\times 525$

Fig. 11 Combined HCC and CCC. The HCC component is bizarre. HCC WHO grade 3 Edmondson grade 3 CCC WHO grade 1, Edmondson grade 2 H & E $\times 525$

Fig. 12 CCC The tubular elements are embedded in abundant collagenous connective tissue. WHO grade 1 Edmondson grade 2 H & E $\times 210$

As to the histological typing of HCC, the 3 latest classification systems have been applied in the present study. The one described by WHO was found very useful, and the most applicable.

The most characteristic of the observed histological features of HCC was its trabecular structure. It was always present, most often in the form of a compact arrangement of microtrabeculae.

The histological pattern did not differ essentially from what was found in African (Anthony 1973, Berman 1941, Norredam 1977 B) and other Caucasian series (Edmondson 1958, Peters 1976). However, in his African material the author found relatively more cases with a sinusoidal structure of the trabeculae than in the present study (Norredam 1977 B).

As was the case in a study from Africa (Norredam 1977 B) the reticulin stain was found very valuable for descriptive and diagnostic purpose. The reason is that this staining technique always elucidates the trabecular structure in HCC, in some cases where H & E shows complete lack of structure; this stain is the only means of showing that the tumour tissue, in effect, is composed of well defined trabeculae.

By help of the reticulin stain the tumour tissue of HCC was observed to consist of one or more of the following structural elements: 1. Reticulin-covered microtrabeculae. These were always at least 2 cells thick. 2. Reticulin-covered macrotrabeculae. 3. Elements so poor in reticulin that the trabecular structure was only suggested.

For these reasons it was, in the present material, always possible to distinguish HCC from normal liver tissue and almost always from cirrhotic regeneration nodules. In only 2 cases were some areas in the specimen seen where the differential diagnosis between tumour tissue and cirrhotic liver tissue was impossible.

In some cases trabeculae consisting of cells without criteria of malignancy were seen to be directly continuous with trabeculae with such criteria. This was often seen to occur simultaneously in many sites in the same tumour. These observations support the hypothesis that

the tumour spreads in a way that speaks in favour of this hypothesis (Anthony 1973). It is, however, a well known fact that the tumour can spread vascularly inside the liver; this was also observed in the present study, where the parenchyma often contained tumour thrombi.

The cytological features of HCC did not differ from those found in materials from sub-Saharan Africa or from the Western Hemisphere. Clear-cell

tumours have been reported from Africa (Anthony 1973, Norredam 1977 B).

The histological and cytological findings were identical in CCC and the CCC-components of the combined tumours, and did not differ from those reported from USA (Edmondson 1958) or Uganda (Anthony 1973).

7763 autopsies were performed in Greater Copenhagen in 1973. Cirrhosis of the liver was found in 309 cases (4.0 per cent). PCL was found in 52 cases (0.7 per cent) of which 45 (0.6 per cent) were HCC. The incidence of cirrhosis is a little lower than the 5.9 per cent that was reported from a

1960)

The incidence of HCC in cirrhosis of 7.8 per cent is similar to what other workers have found in the Western Hemisphere, but is far below the about 40 per cent, reported in several studies from Africa south of the Sahara (Huitt 1971). The incidence of cirrhosis is about 50 per cent higher in that area than in the Western Hemisphere (Davies 1961, Steiner 1961). The coexistence of HCC and

however, this frequency is about 90 per cent (Huitt 1971, Norredam 1977 B).

The present material is too small to decide whether cirrhosis also predisposes to the development of CCC, but the general consensus is that such a relationship does not exist, and that the occasionally reported cases presumably have been secondary biliary cirrhosis caused by the malignant bile duct tumour (Mori & Nagasaki 1976).

Alcohol plays an important role as etiologic agent in cirrhosis and HCC in the industrialized world. This generally accepted view is supported by the present study, in which half of the cirrhotic patients with cirrhosis and HCC were alcoholics. The diagnosis of alcoholism, obtained through the hospital files, was confirmed by the presence in liver tissue of steatosis, Mallory bodies and small

The incidence of orcein positivity in the present material was higher than would be expected in normal or cirrhotic livers, but the series is too small to draw any conclusions. In Africa, evidence of infection with HB_sAg can be found in serum or in liver tissue in almost all cases of HCC (Blumberg et al 1975).

a distinct basement membrane that was positive in the reticulin stain. Necroses of tumour tissue were seen in 5 cases.

Grade of Differentiation and Cytology of CCC

Table 3 shows the results of the grading. The tumour epithelium varied from cuboidal (Fig. 12) to columnar cells with varying amounts of cytoplasm (Fig. 11). In sections stained with Alcian blue varying amounts of mucus were seen in the lumina in all 7 cases and intracellularly in 2 cases. One of the latter contained signet ring cells.

There were no adenosquamous variants in the present material.

Liver Parenchyma

HCC was accompanied by cirrhosis in 24 out of 42 determinable cases (57.1 per cent). The cirrhosis was characterized in the following way. The regeneration nodules were in 16 cases mostly less than 3 mm in size, in 8 mostly more than 3 mm. The amount of connective tissue was slightly, moderately and much increased in 4, 4 and 10 cases respectively.

Steatosis was found in 12 cases, in 3 of these to a severe degree. Seven of the 12 also contained Mallory bodies and 2 weakly PAS positive globular hyalin bodies. Orcein positive ground glass change was seen in the cytoplasm of clusters of parenchymal cells in 5 cases.

Inflammatory changes invariably present were pronounced in 8 cases. Piecemeal necroses were seen in 6 of these cases.

Liver cell dysplasia was found in 7 cases. Cholestasis was seen in 8 cases.

In the 18 cases of HCC without cirrhosis the following diagnoses were made: Mild portal fibrosis in 7 cases (in 2 of these also steatosis, Mallory bodies and weakly PAS positive globular hyalin bodies) and mild non-specific reactive hepatitis in 11 cases.

In the 4 cases of combined tumour 1 was accompanied by cirrhosis, 2 were without cirrhosis and 1 was indeterminable. Two of the 3 patients with CCC also had cirrhosis.

Clinical Data

The age and sex distribution related to the histological type of the tumour and to the presence of cirrhosis and alcoholism is shown in Table 4.

According to the hospital files, out of the 24 patients with HCC and cirrhosis 11 (45.8 per cent) were chronic alcoholics (including 2 cases with

cytological signs of alpha 1 antitrypsin deficiency). 1 had haemochromatosis and 1 chronic active hepatitis of lupoid type that later developed into cirrhosis. The etiology was unknown in 11 cases. None of the patients had had acute hepatitis. The patient with chronic hepatitis had been treated with glucocorticoids for 5 years prior to the appearance of the liver tumour.

Of the 18 patients with HCC without cirrhosis had had acute hepatitis. None of them were alcoholics.

In the 2 cases of combined tumour with cirrhosis the etiology of the latter was unknown. One of the patients with CCC and cirrhosis was an alcoholic.

The duration of symptoms attributable to PC was prior to admission from 2 weeks to 8 months with a mean of 3.2 months, and from admission to death from 1 week to 4 months with a mean of 3 weeks.

On admission for PCL the diagnosis of cirrhosis was known in 13 cases in which it had been made from 14 months to 11 years, mean 7.5 years previously. In the remaining 14 cases the cirrhosis was not diagnosed until autopsy.

None of the patients with PCL had ever been treated with estrogenic or androgenic steroids.

DISCUSSION

The age and sex distribution of HCC corresponds to that found by other workers in the West Hemisphere (Glenert 1961, Patton & Horn 1964). It is a disease of the elderly and old, and 2/3 of the afflicted are men. In an African series the male:female ratio was 3.5:1. The average age, however, was only 43 years (Norredam 1977 A).

Out of 427 cases of PCL from 6 different centres in USA 75.9 per cent were HCC and 24.1 per cent CCC. Combined tumours are not mentioned (Patton & Horn 1964). The high frequency of CCC and lack of combined tumours in these series may be due to the fact that CCC tends to be overdiagnosed at the expense of HCC (Edmondson 1958).

The relative frequency of HCC is high in Saharan Africa. Anthony (1973) in his series of 2 cases of PCL from Uganda found 93.3 per cent to be HCC, the rest was CCC. The author's material from Malawi consisted of HCC exclusively (Norredam 1977 B).

Combined tumours providing 7.7 per cent of the present material are generally regarded as rare. However, Allen & Lisa (1949) found that 10 per cent and Glenert (1961) that 18 per cent of PCL were combined tumours. These tumours have not been reported from Africa.

OCHRATOXIN A-INDUCED MYCOTOXIC PORCINE NEPHROPATHY ALTERATIONS IN ENZYME ACTIVITY IN TUBULAR CELLS

FOLMER ELLING

Department of Pathology Rigshospitalet and University Institute of Pathological Anatomy
Copenhagen Denmark

Folmer Elling Ochratoxin A induced mycotoxic porcine nephropathy Alterations in enzyme activity in tubular cells Acta path microbiol scand Sect A 87 237-243 1979

Mycotoxic porcine nephropathy was induced by p.o. administration of crystalline ochratoxin A for periods of 5 days 3 months and 2 years Enzyme activities of the renal tissue were studied histochemically These were NADH tetrazolium reductase NADPH tetrazolium reductase lactate dehydrogenase isocitrate dehydrogenase succinate dehydrogenase glucose-6 phosphate dehydrogenase a glycerophosphate dehydrogenase unspecific acid phosphatase and unspecific alkaline phosphatase The activity of NADH tetrazolium reductase and succinate dehydrogenase was reduced in the proximal tubule of all neph-

years exposure
proximal tubular
A induced myc-

corresponds to the localization of ochratoxin A previously demonstrated in the kidney The activities of NADPH tetrazolium reductase lactate dehydrogenase glucose 6 phosphate dehydrogenase and unspecific alkaline phosphatase were reduced focally corresponding to the areas with focal tubular atrophy and the degree of reduction was roughly parallel to the degree of atrophy

Key words Ochratoxin A nephropathy mycotoxic enzyme histochemistry pig

Folmer Elling University Institute of Pathological Anatomy Frederik V's Vej 11 DK 2100 Copenhagen
Ø Denmark

Received 30 xi 78 Accepted 8 iii 79

Ochratoxin A is a nephrotoxin elaborated by certain species of the fungal genera *Aspergillus* and *Penicillium* A porcine nephropathy has been associated with spontaneously occurring toxic nephropathy in pigs and poultry in Denmark (Elling & Møller 1973 Elling *et al* 1976) and its nephrotoxic effect has been demonstrated experimentally using crystalline ochratoxin A (Krog *et al* 1976) The histopathological changes which have been described included tubular degeneration and atrophy accompanied by interstitial fibrosis The changes in renal function

were characterized by impairment of proximal tubular function It was shown recently by immunofluorescence microscopy that the proximal tubule is the target part of the nephron in ochratoxin A induced mycotoxic nephropathy (Elling 1977)

In a previous enzyme histochemical study the present author described the changes in activity of a number of dehydrogenases and phosphatases in mycotoxic porcine nephropathy induced by feeding naturally ochratoxin A-contaminated barley (Elling 1974) The aim of the present study was to examine the toxic effect of ochratoxin A on a number of dehydrogenases and phosphatases in the pig kidney after p.o. administration of the toxin for 5 days 3 months and 2 years

The survival time from the onset of symptoms was not significantly different from that found in an African material (Norredam 1977 A)

The author is grateful to the institutes of pathology of Bispebjerg Hospital, Finsensinstituttet, Frederiksberg Hospital, Københavns Amts Sygehus in Gentofte and Glostrup, Kommunehospitalet, Rigshospitalet and Sundby Hospital. This work was supported by a grant from the Danish Cancer Society

REFERENCES

- 1 Allen, R A & Lisa, J R Combined liver cell and bile duct carcinoma Am J Path 25 647-655, 1949
- 2 Anthony, P P Primary carcinoma of the liver A study of 282 cases in Ugandan Africans J Path 110 37-48, 1973
- 3 Anthony, P P, Ishak, K G, Nayak, N C, Paulsen H E, Scheuer, P J & Sobin, L H The morphology of cirrhosis definition, nomenclature, and classification Bull WHO 55(4) 521-540, 1977
- 4 Anthony P P (Rapporteur) Report of the meeting of investigators on the histological classification of tumours of the liver, biliary tract and pancreas World Health Organization In press, 1978
- 5 Berman C The pathology of primary carcinoma of the liver in the Bantu races of South Africa S Afr J Med Sci 6 11-26, 1941
- 6 Blumberg B S, Larouze B, London W T, Werner B, Hesser J E, Millmann I, Saimot G & Payet M The relation of infection with the hepatitis B agent to primary hepatic carcinoma Am J Path 81 669-682 1975
- 7 Davies J N P Cirrhosis in Uganda Un Internat Cancr Acta 17 781-786, 1961
- 8 Edmondson H A Tumours of the liver and intrahepatic bile ducts 1 ed Armed Forces Institute of Pathology Washington, D C 1958 pp 32-90
- 9 Gall E A Primary and metastatic carcinoma of the liver Relationship to hepatic cirrhosis Arch Path 70 226-232 1960
- 10 Glenart, J Primary carcinoma of the liver A postmortem study of 104 cases Acta Path Microbiol Scand 53 50-60, 1961
- 11 Gordon, H & Sweet, H H A simple method for silver impregnation of reticulum Am J Path 545-551, 1936
- 12 Hutt, M S R Epidemiology of human primary liver cancer In Liver cancer, p 21-29 I.A. Scientific Publications No 1 World Health Organization, 1971
- 13 Lillie, R D & Fullmer, H M Histopathologic Technique and Practical Histochemistry 4 McGraw-Hill Book Co New York 1976 544-545
- 14 Mori W & Nagasako K: Cholangiocarcinoma related lesions In Okuda K & Peters, R L (Ed) Hepatocellular carcinoma, 1 ed John Wiley & Sons New York London, Sidney and Toronto 1976 227-246
- 15 Norredam K Primary carcinoma of the liver 1977 A
- 16 Norredam, K Primary carcinoma of the liver histological study of 27 cases of primary carcinoma of the liver from Malawi Acta Path Microbiol Scand Sect A 85 461-469, 1977 B
- 17 Norredam K Unpublished work
- 18 Patton, R B & Horn R C Primary liver carcinoma Autopsy study of 60 cases Cancer 17 757-768 1964
- 19 Perlz M Nachweis von eisenoxyd in geweben pigmenten Arch Pathol Anat Phys 39 42-43 1867
- 20 Peters, R L Pathology of hepatocellular carcinoma In Okuda, K & Peters R L (Eds) Hepatocellular carcinoma, 1 ed John Wiley Sons New York London Sidney & Toronto 1976 pp 107-163
- 21 Shikata T, Uzawa T, Yoshimura N, Akatsuka & Yamazaki S Staining methods of Australia antigen in paraffin sections Detection of cytoplasmic inclusion bodies Jap J Exp Med 44 25-31 1974
- 22 Siener P E Comparison of liver cancer and cirrhosis in nine areas in trans-saharan Africa U Internat Cancr Acta 17 799-825, 1961

Enzymes	Substrate	Product	Method	Buffer	Temp °C	Time (min)	pH	Colorant	Mounting
NADPH tetrazolium reductase	β nicotinamide adenine dinucleotide reduced form disodium salt	Sigma N 8129	Thomas & Pearce (1961)	phosphate	37	4	7.4	NBT* Sigma N 6876	glycerol gelatine
NADPH tetrazolium reductase	Nicotinamide adenine dinucleotide phosphate reduced form tetra sodium salt	Sigma N 1630	-	-	37	4	7.4	NBT	-
Lactate dehydrogenase	DL lactic acid sodium salt β nicotinamide adenine dinucleotide	Sigma L 1375 Sigma N 7004	-	-	37	4	7.4	NBT	-
Isocitrate dehydrogenase	DL-isocitric acid trisodium salt β nicotinamide adenine dinucleotide	Sigma I 1252 Sigma N 7004	-	-	37	20	7.4	NBT	-
Succinate dehydrogenase	Succinic acid tetrahydrate disodium salt	Fluka 14170	-	-	37	20	7.4	NBT	-
Glucose 6 phosphate dehydrogenase	D glucose 6 phosphate dipotassium salt Nicotinamide adenine dinucleotide phosphate	Sigma G 7375 Sigma N 0505	-	••	37	20	7.4	NBT	-
α glycerol phosphate dehydrogenase	DL α glycerophosphate hexahydrate disodium salt β nicotinamide adenine dinucleotide	Sigma G 6126 Sigma N 7004	-	-	37	20	7.4	NBT	-
Unspecific acid phosphatase	α naphthylacid phosphate sodium salt	Sigma N 7000	Bartha & Anderson (1963)	veronal	20	20	6.0	p rosaniline hydrochloride Allied Che mical NA 0664	Eukitt
Unspecific alkaline phosphatase	α naphthylacid phosphate sodium salt	Sigma N 7000	Pearse (1968)	Tris	20	20	8.5	Fast Red TR salt Sigma F 1500	Glycerol gelatine Sigma

* NBT Nitro Blue Tetrazolium

•• Modified according to Andersen & Højer (1974)

The activity of the following enzymes were estimated histochemically NAD(P)H-tetrazolium reductase, lactate dehydrogenase, isocitrate dehydrogenase, succinate dehydrogenase, glucose 6-phosphate dehydrogenase, α -glycerophosphate dehydrogenase, unspecific acid phosphatase, and unspecific alkaline phosphatase

The changes in activity are related to the changes in renal function and morphology and to the localization of ochratoxin A

MATERIAL AND METHODS

The experimental animals were all female pigs of the Danish landrace and 8-10 weeks old at initiation of the experiments. They were given crystalline ochratoxin A po as previously described (Arogh *et al* 1976). The number of animals, dose levels and length of exposure are indicated in Table 1

TABLE 1 No of animals dose levels and length of exposure of crystalline ochratoxin A

	No of pigs Dosed	Dose	Exposure time	No of pigs Controls
Group 1	3	400 μ g/kg bw corresponding to 5 mg/kg feed	5 days	3
Group 2	3	1 mg/kg feed	3 months	3
Group 3	6	1 mg/kg feed	2 years	6

The dose level in group 1 corresponded to the high levels found in feed associated with spontaneous mycotoxic nephropathy in pigs while the level in group 2 and 3 correspond to the intermediate levels (Arogh *et al* 1974). The controls were fed on a diet free from ochratoxin A and were all of the same age as the experimental animals in the 3 groups. The animals in group 2 and 3 are deriving from the experiments previously published (Arogh *et al* 1976, Arogh *et al* in press). At termination of the experimental period the animals were anesthetized and nephrectomy of the right kidney was performed as previously described (Elling *et al* 1977). Tissue blocks comprising renal cortex and medulla were snap frozen in isopentane cooled to -80°C in a freezing mixture consisting of acetone and dry ice and stored at -80°C . Four μ m thick cryostat sections cut on a Bright cryostat were placed on cover slips and placed in Columbia dishes containing the substrate. The histochemical methods employed are shown in Table 2

Controls

As controls in each enzyme reaction a section was incubated in substrate - deficient media

In order to determine a possible diffusion of the soluble dehydrogenases the maleimide blocking method was used in the reactions for lactate dehydrogenase and α -glycerophosphate dehydrogenase (Høyer & Andersen 1970). In the reaction for glucose-6-phosphate dehydrogenase a gel medium containing polyvinyl alcohol and the specific substrate was used (Andersen & Høyer 1974).

The enzyme reactions of the pigs receiving ochratoxin A were compared with those of the controls. As documentation polaroid micrographs were taken of the kidney sections from the control on one half of the picture and of the dosed animal on the other half employing the same exposure time and light intensity. The film used was Polaroid Type 665 positive/negative land film 8.3 \times 10.8 cm

RESULTS

Group 1 - ochratoxin A for 5 days. The structural changes comprised desquamation and focal necrosis of epithelial cells in the proximal tubule of some nephrons (Elling 1977). The alterations in activity of the examined enzymes are shown in Table 3. The activity of NADH tetrazolium reductase was markedly reduced in pars convoluta and pars recta of the proximal tubules of III nephrons. The succinate dehydrogenase activity was reduced in the convoluted part of the proximal tubule of all nephrons while the activity of α -glycerophosphate dehydrogenase was increased throughout the proximal tubule of some nephrons. Acid phosphatase activity was reduced in pars recta in the proximal tubules of nephrons.

The activity of all the examined enzymes was reduced in the areas of the proximal tubules. It showed morphological changes. Changes in enzyme activity were not observed in other parts of the nephron.

Group 2 and 3 (ochratoxin A for 3 months and 2 years respectively). The histological changes observed were focal degeneration and necrosis of proximal tubular cells leading to tubular atrophy. Some nephrons accompanied by focal interstitial fibrosis of the cortex after 3 months exposure (Arogh *et al* 1976). The lesions after 2 years exposure were virtually the same as after 3 months except that in some of the animals the tubular atrophy and the interstitial fibrosis were more widely distributed in the renal cortex. In addition a infiltration of mononuclear cells between atrophic tubular epithelial cells was observed in severely damaged kidneys (Arogh *et al* in press).

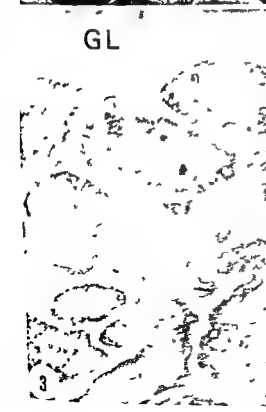


TABLE 3 The Changes in Enzyme Activity in Pars Convoluta (PCT) and Pars Recta (PRT) of the Proximal Tubules in the Kidneys from the 3 Dosed Groups Compared with the Control Kidneys in Each Group

	Group 1		Group 2		Group 3	
	PCT	PRT	PCT	PRT	PCT	PRT
NADH tetrazolium reductase	↓	↓	↓	↓	↓	↓
NADPH tetrazolium reductase						
Lactate dehydrogenase						
Isocitrate dehydrogenase						
Succinate dehydrogenase	↓		↓	↓	↓	↓
Glucose 6 phosphate dehydrogenase						
α-glycerophosphate dehydrogenase	↑*	↑*				
Acid phosphatase		↓		↓		↓
Alkaline phosphatase			↓	↓	↓	↓

↑ increased activity ↓ reduced activity * focally

In addition to the indicated changes a focal reduction in activity of all enzymes corresponding to the atrophic tubul was observed in all 3 groups

The alterations in activity of the examined enzymes in group 2 and 3 were virtually identical (Table 3). The activities of NADH-tetrazolium reductase and succinate dehydrogenase were reduced in the proximal tubules of all nephrons of the experimental animals (Fig 1 and 3), and most outspoken in the areas showing tubular atrophy. The activities of NADPH-tetrazolium reductase, lactate dehydrogenase, glucose-6-phosphate dehydrogenase and α-glycerophosphate dehydrogenase were reduced focally corresponding to the areas with tubular atrophy and the degree of reduction corresponded to the degree of atrophy. Acid phosphatase activity was reduced in the pars recta of the proximal tubules. Alkaline phosphatase activity was reduced in all the proximal tubules, and sometimes virtually absent in the most severely damaged proximal tubules. Also some of the cells in the interstitial cell infiltrations demonstrated alkaline phosphatase activity in the cytoplasm. In the maleimide blocked reactions only lactate dehydrogenase showed diffusion.

DISCUSSION

The main alterations in enzyme activity in ochratoxin A-induced porcine nephropathy were localized to the proximal tubule. This corresponds to the site

of deposition of ochratoxin A as shown previously by immunofluorescence microscopy (Elling 1971). The activities of NADH tetrazolium reductase and succinate dehydrogenase were reduced in the proximal tubule after 5 days exposure and remain reduced after 3 months and 2 years exposure. The reduction suggests decreased function of the Tricarboxylic Acid Cycle and of the respiratory chain resulting in a reduction in the oxidative phosphorylation.

Fig 1 Kidney from pig which had received 1 mg ochratoxin A per kg feed daily for 3 months (Group 1). NADH tetrazolium reductase activity in proximal tubules appears reduced as compared with the activity in the proximal tubules in control animals (Fig 2) (GL = glomerulus) × 325

Fig 2 Kidney from control animal in Group 2. NADH tetrazolium reductase activity in proximal tubule × 325

Fig 3 Kidney from pig which had received 1 mg ochratoxin A per kg feed daily for 3 months (Group 1). The activity of succinate dehydrogenase is reduced in proximal tubules when compared with control (Fig 4) (GL = glomerulus) × 325

Fig 4 Kidney from control group 2. Succinate dehydrogenase activity × 325



lation. This reduction in energy production in the epithelial cells of the proximal tubule could account for the impairment in function of this part of the nephron characterized by decreased reabsorption of glucose and decreased excretion of paraamino hippuric acid (Krogh *et al* 1976) and also for the histologically observed lesions. It remains unclear however why the histological lesions are focally distributed throughout the renal cortex involving only some of the proximal tubules. In contrast to these morphological changes the reduction in activity of the above enzymes occurs in the proximal tubules of every nephron. Cuppage *et al* (1977) described parallel observations in gentamicin nephrotoxicity in rats without being able to explain the focal distribution of lesions. A hypothetical explanation would be that morphological lesions do not appear until the biochemical alterations have reached a threshold level.

The systematic reduction of NADH tetrazolium reductase and succinate dehydrogenase activity of the proximal tubular epithelial cells in this study was not observed in a previous study of the same enzymes in mycotoxic porcine nephropathy induced by ochratoxin A contaminated barley (Ejlert 1974).

This discrepancy is probably due to differences in length of incubation. In the previous study the incubation time for all dehydrogenases was 20 min. In the present study the incubation time for NAD(P)H tetrazolium reductase was 4 min (Table 2). This shorter time of incubation markedly facilitated the evaluation of enzyme activity because the less dense formazan granula were more clearly discernable.

The increase in activity of a glycerophosphate activity observed in group 1 would indicate an increased electron transport via the glycerophosphate shuttle and thus compensate for the above suggested reduction in the TCA cycle

The reduction of activity of NADPH tetrazolium reductase lactate dehydrogenase glucose 6 phosphate dehydrogenase and α glycerophosphate dehydrogenase in the atrophic tubules would indicate that the atrophy is accompanied by a reduced tubular function

Alkaline phosphatase was reduced corresponding to the reduction in brush border of the proximal tubules (Krogh *et al* 1976 Krogh *et al* in press). The physiological significance of the reduced alkaline phosphatase is unclear. The marker enzyme for lysosomes, acid phosphatase, showed a reduced activity in the pars recta of the proximal tubule in all three groups. Whether this reduced activity is due to a reduced number of lysosomes is not known at present.

CONCLUSION

Ochratoxin A induced a reduction in activity of enzymes of the Tricarboxylic Acid Cycle and the respiratory chain in the proximal tubule corresponding to the previously demonstrated localization of ochratoxin A in the kidney. The reduced enzyme activity could account for the alteration in renal function and the histological lesions in the same part of the nephron.

This study was supported by *State Research Council* grant no 513 6554

REFERENCES

- Andersen H & Høyer P E Simplified control experiments in the histochemical study of coenzyme-linked dehydrogenases Histochem 38 71 81 1974
- Bar
- Cuppige F E Setter K S Sullivan L P Keres J & Melnikovich A O Gentamicin Nephrotoxicity II Physiological biochemical and morphological effects of prolonged administration to rats Archows Arch B Cell Path 24 121-138 1977
- Elling F & Møller T Mycotoxic nephropathy in pigs Bull Wild Hlth Org 49 411-418 1973
- Elling F Ph D thesis Roy Vet Agr Univ Copenhagen Denmark 1974
- Elling F & Møller T Enzyme histochemical studies of the normal pig kidney Acta vet. scand 16 153 162 1975
- Elling F
pigs ar
Acta pathol microbiol scand 1977
- Elling F Hasselager E & Fris C Perfusion fixation of kidneys in adult pigs for electron microscopy Acta anat 93 340-342 1977
- Høyer P E & Andersen H Specificity in steroid histochemistry with special reference to the use of steroid solvents Distribution of 11 β hydroxy steroid dehydrogenase in kidney and thymus from the mouse Histochemie 24 292 306 1970
- Krogh P Axelsen N H Elling F Gyrd Hansen A Hald B Hyldgaard Jensen J Larsen A E Madsen A Mortensen H P Møller T Petersen O K Ravnshov U Rosgaard M & Aalund O Experimental porcine nephropathy Changes of renal function and structure induced by ochratoxin A contaminated feed Acta pathol microbiol scand Sect. A Supplementum No 246 21 pp 1974
- Krogh P Advances in veterinary science and comparative medicine Academic Press Inc New York San Francisco London 20 147-168 1976

- Krog P Elling F Gyrd Hansen N Hald B Larsen A E Lillehøj E B Madsen A Mortensen H P & Ravnskov U* Experimental porcine nephropathy. Changes of renal function and structure perorally induced by crystalline ochratoxin A. *Acta path microbiol scand Sect, A* 84 429-434 1976
- Krog P Elling F Friis Chr Hald B Larsen A E Lillehøj E B Madsen A Mortensen H P Rasmussen F & Ravnskov U* Porcine nephropathy induced by long term ingestion of ochratoxin A. *Vet Path* (In press)
- Pearse A G E* Histochemistry Theoretical and applied Vol 1 3rd J A Churchill Ltd London 1968
- Thomas E & Pearse A G E* The fine localization of dehydrogenases in the nervous system. *Histochem* 2 266-282 1961

TUMORIGENICITY AND KARYOTYPE OF RAT EMBRYO CELL LINES TRANSFORMED BY BK VIRUS

H E KARJALAINEN A SALMI and R A MANTYJARVI

The Department of Clinical Microbiology University of Kuopio Kuopio and the Department of
Virology University of Turku Turku Finland

Karjalainen H E Salmi A & Mantyjarvi R A Tumorigenicity and karyotype of rat embryo cell
lines transformed by BK virus. Acta path microbiol scand Sect. A 87 245-253 1979

A rat embryo cell line transformed by BK virus was used to induce tumors in rats. Cell lines were
established from these tumors. Other sublines were obtained by *in vitro* cloning of the parental line.
Growth characteristics and karyotypes were compared to the tumorigenicity of these cell lines. The *in*
ro cloned sublines had a low tumorigenicity. Tumorigenicity of the tumor cell lines varied from high
to undetectable. The tumor cell line with the highest tumorigenicity also had the highest saturation
density *in vitro* but otherwise there was little correlation between tumorigenicity and the *in vitro*
characteristics of the cells. Karyotype analysis was done for two cell lines with high or low
tumorigenicity which both had a near-diploid complement of chromosomes. The findings were in
agreement with the expression suppression model of Robinson and Sachs (1970). The suppression
chromosomes seemed to be confined in group A, the expression chromosomes in group B.

Key words: Rat embryo cell lines, transformation, karyotyping, oncogenic viruses, BK virus.

H E Karjalainen, Department of Clinical Microbiology, University of Kuopio, POB 138, 70101 Kuopio,
10 Finland.

Accepted as submitted 17.1.79

BK virus (BKV), a human polyoma virus,
induces tumors when injected *in vivo* in

20 3
ham-

are tumorigenic upon transplantation in hamsters.
Hamster cells can also be transformed *in vitro* with
BKV or with viral DNA, and transformed cells
grow to tumors when injected in syngeneic animals
(23, 30, 33, 34). In the same way, nude mouse
kidney cells transformed by BKV grow in tumors
when transplanted back to mice (7). Both tumorige-
nic and nontumorigenic transformants of cells from
other strains of mice have been described (24, 29).
Rat embryo fibroblasts transformed *in vitro* by
BKV have a low tumorigenicity (29). Even in
irradiated, weanling rats, the latent period of the
tumors was 7-18 months. Sublines established
from the tumors were, however, highly tumorige-
nic.

One characteristic frequently encountered in
transformed cell lines is the abnormality of the
karyotype of these cells. In most cases, cell lines
derived from *in vitro* transformation or from
primary tumors induced by papovaviruses are
heteroploid with wide modal peaks in the near-
tetraploid range, especially at later passage levels
of the cells (6, 9, 16, 19, 39). An increase in the
chromosome number seems to be an early event in
diploid cells infected with SV40 (15, 17). On the
other hand, several transformed cell lines with a
near-diploid or diploid modal number of chromoso-
mes have been described (9, 14), and therefore
polyploidization does not seem to be necessary for
tumorigenicity.

We have previously analyzed the distribution of
chromosome numbers in cell lines from BKV-
induced hamster tumors (32). These cell lines were
all heteroploid with subtetraploid modal numbers.
In a similar analysis of a BKV-transformed rat cell

line (RE-BK, 29) a different pattern was found. We used this cell line to induce tumors in rats and established cell lines from these tumors. We also cloned these cells *in vitro* to get sublines with different karyotypes. In this report we describe some of these cell lines especially by comparing the relationship between their karyotype and tumorigenicity.

MATERIAL AND METHODS

Cell Cultures

The parental cell line, REBK, was obtained by transforming rat embryo fibroblast cultures (Sprague-Dawley) with BK virus (29). Cells were cultured *in vitro* in Eagle's MEM (GIBCO) supplemented with 10% fetal calf serum and passaged by trypsinization (0.25% trypsin, Difco). Cell cultures from tumors were also established by trypsinization of minced tumor tissue and by seeding the cells in the medium mentioned above.

For cloning experiments trypsinized cells in growth medium were diluted to 10 cells/0.2 ml. Cell suspension was dispensed in 0.2 ml volumes in the wells of a microtiter tissue culture plate (Titertek II, Falcon Plastics). After an incubation of one to two weeks the wells with only one focus of cells were selected for trypsinization and subcultures.

Staining Techniques

The cells were grown on cover slips to sparse monolayers. After washing in 0.05M phosphate-buffered saline, pH 7.6 cells were air dried, and fixed at room temperature in acetone (for immunofluorescent staining) or methanol (for Giemsa staining). Indirect immunofluorescent staining for T antigen was done as described previously (20). Giemsa staining (Merck) was used for cellular morphology.

Chromosome Analysis

Actively growing cells on cover slips were arrested in metaphase with colchicine (Merck, 0.4 µg/ml, 2-4 h). The cells were swollen in hypotonic KCl, fixed and stained with Giemsa stain (27). Metaphase spreads for karyotypes were photographed with a Leitz microscope and 100× lens on Agfa Ortho film. Chromosomes of

the karyotypes were numbered according to Uvalde and Hsu (37).

Tumorigenicity Tests

The cells were detached from cultures by trypsinization, counted, resuspended in Hanks' salt solution and injected subcutaneously in rats. The rats were of the same inbred strain of Sprague-Dawley from which the REBK cells originated. Both new-born and adult rats were used. A total body x-ray irradiation of 400 rads was given to new-born rats used for the tumorigenicity experiment of the parental REBK line.

Histology

Tumors were excised and pieces from different parts of the tumor were fixed in 10% formalin in neutral phosphate-buffered saline. Fixed pieces were embedded in paraffin, sectioned, and stained with hematoxylin-eosin.

RESULTS

Origin of the Sublines of REBK Cells

Our early chromosome studies revealed that the REBK line was heterogenous containing both diploid and aneuploid cells (cf. Table 3). To select from this mixed population sublines which would be more tumorigenic than the parental line, we inoculated 10⁶ REBK cells in 113 irradiated new-born rats. The first tumor was observed 16 weeks after the inoculation. Only two of the tumors grew subcutaneously at the site of the injection. Of the others, one was located in the neck and one in the inguinal region. The rest of the tumors were all intraperitoneal nodules of various sizes often adhering to the organs of the peritoneal cavity. Cell cultures were made by trypsinization of three of the tumors. Cell lines established from these tumors were designated REBK-A, REBK-B and REBK-C. Line REBK-A was derived from the first tumor which appeared as a solid, circumscribed nodule in the inguinal region. Lines REBK-B and REBK-C came from large intraperitoneal tumors.

TABLE 1 Growth Characteristics of the Cell Lines Studied

	Cell line					
	REBK	REBK-A	REBK-B	REBK-C	REBK-2	REBK-12
Morphology	Fibrobl	Epith	Fibrobl	Fibrobl	Fibrobl	Fibrobl
T antigen ¹	+++	±	+++	++	++	++
Saturation density ²	3.6	4.4	1.3	2.0	2.4	2.2

¹ On an arbitrary scale of - to + + + +

² x 10⁵ cells/cm²

Several sublines were cloned *in vitro* from the REBK line as described in Methods. These clones were designated by numbers. Two of the clones REBK 2 and REBK 12 were included in this study.

Growth Characteristics and T Antigen

Some characteristics of the cell lines studied are summarized in Table 1. The parental REBK line grown *in vitro* was made of fibroblast like cells with occasional multinucleated giant cells. All the cells were T antigen positive, although there was some variation in the intensity of the staining from cell to cell. The *in vitro* cloned sublines of REBK were morphologically similar to the parental line (Fig. 1a) and they also showed a similar reaction in the immunofluorescent staining for T antigen. Cell morphology and growth pattern of two of the tumor cell lines REBK B and REBK C were also similar to that of the parental line. The third tumor cell line REBK A behaved differently. The cells were flat polygonal and they grew to dense monolayers (Fig. 1b). This was reflected in the saturation density which was highest for the REBK A cells (Table 1). All three tumor cell lines were T antigen positive. There was however a marked difference between them in the intensity of the immunofluorescent staining. REBK B had a strongly immunoreactive T antigen whereas the T antigen of REBK A cells was barely detectable with the T antisera used.

Tumorogenicity

Tumorigenicity of the sublines was tested in unirradiated rats. Of the tumor cell lines REBK B was not tumorigenic under these conditions; no tumors were observed during 44 weeks in 11 rats injected with 10^6 cells as newborn (Table 2). On the other hand REBK A and REBK C were highly tumorigenic in newborn rats. The first tumors appeared in two weeks after a transplantation of $1-3 \times 10^6$ cells. The tumor producing number of cells of these two cell lines was titrated in adult rats. TD_{50} for REBK A was 4.3×10^5 cells but there were no tumors in rats which had received REBK C cells.

Cell clones REBK 2 and REBK 12 were also tested for tumorigenicity. Their tumorigenicity was low or absent; a tumor appeared only in one animal after a transplantation of 2×10^6 REBK 12 cells as newborn (Table 2).

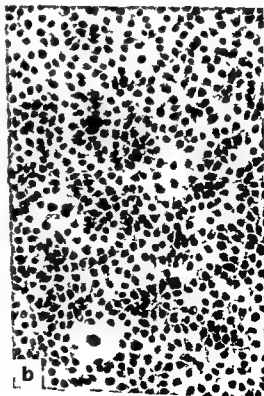


Fig. 1. *In vitro* growth patterns of two sublines of REBK cells. (a) REBK 12. (b) REBK A. Giemsa staining $\times 150$.

TABLE 2 Tumorigenicity of REBK Sublines

Cells	No. of cells injected	Age when injected (weeks)	Tumorigenicity	TPD ₅₀	Observation time (weeks)
REBK-A	1.5 to 3.5 × 10 ⁶	0	31/36 ¹	<1.5 × 10 ⁵	6
REBK-A	10 ² to 3.0 × 10 ⁶	4	4/15	4.3 × 10 ⁵	42
REBK-12	1.0 to 2.0 × 10 ⁶	0	1/29	>2.0 × 10 ⁶	25
REBK-12	1.0 × 10 ⁷	18	0/4	—	15
REBK-B	1.0 × 10 ⁶	0	0/11	—	44
REBK-C	1.0 to 3.0 × 10 ⁶	0	18/19	<1.0 × 10 ⁵	5
REBK-C	6.0 × 10 ⁴ to 3.0 × 10 ⁶	20	0/6	>3.0 × 10 ⁶	23
REBK-2	0.7 or 1.0 × 10 ⁶	0	0/13	—	14

¹ No. of tumors / No. of animals injected

Tumors induced by transplantation of REBK-A or REBK-C cells were round, solid and encapsulated, and they were located at the site of the injection. The histopathological picture of the tumors was that of fibrosarcoma (Fig. 2). The cells were mostly spindle-shaped, giant cells were encountered occasionally. In some parts of a tumor the presence of

collagen fibers was characteristic. Mitotic figures were frequent.

Chromosome Analysis

Chromosome number distribution in some of the cell lines tested is shown in Table 3. Fifty cells of each of the lines were counted except of REBK-B of which only ten cells were counted accurately, for the rest of the REBK-B cells a rough count was made to make sure that 50 cells all contained more than 90 chromosomes. The parental REBK line was heteroploid with two modal peaks, one in the diploid the other one in the tetraploid region. About 30% of the cells had a diploid or near diploid chromosome complement at the passage levels at which normal fibroblasts possibly contaminating the culture should no longer be present.

Chromosome numbers of each clone in the three tumor lines were as follows: REBK-A, 43 chromosomes or less, all the cells of the line had more than 90 chromosomes. The heteroploid distribution of chromosomes in the REBK-C line was between those two extremes.

REBK-2 is an example of the clones isolated from REBK *in vitro*. Ten of the clones tested had a similar distribution pattern to that of REBK-1 they were all heteroploid with chromosome numbers spread in the triploid-tetraploid region. None of them had more than 1–2% diploid cells. The one exception of this was the REBK-12 clone (Table 3). The distribution of chromosomes was similar to that of the parental REBK line but the amount of cells in the diploid range was 72%. A more detailed comparison of chromosome number distributions in the modal peaks of REBK-12 and REBK-A cells is given in Table 4. This distribution pattern of the chromosomes of REBK-12 was however, labile. When tested ten passages later, the chromosome

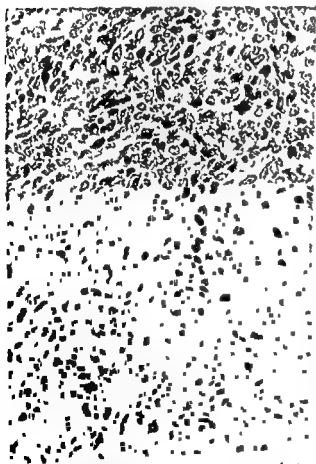


Fig. 2 Histology of a rat tumor induced by transplantation of REBK-A cells. Hematoxylin-eosin staining. × 250.

TABLE 3 Percentage of Cells with Various Chromosome Numbers in REBK Cell Lines

Cells Passage no	REBK 36	REBK 73	REBK A 12	REBK 12 4	REBK H 11	REBK-C 20	REBK 2 8
Number of chromosomes							
35-39	2		10				
40-44	28	34	90	72			
45-49		4					
50-54	6	2				6	
55-59		2					
60-64		4				6	2
65-69		4				6	4
70-74		2				12	28
75-79	14	16		4		22	38
80-84	44	22		20		24	26
85-89	6	10		4		20	2
90-94					30		
95-99					10	4	
100-104					10		
> 105					50		

distribution had returned to a heteroploid pattern similar to that of the REBK line

Karyotypes

Karyotypes were constructed of the REBK cells of tumor lines REBK A and REBK-C and of clones REBK 2 and REBK 12. The two most interesting ones to compare were REBK A and REBK 12. Both lines had a near diploid number of chromosomes in a majority of cells but the tumorigenicity of REBK A was high whereas that of REBK 12 was low (Table 2). Representative karyotypes of these cell lines are shown in Fig. 3 compared to the normal karyotype of a rat embryo fibroblast. A summary of the karyotype analysis is shown in Table 5. Both REBK A and REBK 12 showed variation in the number of chromosomes in all three

chromosome groups. However, there seemed to be one apparent difference between the two lines. When extra chromosomes were present they tended to be ungroupable or of group B in the REBK A cells whereas extra chromosomes in REBK 12 were of group A.

as the corresponding figure for REBK A cells was only 2/12. The modal peaks of 42-43 chromosomes represent 60% and 64% of the total cell population of the REBK A and REBK 12 lines respectively (Table 4). Therefore, there were extra chromosomes of group A in about 10% of REBK A cells and in about 40% of REBK 12 cells. The latter figure is probably too low because extra group A chromosomes may be present also in the 30% of REBK 12 cells with more than 43 chromosomes. No cells with more than 43 chromosomes were found in the REBK A line. For extra chromosomes in group H the situation was reversed. In cells with 42-43 chromosomes extra group H chromosomes were present in 9/18 REBK A cells and in 3/15 REBK 12 cells. These figures represent 30% and 13% of the corresponding total cell populations.

Because of their heteroploidy the analysis of REBK REBK-C and REBK 2 cells was not very fruitful. They seemed to have an increased number of chromosomes in every chromosome group. An exception to this was REBK-C in which the number of chromosomes of group C was normal.

TABLE 4 Chromosome Numbers in the Modal Peaks of REBK 12 and REBK A Cells

	Number of chromosomes				
	40	41	42	43	44
REBK 12	2	4	18	46	2
REBK A	8	22	44	16	-

per cent.



Fig 3 Karyotypes of representative cells of a normal rat embryo fibroblast (top) of REBK-12 (middle) and of REBK-A (bottom)

DISCUSSION

The results of tumorigenicity tests of transformed cells depend on several factors (22) which can be roughly grouped as properties of the transformed cells, the technique used, and the reaction of the host animal. The latter variable may explain why BKV-transformed hamster cells are regularly tumorigenic (23,30,33,34), whereas mouse cells often are not (24,29). Any of the factors may be the reason for

the relatively low tumorigenicity of the BKV-transformed rat embryo cell line REBK. From this parental cell line we were able to establish sublines by *in vivo* and *in vitro* selection, which had high or low tumorigenicity. Since the host and the procedure of the tumorigenicity tests of these sublines remained the same, the difference must have been related to the properties of the cells: growth capacity, immunogenicity and/or immunosensitivity.

TABLE 5 Chromosome Analysis of Two Cell Lines Derived from REBK

REBK-A						REBK-12					
Mouse No	No of chromosomes in groups			Abnormal chromosomes	Total No of chromosomes	No of chromosomes in groups	A	B	C	Abnormal chromosomes	Total No of chromosomes
	A	B	C								
1	6 XY	18	16	1	43	10 XY	17	14			43
2	8 XY	20	13		43	10 XY	18	13			43
3	7 XY	19	14		43	11 XY	16	14			43
4	8 XY	19	14		43	10 XY	17	14			43
5	8 XY	19	14		43	9 XY	18	14			43
6	9 XY	18	14		43	9 XY	18	14			43
7	8 XY	19	14		43	10 XY	18	13			43
8	7 XY	19	14	1	43	9 XY	18	14			43
9	9 XY	18	14		43	9 XY	18	14			43
10	8 XY	18	14		43	7 XY	19	14	1		43
11	5 XY	22	14	43	10 XY	17	13				42
12	8 XY	19	14	43	8 XY	18	14				42
13	9 XY	18	13		42	7 XY	19	14			42
14	8 XY	18	14		42	8 XY	19	13			42
15	8 XY	18	14		42	8 XY	18	13	1		42
16	8 XY	18	14		42	8 XY	18	13			41
17	8 XY	18	14		42	7 XY	18	13			40
18	7 XY	19	14		42	8 X	17	14			40
19	7 XY	18	14		41	9 XY	17	12			40
20	8 XY	18	11	2	41	9 XY	17	12			40
21	8 XY	17	13		40	6 XY	18	11			37
22	6 XY	18	14		40						
23	8 XY	16	13		39						
24	5 X	18	13		37						
25	6 X	15	12		34						
26	7 X	14	12		34						

Apparently no single *in vitro* characteristic of a transformed cell line can be relied upon as an indicator for tumorigenicity.

is correlated with an increased saturation density (1). Furthermore, in the so-called flat revertant cell lines isolated by selection on 3T3 cell.

we tested the REBK-A line showed both the highest saturation density and the highest tumorigenicity. On the other hand three other cell lines similar to each other in saturation densities had quite different tumorigenic capacities.

T antigen of SV40 is necessary for the initiation and probably also for the maintenance of transformation (18). It stimulates cellular DNA synthesis (35) but the significance of this property for transformation is unknown. The amount of T antigen in our BKV transformed rat cells was

almost inversely proportional to the tumorigenicity. Therefore, an increased amount of T antigen, at least as measured by immunological methods, does not make transformed cells more tumorigenic.

Cytogenetic examination of transformed cells has produced little evidence for a correlation between tumorigenicity and a specific change in the karyotype (10). However, in some cases the karyotype has been found to reflect the tumorigenicity of a cell line. Based on studies of polyoma virus transformed golden hamster cell lines Rabinowitz and Sachs (1970) proposed a model of the chromosomal control of malignancy. According to this model

hamster chromosomes 5₆, 5₇ and 5₁₂ the S genes in chromosomes 5₇ and 7₂ (3, 38). Similar results were obtained in studies on chemically transformed hamster cells (2). Also in a mouse tumor system suppression of malignancy

was linked to the presence of a marker chromosome (4) Our observations of the correlation between the karyotype and tumorigenicity seem to be in agreement with the suppression-expression model In terms of that model our results would mean that in BKV transformed rat embryo cells E chromosome(s) localize in group II and S chromosome(s) in group A of the classification of *Unakul and Hsu* (37) In an international nomenclature (5) the S chromosomes resemble acrocentric chromosomes number 12 and 13 A more accurate identification of the E and S chromosomes will require a banding pattern analysis

This work has been supported by the Sigrid Jusélius Foundation and the Finnish Foundation for Cancer Research

The transformed REBA cell line was isolated when one of us (AS) was a recipient of a University of Alberta Killam Postdoctoral Fellowship

REFERENCES

- 1 Aaronson S A Todaro G J Basis for the acquisition of malignant potential by mouse cells cultivated *in vitro* Science 162 1024-1026 1968
- 2 Benedict W F Rucker N Mark C Kouri R E Correlation between balance of specific chromosomes and expression of malignancy in hamster cells J Natl Cancer Inst 54 157-162 1975
- 3 Bloch Shtacher N Sachs L Chromosome balance and the control of malignancy J Cell Physiol 87 89-100 1976
- 4 Codish S D Paul B Reversible appearance of a specific chromosome which suppresses malignancy Nature (Lond) 252 610-612 1974
- 5 Committee for a Standardized Karyotype of *Rattus norvegicus* Standard karyotype of the Norway rat *Rattus norvegicus* Cytogenet Cell Genet 12 199-205 1973
- 6 Cooper H L Black P H Cytogenetic studies of hamster kidney cell cultures transformed by the simian vacuolating virus (SV40) J Natl Cancer Inst 30 1015-1043 1963
- 7 Costa J Howley P M Legallais F Yee C Young N Rabson A S Oncogenicity of a nude mouse cell line transformed by a human papovavirus J Natl Cancer Inst 58 1147-1149 1977
- 8 Costa J Yee C Traika T S Rabson A S Hamster ependymomas produced by intracerebral inoculation of a human papovavirus (MMV) J Natl Cancer Inst 56 863-864 1976
- 9 Defendi Y Lehman J M Transformation of hamster embryo cells *in vitro* by polyoma virus morphological karyological immunological and transplantation characteristics J Cell Comp Physiol 66 351-410 1965
- 10 DiPaolo J A Popescu N C Relationship of chromosome changes to neoplastic cell transformation Amer J Pathol 85 709-738 1976
- 11 Dougherty R M Induction of tumors in Syrian hamsters by a human renal papovavirus RF strain J Natl Cancer Inst 57 395-400 1976
- 12 Greenlee J E Narayan O Johnson R T Herndon R M Induction of brain tumors in hamsters with BK virus a human papovavirus Lab Invest 36 636-641 1977
- 13 Hitotsumachi S Rabinowitz Z Sachs L Chromosomal control of reversion in transformed cells Nature (Lond) 231 511-514 1971
- 14 Lavielle C Stévenet J Morris A G Suarez H G Estrade S Salomon J C Cassingena R Simian virus 40 Chinese hamster kidney cell interaction I Relationship of chromosome changes to transformation Arch Virol 49 127-139 1974
- 15 Lehman J M Early chromosome changes in diploid Chinese hamster cells after infection with simian virus 40 Int J Cancer 13 164-172 1974
- 16 Lehman J M Bloustein P Chromosome analysis and agglutination by concanavalin A of primary simianvirus 40 induced tumors Int J Cancer 14 771-778 1974
- 17 Lehman J M Defendi Y Changes in deoxyribonucleic acid synthesis regulation I Chinese hamster cells infected with simian virus 40 J Virol 6 738-749 1970
- 18 Levine A J SV40 and adenovirus early functions involved in DNA replication and transformation Biochim Biophys Acta 458 213-241 1976
- 19 Nachtigal M Lungeanu A Nachtigal S Aderca I Cytogenetic study of two tumor lines induced in the golden hamster by SV40 virus Rev Roum d'Inframicrobiol 5 119-127 1968
- 20 Nase L M Karkkainen M Mannjärvi R Transplantable hamster tumors induced with the BK virus Acta path microbiol scand Sect B 83 347-352 1975
- 21 Pollack R E Teebor G W Relationship of contact inhibition to tumor transplantability morphology and growth rate Cancer Res 29 1770-1772 1969
- 22 Pontén J The relationship between *in vitro* transformation and tumor formation *in vivo* Biochim Biophys Acta 458 397-422 1976
- 23 Portolami M Barbanti Brodano G La Placa M Malignant transformation of hamster kidney cells by BK virus J Virol 15 420-422 1975
- 24 Portolami M Borgatti M Corallini A Cassa E Grossi M P Barbanti Brodano G Possati L Stable transformation of mouse rabbit and monkey cells and abortive transformation of human cells by BK virus a human papovavirus J Gen Virol 38 369-374 1978
- 25 Rabinowitz Z Sachs L Reversion of properties in cells transformed by polyoma virus Nature (Lond) 220 1203-1206 1968
- 26 Rabinowitz Z Sachs L Control of the reversion

of properties in transformed cells *Nature (Lond)* 225 136-139 1970

- 27 Rapp F Geder L Murasko D Lausch R Ladda R Huang E S Webber M M Long term persistence of cytomegalovirus genome in cultured human cells of prostatic origin *J Virol* 16 982-990 1975
- 28 Sanford K K Malignant transformation of cells *in vitro* *Int. Rev. Cytol* 18 249-311 1965
- 29 Seehafer J Downer D N Salmi A Colter J S Isolation and characterization of BK virus - transformed rat and mouse cells *Virology* in press 1979
- 30 Seehafer J Salmi A Colter J S Isolation and characterization of BK virus transformed hamster cells *Virology* 77 356-366 1977
- 31 Shoh K V Daniel R W Strandberg J D Sarcoma in a hamster inoculated with BK virus a human papovavirus *J Natl Cancer Inst* 54 945-950 1975
- 32 Sien M Tolonen A Pitko V M Nevalainen T Mantjarvi R A Characterization of cell lines derived from hamster tumors induced with the BK virus *Arch Virol* 50 73-82 1976
- 33 Takemoto K K Martin M A Transformation of hamster kidney cells by BK papovavirus DNA *J Virol* 17 247-253 1976
- 34 Tanaka R Koprowski H Iwasaki Y Malignant transformation of hamster brain cells *in vitro* by human papovavirus BK *J Natl Cancer Inst* 56 671-673 1976
- 35 Tjian R Fey G Graessman A Biological activity of purified simian virus 40 T antigen proteins *Proc Natl Acad Sci USA* 75 1279-1283 1978
- 36 Uchida S Watanabe S Aizawa T Kato K Furuno A Muto T Induction of papillary ependymomas and insulinomas in the Syrian golden hamster by BK virus a human papovavirus *Gann* 67 857-865 1976
- 37 Unakul W Hsu T C The C and G banding patterns of *Rattus norvegicus* chromosomes *J Natl Cancer Inst* 49 1425-1431 1972
- 38 Yamamoto T Hayashi M Rabinowitz Z Sachs L Chromosomal control of malignancy in tumors from cells transformed by polyoma virus *Int J Cancer* 11 555-566 1973
- 39 Zuna R E Lehman J M Heterogeneity of karyotype and growth potential in simian virus 40 transformed Chinese hamster cell clones *J Natl Cancer Inst* 58 1463-1472 1977

was linked to the presence of a marker chromosome (4) Our observations of the correlation between the karyotype and tumorigenicity seem to be in agreement with the suppression-expression model In terms of that model our results would mean that in BKV-transformed rat embryo cells E chromosome(s) localize in group II and S chromosome(s) in group A of the classification of *Unakul and Hsu* (37) In an international nomenclature (5) the S chromosomes resemble acrocentric chromosomes number 12 and 13 A more accurate identification of the E and S chromosomes will require a banding pattern analysis

This work has been supported by the *Sigrid Juselius Foundation* and the *Finnish Foundation for Cancer Research*

The transformed REBK cell line was isolated when one of us (AS) was a recipient of a University of Alberta Killam Postdoctoral Fellowship

REFERENCES

- 1 Aaronson S A Todaro G J Basis for the acquisition of malignant potential by mouse cells cultivated *in vitro* Science 162 1024-1026 1968
- 2 Benedict W F Rucker N Mark C Kouri R E Correlation between balance of specific chromosomes and expression of malignancy in hamster cells J Natl Cancer Inst 54 157-162 1975
- 3 Bloch-Shtacher N Sachs L Chromosome balance and the control of malignancy J Cell Physiol 87 89-100 1976
- 4 Codish S D Paul B Reversible appearance of a Rattus norvegicus Cytogenet Cell Genet 12 199-205 1973
- 5 Cooper H L Black P H Cytogenetic studies of hamster kidney cell cultures transformed by the simian vacuolating virus (SV40) J Natl Cancer Inst 30 1015-1043 1963
- 6 Costa J Howley P M Legallais F Yee C Young N Rabson A S Oncogenicity of a nude mouse cell line transformed by a human papovavirus J Natl Cancer Inst 58 1147-1149 1977
- 7 Costa J Yee C Traika T S Rabson A S Hamster ependymomas produced by intracerebral inoculation of a human papovavirus (MMV) J Natl Cancer Inst 56 863-864 1976
- 8 Defendi V Lehman J M Transformation of hamster embryo cells *in vitro* by polyoma virus morphological karyological immunological and transplantation characteristics J Cell Comp Physiol 66 351-410 1965
- 9 DiPaolo J A Popescu N C Relationship of chromosome changes to neoplastic cell transformation Amer J Pathol 85 709-738 1976
- 10 Dougherty R M Induction of tumors in Syrian hamsters by a human renal papovavirus RF strain J Natl Cancer Inst 57 395-400 1976
- 11 Greenlee J E Narayan O Johnson R T Herndon R M Induction of brain tumors in hamsters with BK virus a human papovavirus Lab Invest 36 636-641, 1977
- 12 Hutoisumachi S Rabinowitz Z Sachs L Chromosomal control of reversion in transformed cells Nature (Lond) 231 511-514 1971
- 13 Lavielle C Stevenet J Morris A G Suare H G Estrade S Salomon J C Cassingena R Simian virus 40 Chinese hamster kidney cell interaction I Relationship of chromosome changes to transformation Arch Virol 49 127-139 1975
- 14 Lehman J M Early chromosome changes in diploid Chinese hamster cells after infection with simian virus 40 Int J Cancer 13 164-172 1974
- 15 Lehman J M Bloustein P Chromosome analysis and agglutination by concanavalin A of primary simian virus 40 induced tumors Int J Cancer 14 771-778 1974
- 16 Lehman J M Defendi V Changes in deoxyribonucleic acid synthesis regulation in Chinese hamster cells infected with simian virus 40 J Virol 6 738 749 1970
- 17 Levine A J SV40 and adenovirus early functions involved in DNA replication and transformation Biochim Biophys Acta 458 213-241 1976
- 18 Nachtigal M Lungeanu A Nachtigal S Aderca I Cytogenetic study of two tumor lines induced in the golden hamster by SV40 virus Rev Roum d Inframicrobiol 5 119-127 1968
- 19 Nase L M Karkkainen M Mantjarvi R A Transplantable hamster tumors induced with the BK virus Acta path microbiol scand Sect B 83 347-352 1975
- 20 Pollack R E Teebor G W Relationship of contact inhibition to tumor transplantability morphology and growth rate Cancer Res 29 1770-1772 1969
- 21 Pontén J The relationship between *in vitro* transformation and tumor formation *in vivo* Biochim Biophys Acta 458 397-422 1976
- 22 " " " " " " La Placa V kidney cells 1975
- 23 Portolani M Borgatti M Corallini A Cassai E Grossi M P Barbanti Brodano G Possati L Stable transformation of mouse rabbit and monkey cells and abortive transformation of human cells by BK virus a human papovavirus J Gen Virol 33 369-374 1978
- 24 Rabinowitz Z Sachs L Reversion of properties in cells transformed by polyoma virus Nature (Lond) 220 1203-1206 1968
- 25 Rabinowitz Z Sachs L Control of the reversion

A RETROSPECTIVE HISTOLOGICAL STUDY OF 669 CASES OF PRIMARY CUTANEOUS MALIGNANT MELANOMA IN CLINICAL STAGE I

5 The Consequences of a Reclassification of the Original Group of Lentigo Maligna Melanomas

TOVE EEG LARSEN and TOVE HELLIESEN GRUDE

Institute of Pathology University of Oslo Rikshospitalet Oslo and The Norwegian Radium Hospital
Oslo Norway

Larsen T E & Grude T H A retrospective histological study of 669 cases of primary cutaneous malignant melanoma in clinical stage I 5 The consequences of a reclassification of the original group of lentigo maligna melanomas Acta path microbiol scand Sect A 87 255-260 1979

A selected series of primary malignant melanoma of the skin clinical stage I was originally classified according to Clark's system. The consistency of this classification was tested by two Brisbane pathologists who indicated that we had misinterpreted some cases of superficial spreading malignant melanoma as lentigo maligna melanoma. We have therefore reclassified the original group of 86 lentigo maligna melanomas. This resulted in a total series of 37 (5.5%) lentigo maligna melanomas, 301 (45%) superficial spreading melanomas, 294 (44%) nodular melanomas, 13 (2%) acral lentiginous melanomas and 1 case of melanoma in situ.

was not
group of lentigo maligna melanomas is dominated by cases on the head among patients over 50 years of age (especially women). This is in better agreement with other studies than our previous findings. The relationship with tumour cell type, pigmentation, mitotic count, atypia, transectional profile, level of invasion, ulceration, vascular invasion, lymphocyte infiltration and prognosis shown by the new groups of melanomas is still unclear. The reclassification of the original group of 86 lentigo maligna melanomas represents an intermediate tumour type although it has deviated in the benign direction.

Key words: Melanoma classification.

T E Larsen, Institute of Pathology, Rikshospitalet, Oslo 1, Norway

Received 15 XII 78 Accepted 1 III 79

In order to study the reliability of our melanoma type classification according to Clark's system (Clark 1967, Clark *et al* 1969) presented earlier (Larsen & Grude 1978a) we have sent some of our sections to two Brisbane pathologists*. These sections include the first and the last 52 cases of the series of 669 primary cutaneous malignant melano-

mac (MM) ...
... pathologists and ourselves concerning

* Dr J H Little, Director of Pathology and Dr R L Quinn, The Department of Pathology, Princess Alexandra Hospital, Brisbane, Australia.

TABLE 2 *The Relation of Tumour Type to Localization of the Tumour*

Localization	Total		% of LMM		% of SVM	
	No	%	now	orig *	now	orig
Head	164	25	92	57	13	10
Neck and trunk	210	31	5	21	34.5	35
Upper extremity	79	12	3	7	11	12
Lower extremity	161	24	0	13	32	33
Foot	48	7	0	2	9	9
Other + unknown	7	1	0	0	0.5	1
Total	669	100	100	100	100	100

* Originally

TABLE 3 *The Relative Frequency at Each Tumour Type of Various Histological Features Related to a Good Prognosis*

Features related to a good prognosis	Total		% of LMM		% of SVM	
	No	%	now	orig *	now	orig
Flat slightly elevated surface	356	53	95	97	73	69
No ulceration	419	63	92	91	74	71
Level I-II of invasion	147	22	84	71	31	26
No vascular invasion	600	90	100	100	95	94
Pure spindle cells	46	7	24	20	3	2
Atypia grade +	76	11	24	23	17	15
Mitotic count grade +	371	55	92	93	67	63
Pigmentation grade ++	151	23	27	42	30	27
Lymphocyte infiltration grade +	151	23	46	41	26	25

* Originally

TABLE 4 *The Relative Frequency at Each Tumour Type of Various Histological Features Related to a Poor Prognosis*

Features related to a poor prognosis	Total		% of LMM		% of SVM	
	No	%	now	orig *	now	orig
Hemispherical or pedunculated surface	135	20	0	0	9	11
Ulceration	197	29	3	6	20	22
Level IV-V of invasion	229	34	8	6	25	28
Vascular invasion	39	6	0	0	4	5
Pure epithelioid cells	210	32	11	15	34	36
Atypia grade +++	84	13	0	1	9	11
Mitotic count grade +++	77	12	11	0	6	7
No pigmentation	101	15	0	0	7	8
Lymphocyte infiltration grade +	210	31	24	20	29	30

* Originally

the cases which we had originally described as lentigo maligna melanoma (LMM), while there was an almost complete agreement as regards the cases which we had registered as superficial spreading malignant melanoma (SMM) or nodular malignant melanoma (NMM). Among the 13 cases classified by us as LMM 8 were described as SMM by the Brisbane pathologists.

Accordingly we took a second look at all the 86 cases originally classified as LMM. The result of this and the consequences to our previous findings and conclusions are discussed in this paper.

SERIES AND METHODS

The series includes 669 MM: clinical stage I (256 ♂ and 413 ♀). In earlier papers we have presented the grading as well as the interrelationship of the various histological features discussed later in this paper (Larsen & Grude 1978 II and III; Larsen & Grude 1979).

All 86 cases originally classified as LMM were reclassified by both authors independently of each other with no access to any clinical information as usual. In addition to the criteria used earlier we paid attention this time to the thickness of the epidermis. The finding of an atrophic epidermis led to classification as LMM while a thickening of the epidermis led to classification as SMM (Kuhnt-Petzoldt 1974). Further the diagnosis of LMM was not made in the absence of dermal solar elastosis (McGovern 1976). Our individual results were later compared. In cases of disagreement the classification as a LMM was maintained if one of us had reclassified the case as such. Other cases of disagreement led to a diagnosis of unclassifiable malignant melanoma (UMM).

RESULTS

The reclassification resulted in 37 LMM, 34 SMM, 7 UMM, 4 non-invasive SMM and 4 compound naevi with atypia. In order not to complicate the

Tumour type

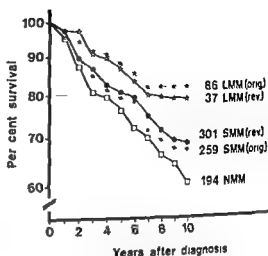


Fig. 1 The observed cumulative survival rates of ex tumour type. Rev = revised series Orig = original series.

calculation compared with the earlier results the cases of non-invasive SMM and compound naevi with atypia were included in the group of SMM. Thereby we have got a series including 37 (3.5%) LMM, 301 (45%) SMM, 194 (29%) NMM and 137 (20.5%) UMM.

The observed cumulative survival rates according to tumour type is illustrated in Fig. 1.

The relation of LMM and SMM to sex and age, the patient and to localization of the tumour is shown in Tables 1 and 2 respectively. Support for the view that the occurrence of these features is independent of each subgroup of these features ought to be the same in the total series as in each tumour type. This concerns also the relation of LMM and SMM to the «benign» and «malignant» grades and types of various histological features which have been studied previously (Tables 3 and 4 respectively).

TABLE 1 The Relation of Tumour Type to Sex and Age of the Patient

Sex and age	Total		% of LMM		% of SMM	
	No.	%	now	orig *	now	orig
<50y ♀	205	31	5	21	37	38
	121	18	3	12	21	21
>50y ♀	208	31	68	49	28	27
	135	20	24	18	14	14
Total	669	100	100	100	100	100

* Originally

DISCUSSION

Auhl Per olds (1974) stressed the diagnostic importance of a thickened epidermis in SVM compared with the atrophic one in LMM and McGovern (1976) that of the presence of dermal solar elastosis in LMM (Fig. 2 and 3). We did not pay any special attention to these features at our original tumour type classification. It seems that originally we had the tendency to classify cases showing a wide spread junctional proliferation of irregular melanocytes or melanocytes with atypia along closely packed deep rete ridges as lentigo maligna or LMM (Fig. 4). We had probably the lentigo senilis in mind as a possible precursor of a lentigo maligna (Pinkus & Mehregan 1969).

The reclassification has led to a smaller group of LMM and a larger group of SVM than earlier. When compared with an American study referred to by Kopf *et al.* (1977) the relative incidence of LMM is the same but our frequency of SVM is lower and that of NVIM is higher. However our series includes a group of UMM. Therefore the figures are not really comparable. The most important finding is the low incidence of LMM in this series. This is in agreement with our experience from the daily routine work (Larsen 1978).

Our problem is: does the reclassification have any effect on our previous findings and conclusions as regards the LMM and SVM?

The Relation of Tumour Type to Prognosis

The observed cumulative survival rates according to LMM and SVM (Fig. 1) do not differ significantly from those found earlier. The prognosis of the new group of patients with LMM has become slightly worse while that of the new group of patients with SVM has become slightly better. This is probably due to the moving of relatively benign cases from the original group of LMM to that of SVM. The observed survival of patients with LMM is however still better than that of patients with SVM although the difference is not significant.

The Relation of Tumour Type to Sex, Age and Localisation

The deviation from our original findings as regards SVM is minimal and shows no special pattern (Tables 1 and 2). There is however an obvious difference in the LMM group. The revised group of LMM includes to a great measure (92%) patients over 50 years of age with the tumour located on the head (especially women). These trends are in much better agreement with other

studies (Clark *et al.* 1969, McGovern 1970) than our previous findings (Larsen & Grude 1978 a).

The Relation of Tumour Type to Various Histological Features

The relation of tumour type to the various benign and malignant grades and types of a series of histological features previously studied (Tables 3 and 4) shows the following tendency. The new group of SVM deviates only slightly from the old one. This is also the case for the LMM. Even if the incidence of LMM with level III of invasion has been much reduced 3 cases with level IV of invasion still remain. Further the revised group of LMM shows a tendency of a lower grade of pigmentation and a higher grade of cellular atypia than the old one (grade + of pigmentation and grade ++ of atypia have become more frequent not illustrated). Also this fits in well with the moving of relatively benign cases from the original group of LMM to that of SVM.

The awareness of a probable misinterpretation of some SVM as LMM certainly influenced our reclassification. However although we had no access to any clinical information it seems that by evaluating epidermal thickness and dermal solar elastosis in addition to the other histological criteria used previously we now have a group of LMM which is in better accordance with the findings in other studies.

Further the trends of our previous findings (Larsen & Grude 1978 b and c, Larsen & Grude 1979) are still valid. The LMM is usually a low grade, the SVM a medium grade and the NVIM a high grade malignant tumour. The SVM may deviate in either direction although mostly in the benign one.

CONCLUSIONS

1) The reclassification has produced a group of lentigo maligna melanomas which are usually found on the head of patients over 50 years of age (especially women). This is in better agreement with previous studies by other investigators.

2) The conclusions of our previous papers are still valid. The new group of lentigo maligna melanomas is still the most benign one and the new group of superficial spreading malignant melanomas still behaves intermediately although it has become more benign.

3) It seems that we overestimated the number of lentigo maligna melanoma in our first series. It was the evaluation of epidermal thickness and of dermal solar elastosis that led to the improvement in classification.

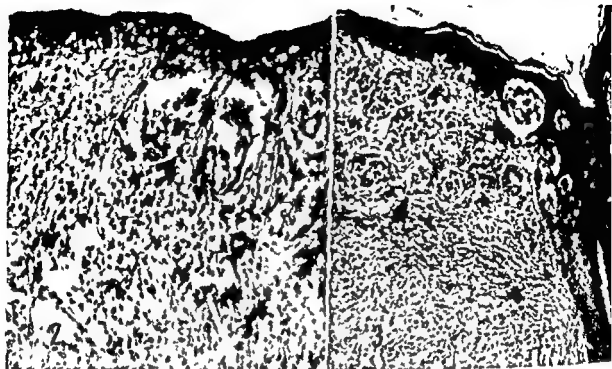


Fig 2 In this case the diagnosis of LMM was maintained. The epidermis is atrophic. To the right early invasive growth of irregular partly spindle shaped tumour cells. Solar elastosis is present in the dermis below (difficult to see) $\times 195$



Fig 3 In this case the diagnosis was changed from LMM to SVM. The epidermis is in fact thin but there is pagetoid growth of single tumour cells in the hair follicle to the right. To the left in the upper part of the dermis nests of small epithelioid slightly atypical tumour cells. No dermal solar elastosis is present $\times 94$

DISCUSSION

attention to these features in our original tumour type classification. It seems that originally we had the tendency to classify cases showing a widespread junctional proliferation of irregular melanocytes or melanocytes with atypia along closely packed, deep rete ridges as lentigo maligna or LMM (Fig. 4). We had probably the lentigo senilis in mind as a possible precursor of a lentigo maligna (Pinkus & Mehregan 1969).

The reclassification has led to a smaller group of LMM and a larger group of SVM than earlier

lower and that of NMM is higher. However, our series includes a group of UMM. Therefore, the figures are not really comparable. The most important finding is the low incidence of LMM in both series. This is in agreement with our experience from the daily routine work (Larsen 1978).

Our problem is: does the reclassification have any effect on our previous findings and conclusions as regards the LMM and SVM?

The Relation of Tumour Type to Prognosis

The observed cumulative survival rates according to LMM and SVM (Fig. 1) do not differ significantly from those found earlier. The prognosis of the new group of patients with LMM has become slightly worse while that of the new group of patients with SVM has become slightly better. This is probably due to the moving of relatively benign cases from the original group of LMM to that of SVM. The observed survival of patients with LMM is however still better than that of patients with SVM although the difference is not significant.

The Relation of Tumour Type to Sex, Age and Localization

The deviation from our original findings as regards SVM is minimal and shows no special pattern (Tables 1 and 2). There is however, an obvious difference in the LMM group. The revised group of LMM includes to a great measure (92%) patients over 50 years of age with the tumour located on the head (especially women). These trends are in much better agreement with other

studies (Clark *et al.* 1969, McGovern 1970) than our previous findings (Larsen & Grude 1978 a).

The Relation of Tumour Type to Various Histological Features

The relation of tumour type to the various »benign« and »malignant« grades and types of a series of histological features previously studied (Tables 3 and 4) shows the following tendency. The new group of SVM deviates only slightly from the old one. This is also the case for the LMM. Even if the incidence of LMM with level III of invasion has been much reduced, 3 cases with level IV of invasion still remain. Further, the revised group of LMM shows a tendency of a lower grade of pigmentation and a higher grade of cellular atypia than the old one (grade + of pigmentation and grade ++ of atypia have become more frequent, not illustrated). Also this fits in well with the moving of relatively benign cases from the original group of LMM to that of SVM.

The awareness of a probable misinterpretation of some SVM as LMM certainly influenced our reclassification. However, although we had no access to any clinical information it seems that by evaluating epidermal thickness and dermal solar elastosis in addition to the other histological criteria used previously, we now have a group of LMM which is in better accordance with the findings in other studies.

Further, the trends of our previous findings (Larsen & Grude 1978 b and c, Larsen & Grude 1979) is still valid. The LMM is usually a low grade, the SVM a medium grade and the NMM a high grade malignant tumour. The SVM may deviate in either direction, although mostly in the benign one.

CONCLUSIONS

- 1) The reclassification has produced a group of lentigo maligna melanomas which are usually found on the head of patients over 50 years of age (especially women). This is in better agreement with previous studies by other investigators.
- 2) The conclusions of our previous papers are still valid. The new group of lentigo maligna melanomas is still the most benign one and the new group of superficial spreading malignant melanomas still behaves intermediately although it has become more benign.
- 3) It seems that we overestimated the number of lentigo maligna melanoma in our first series. It was the evaluation of epidermal thickness and of dermal solar elastosis that led to the improvement in classification.

4) The diagnosis of lentigo maligna melanoma should not be made unless the epidermis is atrophic and solar elastosis is present

5) As the reclassification has turned out to be satisfactory it will be used in the later studies of this series of malignant melanomas

We are grateful to Dr J H Little, Director of Pathology and to Dr R L Quinn, The Department of Pathology Princess Alexandra Hospital, Brisbane, Australia, for their kindly assistance

REFERENCES

- Clark W H A classification of malignant melanoma in man correlated with histogenesis and biologic behavior. In *Montagna II* (Ed) *Advances in Biology of the skin. The pigmentary system* 1 ed Vol VIII Pergamon Press Oxford 1967 pp 621-647
- Clark W H, From L, Bernardino E A & Mihm M C The histogenesis and biologic behavior of primary human malignant melanomas of the skin. *Cancer Research* 29 705-726 1969
- Kopf A W, Bart R S & Rodriguez R S Malignant melanoma. A review. *J Dermatol Surg Oncol* 3 49-55 1977
- Kuhnl Peizoldt C Superficial spreading melanoma. Histological findings and problems of differentiation. *Arch Derm Forsch* 250 309-321 1974
- Larsen T E & Grude T H A retrospective histological study of 669 cases of primary cutaneous malignant melanoma in clinical stage I 1. Histological classification, sex and age of the patients, localization of tumour and prognosis. *Acta Path Microbiol Scand Sect A* 86 437-450 1978
- Larsen T E & Grude T H A retrospective histological study of 669 cases of primary cutaneous malignant melanoma in clinical stage I 2. The relation of cell type, pigmentation, atypia and mitotic count to histological type and prognosis. *Acta Path Microbiol Scand Sect A* 86 513-522 1978
- Larsen T E & Grude T H A retrospective histological study of 669 cases of primary cutaneous malignant melanoma in clinical stage I 3. The relation between the tumour associated lymphocyte infiltration and age and sex, tumour cell type, pigmentation, cellular atypia, mitotic count, depth of invasion, ulceration, tumour type and prognosis. *Acta Path Microbiol Scand Sect A* 86 523-530 1978
- Larsen T E & Grude T H A retrospective histological study of 669 cases of primary cutaneous malignant melanoma in clinical stage I 4. The relation of cross sectional profile, level of invasion, ulceration and vascular invasion to tumour type and prognosis. *Acta Path Microbiol Scand Sect A* 87 131-138 1979
- Larsen T E The classification of primary cutaneous malignant melanoma. A prospective study of 60 cases using Clark's classification. *Acta Path Microbiol Scand Sect A* 86 451-459 1978
- McGovern V J The classification of melanoma and its relationship with prognosis. *Pathology* 2 85 98 1970
- McGovern V J Malignant melanoma. Clinical and histological diagnosis. 1st ed. John Wiley & Sons, New York 1976 pp 59-64

TERATOGENICITY OF INTRAUTERINE COPPER WIRE IN MICE

A Histopathological Study

B BRUUN RASMUSSEN and N CHRISTENSEN

Department of Pathology Frederiksberg Hospital Copenhagen and Eye Pathology Institute Copenhagen Denmark

Rasmussen B Bruun & Christensen N Teratogenicity of intrauterine copper wire in mice A histopathological study Acta path microbiol scand Sect. A 87 261-264 1979

Immediately after the implantation of the fertilized ovum on the 6th day of pregnancy a copperwire was placed in the right hand uterine section on pregnant C3H mice. The left section was similarly surgically traumatized in order to serve as a control. The mice were killed with chloroform on the 19th day of pregnancy and by means of a special histological screening technique the fetuses were examined with special reference to growthreduction, intrauterine fetal death and microscopic malformations. Differences in intrauterine fetal death were shown not to exist nor was there any significant growthretardation in the copperwire containing uterine section. Certain microscopic defects were found with slightly increased incidence in the copper containing section but the differences were not statistically significant.

Key words: Copperwire, fetal death, growthretardation, microscopic malformations.

B Bruun Rasmussen, The Finsen Institute of Pathology, Strandboulevarden 49, DK 2100 Copenhagen B, Denmark.

Accepted as submitted 2 ii 79

The anticonceptual effect of a copper IUD was documented experimentally first in rats by Zipper *et al.* (5) and in rats and hamsters by Chang *et al.* (3). The effect was found to be dependant on the insertion of the copperwire prior to the implantation of the fertilized ovum. Although the exact means of function are not yet fully understood, the fact that a normal implantation process took its course in the contralateral uterine section without copperwire points to a local effect on the endometrium.

The question as to whether a copper IUD placed in the uterus after the implantation will interfere with the normal embryonic development has been examined in preclinical studies by Chang & Tatum (2). The experiments done almost exclusively on rodents so far have shown no teratogenic effect of the copperwire. However, the results have been relying on a macroscopic evaluation of the embryos

only. This and the fact that two cases of fibular dysplasia have been reported by Barrie (1) in children born by mothers with copper IUDs gave us the inspiration to an experiment based on a histological screening of the entire fetus.

MATERIAL AND METHODS

The material comprises 22 pregnant C3H mice and a total of 122 fetuses were examined.

Immediately after the implantation of the fertilized ovum on the day 6 of pregnancy an exploratory laparotomy was done in general anaesthesia with a shortacting barbiturate intraperitoneally. Being assured that the uterus was pregnant a 0.02 mm pure copperwire was sutured inside the upper proximal part of the right uterine section in such a way it would pose no mechanical threat to the implanted ova and yet be inside the cavity. In the proximal part of the left section a

similar surgical procedure was done but no copperwire was left behind. This would serve as a control. The peritoneum and the skin were sutured separately with silk. All of the operated mice were showing normal behaviour approximately 30 minutes after the start of the operation.

On the 19th day of pregnancy the mice were killed with chloroform and the fetuses were removed from the uterus. At the same time a control was made as to whether the copperwire had been in the right position. The fetuses were measured, weighed and screened for malformations under the stereomicroscope. After this decapitation was done and the heads fixed in Bouin's solution, mounted in paraffine and cut in serial sections. The bodies too were fixed in Bouin's solution but hereafter by a sagittal transverse section separated in two at the level of the roots of the extremities. After mounting in paraffine each half was cut in serial sections. All slides were stained with haematoxylin-eosin and admodum van Gieson. Hansen combined with alcian blue.

All the slides were then screened for microscopic malformations in the litters from the copperwire sections as well as the contralateral control sections.

Concerning fetal death and malformations in the two uterine sections we have calculated a statistical index based on the nil hypothesis. This statistical evaluation accounts for the litter effect as well for the controlled experiment. The Wilcoxon test has been used to evaluate the difference in length and weight of the fetuses.

RESULTS

Among the 22 mice in the experiment 3 were found not to be pregnant at the time of caesarean section. Two mice were found dead 2 days after the

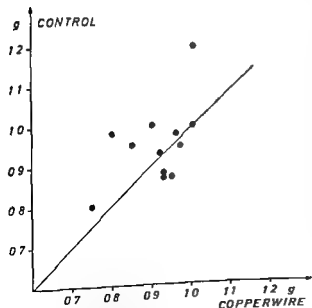


Fig 1 Correlations between mean litter weight in uterine section with and without copper wire. Each spot indicates one pregnant mouse.

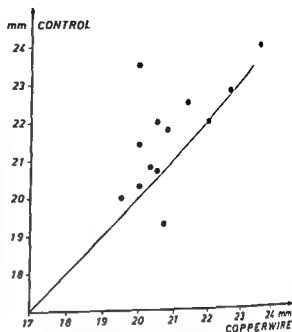


Fig 2 Correlations between mean litter crown-rump length in uterine section with and without copper wire. Each spot indicates one pregnant mouse.

operation because of severe decomposition. Autopsy was not done. In the rest there was found no illnesses, wound infections or wound ruptures.

Pathology

The relationship between mean weight and mean crown-rump length of fetuses in each pregnant mouse is illustrated in Fig 1 and Fig 2 as each spot indicates one pregnant mouse. Statistical analyses revealed no growth reduction in fetuses from copper-containing uterine sections.

At the stereomicroscopic examination one case of microcephalia was found among fetuses from copper-containing uterine horn. No other defects were observed using this method of examination.

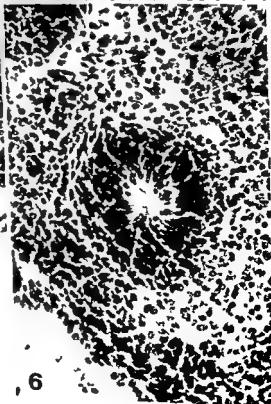
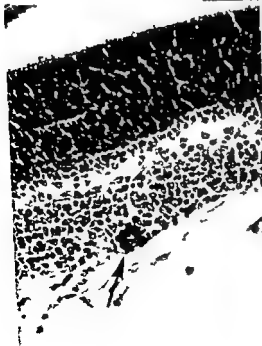
At the histological screening procedure we focused on a detailed examination of all internal organs. Apart from growth reduction in generally small animals we observed changes only in the neuroectodermally derived structures such as the cerebrum and the eyes. These defects were constantly very small, consisting in mainly abnormal retinal vessels, pigmented cells in the optic nerve and single rosettes in the retina and cerebral cortex (Fig 3, 4, 5 and 6).

Fig 3 Abnormal retinal vessel ($\times 400$)

Fig 4 Pigmented cells in the optic nerve ($\times 400$)

Fig 5 Single rosette in the retina ($\times 400$)

Fig 6 Rosette in the cerebral cortex ($\times 400$)



3

5

6

similar surgical procedure was done but no copperwire was left behind. This would serve as a control. The peritoneum and the skin were sutured separately with silk. All of the operated mice were showing normal behaviour approximately 30 minutes after the start of the operation.

On the 19th day of pregnancy the mice were killed with chloroform and the fetuses were removed from the uterus. At the same time a control was made as to whether the copperwire had been in the right position. The fetuses were measured, weighed and screened for malformations under the stereomicroscope. After this decapitation was done and the heads fixed in Bouin's solution, mounted in paraffine and cut in serial sections. The bodies too were fixed in Bouin's solution but hereafter by a sagittal transverse section separated in two at the level of the roots of the extremities. After mounting in paraffine each half was cut in serial sections. All slides were stained with haematoxylin-eosin and admodum van Gieson-Hansen combined with alcian blue.

All the slides were then screened for microscopic malformations in the litters from the copperwire sections as well as the contralateral control sections.

Concerning fetal death and malformations in the two uterine sections we have calculated a statistical index based on the nil hypothesis. This statistical evaluation accounts for the litter effect as well as the controlled experiment. The Wilcoxon test has been used to evaluate the difference in length and weight of the fetuses.

RESULTS

Among the 22 mice in the experiment 3 were found not to be pregnant at the time of caesarean section. Two mice were found dead 2 days after the

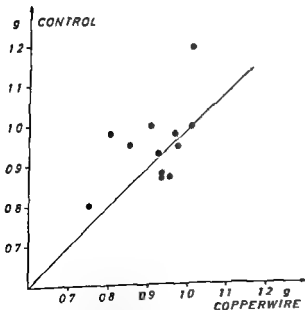


Fig 1 Correlations between mean litter weight in uterine section with and without copper wire. Each spot indicates one pregnant mouse.

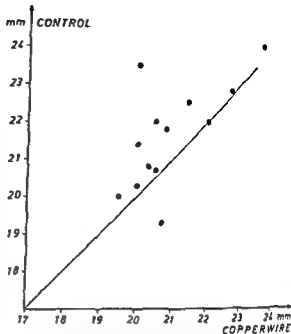


Fig 2 Correlations between mean litter crown-rump length in uterine section with and without copper wire. Each spot indicates one pregnant mouse.

operation because of severe decomposition. Autopsy was not done. In the rest there was found no illnesses, wound infections or wound ruptures.

Pathology

The relationship between mean weight and mean crown-rump length of fetuses in each pregnant mouse is illustrated in Fig 1 and Fig 2 as each spot indicates one pregnant mouse. Statistical analyses revealed no growth reduction in fetuses from copper-containing uterine sections.

At the stereomicroscopic examination one case of microcephalia was found among fetuses from copper-containing uterine horn. No other defects were observed using this method of examination.

At the histological screening procedure we focused on a detailed examination of all internal organs. Apart from growth reduction in generally small animals we observed changes only in the neuroectodermally derived structures such as the cerebrum and the eyes. These defects were constantly very small, consisting in mainly abnormal retinal vessels, pigmented cells in the optic nerve and single rosettes in the retina and cerebral cortex (Fig 3, 4, 5 and 6).

Fig 3 Abnormal retinal vessel ($\times 400$)

Fig 4 Pigmented cells in the optic nerve ($\times 400$)

Fig 5 Single rosette in the retina ($\times 400$)

Fig 6 Rosette in the cerebral cortex ($\times 400$)

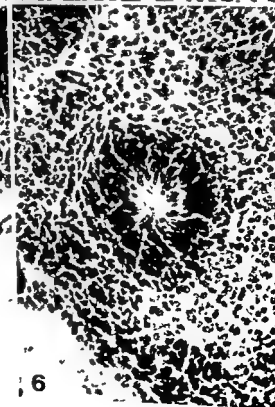
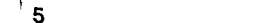
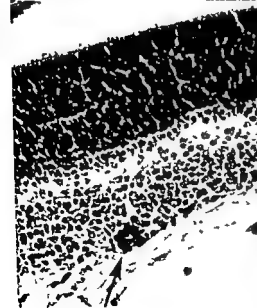
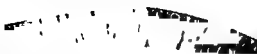


TABLE 1 *Total Number of Fetuses Normal Malformed and Fetal Deaths in the Copperwire containing Uterine Section and the Control Section*

	Fetuses	Normal	Malformed	Fetal deaths
Copperwire section	65	37	15	13
Control section	57	35	11	11

The number of fetuses from the two different groups are shown in Table 1, which also shows the number of dead, malformed and normal individuals. There was no significant difference between the number of fetal deaths, nor was the apparent difference between the number of defects in the two groups significant ($U = 0.83$).

DISCUSSION AND CONCLUSION

If the presence of a copperwire in the uterine cavity would interfere with the normal embryonic development we should expect at least a growth reduction and perhaps an increased number of fetal deaths. This we have not been able to substantiate. In regard to certain malformations we did find a somewhat greater frequency of neuroectodermal defects in animals from the copperwire containing section. The changes were very small though and the frequency did not differ statistically from that of the control section. Moreover all defects demonstrated in this work have previously been described in non treated C3H mice as spontaneously occurring phenomena (Christensen (4)). Taking into account not only the possibility of mass significance but also the diagnostic uncertainty in recording these small defects, we have been unable to regard this a teratogenic effect of copperwire.

One can question whether the microscopic screening of the animal bodies has the same diagnostic certainty as the examination of the heads that are cut in continuous serial sections. We realize that it is certainly possible to miss certain diminutive malformations in the fetal bodies. However, the

method has been devised with special regard to a limited laboratory capacity, but in such a manner that all organs are represented.

Our work confirms the earlier experimental investigations, finding no teratogenic effect on animals developed in a uterine cavity containing a copperwire in spite of the fact, that we have used a histological screening technique. Neither did we find a higher incidence of intrauterine death or growth retardation.

The authors wish to acknowledge the assistance of Kurt Jensen and Eggert Hansen. Laboratory technicians and S. Olesen Larsen. Actuary. Statens Lægevidenskabelige Forskningsråd.

REFERENCES

1. Barrie H. Congenital malformation associated with intrauterine contraceptive device. *Brit Med Jour* *nal* 1 488-490 1976.
2. Chang C C & Tatum H J. Absence of teratogenicity of intrauterine copper wire in rats, hamsters and rabbits. *Contraception* 7 413-434 1973.
3. Chang C C, Tatum H J & Kincl F A. The effect of intrauterine copper and other metals on implantation in rats and hamsters. *Fertil & Steril* 21 274-278 1970.
4. Christensen N. Ocular malformations induced by radiation of the mouse embryo. *Acta path micro biol scand Sect A Suppl* 254 1976.
5. Zipper J A, Mcdel M & Prager R. Suppression of fertility by intrauterine copper and zinc in rabbits - a new approach to intrauterine contraception. *Amer J Obstet Gynec* 105 529-534 1969.

REPAIR IN ARTERIAL TISSUE

I Endothelial Regrowth Subendothelial Tissue Changes and Permeability in the Healing Rabbit Thoracic Aorta

II COLLATZ CHRISTENSEN J CHEMNITZ I TKOCZ and C M KIM*

Winslow Institute of Human Anatomy University of Odense Odense Denmark and the *Department of Pathology School of Medicine Hanyang University Seoul Korea (South)

Collatz Christensen J Chemnitz J Tkocz I & Kim C M Repair in arterial tissue I Endothelial regrowth subendothelial tissue changes and permeability in the healing rabbit thoracic aorta Acta path microbiol scand Sect A 87 265-273 1979

The role of the endothelium and subendothelial connective tissue in the permeability of a healing intima was studied by vital staining with Evans blue and transmission electron microscopy after severe mechanical lesion of the rabbit aorta Reendothelialization decreasing permeability and organization of neointimal connective tissue were concomitant events in the healing processes The determinant factor in decreasing permeability was reendothelialization with the formation of endothelial flaps and junctions Changes in the subendothelial connective tissue seemed also to be factors that influenced the permeability

Key words Experimental arteriosclerosis endothelium vital staining permeability TEM neointima

B Collatz Christensen Winslow Institute of Human Anatomy University of Odense Campusvej 55 DK 5230 Odense M

Received 6 x 78 Accepted 17 ii 79

Reendothelialization is the determinant factor in decreasing permeability of the healing aortic wall (Collatz Christensen *et al* 1976 and 1977 Stemer *man et al* 1977 Clowes *et al* 1978) The importance of endothelial cells (EC) in reconstruction of intimal barrier function was reaffirmed Besides EC junctions the composition and organization of subendothelial connective tissue seemed to be constituents of the barrier An integrated secretory activity of endothelium and smooth muscle cells (SMC) seemed to be essential in sustaining this intimal barrier

MATERIALS AND METHODS

Animals and the embolectomy catheter lesion Twenty five male albino rabbits of the Danish country strain weighing about 3 kg were studied 17 were submitted to a single dilatation trauma of the thoracic aorta by an embolectomy catheter according to a method previously described (Collatz Christensen & Garbarsch 1973) As

controls 8 animals were submitted to a sham-operation viz simple ligation of the left femoral artery

Vital staining Evans blue 0.5% intravenous in ear vein 4 h before autopsy (Collatz Christensen *et al* 1977)

Collatz Christensen 1974) Fixative solution 5% glutaraldehyde and 4% paraformaldehyde buffered with 0.1 M cacodylate buffer supplemented with 4 mM CaCl_2 pH 7.2 fixative vehicle 300 mOsm The animals were perfusion fixed for 30 min at 37°C

Preparation of tissue for TEM The selected specimens (Fig 1) were immersion fixed in the same fixative solution used for perfusion fixation overnight at 4°C Then they were postfixed in osmium tetroxide pH 7.2 fixative vehicle 300 mOsm for 1-2 h at 4°C Forty-six specimens 32 from the experimental animals and 14 from control animals were pre-stained with 1% uranylacetate in re-distilled water for 1 h dehydrated in acetone and embedded in Araldite Ultrathin sections were contrasted with lead citrate

TABLE 1 Total Number of Fetuses Normal Malformed and Fetal Deaths in the Copperwire containing Uterine Section and the Control Section

	Fetuses	Normal	Malformed	Fetal deaths
Copperwire section	65	37	15	13
Control section	57	35	11	11

The number of fetuses from the two different groups are shown in Table 1, which also shows the number of dead, malformed and normal individuals. There was no significant difference between the number of fetal deaths, nor was the apparent difference between the number of defects in the two groups significant ($U = 0.83$).

DISCUSSION AND CONCLUSION

If the presence of a copperwire in the uterine cavity would interfere with the normal embryonic development we should expect at least a growth reduction and perhaps an increased number of fetal deaths. This we have not been able to substantiate. In regard to certain malformations we did find a somewhat greater frequency of neuroectodermal defects in animals from the copperwire containing section. The changes were very small though, and the frequency did not differ statistically from that of the control section. Moreover, all defects demonstrated in this work have previously been described in non treated C3H mice as spontaneously occurring phenomena (Christensen (4)). Taking into account not only the possibility of mass significance, but also the diagnostic uncertainty in recording these small defects we have been unable to regard this a teratogenic effect of copperwire.

One can question whether the microscopic screening of the animal bodies has the same diagnostic certainty as the examination of the heads that are cut in continuous serial sections. We realize that it is certainly possible to miss certain diminutive malformations in the fetal bodies. However, the

method has been devised with special regard to a limited laboratory capacity, but in such a manner that all organs are represented.

Our work confirms the earlier experimental investigations, finding no teratogenic effect on animals developed in a uterine cavity containing a copperwire in spite of the fact, that we have used a histological screening technique. Neither did we find a higher incidence of intrauterine death or growth retardation.

The authors wish to acknowledge the assistance of Kurt Jensen and Eggert Hansen. Laboratory technicians and S. Olesen-Larsen. Actuary. Statens Lægevidenskabelige Forskningsråd.

REFERENCES

1. Barrie H. Congenital malformation associated with intrauterine contraceptive device. *Brit Med Journal* 1 488-490 1976.
2. Chang C C & Tatum H J. Absence of teratogenicity of intrauterine copper wire in rats hamsters and rabbits. *Contraception* 7 413-434 1973.
3. Chang C C, Tatum H J & Kincl F A. The effect of intrauterine copper and other metals on implantation in rats and hamsters. *Fertil & Steril* 21 274-278 1970.
4. Christensen N. Ocular malformations induced by radiation of the mouse embryo. *Acta path microbiol scand Sect A Suppl* 254 1976.
5. Zipper J A, Medel M & Prager R. Suppression of fertility by intrauterine copper and zinc in rabbits - a new approach to intrauterine contraception. *Amer J Obstet Gynec* 105 529-534 1969.



Fig 2a-b 1-4 days after the embolectomy catheter lesion 2a) 4 days after lesion Endothelial regrowth around the mouth of an intercostal artery Cell contacts are incomplete and undifferentiated The subendothelial connective tissue contained small amounts of elastin close to a SMC No extensive reticular Membrana Basalis (rMB) is visible $\times 3800$

2b) 4 days after lesion Incomplete cell contact Condensation of microfilaments (asterisk) in the marginal zones are shown Marginal ruffles (arrowhead) and macrophagocytotic vesicles (arrows) are present $\times 20000$

Sixty nine specimens 48 from experimental animals and 21 from control animals were pre stained in a solution of 1% low molecular weight galloylglucosides (LMGG) in cacodylate buffer (Simionescu & Simionescu 1976) Ultrathin sections from these specimens were contrasted with both zinc uranyl acetate and lead citrate

Transmission light microscopy of semithin sections stained with 1% toluidine blue was performed on a further 13 specimens 10 from the experimental animals and 3 from the control animals not used for TEM investigations

Fluorescence microscopy (Fl) Fl of frozen sections for tracing the Evans blue dye-complex in the arterial wall was performed according to a method previously described by

Altogether

76 from

Selection of tissue for examination and planning of experiments Specimens for TEM and Fl (Fig 1) were excised from close positioned and corresponding areas on the aortic wall to compare the ultrastructure of the intima with its permeability for protein-bound Evans blue Biochemical analyses of the degree of protein

binding of Evans blue have previously been described (Collatz Christensen *et al* 1977) Excision of specimens as shown in Figure 1 made it possible to compare early reendothelialized areas close to intercostal arteries (IA) with later reendothelialized or non reendothelialized areas between IA In Figure 1 specimens from white/blue (Evans blue) transitions are included among specimens excised between IA Transitions between endothelium and pseudoendothelium (modified smooth

RESULTS

Endothelium shamoperated controls The intima was unstained white after vital staining with Evans blue and no red fluorescence was visible by Fl (Collatz Christensen *et al* 1977) EC presented by TEM the well known appearance described by

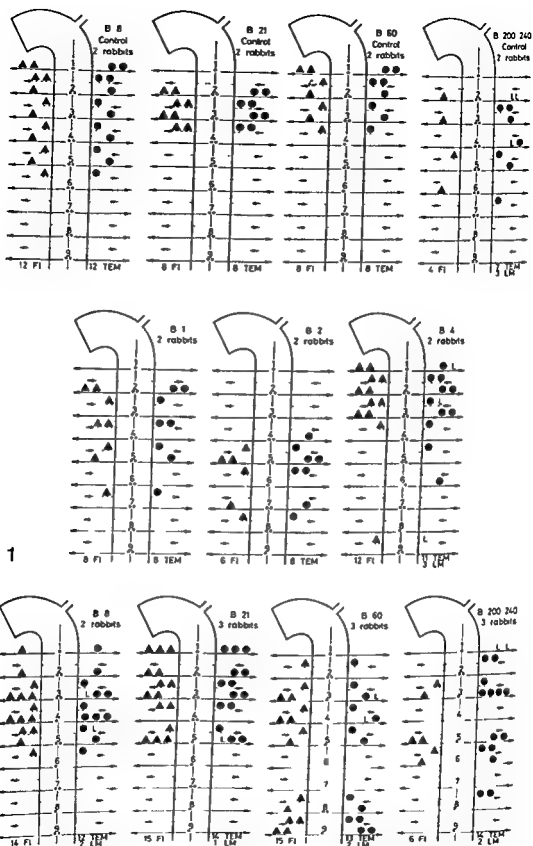


Fig 1 Excision of specimens for transmission electron microscopy light microscopy and fluorescence microscopy B1-B240 indicates rabbits 1-240 days after the embolectomy catheter lesion B8-240 control indicates rabbits 8-240 days after the shamoperation serving as controls TEM transmission electron microscopy FI fluorescence microscopy LM light microscopy Symbols ● TEM and LM L LM only ▲ FI

Young endothelium (4 days after lesion) around IA was permeable for Evans blue with orange red fluorescence present in $\frac{1}{3}$ of the depth of media. TEM of these areas showed that cell junctions between EC were incomplete (Fig. 2a and b) and mitosis was frequently observed. Microfilaments, ruffles and macropinocytotic vesicles were prominent in the thin marginal zones of the cells (Fig. 2b). Polyribosomes and dilated rough endoplasmic reticulum (RER) were prominent whereas Golgi complexes and the number of micropinocytotic vesicles were sparse. The subendothelial tissue contained poorly-condensed amorphous and filamentous substances (Fig. 2a and b) and unripe elastin closely applied to elongated SMC (Fig. 2a).

indicated in the luminal third of media. Close to the IA the cell contacts interdigitated, marginal flaps were frequent and junctions prominent (Fig. 3a, b and c). Microfilaments 100 Å and 60 Å increased in number and the latter were condensed in a spotty manner close to the abluminal plasmamembrane (Fig. 3b). In the 21 days period dilated RER and Golgi complexes, mitochondria and Palade bodies as well as microcytotic vesicles were prominent. The basal caveolae emptied (or engulfed) an amorphous grainy substance belonging to the lattice like rMB (Fig. 3b and d) which was situated between EC and elastin granules surrounding myointimal cells.

Between IA the differentiation of EC and subendothelial tissue varied in accordance with the descriptions given for the young EC (4 days after lesion) and EC 8-21 days after lesion.

Sixty to 240 days after lesion almost the whole intima was covered with endothelium and impermeable to Evans blue with no trace of red fluorescence. EC close to IA had prominent marginal flaps, junctions, aggregations of basal microfilaments and Weibel-Palade bodies and the subendothelial tissue was condensed (Fig. 4a). In some cases EC looked almost ripe covering condensed subendothelial tissue with ripe elastin (Fig. 4a and b). Between IA the differentiation of EC and subendothelial tissue varied. Marginal EC overgrowing pseudoendothelium (see below) were unchanged.

In boundary zones between endothelium and pseudoendothelium...

macropinocytotic vesicles and was crowded with 60 Å filaments (Fig. 5b).

Evans blue stained areas were covered with platelets and blood cells adherent to denuded

surfaces for the first four days. Pseudoendothelium was recognizable after 8 days and dominated blue areas after 21 days covering the intimal surface without apposition of blood elements. Pseudoendothelium was modified SMC with abnormally oriented nucleus, compact zone densely crowded with microfilaments and flattened marginal areas with branched cytoplasmic extensions resembling ruffles. These cells formed incomplete cell contacts (Fig. 6). The connective tissue beneath the pseudoendothelium was a sparse filamentous substance with few randomly dispersed grains of elastin (Fig. 6). The pseudoendothelium was later replaced by an overgrowth of genuine endothelium and 60 to 240 days after lesion only small blue islands persisted. They showed orange red fluorescence around $\frac{1}{3}$ into the depth of media and the luminescence was less intense (Collatz, Christensen *et al.* 1977). Compared with the 21 days experiment the red fluorescence decreased. However, the open communication to the underlying connective tissue between the pseudoendothelial cells was unchanged. The contents of collagen fibres had increased.

DISCUSSION

Sources of Error and Methodological Limitations

Excision of specimens from corresponding horizontal levels was not consequently performed (see Fig. 1). The caudal segments of the thoracic aorta is submitted to a more severe mechanical trauma by the inflated balloon than the cephalic segment because of narrow lumen, thin wall and substantial fixation to the diaphragm. Accordingly, differences in quality, the speed and sequence of healing processes are to be expected in cephalic and caudal segments of the aorta. However, differences in the ultrastructure between specimens from cephalic or caudal levels have not been noticed. On the

Fig. 4a-b. 4a) Endothelium 60 days after lesion. A ripe endothelial cell with 100 Å filaments (F) and Weibel-Palade bodies (arrowheads). The zone between the endothelial cell and the smooth muscle cell (SMC) consists of condensed amorphous and filamentous substance in continuity with the contents in open caveolae (small arrows) both in the endothelial cell and the SMC. $\times 40,000$.

... consists of condensed amorphous and filamentous substance in continuity with ripe elastin (asterisks). $\times 25,000$.



Fig 3a-d 8-21 days after the embolectomy catheter lesion 3a) 8 days after lesion, Endothelial cells close to an intercostal artery. An apparently increased accumulation of rMB is shown $\times 20\,000$
 3b) 21 days after lesion. Well differentiated junction between two endothelial cells. 100 Å filaments (F) are prominent $\times 56\,000$
 3c) 21 days after lesion, differentiated junctions between endothelial cells are seen (arrowheads) $\times 112\,000$
 3d) 21 days after lesion. Caveolae with an apparent opening and probably emptying amorphous substance into the rMB (arrows) $\times 180\,000$

other authors (Buck 1963, Mayno 1965, French 1966). The endothelium could be tightly apposed to the internal elastic membrane by a narrow zone of condensed filamentous material, or separated from it by a subendothelial connective tissue that was

organized with a transition between reticular Membrana Basalis (rMB) emerging from the endothelium and the elastin, forming grainy elastic lamellas around subendothelial SMC.

Endothelium 11-240 days after lesion

Young endothelium (4 days after lesion) around IA was permeable for Evans blue with orange red fluorescence present in $2/3$ of the depth of media. TEM of these areas showed that cell junctions between EC were incomplete (Fig. 2a and b) and mitosis was frequently observed. Microfilaments, ruffles and macropinocytotic vesicles were prominent in the thin marginal zones of the cells (Fig. 2b). Polyribosomes and dilated rough endoplasmic reticulum (RER) were prominent whereas Golgi complexes and the number of micropinocytotic vesicles were sparse. The subendothelial tissue contained poorly-condensed amorphous and filamentous substances (Fig. 2a and b) and unripe elastin closely applied to elongated SMC (Fig. 2a).

Between 8 and 21 days Evans blue white islands expanded from the mouths of IA and confluent. After 21 days red fluorescence was merely indicated in the luminal third of media. Close to the IA the cell contacts interdigitated, marginal flaps were frequent and junctions prominent (Fig. 3a, b and c). Microfilaments 100 Å and 60 Å increased in number and the latter were condensed in a spotty manner close to the abluminal plasmamembrane (Fig. 3b). In the 21 days period dilated RER and Golgi complexes, mitochondria and Palade bodies as well as micropinocytotic vesicles were prominent. The basal caveolae emptied (or engulfed) an amorphous basal substance belonging to the lattice like rMB (Fig. 3b and d) which was situated between EC and elastin granules surrounding myointimal cells.

Between 1A the differentiation of EC and subendothelial tissue varied in accordance with the descriptions given for the young EC (4 days after lesion) and EC 8–21 days after lesion.

Sixty to 240 days after lesion almost the whole intima was covered with endothelium and impermeable to Evans blue with no trace of red fluorescence. EC close to IA had prominent marginal flaps, junctions, aggregations of basal microfilaments and Weibel-Palade bodies and the subendothelial tissue was condensed (Fig. 4a). In some cases EC looked almost ripe covering condensed subendothelial tissue with ripe elastin (Fig. 4a and b). Between 1A the differentiation of EC and subendothelial tissue varied. Marginal EC overgrowing pseudoendothelium (see below) were unchanged.

In boundary zones between endothelium and pseudoendothelium marginal EC overlaid SMC without interposition of connective tissue substance (Fig. 5a and b). Marginal EC looked unripe and presented ruffles, macropinocytotic vesicles and was crowded with 60 Å filaments (Fig. 5b).

Evans blue stained areas were covered with platelets and blood cells adherent to denuded

surfaces for the first four days. Pseudoendothelium was recognizable after 8 days and dominated blue areas after 21 days covering the intimal surface without apposition of blood elements. Pseudoendothelium was modified SMC with abluminally oriented nucleus, compact zone densely crowded with microfilaments and flattened marginal areas with branched cytoplasmic extensions resembling ruffles. These cells formed incomplete cell contacts (Fig. 6). The connective tissue beneath the pseudoendothelium was a sparse filamentous substance with few randomly dispersed grains of elastin (Fig. 6). The pseudoendothelium was later replaced by an overgrowth of genuine endothelium and 60 to 240 days after lesion only small blue islands persisted. They showed orange red fluorescence around $1/3$ into the depth of media and the luminescence was less intense (Collatz, Christensen *et al.* 1977). Compared with the 21 days experiment the red fluorescence decreased. However, the open communication to the underlying connective tissue between the pseudoendothelial cells was unchanged. The contents of collagen fibres had increased.

DISCUSSION

Sources of Error and Methodological Limitations

Excision of specimens from corresponding horizontal levels was not consequently performed (see Fig. 1). The caudal segments of the thoracic aorta is submitted to a more severe mechanical trauma by the inflated balloon than the cephalic segment because of narrow lumen, thin wall and substantial fixation to the diaphragm. Accordingly, differences in quality, the speed and sequence of healing processes are to be expected in cephalic and caudal segments of the aorta. However, differences in the ultrastructure between specimens from cephalic or caudal levels have not been noticed. On the

Fig. 4a–b 4a) Endothelium 60 days after lesion. A ripe endothelial cell with 100 Å filaments (F) and Weibel-Palade bodies (arrowheads). The zone between the endothelial cell and the smooth muscle cell (SMC) consists of condensed amorphous and filamentous substance in continuity with the contents of open caveolae (small arrows) both in the endothelial cell and the SMC $\times 40,000$.

4b) Endothelium 240 days after the lesion. Differentiated contact between two endothelial cells. An abundance of endocytotic vesicles and caveolae are present. The subendothelial tissue consists of condensed amorphous and filamentous substance in continuity with ripe elastin (asterisks) $\times 25,000$.

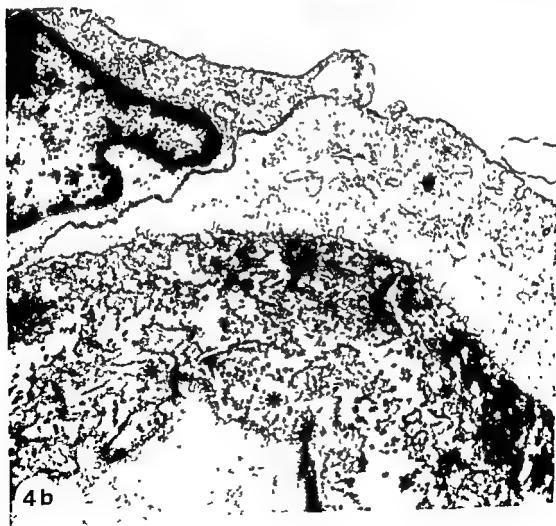




Fig 5a-b Accidental observation of a boundary zone between endothelium and pseudoendothelium 8 days after the lesion.

5a) An endothelial cell apparently migrating over a SMC. No obvious rMB is interposed between the two cells $\times 5000$

5b) A high magnification of the endothelial cell border seen in Figure 5a. Note the condensations of microfilaments (asterisk), marginal ruffles (arrowheads) and a macropinocytotic vesicle (arrow) $\times 50000$

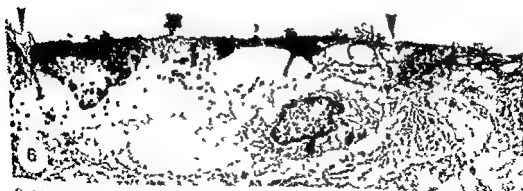
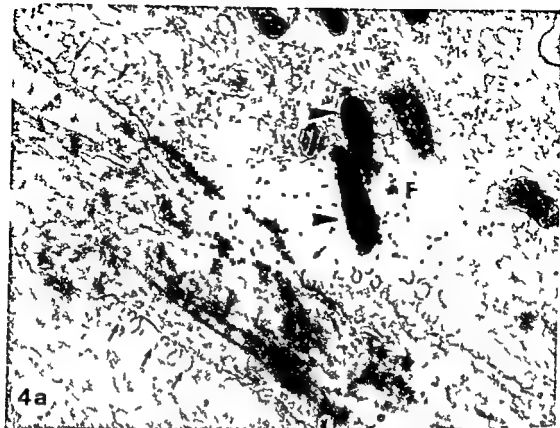


Fig 6 8 days after lesion. Evans blue stained area, pseudoendothelium modified SMC covers the luminal surface, no direct contact between the surface cells is visible (arrowheads). The connective tissue beneath the SMC is a sparse filamentous substance with few randomly dispersed grains of elastin $\times 3600$



- dilatation injury *Virchows Arch Abt A Path Anat* 360 93-106 1973
- Collatz Christensen B Repair in arterial tissue A scanning electron microscopic (SEM) and light microscopic study on the endothelium of the rabbit thoracic aorta following noradrenaline in toxic doses *Virchows Arch A Path Anat and Histol* 363 33-46 1974
- Collatz Christensen B Chemnitz J & Tkocz I Repair in arterial tissue Electron microscopy of Evans blue vital stained embolectomy catheter lesion of the rabbit thoracic aorta *Acta path microbiol scand Sect A* 84 355-357 1976
- Collatz Christensen B Chemnitz J Tkocz I & Glaabjerg O Repair in arterial tissue The role of endothelium in the permeability of a healing intimal surface Vital staining with Evans blue and silver staining of the aortic intima after a single dilatation trauma. *Acta path microbiol scand Sect A* 85 297-310 1977
- Florez Lord & Sheppard B L The permeability of arterial endothelium to horseradish peroxidase *Proc roy Soc B* 174 435-443 1970
- Frenet J E Atherosclerosis in relation to the structure and function of the arterial intima with special reference to the endothelium In Richter G W & Epstein M A International review of experimental pathology vol 5 Academic Press New York 1966 pp 253-353
- Heln P Loren en I Garbarsch C & Mathiesen M Repair in arterial tissue Morphological and biochemical changes in rabbit aorta after a single dilatation injury *Circulat Res* 29 542-554 1971
- Mutner J More R H & Rosa G Fine structural evidence of specific mechanism in increased endothelial permeability in experimental hypertension *Amer J Path* 61 395-411 1970
- Klynsira F B & Boncher J F Permeability patterns in pig aorta Atherosclerosis 11 451-462 1970
- Mayno G Ultrastructure of the vascular membrane In Dow P Handbook of Physiology Section 2 Hamilton W F Circulation vol III chapter 64 Am Physiol Soc Washington DC 1965 pp 2293-2375
- Palade G E Blood capillaries of the heart and other organs *Circulation* 21 368-384 1961
- Schwartz S M & Benditt E P Studies on aortic intima I Structure and permeability of rat thoracic aortic intima *Amer J Path* 66 241-264 1972a
- Schwartz S M & Benditt E P Postnatal development of the aortic subendothelium in rats *Lab Invest* 26 778-786 1972b
- Simionescu N & Simionescu M Galloylglucoses of low molecular weight as mordant in electron microscopy I Procedure and evidence for mordanting effect *J Cell Biol* 70 608-621 1976
- Siemerman M B Spaet T H Pitlick F Cintron J Lejnleis I & Tirl M L Intimal healing The pattern of reendothelialization and intimal thickening *Amer J Path* 87 125-142 1977
- Vracko R & Benditt E P Capillary basal lamina thickening its relationship to endothelial cell death and replacement *J Cell Biol* 47 281-285 1970
- Webster W S Bishop S P & Geer J C Experimental aortic intimal thickening II Endothelialization and permeability *Amer J Path* 76 263-284 1974
- Wight T N & Ross R Proteoglycans in primate arteries I Ultrastructural localization and distribution in the intima *J Cell Biol* 67 660-674 1975

contrary, the variations in ultrastructure throughout the experimental periods were similar in specimens from various horizontal levels. Specimens excised near the mouths of IA probably contain endothelium formed during the first days of repair, whereas specimens taken between IA may include endothelium formed days, weeks or months after the lesion, as a consequence of the irregular and varied pattern of reendothelialization (Collatz Christensen *et al* 1977). In the boundary zones between endothelium and pseudoendothelium reendothelialization is in actual progress.

The Role of EC and Subendothelial Tissue in Vascular Healing and Permeability

The importance of regrowth of genuine endothelium on the decreasing permeability of a healing aortic wall was reaffirmed (Collatz Christensen *et al* 1977). The perfection of the initially imperfect intimal barrier coincided with differentiation of EC cell contacts and junctions, resumption of secretory activity in EC and SMC and differentiation of subendothelial rMB and elastic tissue components. Accordingly, EC as well as connective tissue constituents may play their roles in the barrier function.

The route of penetration of Evans blue remained unknown in the present work. Experiments with tracers have indicated that macromolecules cross the endothelial barrier by intercellular as well as vesicular transport (Florey & Sheppard 1970, Hüttner *et al* 1970, Schwartz & Benditt 1972a). The permeability of damaged and reformed endothelium is increased, but an intimal barrier is re-established during healing after a mechanical lesion (Webster *et al* 1974, Clowes *et al* 1978). Our results have shown that young endothelium with incomplete cell contacts presented considerable permeability for the Evans blue protein complex while differentiated endothelium (21 days after lesion) with flaps and tight junction was impermeable. Pseudoendothelium with open intercellular communications to underlying tissue remained permeable. However, the actual route of penetration of Evans blue protein complex remained unknown, differentiation of cell contacts and junctions seemed to contribute to barrier function.

In the transport of macromolecules across vascular membranes connective tissue constituents play a role. In capillaries the Membrana Basalis (MB) plays a significant role as a filter (Palade 1961), and glykosaminoglycans seem to be integrated in the intimal barrier (Klynsstra & Botcher 1970). In the healing of an embolectomy catheter lesion the metabolism of macromolecules and their organization as a charged filter are important to the

permeability of the healing arterial wall (Helin *et al* 1971, Wight & Ross 1975).

In accordance with our observation of concomitant differentiation of EC and organization of subendothelial tissue Clowes *et al* (1978) give support to our assumption that the intimal barrier depends on both. In their study on the carotid artery drying model, normal and ripened reformed endothelium were impermeable to horse radish peroxidase (HRP). Reformed endothelium was permeable, however, and the HRP was arrested just beyond the endothelium. On the contrary in areas covered with pseudoendothelium HRP penetrated into the media. It may be deduced that connective tissue underlying genuine endothelium has barrier qualities that are absent in connective tissue underlying pseudoendothelium.

The intimal barrier function may be attributed to a double role of the EC as constituents of the intimal barrier and determining the connective tissue formation at the same time. EC are capable of secreting MB substances (Vracko & Benditt 1970) and according to Schwartz & Benditt (1972b) it is likely that the rMB in the aortic subendothelium of growing rats is synthesized by the endothelium. The regular organization of young connective tissue between secreting EC and myointimal cells leads us to suggest that interaction between the two cell types plays a role in sustaining a filter to macromolecules.

Functional or anatomical disturbances of endothelium or subendothelial tissue may affect permeability as well as the connective tissue formation and thus start a vicious circle facilitating the atheromatous process.

This work was supported by grants from the Danish Heart Foundation and Danida. The excellent technical assistance of Mrs E. Berg, Mr E. Pantion, Mrs R. Lonsrup, Mrs J. Holst, Miss I. Rasmussen and Mr J. Vraa is gratefully acknowledged.

REFERENCES

- Buck R. C. Histogenesis and morphology of arterial tissue. In Sandler M. & Bourne G. H. *Atherosclerosis and its origin*. Academic Press, New York and London 1963, pp. 1-38.
- Clowes A. W., Collazzo R. E. & Karnovsky M. J. A morphologic and permeability study of luminal smooth muscle cells after arterial injury in the rat. *Lab. Invest.* 39: 141-150, 1978.
- Collatz Christensen B. & Garbarsch C. Repair in arterial tissue. A scanning electron microscopic (SEM) and light microscopic study on the endothelium of rabbit thoracic aorta following a single

- dilatation injury *Vrchows Arch Abt A Path Anat* 360 93-106 1973
- Collier Christensen B Repair in arterial tissue A scanning electron microscopic (SEM) and light microscopic study on the endothelium of the rabbit thoracic aorta following noradrenaline in toxic doses *Vrchows Arch A Path Anat and Histol* 363 33-46 1974
- Collier Christensen B Chemnir J & Tkocz I Repair in arterial tissue Electron microscopy of Evans blue vital stained embolectomy catheter lesion of the rabbit thoracic aorta *Acta path microbiol scand Sect A* 84 355-357 1976
- Collier Christensen B Chemnir J Tkocz I & Blaabjerg O Repair in arterial tissue The role of endothelium in the permeability of a healing intimal surface Vital staining with Evans blue and silver staining of the aortic intima after a single dilatation trauma *Acta path microbiol scand Sect A* 85 297-310 1977
- Flory Lord & Sheppard B L The permeability of arterial endothelium to horseradish peroxidase *Proc Roy Soc B* 174 435-443 1970
- French J E Atherosclerosis in relation to the structure and function of the arterial intima with special reference to the endothelium In Richter G W & Epstein M A International review of experimental pathology vol 5 Academic Press New York 1966 pp 253-353
- Helin P Lorenzen I Garbarsch C & Matthiessen M E Repair in arterial tissue Morphological and biochemical changes in rabbit aorta after a single dilatation injury *Circulat Res* 29 542-554 1971
- Huimer J More R H & Rona G Fine structural evidence of specific mechanism in increased endothelial permeability in experimental hypertension *Amer J Path* 61 395-411 1970
- Klynstra F B & Bottcher J F Permeability patterns in pig aorta Atherosclerosis 11 451-462 1970
- Majno G Ultrastructure of the vascular membrane In Dow P Handbook of Physiology Section 2 Hamilton W F Circulation vol III chapter 64 Am Physiol Soc Washington DC 1965 pp 2293-2375
- Palade G E Blood capillaries of the heart and other organs *Circulation* 21 368-384 1961
- Schwartz S M & Benditt E P Studies on aortic intima I Structure and permeability of rat thoracic aortic intima *Amer J Path* 66 241-264 1972a
- Schwartz S M & Benditt E P Postnatal development of the aortic subendothelium in rats *Lab Invest* 26 778-786 1972b
- Simionescu N & Simionescu M Galloylglucoses of low molecular weight as mordant in electron microscopy I Procedure and evidence for mordanting effect *J Cell Biol* 70 608-621 1976
- Stemerman M B Spaet T H Pillick F Cintron J Lejnleks I & Tiell M L Intimal healing The pattern of reendothelialization and intimal thickening *Amer J Path* 87 125-142 1977
- Vracko R & Benditt E P Capillary basal lamina thickening Its relationship to endothelial cell death and replacement *J Cell Biol* 47 281-285 1970
- Webster W S Bishop S P & Geer J C Experimental aortic intimal thickening II Endothelialization and permeability *Amer J Path* 76 265-284 1974
- Wight T N & Ross R Proteoglycans in primate arteries I Ultrastructural localization and distribution in the intima *J Cell Biol* 67 660-674 1975

REPAIR IN ARTERIAL TISSUE

2 Connective Tissue Changes Following an Embolectomy Catheter Lesion. The Importance of the Endothelial Cells to Repair and Regeneration

B. COLLATZ CHRISTENSEN, J. CHEMNITZ, I. TKOCZ and C. M. KIM*

Winslow Institute of Human Anatomy, University of Odense, Odense, Denmark, and the *Department of Pathology, School of Medicine, Hanyang University, Seoul, Korea (South)

Collatz Christensen B, Chemnitz J, Tkocz I & Kim C M. Repair in arterial tissue. 2. Connective tissue changes following an embolectomy catheter lesion. The importance of the endothelial cells to repair and regeneration. *Acta path. microbiol. scand. Sect. A* 87: 275-283, 1979.

The neointimal hyperplasia following a severe mechanical lesion of the rabbit thoracic aorta was studied by vital staining with Evans blue and transmission electron microscopy. Neointimal tissue covered with endothelium contained organized laminated elastin-rich connective tissue. On the contrary, neointimal connective tissue covered with pseudoendothelium was disorganized with a tendency to fibrosis. Reendothelialization, re-establishment of intimal barrier function and formation of lamellated neointimal connective tissue were parallel events. The importance of an intact subendothelial zone controlling healing processes is discussed. Interaction of endothelium and smooth muscle cells seems to be essential in the regulation of neointimal tissue formation and is probably implicated in a general vascular reactive pattern.

Key words: Experimental arteriosclerosis, TEM, neoinima, SMC.

B. Collatz Christensen, Winslow Institute of Human Anatomy, University of Odense, Campusvej 55, DK-5230 Odense M.

Received 6 x 78 Accepted 17.11.79

Neointimal hyperplasia based on proliferation of connective tissue formation by smooth muscle cells (SMC) is a common and unspecific response of arterial tissue to various damaging influences. Proliferation of SMC seems to be a key event in atherogenesis (Ross & Glomset 1973). Deendothelialization or injury to endothelium triggers off a neointimal hyperplasia (Siemerman & Ross 1972, Schwartz *et al.* 1975, Spaet *et al.* 1975) and reendothelialization brings about a regression (Siemerman *et al.* 1977). Regression of a neointimal hyperplasia perhaps depends on restoration of the endothelial barrier with exclusion from the blood stream of substances e.g. platelet releasing factor which stimulates growth of neointimal connective tissue (Fishman *et al.* 1975, Clowes & Karnovsky 1977, Clowes *et al.* 1978).

The present investigation has lead us to suggest that an integrated secretory activity of SMC and endothelial cells (EC) is essential in maintenance of an intimal barrier, as well as being determinative in the regulation of neointimal connective tissue formation.

MATERIALS AND METHODS

Animals and embolectomy catheter lesion. Vital staining with Evans blue, perfusion fixation, preparation of tissue for transmission electron microscopy (TEM), fluorescence microscopy (FM), radioimmunoassay (RIA).

REPAIR IN ARTERIAL TISSUE

2 Connective Tissue Changes Following an Embolectomy Catheter Lesion. The Importance of the Endothelial Cells to Repair and Regeneration

■ COLLATZ CHRISTENSEN, J. CHEMNITZ, I. TKOCZ and C. M. KIM*

Winslow Institute of Human Anatomy, University of Odense, Odense, Denmark, and the *Department of Pathology, School of Medicine, Hanyang University, Seoul, Korea (South)

Collatz Christensen B, Chemnitz J, Tkocz I & Kim C M. Repair in arterial tissue. 2. Connective tissue changes following an embolectomy catheter lesion. The importance of the endothelial cells to repair and regeneration. *Acta path. microbiol. scand. Sect. A* 87: 275-283, 1979.

The neointimal hyperplasia following a severe mechanical lesion of the rabbit thoracic aorta was studied by vital staining with Evans blue and transmission electron microscopy. Neointimal tissue covered with endothelium contained organized lamellated elastin-rich connective tissue. On the contrary, neointimal connective tissue covered with pseudoendothelium was disorganized with a tendency to fibrosis. Reendothelialization, re-establishment of intimal barrier function and formation of lamellated neointimal connective tissue were parallel events. The importance of an intact subendothelial zone controlling healing processes is discussed. Interaction of endothelium and smooth muscle cells seems to be essential in the regulation of neointimal tissue formation and is probably implicated in a general vascular reactive pattern.

Key words: Experimental arteriosclerosis, TEM, neointima, SMC.

B. Collatz Christensen, Winslow Institute of Human Anatomy, University of Odense, Campusvej 55, DK-5230 Odense M.

Received 6 x 78 Accepted 17 n 79

Neointimal hyperplasia based on proliferation of cells and connective tissue formation by smooth muscle cells (SMC) is a common and unspecific response of arterial tissue to various damaging influences. Proliferation of SMC seems to be a key event in atherosclerosis (Ross & Glomset 1973). Reendothelialization or injury to endothelium triggers off a neointimal hyperplasia (Siemerman & Ross 1972; Schwartz *et al.* 1975; Spaet *et al.* 1975) and reendothelialization brings about a regression (Siemerman *et al.* 1977). Regression of a neointimal hyperplasia perhaps depends on restoration of the endothelial barrier with exclusion from the blood stream of substances such as platelet releasing factor which stimulates growth of neointimal connective tissue (Fishman *et al.* 1975; Clowes & Karnovsky 1977; Clowes *et al.* 1978).

The present investigation has led us to suggest that an integrated secretory activity of SMC and endothelial cells (EC) is essential in maintenance of an intimal barrier as well as being determinative in the regulation of neointimal connective tissue formation.

MATERIALS AND METHODS

Animals and embolectomy catheter lesion, vital staining with Evans blue, perfusion fixation, preparation of tissue for transmission electron microscopy (TEM), fluorescence microscopy (FM), selection of tissue for examination and the planning of experiments are described in our first paper of this series (Part 1) (Collatz Christensen *et al.* 1979).

RESULTS

TEM of Connective Tissue Sham-operated Controls

TEM of the normal rabbit aorta has previously been described by Yamamoto (1962) Bjerring & Kobayashi (1963) and Seifert (1963). In our controls the endothelium was either tightly applied to the internal elastic membrane or separated from it by a subendothelial space with myointimal cells surrounded by Membrana Basalis (MB) and unripe elastin. The filamentous component in the subendothelial reticular Membrana Basalis (rMB) was transformed via a lattice like pattern imperceptibly into the filamentous substance of elastin. SMC sporadically occurred in fenestra and frequently in lacunae of elastic tissue on the luminal side of the internal elastic membrane.

Connective Tissue 1-240 Days after Lesion

The first two days devitalized cells were prominent as was also disrupted connective tissue and adhesion of platelets, granulocytes and monocyte like cells to the surface. In addition phagocytosis of cell debris by granulocytes and macrophages in deeper layers was frequently found. Mitoses were frequent in the media and a variety of free mesenchymal cells, probably de differentiated SMC were prominent in the luminal zone of media. These cells were apparently migrating between elastic membranes and through their fenestra. Four days after lesion close to the intercostal arteries (IA) unripe EC with incomplete cell contacts covered a subendothelial space with 1-3 layers of secretory myointimal cells surrounded by unripe elastin (Fig 1). Between 8 and 21 days after lesion the



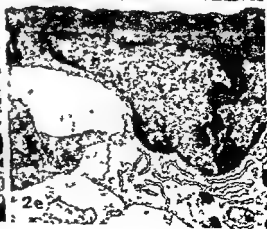
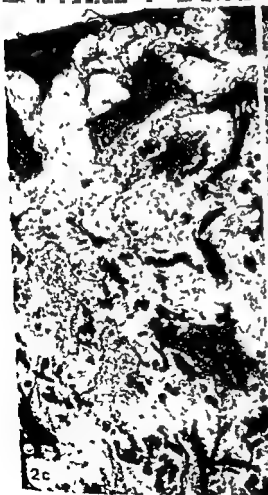
Fig 1 4 days after the embolectomy catheter lesion. Unripe endothelium close to the mouths of intercostal arteries cover a subendothelial space with secretory smooth muscle cells (SMC) surrounded by unripe elastin. $\times 3\ 800$

endothelium had expanded from the mouths of IA and a thick neointima of several cell layers had developed. Conspicuous was a marked qualitative difference between connective tissue covered with endothelium respectively with pseudoendothelium modified SMC (Fig 2a and c). Neointima covered with endothelium generally consisted of laminated connective tissue rich in elastin (Fig 2a) whereas neointima covered with SMC was disorganized with impaired elastogenesis and a tendency to fibrosis (Fig 2c).

The composition of the subendothelial zone varied as described in the control animals. The gradual transition between filamentous grainy substance in continuity with the contents of caveolae in EC (see Part 1) probably rMB, and the filamentous substance on the surface of elastin grains was the same as in the control material. Glycosaminoglycans seemed to be integrated in the filamentous substance of rMB and in the precursors of elastin (Fig 2d inset). Elastin grains were closely applied to the myointimal cells and consisted of a mixture of amorphous and filamentous substance (Fig 2d).

The deeper layers of the neointimal thickening mostly consisted of alternating layers of secretory SMC and an intercellular substance of varying density (Fig 2a see also Fig 3a and b). The SMC were surrounded by a discontinuous MB and there

Fig 2a-e 8-21 days after the embolectomy catheter lesion. 2a) 8 days after lesion close to intercostal arteries (IA) Endothelium closely applied to laminated SMC and elastin rich connective tissue $\times 5\ 000$. 2b) 21 days after lesion. Unripe endothelium close to transitional zone between endothelium and pseudoendothelium. The subendothelial connective tissue is poorly condensed and myointimal cells and elastin grains are randomly distributed $\times 3\ 200$. 2c) 21 days after lesion. Pseudoendothelium with incomplete cell contacts. In the luminal zone predominance of poorly condensed amorphous substances whereas in the deeper layers coarse elastic clumps collagen and myointimal cells are randomly dispersed $\times 4\ 400$. 2d) 21 days after lesion. Between endothelium (above) and SMC the reticular Membrana Basalis (rMB) is integrated into elastic grains (arrowhead) $\times 18\ 000$. Inset: Stellate figures probably glycosaminoglycans (arrow) are integrated in the filamentous grainy substance (arrowheads) of rMB and suggested precursors of elastin (el) $\times 200\ 000$. 2e) 21 days after lesion. Pseudoendothelial cell probably modified SMC heavily contrasted zone with myofibrils inside the luminal plasmamembrane prominent. RER sparse endocytotic vesicles and nucleus placed abnormally. Amorphous connective tissue substances are poorly condensed $\times 11\ 500$.





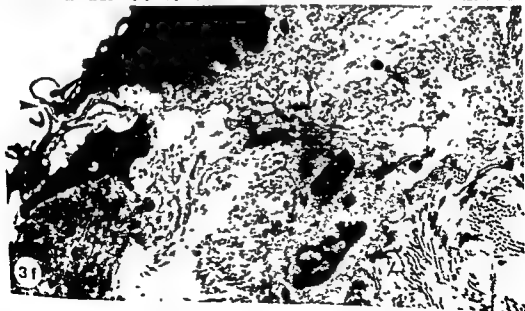


Fig 3a-f 60-240 days after embolectomy catheter lesion 3a) 60 days after lesion Neointima close to transitional zone between endothelium/pseudoendothelium Endothelium looks unripe with incomplete junctions Laminated myoelastic tissue of rather a loose texture $\times 4,200$ 3b) 240 days after lesion, neointima close to an IA Endothelial cells are ripe, subendothelial tissue elastin rich and laminated $\times 5,600$ 3c) 60 days after lesion Neointima with pseudoendothelium In complete stratification of elastic tissue, prominent fibrosis Defect fusion together of elastin granules $\times 4,200$ 3d) Transition endothelium (right) and pseudoendothelium, which is overgrown by endothelium without interposition of connective tissue Elongated branched myointimal cells and unripe elastin $\times 4,200$ 3e) Subendothelial SMC myofilaments, dense bodies microcytic vesicles, discontinuous Membrana Basalis (MB) amorphous grainy substance in caveolae in continuity with elastin surrounding SMC (arrows) Collagen fibers remote from SMC $\times 80,000$ 3f) Pseudoendothelium branched interdigitations with open communication into the deeper layers Myointimal cells integrated in the surface Collagen closely apposed to myointimal cells, amorphous substance and elastin dispersed $\times 16,000$

endothelium and pseudoendothelium, SMC and elastin granules were randomly oriented (Fig 2b)

Sixty - 240 days after the lesion the basic difference in the composition of connective tissue related to endothelium and to pseudoendothelium remained unchanged Generally the contents of collagen had increased Close to IA the subendothelial tissue was condensed with ripe elastin (cf Part I) and in the deeper layers a regular lamination of SMC and connective tissue was prominent (Fig 3b) In boundary zones between endothelium and pseudoendothelium (Fig 3d) the organization of neointima was unchanged (see above) In neointima covered with pseudoendothelium the content of collagen fibres had substantially increased and the coarse irregular grains of elastin tended to be arranged in a laminar fashion (Fig 3c) However the fusion of elastin granules remained defective compared with neointima covered with endothelium Collagen fibers were closer to the myointimal cells (Fig 3f) than in neointima covered with endothelium (Fig 3e)

Semiquantitation of the Occurrence of Lamellated and Non-lamellated Connective Tissue (Table 1)

see also p. 101

was a tendency to a spacing of the connective tissue constituents MB and the filamentous substance were closest to the SMC, followed by the elastin, and more remote banded collagen fibres were found (see Fig 3e)

In the media of the 21 days experiments the number of mitoses, free mesenchymal cells and «migrating» SMC was markedly reduced Neointima covered with pseudoendothelium showed a random arrangement of cells and connective tissue (Fig 2c) In the luminal layers the amorphous substances of connective tissue were indistinct and poorly condensed (Fig 2c and e) In the deeper layers coarse clumps of elastin, collagen, and myointimal cells were randomly dispersed (Fig 2c) and delamination of the internal elastic membrane was prominent

Related to the sites of specimen excision, the ultrastructure of the subendothelial connective tissue showed no differences between specimens excised close to IA or between them Transitional zones between endothelium and pseudoendothelium always presented poorly-condensed subendothelial connective tissue (Fig 2b), and under marginal EC overgrowing pseudoendothelium no connective tissue was interposed (Fig 3d) In the deeper layers of neointima, SMC and elastin tended to be regularly laminated and fairly condensed close to the IA (Fig 2a), whereas between IA the lamination varied Close to the boundary zones between

specimens excised close to the IA, obtained from boundary zones (white/blue stained intima) in the experimental phases 8-240 days after the lesion (Table 1)

Close to the IA the endothelium dominated and the connective tissue was predominantly lamellated Between the IA the frequency of endothelium and pseudoendothelium was equal, and laminated connective tissue most often coincided with endothelium on the surface Beneath the pseudoendothelium only non-lamellated connective tissue was registered In boundary zones with endothelium and pseudoendothelium the correlations endothelium/laminated connective tissue and pseudoendothelium/non laminated connective tissue were inconspicuous

DISCUSSION

Reendothelialization and Lamination of Neointimal Connective Tissue

Our investigations indicated that the unspecific processes of injury and repair (Helin et al 1971) are influenced by the presence of endothelium Expansion of endothelium over neointimal areas covered with pseudoendothelium (SMC) apparently brought about organization, lamination and controlled cellogenesis

TABLE 1 Occurrence of Laminated and Non Laminated Neointimal Connective Tissue

*Aortic segments beneath intercostal arteries
8-240 days after the lesion*

Number of aortic segments with occurrence of		laminated connective tissue	non laminated connective tissue
endothelium	25	25	0
pseudoendothelium	3	0	3

*Aortic segments between intercostal arteries
8-240 days after the lesion*

Number of aortic segments with occurrence of		laminated connective tissue	non laminated connective tissue
endothelium	9	6	3
pseudoendothelium	10	0	10

*Aortic segments with white/blue * transitions
8-240 days after the lesion*

Number of aortic segments with occurrence of		laminated connective tissue	non laminated connective tissue
endothelium	7	4	3
pseudoendothelium	6	2	4

* Aortic segments with white/blue transitions were selected in 7 animals after vital staining with Evans blue

The coincidence however of endothelium and laminated elastin might depend on incidental occurrence at the same time as two mutually independent processes reendothelialization and organization of connective tissue. Furthermore the organization of connective tissue might even be the event of prime importance possibly dependent on the degree of severity of trauma (Bjorkerud 1969, Bjorkerud & Bonders 1971) whereas reendothelialization was a secondary process following up the organized connective tissue.

If reendothelialization was secondary to reconstruction of organized connective tissue then the pattern of expanding endothelium would hardly as found in the present study start as isolated islands around the IA confluence as observed and then further expand in continuity with pre-existing endothelium. Accordingly the correlation of connective tissue organization with the «age of reendothelialization» and its coincidence with the frontiers of the expanding endothelium make it improbable that connective tissue organization is the primary event and that the expansion of the endothelium is secondary to it.

The Intimal Barrier and Organization of Neointimal Connective Tissue

The influence of endothelial regrowth on the course of the healing processes may depend on the function of the intimal barrier, i.e. exclusion from the blood stream of substances, that disturb the formation of connective tissue. In accordance with this assumption is the fact that the connective tissue formation under the highly permeable pseudoendothelium is severely compromised in the zone closest to the lumen, but more intact in the deeper layers. In areas of potentially short lasting decreased permeability in trans-

lu
is
lar
than connective tissue related to areas of «higher age of reendothelialization» close to IA. The barrier function seems to become effective, when the reendothelialization has lasted some time.

Ultrastructural Differences between Neointima Covered with Endothelium and Pseudoendothelium (SVC)

Fig 3a-f 60-240 days after embolectomy catheter lesion 3a) 60 days after lesion Neointima close to transitional zone between endothelium/pseudoendothelium Endothelium looks unripe with incomplete junctions Laminated myoelastic tissue of rather a loose texture $\times 4,200$ 3b) 240 days after lesion, neointima close to an IA Endothelial cells are ripe, subendothelial tissue elastin rich and laminated $\times 5,600$ 3c) 60 days after lesion Neointima with pseudoendothelium Incomplete stratification of elastic tissue, prominent fibrosis Defect fusion together of elastin granules $\times 4,200$ 3d) Transition endothelium (right) and pseudoendothelium, which is overgrown by endothelium without interposition of connective tissue Elongated branched myointimal cells and unripe elastin $\times 4,200$ 3e) Subendothelial SMC myofilaments, dense bodies, microcytotic vesicles, discontinuous Membrana Basalis (MB), amorphous grainy substance in caveolae in continuity with elastin surrounding SMC (arrows) Collagen fibers remote from SMC $\times 80,000$ 3f) Pseudoendothelium, branched interdigitations with open communication into the deeper layers Myointimal cells integrated in the surface Collagen closely apposed to myointimal cells, amorphous substance and elastin dispersed $\times 16,000$

was a tendency to a spacing of the connective tissue constituents MB and the filamentous substance were closest to the SMC, followed by the elastin, and more remote banded collagen fibres were found (see Fig 3e)

In the media of the 21 days experiments the number of mitoses, free mesenchymal cells and «migrating» SMC was markedly reduced Neointima covered with pseudoendothelium showed a random arrangement of cells and connective tissue (Fig 2c) In the luminal layers the amorphous substances of connective tissue were indistinct and poorly condensed (Fig 2c and e) In the deeper layers coarse clumps of elastin, collagen, and myointimal cells were randomly dispersed (Fig 2c), and delamination of the internal elastic membrane was prominent

Related to the sites of specimen excision, the ultrastructure of the subendothelial connective tissue showed no differences between specimens excised close to IA or between them Transitional zones between endothelium and pseudoendothelium always presented poorly-condensed subendothelial connective tissue (Fig 2b), and under marginal EC overgrowing pseudoendothelium, no connective tissue was interposed (Fig 3d) In the deeper layers of neointima, SMC and elastin tended to be regularly laminated and fairly condensed close to the IA (Fig 2a), whereas between IA the lamination varied Close to the boundary zones between

endothelium and pseudoendothelium, SMC and elastin granules were randomly oriented (Fig 2b) Sixty - 240 days after the lesion the basic difference in the composition of connective tissue related to endothelium and to pseudoendothelium remained unchanged Generally the contents of collagen had increased Close to IA the subendothelial tissue was condensed with ripe elastin (cf Part 1) and in the deeper layers a regular lamination of SMC and connective tissue was prominent (Fig 3b) In boundary zones between endothelium and pseudoendothelium (Fig 3d) the organization of neointima was unchanged (see above) In neointima covered with pseudoendothelium the content of collagen fibres had substantially increased, and the coarse irregular grains of elastin tended to be arranged in a laminar fashion (Fig 3c) However, the fusion of elastin granules remained defective compared with neointima covered with endothelium Collagen fibers were closer to the myointimal cells (Fig 3f) than in neointima covered with endothelium (Fig 3e)

Semiquantitation of the Occurrence of Lamellated and Non-lamellated Connective Tissue (Table 1)

The occurrence of lamellated connective tissue and non lamellated connective tissue is registered in specimens excised close to the IA, between IA and from boundary zones (white/blue stained intima) in the experimental phases 8-240 days after the lesion (Table 1)

Close to the IA the endothelium dominated and the connective tissue was predominantly lamellated Between the IA the frequency of endothelium and pseudoendothelium was equal, and laminated connective tissue most often coincided with endothelium on the surface Beneath the pseudoendothelium only non-lamellated connective tissue was registered In boundary zones with endothelium and pseudoendothelium the correlations endothelium/laminated connective tissue and pseudoendothelium/non laminated connective tissue were inconspicuous

DISCUSSION

Reendothelialization and Lamination of Neointimal Connective Tissue

Our investigations indicated that the unspecific processes of injury and repair (Heilm et al 1971) are influenced by the presence of endothelium Expansion of endothelium over neointimal areas covered with pseudoendothelium (SMC) apparently brought about organization, lamination and controlled blastogenesis

Study of the development of elastic elements in intimal proliferation *Exp molec Path* 11 212-223 1969

Kasuda S & Kajikawa K Elastogenesis in experimental arteriosclerosis in rabbits *J Electron Microsc* 26 111-119 1977

Kaerem H J, Bondjers G & Björkerud S Electron microscopy of intimal plaques following induction of large superficial mechanical injury (transverse injury) in the rabbit aorta *Virchows Arch Abt. A Path Anat* 359 267-282 1973

Mosher B F & Vaheri A Thrombin stimulates the production and release of a major surface-associated glycoprotein (fibronectin) in cultures of human fibroblasts *Exp Cell Res* 112 323-334 1978

Paule W J Electron microscopy of the newborn rat aorta *J Ultrastruct Res* 8 219-235 1963

Pese D C, Molnar S Electron microscopy of muscular arteries: pial vessels of the cat and monkey *J Ultrastruct Res* 3 447-468 1960

Ross R & Glomset J A Atherosclerosis and the arterial smooth muscle cell Proliferation of smooth muscle is a key event in the genesis of the lesions of atherosclerosis *Science* 180 1332-1339 1973

Schwartz S M & Benditt E P Postnatal development of the aortic subendothelium in rats *Lab Invest* 26 778-786 1972

Schwartz S M, Stiemerman M B & Benditt E P The aortic intima II Repair of the aortic lining after mechanical denudation *Amer J Path* 81 15-42 1975

Seifert K Elektronenmikroskopische Untersuchungen der Aorta des Kaninchens *Z. Zellforsch* 60 293-312 1963

Spaet T H, Stiemerman M B, Veith F J & Lejnicks I Intimal injury and regrowth in the rabbit aorta Medial smooth muscle cells as a source of neointima *Circulat. Res* 36 58-70 1975

Stiemerman M B & Ross R Experimental arteriosclerosis I Fibrous plaque formation in primates: an electron microscope study *J exp Med* 136 769-789 1972

Stiemerman M B, Spaet T H, Pulick F, Cintron J, Lejnicks I & Tiell M L Intimal healing The pattern of reendothelialization and intimal thickening *Amer J Path* 87 125-142 1977

Wight T N & Ross R Proteoglycans in primate arteries I Ultrastructural localization and distribution in the intima *J Cell Biol* 67 660-674 1975

Yamamoto I An electron microscope study of rabbit arterial wall Smooth muscle and the intercellular components with special reference to the elastic fiber *J Electron Microsc* 11 212-225 1962

Our observations indicated that the content of MB substances, glykosaminoglycans and elastin in neointima covered with endothelium was high and submitted to some control mechanisms rendering SMC and connective tissue organized as lamellated myoelastic tissue. In the absence of endothelium a defective organization of the connective tissue was evident. The secretory function of vascular SMC and the mechanisms of elastogenesis remain as yet unclarified (Pease & Molinary 1960, Yamamoto 1962, Paule 1963, Bierring & Kobayasi 1963, Haust & More 1967, Kadar *et al* 1969, Wight & Ross 1975, Katsuda & Kajikawa 1977). The present study leads us to suggest that the intimal barrier function depends on both endothelium and subendothelial connective tissue, (see Part I) and that the latter was probably formed and organized by an integrated secretory activity of SMC and endothelium. However, there were no plausible suggestions concerning the question whether the endothelium besides the barrier function exerted any direct influence e.g. by induction on the organization of connective tissue beyond the subendothelial space. The barrier function alone may sufficiently explain the influence on the course of healing processes.

SMC of the neointima covered with endothelium reflected the intense secretory activity and modelling of lamellar myoelastic tissue which is described in the developing aorta (Cliff 1967, Schwartz & Benditt 1972, Gerrity & Cliff 1975, Gerrity *et al* 1975) and following «regressive lesion» described by Björkerud (1969) and Björkerud & Bondjers (1971). On the contrary the repair of neointima in the absence of endothelium was little reconstructive leading to fibrosis and scar tissue like the «non regressive lesion» (Björkerud & Bondjers 1971). In our study neointima covered with pseudoendothelium presented an ultrastructure much like the «non regressive lesion» (Knierrni *et al* 1973).

In conclusion our results indicate that an interaction between endothelium and SMC is responsible for the maintenance of an intimal barrier as well as being determinative in governing the healing processes in a fashion of remodelling and reconstructing the basic pattern of vascular tissue. It is possible that LETS protein (Gospodarowicz *et al* 1978) also called fibronectin (Mosher & Vaheri 1978) produced in large quantities by vascular endothelium in addition to the EC attachment also has an influence on the organization of the neointimal connective tissue. Further investigations into the observed interaction between EC and SMC are relevant in elucidating the sequence of events in atherogenesis.

REFERENCES

- Bierring F & Kobayasi T. Electron microscopy of the normal rabbit aorta. *Acta path microbiol scand* 57: 154-168, 1963.
- Björkerud S. Reaction of the aortic wall of the rabbit after superficial longitudinal mechanical trauma. *Virchows Arch Abt A Path Anat* 347: 197-210, 1969.
- Björkerud S & Bondjers G. Arterial repair and atherosclerosis after mechanical injury. Part 2. Tissue response after induction of a total local necrosis (deep longitudinal injury). *Atherosclerosis* 14: 259-276, 1971.
- Cliff W J. The aortic tunica media in growing rats studied with the electron microscope. *Lab Invest* 17: 599-615, 1967.
- Clowes A W & Karnovsky M J. Failure of certain antiplatelet drugs to affect myointimal thickening following arterial endothelial injury in the rat. *Lab Invest* 36: 452-464, 1977.
- Clowes A W, Collazo R E & Karnovsky M J. A morphologic and permeability study of luminal smooth muscle cells after arterial injury in the rat. *Lab Invest* 39: 141-149, 1978.
- Collatz Christensen B, Chemnitz J, Tkocz I & Kim C M. Repair in arterial tissue. Part I. Endothelial regrowth, subendothelial tissue changes and permeability in the healing rabbit thoracic aorta. *Acta path microbiol scand Sect A* 87: 265-273, 1979.
- Fishman J A, Ryan G B & Karnovsky M J. Endothelial regeneration in the rat carotid artery and the significance of endothelial denudation in the pathogenesis of myointimal thickening. *Lab Invest* 32: 399-411, 1975.
- Gerrity R G & Cliff W J. The aortic tunica media of the developing rat. I. Quantitative stereologic and biochemical analysis. *Lab Invest* 32: 585-600, 1975.
- Gerrity R G, Adams E P & Cliff W J. The aortic tunica media of the developing rat. II. Incorporation by medial cells of ^3H proline into collagen and elastin. Autoradiographic and chemical studies. *Lab Invest* 32: 601-609, 1975.
- Gospodarowicz D, Greenburg G, Bralacki H & Zetter B R. Factors involved in the modulation of cell proliferation *in vivo* and *in vitro*. The role of fibroblast and epidermal growth factors in the proliferative response of mammalian cells. *In vitro* 14: 85-118, 1978.
- Haust M D & More R H. Electron microscopy of connective tissues and elastogenesis. International Academy of Pathology Monograph No 7. The Connective Tissues. Ed by B. Wagner & D. Smith. Baltimore: The Williams and Wilkins Co. 1967. pp. 352-376.
- Helin P, Lorenzen I, Garbarsch C & Matthiessen M E. Repair in arterial tissue. Morphological and biochemical changes in rabbit aorta after a single dilatation injury. *Circulat Res* 29: 542-554, 1971.
- Kadar A, Veress B & Jelinek H. Ultrastructural elements in experimental intimal thickening. II.

RELEASE OF INSULIN *IN VITRO* FROM NORMAL AND DUCT-LIGATED RAT PANCREAS

ARNE ANDERSSON ANDERS HALLBERG CLAES HELLERSTRÖM GÖSTA HULTQUIST and LEIF JANSSON

Departments of Histology and Pathology University of Uppsala Sweden

Andersson A Hallberg A Hellerstrom C Hultquist G & Jansson L. Release of insulin *in vitro* from normal and duct ligated rat pancreas Acta path microbiol scand Sect. A 87 285-288 1979

Ligation of the pancreatic duct causes atrophy of the acinar cells but leaves the endocrine tissue intact. In the present study a partial ligation of the pancreatic duct was performed in the rat, and the *in vitro* insulin response to glucose was compared from both the atrophic and non atrophic portions of the pancreas. Subsequent morphological studies of the ducted portion of the pancreas indicated a complete lack of acinar cells and a possible neoformation of ducts fat cells and connective tissue. However islets were present in normal amounts and appeared well preserved. Measurements of the insulin release *in vitro* from this ligated pancreatic tissue showed that an increase of the glucose concentrations from 3.3 to 16.7 mmol/l resulted in a six fold stimulation. A further two fold stimulation was seen after addition of theophylline to the high glucose incubation medium. In addition only under the latter conditions was there a significantly increased insulin release from both the non atrophic portion of the pancreas and from the pancreas of sham-operated animals. It is concluded that duct ligation does not diminish the glucose sensitivity of rat islet B-cells. Thus the present study does not support the view proposed previously that islet tissue is functionally of a foetal nature following duct ligation.

Key words: Pancreas duct ligation insulin release

A. Andersson Histologiska Institutionen Box 571 75123 Uppsala 1 Sweden

Received 30 III 78 Accepted 19 II 79

It is well known that ligation of the pancreatic duct causes an atrophy of the acinar cells. Ducts and islets are preserved but various types of morphological changes have also been reported in these ligated areas of the gland (Edstrom and Falkmer 1968 Boquist and Edstrom 1970). There is furthermore a resistance to the B-cytotoxic effect of alloxan in the duct ligated pancreas of rabbits (Halpole and Innes 1946). This alloxan resistance has been supposed to reflect a possible foetal nature of the islet tissue after duct ligation (Capellato and Perissinotto 1953 Larsson 1956). Indeed an increased neogenesis of islet cells similar to that observed in the foetus has been demonstrated in the duct-tied pancreas (Hultquist et al 1978).

It was the aim of the present investigation to study the release of insulin *in vitro* from pancreatic

pieces of duct ligated rats to determine whether it corresponds to a foetal or adult pattern of insulin release. Previous studies (Asplund et al 1969) have indicated a poor insulin response to glucose in the foetal rat pancreas as compared with that of the adult.

MATERIALS AND METHODS

Animals and Operation Technique

Female Sprague Dawley rats approximately 4 months old and weighing 300-350 g were used. Partial ligation of the pancreatic duct was performed on 10 rats according to the method of Hultquist and Jonsson (1965). Using this procedure a less extensive atrophy of the pancreas is obtained as the ligature is applied approximately between the duodenal two thirds and the ileal third of the pancreas at the level of the superior dorsal pole of the spleen. Five rats were sham-operated

RELEASE OF INSULIN *IN VITRO* FROM NORMAL AND DUCT-LIGATED RAT PANCREAS

ARNE ANDERSSON ANDERS HALLBERG CLAES HELLERSTROM GÖSTA HULTQUIST
and LEIF JANSSON

Departments of Histology and Pathology University of Uppsala Sweden

Andersson A Hallberg A Hellerstrom C Hultquist G & Jansson L Release of insulin *in vitro* from normal and duct ligated rat pancreas Acta path microbiol scand Sect A 87 285-288 1979

Ligation of the pancreatic duct causes atrophy of the acinar cells but leaves the endocrine tissue intact. In the present study a partial ligation of the pancreatic duct was performed in the rat, and the *in vitro* insulin response to glucose was compared from both the atrophic and non atrophic portions of the pancreas. Subsequent morphological studies of the duct tied portion of the pancreas indicated a complete lack of acinar cells and a possible neoformation of ducts fat cells and connective tissue. However islets were present in normal amounts and appeared well preserved. Measurements of the insulin release *in vitro* from this ligated pancreatic tissue showed that an increase of the glucose concentrations from 3.3 to 16.7 mmol/l resulted in a six fold stimulation. A further two-fold stimulation was seen after addition of theophylline to the high glucose incubation medium. In addition only under the latter conditions was there a significantly increased insulin release from both the non atrophic portion of the pancreas and from the pancreas of sham-operated animals. It is concluded that duct ligation does not diminish the glucose sensitivity of rat islet B-cells. Thus the present study does not support the view proposed previously that islet tissue is functionally of a foetal nature following duct ligation.

Key words: Pancreas duct ligation insulin release

A Andersson Histologiska Institutionen Box 571 75123 Uppsala 1 Sweden

Received 30 III 78 Accepted 19 VI 79

It is well known that ligation of the pancreatic duct causes an atrophy of the acinar cells. Ducts and islets are preserved but various types of morphological changes have also been reported in these ligated areas of the gland (Edstrom and Falkmer 1968 Boquist and Edstrom 1970). There is furthermore a resistance to the B-cytotoxic effect of alloxan in the duct ligated pancreas of rabbits (Wapole and Innes 1946). This alloxan resistance has been supposed to reflect a possible foetal nature of the islet tissue after duct ligation (Capellato and Perissinotto 1953 Larsson 1956). Indeed an increased neogenesis of islet cells similar to that observed in the foetus has been demonstrated in the duct tied pancreas (Hultquist *et al.* 1978).

It was the aim of the present investigation to study the release of insulin *in vitro* from pancreatic

pieces of duct ligated rats to determine whether it corresponds to a foetal or adult pattern of insulin release. Previous studies (Asplund *et al.* 1969) have indicated a poor insulin response to glucose in the foetal rat pancreas as compared to that of the adult

MATERIALS AND METHODS

Animals and Operation Technique

Female Sprague Dawley rats approximately 4 months old and weighing 300-350 g were used. Partial ligation of the pancreatic duct was performed on 10 rats according to the method of Hultquist and Jonsson (1965). Using this procedure a less extensive atrophy of the pancreas is obtained as the ligation is applied approximately between the duodenal two thirds and the ileal third of the pancreas at the level of the superior dorsal pole of the spleen. Five rats were sham-operated

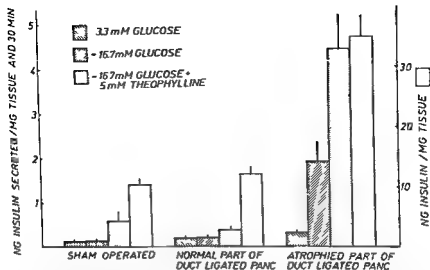


Fig 2 Insulin content and release from different pancreatic tissue specimens. Only the atrophic portion of the duct ligated pancreas was glucose sensitive whereas high glucose plus theophylline stimulated insulin secretion in all tissue specimens. In addition the insulin concentration of the atrophic portion was twice as high as that in the normal portion.

atrophic portion of the pancreas there was no effect of glucose alone whereas addition of theophylline to the high glucose medium resulted in a significant stimulation of the insulin release ($p < 0.01$). A similar pattern of insulin response was observed in the pancreatic pieces of the sham-operated animals. Furthermore in the duct ligated animals the insulin content of the non atrophic pancreatic portion was about one third of that in the atrophic portion of the pancreas (Fig 2). This was the case even when pancreatic samples from the sham operated animals were compared to the duct tied pancreas. These findings support previous observations of a higher volume density of islet tissue in duct ligated rat pancreas (Edsrom 1971b).

Thus the present findings clearly show that the B-cells of a duct tied pancreas are strongly stimulated by glucose to release insulin. Indeed the islet tissue of the atrophic portion of pancreas responded more readily to the acute glucose challenge than did the normal non-atrophic portion. At present we are unable to explain why the normal pancreas showed such a poor insulin response to glucose alone. Possible reasons might be a high proteolytic degradation of insulin in the incubation medium together with extensive diffusion gradients for various compounds including insulin through the large mass of exocrine tissue. The apparent glucose insensitivity of the pancreas of the sham-operated animals rules out an overall effect of duct ligation on the total pancreatic gland. It therefore seems that

the heightened insulin response of the atrophic portion of the pancreas may reflect a better supply of oxygen and perhaps other nutrients rather than a changed glucose recognition brought about by the duct ligation. This hypothesis agrees with the numerous observations of an excellent insulin response to glucose by rat islets isolated from normal pancreas. In conclusion we suggest from the present data that the glucose sensitivity of islet B-cells in the atrophic portion of a partially duct ligated rat pancreas is quite different from the obtunded sensitivity previously observed in the foetal rat pancreas.

We are grateful to Mrs Ing Britt Hallgren and Miss Astrid Nordin for excellent technical assistance. This work was supported financially by the Swedish Medical Research Council (12X 102, 12X 109) and Expressens Prenatal Forskningsfond.

REFERENCES

- Asplund K, Westman S & Hellerstrom C. Glucose stimulation of insulin secretion from the isolated pancreas of foetal and newborn rats. *Diabetologia* 5: 260-262 1969.
- Bencosme S A. Studies on the methods of staining islet cells of the pancreas. *Arch Path* 54: 87-97 1952.
- Boquist L & Edsrom C. Ultrastructure of pancreatic acinar and islet parenchyma in rats at various intervals after duct ligation. *Virchows Arch Abt. A Path Anat* 349: 69-79 1970.

and served as controls. The animals were fed standard laboratory rat pellets for 4–5 months before they were decapitated and used for the incubation experiments.

Light Microscopy

Immediately after sacrifice, non-incubated parts of the pancreas from both the normal and duct-tied rats were blotted, fixed in Bouin solution and embedded in paraffin. Sections, 7 μ m thick, were stained with aldehyde-fuchsin trichrome (Bencosme 1952).

Incubation Procedure

After removal, the pancreas was placed in bicarbonate buffered saline (Gey & Gey 1936), pH 7.4, containing 3.3 mmol/l glucose and 2 mg/ml albumin. The duct tied portion, located close to the spleen, could be distinguished by its more reddish coloration. This portion as well as the non-atrophic duodenal portion was carefully dissected out, blotted and weighed on a torsion balance (sensitivity 1 mg). The wet weight of the duct-tied portion of the gland varied between 80 and 440 mg (200 ± 30 mg, $n = 10$). Pieces of similar size were also prepared from the 'normal' portion of the pancreas of the duct-tied rats and from the pancreas of the sham-operated animals. These tissue samples were further cut into approximately 10 mg pieces, which were transferred in groups of 5 into Warburg vessels containing 2 ml of the bicarbonate buffered medium, as described above. Duplicate incubations were performed on each pancreas preparation. After incubation for 30 min in a gas phase consisting of O_2/CO_2 (95/5) at $+37^\circ C$ the medium was removed and 2 ml of identical fresh medium was added. At the end of a subsequent 30 min incubation period a sample of the medium was taken for assay of immunoreactive insulin (see below) and the remaining medium discarded. The incubation then continued for a further 30 min period in 16.7 mmol/l glucose. This glucose concentration was also employed in a final 30 min incubation period in the presence of 5 mmol/l theophylline. Samples for insulin assay were also taken

tant was then removed and stored at $-20^\circ C$ prior to insulin assay.

Insulin Assay

Measurements of the immunoreactive insulin content of the incubation media and acid ethanol extracts were performed according to the method of Heding (1972) using rat insulin as a standard.

RESULTS AND DISCUSSION

There were numerous islets with well-granulated B-cells visible in the aldehyde-fuchsin stained sections of pancreatic pieces taken from both the atrophic and the non-atrophic portions of the pancreas. In the duct-tied portions (Fig. 1) the acinar cells had



Fig. 1 Aldehyde-fuchsin stained section of the atrophic portion of the pancreas of a duct-ligated animal. There are two dark-stained islets of various size. Fat cells and duct-like structures can also be seen. $\times 250$.

disappeared completely and were replaced by numerous ducts, fat cells and strands of connective tissue surrounding small blood vessels. Mast cells were also present in all these structures. The islets were rounded or kidney-shaped and composed of a core of B-cells surrounded by a thin outer rim of A_2 -cells. Islets of a more irregular shape and with varying distribution of the cell types were often observed. There seemed to be more islets per section surface area in the duct-tied, than in the normal portions of the gland, which is in agreement with the planimetric studies of Edström (1971b). The appearance of the non-ligated portion of the pancreas corresponded, in all respects, to that of the sham-operated animals.

As seen in Fig. 2 an increase of the glucose concentration from 3.3 to 16.7 mmol/l strongly stimulated the insulin release from the duct tied portion of the pancreas ($p < 0.005$). This effect was markedly potentiated by addition of theophylline to the high-glucose medium ($p < 0.001$). In the non-

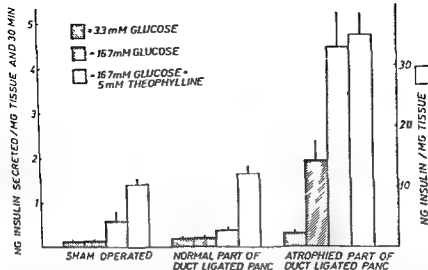


Fig 2 Insulin content and release from different pancreatic tissue specimens. Only the atrophic portion of the duct ligated pancreas was glucose sensitive whereas high glucose plus theophylline stimulated insulin secretion in all tissue specimens. In addition the insulin concentration of the atrophic portion was twice as high as that in the normal portion.

atrophic portion of the pancreas there was no effect of glucose alone whereas addition of theophylline to the high glucose medium resulted in a significant stimulation of the insulin release ($p < 0.01$). A similar pattern of insulin response was observed in the pancreatic pieces of the sham-operated animals. Furthermore in the duct ligated animals the insulin content of the non-atrophic pancreatic portion was about one third of that in the atrophic portion of the pancreas (Fig 2). This was the case even when pancreatic samples from the sham-operated animals were compared to the duct tied pancreas. These findings support previous observations of a higher volume density of islet tissue in duct ligated rat pancreas (Edstrom 1971b).

Thus the present findings clearly show that the B-cells of a duct tied pancreas are strongly stimulated by glucose to release insulin. Indeed the islet tissue of the atrophic portion of pancreas responded more readily to the acute glucose challenge than did the normal non-atrophic portion. At present we are unable to explain why the normal pancreas showed such a poor insulin response to glucose alone. Possible reasons might be a high proteolytic degradation of insulin in the incubation medium together with extensive diffusion gradients for various compounds including insulin through the large mass of exocrine tissue. The apparent glucose insensitivity of the pancreas of the sham-operated animals rules out an overall effect of duct ligation on the total pancreatic gland. It therefore seems that

the heightened insulin response of the atrophic portion of the pancreas may reflect a better supply of oxygen and perhaps other nutrients rather than a changed glucose recognition brought about by the duct ligation. This hypothesis agrees with the numerous observations of an excellent insulin response to glucose by rat islets isolated from normal pancreas. In conclusion we suggest from the present data that the glucose sensitivity of islet B-cells in the atrophic portion of a partially duct ligated rat pancreas is quite different from the obtunded sensitivity previously observed in the foetal rat pancreas.

We are grateful to Mrs. Ing Britt Hallgren and Miss Astrid Nordin for excellent technical assistance. This work was supported financially by the Swedish Medical Research Council (12X 102, 12X 109) and Expressens Prenatal Forskningsfond.

REFERENCES

- Asplund K, Westman S & Hellerstrom C. Glucose stimulation of insulin secretion from the isolated pancreas of foetal and newborn rats. *Diabetologia* 5: 260-262, 1969.
- Bencosme S A. Studies on the methods of staining islet cells of the pancreas. *Arch Path* 54: 87-97, 1952.
- Boquist L & Edstrom C. Ultrastructure of pancreatic acinar and islet parenchyma in rats at various intervals after duct ligation. *Virchows Arch Abt. A Path Anat* 349: 69-79, 1970.

- Cappelato, M & Perissinotto, B* Effetti della introduzione dell'allossana nel dotto di Wirsung Boll Soc Ital biol sperm 29 97-101, 1953
- Edström, C* Alloxan sensitivity of rats at various intervals following ligation of the pancreatic ducts Acta Soc Med Upsal 76 77-86, 1971a
- Edström, C* Further quantitative structural studies of the pancreatic islet parenchyma in rats with duct ligation Acta Soc Med Upsal 76 127-138, 1971b
- Edström, C & Falkmer, S* Pancreatic morphology and blood glucose level in rats at various intervals Virchows Arch Abt A Path Anat 345 139-153, 1968
- Gey, G O & Gey, M K* The maintenance of human normal cells and tumor cells in continuous culture Am J Cancer 27 45-76, 1936
- Heding, L* Determination of total serum insulin (IRI) in insulin treated diabetic patients Diabetologia 8 260-266, 1972
- Hultquist, G, Karlsson, U & Hallner, A C* The regenerative capacity of the pancreas in duct ligated rats Exp Path 17 44-52, 1979
- Hultquist, G & Jönsson, L E* Ligation of the pancreatic duct in rats Acta Soc Med Upsal 70 82-88 1965
- Larsson, Y* Morphology of the pancreas and glucose tolerance in biliary fistula, in common bile duct obstruction and after ligation of pancreatic duct Acta Paediatr Suppl 106 1-271, 1956
- Walpole, A L & Innes, J R M* Experimental diabetes the effect of ligation of the pancreatic duct upon the action of alloxan in rabbits Brit J Pharmacol 1 174-185, 1946

HISTOLOGICAL DIAGNOSIS OF MYOCARDIAL INJURY

*Comparison of Hematoxylin Basic Fuchsin Picric Acid (HBFP)-Stained Sections
Obtained during Autopsy with Isolated Viable Rat Cardiac Myocytes Exposed to
Anoxia*

JOVAN RAJS

Department of Forensic Medicine Karolinska Institutet Medical School Stockholm Sweden

Rajs J Histological diagnosis of myocardial injury Comparison of hematoxylin basic fuchsin picric acid (HBFP)-stained sections obtained during autopsy with isolated viable rat cardiac myocytes exposed to anoxia *Acta path microbiol scand Sect A 87 289-297 1979*

The light microscopic appearances in hematoxylin basic fuchsin picric acid (HBFP)-stained histological sections from cardiac and skeletal muscle tissue were put in relation to the reactions of isolated viable rat cardiac myocytes exposed to anoxia in suspension and their morphology in paraffin embedded sections. Special attention was paid to pre-necrotic phases of myocytic injury which were followed in viable rat cardiac myocytes by light microscopy and confirmed with biochemical assays indicating increased plasma membrane permeability. In cases of sudden death and traumatic injury to the heart and skeletal muscle there was good agreement between alterations demonstrated with the HBFP technique and alterations of viable rat cardiac myocytes exposed to anoxia. In isolated myocytes these alterations were associated with irregular contractility which when occurring *in situ* might have influenced the cardiac function prior to death. Moreover the changes develop at a much faster rate than the inflammatory reaction following tissue injury and may therefore be regarded as an early vital phenomenon of significance in clinico-pathological and medico-legal considerations.

Key words Myocardial injury histological staining

J Rajs Department of Forensic Medicine Karolinska Institutet S-104 01 Stockholm 60 Sweden

Received 7 ix 78 Accepted 19 ix 79

The histological diagnosis of pre-necrotic lesions is a classical problem in human pathology. Although the sequence of pre-necrotic histological changes is well established in the experimental model the appearances in a static section are difficult to relate to functional changes. With regard to the crucial importance of the heart function for the persistence of life and its role in the mechanism of death the confirmation of the pre-necrotic myocardial lesions and their interpretation are of great clinico-pathological and medico-legal importance.

We have previously developed a method for preparation of isolated viable rat cardiac myocytes in order to study the relationship of the histological

and functional changes during anoxia [1]. The results were especially encouraging when we compared morphological and biochemical properties of myocytes in suspension and the morphology of the paraffin-embedded rat cardiac myocytes stained with the hematoxylin basic fuchsin picric acid (HBFP) method [2]. As a result of anoxia there was a gradual increase in plasma membrane permeability noted as an increase in succinate stimulated oxygen uptake, a decrease in the trypan blue exclusion frequency, a leakage of cytosolic lactate dehydrogenase and an increased proportion of swollen irregularly contracting myocytes. The basic fuchsin was taken up by contracted or damaged myocytes which morphologically in

- Cappelato, M & Perissinotto, B* Effetti della introduzione dell'allossana nel dotto di Wirsung Boll Soc Ital biol sperm 29 97-101, 1953
- Edström, C* Alloxan sensitivity of rats at various intervals following ligation of the pancreatic ducts Acta Soc Med Upsal 76 77-86, 1971a
- Edström, C* Further quantitative structural studies of the pancreatic islet parenchyma in rats with duct ligation Acta Soc Med Upsal 76 127-138, 1971b
- Edström, C & Falkmer, S* Pancreatic morphology and blood glucose level in rats at various intervals Virchows Arch Abt A Path Anat 345 139-153, 1968
- Gey, G O & Gey, M K* The maintenance of human normal cells and tumor cells in continuous culture Am J Cancer 27 45-76, 1936
- Heding, L* Determination of total serum insulin (IRI) in insulin-treated diabetic patients Diabetologia 8 260-266, 1972.
- Hultquist, G, Karlsson U & Hallner, A C* The regenerative capacity of the pancreas in duct ligated rats Exp Path 17 44-52, 1979
- Hultquist, G & Jönsson, L E* Ligation of the pancreatic duct in rats Acta Soc Med Upsal 70 82-88 1965
- Larsson, Y* Morphology of the pancreas and glucose tolerance in biliary fistula, in common bile duct obstruction and after ligation of pancreatic duct Acta Paediatr Suppl 106 1-271, 1956
- Walpole, A L & Innes, J R M* Experimental diabetes the effect of ligation of the pancreatic duct upon the action of alloxan in rabbits Brit J Pharmacol 1 174-185, 1946

HISTOLOGICAL DIAGNOSIS OF MYOCARDIAL INJURY

*Comparison of Hematoxylin Basic Fuchsin Picric Acid (HBFP)-Stained Sections
Obtained during Autopsy with Isolated Viable Rat Cardiac Myocytes Exposed to
Anoxia*

JOVAN RAJS

Department of Forensic Medicine Karolinska Institutet Medical School Stockholm, Sweden

Rajs J Histological diagnosis of myocardial injury Comparison of hematoxylin basic fuchsin picric acid (HBFP)-stained sections obtained during autopsy with isolated viable rat cardiac myocytes exposed to anoxia Acta path microbiol scand Sect A 87 289-297 1979

The light microscopic appearances in hematoxylin basic fuchsin picric acid (HBFP)-stained histological sections from cardiac and skeletal muscle tissue were put in relation to the reactions of isolated viable rat cardiac myocytes exposed to anoxia in suspension and their morphology in paraffin embedded sections Special attention was paid to pre necrotic phases of myocytic injury which were followed in viable rat cardiac myocytes by light microscopy and confirmed with biochemical assays indicating increased plasma membrane permeability In cases of sudden death and traumatic injury to the heart and skeletal muscle there was good agreement between alterations demonstrated with the HBFP technique and alterations of viable rat cardiac myocytes exposed to anoxia In isolated myocytes these alterations were associated with irregular contractility which when occurring *in situ* might have influenced the cardiac function prior to death Moreover the changes develop at a much faster rate than the inflammatory reaction following tissue injury and may therefore be regarded as an early vital phenomenon of significance in clinico pathological and medico legal considerations

Key words Myocardial injury histological staining

J Rajs Department of Forensic Medicine Karolinska Institutet S 104 01 Stockholm 60 Sweden

Received 7 ix 78 Accepted 19 ii 79

The histological diagnosis of pre necrotic lesions is a classical problem in human pathology Although the sequence of pre necrotic histological changes is well established in the experimental model the appearances in a static section are difficult to relate to functional changes With regard to the crucial importance of the heart function for the persistence of life and its role in the mechanism of death the confirmation of the pre necrotic myocardial lesions and their interpretation are of great clinico-pathological and medico-legal importance

We have previously developed a method for preparation of isolated viable rat cardiac myocytes in order to study the relationship of the histological

and functional changes during anoxia [1] The results were especially encouraging when we compared morphological and biochemical properties of myocytes in suspension and the morphology of the paraffin-embedded rat cardiac myocytes stained with the hematoxylin basic fuchsin picric acid (HBFP) method [2] As a result of anoxia there was a gradual increase in plasma membrane permeability noted as an increase in succinate stimulated oxygen uptake a decrease in the trypan blue exclusion frequency a leakage of cytosolic lactate dehydrogenase and an increased proportion of swollen irregularly contracting myocytes The basic fuchsin was taken up by contracted or damaged myocytes which morphologically in

suspension revealed irregular contractions, but this was not the case in undamaged or necrotic myocytes

The purpose of this paper is to compare the previously evaluated histological appearances in rat cardiac myocytes exposed to anoxia to the appearances in the human heart and skeletal muscle in paraffin-embedded tissue sections

MATERIALS AND METHODS

Beating cardiac myocytes from adult rats were obtained as previously described [3]. The myocytes were isolated by heart perfusion with a modified Hanks buffer containing 0.83 mg/ml crude collagenase and bubbled with carbogen gas (95% O₂ and 5% CO₂). The procedure yielded about 45×10^6 myocytes which were suspended in Ca²⁺ free Krebs Henseleit buffer (pH 7.4). To induce anoxia the myocyte suspension was bubbled with 100% N₂. Samples from incubates were taken for biochemical assays and for observations in the light microscope every 15 minutes during a 90 minute observation period. The viability of the myocytes in suspension was evaluated using trypan blue exclusion and studying cell morphology and contractility. To evaluate plasma membrane integrity succinate stimulation of oxygen consumption and NADH penetration into the cells were assayed [4].

Samples from oxygenated and anoxic myocytes were also taken every 15 minutes for 90 minutes and prepared for histological examination according to previously described techniques [1]. Sections cut at 3-4 μ were stained with the HBFP technique for detection of recent myocardial lesions [2]. They were evaluated according to previous experiences with this staining procedure taking into account possible artefactual changes as well as experiences with other staining techniques [2-5].

Sections from cardiac and skeletal muscle of selected autopsy cases were similarly examined using the HBFP technique. In the micrographs (Figs 2-17) the black structures were originally in HBFP stained sections crimson red while the grey ones were picrinophilic.

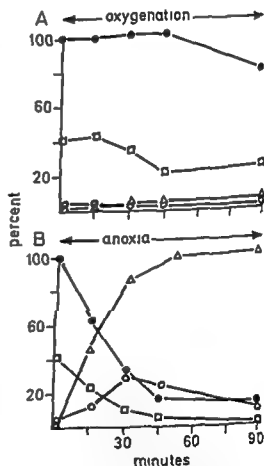
Bodies were kept in the refrigerators of the mortuary (temperatures between +4° and +8°C) and the postmortems were performed within four to six days. The histopathological appearances were related to the gross anatomy, possible physiological events, information about circumstances of death and when available clinical records.

RESULTS AND CLINICO PATHOLOGICAL CORRELATION

incubated in the presence or absence of ... presented in Figs 1A and B and are in accordance with previously published data [1]. A comparison of the appearance of myocytes in suspension and in

histological sections is made in Figs 2-5. On the basis of this comparison the morphological appearances in HBFP stained human myocardial sections may be interpreted in a more functional manner than has hitherto been possible. Examples of this are presented in the following autopsy cases.

I F 1053/77 A 60 year old previously healthy male died suddenly during vigorous physical exercise. The post mortem revealed general organ congestion. The heart size, valves and vessels were normal. Microscopy revealed mural sclerosis and stenosis of the minor coronary artery branches. Sections from the posterior ventricular wall showed resistance to differentiation in solution C when stained with HBFP and irregularities of the striations (Fig. 6). It appeared that these lesions were caused by the myocardial ischemia induced by vigorous



Figs 1A and B Viability of isolated rat cardiac myocytes during oxygenation and anoxia.

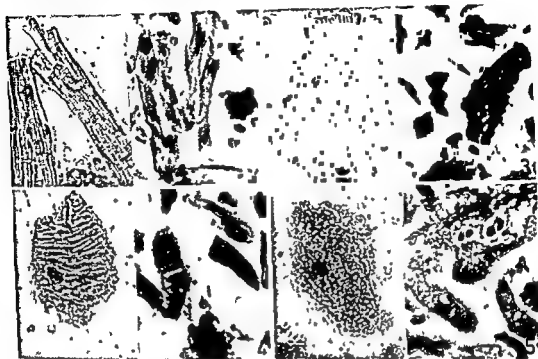
Endogenous oxygen uptake (●) given as per cent of the starting value (10 nmoles/min 10^6 cells); succinate-stimulated oxygen uptake (○) given as per cent of the

the maximal at the total lysis of the cells during oxygenation (suspension bubbled with 95% O₂ - 5% CO₂) (A) and anoxia (bubbled with 100% N₂) (B) of isolated rat cardiac myocytes.

exercise and were due to stenosis of the minor arterial branches it could also seem (taking into account the experience with the isolated rat cardiac myocytes) that they were associated with irregular contractility of the

myofibres and the ventricular wall as a whole presumably leading to heart insufficiency or fibrillation and sudden death

2 F 3498/77 A 53 year old male died suddenly 3



Figs 2-5 Trypan blue (left) and HBFP (right) $\times 800$

Fig 2 Regularly contracting myocyte pellet. Contractions at myocytes in the shortened myocyte in the upper terminal portion and slight uptake of basic fuchsin (dark). On the far right there is one deformed and rounded myocyte stained with basic fuchsin and surrounded by picrinophilic blebs.

Fig 3 Rat cardiac myocytes with alterations following 30 minutes of anoxic incubation. To the left there is a contracted and swollen myocyte in suspension with vacuoles and irregular striations. The upper terminal portion corresponds to a fibrillation while the lower one represents a focus of bradyarrhythmia. Note presence of blebs outside the plasma membrane. In the picture to the right (section of pellet) the largest cell (arrow) is similar to the myocyte in suspension. It is contracted and swollen, there are some picrinophilic blebs, and the striations are not visible due to the massive uptake of basic fuchsin. The other myocytes in the section are also altered.

Fig 4 Rat cardiac myocytes after 45 minutes of anoxic incubation. The picture to the left illustrates the appearance of a myocyte in suspension immediately following bursting. Trypan blue started to penetrate into the cell and the nuclei became blue (here black). The striations are thick and irregular. Prior to bursting there was total arrhythmia with separate foci showing autonomous contractions. In the picture to the right of a section of a pellet there is a similar myocyte in this section and surrounded by dying and dead cells.

Fig 5 Rat cardiac myocytes following 60 minutes of anoxic incubation. The cell is deformed with its plasma membrane blebs. The sarcoplasm was stained with trypan blue (here black). Contractile and picrinophilic myocytes showing intracellular contract. Necrotic and picrinophilic myocytes showing intracellular contract. The photomicrograph of the sectioned pellet (picture to the right).

suspension, revealed irregular contractions, but this was not the case in undamaged or necrotic myocytes

The purpose of this paper is to compare the previously evaluated histological appearances in rat cardiac myocytes exposed to anoxia to the appearances in the human heart and skeletal muscle in paraffin-embedded tissue sections

MATERIALS AND METHODS

Beating cardiac myocytes from adult rats were obtained as previously described [3]. The myocytes were isolated by heart perfusion with a modified Hank's buffer containing 0.83 mg/ml crude collagenase and bubbled with carbogen gas (95% O₂ and 5% CO₂). The procedure yielded about 45×10^6 myocytes which were suspended in Ca²⁺-free Krebs-Henseleit buffer (pH 7.4). To induce anoxia, the myocyte suspension was bubbled with 100% N₂. Samples from incubates were taken for biochemical assays and for observations in the light microscope every 15 minutes during a 90 minute observation period. The viability of the myocytes in suspension was evaluated using trypan blue exclusion, and studying cell morphology and contractility. To evaluate plasma membrane integrity, succinate stimulation of oxygen consumption and NADH penetration into the cells were assayed [4].

Samples from oxygenated and anoxic myocytes were also taken every 15 minutes for 90 minutes and prepared for histological examination according to previously described techniques [1]. Sections cut at 3–4 μ were stained with the HBFP technique for detection of recent myocardial lesions [2] they were evaluated according to previous experiences with this staining procedure taking into account possible artefactual changes as well as experiences with other staining techniques [2, 5].

Sections from cardiac and skeletal muscle of selected autopsy cases were similarly examined using the HBFP technique. In the micrographs (Figs 2–17), the black structures were originally in HBFP stained sections, crimson red, while the grey ones were picrinophilic.

Bodies were kept in the refrigerators of the mortuary (temperatures between +4° and +8°C) and the postmortems were performed within four to six days. The histopathological appearances were related to the gross anatomy, possible physiological events, information about circumstances of death and, when available, clinical records.

RESULTS AND

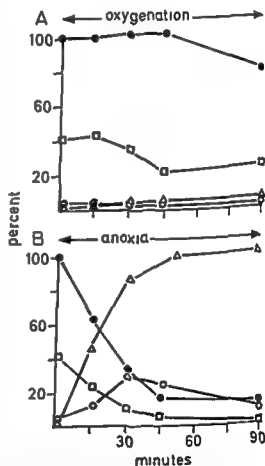
CLINICO-PATHOLOGICAL CORRELATION

incubated in the presence of succinate as follows:

the appearance of myocytes in suspension

histological sections is made in Figs 2–5. On the basis of this comparison, the morphological appearances in HBFP-stained human myocardial sections may be interpreted in a more functional manner than has hitherto been possible. Examples of this are presented in the following autopsy cases.

1 F 1053/77 A 60 year old, previously healthy male died suddenly during vigorous physical exercise. The post mortem revealed general organ congestion. The heart size, valves and vessels were normal. Microscopy revealed mural sclerosis, and stenosis of the minor coronary artery branches. Sections from the posterior ventricular wall showed resistance to differentiation in solution C when stained with HBFP, and irregularities of the striations (Fig. 6). It appeared that these lesions were caused by the myocardial ischemia induced by vigorous



Figs 1A and B Viability of isolated rat cardiac myocytes during oxygenation and anoxia. Endogenous oxygen uptake (●), given as per cent of the starting value (10 nmoles/min 10^6 cells); succinate-stimulated oxygen uptake (○) given as per cent of increase of the oxygen uptake upon addition of succinate; trypan blue exclusion (□) as per cent of cells excluding the dye and NADH penetration (Δ), given as per cent of the maximal at the total lysis of the cells, during oxygenation (suspension bubbled with 95% O₂ - 5% CO₂) (A) and anoxia (bubbled with 100% N₂) (B) of isolated rat cardiac myocytes.



10

Fig 6 Patient no 1 Area of left ventricular wall with myofibres stained with basic fuchsin (black) The cells show presence of numerous contraction bands HBFP $\times 150$

Fig 7 Patient no 2 Photomicrograph of a myocardial section from the left posterior ventricular wall showing crumpled red-stained myofibres in connection with a scar after a healed infarct. HBFP $\times 60$

Fig 8 Patient no 3 Transverse section from the upper part of the ventricular septum showing uptake of basic fuchsin (dark areas) in the subendocardial layer of typical heart muscle HBFP $\times 42$

Fig 9 A higher magnification of the boxed area in Fig 8 Purkinje fibres belonging to the left bundle branches reveal irregular contraction bands HBFP $\times 240$

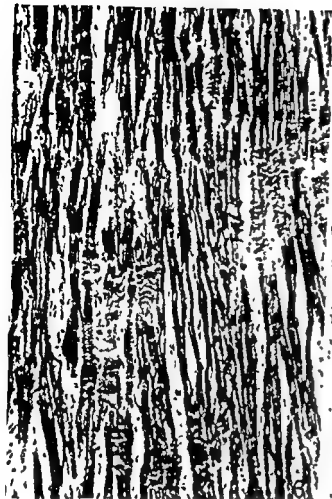
Fig 10 Patient no 4 Photomicrograph of a section from the posterior papillary muscle with transversal segmental uptake of basic fuchsin (dark areas) HBFP $\times 5$

Fig 11 A higher magnification of Fig 10 It is apparent that the myocytes which were stained with basic fuchsin are contracted or fragmented furthermore they show irregularities of contraction bands or uptake of stain in terminal portions changes reminiscent of those in zonal lesions [9]. The picrinophilic myocytes unstained by basic fuchsin are regular in shape and show no alterations HBFP $\times 150$

months after being treated for myocardial infarct with aortocoronary by pass. Post mortem disclosed cardiac hypertrophy, scarring of the left posterior ventricular wall after previous infarct, scarring in the subendocardial tissue of the ventricular septum, stenosis of both coronary arteries and patent grafts between aorta and the coronaries. The scar in the subendocardium was attributed to heart surgery [6]. However, uptake of basic fuchsin was noted only in the vicinity of the scar after the old infarct (Fig 7) and not near the scar in the

subendocardium. It would therefore appear that the patient died due to reinfarction in an area associated with the old infarct rather than to the effect of heart surgery.

3 F 2972/76 A 78 year old male died during an asthmatic seizure. Post mortem disclosed pulmonary emphysema, slight hypertrophy of the heart with right ventricular dilatation and general organ congestion. The coronaries were sclerotic but not occluded. In the HBFP stained sections a positive staining of the subendocardial



chest in a hydraulic press. He was cyanotic and unconscious when arriving at the hospital, exhibiting a low rate of spontaneous respiration. The electrocardiogram revealed wide complexes and low frequency of the heart activity and the patient died soon thereafter. The autopsy disclosed petechial hemorrhages in the face and on the chest and also in the mucous and serous membranes. Furthermore, there were fractures of the third, fourth and fifth ribs on the left side and first and second ribs on the right side. There was also a hematoma of the right atrial anterior wall of the heart and in the interatrial septum. Microscopic examination of the heart (Figs 14 and 15) revealed rupture of the AV bundle. The HBFP technique confirmed the vital origin of the lesion, thus the findings were in good agreement with the clinical symptoms. Moreover, the uptake of stain in the subendocardial region was as expected with regard to the observed circulatory and respiratory disturbances [7].

8 F 1759/78 A 50 year old male shot himself in the right temporal region and died immediately. Sections from the entrance wound of the bullet revealed contracted and hyalinized myofibres belonging to the temporal muscle revealing massive uptake of basic fuchsin (Fig 16) as well as a local hemorrhage.

9 F 1142/78 A 62 year old male survived a suicidal shot injury by 1.5 hours. The routine stained

sections from the entrance wound area revealed contracted, hyalinized and necrotic myofibres, hemorrhage but no inflammatory reaction. The appearance of the HBFP stained sections are shown in Fig. 17.

DISCUSSION

The basis for the demonstration of pre-necrotic changes of the myocytes in tissue sections was the comparison with isolated viable rat cardiac myocytes. The viability of the latter was apparent in the light microscope and confirmed by biochemical assays [1]. Thus, the endogenous oxygen uptake reflects the mitochondrial respiration and is slightly increased during the first period of oxygenation, as opposed to a marked decrease during anoxia (cf. Fig. 1). Augmented NADH penetration and enhanced succinate-stimulated oxygen uptake during anoxia indicates increasing permeability or impairment of the plasma membrane function. During oxygenation the extracellularly located test molecules apparently do not enter the myocardial cells at any significant level. The decrease in succinate stimulation following 45 min of anoxia reflects an

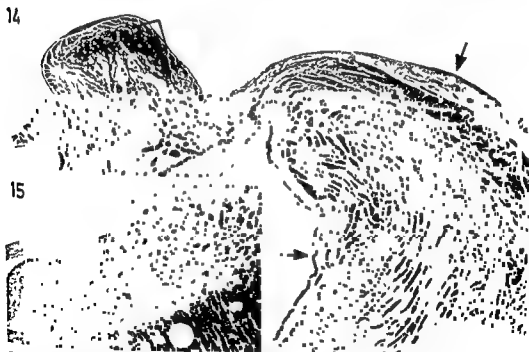


Fig. 14 There is a rupture of unremarkable myocyte.

Fig. 15 The boxed area, similar to Fig. 14, with rupture of the AV bundle, showing contracted and damaged Purkinje fibres revealing uptake of basic fuchsin as well as hemorrhage in the interstices. HBFP $\times 140$.

layer of the typical heart muscle cells was noted (Fig 8) while the layers immediately beneath the endocardium consisting of Purkinje fibres, were picrinophilic. However, some Purkinje fibres belonging to the left bundle branches showed crimson red stained, irregular, contraction bands (Fig 9). It appeared that the asthmatic seizure had caused general hypoxia, a condition in which the subendocardium is especially vulnerable [7]. The alterations could be due to the hypoxia and – in the case of the Purkinje fibres – considered as the pathoanatomic basis for conduction disturbances and death, rat cardiac myocytes with comparable lesions are fibrillating and reveal areas with autonomous contractions [1]. Similar lesions were found in the hearts of intravenous drug addicts who died suddenly in connection with drug administration [8] and of epileptics who died during seizure (unpublished observations).

4 F 640/78 A 58-year old female who had died suddenly during an asthmatic seizure. The post mortem revealed moderate pulmonary emphysema, catarrhal bronchitis and general organ congestion. grossly, the heart was unremarkable. In HBFP-stained sections, a transversal segmental uptake of basic fuchsin was seen (Figs 10 and 11). The papillary muscles are supplied with blood segmentally by penetrating class II vessels [10]. Accordingly, the segmental lesions of the myocytes have their physiological explanation in a situation with general hypoxia which may occur during e.g. an asthmatic seizure. The rat cardiac myocytes with such lesions are fibrillating. Therefore, it is reasonable to assume that a disfunction of the papillaries with consecutive mitral regurgitation occurred and contributed to the heart failure [11].



Fig 12 Patient no 5 Photomicrograph of a section from the anterior papillary muscle. Note uptake of basic fuchsin in the subendocardial layer of the typical heart muscle. HBFP, $\times 30$.



Fig 13 Patient no 6 Section from the ruptured area in the heart. Note the uptake of basic fuchsin (dark) in the damaged and contracted myocytes around the rupture. HBFP $\times 150$.

5 F 1350/77 A 16 year old boy died suddenly in connection with inhalation of trichlorethylene. The autopsy disclosed general organ congestion, pulmonary oedema and hemorrhages, and right ventricular dilatation. The only positive microscopical findings in the heart are shown in Fig 12 and consisted in the uptake of basic fuchsin in the subendocardial layer of the typical heart muscle cells. Such lesions in the papillary muscles might contribute to heart failure in the same way as the lesions in case nr 4.

6 F 3868/76 A 13 year old girl died immediately due to severe organ injury after suicidal jump from a considerable height. The heart showed presence of multiple ruptures. The HBFP stained myocardial sections revealed uptake of basic fuchsin in connection with the injured areas (Fig 13). It can be concluded that such uptake in the periphery of the myocardial section was indicative of a vital process causing the injury, since artefactual alterations due to poor differentiation in solution C show an opposite distribution of the red stain, i.e. the periphery of the sections becomes picrinophilic [5].

7 F 665/77 A 34 year old male was caught by the

chest in a hydraulic press. He was cyanotic and unconscious when arriving at the hospital exhibiting a low rate of spontaneous respiration. The electrocardiogram revealed wide complexes and low frequency of the heart activity and the patient died soon thereafter. The autopsy disclosed petechial hemorrhages in the face and on the chest, and also in the mucous and serous membranes furthermore there were fractures of the third fourth and fifth ribs on the left side and first and

sections from the entrance wound area revealed contracted, hyalinized and necrotic myofibres hemorrhage but no inflammatory reaction. The appearance of the HBFP stained sections are shown in Fig. 17

DISCUSSION

The basis for the demonstration of pre-necrotic changes of the myocytes in tissue sections was the comparison with isolated viable rat cardiac myocytes. The viability of the latter was apparent in the light microscope and confirmed by biochemical assays [1]. Thus the endogenous oxygen uptake reflects the mitochondrial respiration and is slightly increased during the first period of oxygenation as opposed to a marked decrease during anoxia (cf Fig. 1). Augmented NADH penetration and enhanced succinate stimulated oxygen uptake during anoxia indicates increasing permeability or impairment of the plasma membrane function. During oxygenation the extracellularly located test molecules

HBFP technique confirmed the vital origin of the lesion thus, the findings were in good agreement with the clinical symptoms. Moreover the uptake of stain in the subendocardial region was as expected with regard to the observed circulatory and respiratory disturbances [7].

8 F 1759/78 A 50 year old male shot himself in the right temporal region and died immediately. Sections from the entrance wound of the bullet revealed contracted and hyalinized myofibres belonging to the temporal muscle revealing massive uptake of basic fuchsin (Fig. 16) as well as a local hemorrhage.

9 F 1142/78 A 62 year old male survived a suicidal shot injury by 1.5 hours. The routine stained

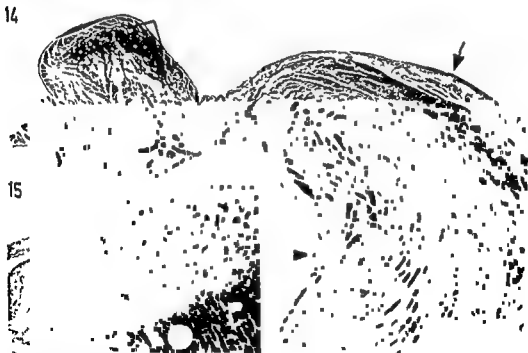


Fig. 14 Section from heart showing a rupture of the AV bundle. There is a rupture of the AV bundle. There are no remarkable myocytes in the section.

Fig. 15 The boxed area from Fig. 14 with rupture of the AV bundle showing contracted and damaged Purkinje fibers revealing uptake of basic fuchsin as well as hemorrhage in the interstices. HBFP x140

impairment of mitochondrial function the cells are evidently severely injured and have probably lost most of their ATP. The trypan blue exclusion frequency parallels rather well these biochemical parameters of cell viability.

When the appearances of HBFP stained myocardial sections are compared with those of viable rat cardiac myocytes it seems that the basic fuchsin uptake may occur in contracted — but otherwise unremarkable — myocytes which in suspension reveal slight irregularities of contractility. There is also uptake in swollen myocytes with more or less irregular contraction bands. In suspension these cells show a whole scale of pathologic contractions. Uptake of stain may also occur in totally deformed or even burst myocytes if fixed shortly after

bursting. This is however not the case in regularly shaped rhythmically contracting or necrotic, non contracting or completely disintegrated myocytes. In contracted or very slightly damaged myocytes the uptake of stain is diffuse in the more deformed myocytes uptake is confined to the irregular contractile elements. Shortly after the cell bursting when the myofibrils are aggregated in clumps the uptake is again diffuse although the peripheral blebs are picrinophilic.

The observations on myocytes in suspension seem to allow the speculation that the altered myocytes noted in autopsy might have contracted irregularly during life and thus influenced cardiac function as a whole. The subendocardium including the AV bundle branches and the papillary

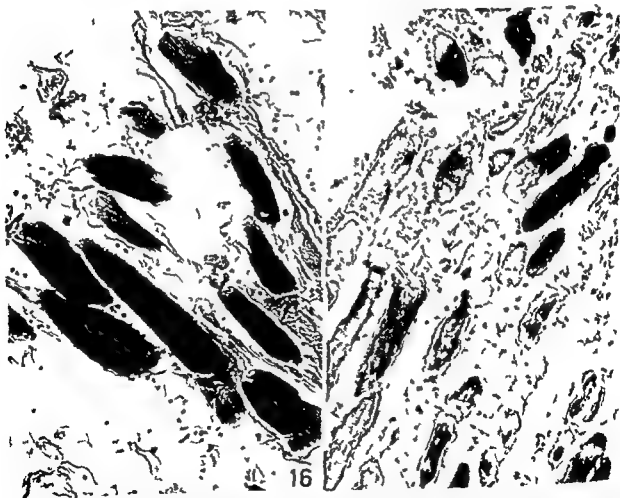


Fig 16 Patient no. 8. Section from entrance wound of firearm bullet in the right temporal muscle. Note monotonous appearance of contracted myofibers heavily stained with basic fuchsin. HBFP $\times 240$.

Fig 17 Patient no. 9. Section from entrance wound of firearm bullet from a patient who survived the injury by 15 minutes. The myocytes are not resembling those of rat cardiac myocytes following variable changes.

are necrotic and picrinophilic. Inflammatory reaction is lacking. HBFP $\times 240$.

muscles are the most common sites for manifestations of general hypoxic cardiovascular injury, lesions in these structures (cf case 3, 4 and 5) have a particular functional importance [12].

The bursting of a cell is assumed to represent the

not the earliest alterations — such as contraction of the myocytes (which might be concomitant with lesions close to intercalated disks) and slight irregularity of the striations — are reversible. However it was apparent in the light microscope that the process of cellular damage varies in rapidity under the same conditions and may develop within minutes or hours. On this basis it appears that a monomorphous occurrence of diffusely crimson red stained non injured or only contracted myocytes may be if not artefactual only of agonal character. Demonstration of myocytes in variable stages of cellular damage would on the other hand constitute rather convincing evidence of a vital process in the causation of the initial lesion and indicate that survival of some of the cells in an injured area might be possible. The alterations within a single anoxically injured myocyte develop much more rapidly than inflammatory lesions and may be taken to signify an early developing vital reaction.

The findings in the cases presented in this study suggest that sections from heart and skeletal muscle when stained according to the HBFP technique [2] and carefully studied and followed [5] may be of diagnostic help in clinical and forensic pathology. This is especially true when the uptake of basic fuchsin and the picrinophilia are adequately related to cellular alterations and localized in specific regions and structures of the myocytes. When the positive staining occurs in regions of the heart which can be expected to be affected on the basis of gross findings and presumed severance of the blood supply under pathological conditions the vital origin of the alterations becomes all the more likely. It should be kept in mind that the uptake of the basic fuchsin was not only observed in apoxic myocytes but also in myocytes exposed to mechanic and thermic (firearm) injury.

In conclusion findings of variable stages of myocytic damage in tissue sections easily demon-

strable with the HBFP technique and not influenced by several days autolysis may be regarded as an early vital reaction to injury in clinico-pathological and medico-legal considerations.

REFERENCES

- 1 Rajs J, Jones D P & Jakobsson S W. Comparison of anoxic changes in isolated rat cardiac myocytes in suspension and histological sections. *Acta path microbiol scand Sect. A* 86: 325-332 1978.
- 2 Lue J T, Holley K E, Kampa W R & Titus J L. New histochemical method for morphologic diagnosis of early stages of myocardial ischemia. *Mayo Clin Proc* 46: 319-327 1971.
- 3 Rajs J, Sundberg M, Sundby G B, Danell N, Tornling G, Biberfeld P & Jakobsson S W. A rapid method for the isolation of viable cardiac myocytes from adult rat. *Experimental Cell Res* 115: 183-189 1978.
- 4 Orrenius S, Thor H, Rajs J & Berggren M. Isolated rat hepatocytes as an experimental tool in the study of cell injury. Effect of anoxia. *Forensic Sci* 8: 255-263 1976.
- 5 Rajs J & Jakobsson S. Experiences with the pematrylin basic fuchsin picric acid staining method for morphologic diagnosis of myocardial ischemia — An experimental study in forensic pathology. *Forensic Sci* 8: 37-48 1976.
- 6 Najafi H, Henson D, Dye W S, David H, Hunter J A, Callaghan R, Eisenstein R & Julian O C. Left ventricular haemorrhagic necrosis. *Ann Thorac Surg* 7: 550-561 1969.
- 7 Guy C & Elliot R S. The subendocardium of the left ventricle: a physiologic enigma. *Chest* 58: 555-556 1970.
- 8 Falconer B & Rajs J. Cardiac lesions in intravenous drug addicts. *Forensic Sci* (in press).
- 9 Martin A M, Green W B & Solomon H B. Human myocardial zonal lesions. *Arch Path* 87: 339-342 1969.
- 10 Harvey Estes E, Dalton F M Jr, Entman M L, Dixon H B & Hackel D B. The anatomy and blood supply of the papillary muscles of the left ventricle. *Amer Heart J* 71: 356-362 1966.
- 11 Gould L, Reddy C V R, Vecchiarelli H J & Gomprecht R F. Observations on papillary muscle dysfunction. *Amer Heart J* 87: 674-675 1974.
- 12 Rajs J. Left ventricular subendocardial haemorrhages. A study of their morphology, pathogenesis and prognosis. *Forensic Sci* 10: 87-103 1977.

AMYLOID-LIKE GREEN BIREFRINGENCE IN CYTOSKELETAL 10 nm FILAMENTS AFTER STAINING WITH CONGO RED

E LINDER¹ V P LEHTO² and I VIRTANEN²

¹Department of Bacteriology and Immunology and ²Department of Pathology University of Helsinki
00290 Helsinki 29 Finland

Linder E, Lehto V P & Virtanen I. Amyloid like green birefringence in cytoskeletal 10 nm filaments after staining with Congo red. *Acta path microbiol scand Sect A* 87 299-306 1979

The commonly accepted markers for amyloid are a fibrillar ultrastructure and congophilia combined with green birefringence when viewed under polarized light. Although a number of cells have been implicated in amyloid formation the detailed events leading to accumulation of amyloid are still unknown. Previous studies have suggested that amyloid shares antigenic properties with cytoskeletal intermediate (10 nm) filaments and connective tissue microfibrils. In the present study we show that such filaments present in fibroblasts and lymphoid cells have an affinity for Congo red, exhibit the typical green birefringence and are ultrastructurally indistinguishable from amyloid fibrils. Intermediate filaments of cultured fibroblasts depleted of nutrient medium retained the Congo red birefringent property and typical ultrastructure despite cell damage. Our observations suggest that amyloid deposits may form locally through abnormal accumulation of bundles of cytoskeletal intermediate filaments under conditions characterized by increased cell proliferation and death.

Key words: Amyloid fibrils, Congo red birefringence, cytoskeletal filaments.

E Linder, Department of Bacteriology and Immunology, Haartmaninkatu 3 SF-00290 Helsinki 29, Finland.

Received 28 ix 78 Accepted 31 i 79

The origin of amyloid deposits in secondary amyloidosis has remained enigmatic despite extensive histological, electronmicroscopical and biochemical studies (5). Two alternative mechanisms have been suggested as leading to amyloid formation: a) local synthesis of a precursor and its subsequent deposition extracellularly; b) extracellular deposition of a circulating amyloid precursor after modification by proteolytic cleavage (11, 29, 2, 1, 33). Morphological studies have implicated that various types of cells, e.g. fibroblasts (32, 30), endothelial cells (6) and reticuloendothelial cells (38, 16) are involved in this process.

The characteristic feature of amyloid is its affinity for Congo red which stains amyloid red and gives green birefringence under polarized light (11, 10). This optical property remains the most useful histological marker for amyloid in tissues (5, 11,

29) although it is also seen in peptide hormones such as insulin and glucagon and some polyaminoacids (11, 10).

Cytoskeletal intermediate filaments (35) and amyloid (7) are birefringent in polarized light. Another feature in common is the ultrastructural appearance and relative insolubility. These similarities appeared even more significant when we observed that serum amyloid A (SAA)-like material is associated with intermediate filaments of cultured fibroblasts (21, 23).

... about intermediate filaments (17). Our results suggest that these filaments may serve as a backbone for amyloid formation in tissues.

MATERIALS AND METHODS

Cells in Tissue Culture

Human embryonal fibroblasts were cultured as described earlier (17). Some of the cultures were grown in the presence of demecolcine (Colcemid, Ciba, Milan, Italy) in a concentration of 0.1 µg/ml for 12 h to produce perinuclear bundles of intermediate filaments. After 2 days of culture the cells were fixed in paraformaldehyde (2.5% in 0.1 M phosphate buffer, pH 7.2) for 20 min followed by -20°C acetone for 10 min. Each batch of demecolcine-treated fibroblasts was examined for formation of bundles of 10 nm filaments. Some of the cultures were depleted of the culture medium after 2 days and were further grown in nutrient-free phosphate buffered saline (PBS) solution which caused extensive cell death in the cultures. Other cultures were extracted with 0.5% Triton X-100 detergent followed by low and high ionic strength actomyosin extraction buffers (34). Homogenates of cultured fibroblasts were prepared using a glass homogenizer. Cells of leukemia cell line K-562 (24) were originally obtained from the Department of Tumor Biology, Karolinska Institutet, Stockholm. These cells, which contain prominent bundles of 10 nm filaments (22) were used in the Congo red staining experiments.

Amyloid Material

The amyloid-laden thyroid from a patient with secondary amyloidosis due to rheumatoid arthritis was removed at autopsy. Crude amyloid fibrils were obtained after extraction of soluble material from the homogenized tissue by repeated washings with 0.1 M NaCl as described by *Pras et al.* (27).

Isolation of Bundles of 10 nm Filaments

Fibroblasts grown in the presence of demecolcine were collected and subjected to extraction of contractile proteins using first 0.5% Triton X-100 followed by low and high ionic strength actomyosin extraction solutions and 1 M KI for 60 min as described by *Small & Sobieszek* (34). The cellular material remaining after the extraction was examined by electron microscopy and analyzed in sodium dodecyl sulphate polyacrylamide gel electrophoresis according to the method of *Laemmli* (18) using 7.5% polyacrylamide gels.

Staining with Congo Red

Puchtler's alkaline (28) and *Pearse's* modified (26) Congo red staining methods were used to stain fibroblasts grown with or without demecolcine, K-562 cells and cryostat sections of an amyloid laden thyroid. Birefringence was studied using a Wild photomicroscope.

Markers for 10 nm Filaments

Intermediate (10 nm) filaments in fibroblasts and lymphoblastoid cells were identified using specific human antibodies in indirect immunofluorescence microscopy as described earlier (17).

Congo Red Binding Test

The method of *Pras et al.* (27) was used to measure the ability of isolated bundles of intermediate filaments to bind Congo red in solution. This test is based on the ability of amyloid to form a stable product with Congo red. This complex can be removed by centrifugation and the binding capacity assayed by measuring the absorbance of the supernatant at 490 nm. Crude thyroid amyloid was used as reference. Washed red cell membranes (9) and cultured, homogenized fibroblasts were used as controls.

Electron Microscopy

The specimens were fixed in 2.5% glutaraldehyde buffered with 0.1 M Na-cacodylate at room temperature for 60 min, and postfixed in 1% osmium tetroxide buffered with 0.1 M phosphate buffer (pH 7.2) for 60 min. After this the specimens were dehydrated and embedded in Epon 812. Thin sections were poststained with uranyl acetate and lead citrate and examined in a Jeol 100 B electron microscope at the Department of Electron Microscopy, University of Helsinki.

RESULTS

Congo Red Birefringent Structures in Cultured Cells

Cultured embryonal fibroblasts often demonstrated Congo red birefringence in cellular extensions.

Fig 1 Human embryonal (HE) fibroblasts in culture show occasionally green birefringence in polarization microscopy after staining with Congo red. Typically the birefringent material was located in long cell extensions. N = Nuclei ($\times 1000$).

Fig 2 HE fibroblast exhibiting long extension similar to the one demonstrating birefringence in *Fig 1*. Indirect immunofluorescence staining using antibodies against intermediate filaments. N = Nucleus ($\times 1000$).

Fig 3 HE fibroblasts treated with demecolcine. A marked increase in cytoplasmic birefringent material compared to *Fig 1* can be seen in polarization microscopy after staining with Congo red. N = Nuclei ($\times 1000$).

Fig 4 HE fibroblasts treated with demecolcine. Thick perinuclear bundles are visible in IFL microscopy after staining with antibodies reacting with intermediate filaments. The location of these bundles is similar to the green birefringent material seen in *Fig 3*. N = Nucleus ($\times 1000$).

Fig 5 K562 leukemia cells demonstrating green birefringence in perinuclear bundles in polarization microscopy after staining with Congo red ($\times 1000$).

Fig 6 Perinuclear bundles in K562 cells can be demonstrated in IFL-microscopy after staining with antibodies against intermediate filaments. Note free bundles of filaments remaining after disruption of some cells ($\times 1000$).

(Fig 1) Intermediate filaments occurred in the same area as shown by IFL (Fig 2) A definite increase in cytoplasmic birefringent material was noted in demecolcine treated cells (Fig 3) This correlated to formation of perinuclear bundles of intermediate filaments which could be demonstrated

by IFL using antibodies against 10 nm filaments (Fig 4)

K562 cells also exhibited Congo red birefringence (Fig 5) They contained bundles of intermediate filaments which could be identified by IFL (Fig 6) and by electron microscopy (Fig 7) Ultrastructu

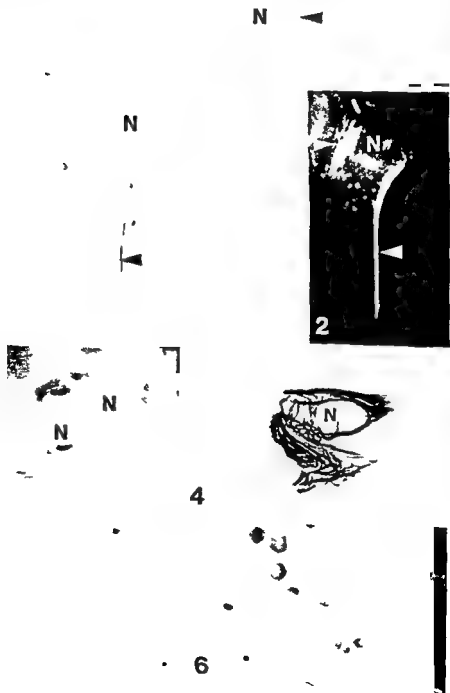




Fig 7 Electron micrograph of a K562 leukemia cell. Perinuclear bundles of filaments with a diameter of approximately 10 nm can be seen (arrows). N = Nucleus ($\times 18000$)

rally the bundles present in K562 cells resembled those seen in colcemid treated fibroblasts (Fig 8)

The birefringent structures were retained in cells subjected to extraction (Fig 9) and in fibroblasts depleted of nutrient medium. The major component of extracted cells appeared to be filaments with an average diameter of 10 nm (Fig 10). This is consistent with the observation that such extracted cells still could be stained by antibodies against intermediate filaments.

Binding of Congo Red by Isolated Bundles of Intermediate Filaments in Solution

The isolated bundles of intermediate filaments were shown in electron microscopy to contain fibrils of 8–10 nm in diameter. There was practically no contaminating material (Fig 11). In polyacrylamide gel electrophoresis a major band of 55 000 MW was seen (Fig 12). The results of the Congo red binding test are presented in Table I. Crude amyloid material added to the Congo red solution produced a definite reduction in the absorbance. The absorbance curve was similar to the one described by *Pras et al* (27). Isolated bundles of intermediate filaments had a higher



Fig 8 Electron micrograph of HE fibroblasts treated with demecolcine. Thick perinuclear bundles consisting of filaments similar to those of K562 cells can be seen (arrows) ($\times 36000$)

capacity to bind Congo red than the crude amyloid preparation. Fibroblasts showed slight binding whereas red blood cell stroma did not bind at all.

Smears prepared of the pelleted amyloid and intermediate filament material displayed green birefringence when examined under polarized light.

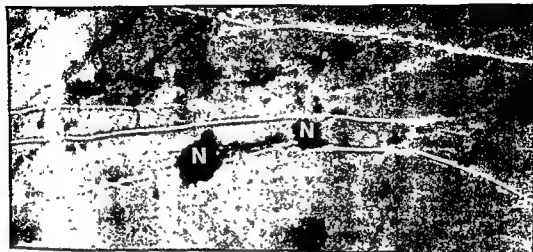


Fig 9 HE fibroblasts solubilized by detergent and actomyosin extraction buffer. Green birefringence can be seen in long cell extensions in polarization microscopy after staining with Congo red. N = Nuclei ($\times 800$)

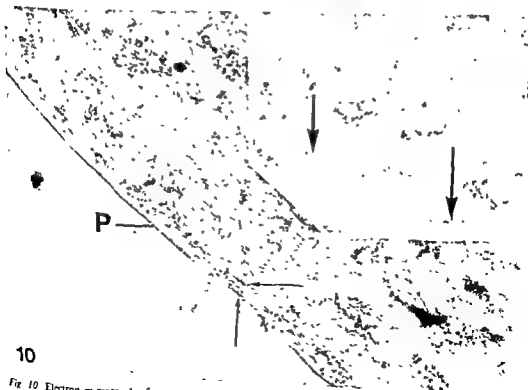


Fig 10 Electron
filaments (arrows)



Fig 7 Electron micrograph of a K562 leukemia cell. Perinuclear bundles of filaments with a diameter of approximately 10 nm can be seen (arrows). N = Nucleus ($\times 18000$)

rally the bundles present in K562 cells resembled those seen in colcemid treated fibroblasts (Fig 8)

The birefringent structures were retained in cells subjected to extraction (Fig 9) and in fibroblasts depleted of nutrient medium. The major component of extracted cells appeared to be filaments with an average diameter of 10 nm (Fig 10). This is consistent with the observation that such extracted cells still could be stained by antibodies against intermediate filaments.

Binding of Congo Red by Isolated Bundles of Intermediate Filaments in Solution

The isolated bundles of intermediate filaments were shown in electron microscopy to contain fibrils of 8–10 nm in diameter. There was practically no contaminating material (Fig 11). In polyacrylamide gel electrophoresis a major band of 55 000 MW was seen (Fig 12). The results of the Congo red binding test are presented in Table I. Crude amyloid material added to the Congo red solution produced a definite reduction in the absorbance. The absorbance curve was similar to the one described by Pras *et al* (27). Isolated bundles of intermediate filaments had a higher



Fig 8 Electron micrograph of HE fibroblasts treated with demecolcine. Thick perinuclear bundles consisting of filaments similar to those of K562 cells can be seen (arrows) ($\times 36000$)

capacity to bind Congo red than the crude amyloid preparation. Fibroblasts showed slight binding whereas red blood cell stroma did not bind at all.

Smears prepared of the pelleted amyloid and intermediate filament material displayed green birefringence when examined under polarized light.

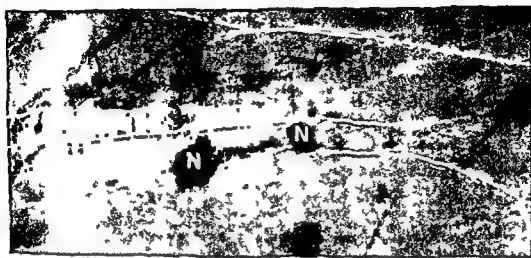


Fig 9 HE fibroblasts solubilized by detergent and actomyosin extraction buffer. Green birefringence can be seen in long cell extensions in polarization microscopy after staining with Congo red. N = Nuclei ($\times 800$)



Fig 10 Electron micrograph of extracted HE fibroblasts show scattered filaments and bundles of intermediate filaments (arrows) P = plasma membrane remnant. No intact cytoplasmic organelles are discernible ($\times 18000$)



Fig 11 Isolated bundles of intermediate filaments Bar indicates 100 nm

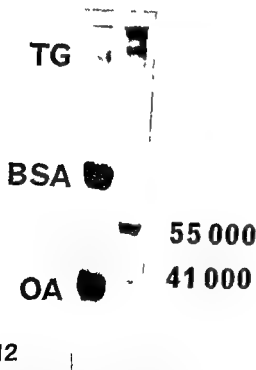


Fig 12 Polyacrylamide gel electrophoresis of isolated bundles of intermediate filaments (right) Major bands MW 41000 and MW 55000 are visible The 55000 MW protein corresponds to desmin (19) the major subunit of intermediate filaments The markers in the standard preparation (left) are from top to bottom thyroglobulin (TG) (MW 105000), bovine serum albumin (BSA) (MW 69000) and ovalbumin (OA) (MW 43000)

TABLE 1 Binding of Congo Red by Test Material

Material added	Absorbance at 490 nm after adding test material	
	1.5 mg	2.5 mg
Isolated bundles of intermediate filaments	0.48	/
Crude amyloid	1.10	0.92
Fibroblasts	2.14	1.66
Red blood cells	2.66	2.56

1.5 mg and 2.5 mg of test material in 1 ml of H₂O were added to 5 ml of 0.15 M NaCl solution containing 10 g/ml Congo red After sonication the solution was incubated at room temperature for 2 h and centrifuged at 1500 g for 15 min The absorbance of the supernatant was measured in a Hitachi Perkin Elmer 124 spectrophotometer using a 1 cm light path The absorbance after adding H₂O only was 2.70
/ = not done

DISCUSSION

In this study we have shown that bundles of intermediate (10 nm) filaments both in cultured fibroblasts and in lymphoid cells display Congo red staining properties and green birefringence which are usually attributed to amyloid material The congophilic material was identified as bundles of intermediate filaments based on IFL microscopy, electron microscopy and biochemical analysis

A number of ultrastructural studies have described a close proximity of amyloid deposits and amyloid like intracellular filaments (15, 31, 3, 25, 8) These intracellular filaments have often been regarded as precursors of the extracellular amyloid deposits but doubts regarding their nature as amyloid precursors have remained especially as amyloid like cytoplasmic fibrils were observed also in cells not directly associated with amyloid deposits (38, 15) The idea of normally occurring intracellular filaments as amyloid precursors is supported by the observations made by Gueft who showed both ultrastructural and biophysical similarities between amyloid and tonofilaments (30, 31) The mechanism whereby cytoplasmic filaments may become deposited extracellularly as amyloid has been discussed by Page & al (25) and recently by David & Buchner (8) These authors suggested that extracellular amyloid in some tumors may arise through spontaneous assembly of cytoplasmic microfibrils of dying tumor cells

An increased knowledge about cytoskeletal intracellular filaments with an average diameter of 10 nm (12) suggested to us that they are similar to amyloid and initiated studies on their conophilic properties. The suggested mechanism for extracellular lar deposition of cytoplasmic filaments is compatible not only with the demonstrated conophilic but also with our knowledge about other physicochemical properties of intermediate filaments. They are resistant to many solubilizing agents and remain intact after disruption of microtubules and microfilaments (34, 19, 20). The insolubility of intermediate filaments may account for extracellular deposition which in the liver seems to occur as hyaline (36). The possibility of extracellular accumulation of intermediate filaments in vivo is also consistent with our present observation that intermediate filaments remain demonstrable in dead cells in cultures depleted of nutrient medium.

The demonstration of Congo red birefringence by intermediate filaments strongly supports the hypothesis that deposition and accumulation of intermediate filaments may result from increased cell proliferation and death. However it is conceivable

dependent upon multiple factors. Deposition may result from break down of defence mechanisms (4) normally capable of eliminating extracellular cytoskeletal material. The extracellular residues of intermediate filaments would constitute a backbone for amyloid deposition which could undergo changes by association with serum proteins such as immunoglobulins, complement and glycoproteins. These changes could account for the typical staining reactions with e.g. thioflavin and toluidine blue (37). Varying localization of amyloid in different types of amyloidosis could reflect both different cellular origin and deposition by various mechanisms.

The skilful technical assistance of Ms Jaana Gluschkoff, Ms Pirko Leikas La'any and Ms Tuire Koro is gratefully acknowledged. Dr Svanne Stenman and Dr Lef Andersson kindly provided cells used in this study. This study was supported by grants from the Sigrid Juselius Foundation, the Finnish Medical Research Council, the Finnish Culture Foundation and the Finnish Lakare sällskapet.

REFERENCES

- Anders R, F. Nørgaard J, B. Michaelsen, T. E. Huxley G. Isolation and characterization of amyloid related serum protein SAA as a low molecular

- weight protein. *Scand J Immunol* 4: 397-401 1975
- Benditt E, P. Eriksen N. Chemical similarity among amyloid substances associated with long standing inflammation. *Lab Invest* 26: 615-625 1972
- Ben Ishay Z, Zlotnick A. The cellular origin of amyloid. Electron microscopic study in a case of amyloidosis. *Isr J Med Sci* 4: 987-994 1968
- Cathari E, S. Mullerky M, Cohen A. S. Amyloidosis. An expression of immunological tolerance? *Lancet* 2: 639-640 1970
- Cohen A. S. Approaches to the study of amyloid and the diagnosis of amyloidosis. Amyloidosis. Proceedings of the fifth Sigrid Juselius Foundation Symposium. Edited by O. Wegelius, A. Pasternack. New York: Academic Press 1976. pp 17-31
- Cohen A. S., Gross E., Skursham T. The light and electron microscopic autoradiographic demonstration of local amyloid formation in spleen explants. *Amer J Path* 47: 1079-1111 1965
- Cooper J. H. "Natural" green birefringence of amyloid. *Am J Clin Path* 66: 1028-1029 1976
- David R., Buchner A. Amyloid stroma in a tubular carcinoma of palatal salivary gland. A histochemical and ultrastructural study. *Cancer* 41: 1836-1844 1978
- Dodge J., Mitchell C., Hanahan D. J. The preparation and chemical characterization of hemoglobin free ghosts of human erythrocytes. *Arch Biochem Biophys* 100: 119-130 1963
- Glenner G. G., Eanes D. E., Bladen H. A., Linke R. P., Termine J. D. β -pleated sheet fibrils: a comparison of native amyloid with synthetic protein fibrils. *J Histochem Cytochem* 22: 1141-1158 1974
- Glenner G. G., Page D. L. Amyloid amyloidosis and amyloidogenesis. *Int. Rev. Exp. Path.* Edited by G. W. Richter and M. A. Epstein. New York: Academic Press 1976. pp 2-93
- Gilbert D. 10 nm filaments. *Nature* 272: 577-578 1978
- Guefi B. The analogy of amyloid and keratin suggested by X ray amino acid and ultrastructural analysis. *Mt. Sinai J. Med* 39: 91-102 1972
- Guefi B. The X ray diffraction pattern of prostatic corpora amyloacea. *Acta Pathol. Microbiol. Scand. A (Suppl. 233)* 80: 132-134 1972
- Hashimoto K. Skin function and amyloidosis. Ultrastructural studies. Proceedings of the fifth Sigrid Juselius Foundation Symposium. Edited by O. Wegelius and A. Pasternack. New York: Academic Press 1976. 515-532
- Heefner W. A., Sorenson G. D. Experimental amyloidosis. I. Light and electron microscopic observations of spleen and lymph nodes. *Lab Invest* 11: 585-593 1962
- Kurki P., Linder E., Virtanen I., Stenman S. Human smooth muscle autoantibodies reacting with intermediate (100 Å) filaments. *Nature* 268: 240-241 1977

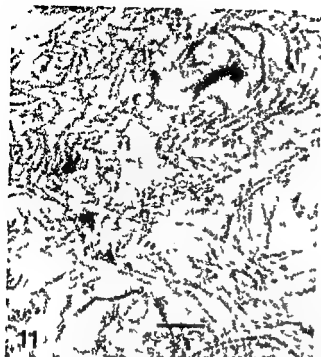


Fig 11 Isolated bundles of intermediate filaments Bar indicates 100 nm

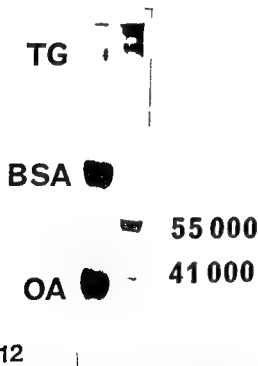


Fig 12 Polyacrylamide gel electrophoresis of isolated bundles of intermediate filaments (right) Major bands MW 41000 and MW 55000 are visible The 55000 MW protein corresponds to desmin (19) the major subunit of intermediate filaments The markers in the standard preparation (left) are from top to bottom thyroglobulin (TG) (MW 105000) bovine serum albumin (BSA) (MW 69000) and ovalbumin (OA) (MW 43000)

TABLE 1 Binding of Congo Red by Test Material

Material added	Absorbance at 490 nm after adding test material	
	1.5 mg	2.5 mg
Isolated bundles of intermediate filaments	0.48	/
Crude amyloid	1.10	0.97
Fibroblasts	2.14	1.66
Red blood cells	2.66	2.56

1.5 mg and 2.5 mg of test material in 1 ml of H₂O were added to 5 ml of 0.15 M NaCl solution containing 10⁻⁴ g/ml Congo red. After sonication the solution was incubated at room temperature for 2 h and centrifuged at 1500 g for 15 min. The absorbance of the supernatant was measured in a Hitachi Perkin Elmer 124 spectrophotometer using a 1 cm light path. The absorbance after adding H₂O only was 2.70.
/ = not done

DISCUSSION

In this study we have shown that bundles of intermediate (10 nm) filaments both in cultured fibroblasts and in lymphoid cells display Congo red staining properties and green birefringence which are usually attributed to amyloid material. The congophilic material was identified as bundles of intermediate filaments based on IFL microscopy, electron microscopy and biochemical analysis.

A number of ultrastructural studies have described a close proximity of amyloid deposits and amyloid-like intracellular filaments (15, 31, 3, 25, 8). These intracellular filaments have often been regarded as precursors of the extracellular amyloid deposits but doubts regarding their nature as amyloid precursors have remained especially as amyloid-like cytoplasmic fibrils were observed also in cells not directly associated with amyloid deposits (38, 15). The idea of normally occurring intracellular filaments as amyloid precursors is supported by the observations made by Gueft who showed both ultrastructural and biophysical similarities between amyloid and tonofilaments (30, 31). The mechanism whereby cytoplasmic filaments may become deposited extracellularly as amyloid has been discussed by Page & al (25) and recently by David & Buchner (8). These authors suggested that extracellular amyloid in some tumors may arise through spontaneous assembly of cytoplasmic microfibrils of dying tumor cells.

LOCAL ARTICULAR AMYLOID DEPOSITION IN PYROPHOSPHATE ARTHRITIS

Histological Aspects

PETER STUBBE TEGLBJÆRG * CHRISTIAN LADEFOGED * K. HARRY SØRENSEN **
and HANS EWALD CHRISTENSEN *

* University Institute of Pathology and ** Orthopedic Department Odense University Hospital

Stubbe Teglbjærg P, Ladefoged C, Sørensen K H & Christensen H F Local articular amyloid deposition in pyrophosphate arthritis. Histological aspects. Acta path microbiol scand Sect A 87 307-311 1979

A material of 15 cases of histologically examined pyrophosphate arthritis (hip joint 7 cases knee joint 8 cases) is presented. Amyloid deposits were found in 14 cases and chondromatosis in the subsynovial connective tissue of all the cases. The significance of this hitherto not previously reported coincidence is discussed together with various pathogenetic possibilities as related to the theories of the genesis of amyloid substance.

Key words: Amyloid deposits, pyrophosphate arthritis.

Hans Ewald Christensen, University Institute of Pathology, Odense University Hospital, DK-5000 Odense, Denmark.

Accepted as submitted 8 II 79

Pyrophosphate arthritis belongs to the crystal associated arthropathies. It occurs in the older age groups and is accompanied by different degenerative or metabolic conditions among these diabetes mellitus (1, 9).

A pathognomonic finding in cases of pyrophosphate arthritis is the presence of characteristic slightly positive polarizing 5 to 15 μ long rhomboid or rod like crystals in the synovial fluid and the subsynovial connective tissue (2, 5).

The present investigation includes 15 cases of pyrophosphate arthritis studied histologically. In 14 of the cases amyloid deposits were also observed in the subsynovial connective tissue.

This combination has not to the best of our knowledge been described earlier.

MATERIAL AND METHODS

The material comprised all the cases studied histologically of pyrophosphate arthritis during the period July 1974 to March 1978 included in the files of the Pathological Institute of the Odense University. A total of 15 cases, five women and ten men. None of the patients had clinical or laboratory signs of hyperparathyroidism.

gout, haemachromatosis, diabetes mellitus, rheumatoid arthritis or generalized amyloidosis.

The tissue histologically examined consisted in seven cases of the synovial membrane and fibrous capsule of the hip joint. In all these cases the tissue had been removed during an alloplastic operation according to the method of Charnley due to arthrosis of the hip joint. In the other eight cases the material consisted of meniscus and synovial membrane from the knee joint. In three of the latter cases the patient had been subjected to meniscectomy due to injury to the meniscus. In the other five cases the patients had been subjected to alloplastic operation of the knee joint. In four cases due to arthrosis and in only one case was the diagnosis pyrophosphate arthritis made prior to operation.

The tissue removed was fixed in 4% neutral buffered formalin for at least thirty hours, dehydrated in ethanol and xylene and embedded in paraffin. Sections of 5 μ in thickness were stained with haematoxylin-eosin (van Gieson's connective tissue stain).

Grading system

The occurrence of pyrophosphate crystals, amyloid deposits and chondromatosis was graded semiquantitatively in the grades: None - 0, slight = +, moderate = ++ and pronounced = +++.

- 18 *Laemmli U K* Cleavage of structural proteins during the assembly of the head of bacteriophage T 4 *Nature* 277 680-685 1970
- 19 *Iazarides E Hubbard B D* Immunological characterization of the subunit of the 100 Å filaments from muscle cells *Proc Nat Acad Sci* 73 4344-4348 1976
- 20 *Lehto I P Virtanen I Kurki P* Intermediate filaments anchor nuclei in nuclear monolayers of cultured human fibroblasts *Nature* 272 175 1978
- 21 *Linder E Anders R F Natvig J B* Connective tissue origin of the amyloid related protein SAA *J Exp Med* 144 1336-1346 1976
- 22 *Linder E Kurki P Andersson L C* Autoantibody to Intermediate Filaments in Infectious mononucleosis *Clin Immunol Immunopathol* in press
- 23 *Linder E Lehto I P Virtanen I Stenman S Natvig J B* Localization of amyloid related serum protein SAA like material to intermediate (10 nm) filaments of cultured human embryonal fibroblasts *J Exp Med* 146 1158-1163 1977
- 24 *Lozzio C B Lozzio B B* Human chronic myelogenous leukemia cell line with positive Philadelphia chromosome *Blood* 45 321 329 1975
- 25 *Page D L Weiss S W Eggleson J C* Ultrastructural study of amyloid material in the calcifying epithelial odontogenic tumor *Cancer* 36 1426-1435 1975
- 26 *Pearse A G E* Histochemistry Theoretical and Applied Vol I Boston Little Brown & C 1968 p 844
- 27 *Pras M Schubert M Zucker Franklin D Rimoin A Franklin F C* The characterization of soluble amyloid prepared in water *J Clin Invest* 47 924-933 1968
- 28 *Puchtler H Sweat F Levine M* On the binding of Congo red by amyloid *J Histochem Cytochem* 10 355-364 1962
- 29 *Rosenthal C J Franklin E C* Amyloidosis and amyloid proteins Recent advances in clinical immunology Edited by H A Thompson New York London Churchill Livingstone 1977 pp 40-76
- 30 *Runne U Ofstanes C E* Amyloid production by dermal fibroblasts Electron microscopic studies of the origin of amyloid in various dermatoses and skin tumours *Brit J Dermatol* 97 155-166 1977
- 31 *Schapiro L Kurban A K Azar H A* Lichen Amyloidosis A histochemical and electron microscopic study *Arch Path* 90 499-508 1970
- 32 *Shiholei S Merker H J Sohar E Gafni J Heller H* Cellular proliferation during the development of amyloid - Electron microscopic observations on the kidneys of Leishmania infected hamster *Brit J Exp Path* 49 244-249 1967
- 33 *Shurahama T Cohen A S* Ultrastructural aspects of the reticuloendothelial cells in amyloidogenesis Amyloidosis Proceedings of the fifth Sigrid Juselius Foundation Symposium Edited by O Wegelius and A Pasternack New York Academic Press 1976 361-369
- 34 *Small J Sobieski A* Studies on the function and composition of the 10 nm (100 Å) filaments of vertebrate smooth muscle *J Cell Sci* 23 243 268 1977
- 35 *Starger J M Goldman R D* Isolation and preliminary characterization of 10 nm filaments from baby hamster kidney (BHK 21) cells *Proc Nat Acad Sci USA* 74 2422-2426 1977
- 36 *Virtanen I Lehto I P Kurki P Meinen A Linder E Stenman S* Intermediate filaments in alcoholic hyaline Virchows Arch B in press 1978
- 37 *Holman M* Amyloid its nature and molecular structure Comparison of a new toluidine blue polarized light method with traditional procedures *Lab Invest* 25 104-110 1971
- 38 *Zucker Franklin D Franklin E C* Intracellular localization of human amyloid by fluorescence and electron microscopy *Amer J Path* 59 23-41 1970



Fig 1

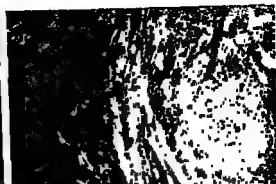


Fig 2

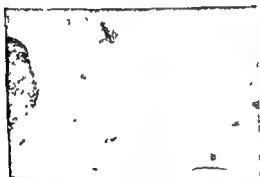


Fig 3



Fig 4

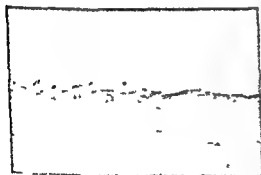


Fig 5



Fig 6

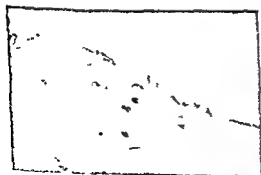


Fig 7



Fig 8

TABLE 1 *Interrelationship between Pyrophosphate Crystal Deposition Amyloid Content and Degree of Chondromatosis*

Case	Sex	Age	Joint	Tissue	Pyrophosphate	Amyloid	Chondromatosis
1	m	63	knee knee	meniscus synovium	+++ +	+ +	+ ++
2	m	46	knee knee	meniscus synovium	+++ +++	+ +	+++ ++
3	m	65	knee	synovium	++	++	+
4	m	71	hip	synovium	++	++	+++
5	f	68	knee	synovium	+++	+	+
6	f	49	hip	synovium	++	0	++
7	m	72	hip	synovium	++	++	++
8	m	39	knee	meniscus	+++	+	+
9	f	46	hip	synovium	++	+++	++
10	m	60	hip	synovium	++	+++	++
11	m	57	knee	meniscus	+++	+++	++
12	m	71	hip	synovium	+++	+++	+++
13	f	61	knee knee	meniscus synovium	++ ++	+++ +++	+++ +++
14	m	75	hip	synovium	+++	+++	+++
15	f	57	knee knee	meniscus synovium	++ +++	+ +	+ +

0 = no, +, ++ and +++ = mild moderate and severe degree of change respectively m = male, f = female.

Fig 1 Deposits of pyrophosphate crystals in the subsynovial connective tissue (Haematoxylin-eosin, $\times 40$)

Fig 2 The same area as in Fig 1 using polarized light (Haematoxylin-eosin, $\times 40$)

Fig 3 Amyloid deposits in the subsynovial connective tissue (Alkaline Congo red, $\times 250$)

Fig 4 The same area as in Fig 3 showing green dichroism using polarized light (Alkaline Congo red $\times 250$)

Fig 5 Ribbon like amyloid deposits just below the synovial cell layer (Alkaline Congo red, $\times 100$)

Fig 6 The same area as in Fig 5 showing green dichroism using polarized light (Alkaline Congo red $\times 100$)

Fig 7 Corona-like amyloid deposits around the chondrocyte-like cells in an area of chondromatosis (Alkaline Congo red $\times 400$)

Fig 8 The same area as in Fig 7 showing green dichroism of the amyloid corona, using polarized light (Alkaline Congo red, $\times 400$)

- 8 *Fuchster H Sweet F & Levine M* On the binding of Congo red by amyloid *J Histochem cytochem* 10 355-364 1962
- 9 *Skinner M & Cohen A S* Calcium pyrophosphate dihydrate crystal deposition disease *Arch Intern Med* 123 636-644 1969
- 10 *Tellum G* Pathogenesis of amyloidosis The two phase cellular theory of local secretion *Acta path microbiol scand* 61 21-45 1964
- 11 *Tellum G* Origin of amyloidosis from PAS positive reticulo-endothelial cells *in situ* and basic factors in pathogenesis In *Mandema E Ruinen L Scholten J H & Cohen A S* (eds) *Amyloidosis* Excerpta Medica Amsterdam 1968 p 37-44

RESULTS

The age and sex of the patients as well as the affected joint are shown in Table 1. In all fifteen cases typical calcium pyrophosphate crystals were observed in the subsynovial connective tissue and/or in the meniscus of the knee. Microscopy using polarized light permitted identification of these as massive deposits of rhomboid shaped or rod like 5 to 15 μ long slightly polarizing crystals (Fig 1 and 2). In one case a reaction to the crystal deposits was observed in the connective tissue in the form of macrophages and multi nuclear foreign body giant cells containing phagocytosed crystals in the cytoplasm. In the remaining cases the crystals were deposited in an inert hyalinized collagen connective tissue which stained red with the van Gieson method. Larger or smaller slightly basophilic areas staining a reddish colour with alkaline Congo red were seen scattered here and there in the hyalinized collagen connective tissue. These areas showed using microscopy with polarized light green dichroism characteristic of amyloid (4) (Fig 3 and 4).

The synovial cell layer above the areas with calcium pyrophosphate deposits was the site of pronounced atrophy with hyalinization of the underlying connective tissue. In these areas the amyloid deposits were often seen as a distinct ribband running parallel to the basal membrane and just below this (Fig 5 and 6).

In all cases chondromatosis was observed in the subsynovial tissue (Table 1) this consisted of a weakly basophilic alcianophilic ground substance in which small round cells with light cytoplasm could be seen these were chondrocyte like and appeared in lagunes. Often deposits of amyloid could be seen in the immediate vicinity or in some instances as a small corona around them (Fig 7 and 8).

DISCUSSION

The present investigation shows a significantly frequent occurrence of amyloid deposits in the subsynovial connective tissue in patients suffering from pyrophosphate arthritis requiring operation inasmuch as fourteen of the fifteen cases demonstrated this pathological finding. This would suggest a pathogenetic relationship.

It is thus possible that the primary deposition of

more prolonged course of the condition in human beings than in experimental animals.

Another possibility is that the high frequency of chondromatosis in our material may be of pathogenetic importance. Recent studies in our laboratory (6) have demonstrated that cartilage from the hip joint in an unselected autopsy material can be the site of local amyloid degeneration and that chondrocytes may comprise one of the sources of amyloid precipitation.

Finally the possibility cannot be excluded that the deposition of pyrophosphate crystals and amyloid are two independent processes running in parallel course.

We have earlier reported a material (3) consisting of forty three patients operated on for arthrosis of the hip joint according to the method of Charnley in which we found amyloid deposits in the joint capsule in sixteen cases. This is however a significantly lower frequency than in the present material ($P < 0.002$ Fisher's exact test).

It is in addition well known that amyloid deposits can be present in the articular tissue of patients suffering from generalized amyloidosis (7). However generalized amyloidosis was not demonstrated in any of the patients in the present material.

Finally it should be noted that the diagnosis of pyrophosphate arthritis was only made preoperatively in one case and therefore it would appear advisable to carry out routine microscopy of all tissue removed from the joints or their immediate surroundings irrespective of the clinical diagnosis.

REFERENCES

1. Bjelle A E & Sundén G. Pyrophosphate synovitis. *Acta Orthop Scand* 47: 131-141 1971.
2. Bjelle A E & Sundén G. Pyrophosphate Arthropathy. A clinical study of fifty cases. *J Bone Jt Surg* 56 B: 246-255 1974.
3. Christensen H E & Sørensen A H. Local amyloid formation of capsula fibrosa in arthrosis coxae. *Acta path microbiol Scand Sect A* 80 suppl 233: 128-131 1972.
4. Cohen A S. In: Laboratory diagnostic methods in the rheumatic diseases. Little Brown and Co. Boston 1975. p. 295-412.
5. Gatter R A. The use of the compensated polarizing microscope. Crystal induced arthropathies. In: *Arthritis* B A (ed.) Clinics in rheumatic disease vol 3 No 1. W B Saunders Company Ltd London 1977. p. 91-103.
6. Ladefoged C & Christensen H E. Amyloid deposition in hip joints in autopsy material. In preparation.
7. Pirani C L. Tissue distribution of amyloid. In: *Wegelius O & Pasternack A (eds) Amyloidosis*. Academic Press London 1976. p. 33-49.

Whether or not this amyloid production is in accordance with the biphasic scheme as described by Teilmann (10, 11) is not quite clear. The fact that we have not found the active cellular elements described in Teilmann's hypothesis may be due to the

GLOMERULAR IMMUNE DEPOSITS IN KIDNEYS FROM PATIENTS WITH NO CLINICAL OR LIGHT MICROSCOPIC EVIDENCE OF GLOMERULONEPHRITIS

Assessment of the Influence of Autolysis on Identification of Immunoglobulins and Complement

SVEND LARSEN

Clinical Chemistry Department, Kommunehospitalet Copenhagen and Institute of Pathology Herlev Hospital University of Copenhagen

Larsen S Glomerular immune deposits in kidneys from patients with no clinical or light microscopic evidence of glomerulonephritis. Assessment of the influence of autolysis on identification of immunoglobulins and complement. *Acta path microbiol scand Sect A* 87 313-319 1979

Using a direct fluorescent staining technique immunofluorescent microscopy (IFM) demonstrated glomerular deposits of IgG and IgM and/or fractions of complement in kidney tissue from 24% of 33 patients examined post mortem and in 39% of kidney biopsies obtained from 23 patients on lithium treatment. All the patients investigated had a normal blood pressure. There was no evidence of glomerulonephritis (GN) neither clinically at light microscopy nor on laboratory investigation. These spontaneously deposited immunoglobulins and complement fractions in glomeruli will obviously be demonstrated in kidney biopsies from patients with GN even though they bear no relation to the disease. This will therefore preclude an immunopathological classification which relates to histological and clinical findings. A control study of the IFM findings in glomeruli on 13 surgically removed kidneys showed optimal identification and no further glomerular deposition of immunoglobulins during the 72 hours following nephrectomy at temperatures below 10° C. C_{1q} and C₃ were less stable and were only demonstrated with certainty up to 24 hours after nephrectomy.

Key words: Immunofluorescent microscopy, kidney disease, normal glomeruli.

S. Larsen, Department of Clinical Chemistry, Kommunehospitalet, Øster Farimagsgade 5, DK 1399 Copenhagen K, Denmark.

Received 14 II 79 Accepted 23 II 79

More than 85% of human glomerulonephritis (GN) is caused by immune mechanisms (Wilson & Dixon 1974). These are to some degree analogues to those in immunological experimental GN (McCluskey *et al* 1960; Sieblav 1962) where GN is induced either by glomerular deposition of nephritogenic immune complexes (antigen antibody complex) or by antibody directed against the glomerular basement membrane.

The appearance of the deposits and composition of different immunoglobulin classes and complement fractions in human GN have shown no

specific relation to either the glomerular lesions or the clinical picture and in only a few cases has the antigen been demonstrated with certainty in deposited immune complexes (Koffler *et al* 1967; Kaufman & McIntosh 1971).

Unknown antigens of various types could therefore be one reason for the lack of correlation between immunopathological findings and the histological and clinical picture. Another possibility is that deposited immunoreactants in glomeruli are not specific for the disease 'glomerulonephritis'. The widespread use of immunofluorescent microscopy (IFM) on kidney biopsies in human kidney

TABLE 1 IFM Findings on 13 Surgically Removed Kidneys Deposits of Immunoglobulins and Complement in Glomeruli

Immunofluorescent study						5° C					10° C					Comments	
IgG cm	IgM cm	IgA cm	C ₃ cm	C ₅ cm	Days after nephrectomy	IgG cm	IgM cm	IgA cm	C ₃ cm	C ₅ cm	IgG cm	IgM cm	IgA cm	C ₃ cm	C ₅ cm		
+	+	+	+	+	1	+	+	+	+	+	+	+	+	+	+	Carcinoma of the kidney	
					2	+	+	+	+	+	+	+	+	+	+		
					3	+	+	+	+	+	+	+	+	+	+		
+	+	+	+	+	1	+	+	+	+	+	+	+	+	+	+	Carcinoma of the kidney	
					2	+	+	+	+	+	+	+	+	+	+		
					3	+	+	+	+	+	+	+	+	+	+		
+	+	+	+	+	1	+	+	+	+	+	+	+	+	+	+	Carcinoma of the kidney	
					2	+	+	+	+	+	+	+	+	+	+		
					3	+	+	+	+	+	+	+	+	+	+		
					1											Carcinoma of the kidney	
					2												
					3												
					1											Renal stones (Diabetes Mellitus)	
					2												
					3												
+	+	+	+	+	1	+	+	+	+	+	+	+	+	+	+	Reno-vascular hypertension (Renal artery stenosis)	
					2	+	+	+	+	+	+	+	+	+	+		+
					3	+	+	+	+	+	+	+	+	+	+		+
+	+	+	+	+	1	+	+	+	+	+	+	+	+	+	+	Calcification of the kidney	
					2	+	+	+	+	+	+	+	+	+	+		+
					3	+	+	+	+	+	+	+	+	+	+		+

9	Negative	Negative	Negative
---	----------	----------	----------

Negative

Negative

Negative

IFM - Immunofluorescent microscopy
c = Within/along the capillary basement membrane
m - Mesangium

membrane in the capillary loops Results of the IFM findings are listed in Table 1 and show

- 1) Immunoglobulins or complement fractions were demonstrated in 5 of the 13 kidneys (38%) but in only 3 of the kidneys were immunoglobulin and complement both demonstrated together in glomeruli
- 2) Kidneys with no glomerular deposits were from patients with the same disorders as patients where glomerular deposits were demonstrated
- 3) IgG IgM and IgA can be demonstrated for at least 72 hours at 10° C
- 4) No subsequent deposition of immunoglobulin or complement occurred during the postoperative period of 72 hours
- 5) C₃ and C_{1q} were less constantly preserved in the glomeruli and could be demonstrated with certainty for 24 hours when tissue was stored at a temperature lower than 10° C

RESULTS

Twenty three biopsies were from lithium treated patients whose ages ranged from 25-71 yr (mean 48 yr) There were 15 women and 8 men

LM examination showed no evidence of GN

IFM showed no glomerular deposits in 14 cases Glomerular deposits were demonstrated in 9 patients (39%) Table 2, where immunoglobulins were found in 8 instances and complement fractions in 8 Deposits with a granular pattern were

capillary loops (IgM) The average number of glomeruli examined by IFM was 5 (range 2-11) The distribution of deposits were almost generalised

disease has demonstrated that glomerular deposits of immunoglobulin can be demonstrated not only in GN but also in kidney disease of non immunological origin \equiv cystinosis (Berger *et al* 1971), bilateral cortical necrosis (Mahieu *et al* 1972) and diabetic nephrosclerosis (Hjman *et al* 1973, Thomson 1972) Furthermore glomerular bound C_3 has been demonstrated in small amounts in 35% of normal living kidney donors (Velsa *et al* 1976) Deposits of immunoglobulins and complement have also been demonstrated in glomeruli of patients with cancer of non renal origin (Pascal *et al* 1976, Sutherland *et al* 1974 a) where there was no demonstrable clinical or histological evidence of GN It is therefore possible that these »spontaneous« deposits in glomerular capillaries and mesangium result from clearance of circulating non nephritogenic immune complexes, analogous to mechanisms which occur in the reticulo-endothelial system

Investigation of the incidence of glomerular deposits of immunoglobulin and complement in a normal population is of course impossible IFM studies were therefore performed on kidney tissue obtained from patients with normal blood pressure (BP) and with no clinical or histological evidence of GN

Renal biopsies from lithium treated patients and kidney tissue obtained at autopsy were used as a reference material of normal glomeruli The biopsies from patients on lithium treatment were included in a running investigation of this specific problem and no clues indicated that these patients had glomerular disease As part of the study was performed on autopsy material a control was set up to examine the influence of autolysis on the identification of deposited immunoglobulin and complement by IFM in relation to time and temperature in the »agonal« period

MATERIAL AND METHODS

Selection

Kidney tissue from two different sources was investigated

- 1) Renal biopsy specimens from 43 lithium treated patients (Rigshospitalet, Copenhagen 1977-1978)
- 2) Kidney tissue obtained 9-48 hours post mortem from 100 consecutive autopsies (Kommunehospitalet Copenhagen 1976)

Patients included in this study were required to have a normal blood pressure (BP) and no clinical or light microscopic (LM) evidence of glomerulonephritis One of the following clinical observations constituted grounds for rejection

A history of previous renal disease

Haematuria > 2 erythrocytes/high power field
Proteinuria > 0.5 g/day or in some cases from the autopsy material where lab sticks (Redia Test[®] Boehringer) were positive for more than a trace (+)
Reduced kidney function serum creatinine concentration > 1.5 mg% or creatinine clearance < 1 ml/sec
Elevated BP ≥ 100 Hg diastolic

Biopsies or autopsy specimens examined by LM had to include at least 10 glomeruli whilst for IFM at least 2 were required

Fifty six cases fulfilled the above conditions for inclusion in the study 23 were biopsies and 33 were autopsy specimens

Methods

Immediately after the kidney specimen was obtained it was divided and prepared for IFM and LM examination

Immunofluorescent Microscopy

Kidney specimens were frozen using dry ice embedded in Tissue Tek[®] gelatine (Ames Laboratory) and sections of $1 \mu\text{m}$ were cut at -24°C on a Leitz Histo-crytome[®] Throughout the investigation all kidney sections were examined by a direct immunofluorescent staining technique using FITC-conjugated rabbit or goat antisera specifically reactive to human IgG IgM IgA as well as complement C_{1q} C_3 C_4 in dilutions (end point) 1:20 to 1:40 Details of the procedure and controls have been previously described (Larsen 1978a)

A Zeiss universal fluorescent microscope with transmitted light and Dark Field Ultracondenser $\times 4$ 1.2/1.4 and objective 0.75 to 1.0 N.A. $\times 40$ Oil with

Light Microscopy

The tissue was fixed in 4% formaldehyde buffered to pH 7.0 (Lillies fluid) embedded in Paraplast[®] cut into 4 \times 3 and 2 μm sections and stained with H & E PAS + H picric acid + sirius red Masson's trichrome and silver methenamine (Jones 1951) + H & E

Investigation of the influence of autolysis on the IFM findings of deposited immunoglobulins and complement fractions in human kidneys during an artificial post mortem (agonal) period

IFM studies were performed on consecutive nephrectomy specimens from February to August 1978 These were from 13 patients 8 with renal carcinoma 2 with renal stones 2 with renal artery stenosis and renovascular hypertension and one patient with renal infarcts

Biopsies for IFM and LM were obtained immediately after nephrectomy The kidney (minus tumour) was divided into two parts and kept in plastic bags at 5°C and 10°C respectively

Every day for 3 days tissue including at least 1 glomeruli was removed and examined by IFM

LM examination of the kidneys showed no evidence of GN

The deposits demonstrated by IFM were granular and localised in the mesangium or along the basement

normal horses (Banks & Henderson 1972) and normal laboratory mice (Markham *et al* 1973). In a high percent of these animals immunoglobulin deposits can be demonstrated without any evidence of GN.

In the material presented here glomerular deposits of IgG, IgM and complement fractions were found in 33% of 56 patients showing no evidence of GN, hypertension or impaired kidney function. No deposits of IgA were demonstrated. Sutherland *et al* (1947b) reported similar findings of deposited immunoglobulins and C₃ in glomeruli and small amounts of C₃ were described by Velosa *et al* (1976) in glomeruli of approximately 35% of normal kidneys from living donors. Non specifically bound IgG was also demonstrated by Hesenberg & Tonder (1978) in eluted from normal kidneys of elderly patients.

It is therefore quite possible that the deposits demonstrated in the material presented here represent the frequency and quality of glomerular deposits which can be expected to occur in a «normal» population. 23 of the patients were on lithium treatment but as immunoglobulin and/or complement were demonstrated only in 1/3 of these it is hardly likely that the deposits represent immune complexes with lithium ion as an antigenic determinant. On the other hand it is well known that lithium ion is excreted in uncombined form via the kidneys (Steele *et al* 1975) and Hestbeck *et al* (1977) have shown that long term treatment with lithium can result in chronic kidney lesions with focal interstitial fibrosis and tubular atrophy. In this latter study the number of sclerotic glomeruli was found to be 4 times greater than in control material but there was no evidence of an immunological mechanism being involved in their pathogenesis. The increased numbers of sclerotic glomeruli in the kidney tissue of patients on long term treatment with lithium salts may indicate that the lithium ion can induce functional changes in glomerular structures. It is therefore possible that any glomerular clearance of circulating non nephritogenic immune complexes is altered so that the frequency with which demonstrable deposits of immunoglobulin and complement occur in glomeruli will differ in patients undergoing lithium treatment from those not on such therapy.

Glomerular deposits of IgG, IgM and C₃ were found in 24% of 33 kidneys obtained at autopsy from patients with no clinical or light microscopic evidence of GN. The same disease processes were present in patients with and without these deposits so that the underlying disease in these instances cannot be immediately accepted as the cause of the glomerular deposits. Identical findings were repor-

ted by Sutherland *et al* (1974b) who found glomerular deposits of immunoglobulin in 25%, and C₃ in 11% of autopsy kidneys from 33 patients with no evidence of tumour or GN.

As a part of the IFM studies were carried out on autopsy material it was possible that autolysis might have been responsible for both «false positive» and «false negative» results.

A) «False negative» results could have been caused by lack of binding of the antisera used to glomerular structures or to globulin deposits which had been altered by proteolytic enzyme action.

B) «False positive» results could have been caused by non specific binding to devitalised tissue (membranes) or immune reactants which had sedimented from the blood in the period following death.

Immunofluorescent microscopic studies on nephrectomy specimens, used as controls for the autopsy material showed

with regard to A) that immunoglobulins demonstrated in glomeruli immediately after nephrectomy were demonstrable throughout the whole 72 hours of the investigation, but that in contrast C_{1q} and C₃ were only demonstrated with certainty during the first 24 hours.

With regard to B) that (in the «agonal» period) up to 72 hours after nephrectomy no subsequent deposits of other immune reactants were seen other than those demonstrated immediately after nephrectomy.

This means that the immunoglobulin deposits demonstrated in the autopsy material must be accepted as genuine for autopsies in every instance were performed within 48 hours thus excluding the possibility of both «false positive» and «false negative» demonstration of IgG, IgM and IgA. This is in keeping with other immunological studies which have similarly shown that autolysis has no influence on deposited immunoglobulins in the kidneys of rats up to 72 hours post mortem (Seelig *et al* 1975).

In the nephrectomy controls complement fractions C_{1q} and C₃ were in contrast unstable for these deposits were only demonstrated with certainty in the first 24 hours. It must therefore be assumed that sometimes complement is altered or destroyed by autolytic processes within 24 hours post mortem.

As in more than half of the cases autopsy was performed between 24 and 48 hours after death «false negative» results for complement C_{1q} and C₃ cannot be excluded. This may explain the difference in the frequency of deposited C_{1q} and C₃ demonstrated in kidney tissue from lithium patients compared with the autopsy kidneys.

The frequency of demonstrable immune reactants

TABLE 2 Patients on Treatment with Lithium Deposits in 9 Pts with no Evidence of Glomerulonephritis

Code no	Glomerulus			
	IgG	IgM	C ₃	C ₄
3360		+	+	
3444			(+ +)	
3484	(+)			+
3531		+		
3536		+		
3587		+		
3602	(+)		(+)	
3623		+	+	
3638	(+ +)	+		

Intensity of fluorescence = 0 (+) + (+ +) + +

as deposits were found in more than 80% of the glomeruli

Thirty three kidney specimens were obtained from 33 patients at autopsy. The age ranged from 51-87 yr (mean 67.7 yr). Autopsy was performed within at least 48 hours of death.

LM examination showed no evidence of GN.

IFM examination showed no glomerular deposits in 25 cases (9 cancers of non renal origin, 5 cerebral thromboses/haemorrhages, 6 myocardial infarctions, 3 bronchopneumonias, 1 pancreatitis, 1 severe burns). Glomerular deposits were found in 8 patients (24%). Table 3 where immunoglobulins were found in 7 instances and C₄ in 7. In 3 cases the deposits were granular and localised to both the mesangium and the basement membranes of the capillary loops (cases 25, 28 and 43). In 5 others the deposits had a granular or interrupted linear pattern

and were localised subendothelially to the basement membranes of the capillary loops.

The average number of glomeruli examined by IFM was 11 (range 7-21). Distribution was almost generalised as deposits were found in 86% of the glomeruli in these specimens.

DISCUSSION

There have been numerous reports on immunofluorescent microscopic (IFM) findings of deposited immunoglobulin and complement in glomeruli of kidney biopsies from patients with glomerulonephritis (GN). These show that immune mechanisms analogous to those in experimental immunological induced GN (McCluskey *et al* 1960, Steblay 1962) can be a pathogenetic factor in human GN. The demonstration of granular deposits of immunoglobulin and complement in glomeruli of patients with GN is therefore widely accepted as evidence for immune complexes being involved in the pathogenesis of this disorder. However in human GN deposited combinations of different classes of immunoglobulin and complement fractions show only slight correlation with the glomerular lesions and the clinical symptoms and course of the disease (Larsen 1978a, Larsen 1978b, Cameron 1975). One of the reasons for this can be that circulating immune complexes, immune reactants or immune aggregates present in the blood stream following everyday contact with infection are filtered and phagocytosed in the glomerular filter system which may therefore have a function similar to that of the remainder of the reticulo-endothelial system. A phagocytic function has been demonstrated in the mesangium in humans (Vernier *et al* 1971) and similar glomerular filter functions are found in both

TABLE 3 Deposits in 8 Pts with No Evidence of Glomerulonephritis (Post Mortem)

Case no	Glomerulus			Comments
	IgG	IgM	C ₄	
9		+	(+)	Myocardial infarction
56			(+)	Cerebral haemorrhage
18	+		+	Malignant neoplasm of testis
20	+		+	Carcinoma of the oesophagus
28	+		+	Cirrhosis of the liver (alcoholic)
43	+	+	+	Cirrhosis of the liver (alcoholic)
25	+		+	Chronic bronchitis
60	(+)		+	Bronchopneumonia

Intensity of fluorescence = 0 (+) + (+ +) + +

- 15 Rygaard J & Olsen W Towards quantitation of excitation *Ann N Y Acad Sci* 177 410-413 1971
- 16 Seelig H P Seelig R & Drescher M Der Einfluss der Autolyse auf die immunohistologische Darstellbarkeit gewebgebundener Immunglobuline in der Niere *Virchows Arch A Path Anat and Histo* 365 151-161 1975
- 17 Sieblay R W Glomerulonephritis induced in sheep by injection of heterologous glomerular basement membrane and Freund's complete adjuvant *J exp Med* 116 253 1962
- 18 Steele T H Marvel M A Newton M & Boner G Renal lithium reabsorption in man: physiologic and pharmacologic determinants *Am J Med Sci* 269 349-363 1975
- 19 Sutherland J C Markham R V Jr Ramsey H E & Mardiney M R Jr Subclinical Immune Complex Nephritis in Patients with Hodgkins Disease *Cancer Res* 34 1179-1181 1974a
- 20 Sutherland J C Markham R V Jr Mardiney M R Jr Subclinical Immune Complexes in the Glomeruli of Kidneys Postmortem *Am J Med* 57 536-541 1974b
- 21 Thomsen O F Studies of Diabetic Glomerulosclerosis Using an Immunofluorescent Technique *Acta path microbiol Scand Sect A* 80 193-200 1972
- 22 Velosa J Miller K & Michael A F Immunopathology of the End Stage Kidney *Am J Path* 84 149-160 1976
- 23 Vermer R L Mauer S M Fish A J & Michael A F The Mesangial Cell in Glomerulonephritis *Advan Nephrol* 1 31-46 1971
- 24 Wesenberg F & Tonder O Evidence for non specifically bound IgG in human tumours *Acta path microbiol scand Sect C* 86 251-258 1978
- 25 Wilson C B & Dixon F J Immunopathology and Glomerulonephritis *Ann Rev Med* 25 85-98 1974

in autopsy material must therefore be accepted as representing a minimum. It is possible that the immune reactants found deposited in glomeruli of patients treated with lithium reflects that frequency with which deposition of IgG, IgM, C_{1q} and C₃ can be demonstrated in normal individuals.

As C₄ is only demonstrable in autopsy kidneys this suggests that this complement fraction represents a »false positive result«, C₄ in contrast to IgG, IgM, C_{1q} and C₃ was neither demonstrated in lithium treated patients nor in the nephrectomy controls. Thus when kidneys remain in situ after death, complement fraction C₄ must presumably sediment out or, alternatively, anti human C₄ must bind non specifically to glomerular structures in autolysed or devitalised tissue. This is not an altogether unknown occurrence for C₄ is often demonstrated in ordinary routine studies on autopsy material (unpublished results).

The frequency with which deposits of IgG, IgM, C_{1q} and C₃ were demonstrated in the present study may thus be considered to approach the frequency of glomerular deposits which appear in a normal population. These deposits possibly occur as a result of glomerular clearance of circulating non nephritogenic immune complexes occurring in an organism as a result of everyday infections. If such spontaneously deposited immune complexes are a relatively normal occurrence, then in some cases of human GN these deposits will obviously be demonstrated by IFM techniques even though they bear no relation to the disease. This will therefore preclude an immunopathological classification of GN which correlates with the histological and clinical findings.

The established finding of glomerular deposits of immune reactants in about 1/3 of the patients in the study presented here who may be presumed to be comparable to a normal population suggests that the frequency of primary human GN caused by immunopathogenetic mechanisms may be considerably lower than 85% as reported by Wilson & Dixon (1974). This, however, does not exclude the possibility that the presence of glomerular deposits of both immunoglobulin and complement may have some influence, at a purely secondary level, on both the clinical symptoms and course of the disease and perhaps in some instances that deposits may be responsible for the changes in glomeruli which lead to sclerosis.

REFERENCES

I acknowledge financial support from the Danish Medical Research Council.
 Christian X
 Berg
 ul technical

- 1 Banks K L & Henderson J B Immunologically Mediated Glomerulitis of Horses II Antiglomerular Basement Membrane Antibody and Other Mechanisms in Spontaneous Disease. *Lab Invest* 26 708-715 1972
- 2 Berger J Yaneva H & Hindglas N Immunohistochemistry of Glomerulonephritis. *Advan Nephrol* 1 11-30 1971
- 3 Cameron J S Clinicopathological Correlates in Glomerulonephritis. Problems and Limitations. *Clin Nephrol* 4 1-7 1975
- 4 Hyman L R, Wagnhild J P, Byrne G J & Burkholder P M Immunoglobulin A distribution in glomerular disease. Analysis of immunofluorescent localization and pathogenetic significance. *Kidney International* 3 397-408 1973
- 5 Jones D B Amer J Path 27 991-1009 1951
- 6 Hestbech J, Hansen H E, Amdisen A & Olsen S Chronic renal lesions following long term treatment with lithium. *Kidney International* 12 205-213 1977
- 7 Kaufman D B & McIntosh R The pathogenesis of the renal lesion in a patient with streptococcal disease infected ventriculo atrial shunt cryoglobulinemia and nephritis. *Am J Med* 50 262-268 1971
- 8 Koffler D, Schur P H & Kunkel H G Immunological studies concerning the nephritis of systemic lupus erythematosus. *J exp Med* 126 607-624 1967
- 9 Larsen S Immunofluorescent microscopy findings in normal glomeruli: minimal lesion and slight generalised mesangioproliferative glomerulonephritis. *Acta path microbiol Scand Sect A* 86 531-542 1978a
- 10 Larsen S Immune deposits in generalised mesangioproliferative glomerulonephritis. Fluorescent microscopy findings correlated in symptoms, clinical course and immunosuppressive therapy. *Acta path microbiol scand Sect A* 86 543-552 1978b
- 11 Mahieu P, Dardenne M & Bach J F Detection of humoral and cell mediated immunity to kidney basement membranes in human renal diseases. *Am J Med* 53 185-192
- 12 Markham R V Jr, Sutherland J C & Mardiney M R Jr The ubiquitous occurrence of immune complex localization in the renal glomeruli of normal mice. *Lab Invest* 29 no 1 111-120 1973
- 13 McCluskey R T, Benacerraf B, Potter J L & Miller F The pathologic effects of intravenously administered soluble antigen antibody complexes. *J exp Med* 111 181-194 1960
- 14 Pascal R R, Iannaccone P M, Rollwagen F M, Harding T A & Bennett S J Electron microscopy and immunofluorescence of glomerular immune complex deposits in cancer patients. *Cancer Res* 36 43-47 1976

IMMUNE DEPOSITS IN HUMAN GLOMERULOPATHY

Fluorescent Microscopy Findings in 366 Kidney Biopsies Correlated to Symptoms Clinical Course and Immunosuppressive Therapy

SVEND LARSEN and CLAUD BRUN

Department of Clinical Chemistry Kommunehospitalet Copenhagen Denmark

Larsen, Svend & Brun, Claus. Immune deposits in human glomerulopathy. Fluorescent microscopy findings in 366 kidney biopsies correlated to symptoms clinical course and immunosuppressive therapy. *Acta path microbiol scand Sect A* 87 321-333 1979

Findings at the time of examination. The IFM findings in the glomeruli were correlated to (1) the LM diagnosis (2) the clinical symptoms (3) the clinical course and (4) the effect of immunosuppressive treatment. A few IFM results were found to correlate significantly with the LM diagnosis and clinical symptoms but not to the effect of immunosuppressive treatment. It was impossible using IFM alone to group patients into any specific categories with uniform symptomatology and prognosis. Defined by IFM immune deposits were found in the patients with SLE (60% glomerulonephritic nephropathy). Demonstration of IgA is therefore a good indicator for corroborating the LM diagnoses of GN. Demonstration of IgG and/or IgM in GN was not found to be sufficient evidence for GN because these deposits also appeared in 40% of patients with non glomerulonephritic nephropathy. An immunopathological classification based solely on glomerular deposits of immunoglobulin/C₃ appears to have no practical importance. The demonstration of glomerular deposits of immunoglobulin/C₃ however showed to be a necessary supplement to clinical and morphological findings in some instances in order to attain practical diagnostic boundaries within the very ill-defined concept which today constitutes GN.

Key words: Immunofluorescent microscopy kidney disease glomerulonephritis

S. Larsen, Department of Clinical Chemistry Kommunehospitalet Øster Farimagsgade 5 DK-1399 Copenhagen K, Denmark

Received 25 iv 79 Accepted 22 v 79

Immunofluorescent microscopy (IFM) used in parallel with light microscopy (LM) examination of kidney biopsies has shown glomerular deposits of immunoreactants which indicate that immunological mechanisms may be involved in some human kidney diseases. There is much supporting evidence for the two main types of immunological mechanisms seen in experimental models of glomerulonephritis (GN) (Mc Cluskey *et al* 1960 Dixon *et al* 1961 and Steblay 1962) being similar to those in human GN reviewed by Lewis and Couser (1971).

In the rarer of these - linear nephritis - a continuous linear deposit of antibody is found in the glomerular basement membrane (GBM) due to circulating antibody directed against the GBM. The other and much more common mechanism involves retention of granular deposits of immune complexes in the wall of the capillary loops and/or mesangium due to antigen antibody complexes formed in the circulating blood (complex nephritis). Clinically as well as on LM it is difficult and in some instances impossible to distinguish between these two different immunological mechanisms and the differ-

information or results of the LM examination being available the time of the investigation

In order to be included in the material patients with GN had to have been observed for at least 3 months and have had at least one of the following symptoms

Hematuria macroscopic or microscopic, with at least 2 erythrocytes in the urine/high power field (Larcom and Carter 1948) without any urological disease

Proteinuria more than 0.5 g/day (Relman and Levinsky 1971)

Reduced kidney function serum creatinine > 1.5 mg % or creatinine or ^{51}Cr EDTA clearance < 1 ml/sec.

The following definitions of clinical symptoms were used elevated blood pressure (BP) was defined as diastolic ≥ 100 mm Hg the term nephrotic syndrome (NS) was used when the serum albumin was ≤ 20 g/l (Scremer 1971) with proteinuria > 5 g/day (Robson 1967)

Infection history of upper respiratory tract infection shortly before the kidney disease presented and/or antistreptolysin titre (ASO) > 200

Needle biopsies were immediately divided under a stereomicroscope for study by LM and IFM

Throughout the investigation all kidney sections were examined by a direct immunofluorescent staining technique using FITC-conjugated rabbit or goat antisera specifically reactive to human IgG IgM IgA as well as complement C₃ and fibrin/fibrinogen

From January 1974 the studies were supplemented by anti IgD -IgE -C₄ -C_{1q} and anti properdin

Details of the procedure and controls have been described previously (Larsen 1978 a)

A Zeiss universal fluorescent microscope with transmitted light and Dark Field Ultracondenser NA 1.2/1.4 oil with iris and objective $\Phi 75/1.0 \text{ NA } \times 40$ and eye piece $\times 10$ Kpl was used in the study with HBO 200 W/4 pressure mercury lamp and filter (R) goard & Olsen 1971)

Light Micro-

Statistical Methods

The Chi square test was used to test for any correlation between the fluorescent findings and the clinical symptoms and clinical course of the disease

RESULTS

The clinical data and the LM diagnosis of kidney biopsies from 339 patients are related to one

another in Table 1 where any significant correlation ($P < 0.01$) is indicated. The period of observation in the groups of patients with minimal lesion, acute tubulo-interstitial nephropathy and acute interstitial nephritis is short because follow-up was carried out by the patients' own practitioner after complete remission or where there were only minimal signs of kidney disease

The short period of observation in patients with extracapillary GN with $> 50\%$ crescents accounted for by the fast progression of the disease to uremia within three months of the first appearance of the kidney disease. Nine of these patients began long-term hemodialysis, (1 died with intractable uremia, in 4 cases kidney transplantation was performed)

In patients classified as GN the length of time between presentation of kidney disease and biopsy was on average 2 months ($\frac{1}{2}$ -3 months) in 1/3 of the patients, and 19 months (3 months-19 years) in 2/3 of the patients. There was no demonstrable difference in the frequency of a clinical history of infection or elevated ASO between the groups of patients classified as GN and the groups of patients with non glomerulonephritic nephropathy

Fluorescent Microscopy Findings

IFM examination in the present study was based on sections of $1 \mu\text{m}$ in contrast to IFM observations published by other investigators on $4 \mu\text{m}$ sections. The difference in the granular pattern in specimens of $1 \mu\text{m}$ and $4 \mu\text{m}$ are seen in Fig. 1 and Fig. 2

IFM findings of glomerular deposits of classes of immunoglobulin and C₃ are related to the LM diagnosis in 339 patients and appear in Table 2, where any significant correlation ($P < 0.01$) is indicated

In patients classified as GN, deposits of IgA/C₃ were more frequently found in «normal glomeruli» and deposits of IgG-IgA/C₃ were found more frequently in mesangioproliferative GN, whilst «no-deposits» correlated with minimal lesion

Apart from this no significant correlation was found between the IFM findings and the groups of GN classified on LM. The frequency with which different immunoglobulin classes were demonstrated in patients with GN was as follows: IgG = 61%, IgM = 43% and IgA = 43%

In 49 patients with non glomerulonephritic nephropathy the following results were obtained:

24%, IgM = 20% and IgA = 10%

renal diagnosis depends on the IFM examination. The widely accepted theory that these two immune mechanisms are responsible for human GN should be taken with some reservation. Firstly, antigens in the immunoglobulin deposits (antigen antibody complex) are very rarely demonstrated. Secondly, the theory does not explain how these two mechanisms can induce such widely different morphological lesions in glomeruli, especially since re-biopsies have shown that the lesions are not different phases of the same glomerular disease. Thirdly, granular deposition of immunoglobulin and C₃ may also appear in glomeruli, where the disease is allegedly on non immunological origin, e.g. in cystinosis and hereditary nephropathy (Berger 1971) and in kidneys from patients with no evidence of GN or nephropathy at all (Larsen 1979).

The present investigation was carried out in an attempt to examine

1) the possibility that the IFM findings correlate with the clinical symptoms, the course of the disease, the response to immunosuppressive treatment, or that they could define some significantly

different pathogenetic group of patients with GN
a) partly independent of the morphological changes in glomeruli

b) partly individual groups of patients with uniform morphological changes in glomeruli on light microscopy

2) in what way the IFM findings in glomeruli in patients with non glomerulonephritic nephropathy differ from those in patients classified as GN. The investigation was performed in the Department of Clinical Chemistry, Kommunehospitalet Copenhagen, from 1972-76.

MATERIAL AND METHODS

The material for the IFM study included 366 kidney biopsies taken from 339 patients. There were 290 biopsies with various types of GN classified on LM according to Pirani and Salinas Madrigal (1968) and Habib (1970) with slight modifications and 49 biopsies with nephropathy not classified as GN (Table 1). Twenty seven biopsies were re-biopsies (Table 6). The LM diagnosis and classification was based on at least 10 glomeruli whilst for IFM at least 2 were required. The IFM investigation was performed without any clinical

TABLE 1 Pertinent Data for Light Microscopic Diagnosis in 339 Patients

Symptoms or diagnosis	No. Pts	Year										Total %	Year (n = max)	Obs. rate (n/pts)	Compl. remission %	Haematuria %	Proteinuria %	Nephritic syndrome %	BP elev. at diagnosis %	GFR decreased %	Tubulonephrosis %	Symptomatic hypertension %
		0-10	11-20	21-30	31-40	41-50	51-60	61-70	71-80													
Normal	18	1	1	3	2	1		1	2		61	44.2 (18/41)	43.1	44	50	78	6	17	11	33	23	
Minimal lesion	15	2	1	1	1		1	1	1		31	32.8 (15/46)	8.5	47	27	87	53.3	13	13	21	7	
Proliferative (GN)	106	10	14	7	14	7	7	4	1		67	29.9 (10/33)	12.6	24	71	90	19	26	147	30	20	
Proliferative (exudative)	9	2	1	2	1	1		1	1		78	33.3 (9/27)	11.1	56	100	100	44	33	31	67	9	
Proliferative (Focal)	43	3	5	10	4	1	4	1			22	28.1 (43/153)	13.5	9	79	93	14	26	16	46	9	
Proliferative (Lobular)	18	2	3	1	1			3			64	30.4 (18/59)	19.1	7	79	100	21	57	36	14	21	
Membranoproliferative	18	1	1	1	2	2		4			51	40.8 (18/46)	19.6	27	73	100	33	20	31	20	9	
Focal glomerulonephritis (<50%)	4			1				1			30	45.8 (22/49)	22.7	73	100	100	0	50	0	25	50	
Extra capsular (>50%)	21	1	1	1	2	2		5			43	46.1 (21/46)	6.4	0	81	93	14	43	11.4	43	4	
Epithelial membranous	9		1	1	1	3		1	1		57	47.8 (9/19)	15.5	53	22.9	100	33	22	22	11	0	
Focal segmental	5			2		1			1		40	44.6 (5/11)	20.0	0	80	100	0	40	60	60	0	
Non classifiable	31	1	3	2	1	1	1	1	2		65	47.2 (31/66)	10.6	10	77	94	16	58.0	58.0	14	23	
Diabetic nephropathy	6		2	1	1	1	1	1			100	42.3 (6/14)	7.7	0	67	100	17	50	67	35	0	
Acute tubulointerstitial nephritis	7		2	2		1		2			78	35.3 (7/19)	2.5	84	71	100	0	29	100	57	0	
Renal amyloidosis	15			1		1	5	2			47	58.5 (15/26)	10.4	0	40	100	33	7	33.7	53	0	
Hereditary nephropathy	4	3	2	1	1	1			1		25	26.3 (4/15)	10.8	25	23	88	0	38	75	0	0	
Acute interstitial nephritis	13		3	2	1	2	1		1		54	42.0 (13/31)	4.1	34	31	88	0	31	69	55.4	0	

1 Significantly elevated } $P < 0.01$
7 Significantly decreased }



Fig 2 (1 μ m) \times 525

Photograph of the next consecutive section of the same glomerulus as shown in Fig 1. Granular deposits of IgG are seen here with the same distribution but the granular pattern of deposits is more finely granular and a more precise description of localisation to the mesangium and the capillary loops is possible.

Distribution of Deposits

Definitions and terminology used are shown in Table 3. The average number of glomeruli examined by IFM was 4.8 per biopsy (range 2-19). The deposits were generalised in the LM groups of GN apart from in a single case where they were focal.

Segmental deposits were demonstrated in a few instances in all the LM classes of GN apart from minimal lesion. Segmental deposition was often found where the GN was secondary to SLE (26%) in the remaining biopsies the deposits were global.

Pattern

Linear deposits were found in biopsies from 5 patients classified as GN and they were distributed to 4 different groups on LM (indicated in Table 2). The deposits had a continuous linear pattern and were localised in the basement membrane of the capillary loops as shown in Fig 3. Deposits in the remaining biopsies were granular. Fine granular deposits were demonstrated most often along the capillary walls in epimembranous GN and more coarse granular deposits were found in lobular and mesangioproliferative GN. In all other instances

deposits had a mixed fine and coarse granular pattern. Interrupted linear deposits were seen along with granular deposits in some of the capillary loops in diabetic nephropathy (75%) in proliferative GN of lobular type, membranoproliferative GN and

Correlation was performed independent of the types of GN and significant correlations are indicated in the table. With deposits of IgG, IgA hematuria was more frequent whilst there was less tendency to reduced kidney function. With IgA/C₃ infection was more frequent and with IgM/C₃ there was less tendency to hematuria and the duration of the disease before biopsy was at least 3 months. Nephrotic syndrome was more frequent where no glomerular deposits were found. Apart from this no significant correlation between the IFM findings, the clinical symptoms and the course of the disease could be found.

Correlation between deposits of different immunoglobulin classes and their localisation appears in Table 4. Ig (G, M, A) were found most frequently



Fig 1 (4 μ m) \times 525

The granular pattern where deposits of IgG are distributed equally to the mesangium and the basement membrane in the capillary loops

TABLE 2 Kidney Biopsy from 339 Patients Glomerular Deposits Correlated to the Light Microscopic Diagnosis

Deposits	290 patients Glomerulonephritis													49 patients Nephropathy non Glomerulonephritic					
	Normal	Minimal lesion	Prolif (gen)	Prolif (extensive)	Prolif (focal)	Prolif (flobular)	Membranoprolif	Extracapillary (<50%)	Extracapillary (>50%)	Epimembranous	Focal (mgm sc)	Non classifiable	TOTAL	Diabetic nephropathy	Ac tub interst neph	Renal amyloidosis	Hereditary nephropathy	Nephrit interst acuta	TOTAL
	18	15	106	9	43	14	15	4	21	9	5	31	290	6	7	15	8	13	49
	Total/													Total/					
Ig (G M A) + C ₃	1	2	15	1	14	3	1	1*	7	3	2	8	58/20	1	0	2	0	0	3/6
Ig (G A) + C ₃	2	2	24*	1	7	1	1	1	2	0	0	2	43/15	0	0	0	0	0	0/
Ig (A) + C ₃	4*	0	3	0	1	1	0	0	0	0	0	2	11/4	0	0	0	0	0	0/
Ig (M A) + C ₃	1	0	3	0	3	3	1	0	0	0	0	2	13/4	0	0	0	1	1	2/4
Ig (G M) + C ₃	0	1	14	1	3	2	3	0	5	3	0	8*	40/14	2	0	1	1	0	4/8
Ig (M) + C ₃	2	0	6	0	1	0	2	0	2	0	1	1	15/5	0	0	0	0	1	1/2
Ig (G) + C ₃	1	2	11	2	6*	2	3	0	4**	1	0	3	35/12	1	1	2	1	2	7/14
C ₃	1	1	8	3	1	1	1	0	0	1	0	3	21/7	1	1	0	1	2	5/10
Ig (GXM)XG A)	2	1	6	0	3	0	1	0	0	1	0	0	16/6	1	1	2	0	1	5/10
No glom deposits	4	6*	16	1	4	0	2	2	1	0	2	2	38/13	0	4	8	4	6	22/45

* = P < 0.05 (significant elevated)

* = Patient with continuous linear deposits (total 5 pts) (One asterisk indicates one patient in the group Two asterisks indicate two patients in the group)



Fig 2 (1 μ m) \times 525

Photograph of the next consecutive section of the same glomerulus as shown in Fig 1. Granular deposits of IgG are seen here with the same distribution but the granular pattern of deposits is more finely granular and a more precise description of localisation to the mesangium and the capillary loops is possible.

Distribution of Deposits

Definitions and terminology used are shown in Table 3. The average number of glomeruli examined by IFM was 4.8 per biopsy (range 2–19). The deposits were generalised in the LM groups of GN apart from in a single case where they were focal.

Segmental deposits were demonstrated in a few instances in all the LM classes of GN apart from minimal lesion. Segmental deposition was often found where the GN was secondary to SLE (26%). In the remaining biopsies the deposits were global.

Pattern

Linear deposits were found in biopsies from 5 patients classified as GN and they were distributed to 4 different groups on LM (indicated in Table 2). The deposits had a continuous linear pattern and were localised in the basement membrane of the capillary loops as shown in Fig 3. Deposits in the remaining biopsies were granular. Fine granular deposits were demonstrated most often along the capillary walls in epimembranous GN and more coarse granular deposits were found in lobular and mesangioproliferative GN. In all other instances

deposits had a mixed fine and coarse granular pattern. Interrupted linear deposits were seen along with granular deposits in some of the capillary loops in diabetic nephropathy (75%) in proliferative GN of lobular type, membranoproliferative GN and non-classifiable GN (35–40%) and in other classes of GN (< 27%). IFM findings are correlated to the clinical data in Table 4 in patients classified as GN. Correlation was performed independent of the types of GN and significant correlations are indicated in the table. With deposits of IgG, IgA, hematuria was more frequent whilst there was less tendency to reduced kidney function. With IgA/C₃ infection was more frequent and with IgM/C₃ there was less tendency to hematuria and the duration of the disease before biopsy was at least 3 months. Nephrotic syndrome was more frequent where no glomerular deposits were found. Apart from this no significant correlation between the IFM findings, the clinical symptoms and the course of the disease could be found.

Correlation between deposits of different immunoglobulin classes and their localisation appears in Table 4. IgG, IgM, IgA were found most frequently

TABLE 3 Terminology and Definition

Terminology	Abbreviation	Definition
Fluorescence		
Positive = (+) + (+ +)	+	Bright fluorescence weak moderate and heavy
Negative =	-	Complete absence of fluorescence
Localisation		
Mesangial	(Mes)	Glomerular intercapillary region
Capillary basement membrane	(Cap)	Within/along the capillary basement membrane
Bowman's capsule	(Bow)	In Bowman's capsule
Distribution		
Generalised	(G)	All glomeruli in specimen
Focal	(F)	One/some glomeruli in specimen
Global	(Glo)	Including all portions of the individual glomerulus
Segmental	(S)	Including only parts of the individual glomerulus
Pattern		
Granular	(Gr)	Fine/coarse granular fluorescence
Linear	(L)	Linear continuous or discontinuous fluorescence within/along the basement membrane

localised in the mesangium as well as along the capillary walls. IgG, IgA and IgM were more often localised to the mesangium and IgM to the capillary loops. Correlation between localisation of deposits and the clinical data appears in Table 4.

There was an increased incidence of reduced kidney function, elevated BP and hematuria in patients with deposits localised to both the mesangium and along the capillary loops, whilst patients with deposits localised solely to the capillary loops had a decreased incidence of hematuria and infection.

Correlation between deposits of immunoglobulins and deposits of fibrinogen and properdin appears in Table 4. The only significant finding was

of GN classified on LM were correlated to clinical data and localisation and localisation was correlated to

symptoms in each of the different classes of GN classified on LM.

Significant findings in normal glomeruli, minimal lesion and generalised mesangio proliferative GN have been described previously (Larsen 1978 a, Larsen 1978 b). Significant correlations in the other LM classes are not shown in the tables but these were as follows.

Proliferative GN (focal) Hematuria was found more frequently in patients with deposits of Ig (G, M, A)/C₃ ($P < 0.01$) and when deposits were localised to both the mesangium and along the capillary loops ($P < 0.01$).

Extracapillary GN > 50% crescents With deposits of Ig (G, M, A)/C₃ reduced kidney function was more frequently ($P < 0.05$) and the same held true when deposits were localised both to the mesangium and along the capillary loops ($P < 0.01$).

Epimembranous GN Patients with deposits localised solely to the capillary walls had less tendency to hematuria ($P < 0.05$).

Non-classifiable GN With deposits of Ig (G, M, A)/C₃ elevated BP was found more frequently ($P < 0.05$).

The lowest intensity of fluorescence accepted as a positive finding of deposits in the present IFM study was indicated as (+). A spot check was performed to investigate changes in the significant correlation between the IFM findings and the clinical data in the borderline area of positive and negative IFM findings, indicated as (+) and 0. All findings indicated as (+) were altered to 0 (negative) in 4 groups of GN: (normal glomeruli, minimal lesions, generalised mesangio proliferative GN and extracapillary GN > 50% crescents). Following this change on correlating the IFM findings and clinical data, there were fewer significant interassociations and the groups of patients with no glomerular deposits increased by 50–100% with fewer significant correlations with the clinical data.

In the 49 patients classified as non glomerulonephritic nephropathy there was no significant correlation between the IFM findings and the clinical data.

Less than 2 months after biopsy 127 of the patients (43%) classified as GN were on corticosteroid or cytostatic treatment. Complete remission occurred in 69 patients (24%). Correlation between the IFM findings and complete remission in both treated and untreated patients appears in Table 5. Complete remission was seen in 31% of treated patients compared with 18% of untreated patients. This higher remission rate is statistically significant in the treated group ($P_e = 0.0216$). No significant difference in complete remission was found between the groups of treated patients with deposits of



Fig 3 (1 μ m) \times 525

Deposits of IgG with a continuous linear pattern localised to the basement membrane of the capillary loops

TABLE 4 *Kidney Biopsies from 290 Patients with Glomerulonephritis: Deposits Correlated to Symptoms and Localisation/ Localisation Correlated to Symptoms*

Deposits	Symptoms										Glomerular Localisation				Deposits other than Ig (I) and C			
	No. pos	Haematuria	Proteinuria	Nephrotic Syndrome	III elevated	GFR decreased	Infect on	Systolic D. raised	Complete Remission	Duration of disease BEFORE biopsy (IN yrs)	Mes + Cap	Cap	Mes	Bow	Fibrinogen tested	Proteinuria tested	% Mem In.	
IgG, M, A, I + C ₃	III	71	97	17	34	11	77	74	71	34	66	86*	13	0	72	74/58	4/77	15.7
IgG, A, I + C ₃	43	84*	88	17	71	14	37	71	17	40	60	74	17	14*	71	16/43	3/70	7.3
Ig (A) + C ₃	11	87	91	0	77	18	64*	18	77	55	45	45	18	36*	18	3/11	3/7	70.1
Ig M, A, I + C ₃	13	92	92	8	38	11	15	0	73	31	69	85	15	0	15	4/13	0/1	16.3
Ig G, M, I + C ₃	40	70	88	30	78	41	30	15	78	45	55	78	23	0	25	19/40	4/17	10.9
Ig (M) + C ₃	15	40	87	70	47	27	77	17	7	7	93	53	47*	0	70	4/15		70.3
Ig G, I + C ₃	35	71	97	14	37	29	26	14	70	43	57	80	14	6	14	10/35	5/13	10.6
C ₃	21	71	86	10	29	33	79	18	79	33	67	57	43*	0	0	6/71	0/3	15.9
IgG, M, A, I, G, A, I	18	69	100	19	31	25	80	10	31	38	68	61	75	13	0	3/16	0/7	13.9
No glom. deposits	38	55	84	34*	26	18	34	11	29	37	68				3	90/38*	0/5	37.5
Total	290	70	92	70	31	27	31	18	72	37	63	74	70	6	14	90/190	21/90	14.3
LOCALISATION																		
Mes + Cap	187	82*	93	18	16*	33*	33	14	72									
Cap	51	57*	96	16	24	18	70	17	88									
Mes	14	86	93	14	14	7	57	21	7									
Total	252	77	93	17	32	79	32	14	22									

\bar{X} = Mean obs. period

* = Significantly elevated
 * = Significantly decreased } $P < 0.05$

TABLE 3 *Terminology and Definition*

Terminology	Abbreviation	Definition
Fluorescence		
Positive = (+) + (+ +)	+	Bright fluorescence, weak, moderate and heavy
Negative =	-	Complete absence of fluorescence
Localisation		
Mesangial	(Mes)	Glomerular intercapillary region
Capillary basement membrane	(Cap)	Within/along the capillary basement membrane
Bowman's capsule	(Bow)	In Bowman's capsule
Generalised	(G)	All glomeruli in specimen
Focal	(F)	One/some glomeruli in specimen
Global	(Glo)	Including all portions of the individual glomerulus
Segmental	(S)	Including only parts of the individual glomerulus
Pattern		
Granular	(Gr)	Fine/coarse granular fluorescence
Linear	(L)	Linear continuous or discontinuous fluorescence within/along the basement membrane

localised in the mesangium as well as along the capillary walls IgG IgA and IgA was more often localised to the mesangium and IgM to the capillary loops. Correlation between localisation of deposits and the clinical data appears in Table 4.

There was an increased incidence of reduced kidney function, elevated BP and hematuria in patients with deposits localised to both the mesangium and along the capillary loops whilst patients with deposits localised solely to the capillary loops had a decreased incidence of hematuria and infection.

Correlation between deposits of immunoglobulins and deposits of fibrinogen and properdin appears in Table 4. The only significant finding was

localisation and localisation was -

symptoms in each of the different classes of GN classified on LM.

Significant findings in «normal glomeruli» minimal lesion and generalised mesangioproliferative GN have been described previously, (Larsen 1978 a, Larsen 1978 b). Significant correlations in the other LM classes are not shown in the tables but these were as follows.

Proliferative GN (focal) Hematuria was found more frequently in patients with deposits of Ig (G, M, A)/C₃ ($P < 0.01$) and when deposits were localised to both the mesangium and along the capillary loops ($P < 0.01$).

Extracapillary GN > 50% crescents With deposits of Ig (G, M, A)/C₃ reduced kidney function was more frequently ($P < 0.05$), and the same held true when deposits were localised both to the mesangium and along the capillary loops ($P < 0.01$).

Epimembranous GN Patients with deposits localised solely to the capillary walls had less tendency to hematuria ($P < 0.05$).

Non-classifiable GN With deposits of Ig (G, M, A)/C₃ elevated BP was found more frequently ($P < 0.05$).

The lowest intensity of fluorescence accepted as a positive finding of deposits in the present IFM study was indicated as (+). A spot check was performed to investigate changes in the significant correlation between the IFM findings and the clinical data in the borderline area of positive and negative IFM findings indicated as (+) and 0. All findings indicated as (+) were altered to 0 (negative) in 4 groups of GN («normal glomeruli» minimal lesions generalised mesangioproliferative GN and extracapillary GN > 50% crescents). Following this change on correlating the IFM findings and clinical data there were fewer significant interassociations and the groups of patients with «no glomerular deposits» increased by 50–100% with fewer significant correlations with the clinical data.

In the 49 patients classified as non glomerulonephritic nephropathy there was no significant correlation between the IFM findings and the clinical data.

Less than 2 months after biopsy 127 of the patients (43%) classified as GN were on corticosteroid or cytostatic treatment. Complete remission occurred in 69 patients (24%). Correlation between the IFM findings and complete remission in both treated and untreated patients appears in Table 5. Complete remission was seen in 31% of treated patients compared with 18% of untreated patients. This higher remission rate is statistically significant in the treated group ($P_e = 0.0216$). No significant difference in complete remission was found between the groups of treated patients with deposits of

TABLE 7 IFM Findings and LM Diagnosis of GN Related to the Clinical Diagnosis of Systemic Disease

	No Pts	Clinical diagnosis								
		Myelomatosis	Scleroderma	SLE	HSP	Periart Nod	WG	Mb Crohn	Goodpasture	SD obs
Deposits		3	2	11	17	4	1	1	2	7
Ig (G M A) + C ₃	14			6	7					1
Ig (G A) + C ₃	9		1		7			1		
Ig (A) + C ₃	2	1*			1					
Ig (G M) + C ₃	6			2		3*	1			
Ig (M) + C ₃	2									2
Ig (G) + C ₃	5			1	1*				2*	1
C ₃	3			1						2
Ig (GVA)	2		1		1					
No deposits	4	2				1				1
LM diagnosis										
Normal	6	2	2	1				1		
Minimal Lesion	1	1								
Prolif GN (gen)	21			5	11	1				4
Prolif GN (focal)	4			1	2				1*	
Prolif GN (lobular)	3			2	1					
Extracapillary GN	2				2					
<50% crescents										
Extracapillary GN	5				1*	2	1		1*	
>50% crescents										
Non Classifiable	5			1		1*				3

SLE = Systemic Lupus Erythematosus

HSP = Henoch Schoenlein's Purpura

WG = Wegener's Granulomatosis

SD = Systemic Disease

* = IgA IgD

• = Linear Nephritis demonstrated in this groups

immunoglobulin/C₃ and those without these deposits. The same held true in patients who were not treated. Treated patients therefore showed more frequent complete remission than those who were untreated, irrespective of whether glomerular deposits of immunoglobulin/C₃ were present or not.

The IFM findings in 27 re biopsies from 24 patients indicate

- 1) that the LM morphological classification of GN did not change
- 2) that deposits of immunoglobulins were not always followed by deposits of C₃ during the period of observation
- 3) that negative IFM findings in the first biopsy did not exclude deposition of immunoglobulins and C₃ later in the course of the disease

4) that changes of deposits (of different immunoglobulin classes and C₃) occurring during the disease are not related to the clinical course

5) that neither presence nor absence of deposits gives any direct information about the clinical course

Glomerular deposits of immunoglobulin/C₃ in GN secondary to systemic disease (SD) Two hundred and nineteen patients were classified as GN. In 47 cases (16%) the GN was secondary to SD. Relations between IFM findings, the LM and the clinical diagnosis appear in Table 7. Continuous linear deposits of IgG/C₃ in the glomerular basement membrane (GBM) were demonstrated in 4 instances (9%), indicated in the table. In addition

TABLE 5. 290 Patients Fluorescent Microscopic Findings in Glomeruli Correlated to Complete Remission in Treated and Untreated Patients

Deposits	No pts.	Treated		Untreated	
		No	Complete remission	No	Complete remission
Ig [G,M,A] + C ₃	58	27	6	31	6
Ig [G,A] + C ₃	43	15	2	28	3
Ig [A] + C ₃	11	4	2	7	1
Ig [M,A] + C ₃	13	5	1	8	2
Ig [G,M] + C ₃	40	22	10	18	3
Ig [M] + C ₃	15	7	1	8	1
Ig [G] + C ₃	35	16	4	19	3
Total	215	96	26 (27%)	119	19 (16%)
C ₃	21	10	2	11	5
Ig [G][M][A][G,A]	16	5	4	11	2
No deposits	38	16	7	22	4
Total	75	31	13 (42%)	44	11 (25%)
Total	290	127	39 (31%)	163	30 (18%)

• $P_e = 0.0216$

TABLE 6 27 Re-Biopsies (24 Patients)

Code	Light micr diagnosis	Duration of Disease before first biopsy > 1 mths.	1 biopsy Deposits				Interval (mths)	2 biopsy Deposits				Interval (mths)	3 biopsy Deposits				Fate of Patients			
			G	M	A	C ₃		G	M	A	C ₃		G	M	A	C ₃	Obs. time (mths)	Complete Remission	Progression	Survival
459	Minimal lesion	+	+	+	+	+	9	+	+	+	+						30	0		
88	Prolif (gen)		+	+	+	+	6	no deposits									40	+		
95	Prolif (gen)	+					6	+	+	+	+						42	0		
105	Prolif (gen)	+	+	+	+	+	6	+	+	+	+						36			+
185	Prolif (gen)	+	+	+	+	+	6	+	+	+	+						26	0		
186	Prolif (gen)		+	+	+	+	24	+	+	+	+						62	0		
231	Prolif (gen)		+	+	+	+	11	+	+	+	+						16	0		
370	Prolif (gen)	+	+	+	+	+	11	no deposits									22	0		
452	Prolif (gen)		no deposits				15	+	+	+	+						30	0		
100	Prolif (focal)		no deposits				12					22					38	0		
87	Prolif (lobular)	+	+	+	+	+	6	+	+	+	+						42			+
193	Prolif (lobular)	+					<1					8					15	0		+/Pain
238	Prolif (lobular)		+				22	+	+	+	+						44			
24	Membranoprolif	+	+				6	+	+	+	+						10	III		
28	Membranoprolif		no deposits				5	no deposits									46	+		
42	Membranoprolif		no deposits				9	+	+	+	+						30	0		
130	Membranoprolif	+	+	+	+	+	2					5					17	0		
255	Membranoprolif	+	+	+	+	+	15	+	+	+	+						40	0		
146	Extracapillary (<50%)	+	+	+	+	+	5	+	+	+	+						29	+		
244	Extracapillary (>50%)	+	+	+	+	+	2	+	+	+	+						27			+/L rx
249	Extracapillary (>50%)	+	+	+	+	+	<1	+	+	+	+						3			
71	Epimembranous	+	+	+	+	+	7	+	+	+	+						29	+		
453	Non classifiable		+	+	+	+	<1	+	+	+	+						2	0		
70	Hereditary nephropathy	+	+	+	+	+	1	+	+	+	+						3			+/L rx

in one of them (with periarthritis nodosa) circulating anti GBM immunoglobulin was demonstrated. The same IFM findings of linear deposits of IgG/C₃ solely localised to the BM of the capillary loops in these 5 patients suggest a common pathogenesis. This group however represented 4 different types of glomerular lesions and different extrarenal features which supports a heterogeneous pathogenesis. On its own therefore IFM was able to demonstrate linear nephritis but an exact diagnosis was achieved only with further information about morphological and clinical data.

Granular deposits of immunoglobulin/C₃ in glomerular immune complexes

secondary to systemic disease (Hjman *et al* 1973). Deposition of circulating antigen antibody complexes (immune complexes) in the glomerular tissue is the immune pathogenetic mechanism (McCluskey 1970) which is generally accepted today as the most common cause of human GN. The aetiology was unknown in approximately 70% of the 210 patients with «complex nephritis» whilst in 30% there was clinical evidence for streptococci being an aetiological factor for GN. However the frequency of clinical evidence of streptococcal infection was shown to be the same in 49 patients with nephropathy where there was no evidence of GN. The number of patients with GN of streptococcal origin must therefore be presumed to be lower than that suggested by the clinical data which is in agreement with what Meadow (1975) demonstrated in children with GN. In GN deposits of different classes of immunoglobulin or their combinations were not specifically related to any type of glomerular lesion, clinical symptoms or the clinical course. The clinical features which were seen in patients with deposits of immunoglobulin/C₃ were also found in patients with no deposits. The diversity of the IFM findings when related to symptoms and to each individual morphological type of glomerular lesion suggests a heterogeneous pathogenesis where the immunoglobulin fraction has apparently no dominant influence on the type of glomerular lesion or nature of the symptoms produced. This is in accordance with what Donadio *et al* (1978) have reported in GN secondary to SLE. Several possible reasons can be given for the lack of correlation between deposits, morphology and the clinical picture. First the LM diagnoses were concordant in the first biopsy examined and in the later re biopsy but in several cases where the first biopsy was taken less than 3 months after recognition of the disease no deposits were demonstrable. However such deposits could be

demonstrated later in the re-biopsies from some of these patients. The same must be presumed to have occurred in other patients in the material even though this was not confirmed by re-biopsy. The deposits in these cases possibly could be superimposed on previous lesions or caused by a normal clearance of non nephritogenic immune complexes from the blood stream in the glomeruli (Larsen 1979). Secondly as shown in the re biopsies alterations in deposits (change in the type of immunoglobulin which was deposited or disappeared) during the course of the disease result in IFM findings which can differ widely from biopsy to biopsy in the same patient depending on the timing of the biopsy in relation to the first appearance of the disease. These factors may be contributory to the demonstrated lack of correlation between deposits, morphology and the clinical picture in the study presented here but they must be equally applicable in other reported material of a similar nature. Glomerular deposits of different immunoglobulin types could not be used as an indicator for or against immunosuppressive therapy as the effect of treatment was independent of whether deposited immunoglobulins were present or not. This findings may be an indirect answer suggesting that cell mediated immune mechanisms are also involved in human GN.

Deposits of IgA/C₃ and IgG IgA/C₃ were found significantly more often localised solely to the mesangium than other types of deposits and IgM/C₃ was significantly localised solely to the BM of the capillary loops. This distribution of IgA and IgM may be dependent on the molecular size of the immunoglobulins (Germuth and Rodriguez 1973) but IgA eluted from kidneys containing such complexes as in addition shown biological properties by having a weak reactivity to normal mesangial tissue (Lowance 1973). It may therefore be supposed that IgA and IgM will always have a preference for mesangium and capillary loops respectively, and therefore the demonstration of these cannot be used as an indicator for possible different antigens being present in a presumed immune complex.

Lowance (1973) mentions the possibility that IgA is the effector for GN (proliferative GN). However we found in 2 cases that IgA was not present in the re biopsies. IgA had therefore hardly been responsible for the induction of GN in all the cases where IgA was demonstrated. On the other hand a high frequency of IgA was found in patients with GN (43%) and was highest in patients with GN secondary to SLE (60%) and Henoch Schonlein purpura (88%). This is in contrast to patients with

in one of these patients granular deposits of IgM were demonstrated on the endothelial side of the GBM but without C₃. Only in one of the cases (periarthritis nodosa) was it possible to identify antibody in the patients blood directed against GBM (demonstrated in cryostat sections of kidney tissue from normal humans - living kidney donors).

Granular deposits were found in 39 patients (83%). In addition in 22 instances (56%) small amounts of discontinuous linear deposits were demonstrated in or along the basement membrane in the capillary loops. In patients with SLE and HSP the distribution of deposits was characteristic. In SLE the granular deposits of IgG and IgM had a global distribution, while linear deposits of IgA were localised at the periphery of some of the capillary walls in a more segmental fashion. In HSP the deposits were generalised and global, but solely localised to the mesangium and in a few cases along the GBM near the mesangium.

The frequency of immunoglobulin classes in GN (secondary to SD) was as follows: IgG = 74%, IgM = 47%, IgA = 55%, where the highest frequency of IgA was found in SLE (60%) and in HSP (88%).

In GN (without SD) the frequency of the immunoglobulin classes was as follows: IgG = 62%, IgM = 44% and IgA = 41%.

DISCUSSION

In recent years intensive morphological study of kidney biopsies from patients with kidney disease has uncovered an abundance of detailed morphological changes in glomeruli and resulted in an increased number of clinico-pathological interassociations. It seems clear from this that glomerulonephritis (GN), rather than being considered a distinct disease entity should rather be looked upon as a concept which includes a broad spectrum of clinico-pathological units of disease. An attempt to define the concept GN can be made at different levels from the clinical features, aetiology, morphology or pathogenesis. But, from data available at the present time in this field it is not possible to draw up a concise, clear and unambiguous definition for GN.

In the material presented here 290 patients with clinical evidence of GN were classified at light microscopy (LM) using a slight modification of the

Pirani
70) No

specific, and only a few statistically significant interassociations were demonstrated between the type of glomerular lesion and the clinical features at

the time of biopsy. The percentage distribution of clinical symptoms in the individual LM groups was where morphology was comparable, on the whole in agreement with that reported by Bohle *et al* (1976) in an analysis of morphological and clinical features in 2500 patients with different types of GN. Incongruity between morphology and clinical features in our study may have been caused by the very different time intervals between the kidney disease being recognised and the time of biopsy. In 2/3 of the patients this time interval varied from 3 months to 19 years (mean 19 months) and it is well recognised that clinical symptoms vary very much during the course of the disease (Treser *et al* 1969). However, we found this same lack of correlation between morphology and clinical features even when biopsy was performed less than 3 months after the kidney disorder presented. The many different deposits of immunoreactants which were demonstrated by immunofluorescent microscopy (IFM) in the individual LM groups suggests a heterogeneous pathogenesis which may explain the lack of relationship between morphology and clinical features. In 2/3 of the patients where biopsies were taken more than 3 months after the disease was recognised, the relatively short observation period (3 months to 35 years (mean 12 months)) may be the reason for the different LM types of GN showing no clear prognostic distinctions from one another.

In the present study two characteristic patterns of deposited immunoglobulin/C₃ were demonstrated in glomeruli corresponding with the two main different types of immune mechanisms (see introduction) which are generally accepted as pathogenetic in most cases of human GN (Wilson & Dixon 1974 a). Linear nephritis (anti GBM nephritis) was demonstrated in 5 patients (2%).

The frequency of this type of nephritis is perhaps geographically determined for reports from USA indicate 4-7% (Wilson & Dixon 1974 b) and France 0% (Berger *et al* 1971). The role of circulating antibodies in inducing anti GBM nephritis is established (Lerner *et al* 1967) and a kidney lesion is well known as the basis of Goodpasture's Syndrome and reported by among others, Duncan *et al* (1965) and Koffler *et al* (1969). Two of the 5 patients in our study had Goodpasture's Syndrome. Proof for this requires demonstration of circulating antibody to GBM in the patients serum (Dixon 1968). This could not, however be shown in these two patients. This does not refute the diagnosis for the concentration of serum anti GBM immunoglobulin often first rises to an identifiable level after nephrectomy (Lerner *et al* 1967). In the 3 patients with linear nephritis hemoptysis did not occur but

in one of them (with periarteritis nodosa) circulating anti GBM immunoglobulin was demonstrated. The same IFM findings of linear deposits of IgG/C₃ solely localised to the BM of the capillary loops in these 5 patients suggest a common pathogenesis. This group however represented 4 different types of glomerular lesions and different extrarenal features which supports a heterogeneous pathogenesis. On its own therefore IFM was able to demonstrate linear nephritis but an exact diagnosis was achieved only with further information about morphological and clinical data.

Granular deposits of immunoglobulin/C₃ in glomeruli (complex nephritis) were demonstrated in 210 patients (72%). These deposits can be seen in both primary GN (Michael *et al* 1966) and in GN secondary to systemic disease (Hjman *et al* 1973). Deposition of circulating antigen antibody complexes (immune complexes) in the glomerular tissue in the immune pathogenetic mechanism (McCluskey 1970) which is generally accepted today as the most common cause of human GN. The aetiology was unknown in approximately 70% of the 210 patients with complex nephritis whilst in 30% there was clinical evidence for streptococci being an aetiological factor for GN. However the frequency of clinical evidence of streptococcal infection was shown to be the same in 49 patients with nephropathy where there was no evidence of GN. The number of patients with GN of streptococcal origin must therefore be presumed to be lower than that suggested by the clinical data which is in agreement with what Meadow (1975) demonstrated in children with GN. In GN deposits of different classes of immunoglobulin or their combinations were not specifically related to any type of glomerular lesion, clinical symptoms or the clinical course. The clinical features which were seen in patients with deposits of immunoglobulin/C₃ were also found in patients with no deposits. The diversity of the IFM findings when related to symptoms and to each individual morphological type of glomerular lesion suggests a heterogeneous pathogenesis where the immunoglobulin fraction has apparently no dominant influence on the type of glomerular lesion or nature of the symptoms produced. This is in accordance with what Donadio *et al* (1978) have reported in GN secondary to SLE. Several possible reasons can be given for the lack of correlation between deposits morphology and the clinical picture. First the LM diagnoses were concordant in the first biopsy examined and in the later re biopsy but in several cases where the first biopsy was taken less than 3 months after recognition of the disease no deposits were demonstrable. However such deposits could be

demonstrated later in the re biopsies from some of these patients. The same must be presumed to have occurred in other patients in the material even though this was not confirmed by re biopsy. The deposits in these cases possibly could be superimposed on previous lesions or caused by a normal clearance of non nephritogenic immune complexes from the blood stream in the glomeruli (Larsen 1979). Secondly as shown in the re biopsies alterations in deposits (change in the type of immunoglobulin which was deposited or disappeared) during the course of the disease result in IFM findings which can differ widely from biopsy to biopsy in the same patient depending on the timing of the biopsy in relation to the first appearance of the disease. These factors may be contributory to the demonstrated lack of correlation between deposits morphology and the clinical picture in the study presented here but they must be equally applicable in other reported material of a similar nature. Glomerular deposits of different immunoglobulin types could not be used as an indicator for or against immunosuppressive therapy as the effect of treatment was independent of whether deposited immunoglobulins were present or not. This findings may be an indirect answer suggesting that cell mediated immune mechanisms are also involved in human GN.

Deposits of IgA/C₃ and IgG IgA/C₃ were found significantly more often localised solely to the mesangium than other types of deposits and IgM/C₃ was significantly localised solely to the BM of the capillary loops. This distribution of IgA and IgM may be dependent on the molecular size of the immunoglobulins (Germuth and Rodriguez 1973) but IgA eluted from kidneys containing such complexes as in addition shown biological properties by having a weak reactivity to normal mesangial tissue (Lowance 1973). It may therefore be supposed that IgA and IgM will always have a preference for mesangium and capillary loops respectively and therefore the demonstration of these cannot be used as an indicator for possible different antigens being present in a presumed immune complex.

Lowance (1973) mentions the possibility that IgA is the effector for GN (proliferative GN). However we found in 2 cases that IgA was not present in the first biopsy but was demonstrated in the re biopsies. IgA had therefore hardly been responsible for the induction of GN in all the cases where IgA was demonstrated. On the other hand a high frequency of IgA was found in patients with GN (43%) and was highest in patients with GN secondary to SLE (60%) and Henoch Schonlein purpura (88%). This is in contrast to patients with

in one of these patients granular deposits of IgM were demonstrated on the endothelial side of the GBM but without C₃. Only in one of the cases (periarteritis nodosa) was it possible to identify antibody in the patients blood directed against GBM (demonstrated in cryostat sections of kidney tissue from normal humans - living kidney donors).

Granular deposits were found in 39 patients (83%). In addition in 22 instances (56%) small amounts of discontinuous linear deposits were demonstrated in or along the basement membrane in the capillary loops. In patients with SLE and HSP the distribution of deposits was characteristic. In SLE the granular deposits of IgG and IgM had a global distribution while linear deposits of IgA were localised at the periphery of some of the capillary walls in a more segmental fashion. In HSP the deposits were generalised and global but solely localised to the mesangium and in a few cases along the GBM near the mesangium.

The frequency of immunoglobulin classes in GN (secondary to SD) was as follows: IgG = 74%, IgM = 47%, IgA = 55% where the highest frequency of IgA was found in SLE (60%) and in HSP (88%).

In GN (without SD) the frequency of the immunoglobulin classes was as follows: IgG = 62%, IgM = 44% and IgA = 41%.

DISCUSSION

In recent years intensive morphological study of kidney biopsies from patients with kidney disease has uncovered an abundance of detailed morphological changes in glomeruli and resulted in an increased number of clinico-pathological interassociations. It seems clear from this that glomerulonephritis (GN) rather than being considered a distinct disease entity should rather be looked upon as a concept which includes a broad spectrum of clinico-pathological units of disease. An attempt to define the concept GN can be made at different levels from the clinical features aetiology morphology or pathogenesis. But from data available at the present time in this field it is not possible to draw up a concise clear and unambiguous definition for GN.

In the material presented here 290 patients with clinical evidence of GN were classified at light

microscopy. The classification of the patients was based on the type of glomerular lesion and the clinical features at

the time of biopsy. The percentage distribution of clinical symptoms in the individual LM groups was where morphology was comparable, on the whole in agreement with that reported by Bohle *et al* (1976) in an analysis of morphological and clinical features in 2500 patients with different types of GN. Incongruity between morphology and clinical features in our study may have been caused by the very different time intervals between the kidney disease being recognised and the time of biopsy. In 2/3 of the patients this time interval varied from 3 months to 19 years (mean 19 months) and it is well recognised that clinical symptoms vary very much during the course of the disease (Treser *et al* 1969). However we found this same lack of correlation between morphology and clinical features even when biopsy was performed less than 3 months after the kidney disorder presented. The many different deposits of immunoreactants which were demonstrated by immunofluorescent microscopy (IFM) in the individual LM groups suggests a heterogeneous pathogenesis which may explain the lack of relationship between morphology and clinical features. In 2/3 of the patients where biopsies were taken more than 3 months after the disease was recognised the relatively short observation period (3 months to 35 years (mean 12 months)) may be the reason for the different LM types of GN showing no clear prognostic distinctions from one another.

In the present study two characteristic patterns of deposited immunoglobulin/C₃ were demonstrated in glomeruli corresponding with the two main different types of immune mechanisms (see introduction) which are generally accepted as pathogenic in most cases of human GN (Wilson & Dixon 1974 a). Linear nephritis (anti-GBM nephritis) was demonstrated in 5 patients (2%).

The frequency of this type of nephritis is perhaps geographically determined for reports from USA indicate 4-7% (Wilson & Dixon 1974 b) and France 0% (Berger *et al* 1971). The role of circulating antibodies in inducing anti-GBM nephritis is established (Lerner *et al* 1967) and a kidney lesion is well known as the basis of Goodpasture's Syndrome and reported by among others Duncan *et al* (1965) and Koffler *et al* (1969). Two of the 5 patients in our study had Goodpasture's Syndrome. Proof for this requires demonstration of circulating antibody to GBM in the patients serum (Dixon

bulin often first rises to an identifiable level after nephrectomy (Lerner *et al* 1967). In the 3 patients with linear nephritis hemoptysis did not occur but

- 23 *Meadow R S* Poststreptococcal nephritis - a rare disease? *Arch Disease in Childhood* 50 379-382 1975
- 24 *Michael A F Drummond K N Good R A & Verner R L* Acute poststreptococcal glomerulonephritis Immune deposit disease *J Clin Invest* 45 237-248 1966
- 25 *Pirani C L & Salinas Madrigal L* Evaluation of Percutaneous Renal Biopsy *Path Ann* by Sommers S C Meredith Corporation 1968 pp 249-296
- 26 *Reiman A S & Levinsky N G* Clinical Examination of Renal Function In Strauss M D & Welt L G (Ed.) *Diseases of the Kidney* Little Brown and Company Boston 1971 pp 89-96
- 27 *Robson J S* The nephrotic Syndrome In Black D A K (Ed.) *Renal Disease* Blackwell Scientific Publications Oxford and Edinburgh 1967 pp 275-308
- 28 *Rygaard J & Olsen W* Toward quantitation of excitation *Ann N Y Acad Sci* 177 410-413 1971
- 29 *Schreiner G E* The Nephrotic Syndrome In Strauss M B & Welt L G (Ed.) *Diseases of the Kidney* Little Brown and Company Boston 1971 p 533
- 30 *Sieblay R W* Glomerulonephritis induced in sheep by injections of heterologous glomerular basement membrane and Freund's complete adjuvant *J Exp Med* 116 253-271 1962
- 31 *Treser G Sagel I & Lange K* Natural history of apparently healed acute poststreptococcal glomerulonephritis in children *Pediatrics* 43 1005-1017 1969
- 32 *Wilson C B & Dixon F J* Immunopathology and glomerulonephritis *Ann Rev Med* 25 83-98 1974 a
- 33 *Wilson C B & Dixon F J* Diagnosis of immunopathologic renal disease *Kidney Int* 5 389-401 1974 b

non glomerulonephritic nephropathy where IgA was only demonstrated in 10%. This may support the hypothesis that IgA (possibly as antigen) can be the effector in some cases of GN. The presence of IgA deposits in very different LM types of glomerular lesions does not exclude IgA as an antigen or as possible inducer of GN because it has been clearly demonstrated by Germuth, Dixon, Rodriguez et al (Germuth & Rodriguez 1973) that individual antigen systems in experimental models induce all the various types of glomerular lesions which are seen in human GN. IFM results therefore suggest that the presence of some immunoglobulins may be interpreted as showing involvement of immune mechanisms only at a purely secondary level. However, this does not exclude the possible importance of immunoglobulin deposits in glomeruli to the severity of symptoms or perhaps chronic course of the disease. Deposits of different immunoglobulin classes and their combinations could be used as a basis for an immunopathological classification in patients with GN on LM. Any such classification, however, only seems to be on yet another descriptive level with the same correlative problems as the LM diagnoses.

However, the IFM findings are necessary in some cases as a supplement to the morphological and clinical data in order to obtain practical diagnostic boundaries within the somewhat ill-defined concept which today constitutes GN.

I gratefully acknowledge the financial support of the Danish Medical Research Council (nr 512-2669) and King Christian X Foundation. My thanks are due to Winnie Pedersen, Karin Solberg, Birgit Høj and Helene Jensen for skilful technical assistance.

REFERENCES

- Andres G A, Accinni L, Hsu A C, Zabriskie J B & Seegal B C. Electron Microscopic Studies of Human Glomerulonephritis with Ferritin conjugated Antibody. *J Exp Med* 123: 399-412 1966
- Berger J, Yaneva H & Hinglais N. Immunohistochemistry of Glomerulonephritis. In: Hamburger J, Crosnier J & Maxwell M H (Ed.) *Advances in Nephrology*. Year Book Medical Publishers, Chicago 1971, pp 11-30
- Bohle A, Eichenseker N, Fischbach H, Neild G G, Wehner H, Edel H H, Losse H, Renner E, Reicher W & Schutterle G. The different forms of glomerulonephritis: morphological and clinical aspects analyzed in 2500 patients. *Klin Wschr* 54: 59-73 1976
- Dixon F J, Feldman J D & Vasques J J. Experimental glomerulonephritis: the pathogenesis of a laboratory model resembling the spectrum of human glomerulonephritis. *J Exp Med* 113: 899-920 1961
- Dixon F J. *Am J Med* 44: 493-498 1968
- Donadio J V Jr, Conn D L, Holley A E & Ilstrup D M. Class of Immunoglobulin Deposition and Prognosis in Lupus Nephritis. *Mayo Clin Proc* 53: 366-372 1978
- Duncan D A, Drummond A N, Michael A F & Vernier R L. Pulmonary Hemorrhage and Glomerulonephritis. *Ann Int Med* 62: 920-938 1965
- Germuth F G Jr & Rodriguez E. *Immunopathology of the renal glomerulus*. Little Brown and Company, Boston 1973
- Habib R. Classification anatomique des nephropathies glomerulaires. *Pad Fortbildungskurse* 28: 3-47 1970
- Hyman L R, Wagnild J P, Berne G J & Burkholder P M. Immunoglobulin - A distribution in glomerular disease. Analysis of immunofluorescence localization and pathogenetic significance. *Kidney International* 3: 397-408 1973
- Jones D B, Amer J. *Path* 27: 991-1009 1951
- Koffler D, Sandson J, Carr R & Kunkel H G. Immunologic Studies Concerning the Pulmonary Lesions in Goodpasture's Syndrome. *Ann J Path* 54: 293-305 1969
- Lange A & Treser G. Acute poststreptococcal glomerulonephritis. *Clin Nephrol* 1: 55-60 1973
- Larcom R C Jr & Carter G H. Erythrocytes in urinary sediment: Identification and normal limits. *J Lab Clin Med* 33: 875 1948
- Larsen S. Immunofluorescent microscopy findings in minimal or no change disease and slight generalized mesangio proliferative glomerulonephritis. *Acta path microbiol scand Sect A* 86: 531-542 1978 (a)
- Larsen S. Immune deposits in generalised mesangio proliferative glomerulonephritis. *Acta path microbiol scand Sect A* 86: 543-552 1978 (b)
- Larsen S. Glomerular immune deposits in kidneys from patients with no clinical or light microscopic evidence of glomerulonephritis. *Acta path microbiol scand Sect A* 87: 313-319 1979
- Lerner R A, Glasscock R J, Dixon F J. The role of antiglomerular basement membrane antibody in the pathogenesis of human glomerulonephritis. *J Exp Med* 126: 989 1967
- Lewis E J & Couser W G. The Immunology. *Basis of Human Renal Disease*. *Ped Clin Amer* 18: 467-507 1971
- Lowance D D, Mullins J D & McPhaul J J. Immunoglobulin A (IgA) associated glomerulonephritis. *Kidney Int* 3: 167-176 1973
- McCluskey R T, Benacerraf B, Potter J L & Miller F. The pathologic effects of intravenously administered soluble antigen antibody complexes. *J Exp Med* 111: 181-194 1960
- McCluskey R T. Evidence for Immunologic Mechanisms in Several Forms of Human Glomerular Diseases. *Bull N Y Acad Med* 46: 769-788 1970

HEPATIC CHANGES IN LATE CANINE ENDOTOXIN SHOCK

A Light and Electron Microscopic Investigation

KNUT NORDSTOGA and ANSGAR O AASEN

Institute for Surgical Research Rikshospitalet and Department of Pathology Veterinary College of
Norway Oslo Norway

Nordstoga, K & Aasen A O Hepatic changes in late canine endotoxin shock: a light and electron
microscopic investigation. Acta path microbiol scand Sect A 87 335-346 1979

The patho morphological lesions in the liver in late stages of canine endotoxin shock were studied by light and electron microscopy. Light microscopic lesions included sinusoidal dilatations with accumulation of red cells and leucocytes, varying damage of the sinusoidal lining, microthrombi and widening of the space of Disse. Necrotic foci were in some cases recognized within a varying number of lobuli at times in the centrilobular areas. Electron microscopy revealed severe hepatocytic damage. These lesions included formation of blebs and other surface protrusions corresponding to cytoplasmic ecdyosis. The resulting cytoplasmic fragments seemed frequently to enter the sinusoids. It is suggested that the severe disturbances observed in the proteolytic enzyme systems of plasma during endotoxin shock are influenced by the hepatic parenchymal changes observed.

Key words: Endotoxin shock, dogs, liver, light microscopy, electron microscopy.

Ansgar O Aasen, Institute for Surgical Research, Rikshospitalet, Oslo 1, Norway.

Received 6 x 78 : Accepted 28 ii 79

Severe endotoxaemia mediates marked alteration of several plasma proteins (Hjort & Rapaport 1965; Kadis *et al* 1971 and Urbaschek *et al* 1973). These changes include components of the four main proteolytic enzyme systems of plasma viz. the coagulation system (Hardaway & Johnson 1963), fibrinolytic system (Gans & Krivit 1961 and von Kowalla 1963), the kallikrein-kinin system (Kobold *et al* 1964 and Hirsch *et al* 1974) and the complement system (Spink & Vick 1961 and McCabe 1973).

In previous studies we have noted considerable reduction of several components of these four proteolytic enzyme systems during the late stages of canine endotoxin shock (Aasen *et al* 1977 and 1978a, b, c). Obviously these phenomena might be due to several factors including disturbances of release into plasma and changes of the production

of these substances. The liver is suggested to be responsible for the synthesis of about eighty per cent of the plasma proteins (Rothschild & Waldmann 1970; Romslo 1976 and Deutsch & Gabl 1976). Thus disturbance of the function of this organ might be an important limiting factor that could influence the reduced levels observed. Several studies previously carried out have actually provided evidence for impairment of hepatic function during canine endotoxaemia. These include elevated plasma levels of substances produced by the liver such as GOT, GPT and alkaline phosphatase (Ushinuma *et al* 1976).

In order to further evaluate the influence of endotoxaemia on the liver, the present work was undertaken to study possible morphological changes of the liver in the late stages of lethal canine endotoxin shock (ES).

HEPATIC CHANGES IN LATE CANINE ENDOTOXIN SHOCK

A Light and Electron Microscopic Investigation

KNUT NORDSTOGA and ANSGAR O AASEN

Institute for Surgical Research Rikshospitalet, and Department of Pathology Veterinary College of
Norway Oslo Norway

Nordstoga K & Aasen A O Hepatic changes in late canine endotoxin shock a light and electron
microscopic investigation Acta path microbiol scand Sect A 87 335-346 1979

The patho-morphological lesions in the liver in late stages of canine endotoxin shock were studied by light and electron microscopy Light microscopic lesions included sinusoidal dilatations with accumulation of red cells and leucocytes varying damage of the sinusoidal lining microthrombi and widening of the space of Disse Necrotic foci were in some cases recognized within a varying number of lobuli at times in the centrilobular areas Electron microscopy revealed severe hepatocytic damage These lesions included formation of blebs and other surface protrusions corresponding to cytoplasmic condensation The resulting cytoplasmic fragments seemed frequently to enter the sinusoids It is suggested that the severe disturbances observed in the proteolytic enzyme systems of plasma during endotoxin shock are influenced by the hepatic parenchymal changes observed

Key words Endotoxin shock dogs liver light microscopy electron microscopy

Ansgar O Aasen Institute for Surgical Research Rikshospitalet Oslo 1 Norway

Received 6 x 78 Accepted 28 ii 79

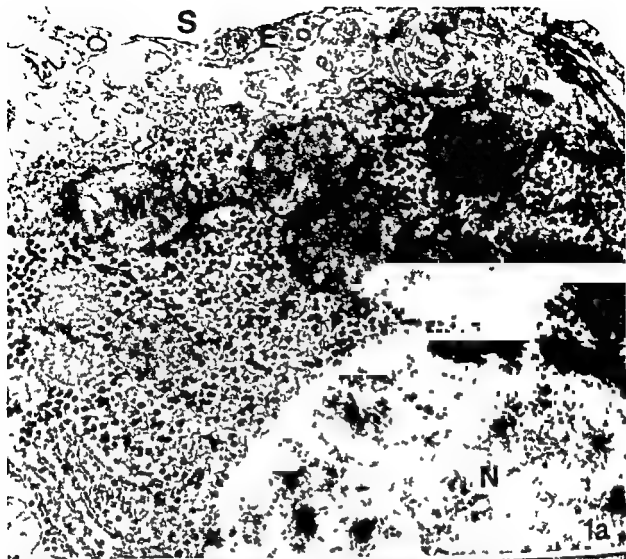
Severe endotoxaemia mediates marked alteration of several plasma proteins (Hjort & Rapaport 1965 Kad's et al 1971 and Urbaschek et al 1973) These changes include components of the four main proteolytic enzyme systems of plasma viz the coagulation system (Hardaway & Johnson 1963) fibrinolytic system (Gans & Kriss 1961 and von Kallia 1963) the kallikrein-kinin system (Aobold et al 1964 and Hirsch et al 1974) and the complement system (Spink & Vick 1961 and McCabe 1973)

In previous studies we have noted considerable reduction of several components of these four proteolytic enzyme systems during the late stages of canine endotoxin shock (Aasen et al 1977 and 1978a, b, c) Obviously these phenomena might be due to several factors including disturbances of release into plasma, and changes of the production

of these substances The liver is suggested to be responsible for the synthesis of about eighty per cent of the plasma proteins (Rothschild & Waldmann 1970 Romslo 1976 and Deutsch & Gabl 1976) Thus disturbance of the function of this organ might be an important limiting factor that could influence the reduced levels observed Several studies previously carried out have actually provided evidence for impairment of hepatic function

Usuyama et al 1976)

In order to further evaluate the influence of endotoxaemia on the liver the present work was undertaken to study possible morphological changes of the liver in the late stages of lethal canine endotoxin shock (ES)



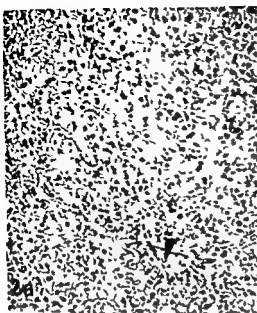


Fig 2 Light micrographs of hepatic tissue A control B experimental dog. Arrows indicate central veins. The translucent appearance of hepatocytes in A is due to a normal content of glycogen while the hepatic tissue in B is severely degenerated. In the upper part of Fig 2B the hepatocytes are intact. Haematoxylin and eosin $\times 100$

MATERIALS AND METHODS

Nine Labrador retriever dogs (14–22 kg) from a veterinary controlled kennel were used during these experiments. Four of the animals were used for control experiments. The experimental procedure has been described in detail elsewhere (Jensen *et al* 1978b). Endotoxin shock was induced by infusion of a lethal dose of *E. coli* endotoxin (2 or 6 mg/kg body weight Lipopolysaccharide B *E. coli* 026 B6 (Difco Laboratories, Detroit, Mich.) over a three hour period. In the control experiments the same amount of sterile isotonic saline was administered i.v. during the first three hours of the observation period. In two of the control animals laparotomy was performed immediately after anaesthesia was induced to obtain liver biopsies. The remaining control experiments lasted for 11 to 14 hours. At the end of these experiments liver specimens were obtained by laparotomy. All these dogs made good recovery. In the dogs receiving endotoxin liver specimens were obtained through a midline incision at the end of the experiments (circulatory collapse) when the aortic blood pressure (Pa)

was below 30 mmHg and marked bradycardia had developed. Dogs receiving endotoxin survived for 11–14 hours after the start of endotoxin infusion. Liver specimens intended for morphological studies were handled in the following manner.

Light microscopic material Pieces of hepatic tissue were fixed in a 10 per cent buffered formaldehyde solution for at least 48 h, embedded in paraffin and sectioned at about 5 μ . Sections were stained with haematoxylin and eosin, Wilder's silver stain, DiPAS, elastin van Gieson, phosphotungstic acid, haematoxylin and with the Marsus scarlet blue method (Lendrum *et al* 1962).

Electron microscopic material Electron microscopic material was selected from areas in immediate proximity of the light microscopic material.

acetone dehydration and infiltration in Araldite the material was embedded in Araldite. Semithin sections were stained with Toluidine blue, ultrathin sections with uranyl acetate and lead citrate, the ultrathin sections were examined in a Siemens Elmiskop 1 A.

RESULTS

Control animals

In some of the controls there seemed to be a modest depletion of glycogen when compared with

Fig 1 Electron micrographs of liver tissue from a control animal showing abundant rosette like glycogen and numerous dense round or oval mitochondria (M) reticular fibres (R) intact microvilli and a distinct endothelium (E) which lines a sinusoid (S) hepatocyte nuclei (N) have a normal chromatin pattern (A) $\times 30\,000$.

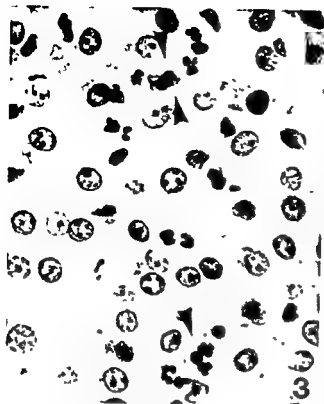


Fig 3 Light micrograph of liver tissue from a dog injected with endotoxin, showing dilatation of the spaces of Disse (arrows) and aggregations of leucocytes within sinusoidal lumina Haematoxylin and eosin $\times 480$

the remaining control animals. Minor aggregates of platelets were infrequently seen in the sinusoidal lumina. Other morphological abnormalities were not noted in any of the controls either by light or electron microscopy (Figs 1a and 1b).

Endotoxin Infused Animals

Light microscopy Evident light microscopic lesions were present in all animals (Figs 2a and 2b), the changes appeared at times but not always, to be most advanced in the centrilobular areas, and consisted of depletion of glycogen, varying degrees of fatty infiltration, and hydropic degeneration of parenchymal cells. PAS positive cytoplasmic inclusion bodies were occasionally seen. Cellular dissociation of hepatocords was common. In the more advanced stages, with incipient cellular necrosis, the spaces of the damaged cells (»cell dropout«) was occasionally recognized. The sinusoids were, as a rule, considerably dilated and contained aggregates of red cells and leucocytes. Sinusoidal microthrombi with staining properties of fibrin, were sometimes recognized. In areas of advanced injury the space of Disse was always greatly extended (Fig 3).

Electron microscopy Hepatocyte damage was a constant finding in all animals receiving endotoxin. The hepatocytes were found to be swollen, with frequent loosening of intercellular attachments, and varying degrees of plasma membrane injury. Depletion of glycogen was striking. Furthermore accumulation of lipids, distortion and disappearance of microvilli, and lysosomal and mitochondrial degeneration occurred, the latter, swelled organelles had frequently an uneven matrix density and fragmented cristae, sometimes bell shaped mitochondria occurred. Electron dense inclusion bodies were commonly seen. Autophagocytic vacuoles containing various cellular components including degenerated mitochondria and unidentifiable debris were numerous (Figs 4–6). Dilation and vesiculation of the endoplasmic reticulum were common findings, in later developmental stages the cisterna seemed to rupture.

The nuclei exhibited as a rule more moderate changes, although a somewhat abnormal chromatin pattern was sometimes recognized.

With increasing involvement the partly necrotic hepatocytes frequently had blebs and vacuoles of various sizes, which at least in some instances seemed to represent degenerated mitochondria located towards the sinusoidal surface (Fig 7). Degenerated mitochondria or more dense projections of hepatocytes were found to protrude from the hepatic cells into the sinusoidal lumina, through wide gaps in the endothelial lining (Figs 8 and 9). These structures, released from hepatocytes, seemed to undergo further fragmentation within the sinusoids (Fig 10). Hepatocytic fragments were also found inside sinusoids and in the space of Disse in areas without severe endothelial lesions (Fig 11). Red cells were often found in the space of Disse.

Endothelial sinusoidal lesions, including proliferative changes and vacuolization were frequent findings. Furthermore, stretching of the endothelium and widened gaps in the endothelial lining seemed to occur at times together with disintegration of endothelium. Phagocytosis of damaged red cells, a fibrin-like material or unidentifiable debris, was occasionally recognized within Kupffer cells and polymorphonuclear leucocytes.

Accumulation of platelets, leucocytes and red cells, sometimes in disintegration, were commonly seen within the sinusoidal lumina (Fig 12). Also a fibrin-like material was found in the sinusoids. However characteristic fibrin periodicity could not be demonstrated in the material. Red cell fragments, »ghosts« and cellular remnants, apparently originating from liver cells, were also found within sinusoidal lumina, but in addition cellular debris impossible to identify was recognized. The hetero-

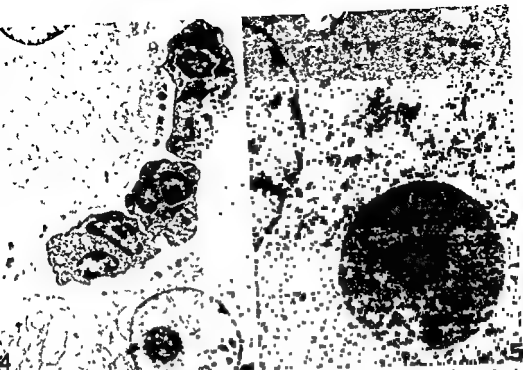


Fig 4 Electron micrograph of liver tissue from an experimental dog showing aggregation of leucocytes within a sinusoidal lumen, and early necrotic changes of hepatocytes $\times 8000$

Fig 5 Electron micrograph of a hepatocyte showing evident degenerative alterations with depletion of glycogen; an electron dense inclusion body is visible in the cytoplasm $\times 12000$

Fig 6 Electron micrograph of a hepatocyte with autophagocytotic vacuoles (AV) probably containing degenerated mitochondria. M indicates less changed mitochondria; a huge bell-shaped mitochondrion is seen to the left $\times 27000$



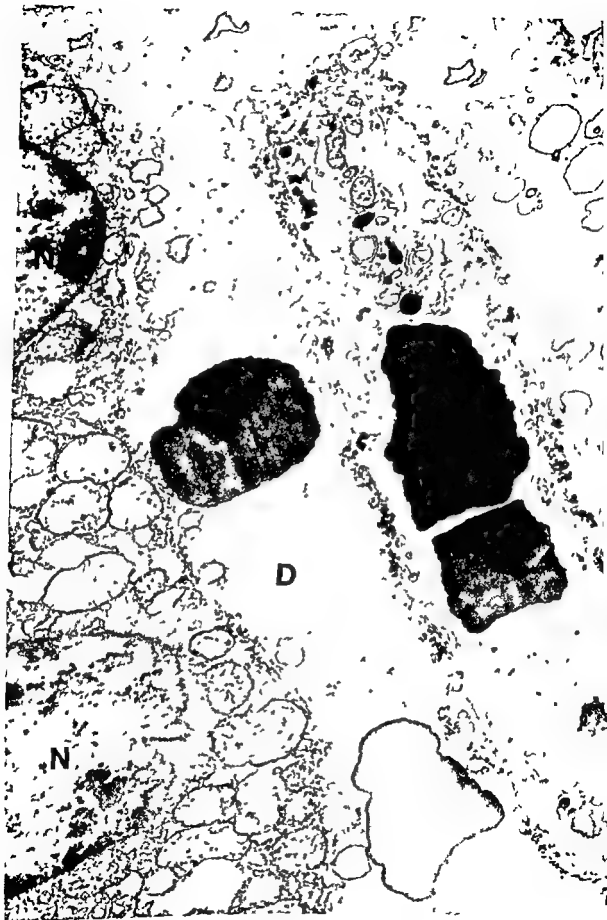
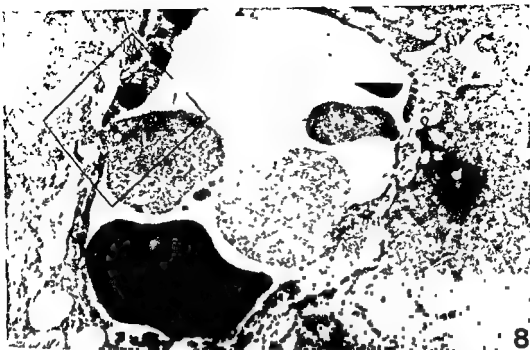
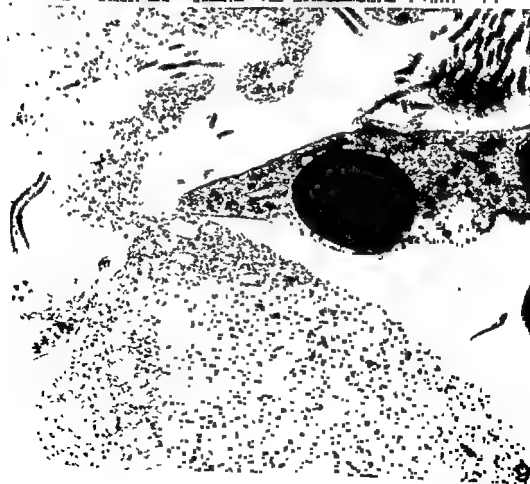


Fig 7 Electron micrograph of hepatic tissue. The space of Disse (D) shows extensive dilation and contains erythrocytes and small vacuoles which probably originate from injured hepatocytes. In the upper part of the sinusoid some mitochondria can be seen together with debris of uncertain origin $\times 12\,000$



8



9

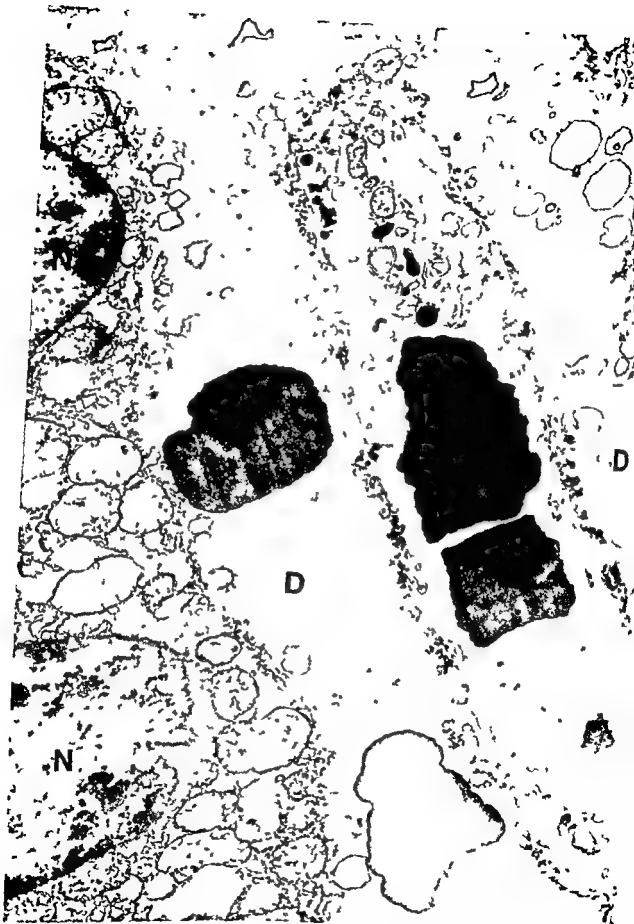


Fig 7 Electron micrograph of hepatic tissue. The space of Disse (D) shows extensive dilation and contains erythrocytes and small vacuoles which probably originate from injured hepatocytes. In the upper part of the sinusoid some mitochondria can be seen together with debris of uncertain origin. $\times 12\,000$

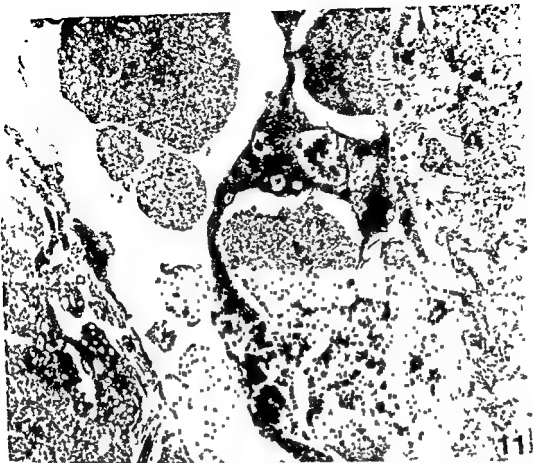


Fig 11 Electron micrograph of hepatic tissue. Several rounded membrane bound structures are seen within a distended space of Disse and a sinusoidal lumen. the endothelium is not obviously damaged. $\times 11\,000$

evidence for an *in vivo* catabolism of energy-rich purines during this ailment. These studies indicate furthermore that endotoxin interferes with basic metabolic cellular processes of the hepatocytes in addition to producing haemodynamic changes leading to altered tissue perfusion of the liver.

A massive release of proteolytic enzymes has been reported in several experimental animals subjected to ES (Gans & Krivit 1961, Spink & Vick 1961 and Hjort & Rapaport 1965) and in humans suffering from septicaemia (Hjort & Rapaport 1965, McCabe 1973 and Hirsch *et al* 1974). Janoff *et al* (1962) demonstrated augmented release of lysosomal enzymes which might cause cell injury from liver specimens obtained from rats and rabbits after injection of endotoxin. Inadequate tissue perfusion is thought to lead to release of lysosomal enzymes (De Duve 1959). Furthermore in our study, an evident accumulation of leucocytes was noted in the liver in the late stages of shock. As reported in detail

elsewhere, we have noticed release of granulocyte elastase during endotoxin shock in dogs (Aasen & Ohlsson 1978). The proteolytic activity of this enzyme is known to cause degradation of basement membranes and arterial walls (Janoff & Zelig 1968). It thus appears likely that release of proteolytic enzymes has significantly influenced the cellular damage observed in this study.

Membrane damage of the hepatocytes leads to release of cytoplasmic material from these cells, as illustrated in Figs 10 and 11. This observation provides evidence for the identification of the described debris material observed in the liver sinusoids and Disse space as cytoplasmic constituents of hepatocytes. Owing to the importance of the hepatocytes for the synthesis of plasma proteins, the marked damage of hepatocytes, leading to subsequent cytoplasmic release is a finding of particular significance for the changes of several plasma proteins previously described in this ES model.

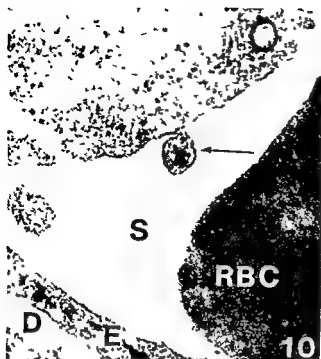


Fig 10 A fragment of a disintegrating hepatocyte is undergoing further fragmentation (arrow) within the lumen of a sinusoid (S) A distinct endothelium (E) is present RBC denotes part of a red blood cell, and D a widened space of Disse $\times 50\ 000$

genous material within the dilated sinusoids sometimes seemed to be included in occlusive microthrombi

DISCUSSION

The present study demonstrates marked ultrastructural changes of the canine liver in the late stages of endotoxin shock. These include severe hepatic and endothelial cell damage, widespread occurrence of sinusoidal microthrombi, and disappearance of liver glycogen, this latter finding in accordance with several other studies, in which marked depletion of liver glycogen and hypoglycaemia characterized the late stages of ES (Levy *et al* 1967 and Filkins & Cornell 1974). The degenerative changes observed in parenchymal cells correspond largely to those occurring in degenerating or necrotizing cells in general. Thus, the process of formation and separation of surface cellular blebs is referred to as cytoplasmic ecdysis in current literature (Cheville

1976). The cytoplasmic inclusion bodies are obviously equivalent to the strongly PAS positive bodies described by others, they are not considered as specific for endotoxic shock (Holmes & Smith 1969).

The noxious effects of endotoxaemia on the hepatic tissue obviously depend on several pathophysiological mechanisms, and the ultimate consequences of these lesions appear to be of significant importance for the lethal outcome of ES. In the dog ES is characterized by marked haemodynamic changes leading to trapping of blood within the portal system during the early stages of shock (Lillehei *et al* 1964). In the low output state due to septicaemia in pigs, hepatic artery flow decreased by 74 per cent, and portal flow by 23 per cent of control values (Imamura & Clowes 1975). Thus circulatory disturbances leading to inadequate tissue perfusion, have obviously influenced the morphological liver changes, this view is also supported by the study of Russo *et al* (1976), who demonstrated substantial ultrastructural changes of hepatocytes in dogs subjected to haemorrhagic hypotension. The widespread occurrence of sinusoidal stasis and microthrombosis may also in all likelihood have contributed to hypoxaemic lesions. The importance of direct effects of endotoxin to cause cellular injuries is emphasized by the study of De Palma *et al* (1967) on endotoxaemia in rats. In this study significant hepatocytic alterations occurred prior to the blood pressure fall as measured in the external iliac artery. These authors suggested a cytotoxic effect of endotoxin upon the cells of various organs including the liver. The liver is thought to be of particular importance for the clearance of endotoxin from the bloodstream both in humans (Bradfield 1974) and in experimental animals (Mori *et al* 1973). Thus an accumulation of endotoxin occurs in the liver during endotoxaemia. Harken *et al* (1975) have in *in vitro* experiments provided evidence for a profound decrease of the oxygen consumption of intact rabbit hepatocytes as a direct response to *E. coli* endotoxin. Endotoxin was also found to decrease the oxygen consumption of hepatocyte homogenates. Furthermore Lunds-gaard-Hansen *et al* (1972) observed a progressive shift from ATP to the di and monophosphorylated compounds in tissue samples obtained from the liver in dogs subjected to ES, thus providing

Fig 8 Electron micrograph of liver tissue: a projection of a hepatocyte is entering a sinusoid through an endothelial gap $\times 11\ 000$

Fig 9 Higher magnification of the framed part of Fig 8 $\times 45\ 000$

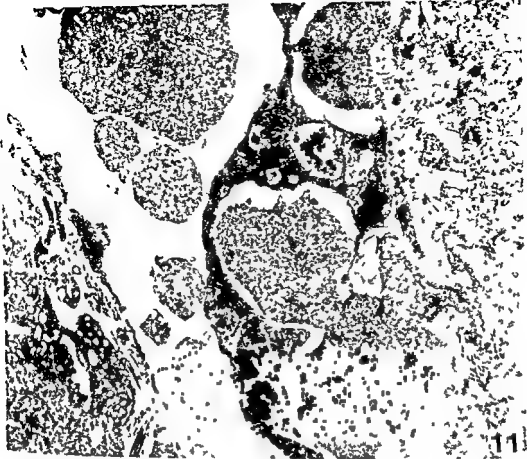


Fig 11 Electron micrograph of hepatic tissue. Several rounded membrane bound structures are seen within a distended space of Disse and a sinusoidal lumen. The endothelium is not obviously damaged. $\times 11\,000$

evidence for an *in vivo* catabolism of energy rich purines during this ailment. These studies indicate furthermore that endotoxin interferes with basic metabolic cellular processes of the hepatocytes in addition to producing haemodynamic changes leading to altered tissue perfusion of the liver.

A massive release of proteolytic enzymes has been reported in several experimental animals subjected to ES (Gans & Krivir 1961; Spink & Vick 1961) and Hjort & Rapaport 1965) and in humans suffering from septicæmia (Hjort & Rapaport 1965; McCabe 1973 and Hirsch et al 1974). Janoff et al (1962) demonstrated augmented release of lysosomal enzymes which might cause cell injury from liver specimens obtained from rats and rabbits after injection of endotoxin. Inadequate tissue perfusion is thought to lead to release of lysosomal enzymes (de Druve 1959). Furthermore in our study an evident accumulation of leucocytes was noted in the liver in the late stages of shock. As reported in detail

elsewhere we have noticed release of granulocyte elastase during endotoxin shock in dogs (Aasen & Ohlsson 1978). The proteolytic activity of this enzyme is known to cause degradation of basement membranes and arterial walls (Janoff & Zelig 1968). It thus appears likely that release of proteolytic enzymes has significantly influenced the cellular damage observed in this study.

Membrane damage of the hepatocytes leads to release of cytoplasmic material from these cells as illustrated in Figs 10 and 11. This observation provides evidence for the identification of the described debris material observed in the liver sinusoids and Disse space as cytoplasmic constituents of hepatocytes. Owing to the importance of the hepatocytes for the synthesis of plasma proteins the marked damage of hepatocytes leading to subsequent cytoplasmic release is a finding of particular significance for the changes of several plasma proteins previously described in this ES model.



Fig 12 Electron micrograph of hepatic tissue part of an occluding microthrombus in a dilated sinusoid the microthrombus consists predominantly of erythrocytes a fibrin like material platelets (P) and debris (D) possibly of hepatocytic origin There is severe injury of the hepatocytes (HC) including formation of lipid droplets (LD) the endothelium (E) is partly necrotic R denotes retilum $\times 14\ 000$

(Aasen *et al* 1977 and 1978a b c) The hepatocytes are responsible for the synthesis of several proenzymes including coagulation factors (Deutsch & Gabl 1976). Thus release of cytoplasmic constituents from hepatocytes might have influenced the coagulation disturbances observed in plasma samples (Aasen *et al* 1978c) and the occurrence of microthrombi described in the present study. It is interesting to note that the masses within the hepatic sinusoids described as microthrombi frequently were found to contain more or less damaged red cells, platelets and leucocytes (Fig. 12). At times also remnants of hepatic parenchymal cells appeared to be a part of microthrombi. The possibility exists that some of the undentifiable debris which so commonly was seen within sinusoidal lumina could originate from other cellular elements than hepatocytes such as endothelial cells. It seems however most probable that the bulk of this material represented disintegrated parenchymal hepatic cells.

Endothelial lesions which were frequently observed in the liver sinusoids in samples obtained during the late stages of shock are also thought to initiate the events leading to coagulation changes (Colman 1974). Recent studies in humans (McHenry *et al* 1971) suggest that septic endovascular lesions are often refractory to medical therapy and that such lesions may be an important factor in the lethal outcome of cases of gram negative septicæmia. Endothelial damage has obviously been a major mechanism for providing the erythrocytes an opportunity to enter the space of Disse (Fig. 7).

The changes of the liver demonstrated in the present study are striking and indicate the participation of several pathogenetic mechanisms. The ultimate consequence of these lesions appears to be of significant importance for the lethal outcome of endotoxin shock.

The present study has been financially supported by Dr Alexander Mathies Fund, Norsk Forening til Krefstens Bekæmpelse and by the Agricultural Research Council of Norway.

REFERENCES

- Aasen A O & Ohlsson K. Release of granulocyte elastase in canine endotoxin shock. *Hoppe Seyler's Z. Physiol. Chem.* 359: 683-690, 1978.
- Aasen A O, Mellbye O J & Ohlsson K. Changes in complement levels during various stages of lethal canine endotoxin shock. *Scand. J. Immunol.* 8: 509-513, 1978a.
- Aasen A O, Frølich W, Saugstad O D & Amundsen E. Plasma kallikrein activity and prekallikrein levels during endotoxin shock in dogs. *Eur. Surg. Res.* 10: 50-62, 1978b.
- Aasen A O, Dale J, Ohlsson K & Gallimore M. Effects of slow intravenous administration of endotoxin on blood cells and coagulation in dogs. *Eur. Surg. Res.* 10: 194-205, 1978c.
- Aasen A O, Gallimore M, J. Ohlsson K & Amundsen E. Alterations of plasmin activity, plasminogen levels and activity of antiplastins during endotoxin shock in dogs. *Thrombos. Haemostas.* 38(1): 46, 1977.
- Bradfield J W B. Control of spillover: The importance of Kupfer-cell function in clinical medicine. *Lancet* II: 883-885, 1974.
- Chevillat N F. Cell Pathology. The Iowa State University Press, Ames, 1976.
- Colman R W. Formation of human plasma kinin. *N. Engl. J. Med.* 5: 509-515, 1974.
- de Duve C. Lysosomes: A new group of cytoplasmic particles in subcellular particles. Ronald Press Company, New York, 1959.
- De Palma R B, Col J, Davis J H & Holden W. Cellular and ultrastructural changes in endotoxemia: A light and electron microscopic study. *Surgery* 62: 505-515, 1967.
- Deutsch Von E & Gabl F. Die Leber als Synthesorgan für Gerinnungs- und Fibrinolysefaktoren. *Med. Labor* 29(2): 23-25, 1976.
- Filkins J P & Cornett R P. Depression of hepatic gluconeogenesis and the hypoglycemia of endotoxin shock. *Am. J. Physiol.* 227: 778-781, 1974.
- Gans H & Krivit W. Effect of endotoxin on the clotting mechanism II. On the variation in response in different species of animals. *Ann. Surg.* 153: 453-458, 1961.
- Hardaway Col R M & Johnson Capp B. Clotting mechanism in endotoxin shock. *Arch. Int. Med.* 112: 775-782, 1963.
- Harken A H, Lallo R S & Hufnagel H V. Direct influence of endotoxin on cellular respiration. *Surg. Gynecol. Obstet.* 140: 858-860, 1975.
- Hirsch E F, Nakajima T, Oshima G, Erdos E G & Herman C M. Kinin system responses in sepsis after trauma in man. *J. Surg. Res.* 17: 147-153, 1974.
- Hjort P F & Rapoport S I. The Shwartzman reaction: Pathogenetic mechanisms and clinical manifestations. *Ann. Rev. Med.* 16: 135-168, 1965.
- Holmes D D & Smith P D. Inclusion bodies in hepatic cytoplasm of dogs and rats after administering endotoxin. *Am. J. Vet. Res.* 30: 811-815, 1969.
- Imamura M & Clowes G H A Jr. Hepatic blood flow and oxygen consumption in starvation, sepsis and septic shock. *Surg. Gynecol. Obstet.* 141: 27-34, 1975.
- Ishiyama S, Nakayama I, Inamoto H, Inai S, Kawabe T & Murata I. Studies on endotoxin shock. In: Williams J D & Geddes A M. *Chemotherapy Vol. 1: Clinical aspects of infec.*

- tions Plenum Press New York and London 1976 pp 169-174
- 21 Janoff A, Weissmann G, Ziefach B W & Thomas L Pathogenesis of experimental shock IV Studies on lysosomes in normal and tolerant animals subjected to lethal trauma and endotoxemia *J exp Med* 116 451-466 1962
 - 22 Janoff A & Zelig J D Vascular injury and lysis of basement membrane *in vitro* by neutral protease of human leucocytes *Science* 161 702-704 1968
 - 23 Aadis S, Weinbaum G & Ayl S J Microbial Toxins Vol V Bacterial Endotoxins Academic Press New York and London 1971
 - 24 Kobold E E, Lovell R, Kar W & Thal A P Chemical mediators released by endotoxin *Surg Gynecol Obstet* 118 807-813 1964
 - 25 Lendrum A C, Fraser D C, Slidders W & Henderson R Studies on the character and staining of fibrin *J clin Path* 15 401-419 1962
 - 26 Levy E, Path F C & Ruebner B H Hepatic changes produced by a single dose of endotoxin in the mouse *Am J Pathol* 51 269-285 1967
 - 27 Lillehei R C, Longerbeam J A, Bloch J H & Manax W G The modern treatment of shock based on physiologic principles *Clin Pharmacol Ther* 5 63-101 1964
 - 28 Lundsgaard Hansen P, Pappova E, Urbaschek B, Heitman L, Laederach A, Molnes N, Oro M & Wirth U Circulatory deterioration as the determinant of energy metabolism in endotoxin shock *J Surg Res* 13 282-288 1972
 - 29 McCabe W R Serum complement levels in bacteraemia due to gram negative organisms *N Eng J Med* 288 21-23 1973
 - 30 McHenry M C, Gavan T L, Van Ommen R A & Hawk W A Therapy with gentamicin for bacteremic infections: results with 53 patients *J Inf Dis* 124 Suppl 164-173 1971
 - 31 Mori K, Matsumoto K & Gais H On the in vivo clearance and detoxification of endotoxin by lung and liver *Ann Surg* 177 159-163 1973
 - 32 Romslo I Regulering av syntesen av enkelte plasmaproteiner - normalt og ved patologiske tilstander *Farmatoterapi* 32 53-64 1976
 - 33 Rothschild M A & Waldmann J Plasma protein metabolism Regulation of synthesis, distribution and degradation Academic Press New York and London 1970
 - 34 Russo M A, Conforti A, Bellavia A & Grasset G Subcellular reactions to injury I Ultrastructural and biochemical investigations on the hepatic cellular damage produced by haemorrhagic shock in dogs *J Pathol* 121 107-113 1976
 - 35 Spink W W & Vick J A labile serum factor in experimental endotoxin shock: cross transfusion studies in dogs *J exp Med* 114 501-508 1961
 - 36 Urbaschek B, Urbaschek R & Neter E Gram negative Bacterial Infections and Mode of Endotoxin Actions Springer Verlag Wien New York 1973
 - 37 von Kaulla A A Chemistry of Thrombolysis Human Fibrinolytic Enzymes Charles C Thomas Springfield Ill 1963 pp 246-247

THE DIAGNOSTIC VALUE OF CYTOCHEMICAL STAINING FOR NON-SPECIFIC ESTERASE IN THE SEARCH FOR CANCER CELLS IN EFFUSIONS

PER P. CLAUSEN, KNUD HØJGAARD and NIELS THOMMESEN

Department of Pathology Hvidovre Hospital University of Copenhagen DK 2650 Hvidovre

Clausen P P, Højgaard K & Thommesen N. The diagnostic value of cytochemical staining for non specific esterase in the search for cancer cells in effusions. *Acta path microbiol scand Sect. A* 87 347-352 1979.

143 consecutive effusion samples were stained for non specific esterase (NSE) in order to test the diagnostic value of the staining method with reference to the diagnosis of carcinosis in pleural and peritoneal cavities. On comparing the results obtained by cytomorphological evaluation and NSE staining the former was proved to have a significant higher diagnostic specificity. The diagnostic sensitivity of the two methods showed no difference. The low diagnostic specificity of the NSE staining was due to occasionally intense staining of macrophages and mesothelial cells in connection with reactive states of the mesothelium. The NSE staining is not recommendable as a diagnostic supplement to the cytomorphological evaluation.

Key words: Effusions, cytochemistry, non specific esterase, cancer diagnosis.

Knud Højgaard, Department of Pathology, Hvidovre Hospital, DK 2650 Hvidovre.

Received 30.1.79 Accepted 29.11.79

The diagnosis of malignant cells in pleural and peritoneal effusions is sometimes difficult. Histochemical staining methods have with variable results been used as a supplement in order to improve the diagnostic efficiency (4, 5, 6).

Bakalos & al (1) claimed that it was possible to distinguish malignant cells from benign cells in effusions by the use of cytochemical staining for non-specific esterase (NSE). It was stated that malignant cells in general have a much higher activity of NSE than benign cells. The purpose of the present investigation is to test the diagnostic value of cytochemical staining for NSE in cells of effusions with reference to the diagnosis of carcinosis of pleural or peritoneal cavities.

MATERIAL AND METHODS

The investigation was performed on a consecutive material of 100 pleural and 44 peritoneal effusions from 112 patients. The samples were examined at the

Pathological Department, Hvidovre Hospital in the period August 1976 to September 1977. The gross specimens were received without additives or fixatives of any kind. After centrifugation of each gross specimen seven smears were made: three stained with haematoxylin-eosin (HE), three with May-Grunwald-Giemsa stain (MGG) and one stained for NSE according to the method of Wachstein (8). In each staining series two negative control preparations have been made: one without substrate, one without diazonium salt.

In the routine diagnostic work three HE and three MGG stained smears have been examined during the period of investigation.

For this investigation

For this investigation a morphological evaluation the following classification has been used: negative, suspicious cells and cancer cells. In the following statement the suspicious cells and the cancer cells have been grouped together as positive cells. The graduation of the activity of NSE has been performed looking at all cells in the smear. The score of the smear was determined according



Fig 1 Graduation of nonspecific esterase according to the scoring system used

A 0 B + C ++ D +++

to the staining intensity in the cell or the cells showing maximum activity. The following scoring system was used (Fig 1) 0 = no activity + one or several fine distinct stained granules in the cytoplasm ++ numerous fine and/or few smaller clumps of granules and +++ numerous granules and several large clumps of granules.

In case of disagreement between the evaluations of the three examiners a definite decision was made following reexamination and discussion.

The final diagnosis and evaluation regarding presence of carcinosis at the moment of examination has in 46

disease. The remaining 79 samples came from patients who had no signs of a malignant condition.

The results of morphologically evaluation and assessment of NSE activity of the effusions are shown in Table I.

On morphological evaluation 13 specimens were positive and 130 negative. In 12 out of 13 positive cases carcinosis was proved. The diagnostic specificity was thus $12/13 = 92.3\%$ (64.0 - 99.8)*.

130 specimens were negative and in 107 cases no carcinosis was demonstrated corresponding to the diagnostic sensitivity $107/130 = 82.3\%$ (74 - 88.4).

On evaluation of NSE activity 10 specimens were unsuitable (in the following statements included in group 0/+). 64 showed activity grade 0 and + 3 were graded ++ and 30 were graded +++.

Using the activities ++ and +++ as an indicator of malignancy the diagnostic specificity is $21/69 = 30.4\%$ (19.9 - 42.7). The corresponding diagnostic sensitivity is $60/74 = 81.1\%$ (70.3 - 89.3). If only the activity grade +++ is used as

clinical history supplemented by laboratory investigations. These cases have been followed for up to two years. The statistical evaluation was based on comparison of 95% confidence limits.

RESULTS

49 of the total 143 effusion samples came from patients with carcinoma. In 35 of these cases the patients were proved to have carcinosis. 15 samples came from patients with a malignant systemic

* (Figures in brackets indicate 95% confidence limits)

TABLE 1 *Evaluation of Cytomorphology and Assessment of Non Specific Esterase in 143 Consecutive Effusions*

Non specific esterase activity (NSE)	Patients with carcinosis		Patients without carcinosis	
	Cytomorphological evaluation		Cytomorphological evaluation	
	Positive	Negative	Positive	Negative
0/+	1	13	0	60
++	7	7	1	24
+++	4	3	0	23

	<i>Diagn specificity</i>	<i>Diagn sensitivity</i>
Cytomorphological evaluation	92.3% (64.0-99.8)*	82.3% (74.6-88.4)
NSE activity (+ + / + + + = positive)	30.4% (19.9-42.7)	81.1% (70.3-89.3)
NSE activity (+ + + = positive)	23.3% (9.9-42.3)	75.2% (66.2-82.8)

*) (Figures in brackets indicate 95% confidence limits)

measure for malignancy the diagnostic specificity is 7/30 = 23.3% (9.9-42.3) and sensitivity 85/113 = 75.2% (66.2-82.8)

The results show that the morphological evaluation has a significantly higher diagnostic specificity than the assessment of activity of cytoplasmatic (NSE). The diagnostic sensitivity of the two methods shows no significant difference.

Furthermore we have tried to evaluate the influence of the degree of verification with reference

to presence of carcinosis on the results in Table 1

In Table 2 the statement has been based on patients on whom autopsy or laparotomy has been made shortly after the cytological examination. On comparing the results obtained in the statements in Table 1 and 2 no significant difference is found.

In Table 3 and 4 the evaluation of morphology and NSE activity is correlated to the diseases of the patients.

TABLE 2 *Evaluation of Cytomorphology and Assessment of Non Specific Esterase in Effusions from Patients with Diagnoses Verified by Autopsy or Laparotomy*

Non specific esterase activity (NSE)	Patients with carcinosis		Patients without carcinosis	
	Cytomorphological evaluation		Cytomorphological evaluation	
	Positive	Negative	Positive	Negative
0/+	1	5	0	24
++	4	5	0	4
+++	4	1	0	11

	<i>Diagn specificity</i>	<i>Diagn sensitivity</i>
Cytomorphological evaluation	100% (66.4-100)	79.3% (65.9-89.2)
NSE activity (+ + / + + + = positive)	43.8% (26.4-62.3)	80.0% (61.4-92.3)
NSE activity (+ + + = positive)	31.3% (11.0-58.7)	67.4% (52.0-80.5)

TABLE 3 *Cytomorphology and Non-Specific Esterase Activity in Pleural Cells Correlated to Diagnoses**Pleura with carcinosis*

Diagnoses	Number	Cytological diagnosis			Non specific esterase			
		Negative	Susp	Tumour cells	0	+	++	+++
C pulm	6	6	0	0	2	3	0	1
C mammae	4	3	0	1	2	0	2	0
C Ovarii	3	1	0	2	1	0	1	1
C prostat	1	1	0	0	1	0	0	0
C renis	1	1	0	0	0	0	1	0
Malignant mesothelioma	2	2	0	0	2	0	0	0
Total	17	14	0	3	8	3	4	2

Pleura without carcinosis

Diagnoses	Number	Cytological diagnosis			Non specific esterase			
		Negative	Susp	Tumour cells	0	+	++	+++
Mb cordis	23	23	0	0	6	5	3	9
Pulmonary embolism	5	5	0	0	2	2	0	1
Pleuritis exsudativa	8	7	1	0	3	1	3	1
Pneumonia	11	11	0	0	0	0	4	1
Carcinoma without carcinosis	11	11	0	0	3	1	1	6
Malignant systemic diseases	14	14	0	0	3	5	5	1
Other diseases	11	11	0	0	4	4	2	1
Total	83	82	1	0	27	18	18	20

DISCUSSION

We have compared the diagnostic value of cytomorphological evaluation and assessment of NSE activity as test methods by measuring their predictive value of positive and negative tests quantitatively expressed as diagnostic specificity and sensitivity

The NSE staining method was proved to have a significant lower diagnostic specificity. As seen from Table 3 and 4 this is due to the fact that macrophages and mesothelial cells in connection with reactive conditions and prolonged exudation in several cases show a high esterase activity. On the other hand although a major part of the cases with carcinosis have a high esterase activity, several

TABLE 4 Cytomorphology and Non Specific Esterase Activity of Peritoneal Cells correlated to Diagnoses

Peritoneum with carcinosis

Diagnoses	Number	Cytological diagnosis			Non specific esterase			
		Negative	Susp	Tumour cells	0	+	++	+++
C ovarii	11	5	0	6	1	11	7	3
C ventriculi	3	2	1	0	11	1	2	0
C vesicae felleae	2	0	0	2	0	0	1	1
Primary tumour unknown	2	2	0	0	0	1	0	1
Total	18	9	1	8	1	2	10	5

Peritoneum without carcinosis

Diagnoses	Number	Cytological diagnosis			Non specific esterase			
		Negative	Susp	Tumour cells	0	+	++	+++
Cirrhosis hepatis	14	14	0	0	1	7	3	3
Mh cordis	4	4	0	0	1	1	2	0
Carcinoma without carcinosis	3	3	0	0	1	0	2	0
Malignant systemic diseases	1	1	0	0	0	1	0	0
Other diseases	3	3	0	0	1	1	0	0
Total	25	25	0	0	5	10	7	3

specimens from patients with histologically verified carcinosis only show slight enzymatic activity. This finding is in agreement with the work of Sandergaard (7) who on a more limited number of specimens found several false positive and false negative results.

Bakalos & al (1) mentioned pulmonary embolism as the only benign condition in which high NSE activity could be found in pleural cells. We have found that almost any reactive condition in the mesothelium may be associated with high esterase activity.

For this reason it is of minor practical value that the NSE activity in our investigation was elevated in 10 cases with false negative cytomorphological evaluation. Although NSE staining in these cases seem usable as a supplementary method, high NSE activity would never in itself be a reliable indicator of malignancy.

Other investigators (2, 3) staining for both NSE and several other enzymes have in agreement with our investigation been unable to demonstrate enzymatic patterns which discern malignant from benign cells.

In order to make the morphological and enzymatic test methods comparable we have in this investigation only examined one smear. Consequently the number of false negative tests was somewhat higher than previously found in the routine diagnostic work.

In conclusion we can confirm the observation that carcinosis often is associated with high NSE activity. Equally high esterase activity may, however, be found in reactive conditions of practically any kind. Therefore, staining for NSE is not recommendable as a supplement to the morphological evaluation.

REFERENCES

- 1 Bakalos D, Constantakis N & Tsiaricas Th. Recognition of malignant cells in pleural and peritoneal effusions. *Acta Cytol* 18: 118-121 1974.
- 2 Bauer Z, Milic N, Handl S, Koprčina M. The results of some cytochemical reactions in metastatic malignant tumor cells in pleural and peritoneal effusions. *Acta Cytol* 21: 141-146 1977.
- 3 Blom D I, Schaberg A & Willighagen R G J. Enzyme cytochemistry of benign and malignant cells in pleural and peritoneal fluid. *Acta Cytol* 11: 460-465 1967.
- 4 Foot N C. The identification of mesothelial cells in sediments of serous effusions. *Cancer* 12: 429-437 1959.
- 5 Marsan C & Cayphas J. The aid of some histochemical stains in the identification of mesothelial cells. *Acta Cytol* 18: 252-258 1974.
- 6 Mavrommatus F S. The identification of mesothelial cells by the technic of Mowry. *Acta Cytol* 6: 443-446 1962.
- 7 Sondergaard A. On the interpretation of atypical cells in pleural and peritoneal effusion. *Acta Cytol* 21: 413-416 1977.
- 8 Wachstein M & Wolf G. The histochemical demonstration of esterase activity in human blood and bone marrow smears. *J Histochem Cytochem* 6: 457 1958.

EXTREME DUCT PAPILLOMATOSIS OF THE JUVENILE BREAST

HENRIK W. KJÆR, WILLIAM W. KJÆR, FOLKE LINELL and STEN JACOBSEN

Department of Pathology, Svenborg Hospital, DK-5700 Svendborg, Denmark; Department of Pathology and Department of Plastic Surgery, General Hospital, Malmö, Sweden

Kjær H. W., Kjær W. W., Linell F. & Jacobsen S. Extreme duct papillomatosis of the juvenile breast. *Acta path. microbiol. scand. Sect. A* 87: 353-359 1979.

Three cases of peculiar and very severe ductal papillomatosis of the breast are reported. This ductal papillomatosis was unusual both in its histological architecture and in occurring in juveniles, viz. girls aged 11, 14 and 17 years. In two of the patients breast cancer was diagnosed 27 and 11 years later. In one of them the ductal papillomatosis must be presumed to have been precancerous, while in the other patient there was possibly from the outset an unusually papilliferous intraductal carcinoma of low malignancy.

Key words: Ductal papillomatosis, breast carcinoma, precancerous breast lesions, young girls.

Henrik W. Kjær, Department of Pathology, University Hospital, DK-5000 Odense, Denmark.

Received 9 XII 78 Accepted 10 III 79

Breast tumours – benign or malignant – rarely occur in children and girls under 20 years of age. Fibroadenomas are most common, solitary ductal papillomas more rare and carcinomas extremely rare (3, 5, 10, 13). Both fibroadenomatosis and ductal papillomatosis (multiple microscopic and possibly grossly visible ductal papillomas) are extremely rare in children and adolescents (5). Our 3 patients, aged 11 to 17 years, with peculiar, severe ductal papillomatosis, in two of whom breast cancer was diagnosed later, seem to warrant publication.

CASE REPORTS

Case 1: L.P., born 7.9.1927

A lump was removed from the right breast in 1938 when the patient was 11. Microscopic examination did not show well-defined tumour formation but widespread and in most sites extremely ectatic ducts partially or completely filled with one or more large papillomas with thick connective tissue stalks. The papillomas were lined with an epithelium which was in most sites stratified cuboidal and columnar with many densely

arranged epithelial proliferations, often confluent and forming small secondary lumina. In places there was a slight variation in cell and nuclear size but no mitoses and no necroses. In some areas there were myoepithelial cells, in other sites a peripheral layer of cuboidal cells. The highly branched papillomas had small clefts apparently packed with epithelium but there were no ductal adenomas. Basement membranes were intact throughout (Figs 1, 2). In 1943 – at the age of 16 – the patient had a ductal papilloma of the usual type with haemorrhagic infarction removed from the left breast.

In 1966, at the age of 38, left mastectomy because of infiltrating duct carcinoma. A biopsy taken at the same time from the right breast revealed severe intraductal epithelial proliferations in most sites cribriform but in places papilliferous with mild epithelial atypia and focal necroses consistent with a cribriform/papilliferous intraductal carcinoma. In smaller areas besides there was invasive tumour tissue made up predominantly of adenomatous gland formations (Fig. 3). No remnants of the ductal papillomatosis demonstrated 27 years previously nor in the mastectomy specimens.

Postoperative radiotherapy and bilateral salpingo-oophorectomy. Since December 1968 several local recurrences of tumour in the scar on the left and skeletal metastases. Received steroid and chemotherapy. Terminal hyperpyrexia. Died on 10.2.1974.



Main post-mortem findings Metastases from a primary breast carcinoma in all ribs on the left in the entire spine, in the liver, bilateral pleural carcinosis and a local left-sided recurrence In addition a primary carcinoma of the right kidney, lobar pneumonia on the right, and pulmonary candidiasis

Case 2 EMG born 11.2.1957

In November 1971 - when the patient was 14 - removal of a lump detected accidentally in the right breast The nodule was $2 \times 3\frac{1}{2} \times 3\frac{1}{2}$ cm greyish white, firm shiny, with a few small cysts Microscopic examination showed widespread and in places severe ectatic ducts containing one or more papillomas varying in size and having highly branched delicate connective-tissue stalks lined with a simple or two layered cuboidal and columnar epithelium This epithelium contained widespread, small luminal proliferations often confluent and forming small secondary lumina In some of the

Fig 1 Case 1 First excision of the right breast at age 11 Ducts filled with large papillomatous structures having broad connective tissue stalks Very pronounced epithelial proliferation with papillary processes In the stroma multiple buds some papillary others solid ($\times 50$)

Fig 2 Same as Fig 1 in higher magnification ($\times 125$)

Fig 3 Case 1 Right breast at age 38 Intraductal carcinoma with invasion of tubular structures ($\times 50$)



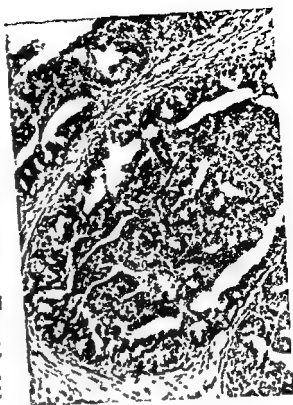


Fig 4 Case 2 Right breast at age 14 Intraductal papillary proliferations ($\times 125$)

Fig 5 Case 2 Right breast at age 14 Very pronounced ovoid and solid intraductal papillary proliferations ($\times 125$)

Fig 6 Case 3 Intraductal papilloma with fibrous stalk and pronounced epithelial proliferations ($\times 50$)



papillomatous areas there were more massive epithelial proliferations in many sites with irregularly branched and complex glandular lumina. In places there was a slight variation in cell size and nuclear size but no atypia and no mitoses or necroses. In smaller areas there were microepithelial cells. In other sites apocrine metaplasia and accumulation of foam cells in the lumina. In most sites the interlobular connective tissue stroma was ample loose cellular with dilated capillaries and mild focal lymphocytic infiltration. No definite evidence of malignancy (Figs 4-5). Ever since the patient has been in good health. No deliveries and no hormone treatment.

Case 3 M.L. born in 1948

In 1965 when she was 17 several tumours in both breasts were noted and one from each breast was removed for microscopic examination. This did not alter the palpatory findings in the breast as a number of more or less solid tumours remained. In 1969 the patient was treated for thyrotoxicosis with subtotal thyroidectomy and thereafter maintained on substitution with thyroxine (Levothyron) and had no further thyroid trouble. The same



Fig 7 Case 3 Mainly solid intraductal proliferation with the appearances of intraductal carcinoma ($\times 50$)

year the patient had several tumours removed from both breasts. On the left very little mammary tissue remained. During follow up new tumours were noted in both breasts but they grew slowly. In 1976 the patient had subcutaneous mastectomy with removal of all remaining mammary tissue. The breasts were reconstructed with Cronin prostheses. The postoperative course was uneventful.

Histological studies of numerous sections were made after all the operations and after the subcutaneous mastectomy the entire breast was cut into large sections. The histological appearances were essentially the same in all operative specimens. In addition to a large fibroadenoma of the peri and intracanalicular type with pronounced epithelial proliferations there were numerous dilated ducts most of which were filled with large papillomas with fibrous connective tissue stalks and vigorous epithelial proliferations. In places the ducts were filled with solid epithelial proliferations showing moderate atypia interpreted in the subcutaneous mastectomy specimens as a fairly well-differentiated intraductal carcinoma. Infiltrating carcinoma was never seen. Essentially the same changes were found on revision of the previous operative preparations in which malignancy could not be definitely ruled out (Figs 6-10).

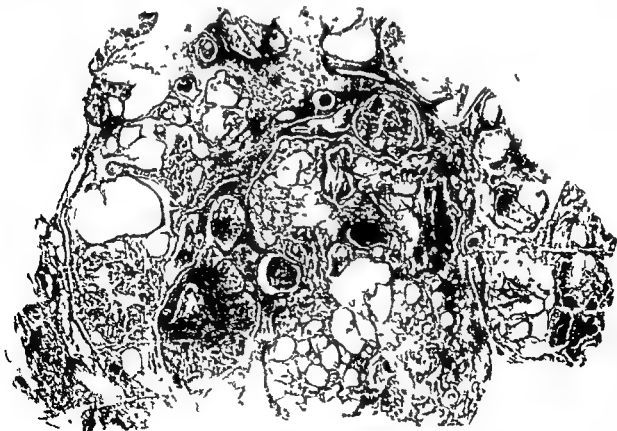


Fig 8 Case 3 Specimen from subcutaneous mastectomy showing multiple large papillomas and solid intraductal proliferations. Also dysplastic lesions with numerous cysts lined with apocrine epithelium ($\times 35$)

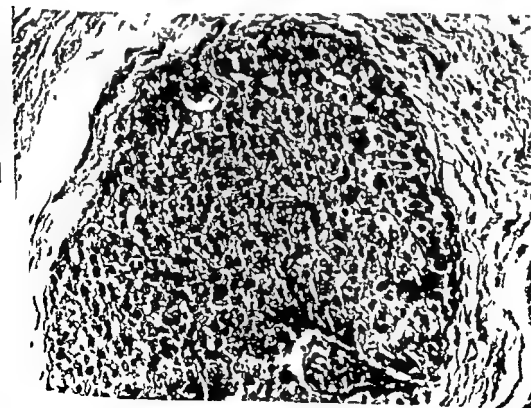




Fig 7 Case 3 Mainly solid intraductal proliferation with the appearances of intraductal carcinoma ($\times 50$)

year the patient had several tumours removed from both breasts. On the left very little mammary tissue remained. During follow up new tumours were noted in both breasts but they grew slowly. In 1976 the patient had subcutaneous mastectomy with removal of all remaining mammary tissue. The breasts were reconstructed with Cronin prostheses. The postoperative course was uneventful.

Histological studies of numerous sections were made after all the operations and after the subcutaneous mastectomy the entire breast was cut into large sections. The histological appearances were essentially the same in all operative specimens. In addition to a large fibroadenoma of the peri and intracanalicular type with pronounced epithelial proliferations there were numerous dilated ducts most of which were filled with large papillomas with fibrous connective-tissue stalks and vigorous epithelial proliferations. In places the ducts were filled with solid epithelial proliferations showing moderate atypia interpreted in the subcutaneous mastectomy specimens as a fairly well differentiated intraductal carcinoma. Infiltrating carcinoma was never seen. Essentially the same changes were found on revision of the previous operative preparations in which malignancy could not be definitely ruled out (Figs 6-10).

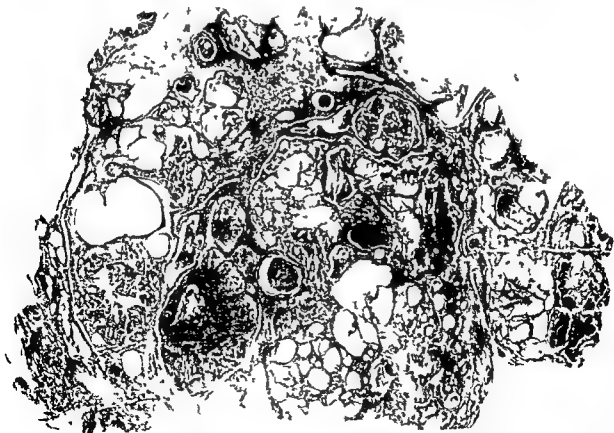


Fig 8 Case 3 Specimen from subcutaneous mastectomy showing multiple large papillomas and solid intraductal proliferations. Also dysplastic lesions with numerous cysts lined with apocrine epithelium ($\times 35$)

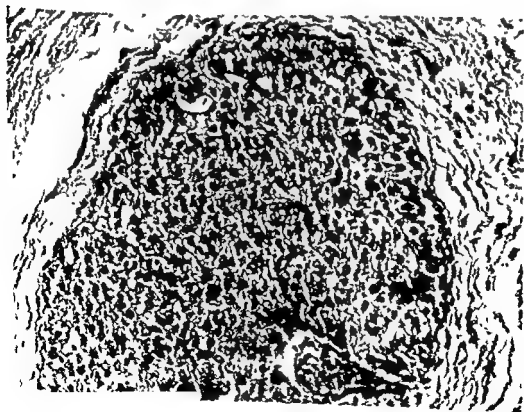
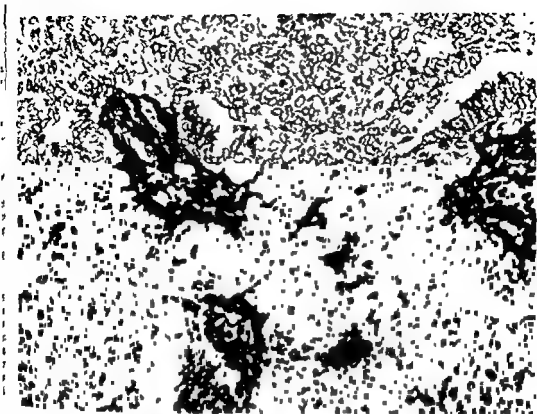


Fig 9 Case 3 Extremely florid intraductal epithelial proliferations on fibrous stalks Biopsy at age 17 years The appearances were essentially the same at 28 years ($\times 320$)

Fig 10 Case 3 Solid epithelial intraductal proliferations showing the appearances of intraductal carcinoma at the age of 17 Unchanged during 11 years ($\times 320$)

DISCUSSION

Breast carcinoma under the age of 20 is very rare. Among *Farrow & Ashkari* (1969) 237 girls aged 10–20 years only 1.3% had malignant tumours and 5.5% ductal papillomatosis. *Bassler* (1973) has collected 49 cases of carcinoma from the literature and *Stone et al* (1977) found only one carcinoma in material of 143 girls aged 14–20 years.

However there is good reason to assume that breast cancer undergoes development of 5–20 years before it is manifest clinically as cancer (*Betsill et al* 1978). It is not unlikely therefore that occasionally precancerous breast changes or peculiar low malignant papilliferous intraductal carcinomas may be found in teenage girls.

Only a few reports on such lesions have been published. The few case reports of papillomatous breast tumours in girls under 20 have concerned solitary intraductal papillomas of the usual type. The patients have been children from 7 months of age up to girls of 19 (3, 5, 6, 8, 9, 12). At the time of publication none of these patients had developed recurrence or cancer but the follow up period has varied widely (from 5 months to 18 years). *Diethrich et al* (1966) have described a case of »prepubertal florid intraductal papillomatosis« in a 10 year-old girl. No recurrence had appeared 2½ years later. The only photomicrograph included in the paper shows 3 dilated lactiferous ducts containing loosely arranged slender branched connective tissue stalks lined with a few rows of cuboidal/columnar epithelial cells. It is somewhat similar to our Case 2 in whom however the epithelial proliferations were much more vigorous. The ductal papillomatosis in our Cases 1 and 3 differs from *Diethrich et al*'s case in the much larger and thicker connective tissue stalks as well as in the far more vigorous epithelial proliferations. *Farrow & Ashkari* (1969) mentioned a patient of 16 with »extremely atypical »papillomatosis« without recurrence 2 years after

condition showed the same slender connective tissue stalks as in our Case 2 but otherwise differed from our cases in the same ways as *Diethrich et al*'s *Haagensen*'s cases had fibrosing adenosis not present in our cases and widespread apocrine metaplasia present among our material only in Case 3.

Although the architecture of the connective tissue stalk in the ductal papillomatosis in Case 2 differs somewhat from that in Cases 1 and 3 and although Case 3 exhibited widespread fibroadenomatosis we do think that the similarities are so marked that these cases must be interpreted as variants of the same lesion.

Case 3 is of particular interest because in the repeated operative specimens there were changes in which »the diagnosis of carcinoma versus atypical papillomatosis is a question of occult distinction and must be accepted or rejected on the grounds of faith or lack of it in the pathologist« (*McDevitt et al* 1968) and because these changes have remained unaltered for 11 years. Cases 1 and 3 did in places show a certain similarity to *Haagensen*'s (1971) »papillary type of mammary carcinoma with broad connective tissue stalks. According to *Haagensen* this type of tumour is the least malignant of all breast cancers and usually affects elderly women.

We are unable to decide whether these tumours detected during adolescence are interpretable as a peculiar juvenile precancerous ductal papillomatosis or as low malignant papilliferous intraductal carcinomas of an unusual type. Our Case 1 might indicate the former possibility. Case 3 the latter. It must be presumed that children and young girls with this form of ductal papillomatosis/low malignant papilliferous intraductal carcinoma do run a certain risk of developing manifest breast cancer after a latent period of many years. The magnitude of this risk is not for us to estimate as our material is very small and the follow up period in Case 2 relatively short (7 years symptom free).

None of our patients had had endocrine disturbances or hormone therapy which might be imagined to bear any causal relation to their breast lesion.

multiple intraductal papillomas 4, 5, 6, 7, 8, 9, 10, 11, 12, 13, 14, 15, 16, 17, 18, and 19. The papillomas in this

REFERENCES

- 1 *Beisil W L, Rosen P P, Lieberman P H & Robbins G F* Intraductal carcinoma: long term follow up after treatment by biopsy alone. *JAMA* 239 1863-1867 1978
- 2 *Bussler R* Pathologie der weiblichen Genital und Mammatumoren in Kindesalter und Adoleszenz. *Gynakologe* 6 49-65 1973
- 3 *Donel W A & Mathews M D* Tumors of the breast in adolescent females. *Pediatrics* 41 743-749 1968
- 4 *Debruch E B, Hammond W W & Holst F* Intraductal papillomatosis of the breast. Report of a case in a ten year old girl. *Amer J Surg* 112 80-82 1966
- 5 *Farrow J H & Ashikari H* Breast lesions in young girls. *Surg Clin N Amer* 49 261-269 1969
- 6 *Haagensen C D, Stout A P & Phillips J S* The papillary neoplasms of the breast. *Ann Surg* 133 18-36 1951
- 7 *Haagensen C D* Diseases of the breast 2nd ed. W B Saunders Company Philadelphia London Toronto 1971 pp 276-291
- 8 *Hendrick J W* Intraductal papilloma of the breast. *Surg Gynec & Obst* 105 215-223 1957
- 9 *Howard M A & Rosenblatt M S* Management of intraductal papilloma. *Amer J Surg* 92 142-150 1956
- 10 *McDivitt R W & Stewart F W* Breast carcinoma in children. *JAMA* 195 388-390 1966
- 11 *McDivitt R W, Stewart F W & Berg J W* Tumors of the breast. Second series. Fascicle 2. Armed Forces Institute of Pathology Washington DC 1968 p 23
- 12 *Simpson J S & Barson A J* Breast tumours in infants and children: a 40 year review of cases at a children's hospital. *Can Med Ass J* 101 100-102 1969
- 13 *Stone A M, Shenker J R & McCarthy K* Adolescent breast masses. *Amer J Surg* 134 275-277 1977

A RETROSPECTIVE HISTOLOGICAL STUDY OF 669 CASES OF PRIMARY CUTANEOUS MALIGNANT MELANOMA IN CLINICAL STAGE I

6 The Relation of Dermal Solar Elastosis to Sex Age and Survival of the Patient and
to Localization Histological Type and Level of Invasion of the Tumour

TOVE EEG LARSEN and TOVE HELLIESEN GRUDE

Institute of Pathology University of Oslo Rikshospitalet Oslo and The Norwegian Radium Hospital
Oslo Norway

Larsen T E & Grude T H A retrospective histological study of 669 cases of primary cutaneous
malignant melanoma in clinical stage I 6 The relation of dermal solar elastosis to sex age and
survival of the patient and to localization histological type and level of invasion of the tumour Acta
path microbiol scand Sect A 87 361-366 1979

A selected series of primary malignant melanoma of the skin clinical stage I was studied The series
includes 37 lentigo maligna melanomas 301 superficial spreading malignant melanomas 194 nodular
malignant melanomas and 137 unclassifiable malignant melanomas Dermal solar elastosis was graded
The most common finding was lack of solar elastosis which together with slight elastosis was mostly
found on the trunks of young men and on the legs of young women in cases of superficial spreading
malignant melanoma Marked and moderate elastosis was found almost exclusively on the head
especially in old women with lentigo maligna melanoma Nodular malignant melanoma was related
neither to any special grade of solar elastosis nor to localization but showed some relation to the male
sex after 50 years of age The present study does not permit any conclusions to be made about a
possible causal relationship between the three types of malignant melanoma and previous sun-exposure
because of lack of clinical information and a control series concerning solar elastosis in the normal
population Level of invasion and prognosis of the patient did not show any covariation with grade of
solar elastosis

Key words Melanoma solar elastosis

Larsen T E Institute of Pathology Rikshospitalet Oslo Norway

Received 16 ii 79 Accepted 17 iii 79

It has been known for many years that lentigo
maligna

Worthington (1952) was the first to point out that all types
of primary cutaneous malignant melanoma (NIM)
are probably related to solar radiation

Mitchell (1963) found abnormal melanocytes in
apparently normal human skin which had been
exposed to prolonged solar radiation and Epstein
(1966) produced malignant blue naevi in hairless

mouse skin with DMBA and UVB light The
carcinogenic range of the UV spectrum includes
especially UVB (290-320 nm) and to a less extent
UVA (320-400 nm) UVB and especially UVA
also cause damage to the papillary dermis and the
dermal interface (Clark's level II and III) Clark *et al*
(1969) The result of solar elastosis (Sams *et al*
1964 Pathak & Epstein 1971)

Solar elastosis is characterized by a reduction and
change in the dermal collagen and elastic fibres
with an increased amount of an interfibrillary
amorphous material (for further references see

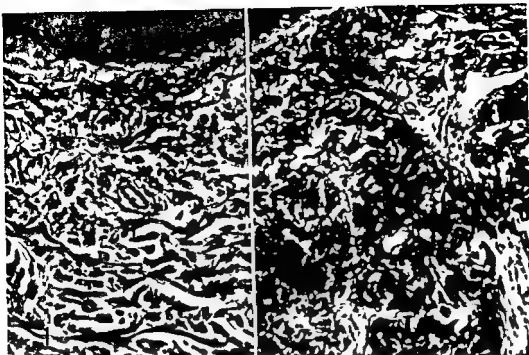


Fig 1 Slight solar elastosis in the upper dermis (Verhoeff's stain) At this grade of change the elastic fibres may be difficult to distinguish from normal elastic fibres when special staining is used $\times 190$

Fig 2 Heavy solar elastosis in the upper dermis (Verhoeff's stain) $\times 110$

The grade of epidermal pigmentation affects the amount of UV light which reaches the nuclei in the basal cell layer and the dermal tissue (Thomson 1955) as well as the incidence of MM and other skin cancers (for further references see Gellin *et al* 1969 Nordlund & Lerner 1977). We have no exact information about previous sun-exposure in each case of the present series. Further we know nothing about individual variations in skin complexion and ability to tan among our patients. Finally at the

moment we have no possibility of comparing the inter relationship between grade of solar elastosis age and localization on the present series with that in a series of otherwise normal individuals. We have however still found it interesting to look for certain trends in these relationships in our series as well as to study the relation of solar elastosis age and localization to histological tumour type.

The chance that in some of our cases an elastotic change is primarily caused by previous X ray

TABLE 2 The Relation of Solar Elastosis to Localization

Grade of solar elastosis	Total		No. in each localization					
	No.	%	Head	Arm	Lower extrem	Neck trunk	Foot	Other
0	353	57.8	10	27	112	163	37	4
+	164	24.3	35	44	46	33	3	2
++	101	15.1	91	3	0	7	0	0
+++	22	3.3	22	11	0	0	0	0
?	30	4.5	6	5	3	7	8	1
Total	669	100.0	164	79	161	210	48	7

Lever & Schaumburg Lever 1975) In HE stained sections solar elastosis appears sub epidermally as swollen greyish fibres which may come together to form an amorphous mass. They stain black with Verhoeff's stain (Figs 1-2)

The present paper deals with the relationship of solar elastosis to sex and age of the patient and to localization and histological type of the tumour in our series. Further we have studied the relation of solar elastosis to level of invasion of the tumours and to prognosis of the patients.

SERIES AND METHODS

The present series includes 669 cases of MM in clinical stage I (413 women and 256 men) registered at the *Cancer Registry of Norway* 1955-72. The tumours have been classified according to Clark (Clark 1967, Clark *et al* 1969*) without access to any clinical information (Larsen & Grude 1978 a). The group of LMM has been reclassified (Larsen & Grude 1979) leading to a total series of 37 LMM, 301 SMM, 194 NMM and 137 UMM. The relation of tumour type to sex, age and prognosis of the patient and to localization and level of invasion of the tumour was reported in our two papers mentioned.

The sections were stained with hematoxylin-eosin-saffron. Special staining was not used in order not to misinterpret normal elastic fibres as elastotic fibres at a low grade of elastosis. The elastotic change was graded 0, +, ++ and ++++. The change in the stroma around the tumour was evaluated rather than in the interstitial stroma of the tumour. Tumour induced collagenization or the presence of granulation or scar tissue after ulceration or clinical regression may give a false impression of a low grade of elastosis. The term 'indefinite' was used whenever the surrounding stroma was insufficient and the interstitial stroma of the tumour could not be evaluated. Grading was done without access to any clinical information.

*) The following abbreviations are used: Lentigo maligna melanoma - LMM, superficial spreading malignant melanoma - SMM, nodular malignant melanoma - NMM and unclassifiable malignant melanoma - UMM.

RESULTS

The relative frequency of the various grades of solar elastosis and the relationship of these to age of the patients and to tumour localization are shown in Tables 1 and 2 respectively. The most common finding was lack of elastotic change (353 ~ 52.8%) which was found especially among patients below 50 years of age and on the trunk and the lower extremities. Among 123 cases with grade ++ or +++ of elastosis 92% were found among elderly patients and on the head. Table 3 shows that these trends are highly significant while no significant pattern is found as regards the relation between elastosis and sex of the patient.

The relation of elastosis to tumour type and level of invasion was also studied (Table 3). There was a highly significant coexistence of LMM and a moderate or marked elastosis while SMM showed a weak tendency to develop in skin with no elastotic change. The occurrence of NMM seemed to be independent of this feature. As regards the relation of solar elastosis to level of invasion only SMM were considered. No trends were found.

Fig. 3 shows the observed cumulative survival rates according to the various grades of solar elastosis. The differences in survival rates are not significant.

DISCUSSION

Solar elastosis is probably a cumulative unavoidable effect of UV sunlight similar to other non-malignant skin alterations caused by ionizing radiation (Marshall 1965, International Commission on Radiological Protection 1977) provided the received dose is large enough (non-stochastic effect). If so, the grade of elastosis increases with the received total dose of UV light. On the other hand, one single dose of UV light may be carcinogenic to melanocytes as well as to keratinocytes by mere chance (stochastic effect) (for further references see United Nations 1977).

TABLE 1 The Relationship of Solar Elastosis with Age

Grade of solar elastosis	Total		No. at each age group						
	No.	%	0-19	20-29	30-39	40-49	50-59	60-69	70-89
0	353	52.8	11	30	90	99	75	28	20
+	163	24.3	3	8	22	44	42	30	14
++	101	15.1	1	1	4	12	21	20	42
+++	22	3.3		1	1	1	3	6	10
++++	30	4.5	1		7	8	3	2	9
Total	669	100.0	16	40	124	164	144	86	95

site between the two series may be referred to the difference in latitude and number of sun hours between Norway and Queensland (for further references see Lancaster 1956 Magnus 1973 Elwood *et al* 1974) Further in the Australian series as well as in ours and that of Kligman (1969) the grade of elastosis increases with growing age (Table 1) In our series the gradual increase takes about 10 years from one grade to the next one This supports the theory that elastosis is an accumulated effect of UV light

As regards the relation of elastosis and localization of tumour type McGovern (1970) concludes that UV light is most important to the LMM and least important to the SMM

In our series LMM is almost exclusively found on the head and especially among 60–80 years old patients Therefore it is not surprising that this tumour is combined with grade ++ and +++ of elastosis The duration of the pre invasive lentigo maligna is approximately 20 years and the invasive LMM may have been present for 10 years at diagnosis (Clark & Mihm 1969 McGovern *et al* 1973) Therefore the growth of a lentigo maligna may have started at the age of 40–50 years in our series

Our patients with SMM are younger than those with LMM viz approximately 30–60 years old Most of our SMM are located on skin areas which are usually exposed to sunlight more irregularly than the face i.e. the lower leg and the trunk It seems therefore reasonable that we have found no trends in the relationship of SMM to grade of elastosis except for a weak linkage to grade 0 Because the pre invasive stage of SMM is assumed to last 10–12 years (McGovern *et al* 1973) and grade + of elastosis takes probably at least 15 years to develop on the trunk and lower leg some patients with SMM may not have had time enough to develop any observable grade of elastosis or at least only grade + As furthermore the invasive SMM may have been present for about 10 years at diagnosis i.e. in our 74 cases with level IV V of invasion (Clark *et al* 1975) the growth of a non invasive SMM may have started at the age of 20–40 years in our series

Our SMM show no special relation to solar elastosis and localization They show however some relation to the male sex after 50 years of age This may contribute to the bad prognosis of old men with MM found by Magnus (1977)

Our findings do not permit any conclusions to be made about a possible causal relationship between the three types of MM and previous sun-exposure None of our findings however preclude that such relationship exists If so the difference in postulated

age at start of tumour growth between LMM and SMM indicates a different susceptibility of the cells of origin to UV light or a different latency time from induction of a neoplastic cell clone to start of tumour growth

The Prognostic Value of Solar Elastosis

In 1958 Mackie & McGovern postulated that solar elastosis led to nutritional defects in the dermis which might mediate tumour induction in the epidermis and enhance dermal invasive growth of malignant non melanotic tumours On the other hand sun induced squamous cell carcinomas of the skin tend to metastasize less than squamous cell carcinomas which are related to chronic ulcers scars and old burns (Stoll 1971) Knutson *et al* (1971) and Little (1972) found as we did that solar elastosis has no prognostic significance in SMM The relatively poor prognosis of our 22 cases with grade +++ of elastosis may first of all be due to the relatively old age of this group of patients

CONCLUSIONS

- 1) Our malignant melanomas were most commonly not associated with dermal solar elastosis in the surrounding stroma No or slight elastosis was particularly found on the trunks of young men and the lower extremities of young women and coexistent with a superficial spreading malignant melanoma
- 2) Marked or moderate solar elastosis was almost exclusively found on the head particularly among elderly women and coexistent with lentigo maligna melanoma
- 3) The nodular malignant melanoma was to some extent related to older men but showed neither relation to any special grade of solar elastosis nor to location of the tumour
- 4) A causal relationship between UV light and the three types of malignant melanoma is neither excluded nor proven by the present study
- 5) Solar elastosis had no prognostic significance in our study

We are grateful to Dr A. Magnus The Cancer Registry of Norway Oslo for invaluable help and advice

REFERENCES

- Beardmore G L Little J H & Anderson P Cutaneous melanocytes in Queensland patients Aust J Derm 17 69–81 1976
- Clark W H A classification of malignant melanoma

TABLE 3 *The Relation of Solar Elastosis to Sex Age Localization Tumour Type and Level of Invasion The Relation of Tumour Type to Sex and Age and to Localization*

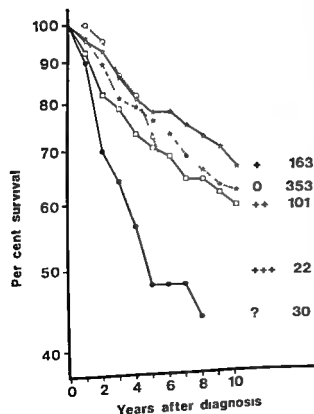
	X ^{2a}	D f ^b	P	Obvious trends among the determinate grades and types
Solar elastosis related to				
Age	112.71	3	<0.001	grade 0 ~ age < 50 years grade + - - - + ~ age > 50 years
Sex	9.66	3	>0.02	
Localization	♀ 298.17 ♂ 151.96	8 6	<0.001 <0.001	♀ grade 0 ~ neck trunk lower extremity ♂ grade 0 ~ neck trunk all grade + ~ arm grade + - - - + ~ head (grade 0 ~ SMM) grade + - - - + ~ LMM
Tumour type	127.65	4	<0.001	
Level of invasion ^c	4.09	4	>0.1	
Tumour type related to				
Sex and age	46.26	6	<0.001	LMM ~ ♀ > 50 years (SMM ~ ♀ < 50 years) (NMM ~ ♂ > 50 years) LMM ~ head SMM ~ lower extremity
Localization	123.16	8	<0.001	

^a The indeterminate grades and types eliminated (the complete tables are available from the author)

^b Degrees of freedom

^c SMM only

Solar elastosis



treatment (Mitchell 1963) ■ considered to be minimal

Grade + of elastosis takes probably at least 10-15 years to develop (Marshall 1965). Therefore in the present series we cannot conclude that a particular skin site has not been exposed at all when no elastotic change is found. Further solar elastosis seems to a limited degree to be reversible (Gerstein & Freeman 1963).

The Grading of Elastosis and Various Inter relations

Most of our tumours were not associated with solar elastosis (52%). Only 3% of the patients showed a marked elastosis. Marked elastosis was found almost exclusively on the head while the trunk and the lower extremities showed less changes (Table 2). This relation to localization fits in well with the findings of Beardmore *et al* (1976). Differences in grade of elastosis according to skin

Fig 3 Survival curves illustrating the observed cumulative survival rates according to different grades of elastosis 0 = no elastosis + = slight elastosis ++ = moderate elastosis +++ = heavy elastosis and ? = indeterminate grade of elastosis

FORMATION OF GRANULATION TISSUE IN SUBCUTANEOUSLY IMPLANTED SPONGES IN RATS

*A Comparison between Granulation Tissue Developed in Viscose Cellulose
Sponges (Visella®) and in Polyvinyl Alcohol Sponges (Ivalon®)*

B HOLMUND P JUNKER C GARBARSCH P CHRISTOFFERSEN and
I LORENZEN

Department of Pathological Anatomy and Department of Medicine Section of Rheumatology Hvidovre
Hospital Laboratory of Histochemistry and Cytochemistry Anatomy Department A University of
Copenhagen

Holmund B Junker P Garbarsch C Christoffersen P & Lorenzen I Formation of granulation
tissue in subcutaneously implanted sponges in rats. A comparison between granulation tissue developed
in viscose cellulose sponges (Visella®) and in polyvinyl alcohol sponges (Ivalon®) Acta path microbiol
scand Sect A 87 367 374 1979

A comparison was made between the granulation tissue formation in two different synthetic sponge
types Visella and Ivalon of different sizes. The granulation tissue formed in the two sponge types did
not differ qualitatively and had the character of wound tissue and inflammatory tissue in man. The
rate of tissue formation in the Visella sponges was faster and the tissue was more homogenous than in
the Ivalon sponges. Fourteen day old Visella implants of either size contained more granulation tissue
than Ivalon sponges, probably owing to the smaller pore size of the former material. This may also
account for the more frequent occurrence of giant cells in the Visella implants. In contrast to the Visella
sponges the trabeculae of the Ivalon polymer showed calcification and positive staining properties with
histological staining procedures and deformation was frequent among the Ivalon implants. Thin
sponges of either type closed in about 21 days, thick ones after about 42 days of implantation.
Calculated per 2 cm³ of implant, thin sponges produced more tissue after 14 days of implantation than
thick ones. It is concluded that the Visella sponge type is best suitable for this experimental model of
inflammation.

Key words: Granulation tissue implanted sponges.

Bert Holmund, Department of Pathological Anatomy, Hvidovre Hospital, University of Copenhagen,
DK 2650 Hvidovre.

Received 20 XII 78 Accepted 18 III 79

25 263

(

Subcutaneous implantation of synthetic sponge
material on experimental animals yields a topogra-
phically and chronologically well defined granu-
lation tissue which can be isolated quantitatively. The
two most commonly used implants are polyvinyl
alcohol sponges (Ivalon®) as first described by
Grindlay & Waugh (15) and viscose cellulose
sponges (Visella®) presented by Vihanto (35).

The biochemical properties of experimentally
induced granulation tissue have been studied in
detail including collagen metabolism (1, 16, 24, 31,

published by each of the sponge types have been
published (4, 15, 28, 35, 40) and the effects of
various drugs and hormones have been investigated
using this experimental model (7, 17, 18, 19, 23,
29, 30, 39).

The aim of the present study was to describe and
morphologically compare the development of gra-
nulation tissue in either of the above mentioned
types of sponge and to evaluate the importance of

- man correlated with histogenesis and biologic behavior In *Montagna W* (Ed) *Advances in biology of the skin The Pigmentary System* 1st ed vol VIII Pergamon Press Oxford 1967 pp 621-647
- Clark W H & Mihm M C* Lentigo maligna and lentigo maligna melanoma *Amer J Path* 55 39-67 1969
- Clark W H From L Bernardino E A & Mihm M C* The histogenesis and biologic behavior of primary human malignant melanomas of the skin *Cancer Research* 29 705-726 1969
- Clark W H Ainsworth A M Bernardino E A Yang C H Mihm M C & Reed R J* The developmental biology of primary human malignant melanomas *Semin Oncol* 2 83-103 1975
- Dubreuilh M W* Lentigo malin des vieillards *Ann Dermatol Syph (Paris)* 5 1092-1099 1894
- Elwood J M Lee J A H Walter S S Mo T & Green A E S* Relationship of melanoma and other skin cancer mortality to latitude and ultraviolet radiation in the United States and Canada *Int J Epidemiol* 3 325-332 1974
- Epstein J H* Ultraviolet light carcinogenesis In *Montagna & Dobson* (Ed) *Advances in biology of the skin Carcinogenesis* 1st ed vol VII Pergamon Press London 1966 pp 215-236
- Gellin G A Kopf A W & Garfinkel L* Malignant melanoma A controlled study of possibly associated factors *Arch Derm* 99 43-48 1969
- Gerstein W & Freeman R G* Transplantation of acutically damaged skin *J Invest Derm* 32 445-450 1963
- Hutchinson J* Lentigo melanosis *Arch Surg* 5 253-256 1894
- International Commission on Radiological Protection* Recommendations of the International Commission on Radiological Protection *Annals of the ICRP* 1 2-3 1977
- Kligman A M* Early destructive effect of sunlight on human skin *J Amer med Ass* 210 2377-2380 1969
- Knutson C O Hori J M & Spratt J S* Melanoma *Curr probl Surg* 12 1-55 1971
- Lancaster H O* Some geographical aspects of the mortality from melanoma in Europeans *Aust Med J* 1 1082-1087 1956
- Larsen T E & Grude T H* A retrospective histological tumour and prognosis *Acta Path Microbiol Scand Sect A* 86 437-450 1978
- Larsen T E & Grude T H* A retrospective study of 669 cases of primary cutaneous malignant melanoma in clinical stage I 5 The consequences of a reclassification of the original group of lentigo maligna melanomas *Acta Path Microbiol Scand Sect A* 87 255-260 1979
- Lever W F & Schaumburg-Lever G* Histopathology of the skin 5th ed J B Lippincott Company Philadelphia 1975 pp 249-251
- Little J H* Histology and prognosis in cutaneous malignant melanoma In *McCarthy W H* (Ed) *International cancer conference Sydney 1972 Melanoma and skin cancer Proceedings* 1st ed Blight N C Government Printer Sydney 1972 pp 107-119
- Mackie B S & McGovern V J* The mechanism of solar carcinogenesis *Arch Derm* 78 218-244 1958
- Magnus A* Incidence of malignant melanoma of the skin in Norway 1955-1970 Variations in time and space and solar radiation *Cancer* 32 1275-1286 1973
- Magnus K* Prognosis in malignant melanoma of the skin Significance of stage of disease anatomical site sex age and period of diagnosis *Cancer* 40 389-397 1977
- Marshall D R* The clinical and pathological effects of prolonged solar exposure 1 The association with ageing of the skin *Austr New Zeal J Surg* 34 161-172 1965
- McGovern V J* Melanoblastoma *Med J Aust* 1 139-142 1952
- McGovern V J* The classification of melanoma and its relationship with prognosis *Pathology* 2 85-98 1970
- McGovern V J Mihm M C Bailly C Booth J C Clark W H Cochran A J Hardy E G Hicks J D Levene A Lewis M G Little J H & Milton G W* The classification of malignant melanoma and its histologic reporting *Cancer* 32 1446-1457 1973
- Mitchell R E* The effect of prolonged solar radiation on melanocytes of the human epidermis *J Invest Derm* 41 199-212 1963
- Nordlund J J & Lerner A B* On the causes of melanomas *Am J Path* 89 443-448 1977
- Pathak M A & Epstein J H* Normal and abnormal reactions of man to light In *Fitpatrick T B Arndt K A Clark W H Eisen A Z Van Scott E J & Vaughan J H* (Ed) *Dermatology in general medicine* 1st ed McCraw Hill Inc New York 1971 pp 977-1036
- Sams W M Smith J G & Burk P G* The experimental production of elastosis with ultraviolet light *J Invest Derm* 43 467-471 1964
- Stoll H L* Squamous cell carcinomas In *Fitpatrick T B Arndt K A Clark W H Eisen A Z Van Scott E J & Vaughan J H* (Ed) *Dermatology in general medicine* 1st ed McCraw Hill Inc New York 1971 pp 407-425
- Thomson W L* Relative efficiency of pigment and horny layer thickness in protecting the skin of Europeans and Africans against solar ultraviolet radiation *J Physiol* 127 236-246 1955
- United Nations* Sources and effects of ionizing radiation United Nations scientific committee on the effects of atomic radiation 1977 report to the General Assembly with annexes United Nations New York 1977 580-582

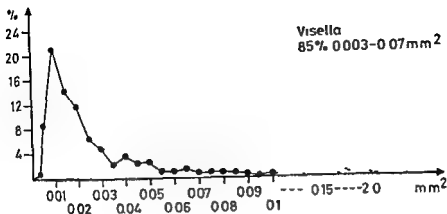


Fig 1 Distribution of pore size of the Visella sponge

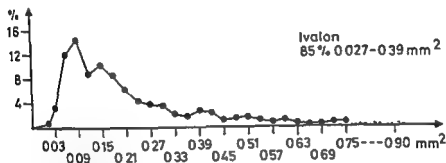


Fig 2 Distribution of pore size of the Ivalon sponge

The sponges are partly surrounded by dense connective tissue with many collagen fibres and scattered fibroblasts. This structure represents the condensed connective tissue in the superficial fascia. The deepest part next to the sponge contains from the second day after implantation many fibroblasts laid down in an amorphous intercellular substance containing scattered collagen fibres and scattered mast cells. Very few mitoses are seen most frequently on days 6-8.

The occurrence and extent of some of the morphological variables observed in the intermediary zone in the thick Visella and Ivalon sponges are given in Fig. 3a + b.

Two days after implantation the granulation tissue is dominated by fibroblasts and histiocytes entering the peripheral part of the sponge. The pores in the central part of the implant are filled with fluid containing a fibrinous network and numerous neutrophils. From the fourth day delicate collagen fibres and capillaries appear in the peripheral part of the sponge and on the tenth day a sparse intercellular substance which is alcianophilic and

stains metachromatically with toluidine blue appears.

The collagen fibres gradually become coarser and from day 42 ha form an

tissue. In some of the Ivalon sponges even in the sponges «closed» with granulation tissue some of the largest pores have a peripheral zone of mature connective tissue and a central zone with amorphous intercellular substance and a few scattered collagen fibres. In most of the Ivalon sponges retraction of the granulation tissue from the trabeculae is prominent. This was not observed in the Viscoelastic sponges.

Fig. 4 shows the width of the zone of granulation tissue in the thick Ivalon and Visella sponges as

«closed» granulation tissue has «closed» the sponge

The granulation tissue contains a few eosinophils and lymphocytes whereas histiocytes occur as the

the size of the implant using two different sizes of each sponge type. In addition the total amount and water content of 14 day old granulation tissue were determined

MATERIAL AND METHODS

Forty male Sprague Dawley rats about 40 days of age and weighing 150–200 g were used

Viscose cellulose sponges (Visella®) and polyvinyl alcohol sponges (Ivalon®) were implanted subcutaneously to produce granulation tissue. The sponges were washed thoroughly with water cut into pieces and sterilized by boiling in physiological saline for 30 minutes before implantation

Two sizes of both types of sponges were used. A large sponge measuring $1 \times 1 \times 2$ cm with a dry weight of 90–100 mg (Visella) and 120–130 mg (Ivalon) and a small sponge measuring $\frac{1}{2} \times 1 \times 2$ cm

At the start of the experiment two sponges of equal size (one Visella and one Ivalon) were implanted symmetrically under the superficial fascia in the infrascapular region of each rat as described by Vilanto (36). The operation was performed under ether anaesthesia. Visella and Ivalon sponges were inserted alternately on either side of the spine. Four rats were kept in each cage with free access to pellets and water. The weight gain was normal during the observation period.

On the 2nd 4th 6th 8th 10th 14th 18th 24th 42nd and 90th day after operation four animals (two with large sponges and two with small sponges) were killed by decapitation. The sponges were removed together with the surrounding connective tissue and each sponge was cut longitudinally and horizontally into two symmetrical parts.

The sponges were fixed for 48 hours in a solution containing 4% formaldehyde and 0.5% cetylpyridinium chloride (41). Dehydrated and embedded in paraffin. Serial horizontal sections were cut at 6–8 μ m starting from the central part of the sponge. The following staining methods were used

- 1) Haematoxylin and eosin
- 2) van Gieson stain for collagen fibres (26)
- 3) Orcein stain for elastic fibres (26)
- 4) ¹Alcian blue for chitin (33)
- 5) to Barger and DeLamater (33)
- 6) 0.3% Alcian blue 8 GX at pH 1 and 2.5 (32) 0.1% Alcian blue 8 GX in 1% acetic acid (21) and 0.1% Alcian blue 8 GX in 1% acetic acid at pH 7.5 (3)
- 7) The calcium red method of Mowbray and Russell (33) for calcification. Control sections were decalcified in a citric acid/sodium citrate buffer at pH 5.7 for 30 min before staining
- 8) A simultaneous demonstration of glycosaminoglycans with Alcian blue, elastic fibres with orcein, collagen fibres with Sirius red, nuclei with haematoxylin and cytoplasm with picric acid. The method was slightly modified after Garbarsch using Sirius red instead of acid fuchsin for collagen fibres (14)

The occurrence in the outer the middle and inner third of the sponge of the following morphological features was registered in a semiquantitative manner (0 + ++ +++) oedema fibrin granular leucocytes lymphocytes histiocytes giant cells fibroblasts collagen fibres capillaries intercellular substance resorption and calcification of the sponge

An estimation of the area of the trabeculae was performed with the Leitz Texture analyzing System (TAS). In addition a classification of the sponge pores was performed with the Leitz ASM Image Analysis System

Finally the propagation of the connective tissue into the sponges was measured. The measurement was performed at a magnification of 40 \times

Twelve other animals were allocated to a separate group in order to determine the total amount and the water content of granulation tissue produced in sponges of different sizes and types after 14 days of implantation. Each of these receives four implants. Sponges of different types were implanted symmetrically and sponges of different sizes in craniocaudal direction: large sponges proximally in half of the animals and distally in the other half thus avoiding differences due to location which may affect the lipid content (5, 12). After the animal had been killed the implants were isolated and adhering tissue was carefully removed. After wet weight determination the tissue was lyophilized to constant weight and the water content was expressed in per cent of dry weight. The net tissue weight was calculated by subtraction of the pre implant weight of the sponges.

Comparison between groups was performed using the Mann Whitney U test

RESULTS

Four animals were excluded from the study owing to infection of the sponges. Deformation of the Ivalon implants was observed in one fourth of the sponges whereas the Visella sponges apart from one sample kept their cubic shape during the period of implantation

In the Visella sponges the trabeculae in mean constitute 13.6% (range 11.5–16) of the total area in the Ivalon sponges 16.3% (range 14.5–21.5). The distribution of the pore size of the Visella sponge is shown in Fig. 1. Most of the pores are small and 85% have an area ranging between 0.0003–0.07 mm² but a few pores up to 2 mm² are seen

In the Ivalon sponge 85% of the pores have an area ranging from 0.027 to 0.39 mm² some large pores up to 0.90 mm² occur (Fig. 2)

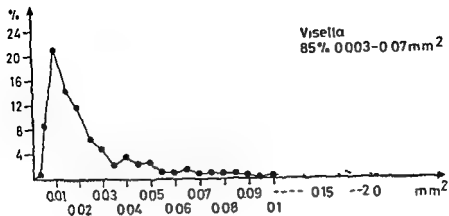


Fig 1 Distribution of pore size of the Visella sponge

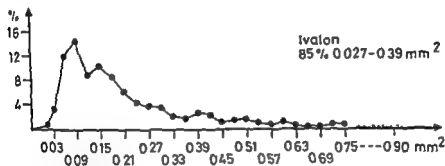


Fig 2 Distribution of pore size of the Ivalon sponge

The sponges are partly surrounded by dense connective tissue with many collagen fibres and scattered fibroblasts. This structure represents the condensed connective tissue in the superficial fascia. The deepest part next to the sponge contains from the second day after implantation many fibroblasts laid down in an amorphous intercellular substance containing scattered collagen fibres and scattered mast cells. Very few mitoses are seen most frequently on days 6-8.

The occurrence and extent of some of the morphological variables observed in the intermediary zone in the thick Visella and Ivalon sponges are given in Fig. 3a + b.

Two days after implantation the granulation tissue is dominated by fibroblasts and histiocytes entering the peripheral part of the sponge. The pores in the central part of the implant are filled with fluid containing a fibrinous network and numerous neutrophils. From the fourth day delicate collagen fibres and capillaries appear in the peripheral part of the sponge and on the tenth day a sparse intercellular substance which is metachromatic and

stains metachromatically with toluidine blue appears.

The collagen fibres gradually become coarser and from day 42 they form a coarse network throughout the sponge. At day 90 all the pores except the largest are filled with a dense mature collagenous tissue. In some of the Ivalon sponges even in the sponges «closed» with granulation tissue some of the largest pores have a peripheral zone of mature connective tissue and a central zone with amorphous intercellular substance and a few scattered collagen fibres. In most of the Ivalon sponges retraction of the granulation tissue from the trabeculae is prominent. This was not observed in the Viscose sponges.

Fig. 4 shows the width of the zone of granulation tissue in the thick Ivalon and Visella sponges as a function of time. The growth is about 0.2 mm/day until the 10th and 14th day respectively after which the rate decreases to about 0.04 mm/day. At day 42 the granulation tissue has «closed» the sponge.

The granulation tissue contains a few eosinophils and lymphocytes whereas histiocytes occur as the

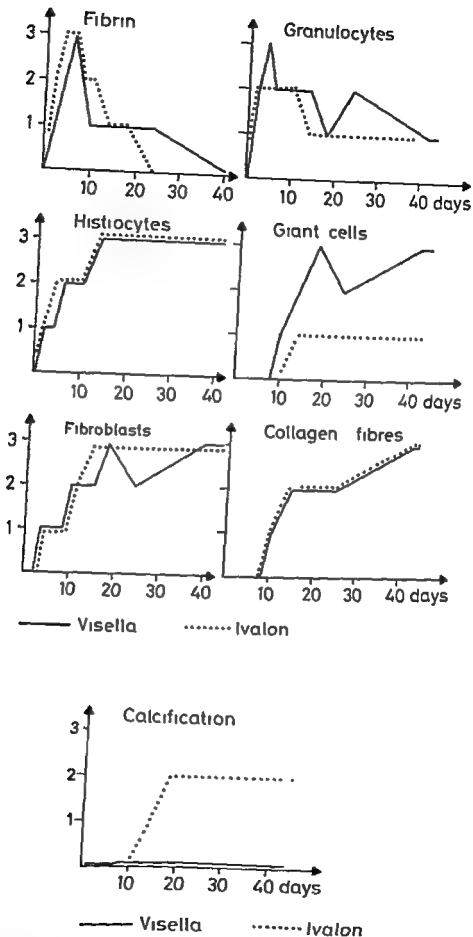


Fig 3 a + b Semiquantitative (0-+ + +) measurements of morphological variables in the intermediary zone in the thick Visella and Ivalon sponge

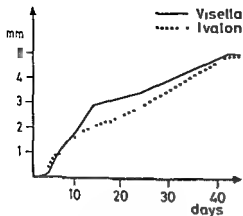


Fig 4 Propagation of granulation tissue into Visella and Ivalon sponges

most predominant cell through the sponge from the 14th day. From day 42 a few granulomatous structures are seen along the trabeculae in the peripheral part.

Giant cells occur in the Viscoelastic sponges as single elements on a few of the most peripheral trabeculae of the sponge from the fourth day. From the 42nd day they occur widespread throughout all zones. At first the giant cells are rather small with 5-6 nuclei. Later on they become larger with up to 20-25 nuclei and a faint basophilic cytoplasmic. On the 90th day large giant cells occur in the intermediary zone and to some degree in the central zone. The Ivalon sponges also contain giant cells but to a much less extent than in the Viscoelastic sponges.

Sponge alterations. The Viscoelastic sponge is unstained by all the staining methods. From the 10th day a slight reduction in thickness of the trabeculae in the Viscoelastic sponges is seen in the peripheral zone. From the 42nd day the reduction occurs throughout the zones. The resorption occurs in relation to giant cells. Calcification of the Viscoelastic sponges is not observed.

In contrast to the Viscoelastic sponge the Ivalon sponge stains basophilic with haematoxylin and toluidine blue and brown with PTAAH and orcein. It is not calcified.

In relation to giant cells. Inclusions with staining properties similar to the trabeculae are seen in the giant cells. The formation and maturing of the granulation tissue in the thin Viscoelastic and Ivalon sponges corresponds in the development in the thick sponges but both acute inflammatory cells and granulation tissue occur earlier in the central part

and the sponges appear «closed» after only 18 to 24 days.

On the 14th post implantation day the total amount of tissue and water in the Viscoelastic sponges of both sizes was higher than in the Ivalon sponges estimated by the net weights before and after drying (Table 1). The same difference was found when the amount of tissue generated by 100 mg of dry implant was calculated for sponges of the same size. A comparison of the amount of granulation tissue contained in 2 cm³ of implant shows that the tissue content in thin sponges exceeds that of thick ones irrespective of sponge type. The water content expressed in per cent of dry weight was higher in thick implants than in thin ones. The difference was however only statistically significant in the Ivalon implants.

DISCUSSION

The pattern of granulation tissue formation was identical in either sponge type and corresponded closely to the phases described by others (24-31). The most marked differences between the two sponge types were the more homogenous structure of the granulation tissue and the faster tissue growth in the Viscoelastic sponge as compared to the Ivalon polymer. The smaller and more homogenous pore size of the Viscoelastic sponge may be important in this respect as the smaller pore size implies a greater surface area thereby facilitating the contact between the implant and the growing tissue. The role of different pore sizes was studied by Salvatore (34) who found increasing growth rate decreasing pore size as in the present study. Most probably the higher water content of the Viscoelastic sponge is due to the larger space available for tissue fluid indicated by the lower dry weight per cm³ and the lower cross sectional area occupied by trabeculae in this sponge type.

The different water percentage in the two sponge sizes may reflect differences of tissue maturity since the water percentage decrease with increasing granuloma age (16).

Ivalon sponges consist of polymerized polyvinyl alcohol cross linked with formaldehyde (6) whereas Viscoelastic sponges are generated from cellulose (36). The colour formation and calcification of the trabeculae in Ivalon sponges in contrast to the non reactive Viscoelastic sponges point to differences of reactive chemical groups. The staining properties of the Ivalon material may present problems in interpreting histochemical sections.

The increased content of foreign body giant cells in the Viscoelastic sponge may be due to both chemical differences between the two sponge types and to

TABLE 1 *Effect of Different Sizes and Types of Sponge Implants on Wet Weight, Dry Weight and Water Content of 14 implants*

	Large sponges		P value	Small sponges		P value
	VISELLA	IVALON		VISELLA	IVALON	
Net wet weight g/granuloma	2 1799 1 9804-2 3299	1 8739 1 7931-2 2684	<0.05	1 1511 1 0703-1 3064	0 9717 0 8960-1 1427	<0.01
Net dry weight g/granuloma	0 2465 0 2214-0 2862	0 2034 0 1747-0 2358	<0.01	0 1461 0 1303-0 1801	0 1185 0 1060-0 1436	<0.01
Dry weight (g) for 100 mg implant	0 2594 0 2331-0 3013	0 1627 0 1398-0 1886	<0.01	0 3076 0 2764-0 3797	0 1896 0 1696-0 2298	<0.01
Net dry weight g/2 cm ² implant	0 2465 0 2214-0 2862	0 2034 0 1747-0 2358		0 2922 0 2606-0 3602	0 2370 0 2120-0 2872	= 0.025 = 0.05
Water content g/granuloma	1 9366 1 7662-2 0459	1 6785 1 6055-2 0392	<0.025	1 0069 0 9427-1 1263	0 8567 0 8019-0 9840	<0.01
H ₂ O % of dry weight	784 677-832	836 747-978	0.05 < P < 1.0	699 625-740	731 656-797	NS 0.05 < P < 0.1 < 0.01

Median values are given with their 95% confidence limits. Each group comprises 10 animals. Implant characteristics: *Visella* 10 × 10 × 20 mm 0.095 g and 5 × 10 × 20 mm 0.0475 g. *Ivalon* 10 × 10 × 20 mm 0.125 g and 5 × 10 × 20 mm 0.0625 g. The net weights were calculated by subtracting the average implant weight from the gross wet weight and dry weight. P values refer to differences between groups underlined at the same level.

differences in pore size (4, 34). Since their presence did not seem to change the character of the granulation tissue in any other respect, they cannot be considered to be an important drawback from a histological point of view.

Deformation was a frequent event among the Ivalon implants. Compression will alter the pore size distribution, which may contribute to the inhomogeneous tissue structure.

Thus, the faster formation of a more homogeneous granulation tissue, the lack of deformation in the Visella sponges and the staining properties and calcification on the Ivalon sponges speak in favour of using the Visella sponge for production of experimental granulation tissue.

Thin sponges closed earlier than thick ones, probably owing to the shorter distance of migration

relatively greater surface area of the former whereby cellular invasion from the adjacent structures is facilitated. Consequently, thin sponges are particularly suited for short-term experiments.

Apart from implant characteristics, animal properties may influence the development of granulation tissue. Of importance in this respect are animal species (9, 27, 43), age (20, 35), sex (10, 12, 27), nutritional state (10, 12, 27) and possibly seasonal variations (43). Therefore, the experimental conditions should be carefully considered before comparisons are made between different studies.

Several experimental models are currently used in the study of inflammatory and reparative processes in connective tissue (13, 36, 37). The sponge model has the advantage that the inflammatory tissue is topographically well defined. Hence it is possible to determine both the quantity of granulation tissue formed and individual constituents at different stages of development. The

- 25 Lehtonen A The mucopolysaccharides in ageing experimental granulation tissue *Acta Physiol Scand* 310 (suppl) 1-78 1968
- 26 Lillie R D Histopathologic technic and practical histochemistry 3rd ed McGraw Hill Book Company New York Toronto Sydney London 1965
- 27 Noble N L & Boucek R J Lipids of the serum and connective tissue of the rat and rabbit *Circ Res* 3 344-350 1955
- 28 Pallin B Ahonen J Rank F & Zederfeldt B Granulation tissue formation in viscose cellulose sponges of different design *Acta Chir Scand* 141 697-701 1975
- 29 Pallin B Ahonen J Rank F & Zederfeldt B Granulation tissue formation in oophorectomized rats treated with female sex hormones I A histological study *Acta Chir Scand* 141 702-709 1975
- 30 Pallin B Ahonen J & Zederfeldt B Granulation tissue formation in oophorectomized rats treated with female sex hormones II Studies on the amount of collagen and on tensile strength *Acta Chir Scand* 141 710-714 1975
- 31 Paulini K Korner B Beneke G & Endres R A quantitative study of the growth of connective tissue Investigations on implanted polyester polyurethane sponges *Connect Tissue Res* 2 257-264 1974
- 32 Pearse A G E Histochemistry Theoretical and applied 3rd ed vol 1 Churchill Livingstone London 1968
- 33 Pearse A G E Histochemistry Theoretical and applied 3rd ed vol 1 J & A Churchill London 1972
- 34 Salvatore J E Gilmer W S Kashgarian M & Barbee W R An experimental study of the influence of pore size of implanted polyurethane sponges upon subsequent tissue formation *Surg Gynecol Obstet* 112 463-468 1961
- 35 Viljanto J & Kulonen E Correlation of tensile strength and chemical composition in experimental granuloma *Acta Pathol Microbiol Scand* 56 120-126 1962
- 36 Viljanto J Biochemical basis of tensile strength in wound healing An experimental study with viscose cellulose sponges on rats *Acta Chir Scand* 33 (suppl) 1-101 1964
- 37 Viljanto J & Rajamaki A Cellular patterns in the early phase of healing wounds in children *Scand J Plast Reconstr Surg* 10 83-89 1976
- 38 Vizoli M R Boileau L & Valdrighi L Alkaline phosphatase activity and the development of rat sponge induced granulation tissue *Acta Anat* 8: 60-69 1972
- 39 Wagner von H & Hauss W H Zur pharmakologische Beeinflussung der Entstehung von Granulationsgewebe *Z Rheumatol* 32 163-168 1973
- 40 Wiener S L Wiener R Platt N Urvelsky M & Meilman E The need for a modification of the polyvinyl sponge model of connective tissue growth *Connect Tissue Res* 3 213-225 1975
- 41 Williams G & Jackson E S Two organic fixatives for acid mucopolysaccharides *Stain Technol* 31 189-191 1956
- 42 Woessner J F & Boucek R J Enzyme activity of rat connective tissue obtained from subcutaneously implanted polyvinyl sponge *J Biol Chem* 234 3296-3300 1959
- 43 Woessner J F jr & Boucek R J Connective tissue development in subcutaneously implanted polyvinyl sponge *Arch Biochem Biophys* 93 85-94 1961

MITOTIC ACTIVITY AND DELAY IN FIXATION OF TUMOUR TISSUE

The Influence of Delay in Fixation on Mitotic Activity of a Human Osteogenic Sarcoma Grown in Athymic Nude Mice

NIELS GRÆM and KARIN HELWEG LARSEN

Pathological anatomical Institutes, Kommunehospital, Rigshospitalet and Frederiksberg Hospital
Copenhagen, Denmark

Græm N & Helweg Larsen K Mitotic activity and delay in fixation of tumour tissue. The influence of delay in fixation on mitotic activity of a human osteogenic sarcoma grown in athymic nude mice. *Acta path microbiol scand Sect A* 87 375-378 1979

The purpose of the present investigation was to study the effect of delay in fixation on the mitotic activity in tumour tissue. A human osteogenic sarcoma, especially suitable for counting of mitoses, grown in athymic nude mice, was fixed with varying delay and the mitotic prophase, metaphase and anaphase indices were determined. An almost exponential decline of the mitotic index was observed with a reduction to 49.4% and 15.0% after respectively 60 and 180 minutes. The proportional incidence of prophases, metaphases and anaphases changed so that a relative accumulation of advanced phases occurred during the 180 minutes of observation. It is concluded that delay in fixation of a magnitude which is not uncommon in routine surgical pathology may allow the majority of mitoses to terminate, resulting in unreliable assessments of mitotic activity.

Key words: Mitosis, malignant tumour, fixation, delay, nude mouse.

Niels Græm, Department of Pathology, Rigshospitalet, Frederiks V's Vej 11, DK 2100 Copenhagen O, Denmark.

Received 9 July 79 Accepted 22 July 79

Assessments of mitotic activity are often used in routine surgical pathology. The diagnosis of malignancy in epithelial tumours is most often given by evident invasion; however, mitotic activity is an important parameter in the grading of carcinomas. Counting of mitoses is thus recommended by the highly authoritative series of WHO's International Classification of Tumours in grading of breast carcinomas (Scarff & Torloni 1968), oral and pharyngeal squamous carcinomas (Wahr *et al* 1971) and adenocarcinomas of the corpus uteri (Poulsen *et al* 1975).

Differentiation between benign and malignant mesenchymal tumours can be difficult because the usual criteria of malignancy, such as invasion and cellular atypia, may be inapplicable. Mitotic activity becomes an important diagnostic help. Thus En-

zinger *et al* (1969) in WHO's International Classification of Tumours state that the presence of mitoses is an important parameter in differentiation between fibromatoses and fibrosarcomas and between leiomyomas and leiomyosarcomas. In routine surgical pathology the validity of assessments of mitotic activity is, however, poor (Siherberg 1976) which may be due to different definitions of mitosis and to the fact that the activity is often given as the number of mitoses per high power field without indication of the exact size of this. But other factors may also depreciate the assessment, e.g. delay in fixation. Fixation is delayed when the specimen is deposited in the operating room or is transported unfixed to the laboratory of pathology. Furthermore, fixation of central areas of big tumours will be delayed owing to slow penetration of fixatives. The duration of the

delay is often unknown but according to our experience it may very well be 1 or 2 hours. In order to assess how delay in fixation influences mitotic activity the mitotic prophase, metaphase and anaphase indices were determined in a human osteogenic sarcoma parts of which were fixed with varying delay. The tumour was grown in athymic nude mice.

MATERIAL AND METHODS

Tumour and Mice

The tumour was an osteogenic sarcoma obtained from the thigh bone of a 28 year old man. The tumour was uniform consisting of densely and irregularly packed polymorphic spindle shaped cells with big and hyperchromatic nuclei. Osteoid formation was very scanty, necroses were inconspicuous. Many mitoses were seen as described in detail below. Following the technique described by Povlsen & Rygaard (1971) solid blocks of the tumour were grafted subcutaneously to nude mice of BALB/c background bred and kept at Pathological anatomical Institute, Kommunehospitalet, Copenhagen under conditions described by Rygaard (1973).

During 20 months until this experiment the tumour tissue has gone through 13 passages of serial transplantation still preserving the original histological structure.

Experimental Design

Seven 14 weeks old female nude mice with 7 weeks old tumour grafts measuring approximately 18 mm in the largest diameter were sacrificed by cervical dislocation without anaesthesia at 10.00 a.m. The 7 tumour grafts were removed immediately by means of atraumatic technique and cut in 2 mm slices. One slice from each tumour graft was instantly fixed at 20°C in 20 ml of 10% neutral buffered formalin (10% aqueous formaldehyde solution buffered with 4 grams of NaH_2PO_4 and 6.5 grams of Na_2HPO_4 per 1000 ml). The remaining 6 slices were placed uncovered on a sterile dry surgical cloth until fixation after 20, 40, 60, 90, 120 and 180 minutes. An equal representation of peripheral and central parts of the tumour graft at varying times of delay in fixation was ensured. The air was calm, the relative humidity 62% and the temperature 20°C.

After 24 hours the fixed tissue was embedded in paraffin, cut in 5 μm sections and stained by haematoxylin-eosin.

Mitosis Counting

Ensuring an equal representation of peripheral and central areas, 3000 nuclei including those in mitosis were counted at 400 times magnification in each of the 7 tumour grafts at the 7 moments of fixation.

The mitoses were registered as prophases, metaphases and anaphases as defined by Bloom & Fawcett (1975). The phases of multipolar and asymmetric mitoses were determined following analogous principles.

Pyknotic and bizarre nuclei as well as isolated fragments of chromosomes were not registered as mitoses. The counting was shared by the two authors. Accordance in the criteria was achieved by discussion and subsequent blind counting in pilot studies. Mitotic index, prophase index, metaphase index and anaphase index were defined as the number of respectively mitoses (all phases), prophases, metaphases and anaphases per 1000 counted nuclei including those in mitosis. The indices in the 7 tumour grafts at each of the 7 moments of fixation, the means and the ranges of distribution of these indices at the 7 moments of fixation were calculated. The nonparametric Friedman test was carried out to analyse the variance statistically.

RESULTS

At the time zero the mean of the mitotic index of the 7 tumour grafts was 12.62 (Fig. 1). After 180 minutes it was reduced to 1.89 or 15.0% of the initial figure. The decline which was almost exponential was statistically significant ($p < 0.0005$).

The mean of prophase index (Fig. 2) was reduced during the 180 minutes of observation from 1.10 to

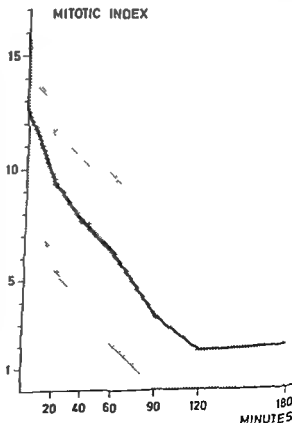


Fig. 1 Mean and range of distribution of the mitotic index in the 7 tumour grafts at varying delay in fixation.

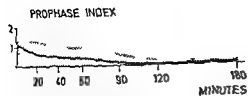


Fig 2 Mean and range of distribution of the prophase index in the 7 tumour grafts at varying delay in fixation

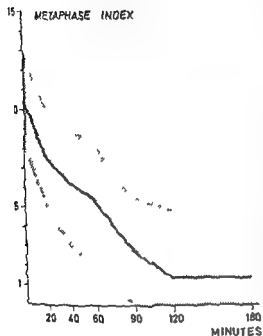


Fig 3 Mean and range of distribution of the metaphase index in the 7 tumour grafts at varying delay in fixation

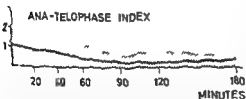


Fig 4 Mean and range of distribution of the ana-telophase index in the 7 tumour grafts at varying delay in fixation

index was reduced from 10.43 to 1.44 or 13.8% of the initial figure, which was statistically significant ($p < 0.0005$).

The decline of the mean of the ana-telophase index (Fig 4) was less regular. During the 180 minutes of observation it was reduced from 1.10 to 0.39 or 35.5% of the initial figure, which was statistically significant ($p < 0.005$).

The proportional composition of the mean of the mitotic index changed during the 180 minutes of observation from 8.7%, 82.6% and 8.7% respectively prophase, metaphase and ana-telophases to 3.2%, 76.2% and 20.6%.

DISCUSSION

Kinetics of Mitoses after Removal of the Tissue

Delay in fixation caused pronounced reduction in the mitotic index. The decline was almost exponential. At 60 and 180 minutes of delay the mitotic index was respectively 49.4% and 15.0% of the initial figure. No further decline could be expected from the curve.

The reduction of the mitotic index was a consequence of the declines of the prophase, metaphase and ana-telophase indices, which, however, during the 180 minutes of observation changed mutual numerical proportions, as the ana-telophase index was relatively increased at the expense of the metaphase and especially the prophase index. In other words, early mitotic phases were seen in reduced numbers, while advanced phases accumulated.

advance through the mitotic phases and enter interphase. The remaining 15% were stopped in mitosis.

Our results are in accordance with those of Bullough (1950) who found a steep decline in the numbers of mitoses in normal tissues and malignant tumours of dead mice during the first 2 hours post mortem.

0.06 or 5.5% of the initial figure. The decline, which was regular and most marked initially, was statistically significant ($p < 0.001$).

The curves of the mitotic (Fig 1) and metaphase index (Fig 3) are much alike. During the 180 minutes of observation the mean of the metaphase

index declined exponentially by a factor of respectively 10 and 17 during 8 hours. The experiment was performed at 4.5°C which may explain the slow decline as compared with our results. On the contrary, Evans (1926) in his early study, found no material variation in the number of mitotic figures during a 24 hours period in two human surgically-

delay is often unknown but according to our experience it may very well be 1 or 2 hours. In order to assess how delay in fixation influences mitotic activity the mitotic prophase metaphase and ana telophase indices were determined in a human osteogenic sarcoma, parts of which were fixed with varying delay. The tumour was grown in athymic nude mice.

MATERIAL AND METHODS

Tumour and Mice

The tumour was an osteogenic sarcoma obtained from the thigh bone of a 28 year old man. The tumour was uniform consisting of densely and irregularly packed polymorphic spindle shaped cells with big and hyperchromatic nuclei. Osteoid formation was very scanty. Necroses were inconspicuous. Many mitoses were seen as described in detail below. Following the technique described by Povlsen & Rjgaard (1971) solid blocks of the tumour were grafted subcutaneously to nude mice of BALB/c background bred and kept at Pathological anatomical Institute Kommunehospitalet Copenhagen under conditions described by Rjgaard (1973).

During 20 months until this experiment the tumour tissue has gone through 13 passages of serial transplantation still preserving the original histological structure.

Experimental Design

Seven 14 weeks old female nude mice with 7 weeks old tumour grafts measuring approximately 18 mm in the largest diameter were sacrificed by cervical dislocation without anaesthesia at 10.00 a.m. The 7 tumour grafts were removed immediately by means of atraumatic technique and cut in 7 mm slices. One slice from each tumour graft was instantly fixed at 20°C in 20 ml of 10% neutral buffered formalin (10% aqueous formaldehyde solution buffered with 4 grams of NaH_2PO_4 and 6.5 grams of Na_2HPO_4 per 1000 ml). The remaining 6 slices were placed uncovered on a sterile dry surgical cloth until fixation after 20, 40, 60, 90, 120 and 180 minutes. An equal representation of peripheral and central parts of the tumour graft at varying times of delay in fixation was ensured. The air was calm, the relative humidity 62% and the temperature 20°C.

After 24 hours the fixed tissue was embedded in paraffin, cut in 5 μm sections and stained by haematoxylin-eosin.

Mitosis Counting

Ensuring an equal representation of peripheral and central areas 3000 nuclei including those in mitosis were counted at 400 times magnification in each of the 7 tumour grafts at the 7 moments of fixation.

The mitoses were registered as prophases, metaphases and ana telophases as defined by Bloom & Fawcett (1975). The phases of multipolar and asymmetric mitoses were determined following analogous principles.

Pyknotic and bizarre nuclei as well as isolated fragments of chromosomes were not registered as mitoses. The counting was shared by the two authors. Accordance in the criteria was achieved by discussion and subsequent blind counting in pilot studies. Mitotic index, prophase index, metaphase index and ana telophase index were defined as the number of respectively mitoses (all phases), prophases, metaphases and ana telophases per 1000 counted nuclei including those in mitosis. The indices in the 7 tumour grafts at each of the 7 moments of fixation, the means and the ranges of distribution of these indices at the 7 moments of fixation were calculated. The nonparametric Friedman test was carried out to analyse the variance statistically.

RESULTS

At the time zero the mean of the mitotic index of the 7 tumour grafts was 12.62 (Fig. 1). After 180 minutes it was reduced to 1.89 or 15.0% of the initial figure. The decline, which was almost exponential, was statistically significant ($p < 0.0005$).

The mean of prophase index (Fig. 2) was reduced during the 180 minutes of observation from 1.10 to



Fig. 1. Mean and range of distribution of the mitotic index in the 7 tumour grafts at varying delay in fixation.

THE ANAL TRANSITIONAL ZONE

Location and Extent

CLAUS FENGER

The Department of Pathology Hvidovre Hospital University of Copenhagen Hvidovre Denmark

Fenger C The anal transitional zone Location and extent Acta path microbiol scand Sect A 87 379-386 1979

The location and extent of the anal transitional zone (ATZ) were investigated in the age group typical for anal canal carcinomas. The methods used were macroscopic determination after whole mount staining with Alcian-dyes as well as conventional histological technique. The results show that the epithelial variants may be found over a larger area than previously reported namely from 6 mm below to 20 mm above the dentate line. Variations in location and extent of the ATZ are described as well as the frequent finding of mature squamous epithelium high in the anal canal. The significance of the findings in relation to the special types of anal canal carcinomas is discussed and on the basis of the macroscopic definition of the anal canal as well as the histological observations in this study it is proposed that anal canal carcinomas should be defined as tumours partly or totally located within a distance of 2 cm above the dentate line.

Key words: Anal transitional zone location extent

C Fenger Institute of Pathology Høstebro Central Hospital DK 7500 Denmark

Received 28.1.79 Accepted 23.11.79

The anal canal extends from the upper to the lower border of the internal anal sphincter. The anal transitional zone (ATZ) is defined as the zone interposed between uninterrupted crypt bearing colo-rectal type mucosa with columnar epithelium above and uninterrupted squamous epithelium below (Fig. 1). Recently a method for macroscopic demonstration of the zone has been described based on observations on the epithelium of the anal glands (5, 6). The present paper deals with the location and extent of the ATZ as estimated by a combination of this method and conventional histological technique, applied to a large series of anal canals.

MATERIAL

The material comprises a one year consecutive series of 113 anal canals obtained by abdomino-perineal resections for adenocarcinomas of the sigmoid colon, rectum and anal canal. The resections were carried out at 11

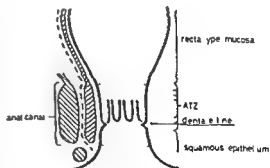


Fig. 1 Location of the anal transitional zone (ATZ)

different hospitals in Greater Copenhagen, Herning and Aalborg. The sex and age distribution related to the location of the tumours is shown in Table 1.

METHOD

The primary fixation and histological examination of the tumours were carried out at the local hospitals. The

removed tumours kept unfixed at various temperatures. It is noticeable that one of the tumours was partially necrotic and that the numbers of mitotic figures were small in the other tumour.

Experimental Model

Our experimental model was approached to the conditions of routine surgical pathology in which the tissue is often not effectively and promptly fixed. Medication and surgical traumas which might influence mitotic activity could be evaded in choosing the nude mouse as a tumour host. The osteogenic sarcoma was chosen among other tumours because of its uniformity, high mitotic activity, small amount of stroma which facilitated the counting, and only few and small necrotic areas. It should be expected that the mitotic activity in other malignant tumours is influenced by delay of fixation within the same order of magnitude and in the same direction. The exact figures may differ because of varying duration of mitosis in different tumours. The fact that the tumour was grown in nude mice does not depreciate the experiment for routine surgical pathology in so far as such tumour grafts retain their human chromosomal structure (Visfeldt *et al* 1972) and cell cycle parameters (Rofstad *et al* 1977).

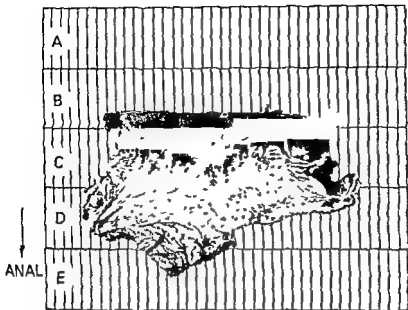
CONCLUSION

Delay in fixation of a magnitude not uncommon in routine surgical pathology may allow the majority of dividing cells to terminate the mitosis resulting in unreliable assessments of mitotic activity.

We thank Dr O. Sneppen and Dr N. Bach Mortensen for their kindness in placing the tumour at our disposal.

REFERENCES

- 1 Bloom W & Fawcett D W. A textbook of histology 10th ed. W. B. Saunders Company, Philadelphia, London, Toronto, 1975, pp 70-73.
- 2 Bullough W S. Mitotic activity in the tissues of dead mice and in tissues kept in physiological salt solutions. *Exp. Cell Res.* 1: 410-420, 1950.
- 3 Edwards J L & Donaldson J T. The time of fixation and the mitotic index. *Am J Clin Pathol* 41: 158-162, 1964.
- 4 Enzinger F M, Lattes R & Torton H. Histological typing of soft tissue tumours. World Health Organisation, Geneva, 1971, pp 28-31.
- 5 Evans N. Mitotic figures in malignant tumours as affected by time before fixation of tissues. *Arch Pathol* 1: 894-898, 1926.
- 6 Poulsen H E, Taylor C W & Sobin L H. Histological typing of female genital tract tumours. World Health Organisation, Geneva, 1975, p 64.
- 7 Povlsen C O & Rygaard J. Heterotransplantation of human adenocarcinomas of the colon and rectum to the mouse mutant nude. A study of nine consecutive transplantations. *Acta path microbiol scand Section A* 79: 159-169, 1971.
- 8 Rofstad E K, Brustad T & Kaalhus O. Cell proliferation kinetics in two human tumours grown in athymic nude mice. *Virchows Arch B Cell Pathol* 24: 219-225, 1977.
- 9 Rygaard J. Thymus & Self Immunobiology of the mouse mutant nude FADL. Copenhagen and John Wiley & Sons, London, New York, Toronto, Sidney, 1973, p 51.
- 10 Scarff R W & Torton H. Histological typing of breast tumours. World Health Organisation, Geneva, 1968, p 19.
- 11 Silberberg S G. Reproducibility of the mitosis count in the histological diagnosis of smooth muscle tumours of the uterus. *Hum Pathol* 7: 451-456, 1976.
- 12 Visfeldt J, Povlsen C O & Rygaard J. Chromosome analyses of human tumours following heterotransplantation to the mouse mutant nude. *Acta path microbiol scand Section A* 80: 169-176, 1972.
- 13 Wahi P N, Cohen B, Luthra U A & Torton H. Histological typing of oral and oropharyngeal tumours. World Health Organisation, Geneva, 1971, pp 17-18.



AKF 15

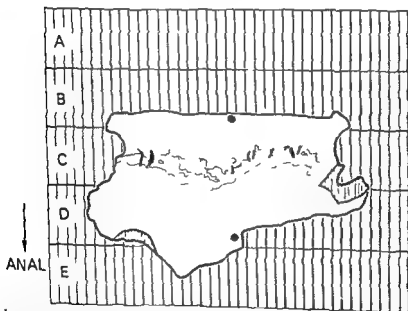


Fig. 2. Various types of ATZ: a - macroscopic specimen; b - diagram based on macroscopic and microscopic measurements. In the diagram the borders of the ATZ are indicated with thin lines. Black areas are anal sinuses and indicate the dentate line. Vertically hatched areas indicate connective tissue. a + b - low location of ATZ.

The ATZ in all cases showed irregular outlines in extent and the lowest and highest point measured in each group of anal canals is also given in Table 2. The highest point measured for each anal varied from 3 to 20 mm above the dentate

line with an average of 8.4 mm. When one includes areas of ATZ found below the dentate line the average extent was 8.9 mm. In the 8 cases with low ATZ the average extent was 11.4 mm, owing to the occurrence of metaplastic squamous epithelium

TABLE 1 Sex, Age, and Tumour Location

Distance of tumour dentate line	Sex		span	Age		Total
	♂	♀		♂ average	♀	
≤ 2 cm	14	12	37-85	66.4	66.6	26
> 2 < 6 cm	29	23	48-85	70.0	65.3	52
≥ 6 cm	25	10	50-82	68.3	71.7	35
	68	45	37-85	68.6	67.1	113

specimens were thereafter sent to Hvidovre Hospital for further examination. The procedure followed here was as described previously (5), all specimens being stained with Alcian Blue or Alcian Green for 40-120 min for macroscopic determination of the ATZ. After photography the whole ATZ and its surroundings were cut up systematically, resulting in 6-40 blocks of tissue, each covering 4 × 25 mm of the surface. In all anal canals the whole ATZ as well as the proximal and distal adjacent mucosa were embedded. A total of 1413 sections of the ATZ were investigated, with an average of 12.5 per anal canal. Extra blocks of tissue were taken from the tumours and their surroundings. The ATZ as well as the borders of the anal canal were then determined microscopically following the previously-mentioned definitions. The results were compared to the photography of the macroscopic specimen in order to correlate the findings to the dentate line as well as to the picture of the ATZ in its whole extent. In cases of lacking correspondence between the macroscopic and the microscopic determination of the extent of the ATZ the latter was chosen as the correct result.

The ATZ shows a great variety of epithelial variants irregularly intermingled with each other. A description of these based on scanning and transmission electron microscopic as well as histochemical observations will be given in following papers. In this study however a marked tendency to areas of mature squamous epithelium being situated at the upper border was observed. Sections exhibiting this feature over a distance of 2 mm or more were therefore registered.

RESULTS

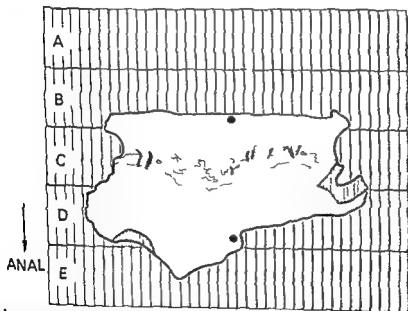
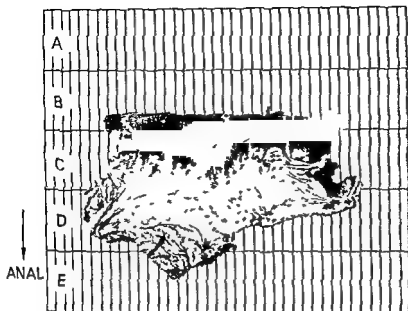
The location of the dentate line (i.e. line of anal valves and sinuses) in relation to the lower border of the anal canal (i.e. lower border of internal sphincter) showed considerable variation from specimen to specimen and even within the same canal. The distance between the two varied from 5 to 19 mm, with an average of 11.4 mm. The upper border of the anal canal (i.e. upper border of internal sphincter) could not be determined with certainty as the internal sphincter gradually merges into the circular muscle coat of the rectum. This transition seems to take place 12-20 mm proximal to the dentate line. So, in this study on fixed material, the anal canal has a length of about 3 cm, with the dentate line located a little below the middle of the canal.

The location of the ATZ in relation to the dentate line could be registered in all 113 canals except one (Table 2). The main part of the ATZ was in all cases located above the dentate line. In 8 canals parts of the ATZ were found 3-6 mm below the dentate line (Fig. 2a + b), in 100 canals the ATZ started at the dentate line and extended upwards (Fig. 3a + b), and in 4 canals the lowest point of the ATZ was found 1-7 mm above the dentate line (Fig. 4a + b). One anal canal showed no ATZ (Fig. 5a + b).

TABLE 2 The Location of the ATZ in Relation to the Dentate Line and the Maximal and Average Extent of the ATZ

Localization of ATZ	No. of anal canals	Relation to dentate line		Extent	
		lowest point	highest point	maximal	average
Low location of ATZ	8	-6 → -3	3 → 12	16	11.4
Intermediate location of ATZ	100	0	3 → 20	20	8.8
High location of ATZ	4	1 → 7	8 → 15	13	7.4
No ATZ	1	-	-	-	-
	113	-6 → 7	3 → 20	0 → 20	8.9

Measurements in millimeters. Negative figures refer to points below the dentate line.

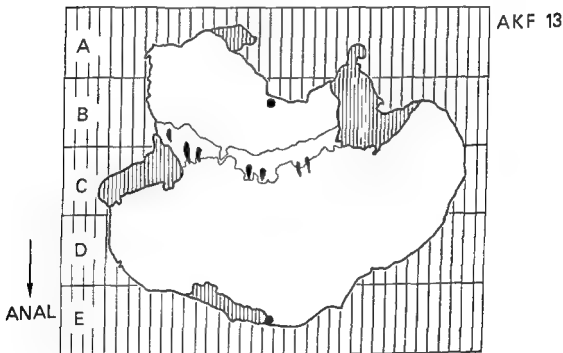
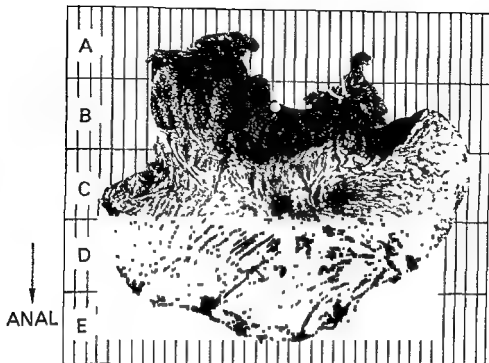


AKF 15

Fig 9 Various types of ATZ a macroscopic specimen b diagram based on macroscopic and microscopic measurements In the diagram the borders of the ATZ are indicated with thin lines Black areas are anal sinuses and indicate the dentate line Vertically hatched areas indicate connective tissue a + b low location of ATZ

The ATZ in all cases showed irregular outlines. The extent and the lowest and highest point measured in each group of anal canals is also given in Table 2. The highest point measured for each canal varied from 3 to 20 mm above the dentate

line with an average of 8.4 mm. When one includes areas of ATZ found below the dentate line the average extent was 8.9 mm. In the 8 cases with low ATZ the average extent was 11.4 mm owing to the occurrence of metaplastic squamous epithelium



AKF 13

Fig 3a + b Intermediate location of ATZ

below the dentate line. In the 4 cases with high ATZ the average was 7.4 mm, and the ATZ did not reach higher in the anal canal in this group than in the others. In one case no ATZ nor dentate line could be demonstrated, and the transition from squamous epithelium to rectal type mucosa took place 17 mm over the lower border of the internal sphincter. In this case anal glands could be demonstrated in 5 out of 18 sections, being localized 4 to 12 mm below the

epithelial transition. The extent of the ATZ related to sex and to location of tumours is shown in Table 3 and shows no significant differences.

Squamous epithelium was found in the ATZ, most often as islands of an epithelium with a histological picture like that of so-called immature metaplastic, less often as mature metaplastic or normal squamous epithelium. At the upper border of the ATZ normal squamous epithelium was,

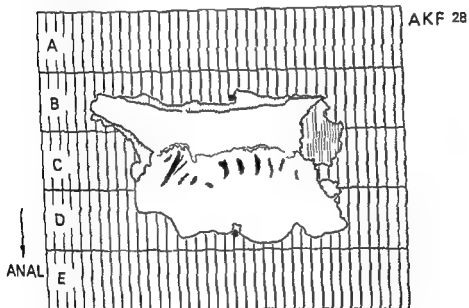
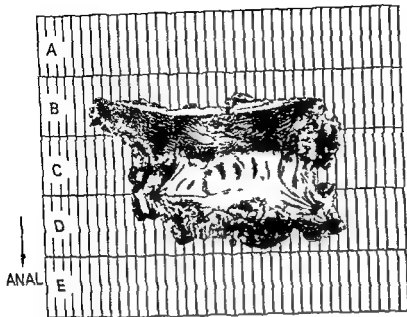


Fig 4a+b High location of ATZ

TABLE 3 Extent of ATZ in Relation to Sex and Tumour Location

Distance of tumour from dentate line	No. of anal canals	span	Extent		average $\bar{O} + \bar{Q}$
			\bar{O}	\bar{Q}	
< 2 cm	26	5-13	9.1	6.7	8.0
> 2 < 6 cm	52	0-20	9.1	8.6	8.7
> 6 cm	35	3-17	9.8	9.5	9.7
	113	0-20	9.4	8.3	8.9

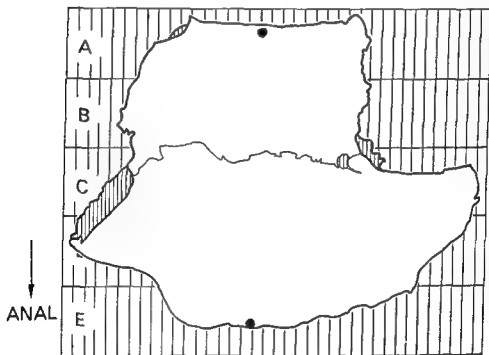


Fig 5a + b No ATZ

however, a frequent finding and present as areas of at least 2 mm's extension in 31.9% of all sections. The figure was lowest for specimens with tumours ≤ 2 cm above the dentate line (21.4%), partly owing to destruction of the ATZ by tumours. The figure for specimens with tumours 2–6 cm above the dentate line was also lower (31.4%) than for the group with tumours ≥ 6 cm above the dentate line (40.6%).

DISCUSSION

The anal transitional zone was first described in 1874 by Robin & Cadiat (15), as a zone of prismatic, i.e. columnar epithelium, devoid of intestinal glands, which extended from the bottom of the anal sinuses upwards to its meeting with the intestinal mucosa 5–8 mm above Hermann & Desfosses (9) wrote in 1880 that »La muqueuse de l'extrémité inférieure du rectum ne se continue pa

TABLE 4 Comparison of Measurements on the ATZ

Ref	Year	Authors	No of anal canals investigated	Extent above dentate line in millimeters
15)	1874	Robin & Cadiat	?	5-8
9)	1880	Hermann & Desfosses	?	6-12
8)	1956	Grinvalsky & Helwig	25	3-11
13)	1956	Parks	?	2.5-10
17)	1958	Walls	20	1-9
4)	1960	Duthie & Cairns	10	2-15
	1978	Fenger	113	-6-20

Negative figures refer to points below the dentate line

directement avec le tegument externe. Il existe a ce niveau une zone circulaire haute de 0^m 006 a 0^m 012 repondant aux saillies musculaires de Mor gagni II qui represente une partie persistante du cloaque de l'embryon. Cette region cloacale est revetue par une muqueuse speciale qui se trouve nettement limitee du cote du rectum et se continue III contraire avec la peau par une transition sensible. Later authors have measured the zone to be 1 to 15 mm (4 8 13 17). A comparison between previous investigations is given in Table 4. The above mentioned measurements have all been carried out on materials consisting of 25 anal canals or less and on a few longitudinal sections.

Material from normal anal mucosa is difficult to obtain. Autopsy specimens are too autolyzed to allow exact determination of the borders and description of the epithelial types. Biopsies from healthy persons would be difficult to get in sufficient numbers and would also as regards the irregular outlines of the ATZ easily give false information on the extent. Surgical specimens from patients with ulcerative colitis, Crohn's disease and adenomatosis of the colon are rare and could not be accepted as representative for normal mucosa. It is debatable whether anal canals resected for colorectal adenocarcinomas represent a normal material. Thus it is known that the histological and ultrastructural picture of the mucosa can be altered in sections taken within a distance of 2 cm (3 14) and that the mucus secretion can show an abnormal pattern in a distance of up to more than 10 cm from a carcinoma. These mucinous changes however only rarely exceed 3.5 cm and the mucosal changes described do not extend to the ATZ.

found in the total material and the lowest border of the tumour. In none of these specimens were there found histological changes typical for mucosa adjacent to carcinoma. The extent of the ATZ in the reference group did not differ significantly from that of the rest of the material.

Primary squamous cell carcinoma and adenocarcinoma may arise in any part of the large intestine but account for less than 0.05 per cent of all colorectal carcinomas. Some cases are seen in patients with ulcerative colitis suggesting an origin from atypical regenerative hyperplasia and metaplasia (2). Basosquamous (basaloid transitional cloacogenic) carcinoma has also been described in the sigmoid colon possibly arising from the totipotent basal cells (16). Cases of squamous metaplasia of the rectum have been reported (1) but the author is not aware of any figures for the occurrence of squamous metaplasia in otherwise normal colon and rectum and has never observed such a change. It would seem reasonable to consider such a phenomenon very rare.

In the anal canal however squamous cell carcinomas and other variants are relatively common. It is generally accepted that the special anal canal carcinomas arise from the ATZ or in a few cases from the anal glands (6). Knowledge of the location and extent of the ATZ is therefore of considerable interest. Information on the location of these tumours reported in the literature is unfortunately often insufficient partly owing to the different use of anatomical terms (5). The St. Mark's series of anal canal carcinomas are useful in this respect.

In the present study the distance between the tumour and the dentate line have been chosen as a 'normal reference' thus leaving a distance of at least 4 cm between the highest extent of the ATZ

The present study shows that the ATZ has

irregular outlines and varying location and extent. Epithelial variants may be found from 6 mm below to 20 mm above the dentate line and normal squamous epithelium is a frequent finding at the upper border. On the basis of the anatomical definition of the anal canal and the above mentioned histological findings it is proposed that anal canal carcinomas should be defined as tumours partly or totally localized within a distance of 2 cm or less above the dentate line. Using this definition the group will inevitably include some carcinomas with origin in rectal mucosa. From a clinical point of view this is however, of minor importance.

My thanks are due to the Departments of Pathology in Copenhagen, Holstebro and Aalborg for providing material for the study of the anal canal.

REFERENCE

- 1 *Cabrera A & Pickren J W* Squamous metaplasia and squamous cell carcinoma of the rectal sigmoid. *Dis Col Rect* 10 288-297 1967
- 2 *Comer T P, Beahrs O H & Dockerty M B* Primary squamous cell carcinoma and adenocarcinoma of the colon. *Cancer* 28 1111-1117 1971
- 3 *Dawson Penelope A & Filipe M Isabel* An ultrastructural and histochemical study of the mucous membrane adjacent to and remote from carcinoma of the colon. *Cancer* 37 2388-2398 1976
- 4 *Duthie H L & Gairns F W* Sensory nerve endings and sensation in the anal region of man. *Brit J Surg* 47 585-595 1960
- 5 *Fenger C* The anal transitional zone. A method for macroscopic demonstration. *Acta Pathol Microbiol Scand Sect A* 86 225-230 1978

- 6 *Fenger C & Filipe M Isabel* Pathology of the anal glands with special reference to their mucin histochemistry. *Acta Pathol Microbiol Scand Sect A* 85 273-285 1977
- 7 *Filipe M Isabel & Branfoot A C* Abnormal patterns of mucus secretion in apparently normal mucosa of large intestine with carcinoma. *Cancer* 34 282-290 1974
- 8 *Grinvalsky H & Helwig E B* Carcinoma of the ano rectal junction. I. Histological considerations. *Cancer* 9 480-488 1956
- 9 *Hermann G & Desfossez L* Sur la muqueuse de la région cloacale de rectum. *CR Acad Sci* 90 1301-1302 1880
- 10 *Morson B C* The pathology and results of treatment of squamous cell carcinoma of the anal canal and anal margin. *Proc Roy Soc Med* 53 416-420 1960
- 11 *Morson B C, Volkstadt H* Mucoepidermoid tumours of the anal canal. *J Clin Pathol* 16 200-205 1963
- 12 *Pang Lillian S C & Morson B C* Basaloid carcinoma of the anal canal. *J Clin Pathol* 20 128-135 1967
- 13 *Parks A G* The surgical treatment of hemorrhoids. *Brit J Surg* 43 337-351 1956
- 14 *Riddell R H & Levin B* Ultrastructure of the 'transitional' mucosa adjacent to large bowel carcinoma. *Cancer* 40 2509-2522 1977
- 15 *Robin Ch & Cadiat* La structure et les rapports de teguments au niveau de leur jonction dans les régions anale, vulvaire et du col utérin. *J Anat Paris* 10 589-605 1874
- 16 *Strate R W, Richardson J D & Bannayan G A* Basosquamous (transitional cloacogenic) carcinoma of the sigmoid colon. *Cancer* 40 1234-1239 1977
- 17 *Walls E W* Observations of the microscopic anatomy of the human anal canal. *Brit J Surg* 45 504-512 1958

NUTRITIONALLY INDUCED NECROTIZING GLOMERULONEPHRITIS AND POLYARTERITIS NODOSA IN PIGS

FOLMER ELLING

University Institute of Pathological Anatomy and Department of pathology Rigshospitalet Copenhagen

Elling F Nutritionally induced necrotizing glomerulonephritis and polyarteritis nodosa in pigs Acta path microbiol scand Sect A 87 387-392 1979

A florid necrotizing glomerulonephritis was found in all 48 pigs that were fed a waste product from the industrial production of the proteolytic enzyme Alcalase® NOVO. In addition three of the animals developed a lesion identical to polyarteritis nodosa. Focal necrosis of the glomeruli was observed in all animals. Electron microscopy showed electron dense deposits at the subendothelial and subepithelial side of the basement membrane of the glomerular capillary wall and in the mesangium. Immunofluorescence microscopy showed IgM in a fine granular pattern in the glomeruli of all 48 pigs. This appears to be the first report on nutritionally induced glomerulonephritis and polyarteritis nodosa in pigs.

Key words: Glomerulonephritis, polyarteritis, pathogenesis, nutritional pigs.

F Elling, University Institute of Pathological Anatomy 11 Frederiksdalsvej DK-2100 Copenhagen Ø, Denmark.

Received 21 79 Accepted 25 11 79

Several chemical compounds have been shown to induce immunologic reactions in some individuals. Thus it has been demonstrated that glomerulonephritis, which is believed to be mediated by immunologic mechanisms, is part of a hypersensitivity reaction to drugs, e.g. penicillamine (Day & Golding 1974). Also polyarteritis nodosa has been associated with hypersensitivity to sulfonamide, penicillin, ouracil and DDT in some cases (Hepinstall 1974).

This report describes for the first time nutritionally induced glomerulonephritis in pigs following administration of a waste product from the industrial production of the enzyme Alcalase®. The lesion was accompanied by polyarteritis nodosa in 3 pigs.

MATERIAL AND METHODS

Alcalase® is an enzyme produced from *Bacillus licheniformis* on a substrate consisting of soybean meal and wheat flour (NOVO Industries, Copenhagen). After

fermentation the broth is centrifuged and the precipitate represents the sludge. The sludge was heated to 90 °C in order to inactivate the enzyme residue and to reduce the cell counts. This sludge product is protein rich and thus its potential value was tested in pigs. The sludge was used in part as a substitute for soybean meal which constitutes the most common protein feed to bacon pigs. The sludge represented 20% of the dry matter of the diet to 48 castrated male pigs during a 12 weeks period. The

to soybean meal as protein feed to bacon pigs.

Of the 48 experimental pigs two from the same litter were necropsied and tissues were fixed and processed for histological examination. Of the remaining pigs tissues from heart, kidney and liver were processed for

sections (4 µm) of the snap-frozen kidneys were washed for 5 min in phosphate buffered saline (PBS) and incubated for 2 h with antisera IgA, IgG and IgM from rabbits diluted

15 at room temperature. The antisera were made available by the State Veterinary Serum Laboratory, Copenhagen. After 2×5 min washings in PBS, the sections were incubated with fluorescein isothiocyanate conjugated goat antirabbit serum IgG (FITC-GAR, Behringwerke) diluted 1:25, for 30 min at room temperature followed by 2 washings in PBS and one washing in distilled water. The sections were air dried and mounted in Eukit®.

The immunofluorescence microscopical examination was made with a Reichert Zetopan equipped with an Osram HBO 200 lamp. In addition to the interference filters (Rigaard & Olsen 1969) a suppression filter ($\lambda < 480$ nm) was used as a primary filter in order to reduce fading.

Formalin fixed tissue blocks from kidneys of 6 pigs were additionally fixed in OsO₄, dehydrated in alcohol and propylene oxide and embedded in epon and processed for electron microscopy. The ultra thin sections of two glomeruli from each animal were stained with uranyl acetate and lead citrate and examined on a JEOL 100 C electron microscope.

Hearts and kidneys of all 60 pigs were weighed after slaughter.

RESULTS

The kidneys of all 48 animals given Alcalase sludge were significantly enlarged (average weight $524 \text{ g} \pm 112$) compared with the controls (average weight $281 \text{ g} \pm 22$) ($p < 0.01$). In all 48 animals microscopical lesions of the renal parenchyma were observed, and based on a grading of the renal lesions the experimental animals could be divided into three groups (Table 1).

Fig 1 Kidney from Group I. Glomerulus showing hypercellularity and focal necrosis (arrow) as well as adhesions between the glomerular tuft and the cells lining the Bowman's capsule. Note also the periglomerular fibrosis. H-E $\times 400$.

Fig 2 Kidney from Group II. Hypercellularity, lobulation and focal necrosis of the glomerular tuft. Fibrin in the glomerular space. Periglomerular and interstitial fibrosis. H-E, $\times 400$.

Fig 3 Kidney from Group III, representing the most severe changes. Large necrotic area in the glomerular tuft (arrow). H-E, $\times 400$.

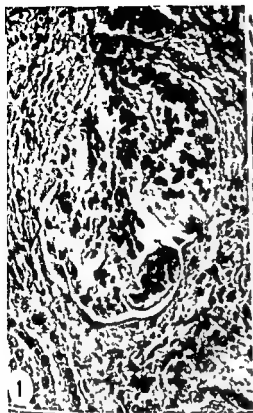
Fig 4 Kidney from Group II. Indirect immunofluorescence staining of IgM deposits appearing in a fine granular pattern in the glomerular tuft. $\times 800$.

Group I (19 Animals with the Slightest Renal Changes) All the glomeruli showed proliferative changes with mesangial hypercellularity and the glomerular tuft often appeared lobulated. Segmental necrosis in a few glomeruli was present in all 19 animals (Fig 1). In all animals adhesions between the glomerular tuft and parietal layer of the Bowman's capsule and periglomerular fibrosis were observed in some glomeruli. The glomerular changes were most severe in the inner $\frac{1}{2}$ of the cortex. Necrosis and desquamation of the epithelial cells were observed in some of the proximal tubules but never in the distal and the collecting tubules.

TABLE 1. Renal Changes in the 3 Groups Given Alcalase Sludge During a 12 Week Period

	Glomerulus					Prox tub	Dist tub	Collecting tub	Interstitialium			Vessels								
	Necrosis	Hypercellularity	Lobulation	Adhesions	Hyalinization	Fibrin in capsules	Necrosis	Atrophy	Necrosis	Cell casts	Necrosis	Cell casts	Edema	Fibrosis	Cell infiltration	Edema	Fibrosis	Cell infiltration	Necrotizing arteritis	Hypertensive changes
Group I 19 animals	+	+	+	+	+		+	+					+	+	+					
Group II 15 animals	++	++	+	+	+	+	++	++					+	++	+	+	+	+		+
Group III 14 animals	+++	++	+	+	+	++	++	++	+	+	+		+	++	++	+	+	+	+	+

+ Slight
++ Moderate
+++ Severe



where only cell casts were seen. No vascular lesions were present. The renal cortex displayed slight edema and focal fibrosis. Focal infiltration with lymphocytes, macrophages and sometimes also a few neutrophils were noticed in both the cortical and the medullary interstitium.

Group II (15 Pigs with Moderate Renal Lesions)

In this group focal necrosis was more frequent than in group I, especially in juxtamedullary glomeruli. Adhesions between the glomerular tuft and the Bowman's capsule were more frequent than in group I. In a few animals fibrin was seen in the capsular space of some glomeruli (Fig. 2). A few hyalinized glomeruli were observed in all animals. Necrosis and desquamation of proximal tubular epithelial cells were more frequent in this group and also atrophic tubules surrounded by a thickened basement membrane were found in the cortex. Necrosis of epithelial cells in the distal and collecting tubules was rare. Desquamated epithelial cells, lymphocytes and sometimes neutrophils could be seen in the tubular casts. Some of the small arteries and some arterioles showed hyperplasia of the

muscular layer. Edema and fibrosis were observed in both the cortical and medullary interstitial tissue. Interstitial cell infiltrations were frequent and consisted of lymphocytes, macrophages and often also neutrophils.

Group III (14 Pigs with the Most Severe Renal Changes)

Glomerular necrosis and hyalinization were frequently present throughout the renal cortex (Fig. 3). Crescent formation and capsular fibrin were seen in a few glomeruli in most pigs. In this group necrosis and desquamation were observed in the distal tubules but to a lesser degree than in the proximal tubules. The collecting tubules appeared normal. Both protein and cell casts were frequent. Hyperplasia of small arteries and arterioles was frequently found. Severe edema was seen in the cortical and medullary interstitium. A widespread interstitial fibrosis was observed in the cortex. Infiltration with lymphocytes, macrophages and neutrophils was seen in both cortical and medullary interstitium. In three animals from the same fibrinoid necrosis and infiltration with neutrophils, lymphocytes and plasma cells was seen in some of the interlobular and arcuate arteries (Fig. 5).

Immunofluorescence microscopy showed deposition of mainly IgM but also IgA and sometimes IgG in a fine granular pattern along the capillary basement membrane and in the mesangium in the kidneys of all 48 pigs (Fig. 4). These findings did not differ significantly from group to group. Immunoglobulin deposits were also found in vascular walls of the three pigs displaying necrotizing arteritis. Immunoglobulin deposits were not observed in any animal of the control group.

Electron microscopical examination was made of two glomeruli from two pigs in each group. Electron dense deposits were observed subendothelially and subepithelially in the capillaries and in the mesangium in almost all lobuli in all examined glomeruli (Fig. 6). In all examined animals neutrophils were found attached to the subendothelial deposits. The capillary basement membranes appeared of normal dimensions. In the control group the glomeruli appeared normal.

Other findings. In the experimental animals the heart was significantly enlarged (average $350 \text{ g} \pm 42$) compared with the controls (average $306 \text{ g} \pm 19$) ($p < 0.01$). Microscopically, however, no lesions were noticed in the hearts of the experimental animals.

The necropsy of two of the experimental pigs from Group III showed identical lesions. The pigs were emaciated and had subcutaneous edema in the extremities. Edema was observed in the perirenal



Fig. 5. Kidney from Group III. Fibrinoid necrosis and inflammatory in the vascular wall. H-E. $\times 400$.

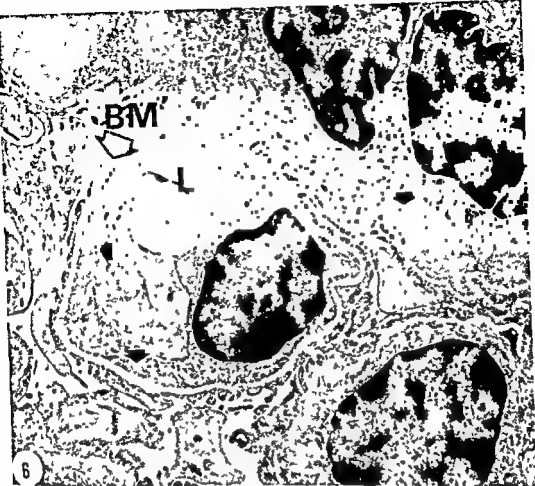


Fig 6 Electron micrograph of glomerular capillary loop. Note the electron dense deposits (arrows) on the subendothelial side of the capillary basement membrane (BM arrow). Lumen of capillary loop (L). UA + Pb. $\times 10,500$

issue and around the ureters and urinary bladder the kidneys were enlarged with a light decapsulated and cut surface. Also numerable minute cysts were seen in the renal cortex of the cut surface. The ears displayed hypertrophy of the left ventricle of the lungs, the liver, the gastrointestinal tract, the nervous system and the spleen appeared normal in both animals.

The remaining 46 experimental animals and the 12 control animals were subjected to routine meat inspection at the slaughterhouse and no macroscopic changes were found.

No microscopic lesions were found in the kidneys and the hearts of the controls.

DISCUSSION

The renal lesions induced by the oral administration of a waste product - sludge - from the production of the proteolytic enzyme Alcalase® could arbitrarily be divided into 3 groups representing an acute necrotizing glomerulonephritis of increasing severity through the groups I-III.

The pathogenesis of this glomerulonephritis is still the present obscure. A possible explanation is that the sludge from the enzyme production contains one or more compounds with antigen properties which get absorbed through the gut mucosa, or if being of a relatively large molecular weight via «membranous» epithelial cells - M cells - which have been demonstrated within the columnar epithelial cells covering the Peyer's patches (Owen & Jones 1974).

where only cell casts were seen. No vascular lesions were present. The renal cortex displayed slight edema and focal fibrosis. Focal infiltration with lymphocytes, macrophages and sometimes also a few neutrophils were noticed in both the cortical and the medullary interstitium.

Group II (15 Pigs with Moderate Renal Lesions)

In this group focal necrosis was more frequent than in group I especially in juxtamedullary glomeruli. Adhesions between the glomerular tuft and the Bowman's capsule were more frequent than in group I. In a few animals fibrin was seen in the capsular space of some glomeruli (Fig. 2). A few hyalinized glomeruli were observed in all animals. Necrosis and desquamation of proximal tubular epithelial cells were more frequent in this group and also atrophic tubules surrounded by a thickened basement membrane were found in the cortex. Necrosis of epithelial cells in the distal and collecting tubules was rare. Desquamated epithelial cells, lymphocytes and sometimes neutrophils could be seen in the tubular casts. Some of the small arteries and some arterioles showed hyperplasia of the

muscular layer. Edema and fibrosis were observed in both the cortical and medullary interstitial tissue. Interstitial cell infiltrations were frequent and consisted of lymphocytes, macrophages and often also neutrophils.

Group III (14 Pigs with the Most Severe Renal Changes)

Glomerular necrosis and hyalinization were frequently present throughout the renal cortex (Fig. 3). Crescent formation and capsular fibrin were seen in a few glomeruli in most pigs. In this group necrosis and desquamation were observed in the distal tubules but to a lesser degree than in the proximal tubules. The collecting tubules appeared normal. Both protein and cell casts were frequent. Hyperplasia of small arteries and arterioles was frequently found. Severe edema was seen in the cortical and medullary interstitium. A widespread interstitial fibrosis was observed in the cortex. Infiltration with lymphocytes, macrophages and neutrophils was seen in both cortical and medullary interstitium. In three animals from the same fibrinoid necrosis and infiltration with neutrophils, lymphocytes and plasma cells was seen in some of the interlobular and arcuate arteries (Fig. 5).

Immunofluorescence microscopy showed deposition of mainly IgM but also IgA and sometimes IgG in a fine granular pattern along the capillary basement membrane and in the mesangium in the kidneys of all 48 pigs (Fig. 4). These findings did not differ significantly from group to group. Immunoglobulin deposits were also found in vascular walls of the three pigs displaying necrotizing arteritis. Immunoglobulin deposits were not observed in any animal of the control group.

Electron microscopical examination was made on two glomeruli from two pigs in each group. Electron dense deposits were observed subendothelially and subepithelially in the capillaries and in the mesangium in almost all lobuli in all examined glomeruli (Fig. 6). In all examined animals neutrophils were found attached to the subendothelial deposits. The capillary basement membranes appeared of normal dimensions. In the control group the glomeruli appeared normal.

Other findings. In the experimental animals the heart was significantly enlarged (average 350 ± 42) compared with the controls (average 306 ± 19) ($p < 0.01$). Microscopically, however, no lesions were noticed in the hearts of the experimental animals.

The necropsy of two of the experimental pigs from Group III showed identical lesions. The pigs were emaciated and had subcutaneous edema in the extremities. Edema was observed in the perirena



Fig. 5 Kidney from Group III. Fibrinoid necrosis and inflammatory in the vascular wall. H-E $\times 400$.

GROWTH STIMULATION OF AGED CELLS IN CULTURE

E BLOMQUIST E ARRO U BRUNK and B WESTERMARK

Department of Pathology and the Wallenberg Laboratory University of Uppsala Uppsala Sweden

Blomquist, E Arro E Brunk U & Westermark B Growth stimulation of aged cells in culture
Acta path microbiol scand Sect A 87 393 399 1979

Human glial cultures of any passage consist of two populations of cells those with mitotic ability and the non-dividers. The fraction of non-dividers increases with age of the culture and dominates in late passages. When cells from midphase II cultures (passage 28) were sparsely seeded in dishes containing agarose partially covered by small isolated palladium squares (haptotactic islands) they settled on the palladium squares but not on the agarose. 58% of the cells divided and formed mini-clones which became density growth inhibited within 10 days in medium with 5% serum. The non-dividers comprised 42%. They showed a characteristic indolent motility pattern. When these cultures were exposed to 15% fetal calf serum and 2 ng/ml mEGF (mouse epidermal growth factor) for another 5 days nine per cent of the solitary cells had divided and DNA measurements showed another 20% to have entered the S phase. About 40% of the initial single cells presented morphological alterations after the stimulation which are known to be early signs of entrance into the cell cycle after blockage in G₁/G₀. The present results in combination with earlier findings suggest that old cells approaching the non-dividing state become increasingly insensitive to stimulation by growth promoting factors.

Key words: Cultured human glial cells ageing *in vitro* phase III phenomenon plasma membrane motility scanning electron microscopy growth stimulation

E Blomquist, Division of Tumor Biology The Wallenberg Laboratory P.O. Box 562 S-751 22 Uppsala Sweden.

Received 5 iv 79 Accepted 23 iv 79

Normal diploid cells can be kept *in vitro* only for a limited number of passages; the growth of the cultures subsequently terminates (a phenomenon termed "entrance into phase III" by Hayflick) (19, 20, 21).

The phase III phenomenon does not seem to involve a sudden stop in a previously rapid cellular proliferation after a certain and defined number of divisions but may rather be the end point of growth capacity which probably declines slowly through several passages (1, 3, 4, 24, 25). It has been demonstrated that the number of cell doublings rather than the total time in culture is of major significance in determining when the cells will cease to divide (6, 15). Different cell types have different pre-determined maximal numbers of divisions. Fibroblasts from species with a short life span divide significantly fewer times than fibroblasts from species with a longer life span and fibroblasts from adult humans grow with less population

doublings than the same cell type from embryos (13). Diploid cells in culture thus seem to be programmed for a certain number of divisions. This program however does not seem to be absolute since variations in the external milieu of the cultures can influence the possible number of divisions. It has thus been known for some years that enlarged volumes of medium and also the addition of hydrocortisone will postpone the phase III phenomenon in fibroblast cultures (12, 32). Furthermore the addition of epidermal growth factor (EGF) was recently found to greatly prolong the life span of

number are composed of a = m + n + p
remain
which h

26) When a culture approaches phase III most of its cells have become non-dividers.

In the present report we describe results of

These M cells have been shown to be able to carry larger molecules like horseradish peroxidase through the gut mucosa and present these to the cells of the immune system (Owen 1977). In the present study the repeated antigen exposure would subsequently cause the formation of antigen-antibody complexes which become deposited in the glomeruli resulting in the observed glomerulonephritis. The electron dense deposits seen in the glomerular capillary walls and the mesangium are in accordance to the immunoglobulins observed by immunofluorescence microscopy. The development of polyarteritis nodosa in 3 pigs from the same litter could be due to an extension of the same process to the vessel wall.

Previous observations have shown that immune complex disease can be induced exogenously. Thus glomerulonephritis was observed in 20% of patients treated with penicillamine (Day & Golding 1974). Similarly polyarteritis nodosa in humans have been associated with hypersensitivity to chemical compounds e.g. sulfonamide, thiouracil, penicillin (Heptinstall 1974).

One striking difference between the referred investigations and the present observations is that in the former only some of the patients exposed to the specific compounds developed immune complex disease. In the present study all animals given the waste developed acute necrotizing glomerulonephritis within 12 weeks of exposure suggesting the presence of a very potent antigen.

The hypertrophy of the heart and the hyperplasia of the muscular layer of the arterioles in the renal cortex suggest arterial hypertension which probably would be of nephrogenic origin.

In conclusion the present observations demonstrate that necrotizing glomerulonephritis and arteritis nodosa can be induced nutritionally. Further work has now been initiated in order to elucidate the mechanism of this anticipated immune complex disease and the nature of the antigen involved.

The author is indebted to P. Thode Jensen and J. Pedersen, State Veterinary Serum Laboratory for providing the antiswine immunoglobulins. Supported by Goldschmidt's Grant and State Research Council's grant no. 513-6554.

REFERENCES

- Day A. T. & Golding I. R. Hazards of penicillamine therapy in the treatment of rheumatoid arthritis. *Post grad med J* 50 (Suppl. August) 71, 197.
- Heptinstall R. H. *Pathology of the kidney* 2nd ed. Little Brown and Company p. 626, 1974.
- Madsen A., Mortensen H. P., Larsen A. E. & Elling A. Alcalase waste to baconpigs. *Meddelelse no. 1977* (In Danish). National Institute of Animal Science, Copenhagen, 1977.
- Owen R. L. & Jones A. L. Epithelial cell specialization within human Peyer's patches. An ultrastructural study of intestinal lymphoid follicles. *Gastroenterology*, 66, 189-203, 1974.
- Owen R. L. Sequential uptake of horseradish peroxidase by lymphoid follicle epithelium of Peyer's patches in the normal unobstructed mouse intestine. An ultrastructural study. *Gastroenterology* 72, 440-447, 1977.
- Rygaard J. & Olsen W. Interference filters improve immunofluorescence microscopy. *Path. microbiol. scand.* 76, 146-148, 1969.

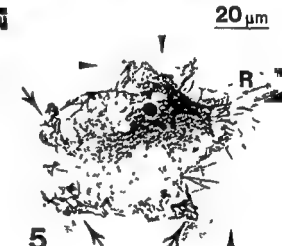
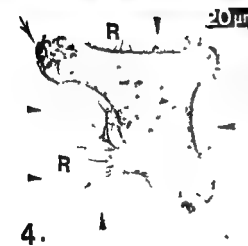
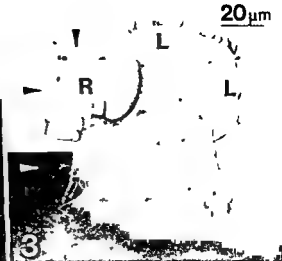
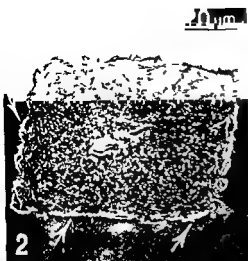


Fig. 2 and 3.

empty when the cells contracted

Fig. 5 Single cell on a haptotactic island after 10 days in EMEM with 5% cs followed by 5 days in EMEM with 15% FCS and 2 ng/ml mEGF. The cell shows strong activation (see also Table 1) with pronounced ruffling activity (arrows) and formation of retraction fibrils (R). The edges of the palladium squares are marked (arrow heads)

compared with the state on day 10. B Slightly to moderately activated with contraction and/or increased ruffling activity. C Highly activated with contraction and formation of a leading edge and a trailing end as a sign of locomotor activity.

DNA measurement

DNA analyses were performed in each experiment on

randomly selected nuclei in cells identified as non-dividers on day 10 and on day 15. The cell bearing coverslips were fixed in 1:1 ethanol acetone for 30 min at room temperature and subsequently prepared according to the ethidium bromide staining method as described previously (2) and the DNA content was measured with a Zeiss microscope fluorometer (2).

experiments showing that a fraction of human glial cells being non dividers under certain conditions will re-enter the cell cycle when exposed to an increased concentration of serum and mouse epidermal growth factor (mEGF)

MATERIAL AND METHODS

Cell Lines and Standard Culture Conditions

All experiments were performed on diploid human glial cells of the line U 787 CG (22) passages 27 to 30 to ensure a suitable number of non-dividing cells (3). The cells were derived and kept in culture as described by Pontén and MacIntyre (30)

Preparation of Haptotactic Islands

Falcon plastic Petri dishes (Ø 35 mm) were filled with a 100°C 1% agarose (Indubiose®) solution in distilled water. The solution was then rapidly sucked off in order to leave a thin film of agarose on the bottom of the dishes which were left to dry at room temperature for 24 hours. EM 200 mesh copper grids were placed on the hardened agarose. The dishes were placed in an Edwards E12E2 vacuum device and palladium was evaporated at 10⁻⁴ torr (3-37)

Round glass coverslips (Ø 25 mm) were used for DNA measurements and rectangular glass slides (12 × 6 × 1 mm) for scanning electron microscopy (SEM). Both types of glass were held at an angle of 45 degrees to the horizontal while the heated agarose was poured over them. For the preparation of SEM glasses, it was found necessary to coat the glass surface with an evaporated layer of palladium prior to the agarose coating (4)

The evaporation procedure created in all the three cases square palladium islands of 7056 µm² area separated by 40 µm wide strips of bare non adhesive agarose film. Cells settled exclusively on the Pd haptotactic islands and could not migrate over the surrounding agarose film

Culture of Cells on Haptotactic Islands and Growth Kinetic Studies

with an electronic cell counter (Celloscope) and 5 × 10⁴ cells were seeded into 35 mm Petri dishes some of which contained cover glasses for DNA measurement and SEM. When the cells had settled and stretched the medium was changed to EMEM with 5% calf serum from a stock used throughout the investigation. The haptotactic islands were studied in an inverted phase contrast microscope and each island inhabited by a single cell was scored and registered. Ten days after seeding the persistent single cells were counted and designated non-dividers (3-37) and their positions were recorded. In the meantime the medium was changed every third day

The medium was then changed from EMEM with 5% c.s. to EMEM with 15% fetal calf serum (FCS) and 2 ng/ml mEGF (36). The same batch of FCS was used in all experiments. After another five days all the initially single cells were scored again and the number of cells which had divided was recorded. In the growth kinetic studies at least 200 cells were followed in each experiment

Preparation for Scanning Electron Microscopy

The rectangular glass slides with cells attached to haptotactic squares were prepared for SEM as previously described in detail (4). The cells were fixed in an aldehyde fixative consisting of 2% glutaraldehyde in 0.1 M Na cacodylate HCl with 0.1 M sucrose (pH 7.2 total osmolality 510 mOsmol; vehicle osmolality 300 mOsmol) (5-11). In order not to initiate withdrawal of ruffling structures by the fixation process this was performed without moving the cultures and without lowering the temperature (4)

After post fixation in 1% OsO₄ in 0.15 M Na cacodylate HCl dehydration in acetone and critical point drying from CO₂ the specimens were goldcoated in a Polaron E 5000 sputter with a 30 nm thick layer

The specimens were studied in a Jeol 100 C electron microscope equipped with a side entrance goniometer and a scanning attachment at 40 kV. Micrographs were taken with the specimens tilted 45°

SEM. The cells that had remained single were classified into three groups. A Morphologically unaltered

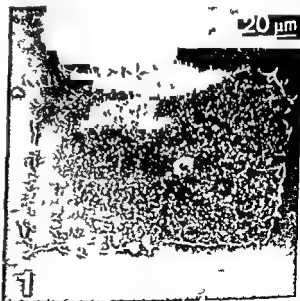


Fig 1 A single cell on a haptotactic island after 10 days in EMEM with 5% c.s. The cell is flat without ruffling activity and occupies the whole of the available palladium square

another 5 days in the medium with 15% FCS and 2 ng/ml mEGF many cells had changed their morphology. Of the still single cells 58% (corresponding to 53% of the single cells at day 10) still presented the aforesaid typical features of the non-divider. The remaining 42% (corresponding to 38% of the single cells at day 10) showed various degrees of activation in the form of ruffling, contraction with formation of retraction fibrils and expanding lamellipodia. The daughter cells of the 9% of the single cells on day 10 which divided during the 5 days of growth stimulation were active with lamellipodia formation and ruffling membranes. The morphological changes are illustrated in Figures 2-5 and summarized in Table 1.

DNA Measurements

One hundred and sixty four single cells from passage number 28 were measured on day 10 and the same number of single cells 5 days after the change from ENEM with 5% c.s. to ENEM with 11% FCS with 2 ng/ml EGF added. The results are illustrated in Table 2. On day 10 about 70% were diploid and most of the rest had a double amount of DNA, no cells being in S phase. This kind of distribution has previously been shown to be typical of non-cycling cells (35-39). After 5 days of stimulation with high serum concentration and mEGF the pattern changed with a reduced number of diploid cells and a population of cells in S phase (see Table 2).

DISCUSSION

Established lines of transformed cells grow indefinitely *in vitro* while normal diploid cells under standard culture conditions either transform spontaneously or eventually slow down their growth rate and finally cannot be further subcultivated (19-20). This difference between normal and neoplastic cells seems to be fundamental and the understanding of malignancy probably demands knowledge of the mechanisms behind this type of growth control. The factors limiting the possible number of divisions for normal cells are only a matter of speculation at present. Irreversible changes in DNA, RNA and protein synthesis are not necessarily involved since hybridization experiments between «young» and «old» fibroblasts and between «old» fibroblasts and established malignant cells have given results indicating that «old» nuclei may regain DNA replication capacity when fused with some malignant cells but not after fusion with «young» diploid cells (16, 23, 27, 28, 36). Furthermore many aspects of the RNA and protein synthesizing mechanisms are intact in aged cells since phase III

cultures have been found to synthesize several non altered lysosomal and mitochondrial enzymes (18) and produce polio and herpes virus to the same extent as phase II cultures (29, 34).

In glial cultures the increase of cells that have lost their mitotic capacity is exponential (3). It has only occasionally been possible to maintain a glial line through more than 45 passages and in passage 40 only about 20% of the cells retain their mitotic capacity while 80% are non-dividers at standard culture conditions (3).

In ordinary mass cultures it is difficult or impossible to follow and characterize individual cells for longer periods of time, while this can easily be achieved using the mini-cloning method in which cells are cultivated on haptotactic islands (10, 17, 37). We have previously shown non-dividers to have a morphology and a motility pattern which distinguish them from dividers. The former are large and flat and incapable of ruffling and locomotion while dividers are mobile and show a leading edge with ruffling and associated pinocytosis (4).

The present study revealed that some cells being non mobile non dividers in a certain milieu can be stimulated to change their morphology and to re enter the cell cycle by changes in the concentration of growth promoting factors. Increased concentration of serum in combination with added mEGF proved to activate about 50% of the non-dividers judging by changes in the cell morphology which are known from earlier studies to accompany the entrance into the cell cycle - start of ruffling activity, macropinocytosis and initiation of cell locomotion (7, 8, 33). The majority of the non dividers which responded to the stimulation did so only with a more active plasma membrane motility during the five days they were stimulated but some also entered the S phase and a few even underwent mitosis. Changes in the surface morphology thus proved to be the most sensitive parameter in evaluating the stimulating effect.

Glial cells have been shown to be dependent on growth promoting factors in order to enter the cell cycle and can easily be blocked in G₁ by serum deprivation (7, 8, 33). The results of the present experiments in combination with earlier findings (3, 4) suggest that aging glial cells become increasingly resistant to growth factor stimulation and eventually stop dividing when exposed to such factors in concentrations which easily keep «younger» cells actively dividing. The growth blockage can to some extent be overcome by increasing the growth stimulation. The understanding of how the ultimate loss of sensitivity to growth promoting factors is created in aged cells

TABLE 1 Morphology of single cells on haptotactic islands after 10 and 15 days culture in EMEM with 5% calf serum (cs) with subsequent activation by transfer for another 5 days to EMEM with 15% fetal calf serum (FCS) with the addition of 2 ng/ml mEGF. For definition of activation: see results and Figs 3, 4 and 5. In all 180 cells were studied.

DAYS	%	non activated cells %	slightly activated cells %	strongly activated cells %
10	5CS	100	0	0
15	5CS	100	0	0
10 + 5	5CS + 15FCS and 2ng/ml mEGF	58	32	10

RESULTS

Growth Kinetics

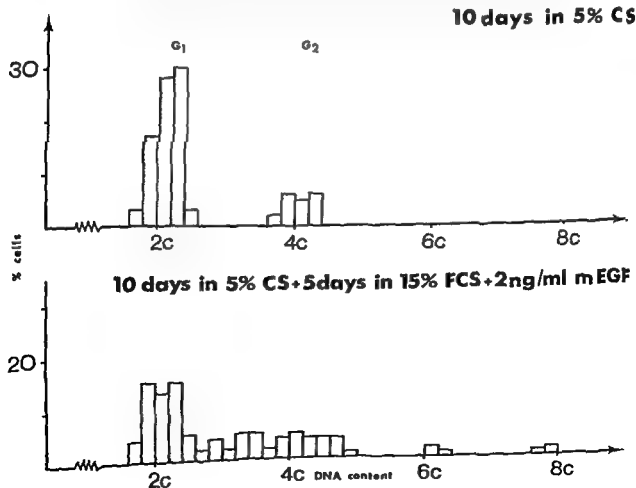
The number of single cells found in the cultures 10 days after seeding on the haptotactic islands in EMEM with 5% cs differed only slightly in passages 27-30 and was 42% of the initially seeded cells in passage 28. No remaining mitotic activity was found after the 10th day.

Five days after the change of medium to EMEM with 15% FCS and 2 ng/ml mEGF it was found that of a total of 212 single cells 20 (9%) had divided while 192 (91%) remained single. Only one of the single cells that divided passed through mitosis more than once (e.g. twice).

Morphological Changes

After cultivation for 10 days in EMEM with 5% cs the single cells were as previously described (4) flat with few microvilli, without membrane motility and occupying the whole square (Fig. 1). After

TABLE 2 Distribution of DNA content in single cells on haptotactic islands after 10 days culture in EMEM with 5% calf serum (cs) and after another 5 days in EMEM with 15% fetal calf serum (FCS) with 2 ng/ml EGF. About 20% of the cells are in S phase after the stimulation. In all 164 cells were studied.



- during aging of human cells in culture. Direction by polio virus. *Exp Cell Res* 94 310-314 1975
- 30 Ponten J & Macintyre E H Long term culture of normal and neoplastic human glia. *Acta Path Microbiol Scand* 74 465-486 1968
- 31 Rheinwald J G & Green H Epidermal growth factor and the multiplication of cultured human epidermal keratinocytes. *Nature* 265 421-424 1977
- 32 Ryan J F Sharf B B & Cristofalo V J The influence of culture medium volume on cell density and life span of human diploid fibroblasts. *Exp Cell Res* 91 389-392 1975
- 33 Schellens J P M Brunk U T & Lindgren A Influence of serum on ruffling activity pinocytosis and proliferation of in vitro cultivated human glia cells. *Cytobiol* 13 93-106 1976
- 34 Tomkins G A Stanbridge E J & Hayflick L Viral probes of aging in the human diploid cell strain WI 38. *Proc Soc Exp Med* 146 385-390 1974
- 35 Westermarck B Induction of a reversible G1 block in human glialike cells by cytochalasin B. *Exp Cell Res* 82 341-350 1973
- 36 Westermarck B Density dependent proliferation of human glia cells stimulated by epidermal growth factor. *Biochem Biophys Res Comm* 69 304-310 1976
- 37 Westermarck B Growth control in miniclones of human glial cells. *Exp Cell Res* 111 295-299 1978
- 38 Wright W E & Hayflick L Nuclear control of cellular aging demonstrated by hybridization of anucleate and whole cultured normal human fibroblasts. *Exp Cell Res* 96 113-121 1975
- 39 Yanushevsky R Mendelsohn M L Mayall B H & Cristofalo V J Proliferative capacity and DNA content of aging human diploid cells in culture. A cytophotometric and autoradiographic analysis. *J Cell Physiol* 84 165-170 1974

must await the clarification of how growth-promoting factors, such as EGF, initiate the start of the cell cycle, presumably after being bound to specific cell membrane receptors (9)

Supported by grants from the Swedish Medical Research Council and the Swedish Cancer Society

REFERENCES

- 1 Absher, P M, Absher, R G & Barnes W D Genealogies of clones of diploid fibroblasts. Cinematographic observations of cell division pattern in relation to population age. *Exp Cell Res* 88 95-104, 1974
- 2 Bengtsson, A, Grumelius, L, Johansson H and Pontén, J Nuclear DNA-content of parathyroid cells in adenomas, hyperplastic and normal glands. *Acta path Microbiol Scand Sect A* 85 455-460, 1977
- 3 Blomquist, E, Brunk, U T, Westermark, B & Arro, E Research Institute, Chicago, Illinois p 13-20, 1977
- 4 Blomquist E, Arro, E, Brunk, U T & Westermark B Plasma membrane motility of cultured human glia cells in phase II and phase III. *Acta Path Microbiol Scand Sect A* 86 257-263, 1978
- 5 Brunk, U T & Ericsson J L E The demonstration of acid phosphatase in *in vitro* cultured cells. Studies of the significance of fixation, tonicity and permeability. *Histochem J* 4 349-363, 1972
- 6 Brunk U T, Ericsson J L E, Pontén J & Westermark B Residual bodies and «aging» in cultured human glia cells. Effect of entrance into phase III and prolonged periods of confluence. *Exp Cell Res* 79 1-14 1973
- 7 Brunk U T, Schellens J P M & Westermark B Influence of epidermal growth factor (EGF) on ruffling activity pinocytosis and proliferation of cultivated human glia cells. *Exp Cell Res* 103 295-302, 1976
- 8 Brunk U T, Schellens J P M, Westermark B & Collins, V P Effect of serum-deprivation on structure. *Acta Path Microbiol Scand Sect A*, 85 157-168, 1977
- 9 Carpenter, G & Cohen S Epidermal growth factor, binding internalization and degradation in human fibroblasts. *J Cell Biol* 71 159-171, 1976
- 10 Carrier, S B Haptotactic islands A method of confining single cells to study individual cell reactions and clone formation. *Exp Cell Res* 48 189-193, 1967
- 11 Collins, V P, Arborth B & Brunk, U T A comparison of the effects of three widely used glutaraldehyde fixatives on cellular volume and structure. *Acta Path Microbiol Scand Sect A*, 85 157-168, 1977
- 12 Cristofalo, V J Metabolic aspects of aging in diploid human cells. In *Aging in Cell and Tissue Culture* E Holzerkova and V J Cristofalo (Eds) Plenum press, New York 1970, p 83-119
- 13 Cristofalo, V J Animal cell cultures as a model system for the study of aging. *Adv Gerontol Res* 4 45-79, 1972
- 14 Cristofalo V J & Sharf, B B Cellular senescence and DNA-synthesis. Thymidine incorporation as a measure of population age in human diploid cells. *Exp Cell Res* 76 419-427, 1973
- 15 Daniel, C W & Young L J T Influence of cell division on an aging process. Life span of mouse mammary epithelium during serial propagation *in vivo*. *Exp Cell Res* 65 27-32, 1971
- 16 Goldstein L & Lin C C Rescue of senescent human fibroblasts by hybridization with hamster cells *in vitro*. *Exp Cell Res* 70 436-439, 1972
- 17 Harris, A Behavior of cultured cells on substrata of variable adhesiveness. *Exp Cell Res* 77 285-297, 1973
- 18 Houben, A & Remacle, J Lysosomal and mitochondrial heat labile enzymes in ageing human fibroblasts. *Nature* 275 59-60 1978
- 19 Hayflick L & Moorhead P S The serial cultivation of human diploid cell strains. *Exp Cell Res* 25 585-621, 1961
- 20 Hayflick L The limited *in vitro* lifetime of human diploid cell strains. *Exp Cell Res* 37 614-636 1965
- 21 Hayflick, L Senescence and cultured cells. *Persp Exp Gerontol* 14 195-211 1966
- 22 Lindgren, A, Westermark B & Pontén J Serum stimulation of stationary glia and glioma cells in culture. *Exp Cell Res* 95 311-319, 1975
- 23 Littlefield J W Attempted hybridizations with senescent human fibroblasts. *J Cell Physiol* 82 129-132, 1973
- 24 Macieira-Coelho A, Pontén J & Philipson L The division cycle and RNA synthesis in diploid human cells at different passage levels *in vitro*. *Exp Cell Res* 42 673-684, 1966
- 25 Macieira-Coelho A Kinetics of the proliferation of human fibroblasts during their lifespan *in vitro*. *Mech Ageing Dev* 6 341-343 1977
- 26 Merz Jr G S & Ross J D Viability of human diploid cells as a function of *in vitro* age. *J Cell Physiol* 74 219-221 1969
- 27 Muggleton-Harris A L & Hayflick L Cellular aging studied by the reconstruction of replicating cells from nuclei and cytoplasm isolated from normal human diploid cells. *Exp Cell Res* 103 321-330 1976
- 28 Norwood T H, Pendergrass W R & Martin G M Reinitiation of DNA synthesis in senescent human fibroblasts upon fusion with cells of unlimited growth potential. *J Cell Biol* 64 551-556, 1975
- 29 Pitha J, Stork E & Wimmer, J Protein synthesis

CORRESPONDENCE

CLINICAL RELEVANCE OF HISTOLOGICAL GRADING OF CANCER OF THE LARYNX

Sir - In Acta path. microbiol. scand. Sect. A 86: 499-504, 1978, Karin Helweg Larsen *et al.* have published an investigation 'Clinical relevance of histological grading of cancer of the Larynx' in which they tested a grading system for evaluation of epidermoid carcinoma of the Larynx originally composed as a point system by Jakobsson (7, 8) later modified to a scoring system by us (Lund *et al.* 9, 10, 11, 12). Karin Helweg Larsen *et al.* conclude that they found no correlation to the clinical course of disease. In their discussion of the discrepancy between this finding and ours, they among other things point to the smallness of their selected material. We would like to add further possibilities as to the cause of discrepancy.

Karin Helweg Larsen *et al.* have changed the system of histological grading used by us in several ways:

- 1) They assess the histological score based upon equal evaluation of superficial and deep parts of the biopsies (e.g. keraunization). We have stressed that the microscopic field with the highest point was counted (12, page 163, 2nd paragraph, lines 3-5).
- 2) Karin Helweg Larsen *et al.* do not differentiate between plasmolymphocytic cellular response on one side and granulocytic infiltration accompanying an ulcerated surface on the other - We consider these as two separate phenomena.
- 3) Karin Helweg Larsen *et al.* evaluate depth of invasion in nearly all their biopsies although they state that many of the biopsies are too small for observing deep invasion - For this reason we have abstained from grading about 70 per cent of our biopsies according to that particular parameter.
- 4) Other minor changes made by Karin Helweg Larsen *et al.* are probably less important.

Conclusion and recommendation. In future attempts to test histological grading systems the procedures quoted being followed with great care, at least as to basic principles.

E. N. T. dep
University Hospital
Odense

K. JØRGENSEN

Institute of Pathology
University Hospital
Odense

C. LUND

Sir - In reply to the letter to the Editors from K. Jørgensen and C. Lund we take the liberty of making the following comments:

re point one

In the evaluation of the keraunization process we followed the principle specified by Jakobsson (8, p. 19) and not the modification of Lund *et al.* which was not defined until 1977 (12).

Consequently this cannot explain the discrepancy.

re point two

We have clearly stated that we have evaluated the total plasmolymphocytic inflammatory response (pp. 501 and 503). We are of the opinion that it is not possible to determine whether the presence of plasma cells or lymphocytes is due to ulceration or defensive reaction of the organism to the carcinoma.

Consequently this does not explain the discrepancy either.

re point three

Unlike Lund *et al.* we have also on this point followed the principle of Jakobsson (8, p. 25) and have evaluated the existing invasion in the given biopsy material. It goes without saying that the applicability of the grading depends on whether the biopsy is representative of the tumour - a fact that applies to all the parameters of the scoring system.

Consequently again this does not explain the discrepancy.

re point four

Since K. Jørgensen and C. Lund have not specified this point we wish to make the following supplementary comments:

It has been difficult to evaluate the papers of C. Lund *et al.* (9, 10, 11, 12). We would have appreciated greater accuracy and delicacy in the handling of the material giving better accordance between the figures of the text and the graphical presentation (e.g. 10, p. 465 and fig. 2). It has also invited reflection that the classification of the material is vague (e.g. 10, fig. 3) and inexact defined (e.g. 12, figs. 1, 2, 3, 4). The statistical method is not stated in the papers 9, 10 and 11. However, in the total description of carcinomas of the lip, tongue and larynx (12) we have also been taken aback by the fact that the authors have applied the chi square test to the group of

TUMOURS IN ICELAND

*Tumours in
Iceland*

2 Tumours and Tumour-Like Lesions of Bone Histological Types and Clinical Course

SIGURDUR V. SIGURJÓNSSON JONAS HALLGRÍMSSON ASMUNDUR BREKKAN and
STEFAN HARALDSSON

The Departments of Pathology Radiology and Orthopedic Surgery University of Iceland Reykjavik
Iceland

Sigurðsson V Hallgrímsson J Brekkan A & Haraldsson S Tumours in Iceland 2 Tumours
and tumour like lesions of bone Histological types and clinical course Acta path microbiol scand
Sect A 87 403-409 1979

Tumours and tumour like lesions of bone occurring in Iceland during the years 1955-1974 were
studied pathologically radiologically and clinically and typed histologically according to the World
Health Organization Classification published in 1972 Cartilage forming tumours were the largest
group or 81 per cent The frequency of primary malignant bone tumours as a group excluding
myelomas resembled that reported from several other countries but the composition of these tumours
in Iceland was different in that chondrosarcomas constituted 47 per cent and osteosarcomas 27 per
cent The chondrosarcomas also were unusual in having a high male/female ratio a high grade of
malignancy and a short survival when located in the long bones of the extremities and the bones of the
foot The bones of the hand were disproportionately frequent sites for chondrosarcomas and
chondromas

Key words Bone tumours histological typing epidemiology chondroma of hand chondrosarcoma of
hand

J Hallgrímsson Dept of Pathology University of Iceland P O Box 150 121 Reykjavik Iceland

Material & Methods

MATERIAL AND METHODS

Received 12 x 78 Accepted 12 x 79

In a brief survey of primary bone tumours
diagnosed in Iceland in the years 1935-1960
cartilage forming tumours were the largest group
constituting 57 per cent of the total (10) Surpri
singly chondrosarcoma was the most frequent
malignant tumour To investigate this further and
to exclude possible errors in histological typing the
subject of bone tumours in Iceland was reviewed
and the results are presented in this paper

This study is a contribution to the international
exchange of data on the epidemiology of bone
tumours which has been called for recently (9) It
falls into a planned series of papers on the
histological typing of tumours in Iceland according
to the classifications proposed by the World Health
Organization This work will represent a standard
approach that is expected to yield valuable data on
tumours such as incidence and comparisons with
other geographic areas

The study involves tumours and tumour like lesions
submitted for histological diagnosis during the 20 years
1955-1974 To ensure the retrieval of the necessary
histological radiological and clinical material for the
review it was considered best not to go farther back in
time than to the year 1955 A great advantage in the
study was that the Department of Pathology at the
University of Iceland is the only laboratory for
anatomical pathology in the country and all available
histological reports slides and tissue blocks are therefore
kept in one institution The names of patients with
malignant bone tumours were obtained from the
Icelandic Cancer Registry and for those with benign
tumours and tumour like lesions from the diagnostic
files of the laboratory of pathology The original
pathological reports
ed and
tumours
with tw
chondro
to those tumours which by the

supraglottic carcinomas covering 33 patients. It should be a well-known fact that this test is applicable only if the number of observations exceeds 40.

Consequently, because of the above-mentioned facts, among other things, we still do not find the grading system clinically relevant.

Conclusion Prior to application of proposed histological grading systems, it is strongly recommended that the basic principles underlying these systems are carefully scrutinized.

References The numbers refer to the list of references in the article by Karin Helweg-Larsen et al

Pathological-anatomical Institute
Kommunehospital
DK-1399 Copenhagen K
Denmark

original pathological descriptions were not clearly of the osteochondroma type. The myelomas were not reviewed as these tumours will be included in a separate study of neoplastic diseases of haematopoietic and lymphoid tissues.

The tumours and tumour like lesions were typed according to the WHO Classification of Tumours (2).

The hospital records and radiograms for the patients with malignant bone tumours were reviewed and correlated with the pathological findings. The radiograms of the benign tumours and tumour like lesions with the exception of many of the osteochondromas were correlated with the pathological findings but a review of the hospital records was not considered necessary in these cases. The information on patient survival was obtained from the cancer registry hospital follow up records and the National Census Bureau. Patients surviving after treatment for malignant bone tumours were re-examined in the orthopedic outpatient clinic and new radiograms were taken to look for recurrences and metastases.

RESULTS

The Icelandic Cancer Registry had registered 58 primary malignant bone tumours other than myelomas in the 20 year period 1955-1974. Of these we excluded 24 tumours from the study. For 1 tumour the histological material was insufficient for typing. 2 tumours were odontogenic in origin. 5 tumours were metastatic carcinomas in bone. 9 tumours were extraskeletal in origin and secondarily invading bone and for one tumour we changed the diagnosis from chondrosarcoma to chondroma. Since the WHO committee considers giant cell tumours to be potentially malignant (2) we added 2 such tumours from the files of the laboratory of pathology to the remaining 34 malignant tumours from the cancer registry. We therefore had a total of 36 malignant and potentially malignant bone tumours to study. From the files of the laboratory of pathology we recovered sufficient material from 178 benign bone tumours and 43 tumourlike lesions.

The results of the histological typing are shown in Table 1. The myelomas are included in the table and reviewed for the sake of completeness to conform to the WHO classification. The cancer registry had registered 71 patients with myeloma in the 20 year period and for 61 of these the diagnosis had been established histologically by bone marrow smears, surgical biopsies and at autopsies. The cartilageforming tumours formed the largest group of primary bone tumours being 174 of 215 or 81 per cent. Among the 36 malignant tumours chondrosarcomas constituted 47 per cent and osteosarcomas 27 per cent.

TABLE 2. Malignant Primary Bone Tumours in Iceland 1955-1974. Incidence Rates per 100 000 Population per Year ¹⁾

Histological type	Sex	Total
Osteosarcoma	M 0.31	0.24
	F 0.16	
Chondrosarcoma	M 0.33	0.45
	F 0.16	
Other malignant tumours ²⁾	M 0.15	0.24
	F 0.32	
Total	M 1.20	0.95
	F 0.60	

¹⁾ Population in Iceland 1 Dec 1964 M 96 111 F 94 117. Standardization to World Population does not alter the incidence rates at the first decimal.

²⁾ All giant cell tumours are included but myelomas are excluded.

The mean annual incidence of the malignant tumours is shown in Table 2.

The localization of the largest groups of tumours i.e. the cartilage forming tumours and the osteosarcomas is shown in Table 3. Eighty seven per cent of

121 had solitary and 7 had multiple tumours resulting in a total of 141 tumours that had been submitted for histological examination.

Histologically the chondromas could be divided into two groups. In the first group 16 tumours were those with uniform small nuclei and abundant ground substance. In the second group 7 tumours were those with more cellularity and slight variation in nuclear size and occasional binucleated cells. Six of the cellular chondromas were in the tubular bones of the hand and one in the distal femur. All these 7 patients had been treated successfully by curettage.

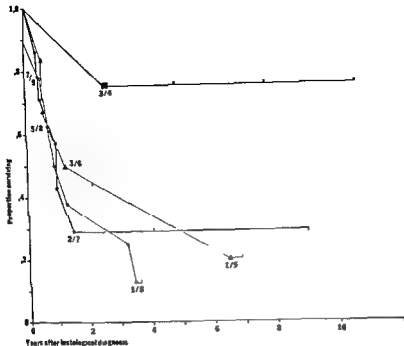
The chondrosarcomas were grouped according to histological grades of malignancy by the method used by Evans *et al* (7). Of the 17 tumours 2 fell into group I, 6 into group II and 9 into group III, that of the highest grade of malignancy.

Among the 9 osteosarcomas 6 were osteoblastic and 3 were chondroblastic.

The duration of symptoms preceding histological diagnosis for the patients with chondrosarcomas

TABLE 1 *Histological Typing of Primary Bone Tumours and Tumour-like Lesions in Iceland 1955-1974*

		Number of patients	Males/ Females
I	Bone-forming Tumours		
A 1	Osteoma	16	8/8
A 2 a	Osteoid osteoma	5	2/3
A 2 b	Osteoblastoma	1	1/0
B 1	Osteosarcoma	9	6/3
B 2	Juxtacortical osteosarcoma	1	0/1
II	Cartilage forming Tumours		
A 1	Chondroma	22	10/12
A 2	Osteochondroma	134	85/49
A 3	Chondroblastoma	0	
A 4	Chondromyxoid fibroma	0	
B 1	Chondrosarcoma	17	14/3
B 2	Juxtacortical chondrosarcoma	0	
B 3	Mesenchymal chondrosarcoma	0	
III	Giant Cell Tumour	3	1/2
IV	Marrow Tumours		
1	Ewing's sarcoma	3	1/2
2	Reticulosarcoma of bone	0	
3	Lymphosarcoma of bone	0	
4	Myeloma	61	38/23
V	Vascular Tumours		
A 1	Haemangioma	0	
A 2	Lymphangioma	0	
A 3	Glomus tumour (glomangioma)	0	
B 1	Haemangioendothelioma	0	
B 2	Haemangiopericytoma	0	
C 1	Angiosarcoma	0	
VI	Other connective tissue Tumours		
A 1	Desmoplastic fibroma	0	
A 2	Lipoma	0	
B 1	Fibrosarcoma	1	0/1
B 2	Liposarcoma	0	
B 3	Malignant mesenchymoma	0	
B 4	Undifferentiated sarcoma	1	0/1
VII	Other Tumours		
1	Chordoma	1	1/0
2	»Adamantinoma« of long bones	0	
3	Neurilemmoma	0	
4	Neurofibroma	0	
VIII	Unclassified Tumours	0	
IX	Tumour like Lesions		
1	Solitary bone cyst	21	14/7
2	Aneurysmal bone cyst	1	0/1
3	Juxta articular bone cyst	5	4/1
4	Metaphyseal fibrous defect	4	3/1
5	Eosinophilic granuloma	6	4/2
6	Fibrous dysplasia	6	2/4
7	»Myositis ossificans«	0	
8	»Brown tumour« of hyperparathyroidism	0	



unrelated causes. The numbers give the ratio of living patients at the time indicated on the abscissa. Symbols: Same as in Figure 1.

and osteosarcomas is shown in Fig. 1. Chondrosarcomas of the long bones of the extremities and the bones of the foot resemble the group of osteosarcomas in having given symptoms which lead to an early diagnosis.

The survival of the patients with chondrosarcomas and osteosarcomas is shown in Fig. 2. Chondrosarcomas of the long bones of the extremities and the bones of the foot again resemble the osteosarcomas in short survival after treatment. The 2 patients with group I chondrosarcomas were cured by surgery. Among those with group II tumours, 4 died with metastases and 2 were cured both having had their tumours in the hand. Among those with group III tumours, 6 died with metastases and 3 were cured, one of them having had the tumour in the hand. Seven of the 9 patients with osteosarcoma died with metastases and one died from postoperative osteomyelitis involving the mandible. One patient with osteosarcoma has survived almost 4 years after an amputation. The only patient with juxtacortical osteosarcoma has survived 18 years after several local recurrences.

One patient with Ewing's sarcoma died of sepsis 10 months after diagnosis and the other two died

with metastases 2 and 5 years after diagnosis. The one patient with chordoma died with disease 5 years after diagnosis. One of the 3 patients with giant cell tumours died with metastases 10 years after the original operation, but the other 2 are living 16 and 17 years later. The one patient with fibrosarcoma is

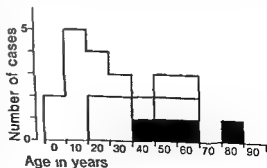


Figure 3 The age distribution of patients with chordoma and chondrosarcoma of the hand. Symbols: Open 13 patients with «normocellular» chondroma. Dotted 6 patients with cellular chondroma. Filled 4 patients with chondrosarcoma.

TABLE 3 Localization of the Four Most Frequent Histological Types of Primary Bone tumours

	Osteosarcoma	Chondroma	Osteochondroma	Chondrosarcoma
Hand				
Metacarpus		3	5	1
Phalanx		17	8	3
Ulna				1
Radius			4	
Humerus		1	22	1
Scapula			5	
Clavicle				1
Vertebra			3	
Mandible	1			
Rib	1		4	2
Innominate	1		8	3
Femur	4	1	26	4
Tibia	2		32	
Fibula			12	
Foot				
Tarsus			2	1
Metatarsus			4	
Phalanx			6	
Total	9	22	141	17

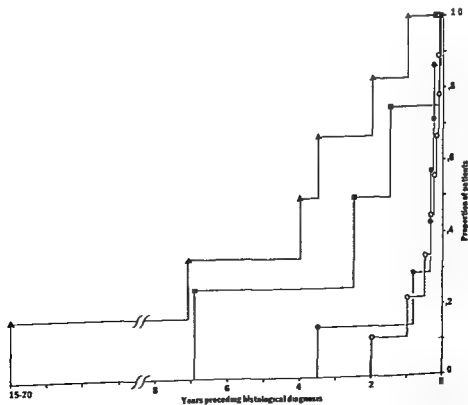


Figure 1 The duration of symptoms preceding histological diagnosis for 17 patients with chondrosarcoma and 9 patients with osteosarcoma. Symbols: Filled triangle chondrosarcoma of trunk. Filled square chondrosarcoma of hand. Filled circle chondrosarcoma of long bones and foot. Open circle osteosarcoma.

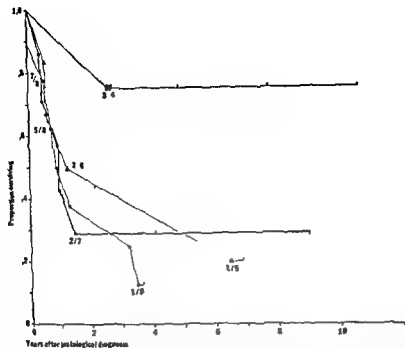


Fig 2 Survival of 17 patients with chondrosarcoma and 9 patients with osteosarcoma. The curves are drawn with a slight modification of the Kaplan-Meier method (11). The vertical lines pointing up from the curves indicate the length of follow-up for living patients. The vertical lines pointing down from the curves indicate the death of patients from unrelated causes. The numbers give the ratio of living patients at the time indicated on the abscissa. Symbols: Same as in Figure 1.

and osteosarcomas is shown in Fig 1. Chondrosarcomas of the long bones of the extremities and the bones of the foot resemble the group of osteosarcomas in having given symptoms which lead to an early diagnosis.

The survival of the patients with chondrosarcoma and osteosarcoma is shown in Fig 2. Chondrosarcomas of the long bones of the extremities and the bones of the foot again resemble osteosarcomas in short survival after treatment. The 2 patients with group I chondrosarcomas were cured by surgery. Among those with group II tumours, 4 died with metastases and 2 were cured both having had their tumours in the hand. Among those with group III tumours, 6 died with metastases and 3 were cured, one of them having had the tumour in the hand. Seven of the 9 patients with osteosarcoma died with metastases and one died from postoperative osteomyelitis involving the mandible. One patient with osteosarcoma has survived almost 4 years after an amputation. The only patient with juxtacortical osteosarcoma has survived 18 years after several local recurrences.

One patient with Ewing's sarcoma died of sepsis 10 months after diagnosis and the other two died

with metastases 2 and 5 years after diagnosis. The one patient with chordoma died with disease 5 years after diagnosis. One of the 3 patients with giant cell tumours died with metastases 10 years after the original operation, but the other 2 are living 16 and 17 years later. The one patient with fibrosarcoma is

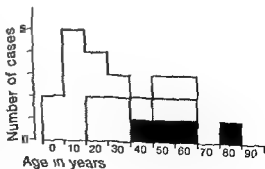


Figure 3 The age distribution of patients with chondrosarcoma.

TABLE 3 Localization of the Four Most Frequent Histological Types of Primary Bone tumours

	Osteosarcoma	Chondroma	Osteochondroma	Chondrosarcoma
Hand				
Metacarpus		3	5	1
Phalanx		17	8	3
Ulna				1
Radius			4	
Humerus		1	22	1
Scapula			5	
Clavicle				1
Vertebra			3	
Mandible	1			
Rib	1		4	2
Innominate	1		1	3
Femur	4	1	26	4
Tibia	2		32	
Fibula			12	
Foot				
Tarsus			2	1
Metatarsus			4	
Phalanx			6	
Total	9	22	141	17

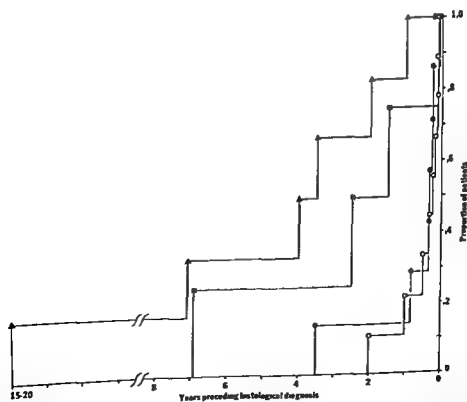


Figure 1 The duration of symptoms preceding histological diagnosis for 17 patients with chondrosarcoma and 9 patients with osteosarcoma. Symbols: Filled triangle chondrosarcoma of trunk; Filled square chondrosarcoma of hand; Filled circle chondrosarcoma of long bones and foot; Open circle osteosarcoma.

clinically in Iceland have come to surgical biopsies in the same way as the benign and malignant tumours

This investigation received financial support from the World Health Organization. The authors are grateful to Professor Hrafn Tulinius, director of the Icelandic Cancer Registry for his assistance

REFERENCES

- 1 Ackerman L V and Rosai J Surgical Pathology 5th ed The C V Mosby CO St. Louis 1974 p 1034
- 2 Ackerman L V, Sissons H A, Sobin L H & Tortona H Histological typing of bone tumours International Histological Classification of Tumours No 6 World Health Organization Geneva 1972
- 3 The Cancer Registry of Norway Trends in cancer incidence in Norway 1955-1967 Universitetsforlaget Oslo Bergen Tromsø 1972 p 45
- 4 Dahlin D C Bone Tumours 2nd ed Charles C Thomas Springfield Illinois 1967 p 11
- 5 Dahlin D C & Salvador A H Chondrosarcomas of bones of the hands and feet - a study of 30 cases Cancer 34 755-760 1974
- 6 Devesa S S & Siherman M T Cancer incidence and mortality trends in the United States 1935-1974 J Natl Cancer Inst 60 545-571 1978
- 7 Evans H L, Ayala A G & Romsdahl M M Prognostic factors in chondrosarcoma of bone A clinicopathologic analysis with emphasis on histologic grading Cancer 40 818-831 1977
- 8 Field J R An analysis of the incidence of bone tumours In Symposium osseum European Association of Radiology Edinburgh London 1970 pp 335-339
- 9 Grundmann E Bone tumors - a challenge for cooperation In Grundmann E (Ed) Malignant bone tumors Recent results in cancer research 1st ed vol 54 Springer Verlag Berlin Heidelberg and New York 1976 pp 1-2
- 10 Hallgrímsson J Illkynja beinaæxli Læknablaðið 52 80-89 1966
- 11 Kaplan E L & Meier P Nonparametric estimation from incomplete observations J Am Stat Assoc 53 457-481 1958
- 12 Larsson S E & Lorentzon R The geographic variation of the incidence of malignant primary bone tumors in Sweden J Bone Joint Surg (Am) 56-A 592-600 1974
- 13 The Netherlands Committee on Bone Tumours "
- 14 O Neal L W & Ackerman L V Chondrosarcoma of bone Cancer 5 551-577 1952
- 15 Price C H G The incidence of primary malignant bone tumours in the South - West of England In Symposium osseum European Association of Radiology Edinburgh London 1970 pp 331-334
- 16 Roberts P H & Price C H G Chondrosarcoma of the bones of the hand J Bone Joint Surg (Br) 59 - B 213-221 1977
- 17 Statistical abstract of Iceland 1974 In Statistics of Iceland II 63 Reykjavik 1976 p 7

alive without ■ recurrence for 10 years and the patient with undifferentiated sarcoma has been well for 16 years following an amputation

The age distribution of the patients with chondromas and chondrosarcomas in the hand is shown in Fig 3 The 6 cellular chondromas fall roughly in between the 13 »normocellular« chondromas and the 4 chondrosarcomas

DISCUSSION

We are not aware of published studies from other countries, where the WHO classification of bone tumours has been used

We found the WHO classification to be a practical guide to the typing of the tumours and tumour-like lesions of bone The explanatory notes are clear The illustrations offer additional support but, understandably, the complex histology of bone lesions cannot be illustrated in detail in a small book

Although the number of tumours in Iceland ■ small, it nevertheless represents the whole population Similar population studies based on the WHO classification are possible in other countries by the use of compiled results from many and preferably all pathological institutes

The mean annual incidence of histologically diagnosed primary malignant bone tumours was according to our review, 0.85 per 100,000 inhabitants in Iceland Results from the Swedish Cancer Registry, also based on histological diagnosis, although not according to the WHO classification, for the years 1958–1968, agree with ours, giving an annual incidence of 0.82 per 100,000 population (12) These calculations for both countries only include those of the giant cell tumours that have had a malignant course Results from Norway (3), England (8, 15) and the United States (6) also agree roughly with ours, but will have to be taken with reservation as they either are not limited to histologically confirmed tumours or do not represent whole populations

The chondrosarcomas in Iceland seem to differ in several respects from chondrosarcomas found ■ elsewhere In the first place, in Iceland they are the most frequent malignant bone tumours comprising 47 per cent, compared to 20–30 per cent found elsewhere (1, 4, 12, 13) Secondly, the male/female ratio in Iceland is 4.7/1.0, compared to 1–2/1.0 found elsewhere (4, 13) Thirdly, their proportion in the bones of the hand is 24 per cent in Iceland, compared to 0.9 to 4.4 per cent found elsewhere (5, 13) Fourthly, in Iceland a larger proportion is of a high histological grade of malignancy than that

found elsewhere (7, 14) Fifthly, in Iceland the chondrosarcomas in the long bones of the extremities and the bones of the foot were all of the highest grade of malignancy and behaved in a fashion similar to that commonly found for osteosarcomas, i.e. had ■ short pre-operative clinical course and a short survival

We found only 20 chondrosarcomas of the hand reported before the year 1964, but by 1977 the number of reported cases had grown to 82, mostly due to 3 large series published in 1966, 1974 and 1977 (13, 5, 16) We think that this sudden increase in the number of reported chondrosarcomas of the hand may be due to a change in the histological criteria for the interpretation of cartilage-forming tumours rather than a true change in their frequency

The proportion of chondromas among benign bone tumours varies between reports, or from 8 to 28 per cent (1, 4, 13) and our finding of 13 per cent falls within that range However, in Iceland chondromas seem to be unusually frequent in the bones of the hand, or 87 per cent of the total compared with 46 per cent found at the Mayo Clinic (4) and 54 per cent in Holland (13) Thus, the high proportions we find of chondrosarcomas and chondromas in the hand may reflect a common origin of these tumours or an origin of chondrosarcomas from pre-existing chondromas possibly through a stage of cellular chondromas In the latter respect, the age distribution of the cellular chondromas shown in Fig 3 may be an important observation

Eighteen per cent of the osteochondromas in our series were in the hand, which agrees roughly with the 14.7 per cent found in England (15) and 14.4 per cent found in Holland (13), but exceeds the 3 per cent found at the Mayo Clinic (4) The origin of osteochondromas in the hand is therefore not likely to be related to that for chondromas and chondrosarcomas, except in the rare instances when chondrosarcomas arise secondarily in osteochondromas

The proportion of osteosarcomas among malignant bone tumours in Iceland, 27 per cent is lower than the 33 to 42 per cent found elsewhere (1, 4, 12, 13) We found nothing unusual regarding the pathology and clinical course for the osteosarcomas in our series

The tumour-like lesions were included in the study to comply with the WHO classification, and our histological review was mainly for differential diagnostic purposes Some of the tumour-like lesions of bone are clinically silent and may therefore never be diagnosed, but we have good reasons to believe that most of those detected

VACUOLIZATION OF THE GLOMERULAR BASEMENT MEMBRANE

GUSTAV TALLQVIST*) TOM TÖRNROTH**) TUOMO VANTTINEN***)
and AMOS PASTERNAK***)

*) Departments of Pathology, Maria Hospital and University of Helsinki; **) Fourth Department of Medicine, University Central Hospital and Department of Electron Microscopy, University of Helsinki; ***) Department of Clinical Science, University of Tampere, Finland

Tallqvist G, Törnroth T, Vantunen T & Pasternack A. Vacuolization of the glomerular basement membrane. *Acta path microbiol scand Sect A* 87 411-419 1979

Immunofluorescence and clinical data were collected retrospectively and renal tissue was examined by electron microscopy 1) for 20 consecutive patients whose glomeruli were normal in light microscopy except for vacuolization of obliquely-cut portions of the glomerular basement membrane (GBM) after periodic acid silver methenamine staining and 2) for 10 control patients with completely normal glomeruli in light microscopy. By electron microscopy the biopsies with vacuolization showed two patterns of abnormalities. In pattern I (10 patients) the changes corresponded to the GBM changes in membranous glomerulonephritis or resolving acute poststreptococcal glomerulonephritis, further confirmed by immunofluorescence and clinical data. In pattern II (10 patients) the GBM showed indentations and intramembraneous lucent areas very similar to but more sparsely distributed than the changes in pattern I. Patients with pattern II lesions had various renal diseases: systemic lupus erythematosus, minimal changes glomerulonephritis, IgA IgG glomerulonephritis, graft rejection and acute anuric tubulointerstitial nephritis, but clinical and immunofluorescence data did not differ from those of the controls. The hypothesis is presented that the indentations and intramembraneous lucent areas in patterns I and II are remnants of former subepithelial deposits.

Key words: Glomerulus, ultrastructure, clinical feature, immunofluorescence, indentations, vacuolization, glomerulonephritis, deposits.

Gustav Tallqvist, Department of Pathology, Maria Hospital SF-00180 Helsinki 18, Finland

Received 23 XI 78 Accepted 9 III 79

In membranous glomerulonephritis (MGN) (14, 5, 10, 17) and in resolving acute poststreptococcal glomerulonephritis (20), obliquely-cut portions of the glomerular basement membrane (GBM) in 3 µm thick histologic sections stained with periodic acid silver methenamine (PASM) (10) have sometimes had a punctate or vacuolated appearance hereafter termed vacuolization. We undertook the present retrospective study to try to identify the ultrastruc-

MATERIALS AND METHODS

From our files on the 1159 renal biopsies from which material was available for electron microscopic study we selected those 377 biopsies which, on initial routine histologic examination, had shown apparently normal glomeruli. All biopsies had been fixed in cacodylate buffered glutaraldehyde, embedded in paraffin, cut to

VACUOLIZATION OF THE GLOMERULAR BASEMENT MEMBRANE

GUSTAV TALLQVIST^{*)} TOM TÖRNROTH^{**)} TUOMO VÄNTTINEN^{***)}
and AMOS PASTERNAK^{***)}

^{*)} Departments of Pathology Maria Hospital and University of Helsinki ^{**)} Fourth Department of Medicine University Central Hospital and Department of Electron Microscopy University of Helsinki
^{***)} Department of Clinical Science University of Tampere Finland

Tallqvist G, Törnroth T, Vanttinen T & Pasternack A. Vacuolization of the glomerular basement membrane. Acta path microbiol scand Sect A 87 411-419 1979

Immunofluorescence and clinical data were collected retrospectively and renal tissue was examined by electron microscopy 1) for 20 consecutive patients whose glomeruli were normal in light microscopy except for vacuolization of obliquely-cut portions of the glomerular basement membrane (GBM) after periodic acid silver methenamine staining and 2) for 10 control patients with completely normal glomeruli in light microscopy. By electron microscopy the biopsies with vacuolization showed two patterns of abnormalities. In pattern I (10 patients) the changes corresponded to the GBM changes in membranous glomerulonephritis or resolving acute poststreptococcal glomerulonephritis further confirmed by immunofluorescence and clinical data. In pattern II (10 patients) the GBM showed indentations and intramembraneous lucent areas very similar to but more sparsely distributed than the changes in pattern I. Patients with pattern II lesions had various renal diseases: systemic lupus erythematosus, minimal changes glomerulonephritis, IgA IgG glomerulonephritis, graft rejection and acute anuric tubulointerstitial nephritis, but clinical and immunofluorescence data did not differ from those of the controls. The hypothesis is presented that the indentations and intramembraneous lucent areas in patterns I and II are remnants or former subepithelial deposits.

Key words: Glomerulus, ultrastructure, clinical feature, immunofluorescence, indentations, vacuolization, glomerulonephritis, deposits.

Gustav Tallqvist, Department of Pathology, Maria Hospital SF 00180 Helsinki 18, Finland

Received 23 xi 78

Accepted 9 iii 79

In membranous glomerulonephritis (MGN) (1, 4, 5, 10, 17) and in resolving acute poststreptococcal glomerulonephritis (20) obliquely-cut portions of the glomerular basement membrane (GBM) in 3 µm thick histologic sections stained with periodic acid silver methenamine (PASM) (10) have sometimes had a punctate or vacuolated appearance hereafter termed vacuolization. We undertook the present retrospective study to try to determine if the

we continued in the study

MATERIALS AND METHODS

From our files on the 1159 renal biopsies from which material was available for electron microscopic study we selected those 377 biopsies which on initial routine histologic examination had shown apparently normal glomeruli. All biopsies had been fixed in cacodylate buffered glutaraldehyde, embedded in paraffin, cut to sections 3 µm thick and stained with hematoxylin-eosin, periodic acid-Schiff and periodic acid silver methenamine (PASM).
In a prospective and retrospective clinicopathologic investigation we selected the biopsies of the first 20 consecutive patients. Ten consecutive patients whose renal biopsy

contained normal glomeruli that were free of vacuolization were used as controls

For electron microscopic study, tissue specimens, about 1 mm in diameter with three to four glomeruli were immersed in cacodylate-buffered glutaraldehyde, postfixed in osmium tetroxide, processed for electron microscopy and embedded in Epon 812. The tissue block were cut to 700–900 Å sections which were then stained with lead citrate and uranyl acetate, and periodic acid-silver-methenamine (PASM) (13), and examined in a JEM 100C electron microscope at 80 kv. In selected cases, the Epon-specimens were cut serially and every second section stained with lead citrate and uranyl acetate, and every second section stained with PASM. For light microscopic examination additional 700–900 Å sections were stained with PASM. The number of indentations and intramembraneous lucent areas of the GBM in each biopsy was quantified in two ways: 1) By means of an oil immersion lens indentations of the GBM and their locations were recorded on a micrograph of the examined section. The number of indentations per unit of square area of the glomerulus was then calculated. 2) In the electron microscope 6–10 random views of each biopsy were photographed at 2000 times enlargement, and the number of indentations and intramembraneous lucent areas of the GBM per micrograph were counted. The significance of the difference between the mean number of GBM lesions in the various patient groups was analysed with the Student's T-test.

All available clinical data, as well as results of immunofluorescence studies, were collected from hospital records and compiled without knowledge of the electron and light microscopic findings.

RESULTS

Light microscopy of paraffin sections In some biopsies, which in electron microscopy often show-



Fig 1 Micrograph of a portion of a glomerulus. Obliquely-cut portions of the GBM have a coarsely-textured stippled appearance (arrows). PASM stained histologic section. Patient No. 5. $\times 800$

ed pattern I (see below), the vacuolizations were easily visible under a dry high-power lens ($40\times$). The densely situated vacuoles, which varied in size, gave some specimens a fine, and others a coarse texture (Fig 1). In some biopsies, which in electron microscopy often showed pattern II (see below), the vacuolization was not readily apparent and as a rule visible only with an oil immersion lens ($100\times$) (Fig 2). It could be dense or sparse (Fig 3).

Light microscopy of Epon sections The GBM had one of two distinctive appearances. Either the GBM was irregular with rows of small knots, spikes and indentations (Fig 4). These changes were present in the biopsies of seven patients in all or most loops, and in the biopsies of three patients (Nos. 5, 6 and 15) in about half of the loops. This finding was called pattern I. Or, the GBM was almost continuously smooth, thin and even, with only occasional indentations (Fig 5). This finding was called pattern II.

Electron microscopy Consistent with the aforementioned light microscopic observations on Epon sections, two patterns could be discerned, which differed from each other more in the number and distribution of glomerular lesions than in their morphologic detail. In pattern I irregularities of the GBM were widespread and consisted of subepithelial deposits, spiky projections of the GBM, indentations, and/or intramembraneous electron dense or lucent areas (Figs 6 and 7). In pattern II the GBM showed indentations and intramembraneous lucent areas or dense deposits rather sparsely, about three lesions in each loop (Fig 8). The distribution of these abnormalities seemed to occur at random in nine patients but regularly in patient No. 2 (Fig 9). In three patients (Nos. 7, 12 and 19), in addition to being irregularly distributed, many abnormalities were concentrated to a few loops producing a picture reminiscent of pattern I (Fig 10). The indentations usually affected the subepithelial, seldom the subendothelial aspect of the GBM. They often had lip-like margins, and they could contain electron-dense amorphous, striated membrane-like, or rounded membrane-bound material (Figs 9, 10a and 10b).

Immunofluorescence and clinical data As shown in Table 1, tissue from seven patients with pattern I had been examined by immunofluorescence and shown a moderate or strong granular fluorescence along the glomerular capillary wall. Tissue from eight patients with pattern II lesions had been examined by immunofluorescence and shown a mostly faint or negative finding except two patients with mesangial deposits, and only one patient (No. 2) showed a linear-granular fluorescence along the capillary wall. Clinically, 9 of the 10 patients with



Fig 2 Micrograph of a portion of a glomerulus. Obliquely-cut portions of the GBM show dense fine vacuolization (arrows). PASM stained histologic section. Patient No. 2. $\times 2,200$.

Fig 3 Micrograph of a portion of a glomerulus. Obliquely-cut portions of the GBM show coarse and sparse vacuolization (arrows). Patient No. 1. $\times 2,500$.





Fig 4 Micrograph of a portion of a glomerulus. The GBM is irregular with multiple knots, indentations and spiky projections (arrows). PASM stained ultrathin section. Patient No 5 $\times 1800$.

Fig 5 Micrograph of a portion of glomerulus in which the GBM is indented (arrows). Patient No 13. PASM stained ultrathin section $\times 1800$.

Fig 6 Electron micrograph of the GBM showing multiple indentations (i) and intramembranous lucent areas (l). Patient No 5. PASM stain $\times 8400$.

Fig 7 Electron micrograph of glomerular capillary loops, one of which contains multiple intramembranous (d) lucent areas and electron dense deposits. Patient No 5 $\times 8300$.

Fig 8 Electron micrograph of a glomerular capillary loop. The GBM shows a number of indentations and intramembranous lucent areas (arrows). Patient No 3. PASM stain $\times 5200$.

Fig 9 Electron micrograph of the glomerular capillary wall. The GBM shows at fairly regular intervals indentations containing electron-dense deposits (arrow heads). Patient No 2 $\times 29000$.

Fig 10 a) Electron micrograph of a glomerular capillary wall that has multiple indentations (thin arrows) and intramembranous lucent areas (thick arrow). Patient No 19. PASM stain $\times 13100$.

b) The same area as in a) viewed in the next consecutive section. Areas that are electron lucent in a) are partly lucent and partly dense in b). Section stained with lead citrate and uranyl acetate $\times 14000$.



TABLE 1 Immunofluorescence and Clinical Data of Patients in Whom the M in PASM stained Histologic Sections Showed Vacuolization

Pattern of GBM lesions in ultrathin sections ^{a)}	Patient No	Sex	Age (yr)	Indication for renal biopsy	Immunofluorescence			Suggested clinicopathological diagnosis after light microscopy immunofluorescence and electron microscopy ^{b)}
					Antisera	Pattern	Intensity	Distribution
I	4	F	23	NS ^{c)} and hematuria	Gammaglobulin and complement	Granular	Strong	Capillary
I	5	F	38	Heavy proteinuria	-	-	(Not done)	-
I	6	M	38	Heavy proteinuria	-	-	(Not done)	-
I	8	M	59	NS and renal vein thrombosis	-	-	(Not done)	-
I	9	F	28	NS	Gammaglobulin and complement	Granular	Strong	Capillary
I	10	F	26	Heavy proteinuria	Gammaglobulin and complement	Granular	Moderate	Capillary
I	13	F	28	SLE and proteinuria	IgG and C3	Granular	Strong	Capillary
I	14	F	22	NS and hematuria	IgG and C3	Granular	Strong	Capillary
I	15	M	38	NS and hematuria	Gammaglobulin	Granular	Moderate	Capillary
I	16	M	47	NS	IgG and C3	Granular	Moderate	Capillary
II	1	M	30	Acute anuria	-	-	(Not done)	-
II	2	F	53	SLE and proteinuria	Gammaglobulin	Linear granular	Moderate	Capillary
II	3	M	30	NS after gold therapy	Gammaglobulin	Linear	Strong	Capillary
II	7	M	41	Acute anuria	Complement	Negative	Negative	Negative
II	11	F	22	Hematuria	Gammaglobulin and complement	Negative	Negative	Negative
II	12	M	21	NS	Gammaglobulin and complement	Negative	Negative	Negative
II	17	F	37	Hematuria after gold therapy	IgG IgM C3	Granular	Moderate	Segm mesangial
II	18	M	32	Hematuria	-	-	(Not done)	Capillary streaks
II	19	M	32	Graft rejection because of chronic GN	Gammaglobulin and complement	Not specified	Moderate	Mesangial
II	20	M	19	Recent acute nephritic syndrome	IgM C3 IgG	Granular	Faint	Capillary streaks
					IgG IgA C3	Negative	Negative	Negative
						Not specified	Moderate	Mesangial
								Chronic rejection
								IgA IgG GN

^{a)} = see text p 412^{b)} = see Discussion^{c)} = nephrotic syndrome^{d)} = membranous glomerulonephritis^{e)} = minimal changes glomerulonephritis^{f)} = systemic lupus erythematosus

TABLE 2 Immunofluorescence and Clinical Data of Control Patients in Whom the GBM in PASM stained Histologic Sections Showed No Vasculization

Patient No	Sex	Age (yr)	Indication for renal biopsy	Immunofluorescence				Suggested clinicopathological diagnosis after light microscopy immunofluorescence and electron microscopy
				Antigen	Pattern	Intensity	Distribution	
21	M	21	Hematuria after gold therapy	Gammaglobulin and complement	Granular	Moderate	Capillary	MCGN
22	F	29	Hematuria after gold therapy	Gammaglobulin Complement	Linear Negative	Faint Negative	Capillary Negative	Hematuria after gold therapy MCGN
23	M	17	Proteinuria and hematuria	Gammaglobulin and complement	Negative	Negative	Negative	MCGN
24	M	19	Proteinuria	Gammaglobulin Complement	Linear	Moderate	Capillary	MCGN
25	F	27	Arterial hypertension	Gammaglobulin and complement	Granular	Moderate	Capillary streaks	Normal finding
26	F	21	Hematuria	Gammaglobulin and complement	Granular	Faint	Capillary streaks	MCGN
27	F	69	Slight renal insufficiency analgesic abuse	Gammaglobulin Complement	Linear Negative	Faint Negative	Capillary streaks	MCGN
28	F	33	Proteinuria and hematuria	Gammaglobulin Complement	Linear	Faint	Capillary streaks	MCGN
29	M	22	Hematuria	Gammaglobulin Complement	Negative	Negative	Capillary	MCGN
30	M	21	Hematuria	Gammaglobulin and complement	Granular	Faint	Capillary streaks	MCGN

pattern I lesions had or had had heavy proteinuria or the nephrotic syndrome. Of the 10 patients with pattern II lesions seven had none or slight proteinuria and two of these suffered from an acute anuric tubulointerstitial nephritis.

Controls Both in light and electron microscopy the GBM appeared completely normal except for occasional indentations in a few capillary loops. In immunofluorescence (see Table 2) eight patients examined had shown a faint or negative finding and only one patient showed a finding suggestive of membranous glomerulonephritis (but in this case no diagnostic subepithelial deposits were seen in electron microscopy). Clinically only two patients (Nos. 23 and 28) had a history of heavy proteinuria. None had ever presented the nephrotic syndrome and the indication for taking a biopsy had generally been microscopic hematuria or slight proteinuria or both.

Quantitative observations The number of light and electron microscopically enumerated lesions differed significantly ($p < 0.01$) between patients belonging to pattern I group and those with pattern II. This applied both when the groups were compared with each other and with the control group. The ratios of the mean numbers of glomerular lesions associated with pattern I, pattern II and controls respectively was approximately 100:10:1.

DISCUSSION

All biopsies which showed vacuolization as the only histological glomerular abnormality also showed on electron microscopy various numbers of indentations and intramembranous lucent areas which were almost totally lacking in control biopsies. We concluded that the ultrastructural counterparts of vacuolization are the indentations and intramembranous lucent areas of the GBM; the number and distribution of which give rise to what we have termed patterns I or II.

As a rule vacuolization was more easily visible in biopsies with pattern I than with pattern II abnormalities. In the former owing to their great frequency indentations and intramembranous lucent areas of the GBM are probably more likely to become superimposed upon each other than in the latter. Another possibility could be that the relative difference between the amount of GBM material on the site of and around the indentations (the spiky projections) was greater in pattern I material than in pattern II where such protruding portions often were lacking.

Ultrastructural immunofluorescence and clinical data of patients with biopsies presenting pattern I

abnormalities were compatible with membranous glomerulonephritis (1, 2, 4, 8, 10, 11) or resolving acute poststreptococcal glomerulonephritis (12, 16, 20). As in the former group the only histologic abnormality of the GBM was vacuolization these patients seem to have a special variant of membranous glomerulonephritis, i.e. nonprogressive histologically mild membranous glomerulonephritis, as previously described (21).

The immunofluorescence and clinical observations in patients with biopsies showing pattern II lesions as among the controls were varying. Only in patient No. 2 the findings were compatible with membranous glomerulonephritis (1, 2, 8) but in electron microscopy there were no spikes around the subepithelial deposits which is an atypical feature. Many patients mimic minimal changes glomerulonephritis (7, 8, 19). As immunofluorescence and clinical data of patients showing pattern II abnormalities did not differ from those of the controls we conclude that the vacuolization seen in light microscopy combined with pattern II in electron microscopy from a nosological point of view must be considered as nonspecific GBM indentations of an appearance similar to that of pattern II have been described previously in experimental and human diabetes mellitus in a variety of kidney diseases as well as in biopsies from healthy controls (9, 14, 15). In morphologic detail the lesions in pattern II and pattern I were remarkably similar (Figs. 3, 4, 8, 9, 10a, 10b). As previously suggested it is our hypothesis that the indentations and intramembranous lucent areas represent the sites of or remnants of former subepithelial deposits, presumably of immune complex origin (3, 6, 9, 16). If this hypothesis proves correct two possibilities exist for their origin. Either the indentations are the sites of former subepithelial deposits on whose epithelial surface no new GBM has been laid down as in stage II or membranous glomerulonephritis (4). Or they are the sites of deposits first buried in the GBM as in stage IV of membranous glomerulonephritis (4) but later "dig up" by a protruding epithelial or endothelial cell. In such a case it could be tempting to extrapolate from the classical staging of membranous glomerulonephritis and call them subepithelial deposits in stage V. In the late stages of membranous glomerulonephritis and often in pattern II lesions (Fig. 8) endothelial cells do protrude into an indentation of the GBM. This can be taken as a support for the latter interpretation. Theoretically our findings thus indicate that GBM lesions possibly related to former subepithelial deposits are found not only in membranous and resolving acute poststreptococcal glomerulonephri-

is but in addition to states quoted above (9, 14, 15). Also in systemic lupus erythematosus IgA IgG mesangial glomerulonephritis minimal changes glomerulonephritis chronic rejection and tubulointerstitial nephritis.

• gratefully acknowledge the technical assistance of Dr. J. A. Holanen. This study was supported by a grant from the S. G. J. Foundation.

REFERENCES

1. Jansen J, Druet P, Lagrue G, Samarcq P & Wile P. Les glomerulopathies membranaires (I, II). Etude morphologique en microscopie optique et electronique III en immunofluorescence. *Pathol Biol (Paris)* 19 3-32 1970
2. Arkholder P W. Atlas of Human Glomerular Pathology 1st ed Harper and Row Hagerstown 1974
3. Couser W G, Spargo B H, Sifman M W & Lew E J. Experimental glomerulonephritis in the rat. Part II Ultrastructural lesions of the basement membrane associated with proteinuria. *Lab Invest* 32 46-55 1975
4. Ehrenreich T & Churg J. Pathology of membranous nephropathy. In Sommers S C (Ed) *Pathology Annual* Appleton Century Croft New York 1968 pp 145-186
5. Gluck M C, Gallo G, Lowenstein J & Baldwin D S. Membranous glomerulonephritis. Evolution of clinical and pathologic features. *Ann Intern Med* 78 1-12 1973
6. Gould D B. Lacunae in glomerular basement membranes. *Lab Invest* 33 207 1975
7. Heib R. Clinicopathological Correlations and prognosis of glomerular nephropathies. In Strauss L (Ed) *Pediatric nephrology* 1st ed vol 1. Symposia Specialists Miami 1974 pp 115-134
8. Hopt U, R H. Pathology of the kidney 2nd ed Little Brown and Company Boston 1974
9. Korn R G, Fauci A S, Rosenthal A S & Wolff S M. Renal biopsy pathology in Wegeners granulomatosis. *Amer J Pathol* 74 423-440 1974
10. Jones D B. Nephrotic glomerulonephritis. *Amer J Pathol* 33 313-329 1957
11. Kinsaid Smith P. The kidney. A clinicopathological study 1st ed Blackwell Scientific Publications Oxford 1975
12. Morel Maroger L, Filastre J P, Gorin F, Gallo P & Richet G. Evolution histologique inhabituelle de 3 cas de glomerulonephrite aigue de l'adulte. *J Urol Nephrol* 76 337-341 1970
13. Movat H Z. Silver impregnation methods for electron microscopy. *Amer J Clin Pathol* 35 528-537 1961
14. Østerby Hansen R & Olsen T S. Moon-crafter formation on the glomerular basement membrane in human and experimental diabetes. *Acta Pathol Microbiol Scand* 71 318-320 1967
15. Østerby Hansen R, Lundbaek A, Olsen T S & Ørskov H. Kidney lesions in rats with severe long term alloxan diabetes III. Glomerular ultrastructure. *Lab Invest* 17 675-692 1967
16. Richet G, Filastre J P, More Maroger L & Barlet J. Change from diffuse proliferative to membranous glomerulonephritis. Serial biopsy in four cases. *Kidney Int* 5 57-71 1974
17. Row P G, Cameron J S, Turner D R, Evans D J, White R H R, Ogg C S, Chantler C & Brown C B. Membranous nephropathy. Long term follow up and association with neoplasia. *Quart J Med* 44 207-239 1975
18. Tallqvist G, Pasterback A & Tornroth R. Indentations of the glomerular basement membrane in renal diseases. A light and electron microscopic study on ultrathin serial sections. *Lab Invest* 35 327-336 1976
19. Thoenes G H. Immunohistochemische Befunde bei Minimalveränderungen und fokaler sklerosierender Glomerulopathie mit nephrotischem Syndrom. *Klin Wochschr* 52 371-378 1974
20. Tornroth T. The fate of subepithelial deposits in acute poststreptococcal glomerulonephritis. *Lab Invest* 35 461-474 1976
21. Tornroth T, Tallqvist G, Pasterback A & Linder E. Nonprogressive histologically mild membranous glomerulonephritis (MGN) appearing in all evolutionary phases as histologically nearly MGN. *Kidney Int* 14 511-521 1978

ORCEIN-POSITIVE GRANULES IN LIVER CELLS

Occurrence in a Consecutive Liver Biopsy Material

MOGENS VYBERG and PER THOMSEN

Department of Pathology Hvidovre Hospital, University of Copenhagen DK 2650 Hvidovre

Vyberg M & Thomsen P. Orcein positive granules in liver cells. Occurrence in a consecutive liver biopsy material. Acta path. microbiol. scand. Sect. A 87: 421-425, 1979.

Orcein positive granules (OPG) assumed to represent a copper storage protein occurring in liver cell lysosomes secondary to copper accumulation have been demonstrated in 139 out of 1002 specimens of a consecutive liver biopsy material (13.9%). OPG are revealed in a variety of lesions which as a common feature exhibit fibrosis often connected with long standing cholestatic liver disease. The highest frequency is found in primary biliary cirrhosis (PBC) where 16 out of 18 biopsies show OPG usually in large amounts and in cirrhosis with alcoholic hepatitis where 38 out of 51 are orcein positive. 37 biopsies showing features of chronic hepatitis are all orcein negative. The fairly constant presence of large amounts of OPG in PBC in contrast to the low frequency in chronic hepatitis seems to be an important diagnostic clue.

Key words: Orcein positive granules, copper accumulation, periportal fibrosis, cholestatic liver disease.

M. Vyberg, Frydenlundsvej 98, DK 2950 Vedbæk.

Accepted as submitted 26 III 79.

In 1974 Shikata *et al* (4) demonstrated that hepatitis B surface antigen (HBsAg) in liver cells was stained by orcein after oxidation of the tissue section. The orcein positive material was seen in the cytoplasm as areas of a uniform finely granular brown material.

Using the same staining method Sipponen *et al* (8) in 1975 found another orcein positive material in the liver cell cytoplasm consisting of discrete rounded black brown granules of a size varying from barely visible to about 5 µm in diameter typically located perinuclearly most often in periportal liver cells. The orcein positive granules (OPG) were first demonstrated in cases of primary biliary cirrhosis (PBC) and chronic aggressive hepatitis (CAH). Subsequently OPG were found in other disorders particularly long standing cholestasis and various forms of cirrhosis (3).

By means of histochemical methods, electron microscopy and X ray microanalysis OPG have been found to represent a copper binding metallo-

protein accumulated in the secondary lysosomes in the liver cells (5, 6, 7).

The aim of the present paper is to describe in which liver diseases and with what frequency OPG occur in a consecutive series of liver biopsies from a Scandinavian metropolis.

MATERIAL AND METHODS

In 1977 The department of Pathology, Hvidovre Hospital received 994 liver biopsies.

Excluded because of either inadequate material (specimens shorter than 5 mm - 22 biopsies), insufficient fixation (3 biopsies) or extensive destruction of the liver tissue due to tumour infiltration (20 biopsies).

The material hereafter comprises 1002 biopsies. Of these 994 are needle biopsies (obtained by a Menghini needle) the average length being about 1 1/2 cm. 8 are surgical biopsies. The specimens are obtained from a total of 930 patients.

The tissue is fixed in 4 per cent buffered formalin embedded in paraffin and cut on a rotary microtome in 6 µm thick serial sections of which three are stained by orcein according to the method of Shikata *et al* (4). The tissue sections are oxidized for 5 minutes in a solution of 1.5 g potassium permanganate in 100 ml distilled water to which 1.5 ml concentrated sulphuric acid is added just before use. Hereafter the sections are bleached in 1.5 per cent oxalic acid for about 1 minute and stained for 4 hours in a solution of 1 g orcein (BDH Batch No 2479310 Product No 34063) dissolved in 100 ml 70 per cent ethanol adjusted to pH 1-2 with 1 ml concentrated hydrochloric acid.

The orcein stained sections are examined by the two authors in cooperation without previous knowledge of the histological diagnoses. The presence of OPG is registered semiquantitatively on basis of the maximal number of granule containing cells per lobule/nodule: 1-5 cells + 6-20 cells ++ > 20 cells +++.

The material is classified according to chief histological diagnosis as shown in Table 1 and 2. The diagnoses have been made by 2 specialists in pathological anatomy with special interest in hepatology.

The diagnosis 'fibrosis' refers to portal and/or periportal increase of connective tissue in livers with preserved architecture. 'Cirrhosis' refers to micro or macronodular cirrhosis without features of biliary cirrhosis or haemochromatosis.

'Large duct biliary obstruction' refers to biopsies with preserved architecture and typical portal changes.

oedema, marginal bile duct proliferation and infiltration with neutrophils with or without parenchymal cholestasis.

The diagnoses PBC, secondary biliary cirrhosis (SBC), primary haemochromatosis and sarcoidosis are confirmed by the clinical features. Seven cases clinically considered as PBC do not show pathognomonic histological changes but the lesions are compatible with PBC and the cases are included in this group.

RESULTS

Orcein positive granules (OPG) have been found in 139 out of 1002 liver biopsies (13.9%). In about half of the biopsies containing OPG the amounts are small (corresponding to +). The rest divided evenly between moderate and large amounts (corresponding to ++ and +++). Table 1 shows the diagnostic groups in which biopsies containing OPG occur and the frequency and the amounts of OPG within each group are shown. Table 2 shows the diagnostic groups in which OPG have not been found.

Conditions in which OPG have been found (Table 1)

Large duct biliary obstruction with fibrosis shows varying amounts of OPG in eleven out of 38 biopsies. Histological cholestasis occurs in about

TABLE 1 Conditions in which Orcein Positive Granules (OPG) Have Been Found

Chief histological diagnosis	Number of biopsies				Per cent biopsies with OPG	
	With OPG			Without OPG	Total	
	+	++	+++	total		
Large duct biliary obstruction						
+ fibrosis	3	6	2	11	17	39
Secondary biliary cirrhosis	1	2	1	4	7	67
Primary biliary cirrhosis	1	1	14	16	2	89
Acute hepatitis	1	1	0	4	197	2
Granulomatous lesions	0	1	0	1	9	10
Fibrosis (without steatosis)	6	1	1	2	21	10
Fibrosis + steatosis	7	2	1	10	61	14
Fibrosis + alcoholic hepatitis	0	3	0	3	16	16
Cirrhosis (without steatosis)	5	3	2	10	34	23
Cirrhosis + steatosis	20	8	6	34	45	43
Cirrhosis + alcoholic hepatitis	23	8	7	38	13	75
Primary haemochromatosis						
cirrhosis	1	0	0	1	3	25
Carcinoma primary	0	0	2	2	3	40
Carcinoma secondary	1	1	1	3	24	11
Total	65	37	37	139	447	24

+ = 1-5 cells with OPG per lobule/nodule ++ = 6-20 cells with OPG per lobule/nodule +++ = > 20 cells with OPG per lobule/nodule (maximal number) Number of patients in brackets

half of the 28 biopsies with the same frequency in orcein positive and orcein negative cases

Secondary biliary cirrhosis OPG are found in four out of six biopsies. The orcein positive biopsies come from patients who have choledochal obstruction at the time of biopsy (three have bile stones one sclerosing cholangitis). The two orcein negative biopsies come from patients in whom choledochal occlusion has been relieved preoperative biopsies (one is included in the above mentioned the other is not in the material) display OPG in both cases. Histological cholestasis is present in two of the orcein positive biopsies.

Primary biliary cirrhosis OPG occur in 16 out of 18 biopsies. Large amounts are seen in 14 of the biopsies. In the two biopsies without OPG only non specific reactive hepatitis is seen. Re biopsies some months later reveal in both cases changes characteristic for PBC as well as large amounts of OPG. None of the biopsies show histological cholestasis. The typical picture of OPG accumulated in perportal liver cells in a case of PBC is shown in Fig 1.



Fig 1 Orcein positive granules in perportal liver cells in primary biliary cirrhosis. Orcein $\times 400$

TABLE 2 Conditions in which Orcein Positive Granules Have not Been Found

Chief histological diagnosis	Number of biopsies
Large-duct biliary obstruction (without fibrosis)	52
Intrahepatic cholestasis	12
Ground glass hepatocytes + non-specific reactive hepatitis	5
Chronic persistent hepatitis	18
Chronic aggressive hepatitis	9
Non specific reactive hepatitis (without fibrosis)	101
Steatosis	117
Haemosiderosis	8
Alpha ₁ antitrypsin accumulation	2
Sinusoidal dilatation	8
Malignant lymphoma and leukemia	5
Other lesions (myeloid metaplasia disseminated intravascular coagulation amyloidosis polyarteritis nodosa)	6
Normal Liver	80
Total	421

Acute hepatitis Out of 196 biopsies small amounts of OPG are found in four. These four biopsies show in addition areas with fibrosis and two of them - coming from an alcoholic - also steatosis.

None of the four biopsies show histological cholestasis.

Granulomatous lesions Out of ten biopsies with granulomas OPG occur in one from a patient with sarcoidosis. This biopsy reveals numerous portal granulomas and severe fibrosis but no

three out of 16 with fibrosis + alcoholic hepatitis the amounts of OPG most often being small.

Histological cholestasis is found in two of the 15 orcein positive biopsies.

Cirrhosis OPG are found in varying amounts in ten cases out of 34 with pure cirrhosis in 33 out of 79 with cirrhosis + steatosis and in 38 out of 51 with cirrhosis + alcoholic hepatitis. In haemochromatosis-cirrhosis OPG occur in one out of four

The tissue is fixed in 4 per cent buffered formalin embedded in paraffin and cut on a rotary microtome in 6 µm thick serial sections of which three are stained by orcein according to the method of Shikata *et al.* (4). The tissue sections are oxidized for 5 minutes in a solution of 1.5 g potassium permanganate in 100 ml distilled water to which 1.5 ml concentrated sulphuric acid is added just before use. Hereafter the sections are bleached in 1.5 per cent oxalic acid for about 1 minute and stained for 4 hours in a solution of 1 g orcein (BDH Batch No 2479310 Product No 34063) dissolved in 100 ml 70 per cent ethanol adjusted to pH 1-2 with 1 ml concentrated hydrochloric acid.

The orcein stained sections are examined by the two authors in cooperation without previous knowledge of the histological diagnoses. The presence of OPG is registered semiquantitatively on basis of the maximal number of granule containing cells per lobule/nodule: 1-5 cells + 6-20 cells ++ > 20 cells +++.

The material is classified according to chief histological diagnosis as shown in Table 1 and 2. The diagnoses have been made by 2 specialists in pathological anatomy with special interest in hepatology.

The diagnosis »fibrosis« refers to portal and/or periportal increase of connective tissue in livers with preserved architecture. »Cirrhosis« refers to micro or macronodular cirrhosis without features of biliary cirrhosis or haemochromatosis.

»Large duct biliary obstruction« refers to biopsies with preserved architecture and typical portal changes

oedema marginal bile duct proliferation and infiltration with neutrophils with or without parenchymal cholestasis.

The diagnoses PBC, secondary biliary cirrhosis (SBC), primary haemochromatosis and sarcoidosis are confirmed by the clinical features. Seven cases clinically considered as PBC do not show pathognomonic histological changes but the lesions are compatible with PBC and the cases are included in this group.

RESULTS

Orcein positive granules (OPG) have been found in 139 out of 1002 liver biopsies (13.9%). In about half of the biopsies containing OPG the amounts are small (corresponding to +). The rest divided evenly between moderate and large amounts (corresponding to ++ and +++). Table 1 shows the diagnostic groups in which biopsies containing OPG occur, and the frequency and the amounts of OPG within each group are shown. Table 2 shows the diagnostic groups in which OPG have not been found.

Conditions in which OPG have been found (Table 1)

Large-duct biliary obstruction with fibrosis shows varying amounts of OPG in eleven out of 28 biopsies. Histological cholestasis occurs in about

TABLE 1 Conditions in which Orcein Positive Granules (OPG) Have Been Found

Chief histological diagnosis	Number of biopsies				Per cent biopsies with OPG	
	With OPG			Without OPG	Total	
	+	++	+++	total		
Large duct biliary obstruction + fibrosis	3	6	2	11	17	28 (25)
Secondary biliary cirrhosis	1	2	1	4	2	6 (5)
Primary biliary cirrhosis	1	1	14	16	2	18 (15)
Acute hepatitis	1	1	0	2	192	196 (165)
Granulomatous lesions	0	1	0	1	9	10 (9)
Fibrosis (without steatosis)	0	1	1	2	21	23 (2)
Fibrosis + steatosis	7	2	1	10	61	71 (66)
Fibrosis + alcoholic hepatitis	0	3	0	3	16	19 (19)
Cirrhosis (without steatosis)	5	3	2	10	34	44 (43)
Cirrhosis + steatosis	20	8	6	34	45	79 (78)
Cirrhosis + alcoholic hepatitis	23	8	7	38	13	51 (50)
Primary haemochromatosis	1	0	0	1	3	4 (3)
Cirrhosis	0	0	2	2	3	5 (4)
Carcinoma primary	1	1	1	3	24	27 (27)
Carcinoma secondary						
Total	65	37	37	139	442	581 (511)
						24

+ = 1-5 cells with OPG per lobule/nodule ++ = 6-20 cells with OPG per lobule/nodule +++ = > 20 cells with OPG per lobule/nodule (maximal number) Number of patients in brackets

of OPG in PBC seems to be an important diagnostic clue in differentiating PBC from CAH and post hepatic cirrhosis and to a certain extent also from large-duct biliary obstruction

REFERENCES

- 1 Jain S, Scheuer P J, Archer B, Newman S P & Sherlock S. Histological demonstration of copper and copper associated protein in chronic liver diseases. *J Clin Pathol* 31: 784-790 1978
- 2 Salaspuro M & Sipponen P. Demonstration of an intracellular copper binding protein by orcein staining in long-standing cholestatic liver diseases. *Gut* 17: 787-790 1976
- 3 Salaspuro M P, Sipponen P & Makkonen H. The occurrence of orcein positive hepatocellular material in various liver diseases. *Scand J Gastroenterol* 11: 677-681 1976
- 4 Shikata T, Umeta T, Yoshinara N, Akatsuka T & Yamaoka S. Staining methods of Australia antigen in paraffin section. *Japan J Exp Med* 44: 1: 25-36 1974
- 5 Sipponen P. Orcein positive hepatocellular material in long standing biliary diseases. I. Histochemical characteristics. *Scand J Gastroenterol* 11: 545-552 1976
- 6 Sipponen P. Orcein positive hepatocellular material in long-standing biliary diseases. II. Ultrastructural studies. *Scand J Gastroenterol* 11: 553-557 1976
- 7 Sipponen P, Hjelt L, Tornkvist T & Salaspuro M. X ray microanalysis of copper accumulation in liver in secondary biliary cirrhosis. *Arch Pathol Lab Med* 100: 664-666 1976
- 8 Sipponen P, Salaspuro M P & Makkonen H. Orcein positive hepatocellular material in histological diagnosis of primary biliary cirrhosis. *Ann Clin Res* 7: 273-377 1975

cases Ten biopsies with cirrhosis show concomitant features of CAH None of these biopsies show OPG Histological cholestasis occurs in eight of the 81 orcein-positive cases

Carcinoma Two biopsies out of five with primary liver cell carcinoma show OPG These two come from the same patient and show concomitant cirrhosis and orcein-positive ground glass hepatocytes This is the only biopsies in our material containing both OPG and HBsAg OPG are seen in three out of 27 biopsies with carcinoma metastases Among the five orcein-positive biopsies in this group, histological cholestasis is found in one and fibrosis in four

Conditions in which OPG have not been found (Table 2)

None of the specimens with intrahepatic cholestasis (12 biopsies) or large-duct biliary obstruction without fibrosis (52 biopsies) reveal OPG Neither are OPG found in specimens with chronic persistent or aggressive hepatitis (27 biopsies) OPG are absent in five cases with HBsAg containing liver cells (and non-specific reactive hepatitis) OPG have not been demonstrated in cases of non-specific reactive hepatitis, steatosis, haemosiderosis, sinusoidal dilatation, malignant lymphoma, leukaemia, and the group other lesions Finally, all of 80 biopsies from normal adult liver are orcein-negative

DISCUSSION

Orcein-positive hepatocellular granules were first demonstrated by *Sipponen et al* (8) in 15 out of 18 cases of PBC and in five out of 25 cases of CAH Later *Salaspuuro et al* (3) in a consecutive material of liver biopsies found OPG in 22 out of 297 specimens and in a material of 103 biopsies representing various liver diseases they found OPG in five biopsies In these materials the orcein-positive biopsies represent PBC cholestatic liver disease related to ulcerative colitis SBC alcoholic and posthepatic cirrhosis Among the cases without OPG, one represents PBC 16 CAH and 36 chronic persistent hepatitis

In our material 139 out of 1002 biopsies contain OPG The common histological feature of the orcein-positive cases, both in our study and in the above mentioned, seems to be periportal fibrosis often in combination with long-standing impediment of the biliary flow

Fibrosis is an almost constant finding, as only one biopsy in our material without fibrosis shows OPG Furthermore, the OPG-containing cells are usually, but not always, situated in fibrotic areas close to the scarring tissue On the other hand

fibrosis, especially in cases with CAH (see below), is often seen without OPG

Impediment of the biliary flow is another prevalent feature Even though histological cholestasis is infrequently seen, the disorders in question often show clinical cholestasis, i.e. increased alkaline phosphatase and bilirubin This goes particularly for PBC and large-duct biliary obstruction, but also for alcoholic liver lesions and neoplastic lesions It is noteworthy, that two cases of SBC become orcein-negative, when the choledochal obstruction is relieved Only cholestatic lesions with concomitant fibrosis show OPG, while lesions with cholestasis of shorter duration and without fibrosis e.g. acute hepatitis, large duct biliary obstruction, and intrahepatic (drug-induced) cholestasis do not show OPG In biopsies with long-standing biliary obstruction, no relationship has been found between the amounts of OPG and degree of fibrosis

In chronic hepatitis the occurrence of OPG is rare In our material, we do not find any positive cases out of 18 with chronic persistent hepatitis and 19 with CAH (including ten where cirrhosis has developed) *Sipponen et al* (8) found OPG in five out of 25 cases of CAH, but four of these were atypical showing cholestatic features *Jain et al* (1) recently found small or moderate amounts of OPG in 7 out of 16 cases of CAH, but did not specify whether these cases were divergent

The orcein-positive granular material is attributed to a copper-binding protein probably the sulphhydryl-rich protein metallothionein (5) The biliary tract is the main excretory route for copper and the copper-protein complex is assumed to accumulate in the lysosomes when the copper content in the liver cells increases, e.g. as the result of impeded bile flow Comparison between orcein and copper staining has shown good agreement (1, 2), the orcein being a little more sensitive than rubanic acid and p-dimethylaminobenzylidine rhodanine (1) The orcein staining thus seems to be a useful method in screening for enhanced copper content in liver biopsies

In conclusion orcein-positive granules are found in a good ten per cent of consecutive liver biopsies The granules - reflecting enhanced liver copper content - can be seen in a variety of lesions generally characterized by features of periportal fibrosis often connected with long-standing impediment of biliary flow Cholestatic liver lesions only reveal OPG when they have persisted long enough for fibrosis to develop It is also possible that fibrosis in some cases act as an obstacle to the excretion of bile from liver cells promoting the copper accumulation and occurrence of OPG

The fairly constant occurrence of large amounts

DIFFERENCE IN GROWTH OF HORMONE DEPENDENT AND HORMONE INDEPENDENT MAMMARY TUMOURS OF GR MICE, *IN VIVO* AND *IN VITRO*

PER BRIAND SUSAN M THORPE and JOHAN L DAENFELDT

The Fibiger Laboratory Copenhagen Denmark

Brand P Thorpe S M & Daehnfeldt J L Difference in growth of hormone dependent and hormone independent mammary tumours of GR mice *in vivo* and *in vitro* Acta path microbiol scand Sect A 87 427-436 1979

Growth *in vivo* of hormone dependent (HD) and hormone independent (HI) GR mouse mammary tumours was evaluated on the basis of doubling time (t_d) and TD_{50} , i.e. the number of tumour cells required to produce a tumour in 50% of inoculated animals within 2 months. TD_{50} was 10-100 times higher for HD than for HI tumour cells whereas t_d was the same for the two types of tumours. By explanting minced tumour tissue in a modified MEM medium supplemented with 10-20% fetal bovine serum and insulin (5 μ g/ml) monolayer cultures consisting of islands of epithelial cells were obtained. Sixty five per cent of primary cultures from 71 tumours were tumourigenic as tested by reinoculation into mice. Nearly all the tumourigenic cultures had retained the hormone dependence or independence of the original tumour. In order to compare the growth of HD and HI tumours *in vitro* 6 primary tumours were transplanted serially to follow the progression from HD to HI growth. Cell proliferation *in vitro* as measured by 3H thymidine incorporation tended to be higher in cultures of HI carcinomas than in cultures of HD carcinomas. The ability of cultures to grow in repeated subcultivations was correlated to the number of transplant generations rather than to the transition from HD to HI growth *in vivo*.

Key words: Mammary tumours, hormone dependence, growth *in vivo* and *in vitro*.

P Brand, The Fibiger Laboratory, Ndr Frhavnsgeade 70, 2100 Copenhagen Ø, Denmark.

Received 16 II 79 Accepted 6 IV 79

It is well established that about one third of the patients with advanced breast cancer respond to some form of endocrine therapy (10). One method of distinguishing hormone responsive (HR) tumours from non responsive is based upon examination of the hormone receptor pattern in the tumour tissue. Another approach would be to investigate whether there are differences in the growth capacities of hormone dependent (HD) and hormone independent (HI) tumour cells in tissue culture. When neither estrogen, progesterone nor prolactin

are added to the culture medium, only HI cells would be expected to be able to proliferate *in vitro*.

In the present communication we have investigated the growth rate of HD and HI mammary tumours of GR mice *in vivo* as well as the ability of cells from these two types of tumours to proliferate *in vitro*.

Abbreviations used

HD hormone dependent
HR hormone responsive
HI hormone independent
 t_d
 TD_{50}

p
o oestrogen

Sponsored by the Danish Cancer Society. Technical assistance of Marianne Hansen, Kirsten Kruger, Janne Krosgaard Petersen and Birthe Antonson.

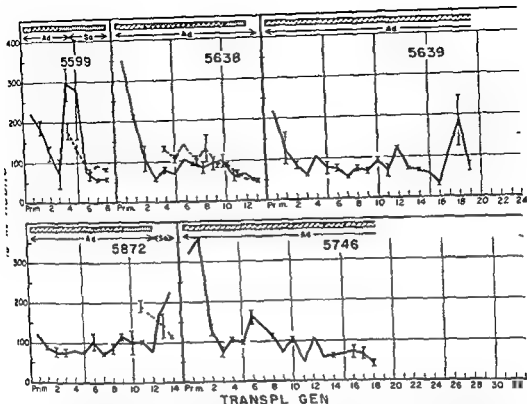


Fig. 2. Doubling time (T_d) of five tumour lines through 8-19 transplant generations *in vivo*. In each transplant generation tumour tissue was transplanted to castrated mice (broken line) some of which were treated with testosterone + oestrone (unbroken line). The tumours were either adenocarcinomas of type B (Ad) or sarcoma like (S). The horizontal bar on top of each curve indicates HD (hatched), HR (cross-hatched) and HI (double-hatched) state of tumour growth.

umber. The tumour maintained its hormone dependence in all of the 9 transplant generations and no significant change was found in the TD_{50} $4-6.5 \times 10^5$ cells per animal).

Monolayer Cultures

All primary cultures were composed of epithelial cells (Fig. 2). In order to demonstrate that the cultures contained tumour cells, primary cultures from 71 tumours were inoculated *in vivo* after one week of cultivation. The animals were inoculated with 0.02 to 4.95 mg of cell protein which responded in 4×10^5 to 10^6 cells per animal. Forty-six (65%) cultures from 71 tumours were tumorigenic (Table 3). Twenty of 26 tumorigenic cultures from HD tumours and 7 of 8 from HI tumours retained the hormonal status of the original tumour.

Histomorphology of tumours produced by inocu-

lated tissue culture cells usually resembled that of the original tumour (Figs. 3A and 3B). Eight (3 HD, 4 HR, 1 HI) of 51 tissue culture derived tumours had a sarcoma like histology.

Our results show that within two transplant generations *in vivo* converted to sarcoma like tumours.

Growth in Monolayer Culture

Tumour cell proliferation was evaluated by the ability of monolayer cultures of the tumours to incorporate 3H thymidine (Fig. 5) and to be propagated in serial subcultivation with a split ratio of 1:2 (Fig. 6).

Six primary tumours were serially transplanted. One of the tumour lines (5663) converted to a HI state in the 3rd transplant generation whereas other tumour lines remained HD for more than 30

MATERIAL AND METHODS

Tumours

Mammary tumours were induced in female GR mice by treatment with 3 pellets (10 mg) weekly of progesterone (p) s.c. + 0.5 µg of oestrone (o) per ml of drinking water according to the method of van Nie (13) and described previously (3, 15). Histologically the tumours are adenocarcinomas of type B (5). Metastases from primary tumours to the lungs were seen in 2 out of 89 animals.

For transplantation either minced tumour tissue or cell suspension was inoculated subcutaneously into castrated male mice some of which were treated with p + o.

Cell suspensions were prepared from minced tumour tissue according to the method of Heppes & Prop (25). The viability as measured by Trypan Blue staining was about 90% in cell suspensions of both HD and HI tumour cells. Usually $5-10 \times 10^6$ Trypan Blue negative cells were inoculated per animal. HD tumour lines were transplanted every 4-6 weeks and HI tumour lines every 2-4 weeks.

The tumours have been defined as HD, HR, and HI as described earlier (3).

Growth Curves and t_d

Tumour growth was registered by measuring the length, width and height (l, w and h) of the tumour with a slide caliper every 1-3 days. The volume (V) of the tumour was calculated from the formula

$$V = 0.5236 \times l \times w \times h \quad (18)$$

No correction was made for skin thickness. Tumours less than 50 mm³ were not scored. On the basis of the tumour volume growth curves were drawn.

The doubling time (t_d) in hours was calculated from the initial near exponential part of the growth curve.

TD₅₀

The number of tumour cells required to produce a tumour within two months in 50% of the animals inoculated with a tumour cell suspension (TD₅₀) was determined by inoculating 3×10^6 , 10^6 , 3×10^5 , 10^5 and 3×10^4 cells respectively into 25 mice/5 in each group. In some experiments groups of 5 mice were also injected with 10^4 and 3×10^3 cells per mouse. TD₅₀ of HR and HI tumours was determined in both p + o treated and in not treated castrated males. A total of at least 50 animals was thus included in a single determination. After inoculation of tumour cells the animals were observed weekly for 2 months and the number of takes recorded. TD₅₀ was calculated as described by Stones (21).

Culture Method

Explantation *in vitro* was carried out either by sequential enzymatic treatment as described by Heppes & Prop (25) excluding the last filtration and the treatment with DNase or by passing minced tissue through a stainless steel grid (mesh size 42 µm). Both methods

led to a suspension of single cells and cell clumps which were seeded into T25 plastic flasks (Falcon Gateway International US or NUNC Roskilde Denmark) or to 250 mm tissue culture roller bottles (RC 41 New Brunswick Scientific Co. Inc. USA). Medium was renewed daily in the flasks used for growth studies and two to three times weekly for subcultivation. The culture medium (Fib 41B) was Eagle's MEM (6) with Earle's Balanced Salt Solution and modified as described previously (2). Five µg insulin per ml and 10% 20% heat inactivated fetal bovine serum were added in the medium.

Incorporation of ³H thymidine

Replicate cultures of tumour cells were explanted in T25 flasks as described above. From 0.5-1.0 mg of cell protein was seeded per flask. After 1, 2, 3 and 4 days ³H thymidine (Radiochemical Center, Amersham, U.K. spec. act. 5 Ci per mmol) was added to two cultures to a final concentration of 1 µCi per ml. After three hours of incubation at 37 °C an excess of unlabeled thymidine (final concentration 2 mM) was added. After a further 30 minutes at 37 °C the medium was discarded and the cell layer was washed twice with ice cold PBS. The protein was determined according to the method of Lowry *et al.* (11) modified by Osama & Eagle (16).

Inoculation of Cultured Cells into Mice

Primary cultures were inoculated subcutaneously into castrated male mice some of which were treated with p + o. The animals were observed once a week for tumour growth at the inoculation site. If no tumour had appeared within a period of 2 months the tumour take was recorded as negative.

RESULTS

In all of 5 serially transplanted tumour lines the doubling time (t_d) decreased considerably from the primary tumour to the third transplant generation although the tumours were still in HD state (Fig. 1). An increase in t_d of tumours growing in p + o treated animals was observed to occur simultaneously to a change from an adenocarcinomatous to a sarcoma like histomorphology in tumour 5599 and 5872. Both these tumours had already progressed to HI growth prior to the alteration of histomorphology and upon further observation the t_d of tumour 5599 was found to return to its previous low value without further histomorphological changes.

The TD₅₀ of HD tumours was fairly uniform with values ranging between 4×10^5 and 10^6 cells per animal whereas TD₅₀ of HI tumours varied from 3×10^3 to 3×10^5 cells. TD₅₀ was followed through 9 transplant generations of the same tumour line (Table 2) in order to observe whether TD₅₀ varies as a function of transplant generation.

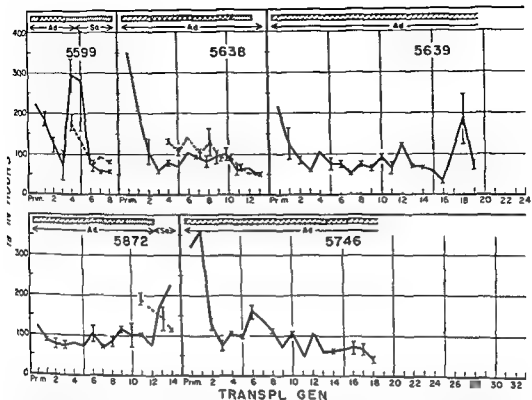


Fig 1 Doubling time (T_d) of five tumour lines through 8-19 transplant generations *in vivo*. In each transplant generation tumour tissue was transplanted to castrated mice (broken line) some of which were treated with progesterone + oestrone (unbroken line). The tumours were either adenocarcinomas of type B (Ad) or sarcoma like (Sa). The horizontal bar on top of each curve indicates HD (hatched) HR (cross hatched) and HI (double hatched) state of tumour growth.

number. The tumour maintained its hormone dependence in all of the 9 transplant generations and no significant change was found in the TD_{50} ($1.4-6.5 \times 10^5$ cells per animal).

Monolayer Cultures

All primary cultures were composed of epithelial like cells (Fig 2) in order to demonstrate that the cultures contained tumour cells. Primary cultures from 71 tumours were inoculated *in vivo* after one week of cultivation. The animals were inoculated with 0.02 to 495 mg of cell protein which corresponded to 4×10^5 to 10^8 cells per animal. Forty six (65%) cultures from 71 tumours were tumorigenic (Table 3). Twenty of 26 tumorigenic cultures from HD tumours and 7 of 8 from HI tumours retained the hormonal status of the original tumour.

Histomorphology of tumours produced by inocu-

lated tissue culture cells usually resembled that of the original tumour (Figs 3A and 3B). Eight (3 HD, 4 HR, 1 HI) of 51 tissue culture derived tumours had a sarcoma like histomorphology (Fig 4A) although the original tumour had been a carcinoma (Fig 4B). Three of these 8 tumours were derived from tumours that within two transplant generations *in vivo* converted to sarcoma like tumours.

Growth in Monolayer Culture

Tumour cell proliferation was evaluated by the ability of monolayer cultures of the tumours to incorporate 3H thymidine (Fig 5) and to be propagated in serial subcultivation with a split ratio of 1:2 (Fig 6).

Six primary tumours were serially transplanted. One of the tumour lines (5663) converted to a HI state in the 3rd transplant generation whereas other tumour lines remained HD for more than 20

TABLE 1 TD_{50} ¹⁾ of Hormone Dependent and Hormone Independent Mammary Tumours of GR Mice

Tumour line	Transplant generation	Hormone ²⁾ dependence	TD_{50} ¹⁾ (Cell number $\times 10^{-6}$ per animal)	
			p + o ³⁾	untreated ⁴⁾
1947	Primary	HD	0.56	no take
3507L	Primary	HD	> 1.1	no take
3508L	Primary	HD	0.38	no take
3545L	Primary	HD	0.83	no take
3833L	Primary	HD	0.49	no take
3402L	Primary	HI	0.11	0.17
243	7	HI	0.066	0.056
243	9	HI	0.066	0.056
481	9	HI	< 0.003	< 0.003
1245L	9	HI	n.i.	0.32
1245L	12	HI	n.i.	0.12
1107L	17	HI	< 0.025	0.032
32	20	HI	< 0.003	0.056

¹⁾ TD_{50} is the number of tumour cells required to produce a tumour in 50% of the animals within an observation time of 2 months

²⁾ HD hormone dependent HI Hormone independent

³⁾ Transplantation to castrated male mice treated with progesterone (p) and oestrone (o)

⁴⁾ Transplantation to castrated male mice receiving no hormonal treatment

n.i. not investigated

TABLE 2 TD_{50} of Tumour 3833 through 9 Serial Transplant Generations¹⁾

Transplant generation	Primary	1	2	3	4	5	6	7	8	9
TD_{50} ¹⁾	0.49	0.56	0.48	0.65	0.17	0.50	0.56	0.14	0.18	0.50

¹⁾ The tumour was hormone dependent in all transplant generations investigated. It was lost in the 9th transplant generation.

²⁾ TD_{50} is the number of tumour cells required to produce a tumour in 50% of recipient animals within an observation period of 2 months. TD_{50} is expressed as cell number $\times 10^{-6}$ per animal.

transplant generations. In all tumour lines the HI growth was preceded by HR state of growth. HI growth never reverted to HR or HD growth.

All 6 primary tumours were adenocarcinomas.

3 of
1 in
..

change from carcinoma to sarcoma-like histomorphology.

The tumour lines 5336, 5510, 5648, and 5663 that progressed to HI growth *in vivo* showed an increased 3H thymidine incorporation in culture associated with the time of conversion to HI. The 3H -thymidine incorporation of two tumour lines (5336 and 5663) decreased when the tumours became sarcoma-like. Although only little 3H -

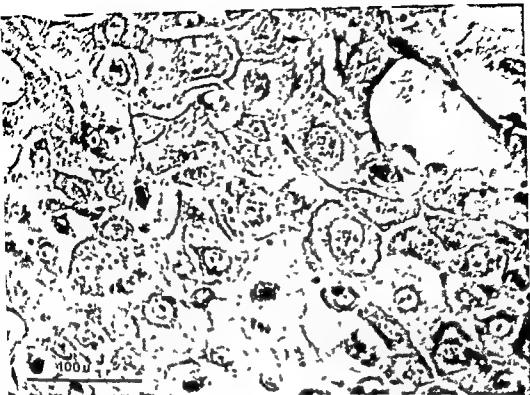


Fig 2 Phase contrast microscopic morphology of GR mouse mammary tumour in primary monolayer culture



Fig 3 Histomorphology of tissue-culture-derived tumour (A) and the tumour of origin (B) Stained with hematoxylin-eosin

TABLE 1 TD_{50} ¹⁾ of Hormone Dependent and Hormone Independent Mammary Tumours of GR Mice

Tumour line	Transplant generation	Hormone ²⁾ dependence	TD_{50} ¹⁾ (Cell number $\times 10^{-6}$ per animal)	
			p + o ³⁾	untreated ⁴⁾
1947	Primary	HD	0.56	no take
3507L	Primary	HD	> 1.1	no take
3508L	Primary	HD	0.38	no take
3545I	Primary	HD	0.83	no take
3833L	Primary	HD	0.49	no take
3402L	Primary	HI	0.11	0.17
243	7	HI	0.066	0.056
243	9	HI	0.066	0.056
481	9	HI	< 0.003	< 0.003
1245L	9	HI	n.i.	0.32
1245L	12	HI	n.i.	0.12
1107L	17	HI	< 0.025	0.032
32	20	HI	< 0.003	0.056

¹⁾ TD_{50} is the number of tumour cells required to produce a tumour in 50% of the animals within an observation time of 2 months

²⁾ HD hormone dependent HI hormone independent

³⁾ Transplantation to castrated male mice treated with progesterone (p) and oestrone (o)

⁴⁾ Transplantation to castrated male mice receiving no hormonal treatment

n.i. not investigated

TABLE 2 TD_{50} of Tumour 3833 through 9 Serial Transplant Generations¹⁾

Transplant generation	Primary	1	2	3	4	5	6	7	8	9
TD_{50} ²⁾	0.49	0.56	0.48	0.65	0.17	0.50	0.56	0.14	0.18	0.50

¹⁾ The tumour was hormone dependent in all transplant generations investigated. It was lost in the 9th transplant generation

²⁾ TD_{50} is the number of tumour cells required to produce a tumour in 50% of recipient animals within an observation period of 2 months. TD_{50} is expressed as cell number $\times 10^{-6}$ per animal

transplant generations. In all tumour lines the HI growth was preceded by HR state of growth. HI growth never reverted to HR or HD growth.

All 6 primary tumours were adenocarcinomas type II according to Dunn's classification (5). In 3 of the 6 tumour lines serial transplantation resulted in the development of fibrosarcoma-like tumours. In two of these tumour lines (5336 and 5510) the progression to HI state of growth coincided with a

change from carcinoma to sarcoma-like histomorphology.

The tumour lines 5336, 5510, 5648, and 5663 that progressed to HI growth *in vivo* showed an increased ³H-thymidine incorporation in culture associated with the time of conversion to HI. The ³H-thymidine incorporation of two tumour lines (5336 and 5663) decreased when the tumours became sarcoma-like. Although only little ³H-

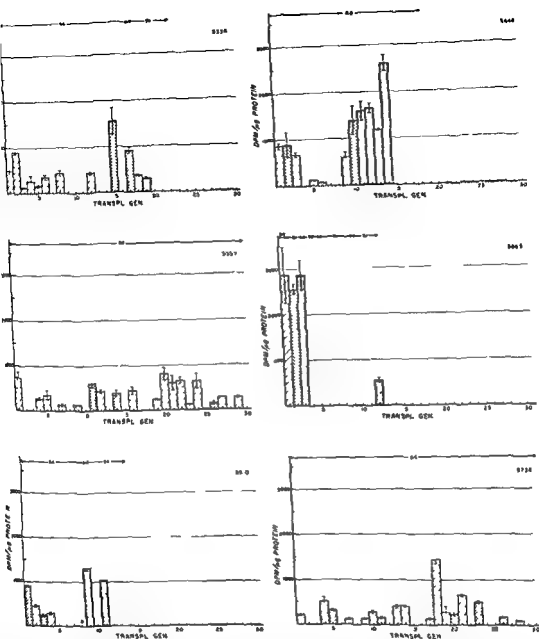


Fig 5 ^3H thymidine incorporation in 3-day-old monolayer cultures of tumours in successive transplant generations. HD tumour hatched bars, HR tumour cross hatched, HI tumour double hatched. Tumour 5510 converted to HI growth in the 8th transplant generation. The histology of the tumours is given at the top of each histogram. AD adenocarcinoma, An anaplastic carcinoma, Sa sarcoma like tumour.

TD₅₀ was 1–2 orders of magnitude higher for HD than for HI tumour cells. This means that if the t_0 s measured in established tumours are also valid for growth of the tumour before it becomes macroscopically measurable, a smaller proportion of HD than of HI cells seems to survive

transplantation. HI cells also seem to be harder

to be more antigenic than HI

TABLE 3 Tumorigenicity of One-Week-Old Monolayer Cultures of HD, HR, and HI Mammary tumours of GR Mice (Serially Transplanted Tumours of the 6 Tumour Lines are included)

Hormone dependence	n ^b	Growth of cultured cells in vivo ^a			
		HD	HR	HI	no growth
HD	49	20	5	1	23
HR	14	7	3	2	2
HI	8	1	0	7	1
	41	46			25

^a HD hormone dependent HR hormone responsive

HI hormone independent

^b n number of tumours explanted

thymidine was incorporated in cultured cells from HD tumours, autoradiography showed that the label was primarily located over the nucleus. The serially transplanted tumours could be grown in culture for more than 10 subculture passages if the

tumour had progressed to HI growth or if the tumour was in a transplant generation higher than 14 (Fig. 6)

DISCUSSION

The growth rate of a HD or a HR tumour - in contrast to a HI tumour - is influenced by the endocrine milieu. Given the proper hormonal environment, the HD tumours of GR mice grow well but they do not attain the same size as HI tumours within the same period of time after transplantation when the same amount of tumour material is transplanted (3, 19). It was suggested (19) that this difference is due to a difference in growth rate of the two types of tumours. However, in this investigation the t_d of the established tumours has been found to be the same for HD and HI tumours provided that they are in the same transplant generation. The increase in the growth rate (shorter t_d) observed here during the first three transplant generations has also been described in both the mammary carcinoma of an AK/Eh mouse (17) and the androgen dependent Shionogi carcinoma of DD/Sio mice (12).

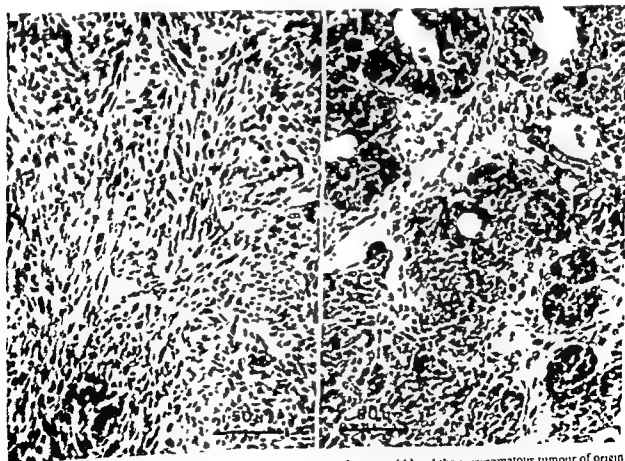


Fig. 4 Sarcoma-like histomorphology of a tissue culture derived tumour (A) and the carcinomatous tumour of origin (B). Stained with hematoxylin-eosin

HD and HI mammary tumours of GR mice have been studied with respect to ability to proliferate *in vitro*. Renoculation of the cultured cells into mice resulted in growth of a tumour that retained its original state of hormone dependence and histology in two-thirds of the cases. Absence of tumour take in the remaining one third of the cases could be due to either inoculum of too small a number of cells or too short a period of observation. In the six tumour lines studied proliferation *in vitro* measured by the ability of the monolayer cultures to be subcultivated was found in all HI tumours. However HD tumours in high transplant generations could also usually be subcultivated. ^3H thymidine incorporation was low in HI tumours of sarcomalike histology and high in a few HD tumours. Therefore neither subcultivation nor ^3H thymidine incorporation could be used to distinguish between HD and HI tumours.

During this study carcinomas have occasionally been observed to dedifferentiate to sarcoma like tumours. Fassel (7) has suggested that such a dedifferentiation may be due to malignant alteration of either tumour stroma or connective tissue at the implantation site by an oncogenic virus in the carcinoma cells. Progression to a HI state of growth simultaneous to a transition to a sarcoma like histology has previously been reported for the DE mammary tumour of the rat (1). While the same phenomenon can be observed in the GR mouse mammary tumours progression to a HI state usually occurs without an alteration in the histology of the tumour.

In conclusion significant differences between HD and HI tumours of the GR mouse have previously been found with respect to activities of glucose 6 phosphate dehydrogenase and hexokinase (3), oestrogen receptor capacity (4, 19), progesterone receptor capacity (4) and uptake of radioactive iodide (22). Differences in the tumour dose (TD_{50}) necessary for a tumour take are reported here. In cell proliferative capacity under our tissue culture conditions was an insufficient criterion to distinguish HD from HI tumours. It may be expected that HD and HI tumour cells react differently to hormones *in vitro* and this is presently under investigation.

Liquid Scintillation Counter used in this work was aided by the Danish National Research Foundation.

REFERENCES

1. Bergh H van den & Verresen H. La progression tumorale dans deux carcinomes mammaires du rat provoques par l'acetylaminofluorene. Bull Assoc. Fr Etud. Cancer 50: 291-303 1963.
2. Briand P. Cultivation of monolayer cell cultures in a continuous perfusion system. Acta Pathol. Microbiol. Scand 66: 31-40 1966.
3. Briand P & Daehnfeldt J L. Enzyme patterns of glucose catabolism in hormone-dependent and -independent mammary tumours of GR mice. Europ. J. Cancer 9: 763-770 1973.
4. Daehnfeldt J L & Briand P. Determinations of high affinity gestagen receptors in hormone-responsive and hormone independent GR mouse mammary tumours by an exchange assay. In McGuire W L et al (eds) Progesterone receptors in normal and neoplastic tissues. Raven Press, New York 1977 pp 59-69.
5. Dunn T B. Morphology of mammary tumours in mice. In Homburger F (ed) Physiopathology of Cancer. Hoeber Harper, New York 1959 pp 38-84.
6. Eagle H. Amino acid metabolism in mammalian cell cultures. Science 130: 432-437 1959.
7. Fassel E, Fetting R, Morgenroth K Jr & The mann H. The sarcomatous transformation of mammary carcinoma of mice in isologous transplantates in cell cultures and in reimplantates. Oncology 21: 189-213 1967.
8. Foulds L. Mammary tumours in hybrid mice: growth and progression of spontaneous tumours. Brit. J. Cancer 3: 345-375 1949.
9. Heston W E, Vlahakis G & Tsubura Y. Strain DD: a new high mammary tumour strain and comparison of DD with strain C3H. J. Natl. Cancer Inst 32: 237-251 1964.
10. Heuson J C. Hormones by administration. In Atkins H (ed) The treatment of breast cancer. MTP, Great Britain 1974 pp 113-163.
11. Lowry O H, Rosebrough N J, Farr A L & Randall R J. Protein measurement with the folin phenol reagent. J. Biol. Chem 193: 265-275 1951.
12. Muesel T & Yamaguchi K. An androgen dependent mouse mammary tumour. Cancer Res 25: 1168-1175 1965.
13. Nie R van. Personal communication 1970.
14. Nie R van & Dux A. Biological and morphological characteristics of mammary tumors in GR mice. J. Nat. Cancer Inst 46: 885-897 1971.
15. Nie R van & Hilgers J. Genetic analysis of mammary tumor induction and expression of mammary tumour virus antigen in hormone treated ovariectomized GR mice. J. Nat. Cancer Inst 56: 27-32 1976.
16. Oyama V I & Eagle H. Measurement of cell growth in tissue culture with a phenol reagent (Folin Ciocalteu). Proc. Soc. Exp. Biol. and Med 91: 305-307 1956.
17. Ringsted J. In vitro study of a mouse mammary carcinoma simulating carcinosarcoma and sarcoma.

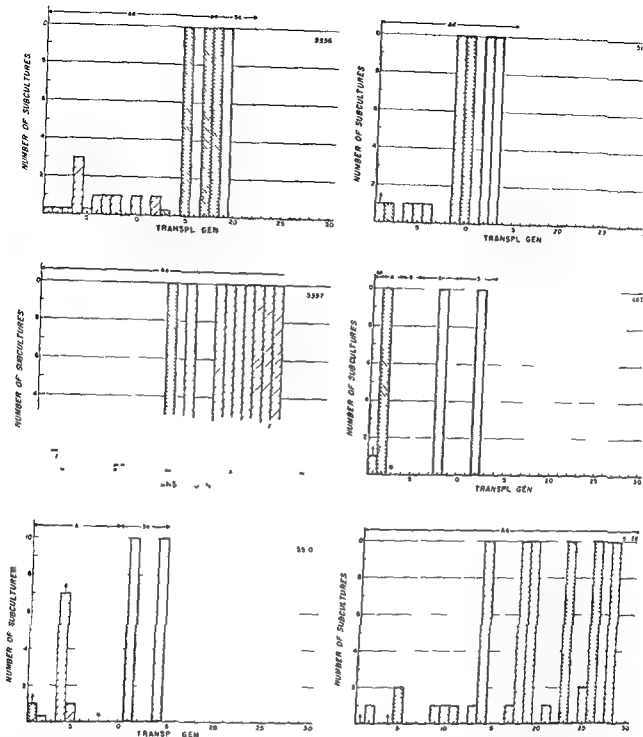


Fig 6 Maximal number of subcultures of tumours in successive transplant generations. All cultures were terminated in the 10th subculture passage. An arrow indicates that the value is a minimum since the culture was lost due to bacterial contamination. An asterisk indicates the transition to HI growth *in vivo*. See also legend to Fig 5.

tumour cells. Vaage (23) has found that the C3H mouse mammary tumour is more immunogenic in early transplant generations than in later generations suggesting a decrease in immunogenicity as the tumour progresses. Although the HD and III tumours referred to here are of the same transplant generation, the HI tumours represent a later state of

tumour progression and may thus be less immunogenic.

HR mammary tumours are known in several strains of mice (8, 9, 14, 20, 24) but growth of these tumours *in vitro* has seldom been the subject of investigation. In the present communication monolayer cultures of epithelial-like cells obtained from

) and HI mammary tumours of GR mice have been studied with respect to ability to proliferate *in vitro*. Repopulation of the cultured cells into mice resulted in growth of a tumour that retained its original state of hormone dependence and histology in two-thirds of the cases. Absence of tumour take in the remaining one third of the cases could be due either to inoculum of too small a number of cells or to a short period of observation. In the six tumours studied proliferation *in vitro* measured by the ability of the monolayer cultures to be subcultivated was found in all HI tumours. However HD tumours in high transplant generations could also readily be subcultivated. ^3H thymidine incorporation was low in HI tumours of sarcomalike histology and high in a few HD tumours. There was neither subcultivation nor ^3H thymidine incorporation could be used to distinguish between HD and HI tumours.

During this study carcinomas have occasionally been observed to dedifferentiate to sarcoma like tumours. Fassel (7) has suggested that such a differentiation may be due to malignant alteration either tumour stroma or connective tissue at the implantation site by an oncogenic virus in the tumour cells. Progression to a HI state of growth is analogous to a transition to a sarcoma like histology has previously been reported for the DE primary tumour of the rat (1). While the same phenomenon can be observed in the GR mouse primary tumours progression to a HI state usually occurs without an alteration in the histology of the tumour.

In conclusion significant differences between HI and HI tumours of the GR mouse have previously been found with respect to activities of glucose 6 phosphate dehydrogenase and hexokinase, oestrogen receptor capacity (4, 19), progesterone receptor capacity (4) and uptake of radioactive iodine (21). Differences in the tumour dose (TD_{50}) are also (21). Differences in the tumour take are reported here. In order to cell proliferative capacity under our tissue culture conditions was an insufficient criterion to distinguish HD from HI tumours. It may be expected that HD and HI tumour cells react differently to hormones *in vitro* and this is presently under investigation.

Liquid Scintillation Counter used in this work was donated by the Danish National Research Foundation. We thank Leo Pharmaceuticals (Ballerup, Denmark) for the supply of oestrogen, progesterone and penicillin, Novo Industry (Bagsværd, Denmark) for the supply of promycin and Nordisk Insulinlaboratorium (Copenhagen, Denmark) for the supply of insulin.

1. Bergh H, van den Bergh H. La progression tumorale dans deux carcinomes mammaires du rat provoqués par l'acétylaminofluorene. *Bull Assoc Fr Etud Cancer* 50: 291-303, 1963.
2. Briand P. Cultivation of monolayer cell cultures in a continuous perfusion system. *Acta Pathol Microbiol Scand* 66: 31-40, 1966.
3. Briand P & Daehnfeldt J L. Enzyme patterns of glucose catabolism in hormone-dependent and -independent mammary tumours of GR mice. *Europ J Cancer* 9: 763-770, 1973.
4. Daehnfeldt J L & Briand P. Determinations of high affinity gestagen receptors in hormone responsive and hormone independent GR mouse mammary tumours by an exchange assay. In McGuire W L et al (eds.) Progesterone receptors in normal and neoplastic tissues. Raven Press, New York, 1977, pp 59-69.
5. Dunn T B. Morphology of mammary tumours in mice. In Homburger F (ed.) *Physiopathology of Cancer*. Hoeber Harper, New York, 1959, pp 38-84.
6. Eagle H. Amino acid metabolism in mammalian cell cultures. *Science* 130: 432-437, 1959.
7. Fassel E, Fetting R, Morgenroth A Jr & The mann H. The sarcomatous transformation of mammary carcinoma of mice in isologous transplantations in cell cultures and in reimplantations. *Oncology* 21: 189-213, 1967.
8. Foulds L. Mammary tumours in hybrid mice: growth and progression of spontaneous tumours. *Brit J Cancer* 3: 345-375, 1949.
9. Heston W E, Vlahakis G & Tsubura Y. Strain DD: a new high mammary tumour strain and comparison of DD with strain C3H. *J Natl Cancer Inst* 32: 237-251, 1964.
10. Heuson J C. Hormones by administration. In Atkins H (ed.) *The treatment of breast cancer*. MTP, Great Britain, 1974, pp 113-163.
11. Lowry O H, Rosebrough N J, Farr A L & Randall R J. Protein measurement with the folin phenol reagent. *J Biol Chem* 193: 265-275, 1951.
12. Mineshima T & Yamaguchi K. An androgen dependent mouse mammary tumour. *Cancer Res* 25: 1168-1175, 1965.
13. Nie R van. Personal communication, 1970.
14. Nie R van & Dux A. Biological and morphological characteristics of mammary tumours in GR mice. *J Nat Cancer Inst* 46: 885-897, 1971.
15. Nie R van & Hilgers J. Genetic analysis of mammary tumor induction and expression of mammary tumour virus antigen in hormone treated ovariectomized GR mice. *J Nat Cancer Inst* 56: 27-32, 1976.
16. Oyama V I & Eagle H. Measurement of cell growth in tissue culture with a phenol reagent (Folin-Ciocalteu). *Proc Soc Exp Biol and Med* 91: 305-307, 1956.
17. Ringsted J. In vitro study of a mouse mammary carcinoma simulating carcinosarcoma and sarcoma.

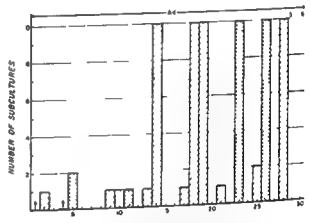
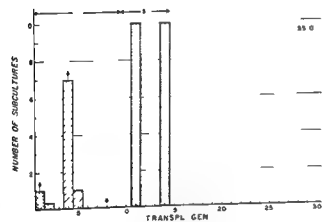
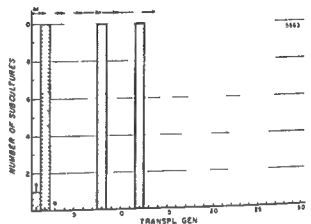
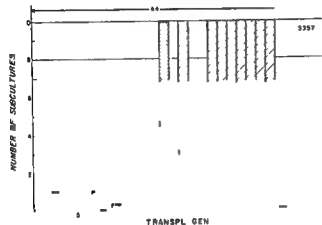
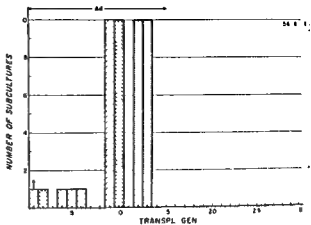
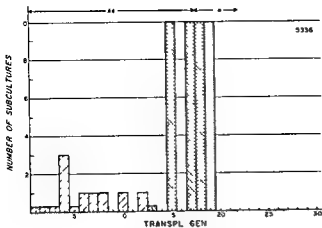


Fig 6 Maximal number of subcultures of tumours in successive transplant generations. All cultures were terminated in the 10th subculture passage. An arrow indicates that the value is a minimum since the culture was lost due to bacterial contamination. An asterisk indicates the transition to HI growth *in vivo*. See also legend to Fig. 5

tumour cells. Vaage (23) has found that the C3H mouse mammary tumour is more immunogenic in early transplant generations than in later generations suggesting a decrease in immunogenicity as the tumour progresses. Although the HD and HI

tumour progression and may thus be less immunogenic.

HR mammary tumours are known in several strains of mice (8, 9, 14, 20, 24) but growth of these tumours *in vitro* has seldom been the subject of investigation. In the present communication mono-layer cultures of epithelial-like cells obtained from

PRIMARY MALIGNANT FIBROUS HISTIOCYTOMA OF BONE AFTER RADIATION

L. ANGERVALL S JOHANSSON L G KINDBLOM and J SAVE SÖDERBERGH

Department of Pathology University of Göteborg Sweden

Angervall L Johansson S Kindblom L-G & Save Soderbergh J Primary malignant fibrous histiocytoma of bone after radiation *Acta path microbiol scand Sect A 87 437-446 1979*

Two cases of primary malignant histiocytoma of bone after irradiation are reported. One tumour developed in the left iliac bone ten years after irradiation for cystadenocarcinoma of the left ovary. The other developed in the left mandible 26 years after irradiation for a »semi malignant« mixed tumour of the left parotid gland. Both tumours had a light microscopic picture of malignant fibrous histiocytoma as described in soft tissues. Fascicular spindle-cell areas resembling leiomyosarcoma were found in both tumours. Ultrastructurally the pelvic tumour was found to be composed of histiocytic and fibroblastic cells and some spindle shaped cells with abundance of myofilaments with dense body like structures indistinguishable from spindle cells of leiomyomatous tumours. The light and electron microscopic observations suggest that a relationship exists between fibroblastic histiocytic and leiomyomatous cell elements of bone and soft tissue tumours.

Key words: Bone tumour malignant fibrous histiocytoma post irradiation sarcoma

L. Angervall Department of Pathology Sahlgrenska Hospital S 413 45 Göteborg Sweden

Received 24 xii 78 Accepted 23 iv 79

The ideas and concept about the diagnosis, classification, occurrence and behaviour of soft tissue tumours have undergone significant changes during the last two decades. Malignant histiocytoma has become a common diagnosis and forms at present a large group with a broad light microscopic spectrum. Until recently malignant fibrous histiocytoma, probably the most common subvariant in this group (Weiss & Enzinger 1978), was often apparently diagnosed and described in the literature under such diagnoses as adult type of rhabdomyosarcoma and fibrosarcoma. During the last years some series of primary intraosseous malignant

or foci that appear typical of malignant fibrous histiocytoma. The problem apparently may be the same for some soft tissue tumours, i.e. pleomorphic liposarcoma, which can contain foci typical of malignant fibrous histiocytoma (Kindblom *et al* 1975).

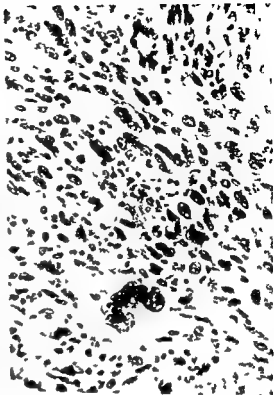
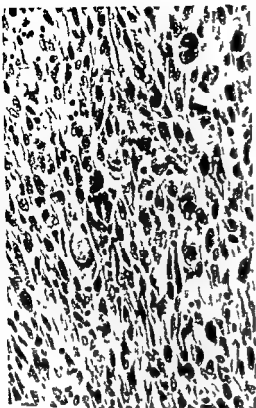
The histogenesis of malignant fibrous histiocytoma of soft tissues has been debated (O'Reilly *et al* 1963; Merkow *et al* 1971; Fu *et al* 1975; Weiss & Enzinger 1978). Light and electron microscopic features and tissue culture characteristics support a fibroblastic histiocytic origin (Merkow *et al* 1971; Fu *et al* 1975; Taxy & Battifora 1977). Ultrastructurally studied malignant fibrous histiocytomas of bone have been reported to be similar to those of soft tissues (Unada *et al* 1976; Johnson *et al* 1978).

Postradiation sarcoma of bone is a concept. These sarcomas have up to 1972 almost exclusively been

al 1978). One can notice some reluctance among bone pathologists to use the diagnosis. According to Dahlin *et al* (1977) the problem is that some bone tumours, i.e. osteosarcoma, fibrosarcoma, dedifferentiated chondrosarcoma, osteo- and fibrosarcomas in previously radiated bones may contain zones

of malignant bone tumours from the Mayo Clinic designated malignant fibrous histiocytoma originally 17 were

- tous overgrowth during transplantation *Acta Path Microbiol Scand* **40** 373-382, 1957
- 18 *Rockwell S C, Kallman, R F & Fajardo, L F* Characteristics of a serially transplanted mouse mammary tumour and its tissue-culture-adapted derivative *J nat Cancer Inst* **49** 735-747, 1972
 - 19 *Sluysen, M, & Nie, R van* Estrogen receptor content and hormone-responsive growth of mouse mammary tumours *Cancer Res* **34** 3253-3257, 1974
 - 20 *Squartini F* Responsiveness and progression of mammary tumours in high-cancer-strain mice *J nat Cancer Inst* **28** 911-926, 1962
 - 21 *Stones P B* Standardization of biological products by microbiological and serological methods. In *Collins C H* (ed) *Progress in Microbiological Techniques* Butterworth London 1967, pp 119-139
 - 22 *Thorpe S M* Increased uptake of iodide by hormone-responsive compared to hormone independent mammary tumours in GR mice *Int J Cancer* **18** 345-350, 1976
 - 23 *Vaage, J* Changing transplantation characteristics with serial *in vivo* passage of C3H/He mammary carcinomas *Cancer Res* **38** 3264-3268 1978
 - 24 *Watson, C, Medina, D & Clark J H* Estrogen receptor characterization in a transplantable mouse mammary tumour *Cancer Res* **37** 3344-3348 1977
 - 25 *Wiepjes G J & Prop F J A* Improved method for preparation of single cell suspensions from mammary glands of adult virgin mouse *Exp Cell Res* **61** 451-454, 1970



iron (Prussian blue) and mucopolysaccharides (as described previously Kindblom *et al* 1975) were also performed

Electron microscopic methods Small pieces of tissue from case 1 were immediately after removal of the tumour put into ice-cold 1 per cent OsO_4 according to Maunsbach (1966) fixed for 2 hours dehydrated in ethanol embedded in Epon 812 and cut in an LKB Ultratome III. Small pieces of tissue were also immersed in 2.5 per cent glutaraldehyde in 0.1 M cacodylate buffer at pH 7.2 for 4 hours at 4°C washed in cold buffer postfixed in ice-cold 1 per cent OsO_4 for 1 hour and then prepared in the same way as the primary OsO_4 fixed pieces. One micron thick sections were stained with toluidine blue. Silver to grey sections were stained by uranyl acetate and lead citrate and examined in a Philips 200 electron microscope.

Fig 3 Case 1 Pleomorphic tumour cells with abundant mitotic figures some of which are polyploid $\times 300$

Fig 4 Case 1 Scattered multinucleated giant cells one of them shows large hyperchromatic nuclei with prominent nucleoli and others show peripherally arranged smaller more uniform nuclei giving a Touton cell like appearance $\times 250$

Fig 5 Case 1 Parallelly arranged spindle shaped tumour cells with cigar shaped nuclei giving a leiomyomatous appearance $\times 300$



considered fibrosarcoma and 18 osteosarcoma. Four of these cases occurred after radiation therapy to the bone (Dahlin *et al* 1977).

This study presents two cases of pleomorphic sarcoma of bone, compatible with the light microscopical appearance of malignant fibrous histiocytoma of soft tissues, occurring in the beam of radiation for tumours outside bone.

CASE REPORTS

Case 1

The patient is a woman born in 1925. In 1967 she underwent bilateral salpingo oophorectomy and hysterectomy because of a well differentiated serous cystadenocarcinoma of the left ovary, 15 cm in diameter. She received 5000 rad of postoperative radiation. In the spring of 1977 she had an episode of lower back pain which disappeared spontaneously. She noticed recurrence of the same symptoms in November 1977. Radiological examination revealed a 6 × 3 cm osteolytic lesion in the left iliac bone. A drill biopsy was performed. As the diagnosis was sarcoma the patient was referred to the department of orthopaedic surgery, Sahlgren's Hospital, Göteborg, and underwent modified leftside hemipelvectomy in January 1978. The patient is alive and well at follow up examination in May 1978.

Case 2

The patient was a woman born in 1916. In 1950 she underwent surgery for a «semimalignant» mixed tumour of the left parotid gland. Postoperative radiotherapy was advised and the patient received 5200 rad. Because of radiation dermatitis over the mandible the patient underwent skin transplantation in 1959. In 1975 she felt pain in her left jaw and radiologic examination revealed destruction of the mandible. An incision biopsy was performed and the diagnosis was fibrosarcoma. The patient was referred to Sahlgren's Hospital and underwent hemimandible ectomy. The operation was not radical therefore in June 1976 extended surgery with further removal of mandibular and soft tissue and subsequent skin transplantation was performed. After 5 months a mass was palpated in the skin transplant. Fine needle biopsy cytologically confirmed local recurrence. Radiological examination revealed destruction of the area lateral of the sphenoidal sinus and foramen ovale and spinosum as well as the tuber maxillae. The tumour extended into the oral cavity to the left tonsil. Surgery was not considered possible and the patient received palliative treatment with vincristine, cyclophosphamide and dactinomycin and another further 3000 rad of radiotherapy. The patient's condition deteriorated rapidly and she expired in April 1977. At the autopsy it was found that the tumour extended into the cranial cavity. There was an extensive destruction of the base of the skull and the maxillae. The tumour involved the meninges but there was no brain involvement. Multiple metastases were present in both lungs.

PATHOLOGY

Light microscopic methods. Material from different parts of the tumours was embedded in paraffin, some after decalcification, and 5 µm sections were stained according to Weigert van Gieson and with hematoxylin and eosin. Stainings for reticulin (Gordon-Sweet) fat (Oil red O).



Fig 1 Case 1. A cut section of the hemipelvectomy specimen showing the nodular tumour which has destroyed part of the iliac bone and protrudes out into surrounding skeletal muscle.

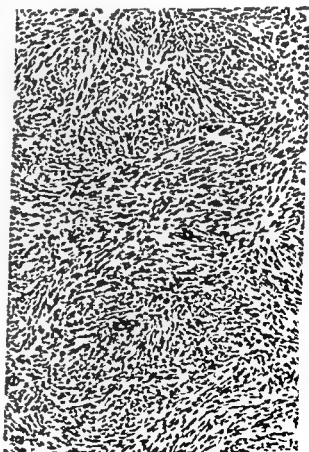


Fig 2 Case 1. Highly cellular tumour area with intertwinning tumour cell bundles forming a whorled pattern, partly storiform. × 120.



Fig 10 Histiocyte like tumour cell showing an indented nucleus with peripherally condensed heterochromatin. The cytoplasm forms abundant pseudopodiae and microvillous projections intertwining with those of neighbouring cells $\times 7500$

Case 1

Gross appearance The tumour involved part of the left iliac bone and infiltrated into the gluteal muscle and subcutaneous fat tissue (Fig 1). The tumour was firm and slightly nodular measuring 9 cm in the largest diameter. The tumour showed greyish white cut surfaces.

Light microscopic appearance The highly cellular tumour was predominantly composed of spindle shaped cells with acidophilic cytoplasm which in places were parallelly arranged forming intertwining bundles (Fig 2). The tumour cells revealed a marked cellular and

Fig 6 Case 1 Area with tumour cells containing hemosiderin $\times 190$

Fig 7 Case 2 Highly cellular tumour area showing a mixture of spindle shaped and polygonal pleomorphic cells and scattered mitotic figures $\times 250$

Fig 8 Case 2 Infiltrates of inflammatory cells predominantly lymphocytes within the tumour $\times 180$

Fig 9 Case 2 An abundant network of reticular fibres forming a whorled pattern $\times 90$

nuclear pleomorphism and throughout the tumour numerous mitotic figures were encountered many of which were atypical - both tri- and quadripolar figures were encountered (Fig 3). The nuclei of these elongated cells were large often irregularly indented and showed a vesicular chromatin structure and one or more prominent nucleoli some of which were distinctly acidophilic and inclusion like. In some areas very large polygonal or irregularly shaped markedly pleomorphic tumour cells predominated. Uninucleated and multinucleated giant cells oriented in a random or haphazard fashion were conspicuous in these areas most of them being of malignant type with prominent nuclear pleomorphism and hyperchromasia but also scattered cells of Touton's cell type with relatively small peripherally arranged nuclei were found (Fig 4).

Fig 11 Less cellular myxoid areas were also found

In some areas slender spindle shaped parallelly arranged tumour cells revealed a suggestive fibrillar structure of the perinuclear and eosinophilic cytoplasm

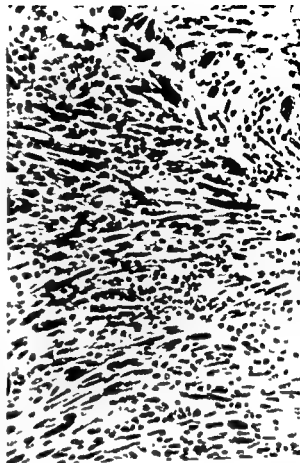
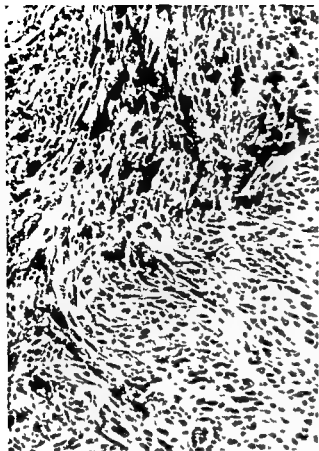




Fig 12 Detail of histiocyte like cell (top) with numerous lysosomal structures and inclusions $\times 15000$

of inflammatory cells were encountered above all in the periphery of the tumour (Fig 8) and in the surrounding fat and muscle tissue. Reticulin fibres were abundant throughout the tumour and enveloped individual spindle shaped tumour cells (Fig 9). There were hyalinized areas including elongated cells with hyperchromatic cigar shaped nuclei and acidophilic cytoplasm; these areas exhibited a leiomyosarcoma like appearance. To a large extent the tumour was hyalinized or necrotic. Special stains revealed neither presence of iron pigment nor mucopolysaccharides within the tumour cells. The tumour grew out into the surrounding skeletal muscle and fat tissue; it also infiltrated a fascia.

Electron microscopic appearance The ultrastructurally studied tumour (case 1) showed cells of mainly two types: histiocyte like and fibroblast like. The histiocyte like cells (Figs 10 and 11) predominated; they were relatively voluminous and had large, folded or irregularly indented nuclei. The nuclei showed peripherally condensed clumps of heterochromatin and one or two prominent nucleoli with a network like structure. The cytoplasm contained abundant systems of vesicles, vacuoles, and lysosomal structures with varying density. Large vacuoles of digestive type containing lipid, hemosiderin like material and multilaminated structures suggestive of auto- and heterophagocytosis were noted (Fig 12). Golgi zones were often prominent. The cells contained numerous mitochondria which were large, oval or rounded. The rough endoplasmic reticulum was sparse and appeared mostly as short profiles of parallel

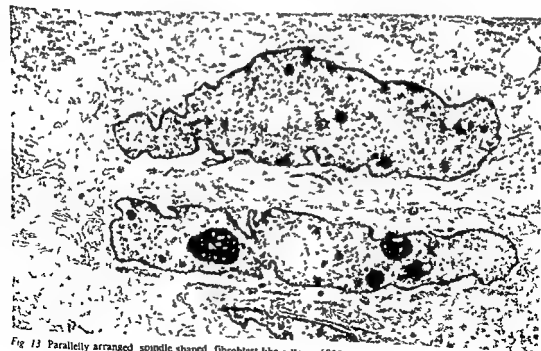


Fig 13 Parallel arranged spindle shaped fibroblast like cells $\times 6000$

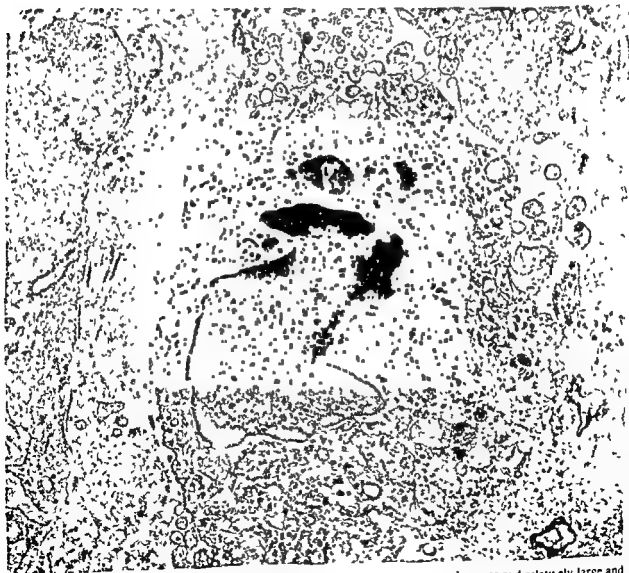
and chromatin-rich elongated nuclei, thereby showing a leiomyosarcoma-like pattern (Fig 5). Areas of the tumour were hyalinized or necrotic. Foci of inflammatory cells, predominantly lymphocytes, were seen throughout the tumour but particularly in the periphery of the tumour. Xanthoma cells intermingling with tumour cells and inflammatory cells were found, not always associated with areas of necrosis. Fat staining disclosed intracytoplasmic lipid droplets. Tumour cells, scattered or in small collections, contained iron-positive pigment (Fig 6). Abundant reticulin fibres and delicate collagen bundles were intimately associated with the tumour cells and were found to run parallelly with bundles of spindle-shaped cells. The mucopolysaccharide stains indicated the presence of hyaluronic acid but not sulphated mucopolysaccharides.

The tumour infiltrated the surrounding fat tissue and skeletal muscle diffusely.

Case 2

Gross appearance The tumour involved and destroyed almost the entire neck of the mandible, which was fractured at the angle. The tumour size was estimated as 5 cm. The tumour extended into the surrounding soft tissue. The cut surfaces were greyish white and had a fibrous texture.

Light microscopic appearance In many respects this tumour resembled that described in case 1. It was thus highly cellular and composed of pleomorphic spindle shaped or large polygonal tumour cells with acidophilic (picrinophilic and eosinophilic) cytoplasm and a large mostly vesicular nucleus with prominent sometimes very large and eosinophilic nucleoli (Fig 7). As in case 1, the tumour cells were in places arranged in a whorled fashion with distinct storiform pattern. There were also nucleated giant cells with strongly pleomorphic nuclei as well as giant cells with peripherally arranged nuclei. Foci



... some and relatively large and
... abundant parallelly arranged

microfilaments and dense body-like struc-

DISCUSSION

Both tumours showed principally the same histologic picture of malignant fibrous histiocytomas pleomorphic acidophilic tumour cells with large vesicular nuclei and prominent nucleoli the presence of giant cells among others such with peripherally arranged nuclei as Touton's type of giant cells a storiform pattern and foci of inflammatory cells Ultrastructurally, the tumours revealed a dual histiocytic and fibroblastic nature as previously has been demonstrated for malignant fibrous histiocytoma of soft tissues (Merkow *et al* 1971 Fu *et al* 1975 Taxy & Battifora 1977) The electron microscopic characteristics seem to be principally the same as those in the six previously studied malignant fibrous histiocytomas of bone (Unada *et al* 1976 Johnson *et al* 1978) and a case of atypical fibrous histiocytoma of the humerus (Saito & Caines 1977)

Both tumours showed leiomyosarcoma like areas on light microscopic examination The electron microscopic examination of case 1 revealed some elongated cells with abundance of cytoplasmic filaments as in myofibroblasts Previous ultrastructural studies on malignant fibrous histiocytoma of soft tissues have demonstrated cells of myofibroblast type and have shown that a clear distinction between the fibroblastic histiocytic cells and leiomyoblastic cells cannot always be made in these tumours (Chung & Kahn 1977)

The difficulties that may rise in the light microscopic differential diagnosis of cutaneous leiomyosarcoma and atypical fibroxanthoma of skin have been pointed out (Dahl & Angervall 1974 Dahl 1976) Fibroblast histiocyte and myofibroblast like cells and intermediate forms have also been demonstrated ultrastructurally in myxofibrosarcoma (Kindblom *et al* 1979) This tumour has also been described as a myxoid variant of malignant fibrous histiocytoma when it has a tendency to include solid areas with a light microscopic appearance typical of malignant fibrous histiocytoma (Weiss & Enzinger 1977) The present study further supports the notion that a relationship may exist between fibroblastic histiocytic and leiomyomatous cell elements of bone and soft tissue tumours

Some 200 cases of sarcoma arising in bone following irradiation have been recorded (Arlen *et al* 1971 Sim *et al* 1972 Dorfman 1973) There are many examples of sarcomas which have appeared after irradiation of benign bone lesions e.g. giant cell tumour aneurysmal bone cyst osteoblastoma and fibrous dysplasia (Sim *et al* 1972) Postradiation sarcomas may also arise in normal bone included in the beam of radiation for malignancies

outside the bone thus 13 of 28 bone sarcomas reported by Arlen *et al* (1971) and 18 of 34 reported by Sim *et al* (1972) were postradiation sarcomas reported as fibrosarcoma and osteosarcoma but also chondrosarcoma and Ewing's sarcoma Recently, Dahlin *et al* (1977) described 4 cases of postradiation malignant fibrous histiocytomas and Gonzalez-Vitale *et al* (1976) reported a case in the base of the skull after irradiation for a chromophobe adenoma A dose of 3000 rad has been considered necessary to induce sarcomas and a latent period of 3-30 years usually separates the irradiation from the time of appearance of the malignant tumour (Dorfman 1973) The present cases are in conformity with these observations they received 5200 and 5000 rad and had a latent period of 10 and 25 years respectively

Ionizing radiation may produce bone necrosis and reparative changes referred to as radiation osteitis which includes a highly cellular stroma reaction (Dorfman 1973) It is interesting that malignant fibrous histiocytomas as well as other

Michael & Dorfman 1976 Galli *et al* 1978) Hence it is possible that the development of sarcomas in patients exposed to radiant energy may be caused both by infarcts produced by the irradiation and the carcinogenicity of ionizing radiation *per se*

Supported by a research grant from the Swedish Cancer Society (530 B78 06XA)

REFERENCES

- Arlen M Higinbotham N L Huvos A G Marcove R C Miller T and Shah J C Radiation induced sarcoma of bone *Cancer* 28 1087-1099 1971
- Chung A M and Kahn T D Atypical fibrous histiocytoma
- Dahl clinical and pathological study of 57 cases *Acta path microbiol Scand Sect A* 84 183-197 1976
- Dahl I and Angervall L Cutaneous and subcutaneous leiomyosarcoma A clinicopathologic study of 47 patients *Pathol Eur* 9 307-315 1974
- Dahlin D C Unni K K and Matsuno T Malignant (fibrous) histiocytoma of bone fact or fancy? *Cancer* 39 1508-1516 1977
- Dorfman H D Malignant transformation of benign bone lesions 7th Nat Cancer Conf Proc p 901-913 1973
- Feldman F and Lattes R Primary malignant fibrous histiocytoma (fibrous xanthoma) of bone *Skeletal Radiol* 1 145-160 1977
- Feldman F and Norman D Intra and extra-osseous



Fig 14 Details of tumour cells revealing abundant parallelly arranged microfilaments with scattered dense body like structures and attachment like sites $\times 16000$



Fig 15 Ordinary and long spaced collagen in the intercellular space $\times 125000$

membranes. Clusters of glycogen like granules were found both in the nucleus and the cytoplasm of some cells. The cell surface often showed numerous microvillous projections and pseudopodia which intertwined with those of adjacent cells.

The fibroblast like cells (Fig 13) characteristically contained elongated, smoothly outlined nuclei with one or two fairly small nucleoli and a relatively sparse peripherally arranged heterochromatin. The cytoplasm was dominated by rough endoplasmic reticulum which appeared as prominent systems of parallel membranes or dilated cisternae containing amorphous moderately osmiophilic material. The Golgi zones were moderate in size or inconspicuous. The mitochondria were oval or elongated and could be seen closely associated with endoplasmic reticulum.

Some cells of both types as well as of intermediate forms contained parallelly arranged cytoplasmic microfilaments 60–90 nm in diameter. The filaments were often parallel to the long axis of the cell (Fig 14). Condensed dense body like areas were associated with these filaments and occasional attachment like sites were encountered. Basement membrane like structures were lacking. Occasional desmosomes were demonstrated.

The narrow intercellular spaces contained some delicate bundles of ordinary cross banded collagen fibres and amorphous moderately dense material. In some areas cross banded fibrillar material of the appearance of long spaced collagen was seen (Fig 15).

DISCUSSION

th tumours showed principally the same histological picture of malignant fibrous histiocytomas: omorphic acidophilic tumour cells with large nuclear nuclei and prominent nucleoli, the presence of giant cells among others such with

a dual histiocytic and fibroblastic nature, as previously has been demonstrated for malignant fibrous histiocytoma of soft tissues (Merkow *et al* 1971, Fu *et al* 1975, Taxy & Battistoni 1977). The electron microscopic characteristics seem to be principally the same as those in the six previously described malignant fibrous histiocytomas of bone (Ada *et al* 1976, Johnson *et al* 1978) and a case of typical fibrous histiocytoma of the humerus (Sario & Cairnes 1977).

Both tumours showed leiomyosarcoma like areas. Light microscopic examination. The electron microscopic examination of case 1 revealed some atypical cells with abundance of cytoplasmic filaments as in myofibroblasts. Previous ultrastructural studies on malignant fibrous histiocytoma of soft tissues have demonstrated cells of myofibroblastic type and have shown that a clear distinction between the fibroblastic histiocytic cells and leiomyosarcoma cells cannot always be made in these tumours (Churg & Kahn 1977).

The difficulties that may rise in the light microscopic differential diagnosis of cutaneous myxosarcoma and atypical fibroxanthoma of skin have been pointed out (Dahl & Angervall 1974, Dahl 1976). Fibroblast, histiocyte and myofibroblast cells and intermediate forms have also been demonstrated ultrastructurally in myxofibrosarcoma (Kindblom *et al* 1979). This tumour has also been described as a myxoid variant of malignant fibrous histiocytoma when it has a tendency to include solid areas with a light microscopic appearance typical of malignant fibrous histiocytoma (Weiss & Enzinger 1977). The present study further supports the notion that a relationship may exist between fibroblastic, histiocytic and leiomyosarcoma cell elements of bone and soft tissue tumours.

Some 200 cases of sarcoma arising in bone following irradiation have been recorded (Arlen *et al* 1971, Sim *et al* 1972, Dorfman 1973). There are many examples of sarcomas which have appeared

outside the bone, thus 13 of 28 bone sarcomas reported by Arlen *et al* (1971) and 18 of 34 reported by Sim *et al* (1972) were postirradiation sarcomas reported as fibrosarcoma and osteosarcoma but also chondrosarcoma and Ewing's sarcoma. Recently, Dahlin *et al* (1977) described 4 cases of postirradiation malignant fibrous histiocytomas, and Gonzalez-Vitale *et al* (1976) reported a case in the base of the skull after irradiation for a chromophobe adenoma. A dose of 3000 rad has been considered necessary to induce sarcomas, and a latent period of 3-30 years usually separates the irradiation from the time of appearance of the malignant tumour (Dorfman 1973). The present cases are in conformity with these observations: they received 5200 and 5000 rad and had a latent period of 10 and 25 years respectively.

Ionizing radiation may produce bone necrosis and reparative changes referred to as radiation osteitis which includes a highly cellular stroma reaction (Dorfman 1973). It is interesting that malignant fibrous histiocytomas as well as other

it is possible that the development of sarcomas in patients exposed to radiant energy may be caused both by infarcts produced by the irradiation and the carcinogenicity of ionizing radiation *per se*.

Supported by a research grant from the Swedish Cancer Society (530 B78 06XA).

REFERENCES

- Arlen M, Higinbotham N L, Huvo A G, Marcove R C, Miller T and Shah J C. Radiation induced sarcoma of bone. *Cancer* 28: 1087-1099, 1971.
- Churg A M and Kahn L B. Myofibroblasts and related cells in malignant fibrous and fibrohistiocytic tumors. *Human Pathology* 8: 205-218, 1977.
- Dahl I. Atypical fibroxanthoma of the skin. A clinicopathological study of 57 cases. *Acta path microbiol Scand Sect A* 84: 183-197, 1976.
- Dahl I and Angervall L. Cutaneous and subcutaneous leiomyosarcoma. A clinicopathologic study of 47 patients. *Pathol Eur* 9: 307-315, 1974.
- Dahlin D C, Ueno K K and Matsuno T. Malignant (fibrous) histiocytoma of bone fact or fancy? *Cancer* 39: 1508-1516, 1977.
- Dorfman H D. Malignant transformation of benign bone lesions. 7th Nat. Cancer Conf. Proc. p. 901-913, 1973.
- Feldman F and Lattes R. Primary malignant fibrous histiocytoma (fibrous xanthoma) of bone. *Skeletal Radiol* 1: 145-160, 1977.
- Feldman F and Norman D. Intra- and extra-osseous

4 sarcomas may also arise in normal bone included in the beam of radiation for malignancies

- malignant histiocytoma (malignant fibrous xanthoma) *Radiology* 104 497-508, 1972
- Fu Y-S, Gabbiani, G, Kaye, G I, and Lattes, R Malignant soft tissue tumors of probable histiocytic origin (malignant fibrous histiocytomas) General considerations and electron microscopic and tissue culture studies *Cancer* 35 176-198, 1975
- Galli, S J, Weintraub, H P, and Proppe, K H Malignant fibrous histiocytoma and pleomorphic sarcoma in association with medullary bone infarcts *Cancer* 41 607-619, 1978
- Gonzales-Vitale, J C, Slavin R E, and McQueen J D Radiation-induced intracranial malignant fibrous histiocytoma *Cancer* 37 2960-2963, 1976
- Huvos, A G Primary malignant fibrous histiocytoma of bone Clinicopathologic study of 18 patients NY State J Med 76 552-559, 1976
- Inada O, Yumoto, T, Furuse, K, and Tanaka, T Ultrastructural features of malignant fibrous histiocytoma of bone *Acta path Jap* 26 491-501, 1976
- Johnson W W, Coburn T P, Pratt C B, Smith, J W, Kumar, A P M, and Dahlin D C Ultrastructure of malignant histiocytoma arising in the acromion *Human Pathology* 9 199-209, 1978
- Kahn, L B, Webber, B Mills E, Anstey, L and Heselson N G Malignant fibrous histiocytoma (malignant fibrous xanthoma xanthosarcoma) of bone *Cancer* 42 640-651, 1978
- Kindblom, L-G, Angervall L, and Svendsen P Liposarcoma A clinico-pathologic radiographic and prognostic study *Acta path microbiol scand Sect A Suppl* 253, 1975
- Kindblom L-G, Merck C and Angervall L The ultrastructure of myxofibrosarcoma A study of 11 cases *Virch Arch A* 381 121-139, 1979
- Maunsbach A B Jr The influence of different fixatives and fixation methods on the ultrastructure of rat kidney proximal tubules cells I Comparison of different perfusion methods and of glutaraldehyde and osmium tetroxide fixatives *J Ultrastr Res* 15 242-282 1966
- Merlow, L P, Irich, J C Jr, Stifkin M, Kyreages C G, and Pardo, M Ultrastructure of a fibroxanthosarcoma (malignant fibroxanthoma) *Cancer* 28 372-383, 1971
- Michael, R H, and Dorfman, H D Malignant fibrous histiocytoma associated with bone infarcts *Clin Orthop* 118 180-183, 1976
- Murra J M, Bullough, P G, Marcove R C, Jacobs B and Huvos A G Malignant fibrous histiocytoma and osteosarcoma in association with bone infarcts Report of four cases, two in caisson workers *J Bone Joint Surg* 56-A 932-940, 1974
- Murra, J M, Gold, R H, and Marafiotte, R Malignant (fibrous) histiocytoma arising in association with a bone infarct in sickle-cell disease Coincidence or cause and-effect? *Cancer* 39 186-194 1977
- Ozzello, L, Stout A P, and Murray M R Cultural characteristics of malignant histiocytomas and fibrous xanthomas *Cancer* 16 331-344 1963
- Sabanias, A O, Dahlin D C, Childs D S Jr, and Ivins J C Postradiation sarcoma of bone *Cancer* 9 528-542, 1956
- Saito R, and Carnes M J Atypical fibrous histiocytoma of the humerus a light and electron microscopic study *Amer J Clin Path* 68 409-415 1977
- Sim F H, Cupps R E, Dahlin D C, and Ivins J C Postradiation sarcoma of bone *J Bone Jt Surg* 54 A 1479-1489, 1972
- Spanier S S, Enneking W F, and Enriques P Primary malignant fibrous histiocytoma of bone *Cancer* 36 2084-2098 1975
- Taxy, J B, and Bathforsa H Malignant fibrous histiocytoma An electron microscopy study *Cancer* 40 254-267, 1977
- Weiss S W and Enzinger F M Myxoid variant of malignant fibrous histiocytoma *Cancer* 39 1672-1685, 1977
- Weiss, S W and Enzinger F M Malignant fibrous histiocytoma An analysis of 200 cases *Cancer* 41 2250-2266 1978

ALPHA-1-ANTITRYPSIN GLOBULES IN LIVERS FROM A MEDICOLEGAL AUTOPSY MATERIAL

INGERMARIE REINTOFT

Institute of Forensic Medicine, University of Odense, DK-5000 Odense C, Denmark

Reintoft, I. Alpha-1 antitrypsin globules in livers from a medicolegal autopsy material. *Acta path. microbiol. scand. Sect. A* 87: 447-450, 1979.

In 32 of 179 consecutive medicolegal autopsies, diastase-resistant periodic acid-Schiff (PAS) positive globules were found inside hepatocytes. Two types of globules were registered. The first type was found in 3 patients, the other in 26, and both in 3 patients. The first type of globules was mainly localized periporally and showed antigenicity for alpha-1 antitrypsin (A1AT) using the immunohistochemical staining method. The 6 subjects with the first type of globules can be assumed to have been carriers of the Z gene for A1AT, i.e. PiZZ or PiMZ. The frequency with which these globules are demonstrated suggests that they are to be found in most, maybe all, Z gene carriers. The other type of globules was localized mainly in the central parts of the hepatic lobules and showed antigenicity for immunoglobulin G in 28 of the 29 cases. These globules correspond to inclusions from plasma proteins. In 2 cases, the last-mentioned globules showed in addition antigenicity for A1AT. Such globules are of a differential diagnostic interest and are probably not related to A1AT deficiency. A comparison with a similar previous study of a hospital autopsy material revealed no statistically significant difference in the frequency of subjects with A1AT globules in hepatocytes, but the mean age and the number of PAS-positive globules were considerably lower in the present material.

Key words: Alpha-1 antitrypsin, PAS-positive, non-glycogenetic globules, forensic pathology.

I. Reintoft, Department of Pathology, Esbjerg Central Hospital, 6700 Esbjerg, Denmark.

Accepted as submitted 25 iv 79

One of the allelic alpha-1 antitrypsin (A1AT) genes, the Z gene, causes accumulation of asialo A1AT inside the endoplasmic reticulum of hepatocytes (4-8). The accumulated A1AT can be demonstrated as diastase-resistant, periodic acid-Schiff (PAS) positive globules which, with immunofluorescence or immunoperoxidase methods, show antigenic characteristics in common with normal allelic A1AT (2, 6, 10, 16, 18). The globules are found in both PiZZ and PiMZ subjects and mainly in periportal hepatocytes or when present alone (9).

or
to
li

The object of the present study was to investigate the frequency and the number of A1AT globules in a medicolegal autopsy material and to compare the results with those of a hospital autopsy material (14, 15).

MATERIAL AND METHODS

The medicolegal autopsy material comprises 179 consecutive autopsies (mean age 46 years) carried out in the Institute of Forensic Medicine of Odense University during 1975-1976. One liver tissue block from each autopsy was present, and one section about 2 cm² from each case was screened for diastase-resistant, PAS-positive intracytoplasmic globules in the hepatocytes. Liver sections from positive cases were subjected to the indirect immunoperoxidase reaction against A1AT and

A1 globules, especially in autopsy materials (15). The immunohistochemical reaction was performed with commercial preparations (12).

Subjects with the Z gene were calculated, and the number of PAS-positive globules was estimated within consecutive areas using a manual optical sample analyser composed of a Leitz grid and drawing tube (ocular GF 12.5). One grid area covered 0.0078 mm² and at least 19 areas were counted in each case.



- g 1 Numerous cytoplasmic globules in periportal hepatocytes PAS following diastase digestion \times approx 450
- g 2 Centrilobular region with cytoplasmic globules in hepatocytes PAS following diastase digestion \times approx 60
- g 3 Annular and diffuse granular cytoplasmic staining in periportal hepatocytes Same case as in Fig 1 A 1 AT immunoperoxidase reaction \times approx 450
- g 4 Centrilobular hepatocytes with diffuse cytoplasmic globules Same case as in Fig 2 A 1 AT immunoperoxidase reaction \times approx 560

The hospital autopsy material has been published earlier (14, 15) and comprises 238 autopsies (mean age 64 years) from a nearby region. 15 subjects were suspected to be carriers of the Z gene. The mean age of these subjects and the number of PAS positive globules were investigated as above. The statistics were based on the Chi square test.

RESULTS

The medicolegal autopsy material In PAS staining after diastase treatment 32 livers showed positive intracytoplasmic globules in hepatocytes. In 3 livers the globules (1–20 pr/cell) were localized inside periportal hepatocytes and showed deeply reddish blue staining. They were of uneven sizes 1–30 μ in diameter (Fig 1). In 26 livers the globules (1–7 pr/cell) were localized inside hepatocytes mainly in centrilobular regions but sometimes throughout the whole lobules. They showed weakly red staining and were of rather even size 6–10 μ in diameter (Fig 2). In 3 livers both types of globules were found.

In the first 3 livers the indirect immunoperoxidase for A 1 AT showed a peripheral annular of diffuse granular dark brown staining of the globules (Fig 3). Between the 26 livers a weak diffuse staining of centrilobular globules was demonstrated in 2 cases only (Fig 4). In the 3 livers periportal globules were positive centrilobular negative.

IgG staining was negative in the first 3 livers and positive in 25 of 26 livers with the centrilobular type of PAS positive globules. The only negative case showed in PAS few typical centrilobular globules, no further attempt to demonstrate IgG was performed. In the 3 livers demonstrating both types of PAS positive globules the periportal globules were positive only in A 1 AT staining the centrilobular only in IgG.

In accordance with the staining results the patients with periportal diastase resistant PAS and A 1 AT were

number of globules and globules per grid unit in the

TABLE 1 Age of Subjects and Number of Periportal PAS Positive Globules in the Two Compared Materials

Case	Medicolegal autopsy material		Hospital autopsy material	
	Age	Average number of globules/unit*	Age	Average number of globules/unit*
1	25	0.4	44	3.1
2	27	2.3	44	insufficient material
3	43	0.4	47	1.3
4	55	0.3	53	1.6
5	58	0.1	54	20.3
6	74	2.1	58	1.5
			62	1.5
			71	2.6
			73	3.0
			74	3.3
			76	5.3
			79	0.3
			81	12.6
			82	31.4
			87	1.1
average	47	0.9	66	5.9

* 1 areal unit = 0.0028 mm²

6 subjects and in the assumed 15 Z gene carriers from the hospital autopsy material. The frequency of subjects was 33 per cent and 63 per cent respectively in the two materials. The difference is not statistically significant ($0.20 < P < 0.30$).

The other type of diastase resistant PAS positive globules, the mainly centrilobular type, appeared in 29 subjects out of 179 in the medicolegal material and in 28 subjects out of 238 in the hospital autopsies.

DISCUSSION

The present study shows that the number of A1 AT globules as well as the mean age was lower in the medicolegal autopsy patients than in the hospital autopsy patients. The findings agree with earlier reports that the number of hepatocytic diastase resistant PAS positive globules in Z gene carriers increases with age (1-7). The number of A1 AT globules can be suspected to increase with diseases associated with enhanced synthesis of protein inside hepatocytes (6, 10) and a medicolegal autopsy material can be assumed to comprise fewer individuals with chronic diseases than hospital autopsy materials do.

The correlation between the occurrence of Z gene and A1 AT globules in hepatocytes is well established, but we do not know if the globules are an obligatory finding together with the Z gene. The frequency of 33 per cent is very similar to the serologically determined frequencies of PiMZ individuals in the Scandinavian regions (3, 5, 17). Thus it can be assumed that globules are to be found in almost all Z gene carriers although in varying amounts.

The PAS positive globules presenting antigenicity for immunoglobulin G correspond well to the inclusions of plasma proteins which have earlier been described in experimental as well as human materials (12, 13, 15). These inclusions might contain A1 AT as seen in 2 occasions in this material. The last observation has not previously been described. These A1 AT positive globules are probably not related to A1 AT deficiency but possibly associated with a high concentration of A1 AT in serum - seen for instance in infection diseases, malignant tumours post operatively. These globules are of differential diagnostic interest.

REFERENCES

1. Berg N O & Eriksson S. Liver disease in adults with alpha₁ antitrypsin deficiency. *New Engl J Med* 287: 1264-1267 1972.
2. DeLellis R A, Balogh K, Merk F B & Chirfe A M. Distinctive hepatic cell globules in adult alpha₁ antitrypsin deficiency. *Arch Path* 94: 308-316 1972.
3. Eriksson S. Studies in alpha₁ antitrypsin deficiency. *Acta med scand Suppl* 432 1965.
4. Eriksson S & Larsson C. Purification and partial characterization of PAS positive inclusion bodies from the liver in alpha₁ antitrypsin deficiency. *New Engl J Med* 292: 176-180 1975.
5. Fagerhol M K. Serum Pi types in Norwegians. *Acta path microbiol scand* 70: 421-428 1967.
6. Gordon H W, Dixon J, Rogers J C, Mittman C & Lieberman J. Alpha₁ antitrypsin (A₁AT) accumulation in livers of emphysematous patients with A₁AT deficiency. *Hum Path* 3: 361-370 1972.
7. Hadchouel M & Gautier M. Histopathologic study of the liver in alpha₁ antitrypsin deficiency.
8. Characterization of alpha₁ antitrypsin in the inclusion bodies from the liver in alpha₁ antitrypsin deficiency. *New Engl J Med* 293: 576-579 1975.
9. Larsson C & Eriksson S. Liver function in asymptomatic adult individuals with severe alpha₁ antitrypsin deficiency (Pi Z). *Scand J Gastroint* 12: 543-546 1977.
10. Lieberman J, Mittman C & Gordon H W. Alpha₁ antitrypsin in the livers of patients with emphysema. *Science* 175: 63-65 1972.
11. Palmer P E, DeLellis R A & Wolfe H J. Immunohistochemistry of liver in alpha₁ antitrypsin deficiency. *Am J Clin Path* 62: 350-354 1974.
12. Pfeifer U & Bannasch P. Zum Problem der chylösen Eiweisstropfen im Cytoplasma der Leberparenchymzellen. *Virchows Arch Abt B* 1: 365-388 1968.
13. Popper H, Paronetto P & Barka T. PAS positive structures of nonglycogenic character in normal and abnormal liver. *Arch Path* 70: 300-313 1960.
14. Reintoft I. Alpha₁ antitrypsin deficiency. Experience from an autopsy material. *Acta Path microbiol scand Sect A* 85: 649-655 1977.
15. Reintoft I. Periodic acid Schiff positive nonglycogenic globules in hepatocytes - Differential diagnostic aspects in screening for alpha₁ antitrypsin globules in an autopsy material. *Acta path microbiol scand Sect A* 86: 325-329 1978.
16. Sharp H L. Alpha₁ antitrypsin deficiency. *Hosp Pract* 92: 83-96 1971.
17. Siver T. Liver disease in alpha₁ antitrypsin deficiency detected by screening of 200 000 infants. *New Engl J Med* 294: 1316-1321 1976.
18. Triger D R, Milward-Sadler G H, Cawowski A A, Trowell J & Wright R. Alpha₁ antitrypsin deficiency and liver disease in adults. *Quart J Med* 45: 351-372 1976.

The author is indebted to Professor Hemming Poulsen, Department of Pathology, Hvidovre Hospital, for fruitful discussions and helpful correction of the manuscript.

THE DISTRIBUTION OF LYSOZYME IN HUMAN GASTRIC MUCOSA IN INFLAMMATORY AND NEOPLASTIC DISORDERS

REITAMO J J REITAMO P SIPPONEN and M KLOCKARS

Fourth Department of Medicine and Fourth Department of Surgery Helsinki University Central Hospital Helsinki and Department of Pathology Jorvi Hospital Espoo Finland

Reitamo J J Reitamo P Sipponen P & Klockars M The distribution of lysozyme in human gastric mucosa in inflammatory and neoplastic disorders Acta path microbiol scand Sect A 87 451-456 1979

An immunoperoxidase staining technique was used to identify lysozyme (LZM) in glutaraldehyde fixed paraffin-embedded tissue sections obtained from patients operated on for a gastric or duodenal ulcer or for a neoplasm of the stomach. As in normal gastric mucosa LZM was identified in neutrophilic granulocytes, cells belonging to the mononuclear phagocytic system and in the glandular cells of the stomach.

LZM was present in the tumour cells of the present study.

From our knowledge of LZM function we conclude that its presence in gastric secretions accords with a definite role of LZM in the nonspecific host defence against exogenous microorganisms. The significance of its presence in tumour associated macrophages needs further studies.

Key words: Gastric ulcer, duodenal ulcer, gastric carcinoma, lysozyme, immunohistochemistry.

S Reitamo, Fourth Department of Medicine, Helsinki University Central Hospital, Unioninkatu 38, 00170 Helsinki, Finland.

Received 28 III 79. Accepted 11 V 79

The cationic antibacterial enzyme lysozyme (LZM) (E.C. 3.2.1.17) has recently been identified by immunoperoxidase techniques in a variety of human tissues. Normal cells and tissues shown to contain LZM include the neutrophilic granulocytes belonging to the mononuclear phagocytic system, the glandular cells of various exocrine glands, Brunner's glands of the duodenum, Paneth cells of the small intestine, cartilage cells and the proximal tubules of the kidney (6, 10, 11, 16, 18). In pathological cells and tissues LZM has been identified in neoplastic cells of patients with myelocytic and monocytic leukaemia (9), in diseases associated with granuloma formation such as sarcoidosis and Crohn's disease. LZM has been identified in various cells of the mononuclear phagocytic cell line, e.g. macrophages, epithelial cells and multinucleated giant cells (7, 11). In

patients with inflammatory bowel disease LZM has also been identified in metaplastic Paneth cells of the colon and rectum (7, 14).

Although LZM has long been known to be present in higher concentrations in gastric fluid than in serum, the cellular sources of gastric fluid LZM are poorly understood. Published reports on the localization of LZM in human gastric mucosa have conflicted. Mason & Taylor (11) were unable to detect LZM in human gastric mucosa and Pinkus & Said (16) identified this enzyme only in occasional epithelial cells. However, by using a shorter fixation time we were able to detect LZM not only in neutrophilic granulocytes but also in the gastric glands (6, 17).

The present study was designed to determine the known distribution of LZM in the gastric mucosa in inflammatory and neoplastic disorders.

MATERIAL AND METHODS

Gastrectomy specimens were obtained from 18 patients operated on for a gastric neoplasm and from five patients with a gastric ulcer. Samples were taken from several sites on each surgical specimen. Biopsies were also taken from the gastrotomy site in 12 patients who underwent a parietal cell vagotomy for a duodenal ulcer. All tissues were fixed for 45 to 90 min in 1.5% aqueous glutaraldehyde pH adjusted with NaOH to 7.2 without a buffer and then dehydrated in several changes of absolute ethanol cleared in xylene and embedded in paraffin. Sections were cut at 5 μ m and mounted on albumin or gelatin coated glass slides and heated at 60°C for 2 hr.

Rabbit anti human LZM antiserum, rabbit anti hen egg white LZM and rabbit anti horseradish peroxidase antiserum were prepared in this laboratory as described in detail elsewhere (6). The specificity of the antisera was tested by immunoelectrophoresis in 1% agarose (Seakem, Maine) in Veronal® buffer ionic strength 0.075 pH 8.6. Sheep anti rabbit globulin antiserum was purchased from Sycco, Sylva Co. (New Jersey).

The localization of LZM was determined by a modification described in detail elsewhere (6) of the immunoglobulin enzyme bridge technique (12). Briefly, tissue sections were treated serially for 30 min with 1) rabbit anti human LZM antiserum (diluted 1:200), 2) sheep anti rabbit globulin antiserum (1:20), 3) rabbit anti horseradish peroxidase antiserum (1:150) and then 4) incubated for 20 min with horseradish peroxidase (Sigma type VI) at a concentration of 250 μ g/ml. The LZM was visualized by staining of the peroxidase as described by Graham & Karnovsky (4). The sections were counterstained with haematoxylin, cresyl violet or Alcian Blue.

For testing the specificity of the LZM staining, the rabbit anti human LZM antiserum was replaced with rabbit anti hen egg white LZM antiserum known to be immunologically distinct from its human counterpart. The intrinsic peroxidase activity of erythrocytes, granulocytes and mononuclear phagocytes was abolished before immunostaining by the methanol H_2O_2 treatment of Sirefherk (19).

TABLE 2 Sites of Immunohistochemically Detectable Lysozyme in 18 Patients Operated on for Gastric Cancer

Site of lysozyme staining	No. of patients
Antral or fundic glands	17
Neutrophils and mononuclear cells in interstitial tissue	9
Metaplastic Paneth cells	6
Tumour macrophages	10
Neoplastic cells	1

RESULTS

The results of this study are summarized in Tables 1 and 2. In controls, in which parallel sections using the anti hen egg white LZM antiserum was used instead of anti human LZM antiserum, no staining specific for LZM was seen.



Fig. 1 Antrum of a patient with a gastric ulcer. Most glands stain positively for LZM (black). Note infiltration by LZM positive cells (granulocytes and mononuclear phagocytes) in the upper part of the mucosa. Cresyl violet counterstain. $\times 120$.

Site of lysozyme staining	No. of patients	
	Gastric ulcer	Duodenal ulcer
Antral or fundic glands	5	10
Neutrophils and mononuclear cells in interstitial tissue	5	4
Metaplastic Paneth cells	4	1



Fig 2 Fundus of a patient with a duodenal ulcer. Most fundic glands are LZM negative. Cresyl violet counterstain $\times 120$

Fig 3 Antrum of a patient with a gastric ulcer. The apical part of most glandular cells stains positively for LZM and the mucosal cellular infiltrate contains LZM positive neutrophils and mononuclear phagocytes. Cresyl violet counterstain $\times 120$

Gastric Glands

In all three pathological conditions LZM was detected in the antral and the fundic glands. The staining for LZM among these two types of cells however varied widely: staining could be strongly positive in all glands (Fig. 1) or strongly positive in one gland and negative in the neighbouring gland (Fig. 2). No staining pattern could be discerned that was typical in tissue from a gastric or duodenal ulcer or from a gastric carcinoma. In all three conditions the antral glands were more consistently

(Figs 1-2)

Cellular Infiltration

In the mucosa the cellular infiltrate consisted of LZM positive granulocytes and mononuclear phagocytes and LZM negative lymphocytes (Fig. 3). Most but not all neutrophils, whether in the blood vessels or in the mucosal infiltrate, stained intensely for LZM. Some specimens of scar tissue from healing ulcers also contained LZM positive mononuclear cells.

Intestinal Metaplasia

Biopsy specimens from all three pathological conditions showed patches of intestinal metaplasia (Tables 1 and 2). Such metaplasia was identified from its typical resemblance to the glandular mucosa of the small intestine with goblet cells staining positively with Alcian Blue or cresyl violet. Paneth cells were observed in all specimens containing goblet cells except one. As in normal Paneth cells, staining was positive for LZM mainly in the suprapical region of the metaplastic Paneth cells (Fig. 4).

Gastric Cancer

Except in one specimen

n

n

Comparative lack of LZM positivity in neoplastic glands was the presence of various numbers of LZM positive macrophages



MATERIAL AND METHODS

Gastrectomy specimens were obtained from 18 patients operated on for a gastric neoplasm and from five patients with a gastric ulcer. Samples were taken from several sites on each surgical specimen. Biopsies were also taken from the gastrotomy site in 12 patients who underwent a parietal cell vagotomy for a duodenal ulcer. All tissues were fixed for 45 to 90 min in 1.5% aqueous glutaraldehyde pH adjusted with NaOH to 7.2 without a buffer and then dehydrated in several changes of absolute ethanol, cleared in xylene and embedded in paraffin. Sections were cut at 5 μ m and mounted on albumin or gelatin coated glass slides and heated at 60°C for 2 hr.

Rabbit anti human LZM antiserum, rabbit anti hen egg white LZM and rabbit anti horseradish peroxidase antiserum were prepared in this laboratory as described in detail elsewhere (6). The specificity of the antisera was tested by immunoelectrophoresis in 1% agarose (Seakem, Maine) in Veronal® buffer, ionic strength 0.075, pH 8.6. Sheep anti rabbit globulin antiserum was purchased from Sycco, Sylva, Co. (New Jersey).

The localization of LZM was determined by a modification described in detail elsewhere (6) of the immunoglobulin enzyme bridge technique (12). Briefly, tissue sections were treated serially for 30 min with: (1) rabbit anti human LZM antiserum (diluted 1:200), (2) sheep anti rabbit globulin antiserum (1:20), (3) rabbit anti horseradish peroxidase antiserum (1:150) and then (4) incubated for 20 min with horseradish peroxidase (Sigma, type VI) at a concentration of 250 μ g/ml. The LZM was visualized by staining of the peroxidase as described by Graham & Karnovsky (4). The sections were counterstained with haematoxylin, cresyl violet or Alcian Blue.

For testing the specificity of the LZM staining, the rabbit anti human LZM antiserum was replaced with rabbit anti hen egg white LZM antiserum known to be immunologically distinct from its human counterpart. The intrinsic peroxidase activity of erythrocytes, granulocytes and mononuclear phagocytes was abolished before immunostaining by the methanol H₂O₂ treatment of Streefkerk (19).

TABLE 1 Sites of Immunohistochemically Detectable Lysozyme in 5 Patients Operated on for Gastric and 12 for Duodenal Ulcer

Site of lysozyme staining	No. of patients	
	Gastric ulcer	Duodenal ulcer
Antral or fundic glands	5	10
Neutrophils and mononuclear cells in interstitial tissue	5	4
Metaplastic Paneth cells	4	1

TABLE 2 Sites of Immunohistochemically Detectable Lysozyme in 18 Patients Operated on for Gastric Cancer

Site of lysozyme staining	No. of patients
Antral or fundic glands	17
Neutrophils and mononuclear cells in interstitial tissue	9
Metaplastic Paneth cells	6
Tumour macrophages	10
Neoplastic cells	1

RESULTS

The results of this study are summarized in Tables 1 and 2. In controls, in which parallel sections using the anti hen egg white LZM antiserum was used instead of anti human LZM antiserum, no staining specific for LZM was seen.



Fig. 1 Antrum of a patient with a gastric ulcer. Most glands stain positively for LZM (black). Note infiltration by LZM positive cells (granulocytes and mononuclear phagocytes) in the upper part of the mucosa. Cresyl violet counterstain. $\times 120$.

LZM by immunoperoxidase techniques it is not yet entirely clear which cells actually synthesize LZM. The observation moreover that LZM is actively synthesized in tissue cultures of gastric biopsy specimens from both normal and inflammatory mucosa (8-13) gives no clue as to which cell in these tissues is responsible for the synthesis. It is well established that cells of the myelocytic series do not normally synthesize LZM outside the bone marrow (2) whereas mononuclear phagocytes synthesize LZM continuously (3). Paneth cells of the small intestine have been shown to secrete LZM (15) but whether normal and metaplastic Paneth cells are also capable of synthesizing LZM is still unclear. The LZM in Paneth cells might originate from the serum or from the neutrophilic granulocytes and mononuclear phagocytes in blood vessels or mucosa—as appeared to be the case with gastric glands. Our observation that LZM staining was especially intense in those glands in which cellular infiltration was heavy points to the possibility that glandular LZM originates from granulocytes and mononuclear phagocytes.

That LZM was detected in the malignant gastric glands of only a single patient contrasts with the frequent observation of some other enzymes both in intestinal metaplasia and neoplastic glands. Amino peptidase for example was reported to be detected in 7 of 20 cases of gastric carcinoma (20). We have stained from more than one hundred various neoplasms of the gastrointestinal and other tissues and except for one highly differentiated jejunal adenocarcinoma that contained neoplastic Paneth cells we detected LZM in no other malignant epithelium (unpublished observation). The only neoplastic cells that have been shown to synthesize LZM are the leukaemic cells of granulocytic and monocytic origin and in these cells the presence of LZM has been verified by immunoperoxidase methods (9).

The gastric mucosal LZM possibly together with secretory immunoglobulins forms a part of an antibacterial defence system. Both LZM and IgA show a similar distribution in various body fluids. Alone LZM cannot lyse other bacteria than gram positive saprophytes in the presence of IgA and complement however LZM can also lyse various pathogenic organisms including some strains of *Escherichia coli* (15). The role of LZM in the tumour macrophages is less well understood. Whether it plays an active role in the defence against tumour growth has yet to be proven.

This study was supported by grants from the Sigrid Jusélius Foundation and Finska Läkaresällskapet.

REFERENCES

- Adinolfi M, Glynn A A, Lindsay M & Milne C M. Serological properties of γ A antibodies in *Escherichia coli* present in human colostrum. *Immunology* 10: 517-526 1966.
- Bainton D F. Neutrophil granules. *Br J Haematol* 29: 17-21 1975.
- Gordon S, Todd J & Cohn Z A. In vitro synthesis and secretion of lysozyme by mononuclear phagocytes. *J exp Med* 139: 1228-1248 1974.
- Graham R C & Karnovsky M J. The early stages of absorption of injected horseradish peroxidase in the proximal tubules of mouse kidney. Ultrastructural cytochemistry by a new technique. *J Histochem Cytochem* 14: 291-302 1966.
- Hill I R & Porter P. Studies of bactericidal activity to *Escherichia coli* of porcine serum and colostrum immunoglobulins and the role of lysozyme with secretory IgA. *Immunology* 26: 1239-1250 1974.
- Klockars M & Reutamo S. Tissue distribution of lysozyme in man. *J Histochem Cytochem* 23: 932-940 1975.
- Klockars M, Reutamo S, Reutamo J J & Møller C. Immunohistochemical identification of lysozyme in intestinal lesions in ulcerative colitis and Crohn's disease. *Gut* 18: 377-381 1977.
- Lai A, Far F M, McClelland D B L & Van Furth R. Intra- and extracellular lysozyme and lactoferrin in myeloproliferative disorders. *J clin Pathol* 30: 541-546 1977.
- Mason D Y, Farrel C & Taylor C R. The detection of intracellular antigens in human leucocytes by immunoperoxidase staining. *Br J Haematol* 31: 361-370 1975.
- Mason D Y & Taylor C R. The distribution of muramidase (lysozyme) in human tissues. *J clin Pathol* 28: 124-132 1975.
- Mason T E, Hifer R F, Spicer S S, Swallow R A & Dreskin R B. An immunoglobulin-enzyme bridge method for localizing tissue antigens. *J Histochem Cytochem* 17: 563-569 1969.
- McClelland D B L, Shearman D J C, Lai A, Far F M & Van Furth R. In vitro synthesis of immunoglobulin secretory component complement and lysozyme by human gastrointestinal tissues II. Pathological tissues. *Clin exp Immunol* 23: 20-27 1976.
- Montero C & Erlandsen S L. Immunocytochemical and histochemical studies on intestinal epithelial cells producing both lysozyme and mucosubstance. *Anat Rec* 190: 127-141 1978.
- Peters T & Vantrappen G. The Paneth cell: a source of intestinal lysozyme. *Gut* 16: 553-558 1975.
- Pinkus G S & Said J W. Profile of intracytoplasmic lysozyme in normal tissues, myeloproliferative



Fig 4 Antrum of a patient with gastric cancer. The intestinal metaplasia of a gland contains many LZM positive metaplastic Paneth cells. Here the normal antral glands are LZM negative. Cresyl violet counterstain $\times 400$



Fig 5 A moderately differentiated gastric cancer. Tubular structures are LZM positive. Cresyl violet counterstain $\times 400$

DISCUSSION

Results of our earlier studies showed that in various cells and tissues the resistance of LZM antigenicity to destruction varied from cell to cell. Even in the same tissue section the LZM in gastric glandular cells is much more rapidly destroyed by fixatives than for example the LZM in neutrophilic granulocytes (17). This cellular variability in the resistance of LZM antigenicity to destruction could explain why Mason & Taylor (11) and Pinkus & Said (16) by using formalin fixed, routinely processed tissues, were unable to detect LZM in human gastric glands. That in the present study some gastric glands were always LZM negative might be explained in one of three different ways: 1) their antigenicity was destroyed by fixation; 2) these glands were not actively synthesizing and/or secreting LZM; or 3) the anionic glycoproteins present in the mucous cells blocked the reactivity for the anti human LZM antiserum (17).

The consistently intense staining for LZM in Paneth cells in intestinal metaplasia of the stomach closely resembled the LZM staining in both normal Paneth cells (6, 11) and in metaplastic Paneth cells in the colon and rectum of patients with inflammatory bowel disease (7, 14). Because LZM is the major cationic protein in Paneth cells, it might be concluded that their eosinophilia is due to the presence of LZM. However, as the biological function of normal and metaplastic Paneth cells is still poorly understood, it is difficult to evaluate the significance of our observation.

The present results suggest that the LZM in gastric fluid originates from the gastric glandular cells, the neutrophilic granulocytes, and the cells of the mononuclear phagocytic system in inflammatory and neoplastic states. Additional sources of gastric fluid LZM are metaplastic Paneth cells and rarely neoplastic glandular cells. Still another source of gastric LZM is saliva, in which the concentration of LZM is similar to that in gastric fluid (unpublished observation). Although all the afore mentioned cells in the gastric mucosa have been shown to contain

REFERENCES

LZM by immunoperoxidase techniques it is not yet entirely clear which cells actually synthesize LZM. The observation moreover that LZM is actively synthesized in tissue cultures of gastric biopsy specimens from both normal and inflammatory mucosa (8-13) gives no clue as to which cell in these tissues is responsible for the synthesis. It is well established that cells of the myelocytic series do not normally synthesize LZM outside the bone marrow (2) whereas mononuclear phagocytes synthesize LZM continuously (3). Paneth cells of the small intestine have been shown to secrete LZM (15) but whether normal and metaplastic Paneth cells are also capable of synthesizing LZM is still unclear. The LZM in Paneth cells might originate from the serum or from the neutrophilic granulocytes and mononuclear phagocytes in blood vessels or mucosa—as appeared to be the case with gastric glands. Our observation that LZM staining was especially intense in those glands in which cellular infiltration was heavy points to the possibility that glandular LZM originates from granulocytes and mononuclear phagocytes.

That LZM was detected in the malignant gastric glands of only a single patient contrasts with the frequent observation of some other enzymes both in intestinal metaplasia and neoplastic glands. Amino peptidase for example was reported to be detected in 7 of 20 cases of gastric carcinoma (20). We have stained from more than one hundred various neoplasms of the gastrointestinal and other tissues and except for one highly differentiated jejunal adenocarcinoma that contained neoplastic Paneth cells we detected LZM in no other malignant epithelium (unpublished observation). The only neoplastic cells that have been shown to synthesize LZM are the leukaemic cells of granulocytic and monocytic origin and in these cells the presence of LZM has been verified by immunoperoxidase methods (9).

The gastric mucosal LZM possibly together with secretory immunoglobulins forms a part of an antibacterial defence system. Both LZM and IgA show a similar distribution in various body fluids. Alone LZM cannot lyse other bacteria than gram positive saprophytes in the presence of IgA and complement however LZM can also lyse various pathogenic organisms including some strains of *Escherichia coli* (15). The role of LZM in the tumour macrophages is less well understood. Whether it plays an active role in the defence against tumour growth has yet to be proven.

This study was supported by grants from the Sigrid Jusélius Foundation and Finska Läkaresällskapet.

- 1 Adinolfi M, Glynn A A, Lindsay M & Milne C M. Serological properties of γ A antibodies in *Escherichia coli* present in human colostrum. *Immunology* 10: 517-526 1966.
- 2 Bainton D F. Neutrophil granules. *Br J Haematol* 29: 17-21 1975.
- 3 Gordon S, Todd J & Cohn Z A. In vitro synthesis and secretion of lysozyme by mononuclear phagocytes. *J exp Med* 139: 1228-1248 1974.
- 4 Graham R C & Karnovsky M J. The early stages of absorption of injected horseradish peroxidase in the proximal tubules of mouse kidney. Ultrastructural cytochemistry by a new technique. *J Histochem Cytochem* 14: 291-302 1966.
- 5 Hill I R & Porter P. Studies of bactericidal activity to *Escherichia coli* of porcine serum and colostrum immunoglobulins and the role of lysozyme with secretory IgA. *Immunology* 26: 1239-1250 1974.
- 6 Klockars M & Reitamo S. Tissue distribution of lysozyme in man. *J Histochem Cytochem* 23: 932-940 1975.
- 7 Klockars M, Reitamo S, Reitamo J J & Møller C. Immunohistochemical identification of lysozyme in intestinal lesions in ulcerative colitis and Crohn's disease. *Gut* 18: 377-381 1977.
- 8 Lai A, Fair R F M, McClelland D B L & Van Furth R. In vitro synthesis of immunoglobulins, secretory component, complement and lysozyme by human gastrointestinal tissues. I. Normal tissues. *Clin exp Immunol* 23: 9-19 1976.
- 9 Mason D Y. Intracellular lysozyme and lactoferrin in myeloproliferative disorders. *J clin Pathol* 30: 541-546 1977.
- 10 Mason D Y, Farrell C & Taylor C R. The detection of intracellular antigens in human leucocytes by immunoperoxidase staining. *Br J Haematol* 31: 361-370 1975.
- 11 Mason D Y & Taylor C R. The distribution of muramidase (lysozyme) in human tissues. *J clin Pathol* 28: 124-132 1975.
- 12 Mason T E, Phifer R F, Spicer S S, Swallow R A & Dreskin R B. An immunoglobulin-enzyme bridge method for localizing tissue antigens. *J Histochem Cytochem* 17: 563-569 1969.
- 13 McClelland D B L, Shearman D J C, Lai A, Fair R F M & Van Furth R. In vitro synthesis of immunoglobulins, secretory component, complement and lysozyme by human gastrointestinal tissues. II. Pathological tissues. *Clin exp Immunol* 23: 20-27 1976.
- 14 Montero C & Erlandsen S L. Immunocytochemical and histochemical studies on intestinal epithelial cells producing both lysozyme and mucosubstance. *Anat Rec* 190: 127-141 1978.
- 15 Peeters T & Vantrappen G. The Paneth cell: a source of intestinal lysozyme. *Gut* 16: 553-558 1975.
- 16 Pinkus G S & Said J W. Profile of intracytoplasmic lysozyme in normal tissues, myeloproliferative



Fig 4 Antrum of a patient with gastric cancer. The intestinal metaplasia of a gland contains many L2M positive metaplastic Paneth cells. Here the normal apical glands are L2M negative. Cresyl violet counterstain $\times 400$.



Fig 5 A moderately differentiated gastric cancer. Tubular structures are L2M positive. Cresyl violet counterstain $\times 400$.

DISCUSSION

Results of our earlier studies showed that in various cells and tissues the resistance of L2M antigenicity to destruction varied from cell to cell. Even in the same tissue section the L2M in gastric glandular cells is much more rapidly destroyed by fixatives than for example the L2M in neutrophilic granulocytes (17). This cellular variability in the resistance of L2M antigenicity to destruction could explain why Mason & Taylor (11) and Pinkus & Said (16) by using formalin fixed routinely processed tissues were unable to detect L2M in human gastric glands. That in the present study some gastric glands were always L2M negative might be explained in one of three different ways: 1) their antigenicity was destroyed by fixation; 2) these glands were not actively synthesizing and/or secreting L2M; or 3) the anionic glycoproteins present in the mucous cells blocked the reactivity for the anti human L2M antiserum (17).

The consistently intense staining for L2M in Paneth cells in intestinal metaplasia of the stomach closely resembled the L2M staining in both normal Paneth cells (6, 11) and in metaplastic Paneth cells in the colon and rectum of patients with inflammatory bowel disease (7, 14). Because L2M is the major cationic protein in Paneth cells it might be concluded that their eosinophilia is due to the presence of L2M. However, as the biological function of normal and metaplastic Paneth cells is still poorly understood, it is difficult to evaluate the significance of our observation.

The present results suggest that the L2M in gastric fluid originates from the gastric glandular cells, the neutrophilic granulocytes and the cells of the mononuclear phagocytic system in inflammatory and neoplastic states. Additional sources of gastric fluid L2M are metaplastic Paneth cells and rarely neoplastic glandular cells. Still another source of gastric L2M is saliva, in which the concentration of L2M is similar to that in gastric fluid (unpublished observation). Although all the aforementioned cells in the gastric mucosa have been shown to contain

MORPHOLOGY AND FUNCTION OF THE GASTRIC MUCOSA IN FIRST-DEGREE RELATIVES OF PROBANDS WITH HISTOLOGICALLY DIFFERENT TYPES OF GASTRIC CARCINOMA

TIMO IHAMAKI and PENTTI SIPPONEN

Gastroenterological Unit, Second Department of Medicine, University of Helsinki, Helsinki, and Department of Pathology, Jorvi Hospital, Espoo, Finland

Ihamaki T & Sipponen P. Morphology and function of the gastric mucosa in first-degree relatives of probands with histologically different types of gastric carcinoma. *Acta path. microbiol. scand. Sect. A* 87: 457-462, 1979.

The occurrence of antral and body gastritis, the prevalence of intestinal metaplasia (IM), epithelial atypia (EA) and circulating antibodies and the maximal acid output (MAO) and fasting serum gastrin level (FSG) were studied in 301 first-degree relatives of probands with histologically different types of gastric carcinoma: intestinal (IC), diffuse spreading (DC) and anaplastic (AC). The results were compared with those obtained from a similar study of 358 first-degree relatives of probands, age and sex matched by computer for each cancer proband from a large Finnish population. The mean score of gastritis changes, the prevalence of atrophic gastritis of antrum and body of IM and the mean FSG were significantly higher and the mean MAO significantly lower in DC relatives than in their controls. No such differences were found between IC relatives and controls. The results suggest that there is a genetic or familial association of chronic gastritis with DC but not with other gastric cancer types.

Key words: Gastric carcinoma, histological types, chronic gastritis, histology, genetics, family study.

Sipponen P. Department of Pathology, Jorvi Hospital, SF-02740 Espoo 74, Finland.

Received 20 May 1979. Accepted 25 May 1979.

Our recent studies indicate that atrophic gastritis, intestinal metaplasia, epithelial atypia and achlorhydria occur more often and at younger age in near relatives of gastric carcinoma than in relatives of age- and sex-matched probands from a general population (Ihamaki *et al.* 1979). Because these signs have often been considered premalignant (Suurala *et al.* 1977; Mosbech 1954; Morson 1955; Ming *et al.* 1957; Nagayo 1971; Sugano *et al.* 1971), the results would explain the increased risk of gastric carcinoma in near relatives with this disease (Videbaek & Mosbech 1956; Woolf 1961; Macklin 1960). However, according to Lehtola (1978), the risk depends on the histological type of the probands' malignancy.

In this paper we have evaluated the morphology and function of the gastric mucosa in first-degree relatives of probands with histologically different types of gastric carcinoma. Relatives of probands computer-matched from a general population for age and sex have been used as controls.

In this paper we have evaluated the morphology and function of the gastric mucosa in first-degree relatives of probands with histologically different types of gastric carcinoma. Relatives of probands computer-matched from a general population for age and sex have been used as controls.

- disorders, hairy cell leukemia, and other pathological processes. An immunoperoxidase study of paraffin sections and smears. *Am J Path* 89, 351-366, 1977
- 17 *Reitamo, S*. Lysozyme antigenicity and tissue fixation. *Histochemistry* 55, 197-207, 1978
 - 18 *Reitamo, S, Klockars, M, Adinolfi, M & Osserman, E F*. Human lysozyme. Origin and distribution in health and disease. *Ric Clin Lab* 8, 211-231, 1978
 - 19 *Streefkerk, J G*. Inhibition of erythrocyte pseudoperoxidase activity by treatment with hydrogen peroxide following methanol. *J Histochem Cytochem* 20, 829-831, 1972
 - 20 *Wattenberg, L W*. Histochemical study of aminopeptidase in metaplasia and carcinoma of the stomach. *Arch Path* 67, 281-286, 1959

MATERIAL AND METHODS

The material consists of 301 first degree relatives of 73 consecutive gastric carcinoma patients diagnosed in the Gastroenterological Unit of Meilahti Hospital, Helsinki. 358 first-degree relatives of 73 probands computer matched for the carcinoma probands as to age, sex, occupation, birth place of residence are used as controls.

The carcinoma probands were divided into two main groups according to *Lauren* (1965): diffuse spreading carcinoma type (20 probands) and intestinal type carcinoma (33 probands). The cases which could not be incorporated into these groups were treated as anaplastic carcinoma (20 probands). The composition of the series and controls as well as their age and sex distribution and the number of relatives in each group are presented in Tables 1 and 2. More details of selection principles and composition of the materials are described elsewhere (*Ihamaki et al 1979*).

It appears that the age and sex distribution of the diffuse and intestinal group is largely similar to their controls (Table 1) indicating a good comparability at least with respect to age and sex. On the other hand, the mean age of relatives of diffuse carcinoma type (DC) was about 5 years lower than that of intestinal type (IC). Because most of the parameters studied are clearly age dependent (*Suurala et al 1977*, *Varis 1971*) a direct comparison of the two main groups is difficult and the main attention is paid upon the comparison of DC and IC relatives with their own controls (Tables 1 and 2).

The following examinations were performed in the series and controls: gastroscopy with multiple biopsies

from antral and body area, pentagastrin test, fasting serum gastrin level and parietal cell and intrinsic factor antibodies (see *Ihamaki et al 1979*).

Biopsy specimens were fixed in neutral buffered 10 per cent formalin and were embedded in paraffin, sectioned and stained with haematoxylin-eosin and Alcian blue (pH 2.5)-PAS. The state of the gastric mucosa and the degree of chronic gastritis were classified as follows: normal, superficial gastritis, slight, moderate or severe atrophic gastritis as described earlier (*Suurala et al 1968*, *Ihamaki et al 1979*). Numerical values of each degree (0-4) of mucosal changes were used in mathematical calculations. The prevalence of intestinal metaplasia and severe epithelial atypia (*Nagayo 1971*, *Sugano et al 1971*, *Ihamaki et al 1979*) were noted separately. Student's *t* test and chi square test were used in statistical analyses.

RESULTS

Comparison of diffuse spreading carcinoma (DC) relatives with their controls. It appears from Table 3 that the prevalence of atrophic gastritis, intestinal metaplasia (IM) and high serum gastrin levels as well as the mean gastritis score in antral and body mucosa were significantly higher in DC relatives than in their controls. In addition, the mean maximal acid output (MAO) was significantly lower and the mean fasting serum gastrin level signifi-

TABLE 4 Comparison of Intestinal Type Carcinoma Relatives with Their Controls

Findings	Intestinal ca Relatives	Controls	Level of Significance
Body mucosa			
Mean gastritis score \pm SD	0.99 \pm 1.23	0.98 \pm 1.06	ns
Atrophic gastritis No	32	36	ns
Antral mucosa			
Mean gastritis score \pm SD	0.94 \pm 1.05	1.04 \pm 1.06	ns
Atrophic gastritis No	36	50	
Intestinal metaplasia No	26	29	ns
Epithelial atypia	5	5	ns
Achlorhydria No	11	10	ns
Mean MAO mmol/hr \pm SD	21.1 \pm 16.4	24.1 \pm 15.8	ns
Serum gastrin > pmol/l No	10	14	ns
Mean basal serum gastrin pmol/l \pm SD	63.6 \pm 74.3	59.1 \pm 69.6	ns
Parietal cell antibodies No	7	13	ns
Intrinsic factor antibodies No	3	6	ns
Total No. of cases	110	142	

TABLE 1 *Number of Cases, mean Age and Male-Female Ratio in Patient Groups Studied*

Patient group	Number of relatives	Mean age \pm SD years	Male female ratio
Intestinal carcinoma	110	48.6 \pm 16.4	51/59 = 0.9
Intestinal carcinoma controls	142	48.5 \pm 17.7	65/77 = 0.8
Diffuse spreading carcinoma	100	44.9 \pm 17.2	47/53 = 0.9
Diffuse spreading carcinoma controls	108	43.5 \pm 15.9	55/53 = 1.0
Anaplastic carcinoma	91	48.9 \pm 15.4	40/51 = 0.8
Anaplastic carcinoma controls	108	46.5 \pm 15.7	49/61 = 0.8

TABLE 2 *Number of Relatives According to Their Family Connections in Carcinoma and Control Groups*

Patient group	Total Number of relatives	Parents		Sisters and Brothers		Children	
		No	%	No	%	No	%
Intestinal carcinoma	110	0		45	41	65	59
Intestinal carcinoma controls	142	3	2	63	44	76	54
Diffuse spreading carcinoma	100	9	9	46	46	45	45
Diffuse spreading carcinoma controls	108	12	11	57	53	39	36
Anaplastic carcinoma	91	0		36	40	55	60
Anaplastic carcinoma controls	108	0		48	44	60	56

TABLE 3 *Comparison of Diffuse Carcinoma Relatives with Their Controls*

Findings	Diffuse ca Relatives	Controls	Level of Significance
Body mucosa			
Mean gastritis score \pm SD	1.18 \pm 1.24	0.49 \pm 0.72	$p < 0.001$
Atrophic gastritis No	26	7	$p < 0.001$
Antral mucosa			
Mean gastritis score \pm SD	1.19 \pm 1.10	0.73 \pm 0.84	$p < 0.01$
Atrophic gastritis No	40	21	$p < 0.01$
Intestinal metaplasia No	29	15	$p < 0.05$
Epithelial atypia No	7	2	ns
Achlorhydria No	9	3	ns
Mean MAO mmol/hr \pm SD	20.1 \pm 13.7	27.3 \pm 13.9	$p < 0.001$
Serum gastrin > 100 pmol/l No	14	7	$p = 0.05$
Mean basal serum gastrin pmol/l \pm SD	44.5 \pm 132.7	46.7 \pm 45.9	$p < 0.01$
Parietal cell antibodies No	5	7	ns
Intrinsic factor antibodies No	4	0	ns
Total No. of cases	100	108	

than IC relatives the mean gastritis score in antrum and body was higher in the former. The difference however was not statistically significant. On the other hand below 50 years of age the mean gastritis score was in DC relatives 1.77 ± 1.69 and in IC relatives 0.70 ± 1.07 . This difference was statistically highly significant ($p < 0.001$). In addition the mean serum gastrin level was significantly higher in DC than in IC relatives. The prevalence of IM and EA was somewhat higher in DC relatives but the prevalence of achlorhydria was similar in both groups. The mean age of subjects with IM, EA and achlorhydria was significantly lower in DC relatives than in IC relatives (Table 6).

DISCUSSION

The present data disclosed significant differences between relatives of diffuse spreading gastric carcinoma (DC) and their controls while no such differences were seen with respect to intestinal and anaplastic types of gastric carcinoma.

In DC relatives the mean score of both antral and body gastritis was significantly higher than in their controls. The mean MAO was also significantly lower and the mean fasting serum gastrin level (SFG) significantly higher in DC relatives than in controls. Intrinsic factor antibodies were also more often seen in DC families than in controls. Thus there is in DC families an increased prevalence of signs characteristic of A type gastritis (Strickland & MacKay 1973) which according to Varis (1971) and Surala *et al.* (1977) is strongly genetically determined.

The comparison of IC relatives directly with DC relatives was handicapped by the 5 years higher mean age of the former group. However there was a tendency to a higher prevalence of atrophic gastritis IM and EA in DC relatives than in IC relatives. There was also a clear trend for these parameters to occur at a younger age in DC than in IC relatives. The results are in line with our earlier dynamic mathematical approaches which suggest that gastritis of the body mucosa is more severe and begins earlier in relatives of DC than IC (Kekki *et al.* 1975).

Atrophic gastritis IM, EA and achlorhydria have often been considered premalignant conditions (Surala & Seppala 1960, Mosbech 1954, Surala *et al.* 1974, 1977, Morson 1955, Ming *et al.* 1967, Nagayo 1971, Sugano *et al.* 1971, Jarvi & Lauren 1951, Fujita & Hattori 1976). The high prevalence of these signs and their occurrence at a younger age could explain the observed high gastric cancer risk

in first-degree relatives of DC patients (Lehtola 1978).

The increased death rate in gastric carcinoma in near relatives with diffuse type may indicate the participation of genetic factors in the pathogenesis of this disease. The hereditary nature of DC is indicated by the younger age of the patients and by the greater proportion of women with DC than with IC (Lauren 1965, Stemmermann & Brown 1974, Sipponen *et al.* 1976). In addition Correa *et al.* (1970, 1973, 1976) and Munoz & Asvall (1971) found a higher than expected prevalence of blood group A among patients with DC. Moreover these authors found some epidemiological differences between the two histological types which suggest a stronger effect of genetic factors in the pathogenesis of diffuse cancer type. The increased prevalence of severe atrophic body gastritis noted in this study could also be regarded as additional evidence for the importance of hereditary factors in the pathogenesis of DC. On the other hand lack of correlation between the various genetic markers and IC would emphasize the greater significance of environmental

accepted by all pathologists. However the present data among many others mentioned above suggest that there are fundamental differences in the biology of the cancer types which favour the classification of gastric carcinomas according to Lauren's principles.

The authors wish to express their thanks to the Finnish Cancer Foundation for financial support.

REFERENCES

1. Correa P. Geographic pathology of cancer in Colombia. *Int Path* 11: 16-22, 1970.
2. Correa P, Cuella C & Haensel W. Pathogenese des Magenkarzinoms. *Epidemiologische Pathologie vorangehender Läsionen Leber Magen Darm* 6: 72-79, 1976.
3. Correa P, Sasano N, Stemmermann G N & Haensel W. Pathology of gastric carcinoma in Japanese populations. Comparison between Miyagi prefecture Japan and Hawaii. *J natl Cancer Inst* 51: 1449-1459, 1973.
4. Fujita S & Hattori T. Cell proliferation, differentiation and migration in the gastric mucosa. A study on a background of carcinogenesis. 7th Int Symp of Princess Takamatsu Cancer Research Fund, 1976, pp 21-34.
5. Ihama T, Varis K & Surala M. Morphological, functional and immunological state of the gastric mucosa in gastric carcinoma families.

TABLE 5 Comparison of Anaplastic Carcinoma Relatives with Their Controls

Findings	Anaplastic ca Relatives	Controls	Level of Significance
Body mucosa			
Mean gastritis score \pm S D	1.06 \pm 1.21	0.75 \pm 0.88	$p < 0.05$
Atrophic gastritis No	27	19	ns
Antral mucosa			
Mean gastritis score \pm S D	1.09 \pm 1.05	0.91 \pm 0.96	ns
Atrophic gastritis No	36	33	ns
Intestinal metaplasia No	26	13	$p < 0.01$
Epithelial atypia No	3	3	ns
Achlorhydria No	8	3	ns
Mean MAO mmol/hr \pm S D	20.3 \pm 15.3	24.1 \pm 14.1	ns
Serum gastrin > 100 pmol/l No	10	11	ns
Mean basal serum gastrin pmol/l \pm S D	81.2 \pm 176.9	48.8 \pm 47.2	ns
Parietal cell antibodies No	9	7	ns
Intrinsic factor antibodies No	0	1	ns
Total No. of cases	91	108	

cantly higher in DC relatives than in controls. The prevalence of epithelial atypia (EA) and achlorhydria was also higher in DC relatives but the difference was statistically insignificant. In addition intrinsic factor antibodies were found in 4% of DC relatives but in none of the controls. As seen from Table 6 there is a tendency to a lower mean age in DC relatives with EA and achlorhydria, the difference being significant only with respect to EA.

Comparison of intestinal type carcinoma (IC) relatives with their controls. Table 4 shows that IC relatives did not differ significantly from their relatives with respect to any of the parameters studied. Neither were there any clear differences in

the mean age of the subjects with IM, EA or achlorhydria between IC relatives and controls (Table 6).

Comparison of anaplastic carcinoma (AC) relatives with their controls. Anaplastic carcinoma relatives showed a significantly higher prevalence of IM and a significantly higher mean score of body gastritis than their relatives (Table 5). In other respects no significant differences were found. The mean age of subjects with different parameters did not essentially differ from those of the controls either.

Comparison of DC relatives with IC relatives. Although the mean age of DC relatives was lower

TABLE 6 Mean Ages of Diffuse Carcinoma and Intestinal Carcinoma Relatives and Their Controls with Intestinal Metaplasia, Epithelial Atypia and Achlorhydria

Findings	Mean Age years \pm S D			
	Diffuse ca Relatives	Diffuse ca Controls	Intestinal ca Relatives	Intestinal ca Controls
Intestinal metaplasia	57.8 \pm 11.9	56.6 \pm 12.7	62.5 \pm 10.7	63.8 \pm 11.6
Epithelial atypia	49.3 \pm 19.5*	71.0 \pm 0.0	63.0 \pm 9.1	58.0 \pm 19.3
Achlorhydria	58.3 \pm 12.0	65.3 \pm 5.5	65.6 \pm 7.0	63.0 \pm 16.9

* Difference statistically significant ($p < 0.05$)

than IC relatives the mean gastritis score in antrum and body was higher in the former. The difference, however, was not statistically significant. On the other hand, below 50 years of age the mean gastritis score was in DC relatives 1.77 ± 1.69 and in IC relatives 1.70 ± 1.07 . This difference was statistically highly significant ($p < 0.001$). In addition the mean serum gastrin level was significantly higher in DC than in IC relatives. The prevalence of IM and EA was somewhat higher in DC relatives but the prevalence of achlorhydria was similar in both groups. The mean age of subjects with IM, EA and achlorhydria was significantly lower in DC relatives than in IC relatives (Table 6).

DISCUSSION

The present data disclosed significant differences between relatives of diffuse spreading gastric carcinoma (DC) and their controls while no such differences were seen with respect to intestinal and anaplastic types of gastric carcinoma.

In DC relatives the mean score of both antral and body gastritis was significantly higher than in their controls. The mean MAO was also significantly lower and the mean fasting serum gastrin level (SFG) significantly higher in DC relatives than in controls. Intrinsic factor antibodies were also more often seen in DC families than in controls. Thus there is in DC families an increased prevalence of signs characteristic of A type gastritis (Strickland & Mackay 1973) which according to Varis (1971) and Siurala *et al* (1977) is strongly genetically determined.

The comparison of IC relatives directly with DC relatives was handicapped by the 5 years higher mean age of the former group. However there was a tendency to a higher prevalence of atrophic gastritis IM and EA in DC relatives than in IC relatives. There was also a clear trend for these parameters to occur at a younger age in DC than in IC relatives. The results are in line with our earlier dynamic mathematical approaches which suggest that gastritis of the body mucosa is more severe and begins earlier in relatives of DC than IC (Kekki *et al* 1975).

Atrophic gastritis IM EA
of
(S
at

Nagata 1971 Sugano *et al* 1971 Jarvi & Lauren 1951 Fujita & Hattori 1976). The high prevalence of these signs and their occurrence at a younger age could explain the observed high gastric cancer risk

in first-degree relatives of DC patients (Lehtola 1978).

The increased death rate in gastric carcinoma in near relatives with diffuse type may indicate the participation of genetic factors in the pathogenesis of this disease. The hereditary nature of DC is indicated by the younger age of the patients and by the greater proportion of women with DC than with IC (Lauren 1965, Stemmermann & Brown 1974, Sipponen *et al* 1976). In addition Correa *et al* (1970, 1973, 1976) and Muñoz & Asvall (1971) found a higher than expected prevalence of blood group A among patients with DC. Moreover, these authors found some epidemiological differences between the two histological types which suggest a stronger effect of genetic factors in the pathogenesis of diffuse cancer type. The increased prevalence of severe atrophic body gastritis noted in this study could also be regarded as additional evidence for the importance of hereditary factors in the pathogenesis of DC. On the other hand lack of correlation between the various genetic markers and IC would emphasize the greater significance of environmental factors in the pathogenesis of this disease.

The Lauren's classification of gastric carcinomas into DC and IC is recognized by WHO but is not

c
t
of the cancer types which favour the classification of gastric carcinomas according to Lauren's principles.

The authors wish to express their thanks to the Finnish Cancer Foundation for financial support.

REFERENCES

- Correa P. Geographic pathology of cancer in Colombia. *Int Path* 11: 16-22, 1970.
- Correa P, Cuello C & Haenszel W. Pathogenese des Magenkarzinoms. *Epidemiologische Pathologie vorangehender Läsionen Leber Magen Darm* 6: 72-79, 1976.
- Correa P, Sasano N, Stemmermann G N & Haenszel W. Pathology of gastric carcinoma in Japanese populations. Comparison between Miyagi prefecture Japan and Hawaii. *J natl Cancer Inst* 51: 1449-1459, 1973.
- Fujita S & Hattori T. Cell proliferation, differentiation and migration in the gastric mucosa. A study on a background of carcinogenesis. 7th Int Symp of Princess Takamatsu Cancer Research Fund 1976 pp 21-34.
- Ihamaki T, Varis K & Siurala M. Morphological, functional and immunological state of the gastric mucosa in gastric carcinoma families.

TABLE 5 *Comparison of Anaplastic Carcinoma Relatives with Their Controls*

Findings	Anaplastic ca Relatives	Controls	Level of Significance
Body mucosa			
Mean gastritis score \pm S D	1 06 \pm 1 21	0 75 \pm 0 88	p < 0 05
Atrophic gastritis No	27	19	ns
Antral mucosa			
Mean gastritis score \pm S D	1 09 \pm 1 05	0 91 \pm 0 96	ns
Atrophic gastritis No	36	33	ns
Intestinal metaplasia No	26	13	p < 0 01
Epithelial atypia No	3	3	ns
Achlorhydria No	8	3	ns
Mean MAO mmol/hr \pm S D	20 3 \pm 15 3	24 1 \pm 14 1	ns
Serum gastrin > 100 pmol/l No	10	11	ns
Mean basal serum gastrin pmol/l \pm S D	81 2 \pm 176 9	48 8 \pm 47 2	ns
Parietal cell antibodies No	9	7	ns
Intrinsic factor antibodies No	0	1	ns
Total No. of cases	91	108	

cantly higher in DC relatives than in controls. The prevalence of epithelial atypia (EA) and achlorhydria was also higher in DC relatives but the difference was statistically insignificant. In addition intrinsic factor antibodies were found in 4% of DC relatives but in none of the controls. As seen from Table 6 there is a tendency to a lower mean age in DC relatives with EA and achlorhydria, the difference being significant only with respect to EA.

Comparison of intestinal type carcinoma (IC) relatives with their controls. Table 4 shows that IC relatives did not differ significantly from their relatives with respect to any of the parameters studied. Neither were there any clear differences in

the mean age of the subjects with IM, EA or achlorhydria between IC relatives and controls (Table 6).

Comparison of anaplastic carcinoma (AC) relatives with their controls. Anaplastic carcinoma relatives showed a significantly higher prevalence of IM and a significantly higher mean score of body gastritis than their relatives (Table 5). In other respects no significant differences were found. The mean age of subjects with different parameters did not essentially differ from those of the controls either.

Comparison of DC relatives with IC relatives. Although the mean age of DC relatives was lower

TABLE 6 *Mean Ages of Diffuse Carcinoma and Intestinal Carcinoma Relatives and Their Controls with Intestinal Metaplasia, Epithelial Atypia and Achlorhydria*

Findings	Mean Age years \pm S D			
	Diffuse ca Relatives	Diffuse ca Controls	Intestinal ca Relatives	Intestinal ca Controls
Intestinal metaplasia	57 8 \pm 11 9	56 6 \pm 12 7	62 5 \pm 10 7	63 8 \pm 11 6
Epithelial atypia	49 3 \pm 19 5*)	71 0 \pm 0 0	63 0 \pm 9 1	58 0 \pm 19 3
Achlorhydria	58 3 \pm 12 0	65 3 \pm 5 5	65 6 \pm 7 0	63 0 \pm 16 9

*) Difference statistically significant (p < 0 05)

PANCREATIC BETA-CELL TUMOURS STUDIED BY IMMUNOFLUORESCENCE AND ELECTRON MICROSCOPY

A Report of Four Cases and a Review of the Literature

OLE FRØKJÆR THOMSEN

University Institute of Pathology Kommunehospitalet Aarhus Denmark

Thomsen O F Pancreatic beta cell tumours studied by immunofluorescence and electron microscopy
A report of four cases and a review of the literature Acta path microbiol scand Sect. A 87 463-468 1979

Pancreatic beta cell tumours from four patients were studied by immunofluorescence for insulin and by electron microscopy. The literature of similar investigations is reviewed. The aim was to ascertain whether the presence of insulin or the morphology of secretory granules could be related to the severity of hypoglycaemia or to the clinical behaviour of the tumour. The results of investigating the four cases did not allow definite conclusions as regards this question. On the other hand perusal of previous publications on this subject indicated that (1) a positive immunofluorescence reaction for insulin in the tumour cells found in most adenomas but not convincingly in any carcinoma appears to spell a favourable prognosis (2) mature secretory granules seen in most adenomas but also in some carcinomas - do not yield sufficient evidence of a good prognosis (3) no association was demonstrated between the severity of hypoglycaemia and the maturity of secretory granules.

Key words: Pancreatic beta cell tumours immunofluorescence electron microscopy

O Frøkjær Thomsen Institute of Pathology Odense Hospital DK 5000 Odense

Accepted as submitted 31 v 79

Tumours originating from insulin producing beta-cells usually cause symptoms of hypoglycaemia of highly varying severity apparently unrelated to the size and histological appearance of the tumour or to its benign or malignant nature.

By immunofluorescence insulin has been demonstrated in some but far from all tumours. Ultrastructurally cytoplasmic secretory granules of varying morphology representing storage forms of insulin can be seen in the tumour cells.

Because of the characteristic clinical symptoms and signs beta-cell tumours are generally diagnosed by internists and radiologists. Therefore electron and immunofluorescence microscopy of beta-cell tumours is not often likely to be of diagnostic significance. But if immature and atypical secretory granules and a lack of immunohistological reactivity

for insulin could be correlated with particularly aggressive forms of beta-cell tumours these methods might be of prognostic value. The results of such studies on four patients are presented below with a review of the literature.

MATERIAL AND METHODS

Pancreatic tumour tissue removed at operation from four patients with a history of hypoglycaemic attacks was studied.

For immunofluorescence tissue specimens were fixed in Bouin's fluid.

For electron microscopy the tissue was fixed in 1% osmium tetroxide, dehydrated in graded ethanol and embedded in Vestopal. Sectioning was carried out on an LKB ultramicrotome.

- comparison with a random family sample Scand J Gastroent 1979 in press
- 6 Jarvi O & Lauren P On the role of heterotopias in intestinal epithelium in pathogenesis of gastric cancer Acta path microbiol scand 29 26-44 1951
 - 7 Kekki M Ihamakı T Sipponen P & Hovinen E Heterogeneity in susceptibility to chronic gastritis in relatives of gastric cancer patients with different histology of carcinoma Scand J Gastroent 10 737-745 1975
 - 8 Lauren P The two histological main types of gastric carcinoma diffuse and so called intestinal type carcinoma Acta path microbiol scand 64 31-49 1965
 - 9 Lehtola J Family study of gastric carcinoma with special reference to histological types Scand J Gastroent 13 Suppl 50 1978
 - 10 Macklin M T Inheritance of cancer of the stomach and large intestine in man J natl Cancer Inst 24 551-571 1960
 - 11 Ming S C Goldman J & Freiman D G Intestinal metaplasia and histogenesis of carcinoma in human stomach Light and electron microscopic study Cancer 20 1418-1429 1967
 - 12 Morson B C Carcinoma arising from areas of intestinal metaplasia in the gastric mucosa Br J Cancer 9 377-385 1955
 - 13 Mosbech J Pernicious anemia and cancer of the stomach Acta med scand 148 309-315 1954
 - 14 Munoz N & Asvall J Time trends of intestinal and diffuse types of gastric cancer in Norway Int J Cancer 8 144-157 1971
 - 15 Nagayo T Histological diagnosis of biopsied gastric mucosa with special reference to the borderline cases GANN Monogr Cancer Res 11 245-256 1971
 - 16 Sipponen P Ihamakı T Saukkonen M Kekki M & Siurala M Histological differentiation of gastric carcinomas and the relation of the different types to endoscopic and clinical parameters Acta et Comment Univ Tartuensis 385 25-29 1976
 - 17 Siurala M Isokoski M Varis K & Kekki M Prevalence of gastritis in a rural population Scand J Gastroent 3 211-223 1968
 - 18 Siurala M Lehtola J & Ihamakı T Atrophic gastritis and its sequelae Results of 19-23 years follow up examination Scand J Gastroent 9 441-446 1974
 - 19 Siurala M & Seppala A Atrophic gastritis as a possible precursor of gastric carcinoma and pernicious anemia Acta med scand 173 455-474 1960
 - 20 Siurala M Villako K Ihamakı T Kekki M Lehtola J Sipponen P & Varis K Atrophic gastritis Its genetic and dynamic behaviour and its relation to gastric carcinoma and pernicious anemia In Pathophysiology of Carcinogenesis in Digestive Organs E Farber et al (eds) Univ of Tokyo Press Tokyo/Park Press Baltimore pp 85-100 1977
 - 21 Sugano H Nakamura K & Takagi A An atypical epithelium of the stomach GANN Monogr Cancer Res 11 257-269 1971
 - 22 Stemmermann G N & Brown C A survival of intestinal and diffuse types of gastric carcinoma Cancer 33 1190-1195 1974
 - 23 Strickland R G & Mackay I R A reappraisal of the nature and significance of chronic gastritis Am J Dig Dis 18 426-440 1973
 - 24 Varis K A familial study of chronic gastritis Histological immunological and functional aspects Scand J Gastroent 6 Suppl 13 1971
 - 25 Videbaek A & Mosbech J The aetiology of gastric carcinoma elucidated by a study of 302 pedigrees Acta med scand 149 137-159 1956
 - 26 Woolf C M The incidence of cancer in the spouses of the stomach cancer patients Cancer 14 199-200 1961



Fig 2 Schematic illustration of the main types of secretory granules as seen in normal beta-cells. The granules are membrane bounded with a central core. Left: immature granules with a round fairly electron-lucent core and only a narrow space between core and membrane. Centre: granule of intermediate maturity with a round electron-dense core and a broad halo between core and membrane. Right: mature granule characterized by electron-dense angular cores often forming several facets. The same types of granules are seen in most beta-cell tumours in highly varying relative numbers.

tumours with a trabecular (cases 1, 2 and 3) and with a solid pattern (case 4). No cellular criteria of malignancy were evident, not even in case 1 in whom liver metastases were present.

A positive immunofluorescence reaction for insulin in the tumour cells present in cases 2 and 4 is illustrated in Fig 1. In case 1 in which the reaction was negative in tumour cells, a positive reaction for insulin was present in beta-cells of normal islets in the adjacent pancreatic tissue.

Electron microscopy revealed cytoplasmic secretory granules in all four tumours varying in

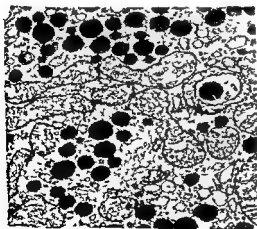


Fig 3 Cytoplasm of tumour cell from case 1. The secretory granules are numerous, uniform with a round electron-dense core and an inconspicuous membrane. These granules are atypical, probably immature. $\times 25,000$.

number from cell to cell. Therefore a definite estimation of their number in the tumours could not be made. Fig 2 schematically illustrates the ultrastructural appearance of secretory granules of varying maturity as seen in normal beta-cells. The same type of granules was found in three of the tumours, whereas one contained only atypical granules. The characteristic ultrastructural appearance of the specific granules is shown in Figs 3-5.

DISCUSSION

Insulin and mature secretory granules were demonstrated in the tumour tissue from the patient with the mildest symptoms of hypoglycaemia (case 4), whereas the patient with the most severe symptoms had a metastasizing tumour with atypical immature granules and no demonstrable insulin (case 1). According to the findings in the other two patients, however, a positive immunofluorescence reaction for insulin may be present in tumour tissue with immature granules and a negative reaction for insulin may occur in tumour tissue with mature granules.

In order to obtain more information on the prognostic value of the two methods applied to beta-cell tumours, the literature of such investigations was reviewed, surveyed in Table 2. The table includes all investigations using immunofluorescence as well as electron microscopy.

From Table 2 it is apparent that 18 of the 24 beta-cell adenomas (i.e. 3/4) gave a positive immunofluorescence reaction for insulin, while a convincing reaction was not found in any of the four carcinomas. Hence the presence of insulin in the tumour tissue, as assessed by the immunofluorescence test, appears to be a favourable prognostic sign.

Creutzfeldt *et al.* (4) studying the ultrastructure of

granules have also been found in four of eight carcinomas, so that the presence of mature secretory granules in a beta-cell tumour does not provide sufficient evidence of its benignity. Atypical granules have been found in both adenomas and carcinomas.

Only a few authors have specifically dealt with the morphology of secretory granules as related to the severity of hypoglycaemia. Goldenberg *et al.* (6) claimed that mild hypoglycaemia was associated with the presence of many and mature secretory granules, whereas Suruki & Matsuyama (14) did

TABLE 1 *Main Clinical Features and Results of Morphological Immunofluorescence (IF) and Electron Microscopic (EM) Examinations of the Four Patients*

Patients	Sex age	Duration of hypoglycaemia	Symptoms and signs	Size and location of tumour	Metastases	Predominant morphologic pattern	Insulin in tumour cells (IF)	Predominant types of secretory granules (EM)
Case 1	F 62	Several years increasing frequency and intensity	Daily fainting relieved by glucose intra venously	10 cm pancreatic head	Numerous in liver	Trabecular	Not present	Atypical immature
Case 2	F 40	One year increasing frequency and intensity	Dizziness confusion	1.2 cm pancreatic body	None	Trabecular	Present	Immature intermediate
Case 3	M 60	Six years increasing frequency and intensity	Weakness sweating spasms	1.5 cm pancreatic tail	None	Trabecular	Not present	Intermediate mature
Case 4	M 45	Two years a few attacks	Dizziness confusion tremor	0.8 cm pancreatic tail	None	Solid	Present	Intermediate mature

Ultrathin sections were mounted on copper grids with Formvar membranes and stained with uranyl acetate and lead citrate. The specimens were examined in a Jeol 100 B electron microscope.

The remaining tissue was fixed in 4% formalin and prepared for light microscopy.

RESULTS

The main findings in the four cases are presented in Table 1.

As in the study of Woodli & Hedinger (18) two principal histological patterns could be discerned

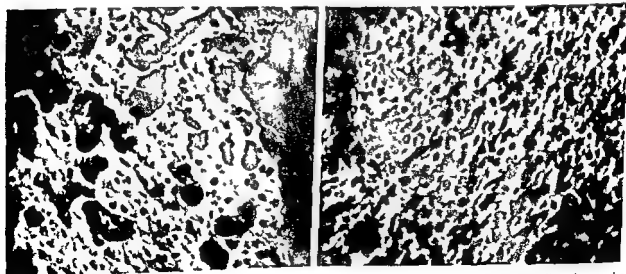


Fig. 1 Tumour tissue from case 2 (left) and case 4 (right). Fluorescence in the cytoplasm of tumour cells indicates the presence of insulin. Section stained for insulin $\times 300$.

Fig 4 Parts of tumour cells from case 2. The secretory granules are immature (long arrow) and intermediate (short arrow) and no mature forms are present $\times 15\ 000$

Fig 5 From the tumour of case 3. Numerous intermediate (short arrow) and mature granules (long arrows). Besides a few atypical forms (arrowhead). Similar intermediate and mature granules were seen in the tumour of case 4 $\times 15\ 000$

not find any correlation between the maturity of granules and the severity of hypoglycaemia. *Toker* (17) observed mature granules in a beta-cell carcinoma of a patient who had no clinical symptoms of hypoglycaemia at all.

A review of the investigations summarized in Table 2 leaves the impression that no simple

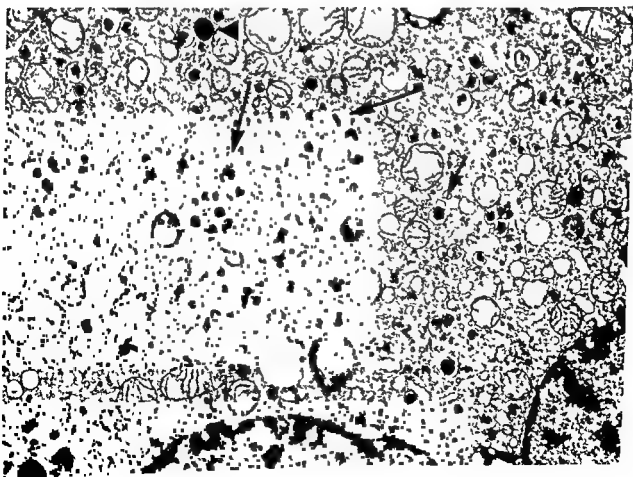
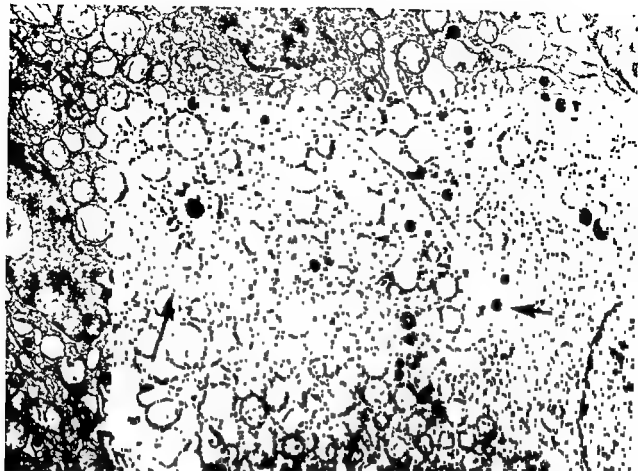
relationship exists between the morphology of secretory granules, the immunofluorescent reactivity of insulin and the nature of the tumour. Obviously combined morphological and functional studies of larger series are needed for further elucidation of these problems.

TABLE 2 Investigations of Beta Cell Adenomas (a) and Carcinomas (c) by Immunofluorescence Microscopy for Insulin and Electron Microscopy

Authors	Year	Tumour	No of tumours	Insulin demonstrated in tumour	Predominant types of secretory granules
Lacy & Williamson (9)	1960	a	2	in 2/2	Mature
Lazarus & Volk (10)	1962	a	1		Int. mat.
Bencosme et al. (3)	1963	a	1		Int. mat.
—	1963	a	1		No granules
Greider & Elliott (7)	1964	a	2		Int. mat.
—	1964	a	2		Atypical
Honjin et al. (8)	1965	a	1		Int. mat.
Georgsson & Wessel (5)	1967	c	1		Atypical
Toker (17)	1967	c	1		Mature
Mancini et al. (12)	1968	a	1	+	
Goldenberg et al. (6)	1969	a	1		Imm. int. mat.
—	1969	a	2		Imm. int.
—	1969	a	1		?
—	1969	c	1		Imm.
Misugi et al. (13)	1970	a	2		Int. mat.
Suzuki & Matsuyama (14)	1971	a	3		Imm. int. mat.
—	1971	a	2		Atypical
—	1971	c	3		Int. mat.
Thomsen (16)	1972	a	1	+	
Sveučelst et al. (14)	1973	a	28		
Woodruff & Hedinger (18)	1976	a	14	+ in 11/14	Mat. in most
—	1976	c	3	+ in 1/3*	Int. mat. (2 examined)
Arnall, Montreal et al. (2)	1977	a	3	+ in 3/3	Imm. (1 examined)
Le Charpenier et al. (11)	1977	a	8		Int. mat. (2 examined)
—	1977	a	1		Int. mat.
An & Kaye (1)	1978	a	1		Atypical
Thomsen (present study)	1979	a	1		Int. mat.
—	1979	a	2	+	Imm. int.
—	1979	c	1	+ in 1/2	Int. mat.
				—	Atypical

imm = immature
int = intermediate
mat = mature

* Described as "weak fluorescence in few cells" in one of the three cases.



A RETROSPECTIVE HISTOLOGICAL STUDY OF 669 CASES OF PRIMARY CUTANEOUS MALIGNANT MELANOMA IN CLINICAL STAGE I

7 *The Relative Prognostic Value of Various Clinical and Histological Features
The Result of a Stepwise Multiple Regression Analysis of 553 of These Cases*

TOVE EEG LARSEN and TOVE HELLIESEN GRUDE

Institute of Pathology University of Oslo Rikshospitalet and the Norwegian Radium Hospital Oslo
Norway

Larsen T E & Grude T II A retrospective histological study of 669 cases of primary cutaneous malignant melanoma in clinical stage I 7 The relative prognostic value of various clinical and histological features The result of a stepwise multiple regression analysis Acta path microbiol scand Sect A 87 469-477 1979

A part of the previously published series of primary cutaneous malignant melanomas in clinical stage I viz 553 cases registered 1955-67 has been the object of a stepwise multiple regression analysis The series includes 33 lentigo maligna melanomas 247 superficial spreading malignant melanomas 156 nodular malignant melanomas and 117 unclassifiable malignant melanomas The dependent variable is 5 year survival while totally 15 clinical and histological variables (among others excluding tumour type and features related to treatment) have been used as independent variables The results are presented for the total series as well as for that of superficial spreading malignant melanomas and nodular malignant melanomas separately When all the independent variables are considered 5 year survival is explained to a degree of 19.8-22% in the 3 series Level of invasion and to some degree also localization to the trunk have the greatest prognostic importance in all 3 series Tumour cell type solar elastosis and atypia are poor indicators of prognosis Age sex mitotic count and to some degree also lymphocyte

infiltration may also be of interest

Key words Malignant melanoma histological features prognosis regression analysis

T E Larsen Institute of Pathology Rikshospitalet Oslo 1 Norway

Received 1 vi 79 Accepted 24 vi 79

In a previous paper (Larsen & Grude 1978a) we presented a series of 669 primary cutaneous malignant melanomas (MM) in clinical stage I which had been registered by the Cancer Registry of Norway 1955-72 These MM were classified

tumour type as well as their age and sex and the localization of the tumour Other papers concerned the grading and classification of various histological features and their interrelationship judged by simple X^2 tests and based on the original tumour type

* Lentigo maligna melanoma (LMM) superficial spreading malignant melanoma (SSMM) nodular malignant melanoma (NMM) and unclassifiable malignant melanoma (UMM)

classified the survival of the patients according to

REFERENCES

- 1 *An T & Kaye G I* Amyloid formation in insulinoma Arch Pathol Lab Med 102 227-232 1978
- 2 *Arnal Monreal F M Goltzman D Knaack J Wang N & Huang S* Immunohistologic study of thyroidal medullary carcinoma and pancreatic insulinoma Cancer 40 1060-1070 1977
- 3 *Bencosme S A Allen R A & Latta H* Functioning pancreatic islet cell tumors studied electron microscopically Am J Path 42 1-22 1963
- 4 *Creutzfeldt W Arnold R Creutzfeldt C Deuticke U Frerichs H & Track N S* Biochemical and morphological investigation of 30 human insulinomas Correlation between the tumour content of insulin and pro insulin like components and the histological and ultrastructural appearance Diabetologia 9 217-231 1973
- 5 *Georgson G & Wessel W* Vergleichende elektron mikroskopische untersuchungen normaler menschlicher pankreasinseln und eines hormonellaktiven inselzellcarcinoms mit hyperinsulinismus Z Krebsforsch 69 70-86 1967
- 6 *Goldenberg I E Goldenberg N S & Benditt E P* Ultrastructural features of functioning alpha and beta cell tumors Cancer 24 236-247 1969
- 7 *Greider M H & Elliott D W* Electron microscopy of human pancreatic tumors of islet cell origin Amer J Path 44 663-678 1964
- 8 *Honjin R Takahashi A Maruyama H Mureno S & Hanyu T* Electron microscopy of a case of insulinoma J Electron Microsc 14 183-188 1965
- 9 *Lacy P E & Williamson J R* Electron microscopic and fluorescent antibody studies of islet cell adenomas Anat Rec 136 227-228 1960
- 10 *Lazarus S S & Volk B H* Histochemical and electron microscopic studies of a functioning insulinoma Lab Invest 11 1279-1294 1962
- 11 *Le Charpentier Y Leger L Chiche B Louvet A Dugue M A Moulle P Lemaigre G & Abelanet R* Insulinomes pancreatiques Etude en microscopie electronique 9 cas Nouv Presse Med 6 3713-3716 1977
- 12 *Mancini A M Costanzi G & Vecchi A* Studio istochimico e istocimmunologico di un insuloma ipoglicemizzante Bollettino delle Società Italiane di Patologia 10 1968
- 13 *Misugi K Howell S L Greider M H Lacy P E & Sorenson G D* The pancreatic beta-cell Demonstration with peroxidase labelled antibody technique Arch Path 89 97-102 1970
- 14 *Sasaki H & Matsuyama M* Ultrastructure of functioning beta cell tumors of the pancreatic islets Cancer 28 1302-1313 1971
- 15 *Thomsen O F* Staining of beta-cells in pancreatic islets by an indirect immunofluorescence method on bouin fixed paraffin embedded tissue Acta path microbiol scand Section A 79 497-500 1971
- 16 *Thomsen O F* Demonstration of insulin in an islet cell pancreatic adenoma using an immunofluorescent technique Acta path microbiol scand Section A 80 689-690 1972
- 17 *Toker C* Observations on the ultrastructure of a metastasizing beta cell islet tumor Diabetes 16 800-803 1967
- 18 *Woodith W & Hedinger C* Histologic characteristics of insulinomas and gastrinomas Value of argyrophilia metachromasia immunohistology and electron microscopy for the identification of gastrointestinal and pancreatic endocrine cells and their tumors Virchows Arch A Path Anat and Histol 371 331-350 1976

TABLE 2 *The Coding of the Various Grades and Types of the Explanatory Variables*

Explanatory variable	Coding
X ₁ Sex	1 ♂ 2 ♀
X ₂ Ulceration	1 = 0 and 2/3 of ? 2 = + and 1/3 of ?
X ₃ Vascular invasion	0 = 0 and 1/2 of ? 1 = + and 1/2 of ?
X ₄ Mitotic count	1 = + and 2/3 of ? 2 = ++ and 1/3 of ? 3 = +++
X ₅ Level of invasion	1 I 2 II 3 III 4 IV 5 V and all ?
X ₆ Lymphocyte infiltration	1 = + and all ? 2 = ++ 3 = +++
X ₇ Age	Age/10
X ₈ and X ₉ Pigmentation	X ₈ = 1 and X ₉ = 0 0 and + X ₈ = 0 and X ₉ = 1 ++ X ₈ = 0 and X ₉ = 0 +++
X ₁₀ and X ₁₁ Cell type	X ₁₀ = 1 and X ₁₁ = 0 epithelioid X ₁₀ = 0 and X ₁₁ = 1 spindle X ₁₀ = 0 and X ₁₁ = 0 mixed cellularity and all ?
X ₁₂ Atypia	1 = + and 1/3 of ? 2 = ++ and 2/3 of ? 3 = +++
X ₁₃ Solar elastosis	1 = 0 and 1/3 of ? 2 = ++ and 1/3 of ? 3 = +++ and 1/3 of ? 4 = +++
X ₁₄ and X ₁₅ Localization	X ₁₄ = 1 and X ₁₅ = 0 trunk X ₁₄ = 0 and X ₁₅ = 1 Foot X ₁₄ = 0 and X ₁₅ = 0 all other localizations
X ₁₆ Survival	0 = alive after 5 years 1 = dead before 5 years

frequency of the latter. At this randomization procedure we also paid attention to certain difficulties in the grading and classification of some of the variables (for further details see discussion).

As our grading of pigmentation does not refer to any homogeneously increased pigmentation

classification (Larsen & Grude 1978b and c 1979a) and on the re classification (Larsen & Grude 1979c) respectively

In this paper we present a stepwise multivariate regression analysis of part of these MM. The purpose has been to find out the relative prognostic value of the features which have been presented earlier

SERIES

The series includes 553 of the original 669 MM i.e. those which have been registered no later than 1967. There are 205 males and 348 females among whom 3 are under 10 years and 4 over 90 years of age. According to the re classification of tumour type mentioned above there are 33 (6.0 %) LMM, 247 (44.7 %) SMM, 156 (28.2 %) NMM and 117 (21.1 %) UMM. The observed 5 year survival rate is 84.9 % among the LMM, 79.4 % among the SMM, 59.0 % among the NMM and 77.8 % among the UMM. The overall observed 5 year survival rate is 73.6 %.

STATISTICAL METHODS

The stepwise multivariate regression analysis used in our study** is based on the assumption that $Y = b_0 + b_1X_1 + \dots + b_pX_p + \text{random variation}$ in which Y is the dependent variable, b_0, \dots, b_p are regression constants to be estimated by the series and X_1, \dots, X_p are the explanatory (independent) variables. The first explanatory variable selected to enter the analysis is the one which correlates best with the dependent variable. The next one is that which correlates best given the first one etc. The degree of explanation to the dependent variable may be expressed as the square of a multiple regression coefficient (R^2) at each step. R^2 increases with the

number of explanatory variables which enter the analysis.

In our study the dependent variable is 5 year survival. The explanatory variables are shown in Table 1. The symbols used to characterize grades and types are the same as those used in previous papers.

In the stepwise procedure we have included only explanatory variables which are partially significant at the 10 per cent level at each step according to a t test. The statistical P values have been computed without the formulation of any null hypothesis concerning the relative prognostic value of the explanatory variables *a priori*. The reason why a variable does not enter the analysis at any significant level may therefore be merely accidental due to a strong covariation with one or several of those variables which have already been chosen to enter the analysis. As such highly intercorrelated explanatory variables often make interpretation difficult a preliminary simple correlation analysis was done (not illustrated) with the object of studying the first order interrelationships between all the clinical and histological features reported earlier. In this analysis a correlation coefficient ≥ 0.40 was found in the correlation of cross sectional profile with tumour type, SMM and NMM, level of invasion, ulceration and mitotic count, of level of invasion with tumour type, NMM and finally of solar elastosis with localization to the face and age. It was decided to exclude cross sectional profile and tumour type as explanatory variables in the final regression analysis.

The series includes only very few cases in which every variable is classifiable. Cases with an indeterminate grade or type of a particular variable have therefore been incorporated among those with determinate sub classes of this variable (Table 2). This has been done by comparing the survival of the cases with the indeterminate sub class with that of those with determinate sub classes according to our previous findings (Larsen & Grude 1978b and c, Larsen & Grude 1979a and c). Further the indeterminate cases were assigned to the determinate ones more or less proportional to the relative

** The analysis was performed with an Univac 1110 computer at the Norwegian Computing Center, Oslo.

TABLE 1 The Frequency of the Various Subgroups of Each of the Explanatory Variables (n = 553)

X ₁ Sex	205 ♂ 348 ♀
X ₂ Ulceration	164 + 344 45 ?
X ₃ Vascular invasion	36 + 492 - 25 ?
X ₄ Mitotic count	308 + 106 + + 65 + + + 74 ?
X ₅ Level of invasion	3 level I 115 level II 198 level III 157 level IV 37 level V 43 level ?
X ₆ Lymphocyte infiltration	171 + 229 + + 125 + + + 28 ?
X ₇ Age	3 age 0-9 10 age 10-19 29 age 20-29 107 age 30-39 136 age 40-49 116 age 50-59 70 age 60-69 52 age 70-79 26 age 80-89 4 age 90-99
X ₈ and X ₉ Pigmentation	82 - 328 + 125 + + 18 + + +
X ₁₀ and X ₁₁ Cell type	177 epithelioid 40 spindle 295 mixed 41 ?
X ₁₂ Atypia	63 + 310 + + 67 + + + 113 ?
X ₁₃ Solar elastosis	295 - 129 + 87 + + 21 + + + 21 ?
X ₁₄ and X ₁₅ Localization	143 head 172 trunk 63 upper extremity 39 foot 131 lower extremity 5 other
X ₁₆ Survival	146 survived less than 5 years 407 survived 5 years or more

RESULTS

The Simple Correlation Analysis

The results of the simple correlation between 5 year survival and the explanatory variables are reported in this paper. The correlation coefficients and their significance values are illustrated as regards the total series of MM as well as the series of SMM and that of NMM* (Table 3). In addition the simple correlation between tumour type SMM and NMM and 1 year survival (n 539) is illustrated.

Deep level of invasion and ulceration are correlated significantly with short survival among all 3 series of MM. In the total series and that of SMM male sex, high mitotic count, low grade lymphocyte infiltration, high grade atypia and localization to the trunk are significantly correlated with poor prognosis while pigmentation grade ++ is similarly correlated with a good prognosis. In the total series of MM and in that of NMM vascular invasion and high age are correlated significantly with short survival. Finally localization to the foot is significantly correlated with poor prognosis among the SMM only and so is tumour type NMM with 1 year survival in the total series of MM.

The Multivariate Regression Analysis

Tables 4-6 illustrate the results of a stepwise multivariate regression analysis concerning the total

series the SMM series and the NMM series respectively. Multiple regression coefficients (R) as well as degree of explanation to 5 year survival (R^2) are given for each set of regression coefficients.

All these tables show that the first independent variable which has been selected to enter the analysis is level of invasion. When variables like age, sex, localization to the trunk, pigmentation grade ++, lymphocyte infiltration and ulceration are also evaluated as regards the total series survival is explained to a degree of 18.7% (Table 4). As regards the SMM series the additional evaluation of mitotic count as well as localization to the trunk and foot gives a degree of explanation of 15.9% (Table 5). Finally concerning the NMM series the degree of explanation to 5 year survival is 18.7% when age, vascular invasion and localization to the trunk are also considered (Table 6).

In the full regression model i.e. when all 15 variables are considered (not illustrated) survival is explained to a degree of 19.7% in the total series, 20.9% among the SMM and 22.0% among the NMM. As regards the total series of MM prognostic significance is maintained in the full regression model by level of invasion, age, localization to the trunk, sex and lymphocyte infiltration (in that order). Where only the SMM is concerned level of invasion and localization to the trunk are still of significant prognostic value in the full regression model while as regards the NMM only level of invasion and age have maintained their prognostic significance.

* The complete correlation tables are available from the author.

TABLE 5 Five year Survival (0-1 Dependent Variable) in Relation to Various Explanatory Variables. A forward Stepwise Regression Analysis Based on 247 Equally Weighted Points (SMM only)

Step No	Regression coeff (b) Sign (P)	b ₁ Level of invasion	b ₂ Mitotic count	b ₃ Local trunk	b ₄ Local foot	Multi corr coeff (R)	Degree of explan R ² (%)
1	b P	0.15 0.000				0.32	10.0
2	b P	0.12 0.000	0.12 0.007			0.36	12.7
3	b P	0.11 0.000	0.12 0.005	0.12 0.018		0.38	14.7
4	b P	0.11 0.000	0.11 0.013	0.14 0.006	0.17 0.062	0.40	15.9

TABLE 3 *The Relationship Between 5-year Observed Survival and the Various Explanatory Variables Simple Correlation Analysis Based on 553 (Total Series) 247 (SMM) and 156 (NMM) Cases*

Explanatory variable	Total series	Correlation coefficient	
		SMM	NMM
X ₁ Sex	-0.16***	-0.16*	-0.12
X ₂ Ulceration (0-+)	0.20***	0.19**	0.16*
X ₃ Vascular invasion (0-+)	0.14***	0.06	0.24**
X ₄ Mitotic count (+-+ + +)	0.20***	0.27***	0.09
X ₅ Level of invasion (I-V)	0.34***	0.32***	0.30***
X ₆ Lymphocyte infiltration (+-+ + +)	-0.16***	-0.16**	-0.11
X ₇ Age	0.18***	0.04	0.28***
X ₈ Pigmentation (0-+)	0.09*	0.03	0.07
X ₉ Pigmentation (+ +)	-0.13**	-0.16*	-0.02
X ₁₀ Cell type (epithelioid)	0.08	0.09	0.001
X ₁₁ Cell type (spindle)	-0.03	-0.04	-0.05
X ₁₂ Atypia (+-+ + +)	0.18***	0.15*	0.04
X ₁₃ Solar elastosis (0-+ + +)	0.02	-0.04	0.03
X ₁₄ Localization (trunk)	0.09*	0.14*	0.11
X ₁₅ Localization (foot)	0.08	0.17**	0.03
Tumour type (SMM)*	-0.08		
Tumour type (NMM)*	0.09*		

*P ≤ 0.05

**P ≤ 0.01

***P ≤ 0.001

*Only 1-year survival considered

TABLE 4 *Five-year Survival (0-1 Dependent Variable) in Relation to Various Explanatory Variables A Forward Stepwise Regression Analysis Based on 553 Equally Weighted Points (All Tumour Types Included)*

Step No	Regression coeff (b) Sign (P)	b ₁ Level of invasion	b ₂ Age	b ₃ Sex	b ₄ Local trunk	b ₅ Pigm + +	b ₆ Lymphoc infiltr	b ₇ Ulcer	Mult corr coeff (R)	Degree expl R ² (%)
1	b P	0.15 0.000							0.34	11.5
2	b P	0.15 0.000	0.05 0.000						0.38	14.2
3	b P	0.14 0.000	0.05 0.000	-0.13 0.000					0.40	16.2
4	b P	0.14 0.000	0.05 0.000	-0.11 0.004	0.09 0.018				0.41	17.1
5	b P	0.14 0.000	0.05 0.000	-0.11 0.004	0.10 0.011	-0.09 0.039			0.42	17.7
6	b P	0.13 0.000	0.05 0.000	-0.11 0.002	0.11 0.007	-0.08 0.049	-0.05 0.052		0.43	18.3
7	b P	0.11 0.000	0.05 0.000	-0.11 0.003	0.10 0.009	-0.08 0.057	-0.05 0.033	0.07 0.086	0.43	18.7

RESULTS

The Simple Correlation Analysis

The results of the simple correlation between 5 year survival and the explanatory variables are reported in this paper. The correlation coefficients and their significance values are illustrated as regards the total series of MM as well as the series of SMM and that of NMM* (Table 3). In addition the simple correlation between tumour type SMM and NMM and 1 year survival (n 539) is illustrated.

Deep level of invasion and ulceration are correlated significantly with short survival among all 3 series of MM. In the total series and that of SMM male sex, high mitotic count, low grade lymphocyte infiltration, high grade atypia and localization to the trunk are significantly correlated with poor prognosis, while pigmentation grade ++ is similarly correlated with a good prognosis. In the total series of MM and in that of NMM vascular invasion and high age are correlated significantly with short survival. Finally localization to the foot is significantly correlated with poor prognosis among the SMM only, and so is tumour type NMM with 1 year survival in the total series of MM.

The Multivariate Regression Analysis

Tables 4-6 illustrate the results of a stepwise multivariate regression analysis concerning the total

* The complete correlation tables are available from the author.

series the SMM series and the NMM series respectively. Multiple regression coefficients (R) as well as degree of explanation to 5 year survival (R^2) are given for each set of regression coefficients.

All these tables show that the first independent variable which has been selected to enter the analysis is level of invasion. When variables like age, sex, localization to the trunk, pigmentation grade ++, lymphocyte infiltration and ulceration are also evaluated as regards the total series survival is explained to a degree of 18.7% (Table 4). As regards the SMM series the additional evaluation of mitotic count as well as localization to the trunk and foot gives a degree of explanation of 15.9% (Table 5). Finally concerning the NMM series the degree of explanation to 5 year survival is 18.7% when age, vascular invasion and localization to the trunk are also considered (Table 6).

In the full regression model i.e. when all 15 variables are considered (not illustrated) survival is explained to a degree of 19.7% in the total series, 20.9% among the SMM and 22.0% among the NMM. As regards the total series of MM prognostic significance is maintained in the full regression model by level of invasion, age, localization to the trunk, sex and lymphocyte infiltration (in that order). Where only the SMM is concerned level of invasion and localization to the trunk are still of significant prognostic value in the full regression model, while as regards the NMM only level of invasion and age have maintained their prognostic significance.

TABLE 5 Five year Survival (0-1 Dependent Variable) in Relation to Various Explanatory Variables. A forward Stepwise Regression Analysis Based on 247 Equally Weighted Points (SMM only)

Step No	Regression coeff (b) Sign (P)	b ₁ Level of invasion	b ₂ Mitotic count	b ₃ Local trunk	b ₄ Local foot	Mult corr coeff (R)	Degree of explan R ² (%)
1	b P	0.15 0.000				0.32	10.0
2	b P	0.12 0.000	0.12 0.007			0.36	12.7
3	b P	0.11 0.000	0.12 0.005	0.12 0.018		0.38	14.7
4	b P	0.11 0.000	0.11 0.013	0.14 0.006	0.17 0.062	0.40	15.9

TABLE 6 *Five-year Survival (0-1 Dependent Variable) in Relation to Various Explanatory Variables A forward Stepwise Analysis Based on 156 Equally Weighted Points (NMM only)*

Step No	Regression coeff (b) Sign (P)	b ₁ Level of invasion	b ₂ Age	b ₃ Vascular invasion	b ₄ Local trunk	Multiple correl coeff (R)	Degree of explan R ² (%)
1	b P	0.19 0.000				0.30	8.9
2	b P	0.16 0.001	0.06 0.004			0.37	13.6
3	b P	0.13 0.008	0.06 0.006	0.23 0.033		0.40	16.1
4	b P	0.14 0.006	0.06 0.003	0.24 0.027	0.17 0.032	0.43	18.7

DISCUSSION

We tried previously deliberately to keep the determinate grades and types of the various histological features which we have studied as well defined and pure as possible. In the process of making a multivariate regression analysis we were forced to incorporate cases with indeterminate sub classes among those with determinate ones. This has been done to the best of our ability by paying attention to the relative prognostic value of the various grades and types combined with a randomisation procedure, as mentioned under Statistical Methods.

Deviation from these two main principles is due to features impairing the grading or classification of some of the variables, e.g. high grade pigmentation interfering with the grading of mitotic count and atypia, shrinkage artefacts disturbing the judgment of tumour cell type as well as that of vascular invasion, lack of surrounding stroma interfering with the grading of level of invasion, lymphocyte infiltration as well as solar elastosis.

The number of cases showing an indeterminate grade or type of some variable is usually not very large (ranging mainly between 21 and 45 cases, Table 1), except for 113 cases with indeterminate atypia and 74 cases with indeterminate mitotic count. The randomisation procedures used for the incorporation of these cases are disputable. We are therefore bound to admit that these procedures may have influenced the result of the multivariate regression analysis in an unpredictable way. This as well as the lack of any formulation of a null

degree of caution necessary in interpreting the results.

The Relative Prognostic Value of the Explanatory Variables

Level of invasion was chosen as the first variable to enter the multivariate regression of all three series of MM because of the strong correlation with 5-year survival (Table 3). Breslow (1975) prefers tumour thickness as a measure of the tumour load. In the multivariate analyses of Malec-Olsson (1978) and Eldh *et al.* (1978) tumour thickness had greater prognostic significance than level of invasion. We have however not measured tumour thickness in our study. We have claimed earlier that level of invasion is of greater importance to survival than tumour associated lymphocyte infiltration (Larsen & Grude 1978 c). This is in agreement with the findings in the present multivariate analysis. We have also shown previously that level of invasion has greater prognostic value than tumour type (Larsen & Grude 1979 a) in agreement with Hermanek *et al.* (1976).

Localization to the trunk is the only other variable which enters the regression analysis of all three series of MM. In the NMM series this explanatory variable is however of relatively low prognostic significance. The relatively poor prognosis of our MM with this localization seems to be independent of the malignant properties of the tumour. Localization to the trunk is not significantly correlated with unfavourable features like deep level of invasion, high mitotic count and ulceration in our simple correlation analysis. There are also more SVM (51.7%) than NMM (28.5%) with this localization in our study. This is in agreement with the findings

of Eldh *et al* (1978) They suggest the possible importance of certain anatomical characteristics concerning vascularization This may well be so even if localization to the trunk is not significantly correlated to vascular invasion among any of our three groups of MM Vascular invasion is one of the most difficult histological features to judge It may as easily be overlooked as overdiagnosed and it was found in only 36 cases of the total series

Age has prognostic significance in the analysis of the total series and the NMM series but not at all in the SMM series Malec-Olovson (1978) made the same observation in their regression analysis of a series of NMM In our preliminary correlation analysis tumour type SMM is significantly correlated to young age This may contribute to the lack of any prognostic value of age in our SMM group There is no such trend in the NMM group

Sex has a significant prognostic value only in the total series of MM in which male sex is correlated with a poor prognosis In the preliminary correlation analysis male sex is correlated significantly with NMM and female sex almost significantly with SMM Further LMM is significantly related to female sex in our previous χ^2 test This relatively strong correlation of sex with tumour type may be a reason for the lack of any prognostic value of sex at one particular tumour type

At a certain point in the series

mitotic count in our previous χ^2 test and in our preliminary correlation analysis respectively while NMM is correlated with high mitotic count Further a high mitotic count is correlated significantly with deep level of invasion in the total series and the SMM series but not in the NMM series We have no explanation for why mitotic count has a different prognostic significance in the various series of MM except that it is accidentally due to intercorrelations like these In a previous paper (Larsen & Grude 1978 b) we reported that mitotic count seemed to be of greater importance to survival than pigmentation This is in agreement with the result of the multivariate analysis of the SMM series Pigmentation enters the regression analysis of the total series but at a lower level of significance than mitotic count in the SMM series

Lymphocyte infiltration pigmentation and ulceration are of some (relatively low) prognostic value only in the total series of MM while localization to the foot enters the multivariate analysis of the SMM series only (not significant) and vascular invasion that of the NMM series only (only slightly significant) The sporadic entrance of these features in the analysis may be merely accidental too

Lymphocyte infiltration is the only one among these explanatory variables which has maintained a slightly significant prognostic value ($P = 0.025$) in the full regression model Further this variable seems to be of even greater importance to 1 year survival in the preliminary analysis ($P = 0.002$ in the full regression model) Our previous finding that lymphocyte infiltration has less prognostic importance than level of invasion in our total series of MM seems to be also true in the final multivariate analysis as mentioned above Eldh *et al* (1978) and Malec-Olovson (1978) did not find any prognostic significance of this variable in their multivariate analysis Such discrepancies may be due to variations in the series which have been studied probably first of all as regards frequency and classification of the various tumour types and levels of invasion

Atypia does not enter the multivariate analyses at all This is in disagreement with our previous impressions (Larsen & Grude 1978 b) and may be accidental e.g. owing to a significant correlation of this variable with level of invasion and mitotic count Further neither tumour cell type nor solar elastosis enters any of the multivariate analyses This is however in good agreement with our previous findings (Larsen & Grude 1978 b Larsen & Grude 1979 c)

In the full regression model all our explanatory variables together explain only 20% of the 5 year survival as regards the total series of MM and 22% as regards the NMM series In the regression analysis of Malec-Olovson (1978) concerning NMM clinical features like stage tumour free margin and lymph node dissection had an explanatory value of 24% All our patients are in clinical stage I i.e. registered without known metastases We know however nothing about the tumour free margin of each specimen or whether lymph node dissection has been done or not

As regards our exclusion of tumour type as explanatory variable Eldh *et al* (1978) found in their multivariate analysis that tumour type had no prognostic importance Further tumour type did not enter our own preliminary regression analysis using 1 year survival as dependent variable Finally we have previously shown (Larsen & Grude 1979 a) that tumour type has less prognostic importance than level of invasion which is also in agreement with Hermanek *et al* (1976)

Guidelines for treatment of MM

Various kinds of »prognostic score sheet« have been recommended including clinical as well as histological features (Cochran 1968 Hardmeier 1970) Recently a »prognostic index« has been

proposed by *Schmoekel & Braun-Falco* (1978) based on tumour thickness and mitotic count. This should be a better guide for treatment than tumour thickness alone (*Breslow* (1975) or combined with level of invasion as recommended by *Wanebo et al* (1975) and also chosen by *Eldh et al* (1978). The guidelines for biopsy and surgical treatment of MM proposed by the American Academy of Dermatology (*Sober et al* 1976) are based on tumour type and level of invasion.

We find that the present results of our multivariate analyses are not suitable for making any »prognostic score sheet«. Neither have we tried to make any »prognostic index«. These ought to be based on persistent observations when several multivariate studies are compared in order to avoid methodological artefacts of a single study. At the moment we will only point to the significant importance of the tumour mass, whether measured by level of invasion or tumour thickness, and of localization found in our study as well as by *Eldh et al* (1978). The significant prognostic importance of mitotic count in the latter study and to some degree in our series of SMM may further support the prognostic index of *Schmoekel & Braun-Falco* (1978).

Tumour type had no prognostic significance to 1-year survival in our preliminary multivariate study and neither to 5-year survival in that of *Eldh et al* (1978). Due to the significant correlation of tumour type to most of the clinical and histological variables in the present study and due to the unsolved problems concerning histogenesis (*Mishima & Matsunaka* 1973, *Paul & Illig* 1976) the registration of tumour type may still be of practical interest to prognosis (see Fig. 1, *Larsen & Grude* 1976 b) as well as of importance to research.

Clinicians recognize variables like sex and age of the patient as well as localization, cross sectional profile, diameter and ulceration of the tumour. We recommend that the pathologists give information to the clinicians at least as regards tumour type and a measure of the tumour mass either by level of invasion or tumour thickness. Information about mitotic count and tumour-associated lymphocyte infiltration may also be of interest.

CONCLUSION

- 1) Level of invasion and to some degree also localization to the trunk have significant importance in the 5-year survival of patients with malignant melanoma whatever tumour type.
- 2) The prognostic significance of localization to the trunk seems not to be related to the malignant properties of the tumour.
- 3) The sporadic instead of general entrance of other

variables in the multivariate analyses of the total series of melanomas, the series of superficial spreading malignant melanomas or that of nodular malignant melanomas, is difficult to interpret. It may be merely accidental owing to the limitations of the statistical method which has been used. Among these variables, age, sex and to some degree also mitotic count and lymphocyte infiltration show varying levels of significance as regards the prognostic value.

- 4) Tumour cell type, solar elastosis and atypia are poor indicators of prognosis in our study. This is probably generally true as regards the first two variables, but may be accidental as regards the last one.
- 5) When all 15 histological and clinical variables are considered, the 5-year survival is explained to a degree of 19.8%–22%.
- 6) We recommend that the pathologist gives the clinician information at least about the tumour type and some measure of the tumour mass as a guide for treatment. Information about mitotic count and tumour-associated lymphocyte infiltration may also be of interest.

We want to thank Actuary *Ingar Holme*, Life Insurance Companies Institute for Medical Statistics, Oslo City Hospital, for valuable help and advice.

REFERENCES

- Breslow A*: Tumour thickness, level of invasion and node dissection in stage I cutaneous melanoma. *Ann Surg* 182: 572–575, 1975.
- Clark W H*: A classification of malignant melanoma in man correlated with histogenesis and biologic behavior. In *Montagna W* (Ed): *Advances in biology of the skin. The pigmented system*, 1 ed, vol. 8. Pergamon Press, Oxford, 1967, p. 621–647.
- Clark W H*, *From L*, *Bernardino E A* & *Mohr V C*: The histogenesis and biologic behaviour of primary human malignant melanomas of the skin. *Cancer Research* 29: 705–726, 1969.
- Cochran A J*: Method of assessing prognosis in patients with malignant melanoma. *Lancet* 2: 1062–1064, 1968.
- Eldh J*, *Boernd B* & *Peterson L E*: Prognostic factors in cutaneous malignant melanoma in stage I. A clinical, morphological and multivariate analysis. *Scand J Plast Reconstr Surg* 12: 243–255, 1978.
- Hardmeier T*: Das maligne Melanom: histologische Befunde und deren Bedeutung für die Prognosestellung. *Schweiz med Wschr* 100: 967–971, 1970.
- Hermanek P*, *Hornstein O P*, *Tonak J* & *Weidner F*: Malignes Melanom: Invasionstiefe und Melanontyp. *Beiträge Pathol* 157: 269–282, 1976.
- Larsen T E* & *Grude T H*: A retrospective histological study of 669 cases of primary cutaneous malignant

- melanoma in clinical stage I 1 Histological classification sex and age of the patients localization of tumour and prognosis *Acta Path Microbiol Scand Sect. A* 86 437-450 1978
- Larsen T E & Grude T H* A retrospective histological study of 669 cases of primary cutaneous malignant melanoma in clinical stage I 2 The relation of cell type pigmentation atypia and mitotic count to histological type and prognosis *Acta Path Microbiol Scand Sect. A* 86 513-522 1978
- Larsen T E & Grude T H* A retrospective histological study of 669 cases of primary cutaneous malignant melanoma in clinical stage I 3 The relation between the tumour associated lymphocyte infiltration and age and sex tumour cell type pigmentation cellular atypia mitotic count depth of invasion ulceration tumour type and prognosis *Acta Path Microbiol Scand Sect. A* 86 523-530 1978
- Larsen T E & Grude T H* A retrospective histological study of 669 cases of primary cutaneous malignant melanoma in clinical stage I 4 The relation of cross sectional profile level of invasion ulceration and vascular invasion to tumour type and prognosis *Acta Path Microbiol Scand Sect. A* 87 131-138 1979
- Larsen T E & Grude T H* A retrospective histological study of 669 cases of primary cutaneous malignant melanoma in clinical stage I 5 The consequences of a reclassification of the original group of lentigo maligna melanomas *Acta Path Microbiol Scand Sect. A* 87 255-260 1979
- Larsen T E & Grude T H* A retrospective histological study of 669 cases of primary cutaneous malignant melanoma in clinical stage I 6 The relation of dermal solar elastosis to sex age and survival of the patient and to localization histological type and level of invasion of the tumour *Acta Path Microbiol Scand Sect. A* 87 361-366 1979
- Malec Olofsson E* Malignant melanoma of the skin in Sweden Epidemiological and clinic histopathological study (A thesis) Stockholm 1978
- Mishima Y & Matsunaka M* Macromolecular pathology of pagetoid melanoma *Pigment Cell* 1 292-299 1973
- Paul E & Illig L* Melanin producing dendritic cells and histogenesis of malignant melanoma *Arch Derm Res* 257 163-177 1976
- Sober A J Fitzpatrick T B Mihm M C & Clark W H* Primary cutaneous malignant melanomas Recognition and management Guideline II An audio visual course in clinical dermatology by the American Academy of Dermatology 1976
- Wanebo H J Woodruff J & Forner J G* Malignant melanoma of the extremities A clinicopathologic study using levels of invasion (microstage) *Cancer* 35 666-676 1975

proposed by *Schmoeckel & Braun Falco* (1978) based on tumour thickness and mitotic count. This should be a better guide for treatment than tumour thickness alone (*Breslow* (1975) or combined with level of invasion as recommended by *Wanebo et al* (1975) and also chosen by *Eldh et al* (1978). The guidelines for biopsy and surgical treatment of MM proposed by the American Academy of Dermatology (*Sober et al* 1976) are based on tumour type and level of invasion.

We find that the present results of our multivariate analyses are not suitable for making any 'prognostic score sheet'. Neither have we tried to make any 'prognostic index'. These ought to be based on persistent observations when several multivariate studies are compared in order to avoid methodological artefacts of a single study. At the moment we will only point to the significant importance of the tumour mass whether measured by level of invasion or tumour thickness and of localization found in our study as well as by *Eldh et al* (1978). The significant prognostic importance of mitotic count in the latter study and to some degree in our series of SMM may further support the prognostic index of *Schmoeckel & Braun Falco* (1978).

Tumour type had no prognostic significance to 1 year survival in our preliminary multivariate study and neither to 5 year survival in that of *Eldh et al* (1978). Due to the significant correlation of tumour type to most of the clinical and histological variables in the present study and due to the unsolved problems concerning histogenesis (*Mishima & Matsunaka* 1973; *Paul & Illig* 1976) the registration of tumour type may still be of practical interest to prognosis (see Fig. 1; *Larsen & Grude* 1976 b) as well as of importance to research.

Clinicians recognize variables like sex and age of the patient as well as localization, cross sectional profile, diameter and ulceration of the tumour. We recommend that the pathologists give information to the clinicians at least as regards tumour type and a measure of the tumour mass either by level of invasion or tumour thickness. Information about mitotic count and tumour associated lymphocyte infiltration may also be of interest.

CONCLUSION

- 1) Level of invasion and to some degree also localization to the trunk have significant importance in the 5 year survival of patients with malignant melanoma whatever tumour type.
- 2) The prognostic significance of localization to the trunk seems not to be related to the malignant properties of the tumour.
- 3) The sporadic instead of general entrance of other

variables in the multivariate analyses of the total series of melanomas, the series of superficial spreading malignant melanomas or that of nodular malignant melanomas is difficult to interpret. It may be merely accidental owing to the limitations of the statistical method which has been used. Among these variables age, sex and to some degree also mitotic count and lymphocyte infiltration show varying levels of significance as regards the prognostic value.

- 4) Tumour cell type, solar elastosis and atypia are poor indicators of prognosis in our study. This is probably generally true as regards the first two variables but may be accidental as regards the last one.
- 5) When all 15 histological and clinical variables are considered the 5 year survival is explained to a degree of 19.8%–22%.
- 6) We recommend that the pathologist gives the clinician information at least about the tumour type and some measure of the tumour mass as a guide for treatment. Information about mitotic count and tumour associated lymphocyte infiltration may also be of interest.

We want to thank Actuary *Ingar Holme*, Life Insurance Companies Institute for Medical Statistics, Oslo City Hospital, for valuable help and advice.

REFERENCES

- Breslow A*. Tumour thickness, level of invasion and node dissection in stage I cutaneous melanoma. *Ann Surg* 182: 572–575, 1975.
- Clark W H*. A classification of malignant melanoma in man correlated with histogenesis and biologic behavior. In *Montagna W* (Ed) *Advances in biology of the skin. The pigmented system* 1 ed, vol. 8. Pergamon Press, Oxford, 1967, p. 621–647.
- Clark W H*, *From L*, *Bernardino E A* & *Mhm W C*. The histogenesis and biologic behaviour of primary human malignant melanomas of the skin. *Cancer Research* 29: 705–726, 1969.
- Cochran A J*. Method of assessing prognosis in patients with malignant melanoma. *Lancet* 2: 1062–1064, 1968.
- Eldh J*, *Boeryd B* & *Peterson L E*. Prognostic factors in cutaneous malignant melanoma in stage I. A clinical, morphological and multivariate analysis. *Scand J Plast Reconstr Surg* 12: 243–255, 1978.
- Hardmeier T*. Das maligne Melanom: histologische Befunde und deren Bedeutung für die Prognosestellung. *Schweiz med Wschr* 100: 967–971, 1970.
- Hermanek P*, *Hornstein O P*, *Tonak J* & *Wendner F*. Malignes Melanom: Invasionsstiefe und Melanomtyp. *Beiträge Pathol* 157: 269–282, 1976.
- Larsen T E* & *Grude T H*. A retrospective histological study of 669 cases of primary cutaneous malignant

ACTA
PATHOLOGICA
ET MICROBIOLOGICA
SCANDINAVICA

INDEX
VOL. 87 A

ETA

THOLOGICA

MICROBIOLOGICA

ANDINAVICA

INDEX

VOL 87 A

ACTA PATHOLOGICA ET MICROBIOLOGICA SCANDINAVICA

Section **A** PATHOLOGY

EDITORIAL BOARD

STEEN OLSEN DENMARK
J RAPOLA FINLAND
O BJARNASON ICELAND
E ARNESEN NORWAY
J L E ERICSSON SWEDEN

EDITOR IN CHIEF

J CHR SIIM

ADVISORY BOARD

J RYGAARD DENMARK
J VISFELDT DENMARK
T NEVALAINEN FINLAND
L TEPPU FINLAND
G GEORGSSON ICELAND
J HALLGRÍMSSON ICELAND
T HOVIG NORWAY
O D LÆRUM NORWAY
T BERGE SWEDEN
K NILSSON SWEDEN

VOL 87 A FASC 1-6 1979

MUNKSGAARD COPENHAGEN

Published by the
Scandinavian Societies for Microbiology and Pathology



Acta Pathologica
et Microbiologica
Scandinavica
1979

All rights reserved

Reproduction in any form
including microfilm, without written permission
of the Editor, is prohibited

Distributed by Munksgaard
International Booksellers and Publishers, Ltd
35 Norre Sogade, DK-1370 Copenhagen K Denmark

Printed by
bording grafik a/s
Copenhagen

INDEX

VOL. 87 A FASC 1-6 1979

<i>Aabo Kristian</i>	165	<i>Elling Folmer</i>	237
<i>Abo Kristian</i>	173	<i>Elling Folmer</i>	387
<i>Akerstrom Goran</i>	91	<i>Ericsson J L E</i>	19
<i>Aasen Ansgar O</i>	335	<i>Faarup Poul</i>	211
<i>Adolfsson Jan</i>	15	<i>Fabricius Bjerre N</i>	139
<i>Andersson Arne</i>	285	<i>Fenger Claus</i>	379
<i>Angervall L</i>	437	<i>Forsberg John Gunnar</i>	151
<i>Arentz P W</i>	63	<i>Forsby N</i>	19
<i>Arjffmann E</i>	143	<i>Fox C H</i>	63
<i>Arro E</i>	393	<i>Fredriksson B-A</i>	29
<i>Bahnsen M</i>	139	<i>Garbarsch C</i>	367
<i>Baunsgaard Philip</i>	51	<i>Græm N</i>	375
<i>Beck Eva I</i>	193	<i>Græm N</i>	401
<i>Beyer Boon M E</i>	63	<i>Grimelius Lars</i>	91
<i>Bing Jens</i>	211	<i>Grude Tove Helliesen</i>	131
<i>Blomquist E</i>	393	<i>Grude Tove Helliesen</i>	255
<i>Boiesen P T</i>	139	<i>Grude Tove Helliesen</i>	361
<i>Bondjers G</i>	201	<i>Grude Tove Helliesen</i>	469
<i>Boquist L</i>	157	<i>Hagerstrand I</i>	223
<i>Breustein Liv Stray</i>	151	<i>Hagen C</i>	139
<i>Brekkan Asmundur</i>	403	<i>Hagmar Bjorn</i>	97
<i>Briand Per</i>	427	<i>Hagstrom S</i>	157
<i>Bruaset Ingolv</i>	185	<i>Hainau Bo</i>	59
<i>Brun Claus</i>	321	<i>Hallberg Anders</i>	285
<i>Brunk U T</i>	19	<i>Hallgrimsson Jonas</i>	403
<i>Brunk U T</i>	29	<i>Hansen Heine H</i>	59
<i>Brunk U T</i>	393	<i>Hansen Knud Bendix</i>	165
<i>Bylock A</i>	201	<i>Hansen Knud Bendix</i>	173
<i>Carlsson Sture</i>	15	<i>Hansen O Hart</i>	217
<i>Chemnitz J</i>	265	<i>Hansson H-A</i>	201
<i>Chemnitz J</i>	275	<i>Haraldsson Stefan</i>	403
<i>Christensen B Collatz</i>	265	<i>Hellerstrom Claes</i>	285
<i>Christensen B Collatz</i>	275	<i>Helweg Larsen K</i>	375
<i>Christensen Hans Ewald</i>	307	<i>Helweg Larsen K</i>	401
<i>Christensen N</i>	261	<i>Hirsch Fred R</i>	59
<i>Christoffersen P</i>	45	<i>Hjorne N</i>	143
<i>Christoffersen P</i>	367	<i>Højgaard Knud</i>	347
<i>Clausen Per P</i>	347	<i>Holund B</i>	367
<i>Collan Y</i>	71	<i>Hultquist Gosta</i>	285
<i>Collins V P</i>	19	<i>Ihamaki Timo</i>	457
<i>Collins V P</i>	29	<i>Jacobsen Sten</i>	353
<i>Cornelisse C J</i>	63	<i>Jansson I</i>	201
<i>Daehnfeldt Johan L</i>	427	<i>Jansson Leif</i>	285
<i>Eckersberg Thomas</i>	185	<i>Jørgensen K</i>	401
<i>Ekelund Peter</i>	179	<i>Johansen Aa</i>	217

<i>Johansson Henry</i>	91	<i>Petersen P</i>	45
<i>Johansson S</i>	179	<i>Rajs Jovan</i>	289
<i>Johansson S</i>	437	<i>Rasmussen B Bruun</i>	261
<i>Junker P</i>	367	<i>Reintoft Ingermarie</i>	447
<i>Karjalainen H E</i>	245	<i>Reinamo J J</i>	451
<i>Kiær Henrik W</i>	353	<i>Reinamo S</i>	451
<i>Kiær William W</i>	353	<i>Ryd Walter</i>	97
<i>Kim C M</i>	265	<i>Save Soderbergh J</i>	109
<i>Kim C M</i>	275	<i>Save Soderbergh J</i>	437
<i>Kindblom L G</i>	109	<i>Salmi A</i>	245
<i>Kindblom L G</i>	437	<i>Sanchez German C</i>	51
<i>Klockars M</i>	451	<i>Schaberg A</i>	63
<i>Ladefoged Christian</i>	307	<i>Schreiner Berit</i>	79
<i>Lahdevirta J</i>	71	<i>Sigurjonsson Sigurdur V</i>	403
<i>Larsen J K</i>	217	<i>Sipponen Pentti</i>	451
<i>Larsen Svend</i>	313	<i>Sipponen Pentti</i>	457
<i>Larsen Svend</i>	321	<i>Skakkebæk Niels E</i>	87
<i>Larsen Tove Eeg</i>	131	<i>Sørensen Harry K</i>	307
<i>Larsen Tove Eeg</i>	255	<i>Svendsen Einar</i>	123
<i>Larsen Tove Eeg</i>	361	<i>Svendsen L B</i>	217
<i>Larsen Tove Eeg</i>	469	<i>Tallqvist Gustav</i>	411
<i>Laursen A M</i>	223	<i>Teglbjærg Peter Stubbe</i>	307
<i>Lehto V P</i>	299	<i>Thommesen Niels</i>	347
<i>Linder E</i>	299	<i>Thomsen Ole Frøkjær</i>	463
<i>Lindholm J</i>	139	<i>Thomsen Per</i>	421
<i>Linell Folke</i>	353	<i>Thorpe Susan M</i>	427
<i>Ljungqvist Arne</i>	15	<i>Tkoc I</i>	265
<i>Lorenzen I</i>	367	<i>Tkocz I</i>	275
<i>Lund C</i>	401	<i>Törnroth Tom</i>	411
<i>Lundborg C J</i>	51	<i>Törnling Goran</i>	15
<i>Lundborg C J</i>	223	<i>Unge Gunnar</i>	15
<i>Manttyjärvi R A</i>	245	<i>Vanntinen Tuomo</i>	411
<i>Magnusson Bjarki</i>	37	<i>van der Voorn denHollander M J A</i>	63
<i>McKnight Charles K</i>	37	<i>Virtanen I</i>	299
<i>Moe H</i>	1	<i>Vyberg Mogens</i>	421
<i>Myhre Jensen Olaf</i>	165	<i>Westermarck B</i>	19
<i>Nilsson Goran</i>	11	<i>Westermarck B</i>	29
<i>Nørgaard Pedersen B</i>	223	<i>Westermarck B</i>	393
<i>Nørredam Kai</i>	227	<i>Wie Henrik</i>	185
<i>Nordby Grete</i>	79	<i>Wie Henrik</i>	193
<i>Nordstoga Knut</i>	335		
<i>Pasternack Amos</i>	411		
<i>Pertoft Håkan</i>	91		

A See Ae Æ See Ae Ö See Oe
 Ø See Oe Å See Aa

Alpha fetoprotein infantile vaginal tumour endo- dermal sinus tumour	223	Embryo cell lines rat transformation karyoty ping oncogenic viruses BK virus	245
Alpha 1 antitrypsin PAS positive non glycoemic globules forensic pathology	447	Endodermal sinus tumour infantile vaginal tu mour alpha fetoprotein	223
Ameloblasts vinblastine cell death ultrastructure	1	Endothelial cell injury aorta cholesterol rabbit	123
4-aminopyrazolopyrimidine, hepatocytes lipopro teins ultrastructure	79	Endothelium experimental arteriosclerosis vital staining permeability TEM neointima	265
Amyloid deposits pyrophosphate arthritis	307	Esterase non-specific cytochemistry effusions cancer diagnosis	347
Amyloid fibrils Congo red birefringence cytoske letal filaments	299	Gastric carcinoma gastric ulcer duodenal ulcer lysozyme immunohistochemistry	451
Anal transitional zone location extent	379	Gastric carcinoma histological types chronic ga stritis histology genetics family study	457
Aorta endothelial cell injury cholesterol rabbit	123	Gastric mucosa gastritis cell division autoradio graphy ³ H thymidine	217
Arteries human ultrastructure smoking	201	Gastric ulcer duodenal ulcer gastric carcinoma lysozyme immunohistochemistry	451
Arteriosclerosis experimental endothelium vital staining permeability TEM neointima	265	Gastritis gastric mucosa, cell division autoradio graphy ³ H thymidine	217
Arteriosclerosis experimental TEM neointima SMC	275	Glia glioma cells cell lines ultrastructure	19
Arthritis pyrophosphate amyloid deposits	307	Glia glioma cells cell lines ultrastructure	29
Ascaris tumors ultrastructure CBA mice	97	Glia cells cultured human ageing <i>in vitro</i> phase iff phenomenon plasma membrane motility scanning electron microscopy growth sumu lation	393
Aspirated goitre nuclear segmentation	11	Glioma cells glia cell lines ultrastructure	19
B-cells pancreatic islets carbonic anhydrase mouse electron microscopy	157	Glioma cells glia cell lines ultrastructure	29
Bone marrow examination small-cell carcinoma of the lung staging	59	Glomerulonephritis immunofluorescent micro- scopy kidney disease	321
Bone tumour malignant fibrous histiocytoma post irradiation sarcoma	437	Glomerulonephritis polyarteritis pathogenesis nu tritional pigs	387
Bone tumours histological typing epidemiology chondroma of hand chondrosarcoma of hand	403	Glomerulonephritis vacuolization glomerulus ill trastructure clinical feature immunofluore science identations deposits	411
Breast carcinoma ductal papillomatosis precancer ous breast lesions young girls	353	Glomerulus vacuolization ultrastructure clinical feature immunofluorescence identations glo merulonephritis deposits	411
Capillary wall cells myocardium rats	15	Goitre aspirates nuclear segmentation	11
Carbonic anhydrase pancreatic islets B-cells mouse electron microscopy	157	" " " " " "	367
Carcinoma <i>in situ</i> testicular neoplasm testicular liminization syndrome	87	" " " " " "	71
Ceramic implants hydroxyproline mechanical pro perties regeneration	193	" " " " " "	79
Cervical carcinoma mouse incidence of carci noma prolactin estradiol bromocriptine	151	" " " " " "	193
Cholesterol endothelial cell injury aorta rabbit	123	Immunofluorescent microscopy kidney disease, normal glomeruli	313
Chronic gastritis gastric carcinoma histological types histology genetics family study	457	Insulin release pancreas duct ligation	285
Cirrhosis primary carcinoma of the liver Den mark	227	Karyotyping rat embryo cell lines transformation oncogenic viruses BK virus	245
Congo red birefringence amyloid fibrils cytoskele tal filaments	299	Kidney disease immunofluorescent microscopy glomerulonephritis	321
Copper accumulation <i>oestro</i> positive granules periportal fibrosis cholestatic liver disease	421	Kidney disease immunofluorescent microscopy normal glomeruli	313
Copperwire fetal death growth retardation micro- scopic malformations	261	" " " " " "	45
Cyclophosphamide wound healing rats skin autoradiography	185	" " " " " "	109
Cystus polypoid urinary bladder catheter	179	Liver chronic alcoholism spermatogenesis testis	51
Cytochemistry effusions non specific esterase cancer diagnosis	347		139
Cytopreparation urothelial cells	63		
Cytoskeletal filaments amyloid fibrils Congo red birefringence	299		
Density determination parathyroid glands	91		
Effusions cytochemistry non-specific esterase cancer diagnosis	347		

Liver, endotoxin shock, light microscopy, electron microscopy, dogs	335	Pancreas, duct ligation, vesicle release	
Liver, lipogranulomas, ultrastructure	45	Pancreatic beta-cell tumours, immunofluorescence, electron microscopy	
Liver, primary carcinoma of, cirrhosis, Denmark	227	Pancreatic islets B-cells, carcinoma, transgenic mouse, electron microscopy	
Lysozyme, gastric ulcer, duodenal ulcer, gastric carcinoma, immunohistochemistry	451	Papillomatosis, ductal breast area - cancerous breast lesions, rat ch	
Malformations, microscopic, copperwired, fetal death, growth retardation	261	Parathyroid glands density determinations	
Malignant fibrous histiocytoma, bone tumour, post-irradiation sarcoma	437	PAS positive non glycoprotein (P-N-G-P) antitrypsin, forensic pathology	
Malignant melanoma, histological features, prognosis, regression analysis	469	Polyarteritis, glomerulosclerosis, glomerular tuft	
Mammary tumours, hormone dependence, growth in vivo and in vitro	427	Post-irradiation sarcoma bone tissue fibrous histiocytoma	
Megakaryocyte morphology, nucleus escape	173	Renin release, submaxillary gland, rat	
Megakaryocytopoiesis, thromboplastin infusion, intravascular coagulation	165	Shock, endotoxin, liver, light microscopy, electron microscopy, dogs	
Melanoma, classification	255	Skin carcinogenesis surface lipids, rats	
Melanoma, cross-sectional profile, level of infiltration, ulceration, vascular invasion prognosis	131	Skin tumours, primary malignant, skin neoplasms	
Melanoma, solar elastosis	361	Small-cell carcinoma of the lung, bronchus examination staging	
Mitosis, malignant tumour, fixation, delay, nude mouse	375	Smoking, human arteries, ultrastructure	
Mycotoxic, ochratoxin A, nephropathy, enzyme histochemistry, pig	237	Spermatogenesis testis chronic alcoholism, rat	
" " " " " "	289	Sponges, implanted granulation tissue	
" " " " " "	15	Submaxillary glands, transplants, renal transplantation	
" " " " " "	51	Surface lipids, skin carcinogenesis, rats	
" " " " " "	71	Testicular feminization syndrome, carcinoma, rat, situ, testicular neoplasm	
Nephropathia epidemica, haemorrhagic fever, kidney, nucleus, inclusions, electron microscopy	237	Testicular neoplasm, carcinoma, intra-testicular feminization syndrome	
Nephropathy, ochratoxin A, mycotoxic, enzyme histochemistry, pig	375	Testis spermatogenesis, chronic alcoholism, rats	
Nude mouse, mitosis malignant tumour fixation delay	237	Transplants, submaxillary glands, renal release	
Ochratoxin A, nephropathy, mycotoxic, enzyme histochemistry, pig	237	Urinary bladder, catheter, polypoid cystitis	
Oncogenic viruses, BK virus rat embryo cell lines transformation, karyotyping	245	Urothelial cells, cytopreparation	
Orcotin positive granules copper accumulation, periparturient fibrosis cholestatic liver disease	421	Vaginal tumour, infantile endodermal sinus tumour alpha-fetoprotein	
		Vinblastine ameloblasts cell death, ultrastructure	
		Wound healing, cyclophosphamide rats skin autoradiography	

ADVICE TO AUTHORS

Usually only articles submitted by Scandinavian authors will be accepted but the Editorial Board may invite contributions from authors outside Scandinavia

Submission of a manuscript for publication in this Journal will be held to imply that the work is original that it has not been published elsewhere and that if accepted it will not be published in any other journal without the Editor's written permission. Contributions should usually be in English but papers in French or German can also be accepted (with English summaries)

The Editorial Board takes no responsibility for contents of or views implied or expressed by the authors or advertisements

Manuscripts should be submitted to the national editor in their final form as top pages not carbon copies in double-spaced type-script in English French or German All written matter illustrations and references should be submitted at the same time

Authors must note and adopt the ACTA's customary arrangement and style failure to do so may lead to delay in publication Instructions to authors are available on request to the Editors

Ordinary articles should generally not exceed 4 printed pages and not more than 5 pages of illustrative material They must contain a summary in English not exceeding 250 words *Brief reports* for immediate publication must not exceed 1½ printed pages Such reports will be published as soon as possible after receipt Manuscripts will be reviewed by appropriate experts Since manuscripts will not be insured against loss or damage contributors are expected to retain duplicate copies of all material submitted for publication Only illustrations of reasonable technical standards will be accepted If the limit of 4 pages is exceeded and if corrections in the proof are particularly numerous or the tabular and illustrative material unusually excessive and/or expensive authors will be requested to contribute to the cost of publication Reference to literature should conform to the standards of *World Medical*

Liver endotoxin shock light microscopy electron microscopy dogs	335	Pancreas duct ligation insulin release
Liver lipogranulomas ultrastructure	45	Pancreatic beta-cell tumours immunofluorescence electron microscopy
Liver primary carcinoma of cirrhosis Denmark	227	Pancreatic islets B cells carbonic anhydrase mouse electron microscopy
Lysozyme gastric ulcer duodenal ulcer gastric carcinoma immunohistochemistry	451	Papillomatosis ductal breast carcinoma pro cancerous breast lesions young girls
Malformations microscopic copperwire fetal death growth retardation	261	Parathyroid glands density determinations
Malignant fibrous histiocytoma bone tumour post irradiation sarcoma	437	PAS positive non glycogenic globules alpha antitrypsin forensic pathology
Malignant melanoma histological features prognosis regression analysis	469	Polyarteritis glomerulonephritis pathogenesis nutritional pigs
Mammary tumours hormone dependence growth <i>in vivo</i> and <i>in vitro</i>	427	Post irradiation sarcoma bone tumour malignant fibrous histiocytoma
Megakaryocyte morphology nucleus escape	173	Renin release submaxillary glands transplants
Megakaryocytopoiesis thromboplastin infusion intravascular coagulation	165	Shock endotoxin liver light microscopy electron microscopy dogs
Melanoma classification	255	Skin carcinogenesis surface lipids rats
Melanoma cross sectional profile level of infiltration ulceration vascular invasion prognosis	131	Skin tumours primary malignant solar radiation
Melanoma solar elastosis	361	Small cell carcinoma of the lung bone marrow examination staging
Mitosis malignant tumour fixation delay nude mouse	375	Smoking human arteries ultrastructure
Mycotoxic ochratoxin A nephropathy enzyme histochemistry pig	237	Spermatogenesis testis chronic alcoholism liver
Myocardial injury histological staining	289	Sponges implanted granulation tissue
Myocardium capillary wall cells rats	15	Submaxillary glands transplants renin release
Needle biopsies double liver changes histopathology	51	Surface lipids skin carcinogenesis rats
Nephropathia epidemica haemorrhagic fever kidney nucleus inclusions electron microscopy	71	Testicular feminization syndrome carcinoma in situ testicular neoplasm
Nephropathy ochratoxin A mycotoxic enzyme histochemistry pig	237	Testicular neoplasm carcinoma in situ testicular feminization syndrome
Nude mouse mitosis malignant tumour fixation delay	375	Testis spermatogenesis chronic alcoholism liver
Ochratoxin A nephropathy mycotoxic enzyme histochemistry pig	237	Transplants submaxillary glands renin release
Oncogenic viruses BK virus rat embryo cell lines transformation karyotyping	245	Urinary bladder catheter polypoid cystitis
Orcein positive granules copper accumulation periportal fibrosis cholestatic liver disease	421	Urothelial cells cytopreparation
		Vaginal tumour infantile endodermal sinus tumour alpha fetoprotein
		Vinblastine ameloblasts cell death ultrastructure
		Wound healing cyclophosphamide rats skin autoradiography

CONTENTS

Vol 87A Fasc 6 1979

Tumours in Iceland 2 Tumours and tumour like lesions of bone Histological types and clinical course <i>Sigurdur V Sigurjonsson Jonas Hallgrimsson Asmundur Brekkan and Stefan Haraldsson</i>	403
Vacuolization of the glomerular basement membrane <i>Gustav Tallqvist Tom Tornroth Tuomo Vanttinen and Amos Pasternak</i>	411
Orcein positive granules in liver cells Occurrence in a consecutive liver biopsy material <i>Mogens Vyberg and Per Thomsen</i>	421
Difference in growth of hormone dependent and hormone independent mammary tumours of GR mice <i>in vivo</i> and <i>in vitro</i> <i>Per Briand Susan M Thorpe and Johan L Daehnfeldt</i>	427
Primary malignant fibrous histiocytoma of bone after radiation <i>L Angervall S Johansson L G Kindblom and J Save Soderbergh</i>	437
Alpha 1 antitrypsin globules in livers from a medicolegal autopsy material <i>Ingermarie Reintoft</i>	447
The distribution of lysozyme in human gastric mucosa in inflammatory and neoplastic disorders <i>S Reitamo J J Reitamo P Sipponen and M Klockars</i>	451
Morphology and function of the gastric mucosa in first degree relatives of probands with histologically different types of gastric carcinoma <i>Timo Ihamaki and Pentti Sipponen</i>	457
✓ Pancreatic beta-cell tumours studied by immunofluorescence and electron microscopy A report of four cases and a review of the literature <i>Ole Frøkjær Thomsen</i>	463
A retrospective histological study of 669 cases of primary cutaneous malignant melanoma in clinical stage I 7 The relative prognostic value of various clinical and histological features The result of a stepwise multiple regression analysis of 553 of these cases <i>Tnve Egg Larsen and Tove Helliesen Grude</i>	469

